UNIVERSIDADE FEDERAL DE SÃO CARLOS
CENTRO DE CIÊNCIAS EXATAS E DE TECNOLOGIA
DEPARTAMENTO DE QUÍMICA
PROGRAMA DE PÓS-GRADUAÇÃO EM QUÍMICA

"Multicomponent Combinatorial Synthesis of Prolyl Peptide-Lipopeptoid Hybrid Catalysts: Application in the Asymmetric Michael Addition under Aqueous Environment."

José Antonio Campos Delgado*

Dissertação apresentada como parte dos requisitos para obtenção do título de MESTRE EM QUÍMICA, área de concentração: QUÍMICA ORGÂNICA

Orientador: Prof. Dr. Márcio Weber Paixão
Co-orientador: Prof. Dr. Marco Antonio Barbosa Ferreira

*bolsista CNPq

São Carlos - SP
2018

UNIVERSIDADE FEDERAL DE SÃO CARLOS

Centro de Ciências Exatas e de Tecnologia
Programa de Pós-Graduação em Química

Folha de Aprovação

Assinaturas dos membros da comissão examinadora que avaliou e aprovou a Defesa de Dissertação de Mestrado do candidato José Antonio Campos Delgado, realizada em 29/11/2018:

Prof. Dr. Márcio Weber Paixão
UFSCar

Prof. Dr. Cristiano Raminelli
UNIFESP

Prof. Dr. Ricardo Samuel Schwab
UFSCar

``Everything should be made as simple as
possible, but not simpler.´´

Albert Einstein

Dedicated to my Family!

Acknowledgments

Firstly, I´m proud to express most of the acknowledgments to my dear parents for so much education, and my brother, Pedro, and Maite for their unconditional support.

I´m profoundly grateful to Dr. Márcio Weber Paixão, for giving me this opportunity and spending his time teaching me. His passion and skill for chemistry are, without a doubt, the best I have ever seen. Besides providing an exciting educational work environment, he has shown true concern and extraordinary lab experience for which I will always be incredibly grateful.

I would like to thank all the professors of the Chemistry Department at the Federal University of São Carlos (UFSCar) for the wonderful class and seminaries. Also, thank my friends in and outside of the lab of LSPN during the years 2016-2018.

Abreviatures

AE	Atom economy
Aib	Aminoisobutyric acid
DCC	Diciclohexylcarbodiimide
DIC	Diisopropylcarbidiimide
DFT	Density Functional Theory
d.r.	Diastereoisomeric ratio
e.e.	Enantiomeric excess
FT-ICR	Fourier transform-ion cyclotron resonance
FOT	Frontier orbital theory
HB	Hydrogen bonding
HBTU	*N, N, N′, N′*-Tetramethyl-O-(1H-benzotriazol-1-yl) uronium hexafluorophosphate
HOBt	1-Hydroxybenzotriazole hydrate
HOMO	Highest occupied molecular orbital
LUMO	Lowest unoccupied molecular orbital
HPLC	High-performance liquid chromatography
I-MCRs	Isocyanide-based multicomponent reactions
$K_{trans/cis}$	*Trans/cis* ratio of conformers
MCR	Multicomponent reaction
MW	Microwave
NMR	Nuclear magnetic resonance
PDA	Passerini three-component reaction
PEG-300	Poliethylenglycol-average molecular mass 300 Da
PMA	Phosphomolybdic acid hydrate
SI	Steric interactions
THF	Tetrahydrofuran
TLC	Thin layer chromatography
TS	Transition states
Ugi-4CR	Ugi four-component reaction
Ugi-3CR	Ugi three-component reaction
UPC^2	Ultra performance convergence chromatography

List of Tables

List of Figures

List of Schemes

Resumo

SÍNTESE COMBINATORIA MULTICOMPONENTE DE CATALISADORES PROLIL PEPTÍDEO-LIPOPEPTÓIDES HÌBRIDOS: APLICAÇÃO NA ADIÇÃO DE MICHAEL ASSIMÉTRICA EM MEIO AQUOSO

Este estudo descreve a síntese de uma nova biblioteca de catalisadores híbridos de peptídeos prolil-lipopeptóides através de uma abordagem combinatória multicomponente. Para o projeto deste catalisador, levamos em consideração o crescente interesse no desenvolvimento de tecnologias mais sustentáveis e a recente contribuição de nosso grupo de pesquisa nessa área. Para este fim, usando o protocolo de Ugi-quatro componentes, incorporamos cadeias laterais lipídicas na arquitetura do catalisador híbrido peptídeo prolil-peptóide. A inserção de funcionalidades com propriedades anfifílicas fornece propriedades surfactante ao organocatalisador. Os compostos foram ainda avaliados como organocatalisadores na adição ambientalmente amigável de aldeídos a nitrostirenos. Os adutos de Michael foram obtidos em altos rendimentos, diastereosseletividades e excelentes enantiosseletividades utilizando baixa carga de catalisador, empregando água como solvente sem a adição de outro aditivo.

Abstract

MULTICOMPONENT COMBINATORIAL SYNTHESIS OF PROLYL PEPTIDE-LIPOPEPTOID HYBRID CATALYST: APPLICATION IN THE ASYMMETRIC MICHAEL ADDITION UNDER AQUEOUS ENVIRONMENTAL

This study describes the synthesis of a new library of prolyl peptides-lipopeptoid hybrids catalysts through a multicomponent combinatorial approach. For the design of this catalyst library, we took into consideration the growing interest in the development of environmentally friendly technologies and the recent contributions of our research group in their field. To this end, by using the Ugi-four component protocol we have incorporated lipidic side chains in the architecture of the proyl peptide-peptoid hybrid catalyst. The insertion of functionalities with amphiphilic properties afford to the organocatalyst surfactant properties. Therefore, they have been further evaluated as an organocatalysts in the environmentally friendly enantioselective addition of aldehydes to nitrostyrenes. The Michael adducts were obtained in high yields, diastereoselectivities and excellent enantioselectivities using low catalyst loading under water as solvent without addition of any other additive.

Summary

1 Introduction

The environmental concerns associated with synthetic organic chemistry have raised rigorous and compelling demands for greener processes. The development of cost-effective and environmentally benign catalytic systems has become one of the main topics of modern chemistry.[1, 2, 3] Traditional organic synthesis relies heavily on organic solvents for a multitude of tasks, including the dissolution of components and the facilitation of chemical reactions, since many reactants and reactive species are incompatible or immiscible with water. Since they are used in large quantities compared to the reactant's solvents have been the focus of environmental concerns due to their hazards.[4] Along with the reduction of the environmental impact of organic synthesis, the use of water as a reaction medium also benefits chemical processes by simplifying operations, allowing moderate reaction conditions and, on occasion, providing unanticipated reactivity and selectivity.[5]

1.1 Green Chemistry

According to United State Environmental Protection Agency, the ´´Green Chemistry´´: *It is the design of chemical products and processes that reduce or eliminate the use or generation of hazardous substances. Green chemistry applies across the life cycle of a chemical product, including its design, manufacture, use, and ultimate disposal. Green chemistry is also known as sustainable chemistry.*

---

[1] TUCKER, J. L.; FAUL, M. M. Industrial research: Drugs companies must adopt green chemistry. *Nature*. **2016**, *534*, 27-29.

[2] SANDERSON, K., It is not easy being green. *Nature*. **2011**, *469*, 18-20.

[3] FEU, K. S.; DE LA TORRE, A. F.; SILVA, S.; DE MORAES JUNIOR, M. A. F.; CORRÊA, A. G.; PAIXÃO, M. W. Polyethylene glycol (PEG) as a reusable solvent medium for an asymmetric organocatalytic Michael addition. Application to the synthesis of bioactive compounds. *Green Chem*., **2014**, *16*, 3169−3174.

[4] ALDER, C. M.; HAYLER, J. D.; HENDERSON, R. K.; REDMAN, A. M.; SHUKLA, L.; SHUSTER, L. E.; SNEDDON, H. F. Updating and further expanding GSK's solvent sustainability guide. *Green Chem*., **2016**, *18*, 3879-3890.

[5] KITANOSONO, T.; MASUDA, K.; XU, P.; KOBAYASHI, S. Catalytic organic reactions in water toward sustainable society. *Chem. Rev*. **2018**, *118*, 679−746.

This concept also involves 12 fundamental principles enunciated below:[6, 7]

- Waste prevention instead of remediation
- **Atom efficiency**
- Less hazardous/toxic chemicals
- Safer products by design
- **Innocuous solvents and auxiliaries**
- Energy efficient by design
- Preferably renewable raw materials
- Shorter syntheses (avoid derivatization)
- **Catalytic rather than stoichiometric reagents**
- Design products for degradation
- Analytical methodologies for pollution prevention
- Inherently safer processes

Beside to these principles, several metrics have been introduced to measure the degree of greenness and sustainability. Two of the most important are the Atomic Economy (AE) and the environmental factor (E). Professor Barry M. Trost was the first researcher to introduce the term AE, [8] which is defining as *"the ability of a chemical process to incorporate as many as possible of the atoms."* and can be calculated by the following equation:[9], (FIGURE 1).

$$AE = \frac{MW\ (product)}{\sum MW\ (reagent)}\ X\ 100$$

FIGURE 1. Atom economy is defined as the ratio between the mass of the product obtained and the mass of all the reagents used, expressed in percent.

In this way, chemical transformations that convert most of the starting materials into a single desired product have a high atomic economy and are highly desired transformations in

[6] ANASTAS, P. T., WILLIAMSON T. C. *ACS* Symp.Ser., ed., **1996**, ch. 1, *626*, 1–17.

[7] SHELDON, R. A. Fundamentals of green chemistry: efficiency in reaction design. *Chem. Soc. Rev*. **2012**, *41*, 1437-1451.

[8] TROST, B. M. The atom economy-A search for synthetic efficiency. *Science*. **1991**, *254*, 1471-1477.

[9] LI, C-J.; TROST, B. M. Green chemistry for chemical synthesis. *Proc Nat Acad Sci.,* **2008**,*105*, 13197–13202.

terms of sustainability, since they reduce the waste generated, and therefore their environmental impact.

Additionally, Professor Rogers Sheldon has formulated another important metrics, the so-called E Factor.[10] Almost over twenty years E factor is an environmental measure that expresses the relationship between the amount of product generated and the amount of waste generated in the process[11], as shown in FIGURE 2.

$$E\ Factor = \frac{kg\ waste}{kg\ product}$$

FIGURE 2. E Factor equation.

High values of E Factor mean more waste so the ideal value of this measure would be zero. An exception to this factor is that it does not include water as waste, only in some cases the residual salts that are present in it are considered. So, the simple substitution in the use of organic solvents for water could be the switch towards sustainability.

1.2   "On Water" or "In Water" Catalysis

In this sense, back to the 1980s, Breslow reported a pioneering work in the acceleration of Diels-Alder reactions performed in water - i.e., 10-15 min versus 35-40 min - between cyclopentadiene **1** and butanone **2** in aqueous emulsion[12] SCHEME 1.

SCHEME 1. [4+2] cycloaddition accelerated by hydrophobic effect in water.

Theoretical models are mainly focused on an explanation of how the rate of the chemical reactions "on water" or "in water" is accelerated by a water molecule. This has been analyzed

[10] SHELDON, R. A., Organic synthesis - Past, present, and future, *Chem. & Ind.*, **1992**, 903-906.
[11] SHELDON, R. A. The E factor: fifteen years on. *Green Chem.*, **2007**, *9*, 1273-1283.
[12] RIDEOUY, D. C.; BRESLOW, R. Hydrophobic acceleration of Diels-Alder reactions. *J. Am. Chem. Soc.*, **1980**, *102*, 7816–7817.

in comprehensive reviews and articles.[13,14] Among them, the driving force that explains the rate increase in the water-oil biphasic system was attributed mainly to hydrogen bonding interactions in the interface and hydrophobic effects.[15]

As such concepts, it is debated several types of terms to describe reactions proceeding "in water", "under water", "in aqueous medium", or "on water", "in concentrated organic phases" but none of those adequately represent the effect of water or the difference seem between conditions with water present and solvent-free conditions. About this dilemma, two general terms can be defined "a reaction in water" as one in which the reactant participating in the reaction are dissolved homogeneously in water whereas "a reaction in the presence of water" should be used for a reaction that proceeds in a concentrated organic phase with water being present as a second phase that influences the reaction in the organic phase.

Moreover, in "on water", or "a reaction in the presence of water" catalysis, the transition state occurs at the organic layer of the organic–water interface, this interaction with water is strongly dependent on the properties of each substrate and can be explained by a simple acid-catalysis mechanism facilitated by the strong adsorption of the hydroxide ion by-product at the oil-water interface[16] (FIGURE 3).
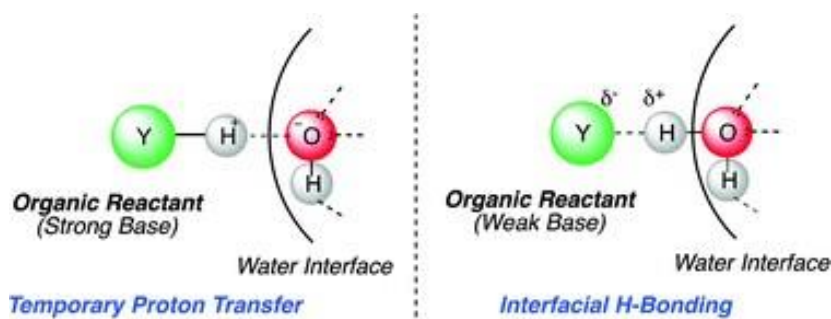
FIGURE 3. "On water" interaction.

1.3 Organocatalysis

Organocatalysis, the catalytic application of small organic molecules or also known as catalysis in the absence of metals and enzymes, has become a well-recognized concept and a highly active field of research. In recent years, reactions catalyzed by purely organic molecules have found an increasing field for the synthesis of complex molecules.[17,18] As a consequence, organocatalysis is unquestionably one of the pillars of asymmetric catalysis together with

---

[13] BUTLER, R. N.; COYNE, G. Organic synthesis reactions on-water at the organic-liquid water interface. *Org. Biomol. Chem.*, **2016**, *14*, 9945-9960.

[14] BUTLER, R. N.; COYNE, A. G. Understanding ´´On-Water´´ catalysis of organic reactions. Effects of H+ and Li+ ions in the aqueous phase and nonreacting competitor H-bond acceptors in the organic phase: On H_2O versus on D_2O for Huisgen cycloadditions. *J. Org. Chem.*, **2015**, *80*, 1809-1817.

transition metal catalysis and biocatalysis.[19] Primary chiral amines, thioureas and proline derivatives are the most common organocatalysts used (FIGURE 4).

FIGURE 4. General methods in aminocatalysis

In organic synthesis, we usually think of catalysts as being transition metals, main elements group, and other elements besides C, H, N, and O. Recently, however, there have been significant advances in the organocatalysis field, with the development of new organic systems that have desirable catalytic behaviors. Part of the motivation for such efforts is the air and water instability often associated with metal-based systems, the environmental benefit of avoiding toxic metals, and the ready availability of many enantiomerically pure orga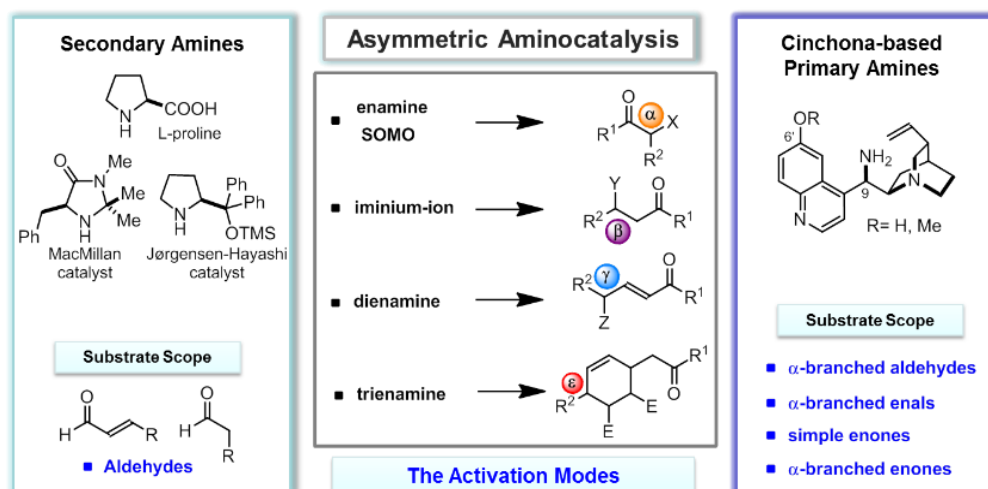nic molecules. The well-defined geometry of the system produces very high stereoselectivities. Furthermore, the benefits of inexpensive catalysts and the ability to run the reaction in the open air with wet solvents often more than compensates. Using this approach, a variety of reactions have succumbed to organocatalysis, including Diels-Alder and Friedel-Crafts reactions, direct alkylations of heterocycles such as furan and indole, and a variety of Michael additions.[19, 20]

1.3.1 Asymmetric Enamine Catalysis

After the pioneering work by List, Lerner, and Barbas employing chiral secondary amines (i.e., proline-type catalysts) to catalyze an intermolecular aldol reactions[21] and the successive

---

[15] GUO, W.; LIU, X.; LIU,Y.; LI, C. Chiral catalysis at the water/oil interface. *ACS Catal*. **2018**, *8*, 328-341.

[16] BEATTIE, J. K., MCERLEAN, C. S. P., PHIPPEN, C. B. W. The mechanism of on-water catalysis. *Chem. Eur. J.,* **2010**, *16*, 8972 – 8974

[17] WASER, M., Asymmetric organocatalysis in natural product syntheses. Springer, Vienna, **2012**.

[18] MARQUEZ-LOPEZ, E., HERRERA, R. P., CHRISTMANN, M., Asymmetric organocatalysis in total synthesis-a trial by fire. *Nat. Prod. Rep*. **2010**, *27*, 1138-1167.

expansion of the research interest in organocatalysis. The general concept of enamine catalysis was extensively applied to a wide variety of α-functionalization of carbonyl compounds, e.g. aldol reactions, α- aminations, α-oxidations and α-halogenations, Mannich reactions as well as Michael and hetero Michael reactions (SCHEME 2).[22]
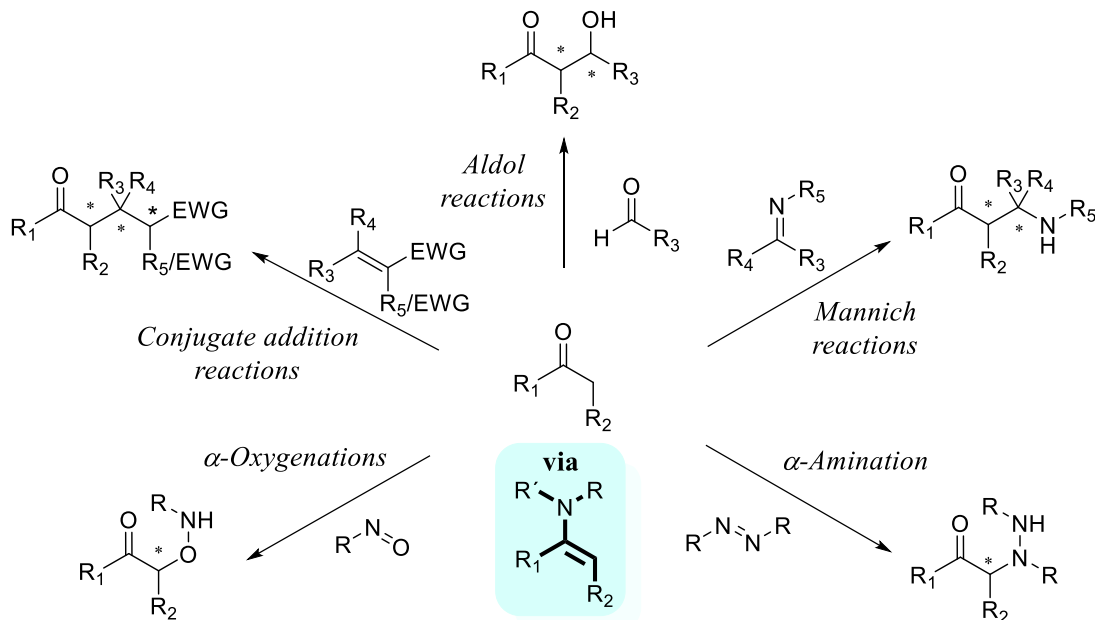
SCHEME 2. Some α-functionalization of aldehydes or ketones promoted by proline-type catalysts via enamine.[23]

A rational design is usually an enormous challenge and directly depends on the chosen of asymmetric reaction to pursue. Rarely, the discovery of potential catalysts is successful. The process often involves a separate synthesis of many catalysts and testing their catalytic properties in individual reaction, like test-error. The development of an effective organocatalyst usually needs further optimization process, in which both, the substituents and position of the catalytic functions have been examined towards the reaction of interest.

[19] ANSLYN, E. V., DOUGHERTY, D. A. Modern physical organic chemistry. University Science Books. **2006**, Chap. 9.

[20] MACMILLAN, D. W. C., The advent and development of organocatalyst. *Nature*., **2008**, *455*, 304-308.

[21] LIST, B., LERNER, R. A., BARBAS, C. F. Proline-catalyzed direct asymmetric aldol reactions. *J. Am. Chem. Soc.* **2000**, *122*, 2395-2396.

[22] MUKHERJEE, S., YANG, J. W., HOFFMANN, S., LIST, B. Asymmetric enamine catalysis. *Chem. Rev.* **2007**, *107*, 5471-5569.

[23] DUSCHMALÉ, J. Peptide catalyzed conjugate addition reactions of aldehydes to nitroolefins-mechanistic investigations and challenging substrates. University of Basel. Ph.D. thesis. **2013**.

However, how the pyrrolidine-type catalysts induce stereoselectivity?

Let´s explain the enamine activation mechanism, the insights of the stereochemistry induction for the substituents and catalytic function.

It is important to understand the basic principles of enantioselectivity induction to design a new catalyst.

1.3.2 Mechanistic aspects

The enamine formation is produced after the condensation between pyrrolidine ring and the correspondent carbonyl group (aldehyde or ketone) as shown in the catalytic cycle (SCHEME 3). The generated enamine has two possible configurational isomers (E and Z), in a thermodynamic equilibrium. Unless other general and specific interactions favor the enamine Z, the enamine E is energetically most favored and always the formation of this configuration is predominantly. Two rotational isomers (*s-trans* and *s-cis*) exist in the enamine E, whereby steric interactions the most favorable is the *s-trans*-enamine E (SCHEME 3). It is generally accepted that the *s-trans*-enamine is the most stable conformer, where the double bond is situated in the opposite direction to the bulky group located in the 2-position of the pyrrolidine ring.
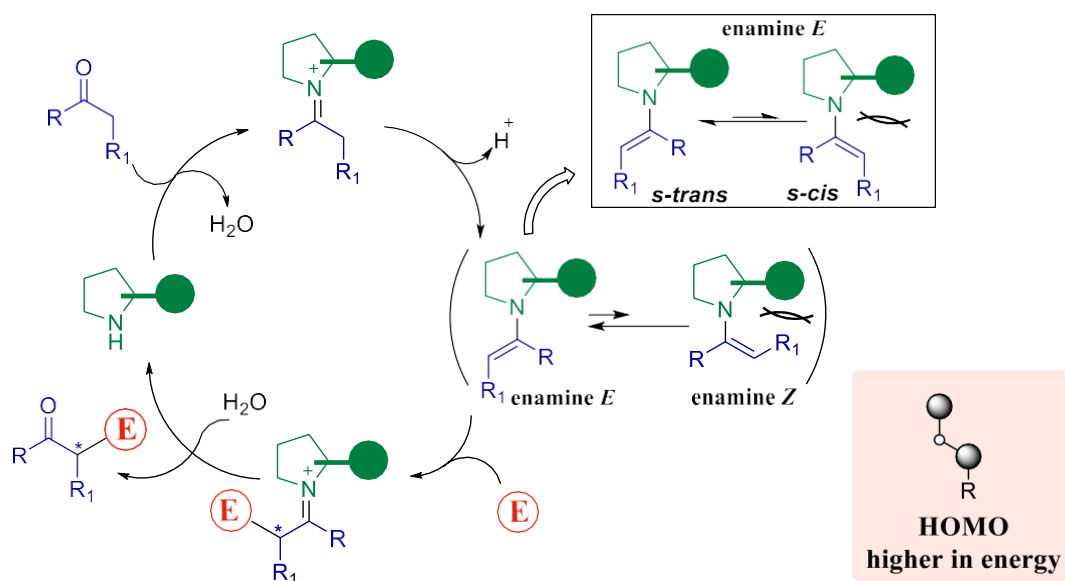
SCHEME 3. Pyrrolidine-catalyzed activation cycle of enamine.

The *s-trans* conformer has also been considered as the most reactive intermediate until now (*vide infra*). So far, the role of the pyrrolidine ring is to activate the oxo component increasing the energy of the high occupied molecular orbital (HOMO) of the substrate when the enamine is formed but not in the trajectory of the electrophile in the formation of the new stereogenic C-C bond. The trajectory of the electrophile depends on the side group attached to the pyrrolidine ring.

The trajectory of the incoming electrophile has traditionally been proposed to follow either of the two different models (A and B, FIGURE 5) based on the nature of catalysts. Model A shows the induction of stereoselectivity by a hydrogen bond (HB) interaction, and model B shows the approach of the electrophile ruled by steric interaction (SI).
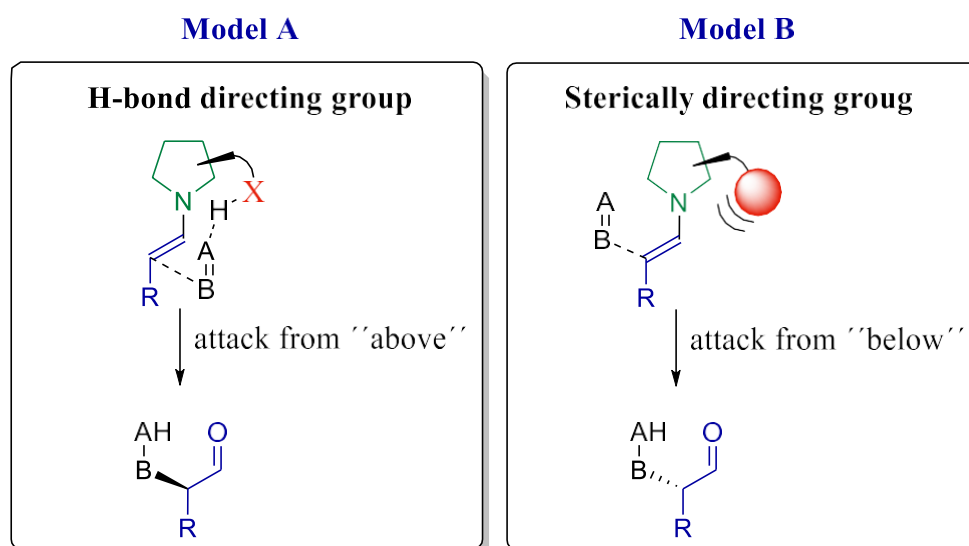

FIGURE 5. Stereocontroller models A and B. Hydrogen Bonding vs. Steric Hindrance

In general, catalysts with a HB directing group (i.e. -CO$_2$H, -OH, -CONH$_2$, etc…)[24, 25, 26, 27, 28] at the position 2 of the pyrrolidine ring, follows model A (see **4**, **5**, **6**, **7**, FIGURE 6). In contrast, bulky substituents in the position 2 of pyrrolidine ring (i.e. -2Ph, -2PhCF$_3$, etc…)[29, 30,

[24] HAJOS, Z. G.; PARRISH, D. R., Stereocontrolled synthesis of trans-hydrindan steroidal intermediates. *J. Org. Chem.,* **1973**, *38*, 3239.

[25] AHRENDT, K. A.; BORTHS, C. J.; MACMILLAN, D. W. C., New strategies for organic catalysis: The first highly enantioselective organocatalytic Diels-Alder reaction´´. *J. Am. Chem. Soc.,* **2000**, *122*, 4243.

[26] WENNEMERS, H., Peptides as asymmetric aatalysis for Aldol reactions. *Chimia.,* **2007**, *61*, 276.

[27] COBB, A. J. A.; SHAW, D. M.; LEY, S. V., 5-Pyrrolidin-2-yltetrazole: A new catalytic more soluble alternative to proline in an organocatalytic asymmetric Mannich-type reaction. *Synlett.,* **2004**, *3*, 558.

[28] VISHNUMAYA, R. M.; GINOTRA, S. K.; SINGH, V. K., Highly enantioselective direct Aldol reaction catalyzed by organic molecules. *Org. Lett.,* **2006**, *8*, 4097.

[29] HALLAND, N., ABUREL, P. S.; Jørgensen, K. A., Highly enantioselective organocatalytic conjugate addition of malonates to acyclic α,β-unsaturated enones. *Angew. Chem. Int.* Ed., **2003**, *42*, 661.

[30] MELCHIORRE, P., JØRGENSEN, K. A., Direct enantioselective Michael addition of aldehydes to vinyl ketones catalyzed by chiral amines. *J. Org. Chem.,* **2003**, *68,* 4151.

[31], [32] where the steric hindrance blocks one face of the enamine, agree with model B of induction of stereoselectivity (see **8**, **9**, **10**, FIGURE 6). Some pyrrolidine-type catalysts are illustrated again in FIGURE 6 for better understanding; the red color in the structures refers to the respective HB or SI groups.
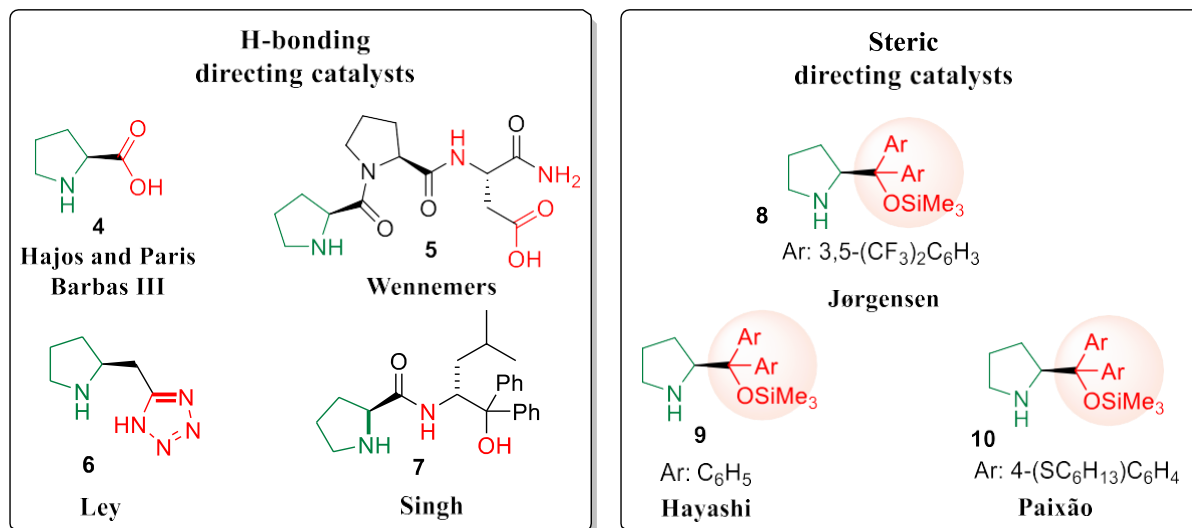

FIGURE 6. Some pyrrolidine-type catalysts with Hydrogen Bonding or Steric directing groups.

1.3.3 Conjugate Michael Addition Reactions of Aldehydes to Nitroolefins

Conjugate addition reactions of carbon nucleophiles to electron deficient double bonds are widely used in organic synthesis in general[33] and in organocatalytic processes with enamine activation.[34], [35], [36] The Michael reaction is one of the most useful methods for the mild formation of C–C bonds that follows an enamine mechanism. It is, amongst other asymmetric reactions, used to test new catalysts based on enamine activation. Nitroalkenes are

---

[31] HAYASHI, Y.; GOTOH, H.; HAYASHI, T.; SHOJI, M. Diphenylprolinol silyl ethers as efficient organocatalysts for the asymmetric Michael reaction of aldehydes and nitroalkenes. *Angew. Chem. Int. Ed.,* **2005**, *44,* 4412.

[32] DEOBALD, A. M., CORRÊA, A. G., RIVERA, D. G., PAIXÃO, M. W., Organocatalytic asymmetric epoxidation and tandem epoxidation/Passerini reaction under eco-friendly reaction conditions. *Org. Biomol. Chem.,* **2012***, 10,* 7681-7684.

[33] PERLMUTTER, P., Conjugate addition reactions in organic synthesis, Pergamon Press, Oxford, **1992**.

[34] VICARIO, J. L., BADÍA, D., CARRILLO, L., Organocatalytic enantioselective Michael and Hetero-Michael reactions. *Synthesis* **2007**, *14*, 2065-2092.

[35] VICARIO, J. L., Organocatalytic enantioselective conjugate addition reactions: a powerful tool for the stereocontrolled synthesis of complex molecules, Royal Society of Chemistry, Cambridge, **2010**.

[36] TSOGOEVA, S. B., Resent advances in asymmetric organocatalytic 1,4-conjugate additions. *Eur. J. Org. Chem.* **2007**, *11*, 1701-1716.

particularly attractive Michael acceptors due to their high electrophilicity[37] and the synthetic utility of the nitro group.[38] The conjugate addition of aldehydes to nitroolefins provides γ-nitroaldehydes that are versatile intermediates for the synthesis of, for example, chiral γ-butyrolactones,[39] pyrrolidines,[40] or γ-amino acids[41] (SCHEME 4).
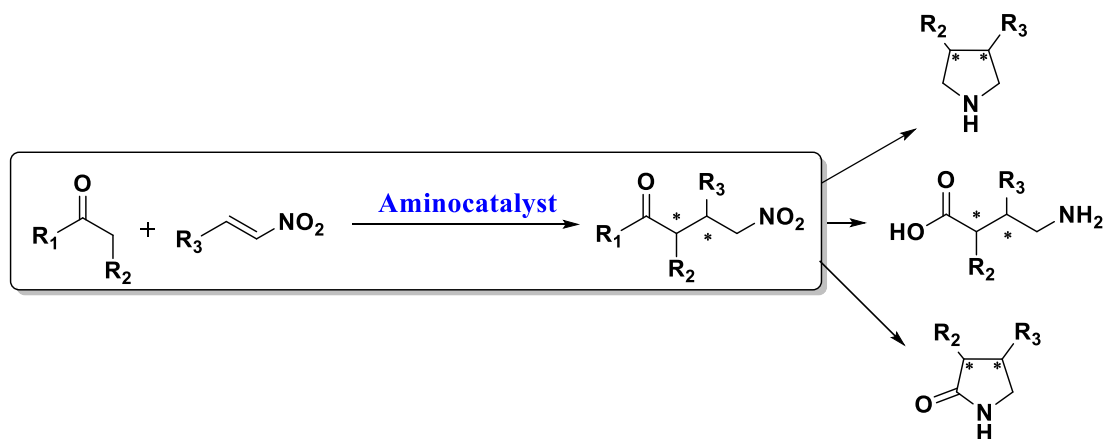
SCHEME 4. Conjugate addition reactions of aldehyde to nitroolefins.

In SCHEME 5 it can be noted that the substituent attached to the pyrrolidine core is important in the direction of the induction in both enantio- and diastereoselectivity of the formed compounds. Four possible transition states (TS) can be drawn for both models (model A and model B, SCHEME 5). These TS show that even with the possibility to form the *s-cis*-enamine *E* (TS III, IV, VII and VIII), the equilibrium is displaced to the formation of the most stable *s-trans*-enamine E (TS I, II, V and VI) of both models, and therefore, the difference in terms of energy between these TS determines the course of stereoselectivity. Model A, also

---

[37] ZENZ, I., MAYR, H., Electrophilicities of trans-β-nitrostyrenes. *J. Org. Chem.* **2011**, *76*, 9370-9378.

[38] ONO, N., The nitro group in organic synthesis, Wiley-VCH, New York, **2001**.

[39] PALOMO, C., VERA, S., MIELGO, A., GÓMEZ-BENGOA, E., Highly efficient asymmetric Michael addition of aldehydes to nitroalkenes catalyzed by a simple 4-*trans*-hydroxyprolylamida. *Angew. Chem. Int. Ed.* **2006**, *45*, 5984-5987.

[40] RUIZ, N., REYES, E., VICARIO, J. L., BADÍA, D., CARRILLO, L., URIA, U., Organocatalytic enantioselective synthesis of highly functionalized polysubstituted pyrrolidines. *Chem. Eur. J.,* **2008**, *14*, 9357-9367.

[41] CHI, Y., GUO, L., KOPF, N. A., GELLMAN, S. H., Enantioselective organocatalytic Michael addition of aldehydes to nitroethylene: efficient access to γ²–amino acid. *J. Am. Chem. Soc.* **2008**, *130*, 5608-5609.

known as Houk-List model,[42, 43] (SCHEME 5, TS I-IV) shows an HB between the proton of the carboxylic acid and the nitro group of *β*-nitrostyrene. This HB directs the *β*-nitrostyrene to the ***Re*** face of the enamine by a like approach, thus forming the *S,R*-diastereomer as the major product. However, model B is determined by SI, the bulky group attached to pyrrolidine core produces a steric hindrance capable of approaching the ***Si*** face of enamine to *β*-nitrostyrene and thus produce the inversed *R,S*-configuration of Michael product (see model B in SCHEME 5). In either case, model A or model B led to the formation of the major diastereomer *syn*.

Two factors are important for good stereoselection: 1) one face of the enamine must be less accessible; 2) the equilibrium between the enamine rotamers must be well displaced to the one side.

According to SCHEME 5, models A and B having the pyrrolidine-type catalyst with the same configuration produce different stereoisomers. The ***Re-Re*** approach is favored for model A and ***Si-Si*** for Model B. This makes us conclude that the stereoselection is totally influenced by the linked functional group in the backbone of the catalyst.

---

[42] BAHMANYAR, S., HOUK, K. N., Transition states of amine-catalyzed Aldol reactions involving enamine intermediates: Theoretical studies of mechanism, reactivity, and stereoselectivity. *J. Am. Chem. Soc.*, **2001**, *123,* 11273.

[43] BAHMANYAR, S., HOUK, K. N., MARTIN, H. J., LIST, B. Quantum mechanical predictions of the stereoselectivities of proline-catalyzed asymmetric intermolecular Aldol reactions. *J. Am. Chem. Soc.*, **2003**, *125*, 2475.
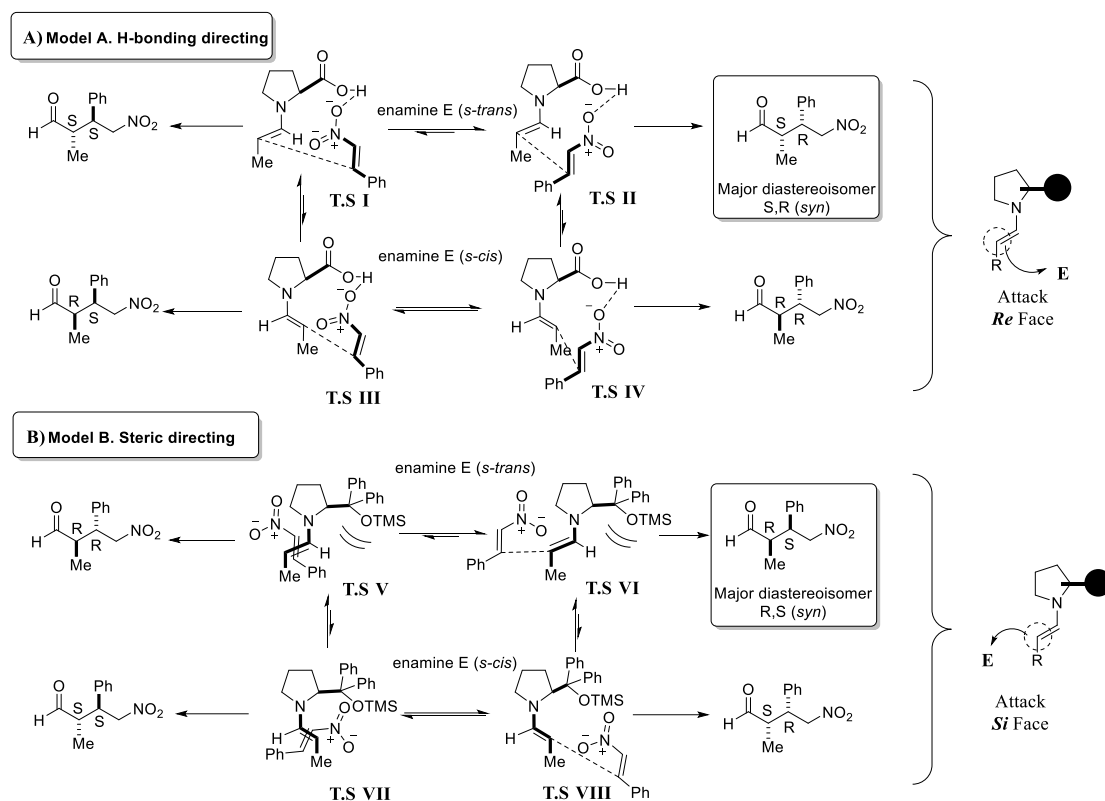
SCHEME 5. Transition states by HB and SI control in Michael addition: A) HB with S-Proline as catalyst, B) SI with Hayashi´s catalyst.

Not only the adopted model of the catalyst and/or backbone of catalysts, but also the intermediates structures formed in the catalytic system can affect the stereoselectivity of the final product. Thereafter, the tridimensional intermediates structure of catalysts and substrates (Transitions States), as well as parasitic intermediates should also be taken in consideration. Blackmond and co-workers[44] reported a kinetic study of the Michael reaction, where they found a parasitic intermediated which influences the stereoisomers of the final product. In this work, the conjugate addition of *n*-propanal to *β*-nitrostyrene, catalyzed by diarylprolinol silyl ether, reveals that the formation of the product (iminium species, SCHEME 6) is the rate-determining step of the reaction, and not the enamine formation as mentioned before. The formation of the cyclobutane intermediate (SCHEME 6), called as `*parasitic intermediate*´ during the catalytic cycle, is very important to keep the high stereoselectivity in the final product. Interestingly, this parasitic intermediate, which should delay the reaction, is important in the stereoselectivity.

---

[44] BUR, J.; ARMSTRONG, A.; BLACKMOND, D. G. Mechanistic rationalization of organocatalyzed conjugate addition of linear aldehydes to nitro-olefins. J. *Am. Chem. Soc.,* **2011**, *133,* 8822.
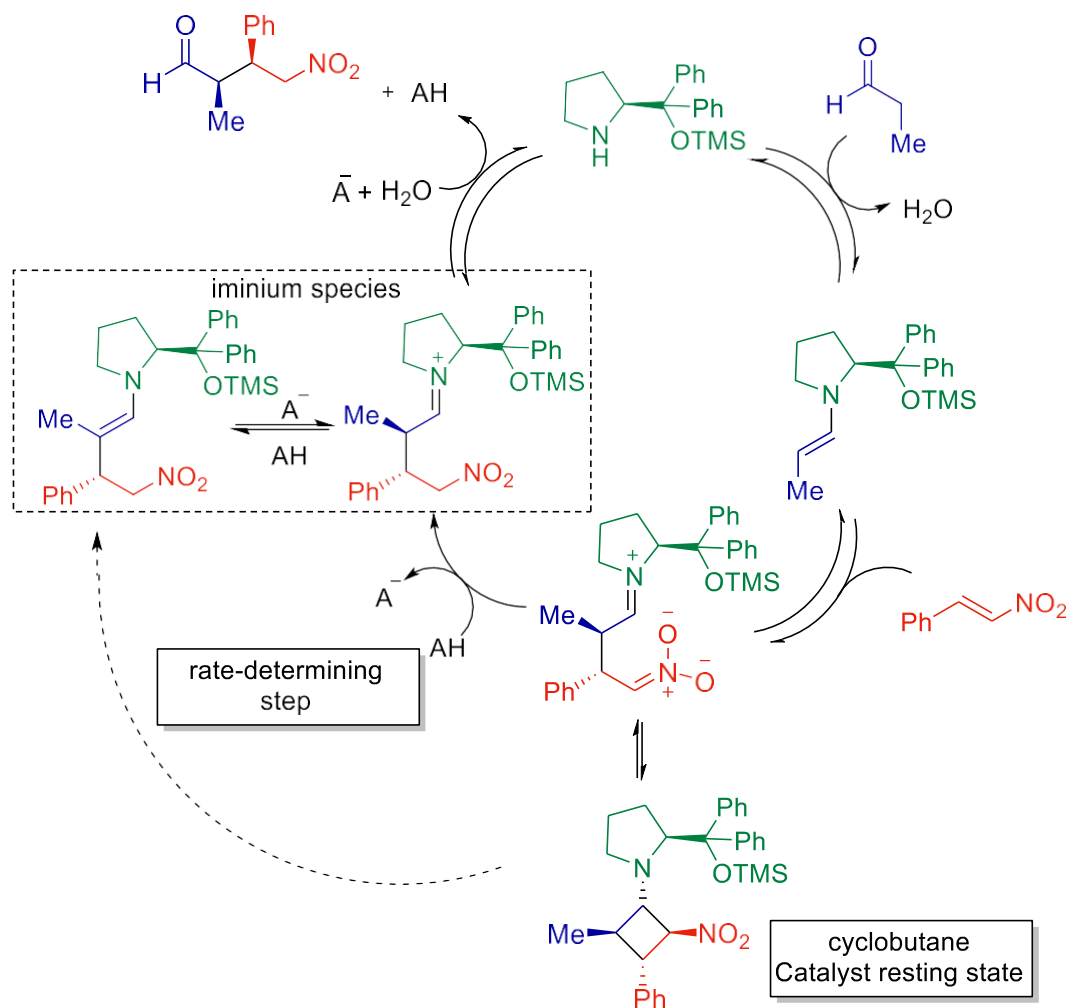
SCHEME 6. Catalytic system for Michael reaction proposed by Blackmond.

These mechanistic principles help us to design new organocatalysts based in the covalent enamine activation. Although a rational design is usually an enormous challenge, major is to develop new ecofriendly and economic route to access a library of catalysts to test.

1.4   Peptides catalysts. A rational design

The invention of peptide synthesis in the 50th stimulated the development of different application areas in which synthetic peptides are now used, including the development of specific antibodies against pathogenic proteins, the study of protein functions, study of enzyme-substrate interactions and catalysis. Every year it is being more evident that combinatorial chemistry can face the synthesis and analysis not only of analogous entities (focused libraries) of previously identified leads but also of truly new catalytic systems based on novel dissimilar chemical functionalities.

Small peptides employed as organocatalysts have molecular weights often comparable to that of typical synthetic catalysts, and they provide the same and, in some cases, better results in asymmetric enamine reactions. [45]How can we design a new peptide (or focused library) catalyst?

In the same way, the first step is thinking of the target reaction (i.e., Aldol, Michael, Mannich reaction, etc…), the mechanism and the reaction conditions. Second: selecting the mode of activation (i.e., enamine, iminium…). This step is very dependent of the first step where the peptide in point should carry a secondary or primary amine depending on the asymmetric reaction selected. Third: improving the backbone in the structure of the peptide catalyst considering model A or B explained in SCHEME 5. Some structural motifs of peptides[46] are represented in FIGURE 8; α-helix and β-turn are the major motifs adopted by small-synthesized peptide catalysts. Fourth: screening peptide catalysts, the catalytic efficiency, stereoselectivity and the scope of catalysts are followed in this step (FIGURE 7).
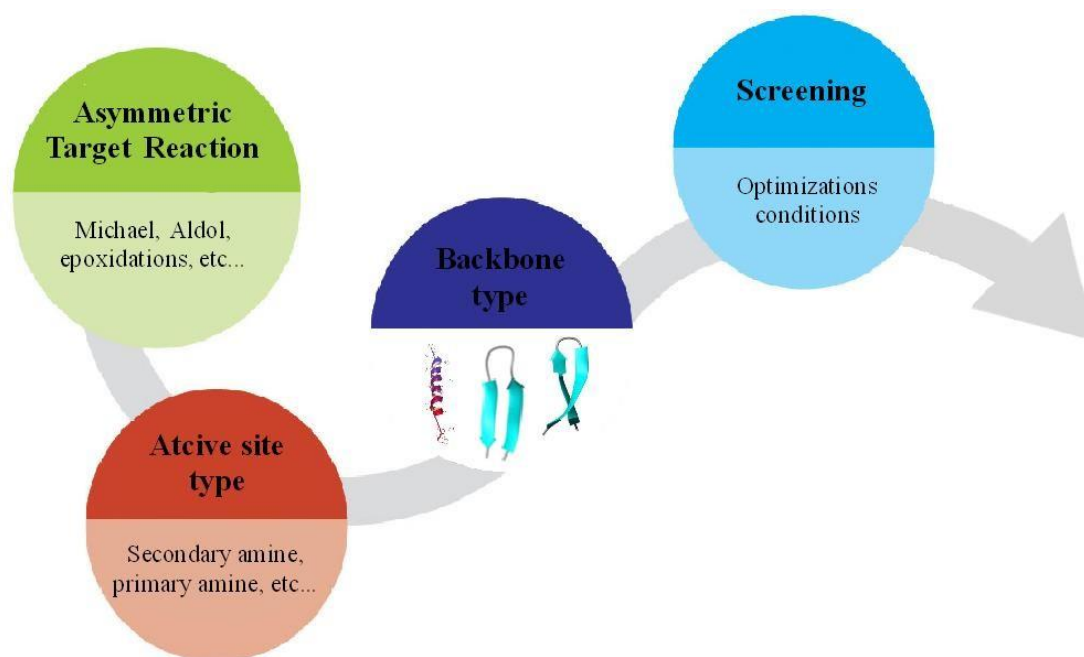

FIGURE 7. Rational design of a new peptide catalyst.

The secondary structure in peptides is the ordered arrangement or conformation of amino acids unfolded spatially to form the lowest energy conformation. The preferred peptide chain conformation under physiological conditions is dominated by the energetically favored torsion angles, together with

[45] COLBY, E. A.; MENNEN, S. M.; XU, Y.; MILLER, S. J. Asymmetric catalysis mediated by synthetic peptides. *Chem. Rev.,* **2007**, *107,* 5759.

[46] VENKATRAMAN, J.; SHANKARAMMA, S.C.; BALARAM, P. Design of folded peptides. *Chem. Rev.*, **2001**, *101,* 3131.

additional stabilizing factors such as HB and hydrophobic contacts. A hydrogen bonding is formed between the NH group (hydrogen bond donor) and the carbonyl oxygen atom (hydrogen bond acceptor) of peptide bonds. The energy of a single HB is quite low ($20\,\text{kJmol}^{-1}$), compared to a covalent bond (200–$400\ \text{kJmol}^{-1}$). However, in most secondary structure elements stabilized by HB it is multiple rather than single hydrogen bonds that are formed, and it is these multiple interactions of such a cooperative system that result in considerable stabilization. These interactions cause three different motifs: α-helix, β-sheet, and coil. [46, 47] Among these secondary structures, α-helix and β-turn motifs are the major structures employed as catalysts.

The α-helix comprises a spiral arrangement of the peptide backbone with 3.6 amino acid residues per turn (n = 3.6). It is stabilized by hydrogen bonds directed backwards from a C-terminal NH to an N-terminal CO ($NH^{i+4} \rightarrow CO^{i}$) forming a 13-membered ring (FIGURE 9). Among the types of local structure in proteins, α-helix is the most regular and the most predictable from sequence, as well as the most prevalent.
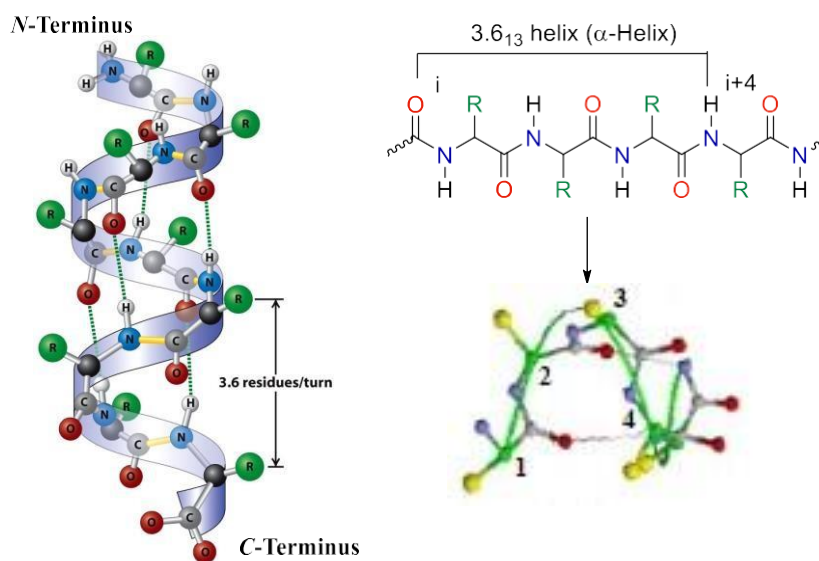

FIGURE 8. Hydrogen bond pattern in α-helical peptides and schematic representation.

A turn (loop) is an element of secondary structure in polypeptide or protein where the chain reverses its overall direction. Often, but not necessarily, they are stabilized by an HB between a C-terminal amino group and an N-terminal carboxy group. Turns are classified according to the number of amino acid residues involved as γ-turns (three amino acids), β-turn (four amino

[47] SEWALD, N., JAKUBKE, H-D., Peptides: Chemistry and Biology. Copyright © 2002 Wiley-VCH Verlag GmbH & Co. KGaA ISBNs: 3-527-30405-3 (Hardback); 3-527-60068-X (Electronic), pp 36.

acids), *α*-turn (five amino acids), or *π*-turn (six amino acids). *β*-turn are very common motifs. A general criterion for the existence of a *β*-turn is that the distance of the atoms C (i) and C (i + 3) is smaller than 7 Å. It is stabilized by hydrogen bonds directed backwards from a C-terminal NH to an N-terminal CO ($NH^{i+3} \rightarrow CO^i$). Also, it could be stabilized by certain alkyl residues presented in position i+2 such as (α,α)-dialkylglycines such as aminoisobutyric acid (Aib) (FIGURE 9).[46]
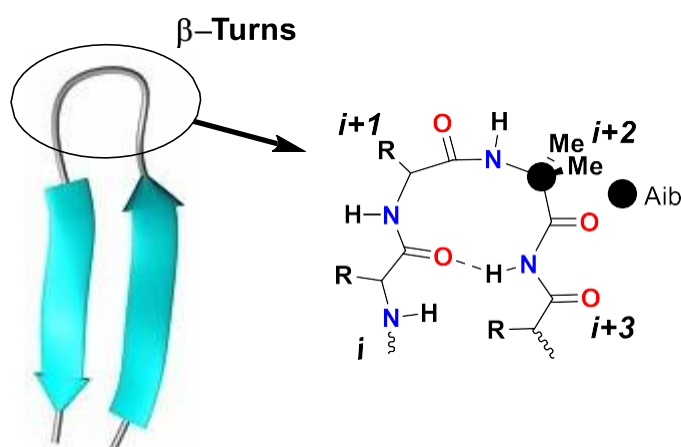

FIGURE 9. Hydrogen bond representative of β-turns. Schematic representation.

1.5 Peptides of the Type Pro-Pro-Xaa as Catalysts in Conjugate Addition Reactions between Aldehydes and Nitroolefins

Due to the high degree of rotational freedom even in short peptides, prediction of the conformational properties and thereby the spatial arrangement of functional groups of potential peptide catalysts is a challenge complicating their rational design. Thus, smart combinatorial methods are attractive for the discovery of peptide catalysts.[48, 49, 50] The modular nature of linearly linked amino acid building blocks combined with the established synthetic protocols in peptide synthesis (solid phase synthesis), allow for straightforward generation of diverse libraries by the split-and-mix method. Such one-bead-one-compound libraries combined with a cleverly designed screening method and an elegant way of identifying active species allow for the discovery of very potent peptide catalysts.[49]

---

[48] BERKESSEL, A., *Curr. Opin. Chem. Biol.* **2003**, *7*, 409-414.

[49] REVELL, J. D., WENNEMERS, H., Peptidic catalyst developed by combinatorial screening method. *Curr. Opin. Chem. Biol.* **2007**, *11*, 269-278.

[50] REVELL, J. D., WENNEMERS, H., *Top. Curr. Chem.* **2007**, *277*, 251-261.

Using the concept of catalyst substrate co-immobilisation (FIGURE 10, a)[51] the two tripeptides H-Pro-D-Ala-D-Asp-NH$_2$ and H-Pro-Pro-Asp-NH$_2$ were identified as excellent catalysts for aldol reactions of acetone with aromatic aldehydes.[52] The corresponding aldol products were obtained in high enantioselectivities using as little as 1 mol% of the peptidic catalyst. Interestingly, in a lowest energy structure obtained by molecular modelling studies the distance between the secondary amine and the carboxylic acid of H-Pro-Pro-Asp-NH$_2$ is approximately 3 Å greater than in proline. Inspired by this fact and hypothesising that these 3 Å might provide enough space for two additional atoms (FIGURE 10, b), H-Pro-Pro-Asp-NH$_2$ and closely related peptides Pro-Pro-Xaa, combining the Pro-Pro motif with a C-terminal amino acid containing a carboxylic acid moiety (Xaa), were examined as catalysts for conjugate addition reactions.
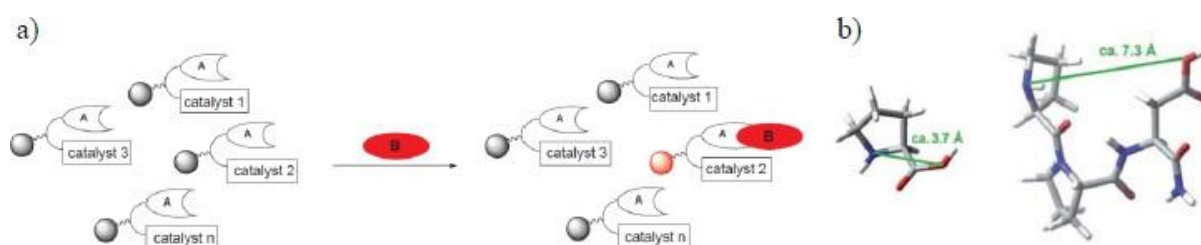
FIGURE 10. a.) The principle of catalyst-substrate co-immobilisation: the bead carrying an active catalyst (catalyst 2) becomes labelled with a red dye. b.) The additional distance between the carboxylic acid moiety and the secondary amine of H-Pro-Pro-Asp-NH$_2$ compared to proline.[28]

Indeed, H-Pro-Pro-Asp-NH$_2$ and in particular its diastereoisomer H-D-Pro-Pro-Asp-NH$_2$ proved to be very good catalysts for the conjugate addition reaction of various aldehydes to aromatic as well as aliphatic β-substituted nitroolefins providing the corresponding products in excellent yields, diastereo- and enantioselectivities.[53] Further studies revealed that the closely related analogue H-D-Pro-Pro-Glu-NH$_2$ is an even better catalyst for conjugate additions

---

[51] KRATTIGER, P., MCCARTHY, C., PFALTZ, A., WENNEMERS, H., Catalyst-substrate coimmobilization: a strategy for catalyst discovery in split-and-mix libraries. *Angew. Chem. Int. Ed.* **2003**, *42*, 1722-1724.

[52] KRATTIGER, P., KOVASY, R., REVELL, J. D., IVAN, S., WENNEMERS, H., Increased structural complexity leads to higher activity: peptides as efficient and versatile catalyst for asymmetric aldol reactions. *Org. Lett.* **2005**, *7*, 1101-1103.

[53] WIESNER, M., REVELL, J. D., WENNEMERS, H., Tripeptides as efficient asymmetric catalysis for 1,4-addition reactions of aldehydes to nitroolefins-a rational approach. *Angew. Chem. Int. Ed.* **2008**, *47*, 1871-1874.

between aldehydes and nitroolefins[54, 55] Detailed investigations revealed that within the catalyst structure the turn-inducing D-Pro-Pro-motif as well as the C-terminal amide and the carboxylic acid moiety in the side chain are crucial for effective catalysis.

In this sense, other studies done by Wennemers and co-worker[56] with the analogue H-D-Pro-Pro-Glu-NH$_2$ showed that the *trans/cis* ratio of the conformers ($K_{trans/cis}$) are determinant for the induction of stereoselectivity (SCHEME 7).
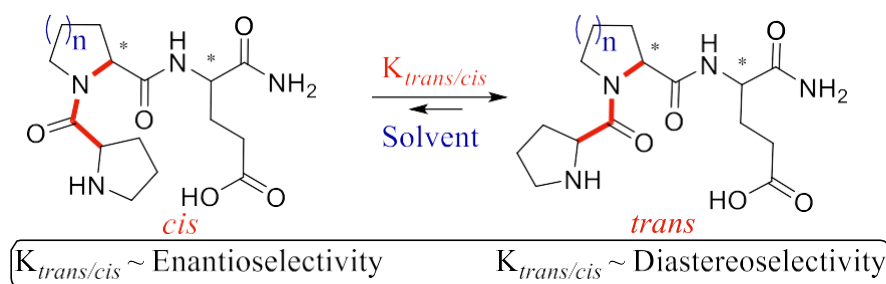
SCHEME 7. *Trans/cis* equilibrium of H-D-Pro-Pro-Glu-NH$_2$ type catalyst.

These studies showed that when the size of the proline ring adjacent to the proline core employed as a catalyst is increased the trans/cis ratio is varied and can be controlled by using a more significant amount of polar aprotic solvents (CHCl3/i-PrOH 9:1) to afford the trans isomer, a marked increase in the trans/cis ratio of their conformers are observed. Tested in a Michael addition of aldehydes to nitroolefins, the best stereoselectivities are obtained for a better $K_{trans/cis}$. In this way, the sequence H-D-Pro-Pip-Glu-NH$_2$ presented the best result.

In counterpart, when the amount of polar protic solvent is increased (CHCl3/i-PrOH 1:1), but in this case for adding aldehydes to maleimides, this ratio decreases, and it stops depending on the size of the ring and decreases the stereoselectivity.

---

[54] WIESNER, M., NEUBURGER, M., WENNEMERS, H., Tripeptides of the type H-D-Pro-Pro-Xaa-NH$_2$ as catalysts for asymmetric 1,4-addition reactions: Structural requirements for high catalytic efficiency. *Chem. Eur. J.* **2009**, *15*, 10103-10109.

[55] WIESNER, M., WENNEMERS, H., Peptide-catalyzed conjugate addition reactions of aldehydes to nitroolefins. *Synthesis* **2010**, *9*, 1568-1571.

[56] SCHNITZER, T., WENNEMERS, H., Influence of the *Trans/Cis* conformer ratio on the stereoselectivity of peptidic catalysts. *J. Am. Chem. Soc.,* **2017**, *139*, 15356−15362.

1.6 Water-Compatible Organocatalysis

The development of organocatalytic processes that use water as the reaction medium has attracted widespread attention over the last years[57, 58, 59, 60, 61] because water is the most abundant solvent on earth, non-toxic, non-flammable and easy to handle and thus generally considered as a "green solvent." Since the conjugate addition reaction of carbonyl compounds to nitroolefins is one of the most useful and widely researched organocatalytic transformations, the development and optimization of secondary amine catalysts that allow this reaction to take place in an aqueous medium has received considerable research interest. In this context, several catalysts have been reported that provide the corresponding γ-nitro carbonyl compounds in

[57] MASE, N., BARBAS, C. F., In water, on water, and by water: mimicking nature's aldolases with organocatalysis and water. *Org. Biomol. Chem.* **2010**, *8*, 4043-4050.

[58] LINDSTRÖM, U. M., Organic reactions in water, Blackwell, **2007**.

[59] RAJ, M., SINGH, V. K., Organocatalitic reactions in water. *Chem. Commun.* **2009**, 6687-6703.

[60] GRUTTADAURIA, M., GIACALONE, F., NOTO, R., Water in stereoselective organocatalitic reactions. *Adv. Synth. Catal.,* **2009**, *351*, 33-57.

[61] PARADOWSKA, J., STODULSKI, M., MLYNARSKI, J., Catalysts based on amino acid for asymmetric reactions in water. *Angew. Chem. Int. Ed.* **2009**, *48*, 4288-4297.

good yields and stereoselectivities (SCHEME 8).[62, 63, 64, 65, 66, 67, 68, 69, 70] As the water-solubility of the substrates is generally low, the reaction mixtures are in homogeneous, and the reactions take place in or at the surface of a highly concentrated organic phase. The development of new catalysts that can work in pure water is a challenge, especially for catalyzed asymmetric reactions. The most used approach is the surfactant type design. Many approaches are based on the introduction of lipid chains and others in the use of catalysts in the form of salts to make it soluble in water. Consequently, the secondary amine catalysts that perform best in an aqueous medium are amphiphilic, allowing for their solubility in the organic phase as well as stabilization of an emulsion of the two phases.

[62] MASE, N., WATANABE, K., YODA, H., TAKABE, K., TANAKA, F., BARBAS, C. F., Organocatalytic direct Michael reaction of ketones and aldehydes with β-nitrostyrene in brine. *J. Am. Chem. Soc.* **2006**, *128*, 4966-4967.

[63] ZU, L., WANG, J., HAO, L., WANG, W., A recyclable fluorous (*S*)-pyrrolidine sulfonamide promoted direct, highly enantioselective Michael addition of ketones and aldehydes to nitroolefins in water. *Org. Lett.,* **2006**, *8*, 3077-3079.

[64] ZHU, S., YU, S., MA, D., Highly efficient catalytic system for enantioselective Michael addition of aldehydes to nitroalkenes in water. *Angew. Chem. Int. Ed.* **2008**, *47*, 545-548.

[65] LOMBARDO, M., CHIARUCCI, M., QUINTAVALLA, A., TROMBINI, C., Highly efficient ion-tagged catalyst for the enantioselective Michael addition of aldehydes to nitroalkenes. *Adv. Synth. Catal.* **2009**, *351*, 2801-2806.

[66] ZHENG, Z., PERKINS, B. L., NI, B., Diarylprolinol silyl ether salts as new, efficient, water-soluble, and recyclable organocatalysts for the asymmetric Michael addition on water. *J. Am. Chem. Soc.* **2010**, *132*, 50-51.

[67] SARKAR, D., BHATTARAI, R., HEADLEY, A., NI, B., A novel recyclable organocatalytic system for the highly asymmetric Michael addition of aldehydes to nitroolefins in Water. *Synthesis* **2011**, 12, 1993-1997.

[68] LUO, S., MI, X., LIU, S., XU, H., CHENG, J.-P., Surfactant-type asymmetric organocatalyst: organocatalytic asymmetric Michael addition to nitrostyrenes in water. *Chem. Commun.* **2006**, 3687-3689.

[69] CAO, Y.-J., LAI, Y.-Y., WANG, X., LI, Y.-J., XIAO, W.-J., Michael additions in water of ketones to nitroolefins catalyzed by readily tunable and bifunctional pyrrolidine–thiourea organocatalysts. *Tetrahedron Lett.,* **2007**, *48*, 21-24.

[70] VISHNUMAYA, SINGH, V. K., Highly Enantioselective Water-Compatible Organocatalyst for Michael Reaction of Ketones to Nitroolefins. *Org. Lett.,* **2007**, *9*, 1117-1119.
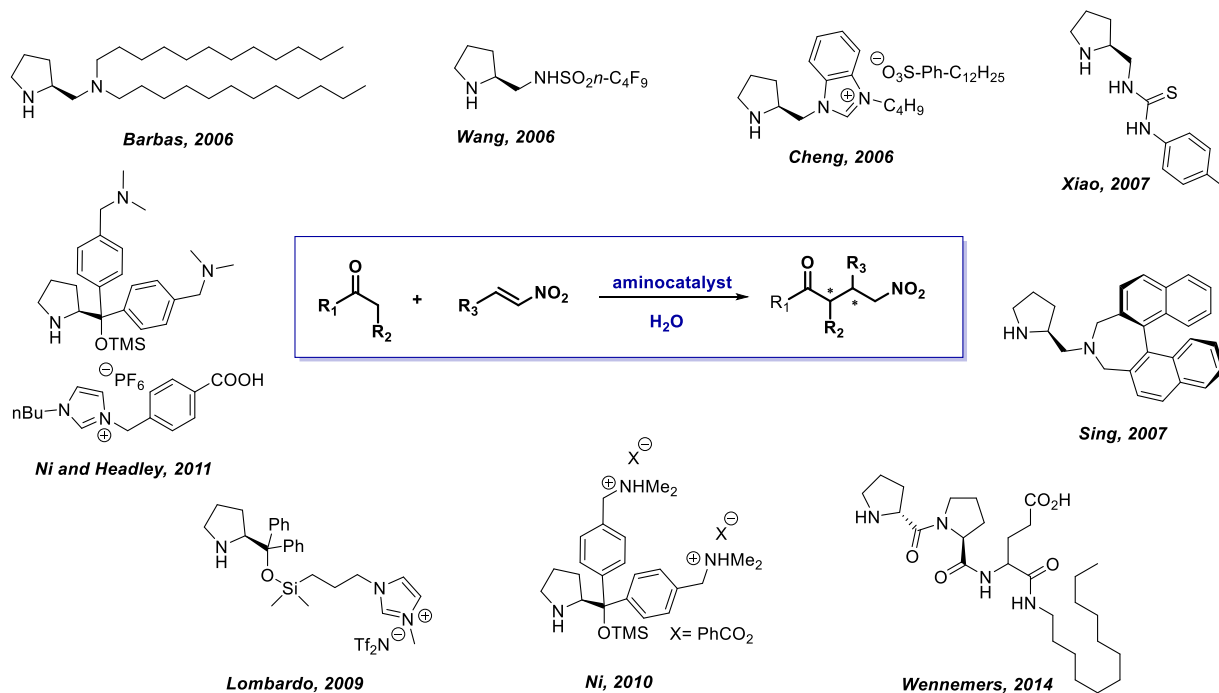
SCHEME 8. Selected examples of water-compatible organocatalysis.

Our research group has designed a new organocatalyst inspired in the seminal one described independently by Hayashi and Jørgensen. The new catalyst type is modified with lipid side chains and has been used effectively in asymmetric transformations using alternative sustainable solvents.[3, 37,71]

Short peptides have low molecular weight when compare with proteins, but at the same time, consist of the same amino acid building blocks as enzymes. Thus, it is a highly interesting question if and in how far enzymes can be mimicked by their low molecular weight analogues. In this context, Wennemers[72] reported the first lipopeptide used as an aminocatalyst in additions of Michael using water as a solvent (SCHEME 9).

---

[71] FEU, K. S., DEOBALD, A. M., NARAYANAPERUMAL, S., CORRÊA, A. G., PAIXÃO, M. W., An eco-friendly asymmetric organocatalytic conjugate addition of malonates to α,β-unsaturated aldehydes: Application on the synthesis of chiral indoles. *Eur. J. Org. Chem.* **2013**, 5917-5920.

[72] DUSCHMALÉ, J., KOHRT, S., WENNEMERS, H., Peptide catalysis in aqueous emulsions. *Chem. Commun.,* **2014**, *50*, 8109-8112.
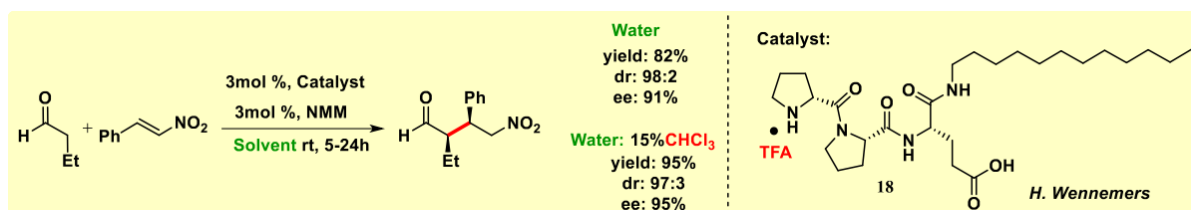
SCHEME 9. Michael addition catalyzed by amphiphilic lipopeptide under aqueous media.

Based on these observations, pyrrolidine-type peptides can be considered as very useful organocatalysts for direct asymmetric catalysis. The major disadvantages of this peptide catalysts remain in the linearity of the synthesis. Peptide synthesis often occurs by coupling the carboxyl group of the incoming amino acid to the N-terminus of the growing peptide chain. The growing peptide chain follows the stepwise method to add amino acids one- at-a-time to the growing peptide chain. This produces low yields and atom economy. Peptide coupling requires the activation of the *C*-terminal carboxylic acid of the incoming amino acid using carbodiimides such as dicyclohexylcarbodiimide (DCC) or diisopropylcarbodiimide (DIC). Carbodiimides form such a reactive intermediate that racemization of the amino acid can occur. Therefore, reagents to avoid or reduce racemization are often added, including 1-hydroxybenzotriazole (HOBt) and 2-(1H-benzotriazol 1-yl)-1,1,3,3-tetramethyluronium hexafluorophosphate (HBTU). These coupling reagents, resin and additives are expensive and sometimes are unrecovered.

1.7   Multicomponent reactions

Multicomponent reactions (MCRs) are convergent processes where three or more compounds react sequentially to form a product that retains most of the atoms of the starting materials. The exact nature of these reactions is difficult to assign given that in the theory of collisions, the simultaneous interaction of three or more molecules results in lower reaction rates. These processes occur through a series of bimolecular reactions, according to a cascade of elementary reactions in equilibrium with a final flow towards an irreversible step that yields the product. Many times, the presence of common substrates allows the occurrence of collateral multicomponent reactions. Conducting a multicomponent reaction in a way that leads to a majority product, will depend on the reaction conditions: solvent, temperature, catalyst, concentration, type of starting materials and functional groups.[73]

---

[73] ZHU, J.; BIENYAMÉ, H., Multicomponent Reactions. *2da* Eds, Wiley-VCH, Weinheim, 2005.

MCRs generally have perfect atom economy and thus represent suitable synthetic tools for addressing the Green Chemistry criterion. Usually, the starting materials of MCRs are readily available, or can easily be prepared.

1.7.1 Isocyanide-based multicomponent reactions (I-MCRs)

The chemistry of isocyanides began in 1859 when Lieke obtained allyl-isocyanide by reaction between allyl iodide and silver cyanide.[74] However, during a whole century, only 12 isocyanides were prepared, whose chemical properties were not investigated in depth due to their unpleasant odor. The isocyanides are characterized by three fundamental chemical properties: i) the acidity of their position α, ii) the easy formation of radicals, and iii) the double addition of electrophiles and nucleophiles; its most important chemical property (Scheme 10).[75,76,77]
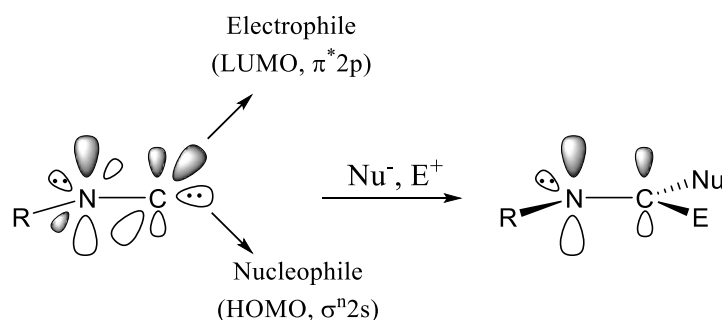
SCHEME 10. Frontier orbital theory (FOT) of an isocyanide showing its ambiphilic reactivity.

Accordingly, in I-MCRs several chemical bonds are formed with high chemical efficiency, and generating high levels of structural diversity and complexity such as *pseudo*-peptide (i.e.,

[74] UGI, I.; Recent progress in the chemistry of multicomponent reactions. *Pure Appl. Chem.*, **2001**, *73*, 187-191.
[75] UGI, I.; *Isocyanide Chemistry*, Academic Press, New York, **1971**.
[76] DÖMLING, A., Recent developments in isocyanide based multicomponent reactions in applied chemistry. *Chem. Rev.*, **2006**, *106*, 17-89.
[77] DÖMLING, A., UGI, I.; Multicomponent reactions with isocyanides. *Angew. Chem.*, **2000**, *39*, 3168-3210.

depsipeptides,[78] peptoids[79,80,81]) and peptidomimetic (e.g., oxa-,[82] dihydroimida-,[83] thia-,[84] and tetrazoles[85]) motifs in a diversity-oriented manner without utilization of coupling agents or additives like in peptide chemistry.

1.7.2 The Ugi-four component reaction (Ugi-4CR)

The reaction of Ugi is undoubtedly the most used I-MCR, not only in the way of obtaining peptidomimetic structures but also in other very varied ones. Most chemical reactions have their own scope and limitation, whereas the Ugi-4CR can convert almost all combinations of starting materials into their products. Its simplest version is the condensation of an aldehyde or ketone, a primary amine, a carboxylic acid, and an isocyanide to form an *N*-substituted dipeptide.[86] The use of a prochiral carbonyl compound leads to the formation of mixtures of stereoimomers, because the reaction is not stereoselective[87,88,89](SCHEME 11).

[78] BANFI, L.; RIVA, R.; The Passerini reaction. *Org. React.*, **2005**, *65*, 1-142.

[79] DÖMLING, A.; UGI, I. Multicomponent reactions with isocyanides. *Angew. Chem. Int. Ed.,* 2000, *39*, 3168.

[80] DÖMLING, A. Recent developments in isocyanide based multicomponent reactions in applied Chemistry. *Chem. Rev.*, **2006**, *106*, 17.

[81] DÖMLING, A.; WANG, W.; WANG, K. Chemistry and Biology of multicomponent reactions. *Chem. Rev.,* **2012**, *112***,** 3083.

[82] XIA, Q.; GANEM, B. Metal-promoted variants of the Passerini reaction leading to functionalized heterocycles. *Org. Lett.*, **2002**, *4*, 1631.

[83] BON, R. S.; HONG, C. G.; BOUMA, M. J.; SCHMITZ, R. F.; DE KANTER, F. J. J.; LUTZ, M.; SPEK, A. L.; ORRU, R. V. A. Novel multicomponent reaction for the combinatorial synthesis of 2-imidazolines. *Org. Lett.*, **2003**, *5,* 3759.

[84] HENKEL, B.; BECK, B.; WESTNER, B.; MEJAT, B.; DÖMLING, A. Convergent multicomponent assembly of 2-acyloxymethyl thiazoles. *Tetrahedron Letters*, **2003**, *44*, 8947.

[85] UGI, I.; WERNER, B.; DÖMLING, A., The Chemistry of isocyanides, their multicomponent reactions and their libraries. *Molecules*, **2003**, *8,* 53.

[86] DÖMLING, A., The discovery of new isocyanide-based multicomponent reactions. *Curr. Op. Chem. Biol.*, **2000**, *4*, 318-323.

[87] RIVERA, D. G., PANDO, O., COLLl, F., Synthesis of peptidomimetic-spirostane hybrids via Ugi reaction: a versatile approach for the formation of peptide–steroid conjugates. *Tetrahedron*, **2006**, *62*, 8327-8334.

[88] WESSJOHANN, L. A., RIVERA, D. G., COLL, F., Synthesis of steroid-biaryl ether hybrid macrocycles with high skeletal and side chain variability by multiple multicomponent macrocyclization including bifunctional building blocks. *J. Org. Chem.*, **2006**, *71*, 7521-7526.

[89] WESSJOHANN, L. A., RIVERA, D. G., Supramolecular compounds from multiple Ugi multicomponent macrocyclizations: Peptoid-based cryptands, cages, and cryptophanes. *J. Am. Chem. Soc.*, **2006**, *128*, 7122-7123.
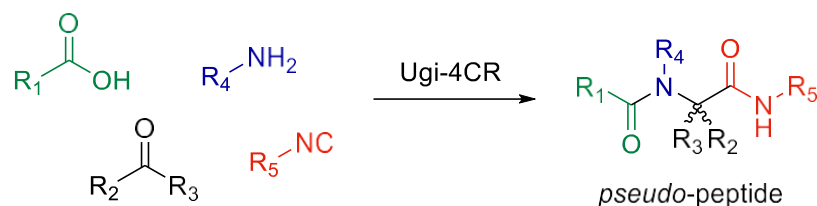
SCHEME 11. The Ugi four-component reaction (Ugi-4CR).

This reaction consists of an ionic mechanism developed in polar protic solvents (such as methanol). The mechanism of Ugi-4CR is shown in (SCHEME 12). [86, 90] In the first step, the amines and carbonyl compounds (aldehyde or ketone) condensed to the imine. The imine is protonated by the carboxylic acid. Depending on the solvent, the ion can be as salt pair or separately. Then, both ions react with the isocyanide component to form an imidate intermediate. The last step is the Mumm rearrangement, consisting in an intramolecular acylation and subsequent rearrangement forming a (C=O) double bond and consequently the Ugi product.
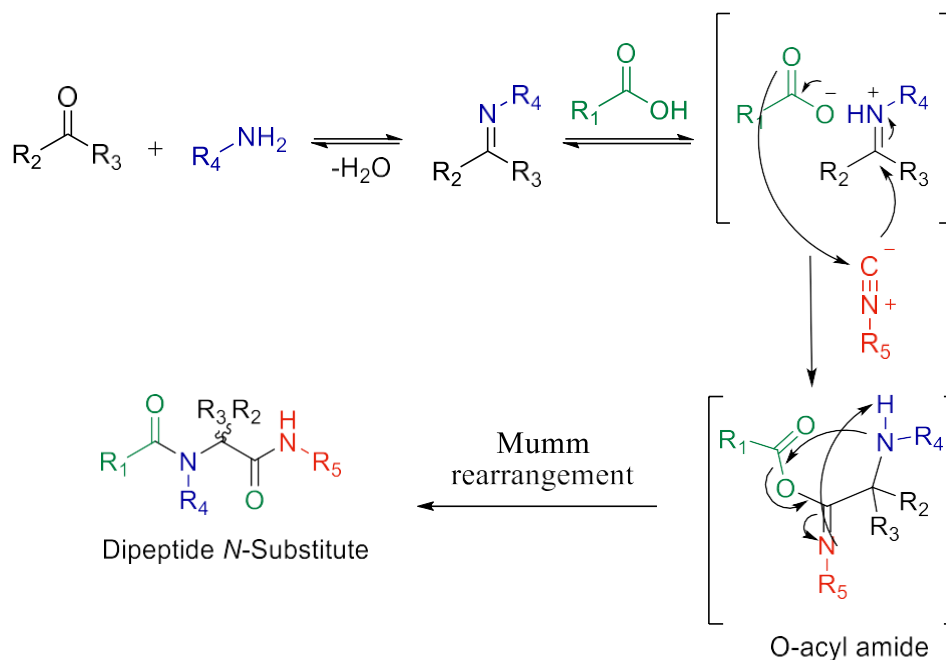
SCHEME 12. General mechanism of the Ugi-4CR.

In accord with the ever-increasing demand for `atom economic´ processes and efficient methods to obtain compounds capable inducing good enantioselectivity, I-MCRs are an unexploited and elegant field that deserve to be studied.

---

[90] RON, N. C.; RAMOZZI, R.; KAÏM, L. E.; GRIMAUD, L.; FLEURAT-LESSARD, P. Challenging 50 years of established views on Ugi reaction: A theoretical approach. *J. Org. Chem.,* **2012**, *77,* 1361.

In 2010, Orru and co-workers[91] published an article with the Ugi type 3CR for the straightforward synthesis of catalyst **20** (SCHEME 13) resembling the structure and catalytic behavior of Wennemer´s catalyst **18**.
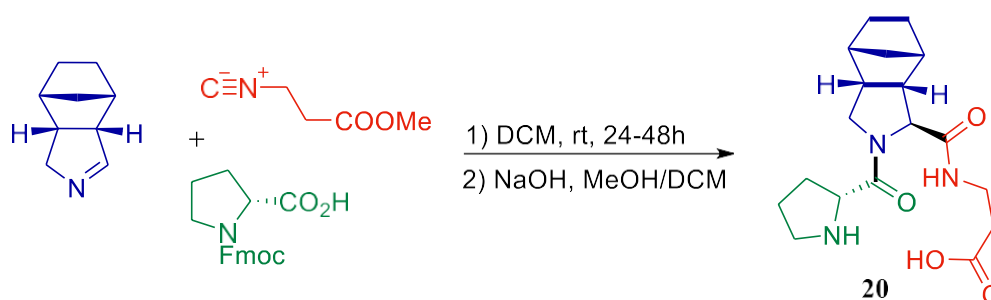
SCHEME 13. Ugi-type 3CR reaction developed by Orru and co-workers.

Recently, our research group using I-MCR developed the synthesis of a combinatorial library of prolyl peptide-peptoid hybrids and their application as aminocatalysts (Scheme 14).[92]
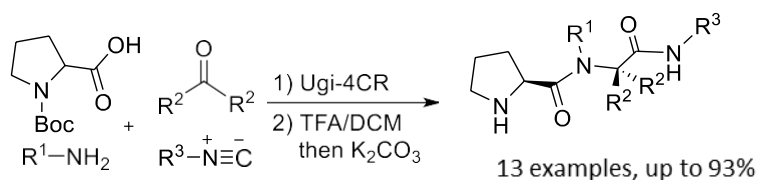
SCHEME 14. Prolyl peptide-peptoid hybrid catalyst library.

The best catalytic motif was obtained when a (L)-proline, (S)-α-methylbenzylamine, acetone and cyclohexyl isocyanide are combined in the Ugi-4CR. The obtained catalyst **24** showed an exceptional performance in the Michael addition of aldehydes to nitrostryrenes having toluene as a solvent system (SCHEME 15).

---

[91] ZNABET, A., RUIJTER, E., de KANTER, F. J. J., KHLER, V., HELLIWELL, M., TURNER, N. J., ORRU, R. V. A., Highly stereoselective synthesis of substituted prolyl peptides using a combination of biocatalytic desymmetrization and multicomponent reactions. *Angew. Chem. Int. Ed.*, **2010**, *49*, 5289 –5292.

[92] de la TORRE, A. F., RIVERA, D. G., FERREIRA, M. A. B., CORRÊA, A. G., PAIXÃO, M. W., Multicomponent combinatorial development and conformational analysis of prolyl peptide−peptoid hybrid catalysts: Application in the direct asymmetric Michael addition. *J. Org. Chem.*, **2013**, *78*, 10221−10232.
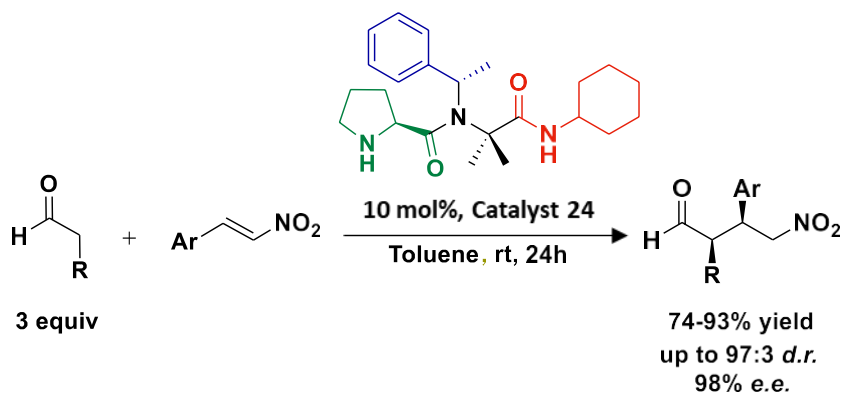
SCHEME 15. Michael addition of aldehydes to nitrostyrenes.

We have determined the optimized lowest-energy structure of the enamine with *E* configuration, in toluene as a best solvent for Michael addition. FIGURE 11 shows a significant overlap of the peptidic skeleton to the ***Re***-face, which according to Seebach's topological model explains the high enantioselection of the catalyst **24**.
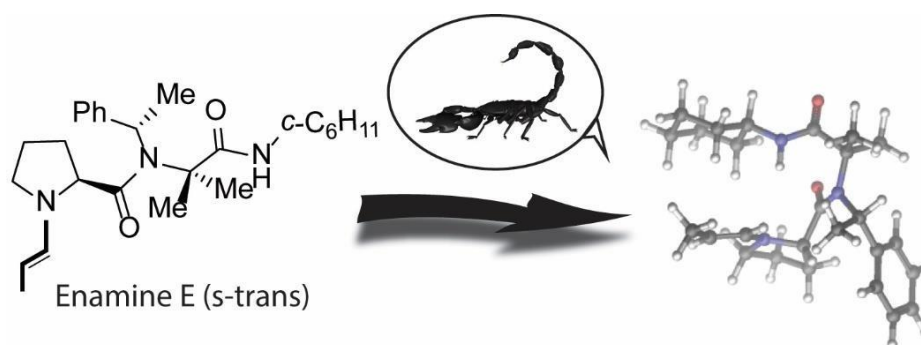
FIGURE 11. Lowest-energy structure of the enamine E (s-trans) derived from catalyst **21**.

FIGURE 11 clearly shows that the face (***Re***-face) of the enamine is totally blocked by the peptidic skeleton (literally as a scorpion). Thus, this clearly justify how this catalyst works in the configuration of enamine E (s-trans) and its influence in the enantioselectivity for Michael adducts.

So, could it be possible to apply I-MCRs, specifically Ugi-4CR, to generate a new class of prolyl peptide-lipopetoid hybrids catalyst library through the introduction of lipidic chains on the same peptide skeleton of the catalyst previously developed by our group, capable to catalyze chemical asymmetric reactions in pure water? Might it be an easy and green way to mix more than one component in a one-pot process to get organocatalysts with surfactant properties?

2 Objectives

The application of Ugi-4CR in the field of organocatalysis is a wonderful tool to generate versatility in combinatorial approaches to rapidly, efficiently, and eco-friendly generate peptide derivatives with catalytic potential in asymmetric catalysis. In accord to Green Chemistry principles, the development of new catalyst synthetized with higher atom economy, can be used in pure water is a true challenge and desirable. Therefore, the main target in this work is a synthesis of a combinatorial library of prolyl peptide-lipopeptide hybrids catalysts by Ugi-4CR. Evaluate its amphiphilic and catalytic properties through catalysis via enamine in an addition of aldehydes to nitrostyrenes under water and other environmentally benign solvents. Finally characterize the catalytic system formed by the interaction of the catalyst-water and DFT calculations of the more stable enamine conformation.

3   Results and Discussion

3.1   Combinatorial multicomponent synthesis of prolyl *pseudo*-lipopeptides hybrid catalysts

An isocyanide multicomponent reaction (I-MCR) approach based on the Ugi-4CR was carried out for the synthesis and development of a new library of prolyl *pseudo*-lipopeptides hybrid catalysts (FIGURE 12).
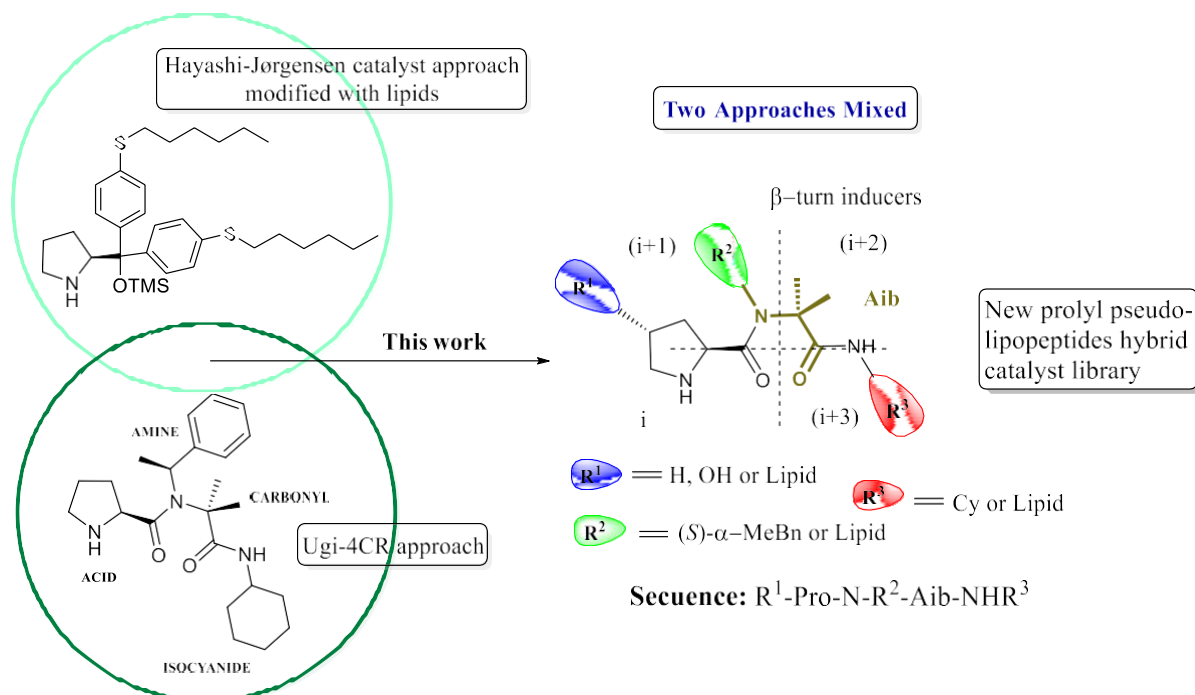
FIGURE 12. Combinatorial multicomponent strategy adopted for the preparation of the prolyl pseudo-lipopeptide catalysts library.

For the catalyst design, we first have taken into consideration the fact that the *N*-substitution at R^2 and the Aib residue derived from the carbonyl component - both beta turn inducers - are responsible for the conformation restrictions (trans/cis equilibrium of the amide bond), therefore shielding one face of the pro-chiral enamine. The influence of the trans/cis conformer ration has been rationalized as one of the main contributors for the high stereoselectivity of this catalyst series. Further, an additional aspect was the high efficiency showed by the Hayashi-Jørgensen type catalyst modified with lipid side chains recently developed and applied by our group. Having these aspects in mind and that three different elements of diversity could precisely be tuned during the multicomponent event (i.e. the amine, the acid and the isocyanide components) we designed a series of prolyl *pseudo*-lipopeptides hybrid catalysts presented in the FIGURE 12. To this end, (*i*) acetone was fixed as the carbonyl

component to furnish the Aib moiety in the backbone; (*ii*) the chiral pyrrolidine core came from *N*-Boc-proline, *N*-Boc-4-hidroxy-proline or from a lipidic derivative of this last one.

(*iii*) on the other hand, dodecylamine and (*S*)-α-methylbenzylamine were employed as amine components alternatives, and cyclohexyl isocyanide and dodecyl isocyanide were evaluated as isocyanide components. Therefore, it is possible to note that the multicomponent nature of this process enables the direct generation of a series of prolyl *pseudo*-lipopeptides having the generic sequences R^1-Pro-*N*-R^2-Aib-NHR^3, being R^1 = H, OH, n-$C_{11}H_{23}COO$; R^2 = (*S*)-α-MeBn, n-$C_{12}H_{25}$, Diphenylmethanamine (Dpm); and R^3 = Cy, n-$C_{12}H_{25}$ (TABLE 1).

Thus, the Ugi-4CR protocol[93] was employed for the one-pot assembly of the lipopeptoid skeleton followed purification of the corresponding *N*-Boc protected Ugi adduct by flash chromatography. Under this concept, eight prolyl *pseudo*-lipopeptides of the type R^1-Pro-*N*-R^2-Aib-NHR^3 were synthesized in moderate to good yields considering the nature and complexity of this one-pot process (TABLE 1). Finally, the corresponding *NH* catalysts **24**-**31** were directly used after the *N*-Boc cleavage.

First, prior to introduce structural changes, the catalyst previously developed by our research group was synthetized employing the already reported protocol.[94] In this way, the catalyst was obtained in the same yield previously reported (77% yield, TABLE 1, compound 24). Among the three possible elements of diversity, initial attention was given to the amine component by exchanging the (*S*)-α-methylbenzylamine to dodecylamine (TABLE 1, compound 25). The synthesis of this compound was carried out at room temperature for 24 hours. First, the imine was pre-formed by mixing dodecylamine with acetone in methanol for 2 hours. Subsequently, *N*-Boc-proline and cyclohexyl isocyanide were added to afford the compound 25 with 70% of yield after additional 22 hours.

The second variation was focused on varying the isocyanide component by exchanging cyclohexyl isocyanide for a lipidic isocyanide. However, dodecyl isocyanide **23** had to be firstly synthesized from dodecylamine **22** in a one-pot two steps sequence in 71% of yield (Scheme 16).

---

[93] UGI, I.; MEYR, R.; FETZER, U.; Steinbrücker, C. Experiments with isocyanides. *Angew. Chem.*, **1959**, *71*, 386.

[94] de la TORRE, A. F., Multicomponent reactions in the discovery of organocatalysts and the diversification of organocatalytic approaches. PhD Thesis. **2015**.
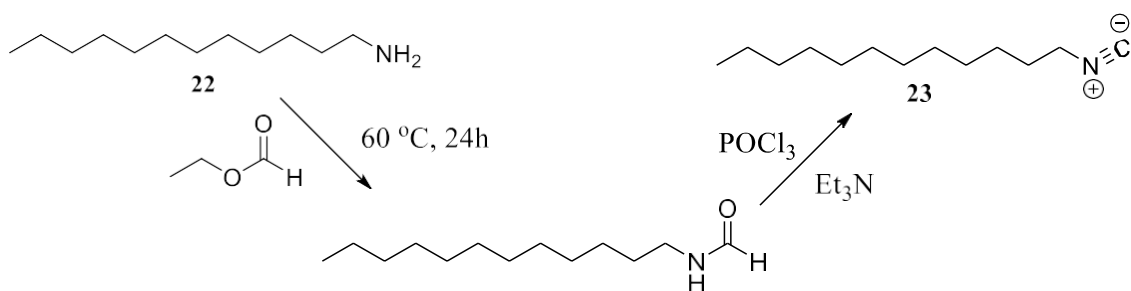
SCHEME 16. Synthesis of commercially not available lipidic isocyanide **23**.

With the isocyanide in hands, the reaction was carried out using (*S*)-α-methylbenzylamine, acetone and *N*-Boc-proline as reaction components under the same conditions previously employed. Thus, compound **26** (TABLE 1) was synthesized in 25% of yield. The observed low yield shall be rationalized due to two fundamental factors: (a) first, there was no effective formation of the imine at room temperature; (b) second, the lipidic isocyanide and final product were poorly soluble in methanol. Those problems were solved using MW heating for both steps and with the use of approximately 30% of THF as a co-solvent. This modification in the reaction protocol afforded compound **26** in 54% of yield.

TABLE 1. Multicomponent combinatorial synthesis of prolyl pseudo-lipopeptides hybrid catalysts using the [a] Ugi-4CR.

prolyl *pseudo*-lipopeptides hybrid catalysts

24 [c] 77%	**25** [b] 70%	**26** [c] 54%
27 [c] 57%	**28** [d] 50%	**29** [d] 73%
30 [d] 48%	**31** [d] 55%	
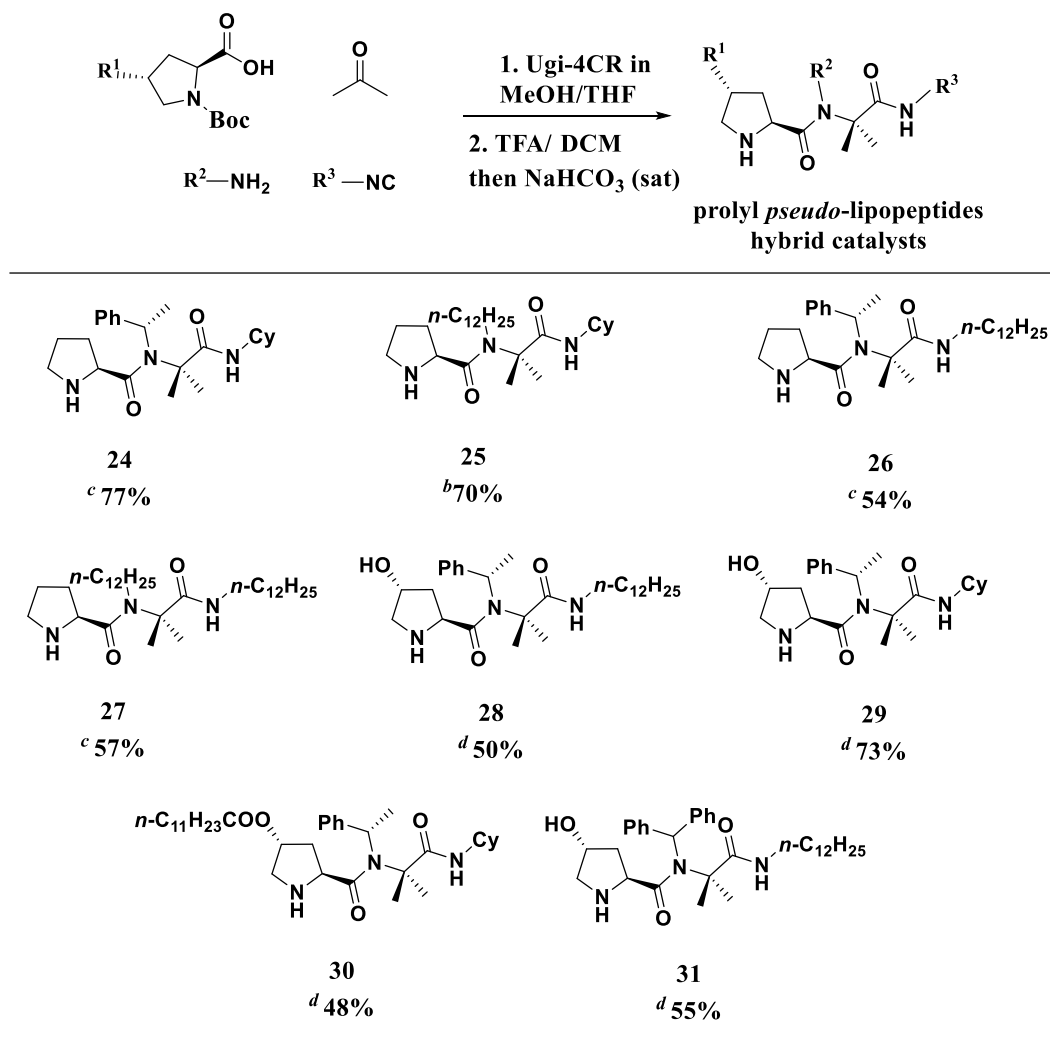
[a] All yield is referred of isolated pure N-Boc protected product. [b] Reaction conducted at room temperature in MeOH for 24h. [c] Reaction conducted under microwave irradiation. [d] Only imine preforming by microwave irradiation.

With the purpose of introducing two lipid chains at the same time in the same peptidic skeleton as in the Barbas III catalyst[67] dodecylamine and dodecyl isocyanide were used in an alternative multicomponent reaction using *N*-Boc-proline and acetone under MW irradiation and THF in MeOH as solvent system (30% v/v), archiving compound **27** (TABLE 1) in 57% of yield. Taking advantage of the main characteristics of surfactants molecules, structures which contain a nonpolar part and a polar part in opposite directions, therefore compound **28** (TABLE 1) was designed. This approach also had the aim to increase the amphiphilic properties of the catalyst. To achieve the desired catalysts, *N*-Boc-proline was substituted for *N*-Boc-trans-4-hydroxy-

proline as the acid component in a fourth modification. Thus, the combination of (*S*)-α-methylbenzylamine, acetone, *N*-Boc-trans-4-hydroxy-proline and dodecyl isocyanide afforded compound **28** in 50 % of yield. This reaction was also carried out using MW heating to preform imine and completed at room temperature to favor the Mumm rearrangement.

The polar pyrrolidine-containing hydroxyl group in the *trans* position was also used to increase the polarity of the catalyst previously developed by our group. Compound **29** (TABLE 1) could be prepared from acetone, (*S*)-α-methylbenzylamine, *N*-Boc-trans-4-hydroxy-proline and cyclohexyl isocyanide in 73% of yield. The presence of a hydroxy group in the pyrrolidine core also opened a new perspective for functionalization. To investigate the effect of the presence of a lipidic portion at this moiety, *N*-Boc-*trans*-4-hydroxy- proline was acylated[95] with lauryl chloride and then used as an acid component, affording compound **30** (TABLE 1) in 48% of yield. In this case, the imine was also pre-formed under MW heating and the reaction could be completed at room temperature.

Finally, one last consideration in the design of the catalytic motifs was carried out. To this end a structural change was made based on compound **28**, that in theory presents the best surfactant type design. In this approach, the chiral amine (*S*)-α-methylbenzylamine incorporated in compound **28** was replaced by the more hindered 2.2-diphenylglycine methyl ester. Interestingly, after preparing the methyl ester and use as an amine component in the Ugi reaction - employing the imine preformation under MW and allowing the completion of reaction at room temperature - the final product undergoes decarboxylation, affording compound **31** (TABLE 1) in 55% of yield. This decomposition probably occurs in the preformation of the imine in methanol at 70 ^{0}C, through a nucleophilic attack of methanol to the methyl ester, which gives rise to dimethylcarbonate and diphenylmethanamine (SCHEME 17).

---

[95] KRISTENSEN, T. E., HANSEN, F. K., HANSEN, T., The selective *O*-acylation of hydroxyproline as a convenient method for the large-scale preparation of novel proline polymers and amphiphiles. *Eur. J. Org. Chem.,*. **2009**, 387–395.
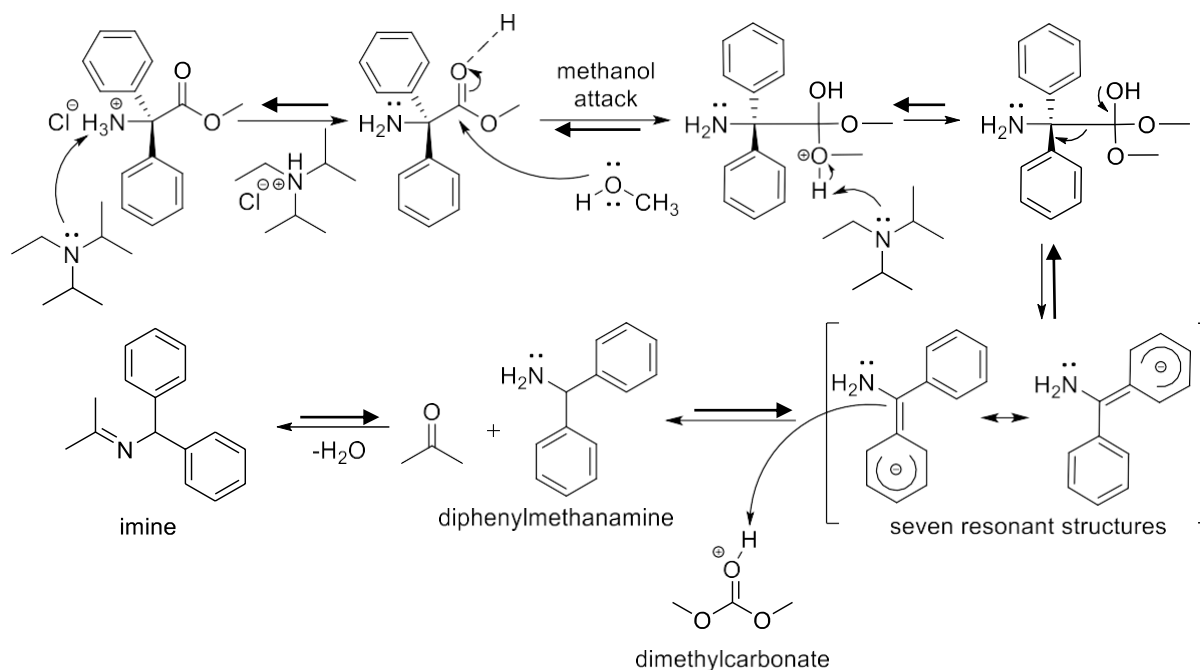
SCHEME 17. Decarboxylation mechanism of the 2.2-diphenylglycine methyl ester hydrochloride during the preformation of imine in methanol.

To summarize, eight aminocatalysts have been synthesized, among then, seven are new in the literature. A peptoid (compound **29**) and six lipopeptoids presenting a wide structural diversity and catalytic motifs.

3.2 Prolyl *pseudo*-lipopeptide hybrid catalysts: Evaluation in the asymmetric Michael reaction under aqueous media

To evaluate the catalytic behavior of the prolyl *pseudo*-lipopeptides in the conjugate addition reactions of aldehydes to nitroolefins, we chose to use *n*-butanal and (*E*)-(2-nitrovinyl) benzene as model reaction (TABLE 2). As standard conditions a mixture of the *β*-nitrostyrene and 2 equivalents of the aldehyde, were vigorously stirred in pure water (0.5 M concentration of the nitroolefin), in the presence of 10 mol% of each catalyst, at room temperature for 24 hours. Prior to beginning the evaluation of the new catalysts synthesized by this new methodology, the catalyst previously synthesized in our group (compound **24**) was evaluated (Entry 1, TABLE 2). As expected, this catalyst showed good results, both enantioselectivity (95% *e.e.*) and diastereoselectivity (98:2 *d.r.*), however a low yield (34%) was observed. The very low yield shall be related to the low solubility of the organocatalyst in water and the lack of surfactant proprieties. With this result in hands, we started to evaluate the new lipopeptoids based organocatalysts. Compound **25** showed significant improvements in terms of

performance (75% of yield), but lower *d.r.* (76:24) and *e.e.* (85%) were observed (Entry 2, TABLE 2). This preliminary result was very encouraging since our proposed methodology seemed to work well in completely aqueous media. Then, compound **26** was further evaluated, the lipid chain in the opposite direction of the pyrrolidine nucleus showed improvements in terms of yield (88%), *d.r.* (89:11) and *e.e.* (92%) (Entry 3, TABLE 2). We expected an excellent result for compound **27** since the design was centered on a structure similar to Barbas III catalyst. However, this catalyst did not work as expected, since good performance (71% of yield) but low selectivity (87% *e.e.* and 87:13 *d.r.*) were observed (Entry 4, TABLE 2). At this point of the catalyst screening, the results obtained were good mainly in terms of yields, but not yet satisfactory in terms of stereoselectivity.

TABLE 2. Asymmetric Michael reaction of *n*-butanal and *β*-nitrostyrene. Screening of different prolyl pseudo-lipopeptide catalysts. [a]
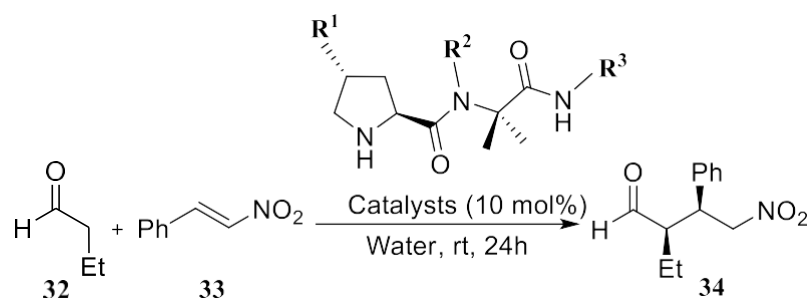
Entry	R^1/ R^2/ R^3	Compound	Yield (%)[b]	*d.r.* (*syn/anti*)[c]	*e.e.* (%)[d]
1	H/ (*S*)-α-MeBn/ Cy	**24**	34	92:8	95
2	H/ *n*-C$_{12}$H$_{25}$/ Cy	**25**	75	76:24	86
3	H/ (*S*)-α-MeBn/ *n*-C$_{12}$H$_{25}$	**26**	88	89:11	92
4	H/ *n*-C$_{12}$H$_{25}$/ *n*-C$_{12}$H$_{25}$	**27**	71	87:13	87
5	OH/ (*S*)-α-MeBn/ *n*-C$_{12}$H$_{25}$	**28**	88	76:24	99
6	OH/ (*S*)-α-MeBn/ Cy	**29**	43	70:30	99
7	*n*-C$_{11}$H$_{23}$COO/ (*S*)-α-MeBn/ Cy	**30**	23	89:11	99
8	OH/ Dpm/ *n*-C$_{12}$H$_{25}$	**31**	84	79:21	89

[a] All reactions were conducted using 2 equivalents of the aldehyde and 0.2 mmol of *β*-nitrostyrene in 0.4 mL of water. [b] Yield determined by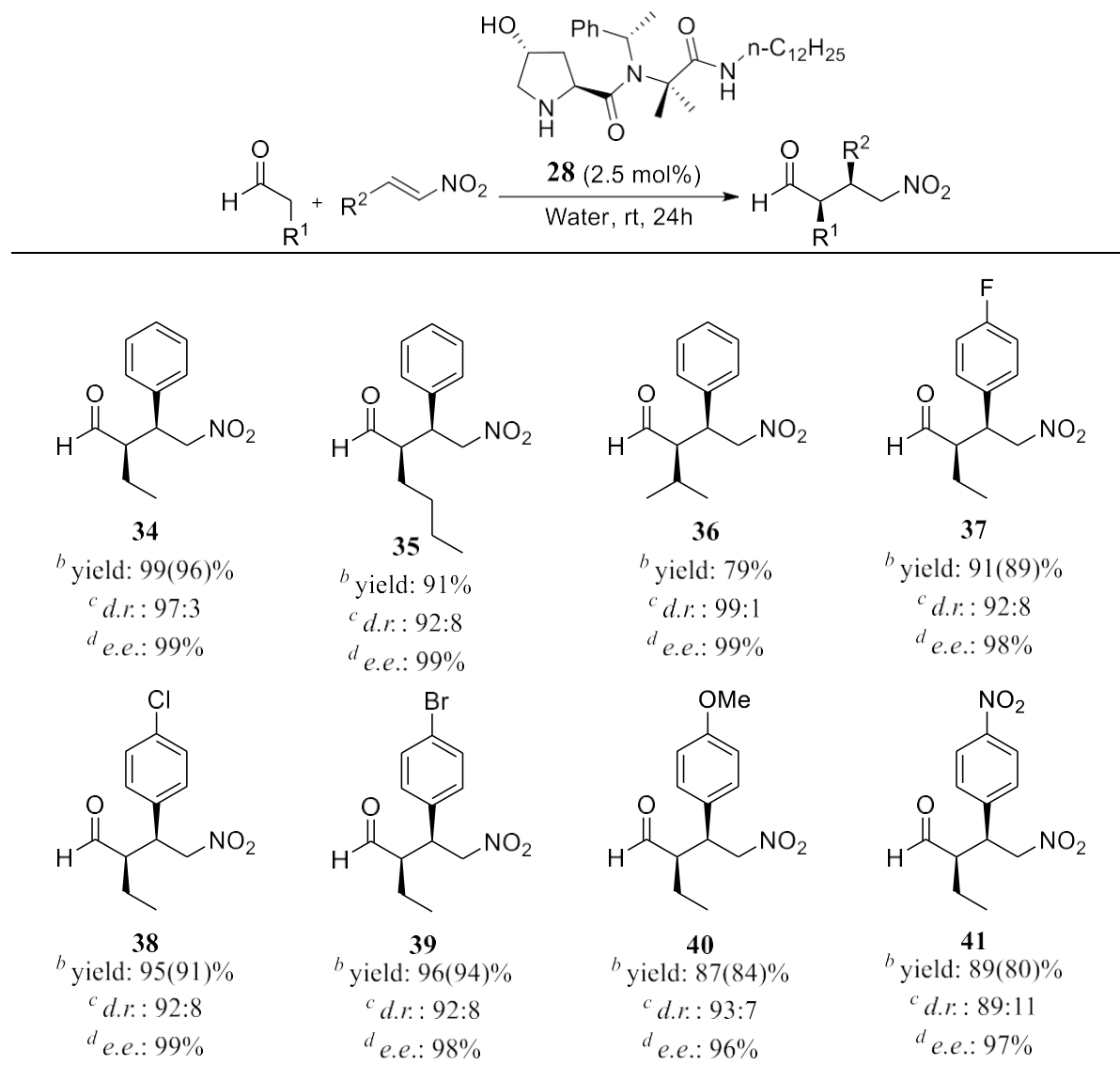 ^{1}H-NMR analysis with 1,2,3-trimethoxybenzene as standard. [c] Determined by ^{1}H NMR analysis of crude of the reaction mixture. [d] Determined by chiral-stationary phase HPLC or UPC^2 analysis.

An excellent performance was also expected for compound **28**, since the presence of a free hydroxyl group in pyrrolidine ring would likely provide a better solubility. To our delight, us

expectative became true, since a high yield accompanied by an excellent *e.e.* (99%) was observe when the reaction was performed using this catalyst (Entry 5, TABLE 2). At that moment, it became clear that the introduction of an additional chiral center was essential to the improvement of the enantioselectivity. To confirm this, we have observed that the introduction of this same chiral center into the catalyst previous developed in our group afforded better results in performance (43% of yield) and enantioselectivities (99% of *e.e.*), although a significant decrease in diastereoselectivity (*d.r.*: 70:30) was observed (Entry 6, TABLE 2). The maintenance of the enantioselectivity and slightly higher *d.r.* was observed when the *O*-substituted *N*-Boc-*trans*-4-C$_{11}$H$_{23}$COO-proline had its catalytic behavior evaluated. However, a very poor yield (23%) was obtained (Entry 7, TABLE 2). In this case, despite the presence of a lipid chain, it is placed on the polar side of the pyrrolidine nucleus, which leads to erosion in terms of amphiphilicity. Additionally, this compound is extremely hydrophobic, so its behavior in water is limited. The reaction performed using catalyst (compound **31**, Entry 8, TABLE 2), afforded the product in 84% of yield, 79:21 *d.r.* and 89% *e.e.* The decrease in selectivity could be attribute to the replacement of a chiral (*S*)-α-methylbenzyl in the side chain of the lipopeptoid backbone by an achiral, but bulky diphenylmethane. These results showed that the presence of a chiral center in this portion of the catalyst is also determinant for the stereoselection.

3.3 Optimization of the catalytic system

From the results presented in TABLE 2, catalyst **28** was chosen for the next set of optimization experiments, since it was considered to have the best combination yield/enantioselectivity. As show in TABLE 3, we next evaluated catalyst loading and the nature of the environmentally benign solvent under room temperature. Most of these reactions were performed in triplicate to evaluate if the results obtained were reproducible (Entry 1, 2; 4-6 and 7-9, TABLE 3). Firstly, we turned our attention to study the amount of catalyst in the Michael reaction. By lowering the catalyst loading to 5 mol%, the desired product **34** was obtained in higher yield and excellent enantioselectivity, however, a moderate diastereoisomeric ratio could be observed (Entry 3, TABLE 3). Further decreasing the catalyst loading to 2.5 mol%, yields above 90% are obtained, again with a concomitant improvement in the diastereomeric ratio and the maintenance of enantiomeric excesses (99%) (Entry 4-6, TABLE 3). The use of 1 mol% of the catalyst leads to an erosion on chemical yields (Entry 7-9, TABLE 3). The main differences in the obtained results in the catalyst loading study shall be

associated to the stability of the self-assembled water-oil catalytic system that is formed in dependence on the quantities of catalyst. The use of 10 mol% of catalyst forms a self-assembled water-oil system that is very stable and emulsified, therefore hydrophobic effects are responsible for the slight decrease in yield and diastereoselectivity. While the use of 1 mol% of catalyst forms an unstable water-oil system, and although the results in terms of *d.r.* and *e.e.* were high, chemical yields are very poor, since the system formed does not allow the solubility of the starting materials (so the intermediates) or the desired product. Thus, 2.5 mol% of catalyst is sufficient to maintain good yields and enantioselectivities in pure water.

TABLE 3. Asymmetric Michael reaction of *n*-butanal and β-nitrostyrene catalyzed by **28**. Optimization of the system. [a]
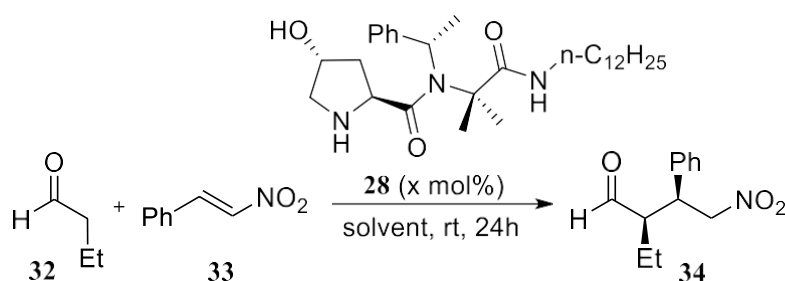
Entry	Catalyst (mol%)	Solvent	Yield (%)[b]	d.r. (syn:anti)[c]	e.e. (%)[d]
1	10	H_2O	76	87:13	98
2	10	H_2O	87	76:24	98
3	5	H_2O	90	90:10	99
4	2.5	H_2O	95	93:7	99
5	2.5	H_2O	96	93:7	99
6	2.5	H_2O	99(96)	93:7	99
7	1	H_2O	46	98:2	99
8	1	H_2O	45	98:2	99
9	1	H_2O	65	98:2	99
10	2.5	Ethanol	26	85:15	98
11	2.5	Brine	84	95:5	99
12	2.5	PEG-300	54	82:18	98

[a] Reactions using 2 equivalents of *n*-butanal and 0.2 mmol of *β*-nitrostyrene in 0.4 mL of solvent. [b] Yield determined by ^{1}H-NMR analysis with 1,2,3-trimethoxybenzene as standard (isolated product).
[c] Determined by ^{1}H NMR analysis of crude of the reaction mixture. [d] Determined by chiral-stationary phase UPC[2] analysis.

Furthermore, we decided to evaluate other green and sustainable solvents, employing 2.5 mol% of catalyst loading. Three systems were examined (ethanol, brine and PEG-300) as alternative solvents of water. When the reaction was performed using ethanol and PEG-300 (Entry 10 and 12, TABLE 3) the desired products are obtained in low yields and good stereoselectivities. The observed yield could be rationalized mainly since these solvents completely dissolve the reagents. Therefore, there is no formation of a water-oil biphasic system. On the other hand, a good result was obtained when brine was evaluated (Entry 11, TABLE 3), showing that our catalytic system depends fundamentally on the formation of a biphasic water-oil system and not of an emulsified or micellar system.

3.4   Scope and Limitations

Encouraged by these results and using the best reaction conditions for our catalytic system, we next explored the scope and limitations of this enamine-type catalytic reaction with a variety of aldehydes and several substituted nitrostyrenes in the *para* position (TABLE 4).

TABLE 4. Scope of catalyst **28** in the asymmetric Michael reaction between different aldehydes and β-nitrostyrenes. [a]

34
[b] yield: 99(96)%
[c] d.r.: 97:3
[d] e.e.: 99%

35
[b] yield: 91%
[c] d.r.: 92:8
[d] e.e.: 99%

36
[b] yield: 79%
[c] d.r.: 99:1
[d] e.e.: 99%

37
[b] yield: 91(89)%
[c] d.r.: 92:8
[d] e.e.: 98%

38
[b] yield: 95(91)%
[c] d.r.: 92:8
[d] e.e.: 99%

39
[b] yield: 96(94)%
[c] d.r.: 92:8
[d] e.e.: 98%

40
[b] yield: 87(84)%
[c] d.r.: 93:7
[d] e.e.: 96%

41
[b] yield: 89(80)%
[c] d.r.: 89:11
[d] e.e.: 97%

---

[a] All reactions were conducted using 2 equivalents of aldehyde and 0.2 mmol of β-nitrostyrene in 0.4 mL of water. [b] Yield determined by ^{1}H-NMR analysis with 1,2,3-trimethoxybenzene as standard and (isolated product). [c] Determined by ^{1}H NMR analysis of crude of reaction mixture. Determined by chiral-stationary phase UPC^2 analysis.

All reactions were conducted in water at room temperature for 24 h in the presence of 2.5 mol% catalyst **28**. In each case, smooth reactions occurred to generate Michael adducts in high yields (80–96%), diastereoselectivities up to 99:1 and excellent enantioselectivities (from 96-to 99% *e.e.*). By increasing the carbon side chain of the aldehyde, the desired product **35** was delivered in the good yield and excellent estereoselectivity. Moreover, performing the reaction in the presence of an aldehyde bearing a bulkier substituent in the *β*-position (i.e.

isovaleraldehyde) afforded lower yield (79%), but 99:1 *dr.* and 99% ee have been observed (product **36**, TABLE 4). As depicted, *β*-nitrostyrenes bearing *β*-aryl substituents with moderate electron withdrawing effect by electronegativity and electron donor due to mesomeric effect (i.e, F, Cl, Br) had a similar behaviour in water. In all these cases, high yields and excellent estereoselectivies were observed (products **37**-**39**, TABLE 4). Besides, the reaction also showed to be non-affected by the presence of strong *β*-aryl electron-rich or electron-withdrawing substituents. Intriguingly, a slight decrease in terms of yield, as well as on the stereoselectivity were observed for the formation of produtcs **40** and **41.**

These results demonstrate that the new prolyl-lipopeptoid hybrid catalyst **28** can be faced as a good catalyst for conjugate addition reactions between a different substituted aromatic nitroolefins and aldehydes. It is also important to emphasize that no additive was needed to assist the catalytic activity, which implies in an even more sustainable process.

3.5 Conformational Study
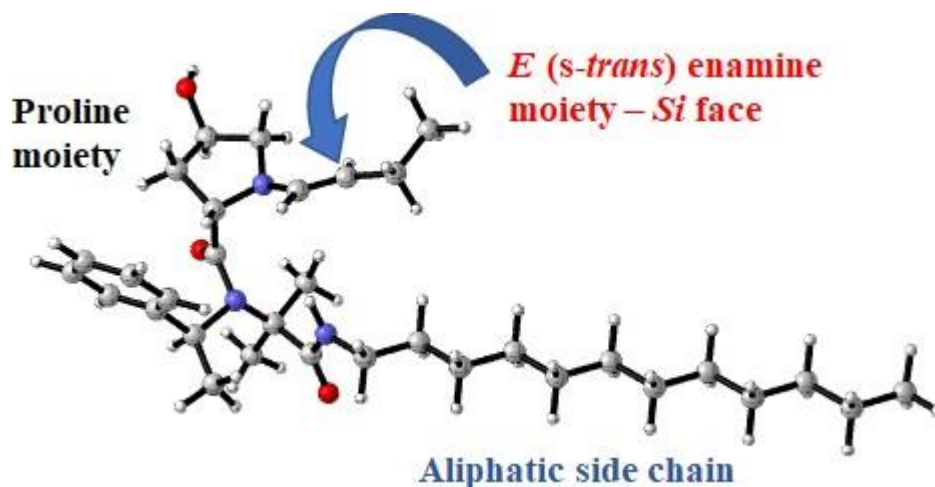
FIGURE 13. Conformational structure of the optimized enamine. In red, the oxygen atoms are represented. In blue are the atoms of nitrogen, in gray the carbon atoms and in white the hydrogen atoms.

The enamine type structure was optimized in a Gaussian 09 program, which afforded the conformation shown in FIGURE 15.[96] Although not so precisely, this simple schematic

---

[96] CYLview, 1.0b; Legault, C. Y., Université de Sherbrooke, 2009 (http://www.cylview.org)

representation of the enamine supports the explanation of the observed enantiomeric discrimination. The enamine configuration is *E* (s-*trans*), which is likely the more stable conformation, where the long alkyl chain is completely blocking one of the faces of the enamine, that is, the *Re*-face. However, since it is a simple approximation proposed, a more accurate DFT calculations still necessary.

4   Conclusions

In conclusion, a new catalyst library based on the prolyl peptide-lipopeptoid hybrid has synthesized by Ugi-4CR. Thus, variation of three elements of diversity at the Ugi-derived *N*-substituted peptide led to eight prolyl *pseudo*-lipopeptides catalysts of the type of Pro-*N*-R^1-Xaa- NHR^3 in moderate to good yields (48-77%). This showed a remarkable improvement in terms of chemical performance, maintaining high stereoselectivity compared to the catalyst previously developed by our research group under these reaction conditions in aqueous media. A low charge of the catalyst **28** (2.5 mol%) was necessary to afford the products with excellent yield, diastereoselectivity and enantioselectivity without any further additive.

5 Perspectives

→ We intend to carry out a conformational study of the catalysts, as well as to increase the number of examples of the scope.

→ The use of *N*-Boc-*trans*-4-hydroxy-proline- as acid component could provide alternatives for the further modifications on the hydroxyl group in this type of catalyst e.g. lipid, pegylated, or support in a solid support that can be polystyrene and polyethylene glycol resins or in silica to be able to recycle it.

→ Due to the results presented for the prolyl *pseudo*-lipopeptide catalyst **28** in Michael reaction under aqueous media we consider that new asymmetric reactions should be evaluated in a sustainable way, especially remote asymmetric funcionalizations (i.e. trienamine).

6 Experimental Section

6.1 General Aspects

Materials and reagents were of the highest commercially available grade purchased from Sigma-Aldrich, Oakwood Chemicals, and Strem Chemicals and used without further purification. Flash chromatography was performed using silica gel 60, particle size 40-63 μm and analytical thin layer chromatography (TLC) was performed using silica gel aluminum sheets. Compounds were visualized on TLC by UV, $KMnO_4$, I_2, $H_3[P(Mo_3O_{10})_4] \cdot xH_2O$ (PMA) and Vanillin solutions. Solvents for extractions and for column chromatography were previously distilled. Chemical yields were given after chromatographical purification. ^{1}H NMR and ^{13}C NMR spectra were recorded at 400 MHz for ^{1}H and 100 MHz for ^{13}C, respectively. Chemical shifts (δ) are reported in parts per million relatives to the residual solvent signals and coupling constants (*J*) are reported in hertz. High resolution ESI mass spectra were obtained from a Fourier transform ion cyclotron resonance (FT-ICR) mass spectrometer, an RF-only hexapole ion guide and an external electrospray ion source. HPLC analysis were carried out on an analytical HPLC with a diode array detector SPD-M20A from Shimadzu using Chiralpak column (OD-H) (250 mm x 4.6 mm) from Daicel Chemical Ind. LTD. UPLC analysis were carrie out on Acquity UPC^2 system from Waters with a 2998 photodiode array (PDA) and Xevo TQD triple cuadrupolo mass spectrometry detectors using Trefoil columns (CEL2 and AMY1) (2.1mm x 50 mm) from Waters. Optical rotations were measured on a Perkin Elmer Polarimeter 341.

6.2 General procedures

6.2.1 Synthesis of commercially not available lipidic isocyanide.

General procedure for the synthesis of isocyanide 23: In a 50 mL bottom flask, commercially dodecylamine (2.00 g, 11 mmol) was dissolved in ethyl formate (20 mL). The resulting solution was refluxed for 24 h at 60 ° C in a silicon bath and the quantitative formation of formamide was checked by TLC (*n*-Hexane/EtOAc 1: 1). The reaction was concentrated by reduced pressure; the crude product was dissolved in triethylamine (30 mL) and cooled down to -70 ºC. Then $POCl_3$ 3 mL (33 mmol) was added drop by drop during 15 min under argon atmosphere. The reaction allowed stirring at room temperature for 48h and after this period the resulting mixture was decanted. The solid obtained was washed with *n*-Hexane (2 × 25 mL), decanted and the fractions of sobrenadant were united. The solvent was removed by reduced pressure and the resulting very viscous oil is directly purified by column chromatography

(Petroleum ether) to obtain pure dodecyl isocyanide as a light-yellow oil (1.50 g, 71%). R_f = 0.83 (*n*-Hexane/EtOAc 10: 1).

Spectroscopic data of dodecyl isocyanide 23:
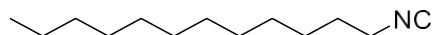
^{1}H NMR (400 MHz, CDCl$_3$) δ = 3.41 – 3.35 (m, 2H), 1.72 – 1.63 (m, 2H), 1.48 – 1.38 (m, 2H), 1.32 – 1.24 (m, 16H), 0.88 (t, *J* = 6.9 Hz, 1H).

^{13}C NMR (101 MHz, CDCl$_3$) δ = 155.43, 60.40, 41.57, 31.91, 29.60, 29.51, 29.37, 29.33, 29.11, 28.71, 26.32, 22.68, 14.12.

6.2.2 Synthesis of prolyl *pseudo*-lipopeptides by Ugi-4CR
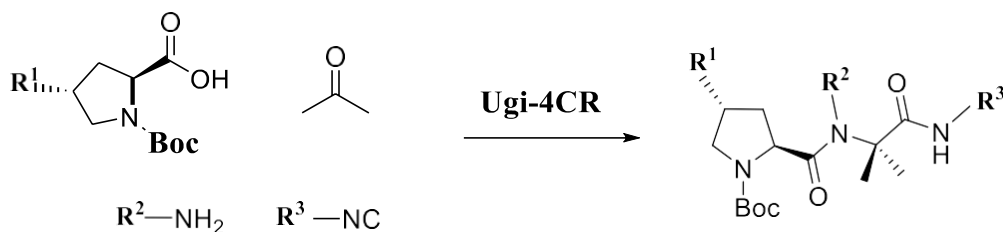
General procedure for the synthesis of compound 25: A solution containing acetone (3 equiv.) and amine (1.5 equiv.) and anhydrous sodium sulfate (3 equiv.) in methanol was stirred at room temperature for 2 hours to preform the imine. After the addition of carboxylic acid (1.2 equiv.) and isocyanide (1 equiv.), the resulting mixture was allowed to stir at room temperature for 24 h. Finally, the solvent was removed under reduced pressure and the residue was purified by column chromatography.

Spectroscopic data of compound 25:
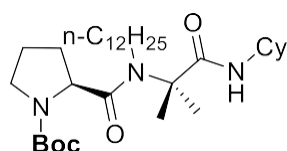
Dodecylamine (56 mg, 0.3 mmol), acetone (44 µL, 0.6 mmol), *N*-Boc-proline (52 mg, 0.24 mmol), cyclohexyl isocyanide (25 µL, 0.2 mmol) and anhydrous sodium sulfate (85 mg, 0.6 mmol) were reacted in MeOH (200 µL) according to the procedure described above. The resulting Boc protected compound was subjected to flash column chromatography purification (EtOAc/*n*-Hexane 7:3) affording the lipopeptoid hybrid **2** (77 mg, 70%) as a colorless oil.

R_f = 0.60 (EtOAc/*n*-Hexanes 7:3).

[α]$_D^{20}$ = n.d.

^{1}H NMR (400 MHz, CDCl$_3$) δ = 5.76 (d, *J* = 7.6 Hz, 1H), 4.48 (dd, *J* = 7.6, 3.5 Hz, 1H), 3.74 – 3.49 (m, 2H), 3.47 – 3.31 (m, 2H), 3.31 – 3.15 (m, 2H), 2.26 – 2.02 (m, 2H), 1.98 – 1.76 (m,

7H), 1.73 – 1.54 (m, 4H), 1.46 – 1.41 (m, 13H), 1.35 – 1.18 (m, 20H), 1.16 – 0.98 (m, 3H), 0.87 (t, J = 6.8 Hz, 3H).

^{13}C NMR (101 MHz, CDCl$_3$) δ = 174.09, 173.29, 154.53, 79.41, 62.82, 56.95, 48.61, 47.17, 44.61, 33.04, 32.74, 32.51, 31.90, 31.25, 30.34, 29.60, 29.32, 29.13, 28.62, 27.01, 25.55, 25.48, 25.21, 24.97, 24.30, 23.82, 23.07, 22.68, 14.11.

General procedure for the synthesis of compound 24, 26 and 27: A solution containing acetone (3 equiv.) and amine (1.5 equiv.) and anhydrous sodium sulfate (3 equiv.) in MeOH/ THF (2:1 v/v) was stirred under microwave irradiation at 70 ^{o}C during 10 min to preform imine. After the carboxylic acid (1.2 equiv.) and isocyanide (1 equiv.) were added, the resulting mixture was stirred under microwave irradiation (at 70 ^{o}C) during 30 min. Finally, the solvent was removed under reduced pressure and the residue was purified by column chromatography. Note: Only THF was used for the synthesis of compounds **3** and **4.**

Spectroscopic data of compound 24:
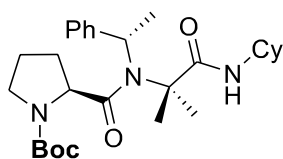
(*S*)-α-methylbenzylamine (39 µL, 0.3 mmol), acetone (44 µL, 0.6 mmol), *N*-Boc-proline (52 mg, 0.24 mmol), cyclohexyl isocyanide (25 µL, 0.2 mmol) and anhydrous sodium sulfate (85 mg, 0.6 mmol) were reacted in MeOH (200 µL) according to the procedure described above. The resulting Boc protected compound was subjected to flash column chromatography purification (*n*-Hexane/EtOAc 7:3) affording the peptoid hybrid **1** (75 mg, 77%) as a colorless oil.

R_f = 0.30 (*n*-Hexane/EtOAc 7:3).

[α] $_D^{20}$ = n.d.

^{1}H NMR (400 MHz, CDCl$_3$) δ = 7.61 (d, J = 7.7 Hz, 2H), 7.40 (t, J = 7.6 Hz, 2H), 7.32 – 7.25 (m, 1H), 5.81 (d, J = 7.3 Hz, 1H), 5.14 (s, 1H), 4.31 – 4.07 (m, 1H), 3.75 – 3.55 (m, 1H), 3.54 – 3.37 (m, 1H), 3.35 – 3.14 (m, 1H), 2.09 – 2.03 (m, 2H), 1.93 (d, J = 7.1 Hz, 3H), 1.89 – 1.73 (m, 2H), 1.72 – 1.53 (m, 8H), 1.53 – 1.38 (m, 11H), 1.39 – 1.26 (m, 3H), 1.21 – 1.09 (m, 3H).

^{13}C NMR (101 MHz, CDCl$_3$) δ = 174.37, 174.27, 154.30, 142.80, 128.68, 127.28, 127.16, 78.96, 64.32, 58.91, 48.73, 47.41, 32.56, 32.31, 28.80, 28.59, 25.48, 25.05, 24.86, 23.67, 18.93, 14.16.

Spectroscopic data of compound 26:
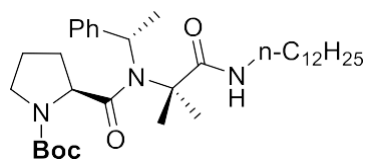
(S)-α-methylbenzylamine (39 µL, 0.3 mmol), acetone (44 µL, 0.6 mmol), N-Boc-proline (52 mg, 0.24 mmol), dodecyl isocyanide (45 µL, 0.2 mmol) and anhydrous sodium sulfate (85 mg, 0.6 mmol) were reacted in MeOH/ THF (200:100 µL v/v) according to the procedure described above. The resulting Boc protected compound was subjected to flash column chromatography purification (n-Hexane/EtOAc 7:3) affording the lipopeptoid hybrid **3** (62 mg, 54%) as a colorless oil.

R_f = 0.4 (n-Hexane/EtOAc 7:3).

[α] $_D^{20}$ = 13.58 (c 0.033, EtOAc, 20 °C).

¹H NMR (400 MHz, CDCl₃) δ = 7.53 (s, J = 48.5 Hz, 2H), 7.39 (t, J = 7.6 Hz, 2H), 7.31 – 7.25 (m, 1H), 6.40 (s, 1H), 5.10 (s, 1H), 4.13 – 3.95 (m, 1H), 3.46 – 3.16 (m, 3H), 2.98 – 2.82 (m, 1H), 2.04 – 1.89 (m, 3H), 1.86 – 1.57 (m, 8H), 1.50 – 1.41 (m, 11H), 1.31 – 1.22 (m, 20H), 0.88 (t, J = 6.8 Hz, 3H).

¹³C NMR (101 MHz, CDCl₃) δ = 175.27, 154.56, 142.71, 128.75, 128.64, 127.24, 79.24, 64.70, 59.21, 51.80, 47.53, 39.76, 31.91, 29.64, 29.39, 29.36, 28.82, 28.51, 26.98, 26.74, 24.37, 23.98, 22.68, 19.06, 14.12.

Spectroscopic data of compound 27:
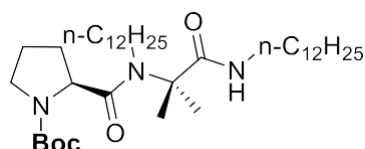
Dodecylamine (56 mg, 0.3 mmol), acetone (44 µL, 0.6 mmol), N-Boc-proline (52 mg, 0.24 mmol), dodecyl isocyanide (45 µL, 0.2 mmol) and anhydrous sodium sulfate (85 mg, 0.6 mmol) were reacted in MeOH/ THF (200:100 µL v/v) according to the procedure described above. The resulting Boc protected compound was subjected to flash column chromatography purification (n-Hexane/EtOAc 7:3) affording the lipopeptoid hybrid **4** (73 mg, 57%) as a colorless oil.

R_f = 0.50 (n-Hexane/EtOAc 7:3).

[α] $_D^{20}$ = -7.33 (c 0.033, EtOAc, 20 °C).

¹H NMR (400 MHz, CDCl₃) δ = 6.31 – 6.16 (m, 1H), 4.47 (dd, J = 7.4, 4.6 Hz, 1H), 3.76 – 3.50 (m, 2H), 3.47 – 3.35 (m, 1H), 3.35 – 3.17 (m, 2H), 3.15 – 2.84 (m, 1H), 2.16 – 2.05 (m, 3H), 1.99 (m, 2H), 1.93 – 1.77 (m, 3H), 1.50 – 1.45 (m, 6H), 1.43 (s, 9H), 1.33 – 1.21 (m, 37H), 0.88 (t, J = 6.9 Hz, 6H).

¹³C NMR (101 MHz, CDCl₃) δ = 175.01, 173.39, 154.75, 79.53, 62.86, 56.79, 47.19, 44.57, 39.80, 32.06, 31.90, 30.20, 29.62, 29.53, 29.41, 29.35, 29.33, 29.14, 28.54, 28.47, 27.00, 26.11, 24.52, 23.56, 22.68, 14.11.

General procedure for the synthesis of compound 28-31: A solution containing acetone (3 equiv.), amine (1.5 equiv.) and anhydrous sodium sulfate (3 equiv.) in MeOH/ THF (2:1 v/v) was stirred under microwave irradiation at (70 °C) during 10 min to perform the imine. After, carboxylic acid (1.2 equiv.) and isocyanide (1 equiv.) were added, the resulting mixture was allowed to stir at room temperature for 24-48 h. Finally, the solvent was removed under reduced pressure and the residue was purified by column chromatography.

Spectroscopic data of compound 28:
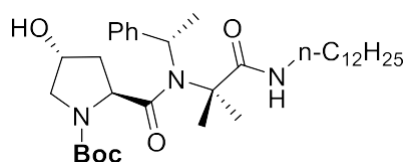
(S)-α-methylbenzylamine (39 µL, 0.3 mmol), acetone (44 µL, 0.6 mmol), N-Boc-trans-4-hydroxy-proline (56 mg, 0.24 mmol), dodecyl isocyanide (45 µL, 0.2 mmol) and anhydrous sodium sulfate (85 mg, 0.6 mmol) were reacted in MeOH/ THF (200:100 µL v/v) according to the procedure described above. The resulting Boc protected compound was subjected to flash column chromatography purification (EtOAc/n-Hexane 8:2) affording the lipopeptoid hybrid **5** (51 mg, 50%) as a colorless oil

Rf = 0.40 (EtOAc/ n-Hexanes 8:2).

[α] ᴅ²⁰ = n.d.

¹H NMR (400 MHz, CDCl₃) δ = 7.52 (s, J = 71.2 Hz, 2H), 7.40 (t, J = 7.5 Hz, 2H), 7.34 – 7.25 (m, 1H), 6.55 (s, 1H), 5.09 (s, 1H), 4.29 – 4.04 (m, 2H), 3.58 – 3.23 (m, 3H), 2.88 (s, 1H), 2.04 (s, 3H), 1.78 – 1.58 (m, 6H), 1.50 – 1.38 (m, 11H), 1.25 (s, 20H), 0.88 (t, J = 6.6 Hz, 3H).

¹³C NMR (101 MHz, CDCl₃) δ = 175.22, 174.46, 154.64, 142.80, 128.80, 127.53, 127.37, 79.65, 69.78, 64.84, 58.15, 55.48, 51.76, 39.77, 37.86, 31.92, 29.66, 29.40, 29.36, 28.47, 26.99, 26.86, 24.21, 22.69, 19.07, 14.13.

Spectroscopic data of compound 29:
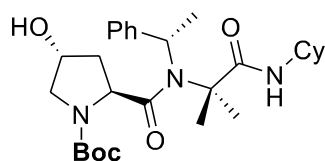
(S)-α-methylbenzylamine (39 µL, 0.3 mmol), acetone (44 µL, 0.6 mmol), N-Boc-trans-4-hydroxy-proline (56 mg, 0.24 mmol), cyclohexyl isocyanide (25 µL, 0.2 mmol) and anhydrous sodium sulfate (85 mg, 0.6 mmol) were reacted in MeOH/ THF (200:100 µL v/v) according to the procedure described above. The resulting Boc protected compound was subjected to flash

column chromatography purification (EtOAc/*n*-Hexane 9:1) affording peptoid hybrid **6** (73 mg, 73%) as a colorless oil.
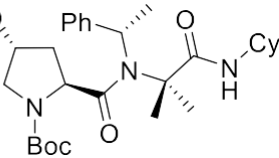
R_f = 0.45 (EtOAc/ *n*-Hexanes 9:1).

$[\alpha]_D^{20}$ = 3.88 (*c* 0.033, EtOAc, 20 °C).

¹H NMR (400 MHz, CDCl₃) δ = 7.62 (d, *J* = 7.6 Hz, 2H), 7.40 (t, *J* = 7.6 Hz, 2H), 7.29 (t, *J* = 7.2 Hz, 1H), 5.87 (d, *J* = 7.5 Hz, 1H), 5.12 (s, 1H), 4.43 – 4.00 (m, 2H), 3.75 – 3.46 (m, 2H), 3.42 – 3.20 (m, 1H), 2.13 – 1.80 (m, 7H), 1.73 – 1.54 (m, 8H), 1.44 (s, 9H), 1.37 – 1.24 (m, 3H), 1.21 – 1.08 (m, 3H).

¹³C NMR (101 MHz, CDCl₃) δ = 174.47, 174.29, 154.46, 142.88, 128.73, 127.43, 127.30, 79.42, 69.68, 64.40, 58.06, 55.44, 48.91, 37.98, 32.54, 32.28, 28.82, 28.62, 25.46, 25.12, 24.93, 19.00.

Spectroscopic data of compound 30:

(*S*)-α-methylbenzylamine (97 µL, 0.75 mmol), acetone (110 µL, 0.6 mmol), *N*-Boc-*trans*-4-C₁₁H₂₃COO-proline (248 mg, 0.6 mmol), cyclohexyl isocyanide (62 µL, 0.5 mmol) and anhydrous sodium sulfate (213 mg, 1.5 mmol) were reacted in MeOH/ THF (400:200 µL v/v) according to the procedure described above. The resulting Boc protected compound was subjected to flash column chromatography purification (*n*-Hexane/EtOAc 8:2) affording the lipopeptoid hybrid **7** (165 mg, 48%) as a colorless oil.

R_f = 0.50 (*n*-Hexane/EtOAc 8:2).

$[\alpha]_D^{20}$ = 17.70 (*c* 0.033, EtOAc, 20 °C).

¹H NMR (400 MHz, CDCl₃) δ = 7.62 (d, *J* = 7.7 Hz, 2H), 7.38 (t, *J* = 7.6 Hz, 2H), 7.29 – 7.24 (m, 1H), 5.85 (d, *J* = 7.6 Hz, 1H), 5.12 (s, 1H), 4.91 (s, 1H), 4.20 (s, 1H), 3.61 (d, *J* = 10.0 Hz, 2H), 3.39 (d, *J* = 10.8 Hz, 1H), 3.37 – 3.30 (m, 1H), 2.18 (t, *J* = 7.1 Hz, 2H), 2.07 – 1.91 (m, 5H), 1.87 (d, *J* = 10.1 Hz, 1H), 1.74 – 1.58 (m, 8H), 1.51 – 1.39 (m, 11H), 1.33 – 1.22 (m, 20H), 1.19 – 1.08 (m, 3H), 0.88 (t, *J* = 6.9 Hz, 3H).

¹³C NMR (101 MHz, CDCl₃) δ = 174.37, 172.91, 154.16, 142.88, 128.71, 127.53, 127.28, 79.63, 72.59, 64.39, 58.10, 53.36, 51.52, 48.86, 35.20, 34.28, 32.61, 32.36, 31.89, 29.61, 29.47, 29.32, 29.30, 29.11, 28.78, 28.56, 25.49, 25.10, 24.92, 24.81, 22.67, 19.03, 14.11.

Spectroscopic data of compound 31:
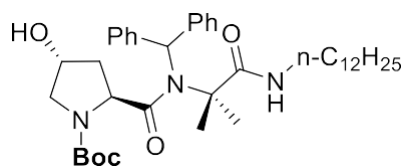
2.2-diphenylglycine methyl ester hydrochloride (241 mg, 1 mmol), DIPEA (174 µL, 1 mmol), acetone (110 µL, 1.5 mmol), *N*-Boc-*trans*-4-hydroxy-proline (139 mg, 0.6 mmol), dodecyl isocyanide (98 µL, 0.5 mmol) and anhydrous sodium sulfate (213 mg, 1.5 mmol) was reacted in MeOH/ THF (400:200 µL v/v) according to the procedure described above. The resulting Boc protected compound was subjected to flash column chromatography purification (*n*-Hexane/EtOAc 1:1) affording the lipopeptoid hybrid **8** (193 mg, 55%) as a colorless oil.

R_f = 0.30 (*n*-Hexanes/EtOAc 1:1).

[α] $_D^{20}$ = -21.76 (*c* 0.033, EtOAc, 20 °C).

^{1}H NMR (400 MHz, CDCl$_3$) δ = 8.07 (d, *J* = 7.5 Hz, 2H), 7.43 (t, *J* = 7.5 Hz, 2H), 7.37 – 7.23 (m, 7H), 6.54 (s, 1H), 6.29 (s, 1H), 4.26 (t, *J* = 7.3 Hz, 1H), 4.04 (s, 1H), 3.49 (dd, *J* = 11.5, 4.2 Hz, 1H), 3.42 – 3.27 (m, 2H), 2.97 – 2.83 (m, 1H), 1.72 (s, 3H), 1.47 (s, 9H), 1.45 – 1.33 (m, 6H), 1.31 – 1.17 (m, 20H), 0.88 (t, *J* = 6.8 Hz, 3H).

^{13}C NMR (101 MHz, CDCl$_3$) δ = 175.39, 174.78, 154.51, 142.28, 139.48, 130.51, 128.81, 128.70, 128.63, 127.98, 127.49, 79.79, 69.37, 65.82, 62.71, 59.76, 55.75, 39.57, 37.68, 31.93, 29.64, 29.62, 29.40, 29.37, 29.25, 28.48, 27.22, 26.90, 23.39, 22.70, 14.14.

6.2.3 Boc deprotection of prolyl *pseudo*-lipopeptides using TFA

General procedure: The *N*-Boc pure product resulting for the Ugi-4CR was cooled and dissolved in 1 mL of a mixture of TFA/CH$_2$Cl$_2$ 9:1 v/v at 0 °C. The reaction mixture was allowed to stir for 30 min and then concentrated to reduced pressure (TFA was removed completely by repetitive addition and evaporation of further CH$_2$Cl$_2$). The crude was dissolved in 10 mL of EtOAc and washed with satured NaHCO$_3$ (3 x 10 ml), brine (10 ml), dried over anhydrous Na$_2$SO$_4$ and filtered evaporated under reduced pressure afforded to desired product.

6.2.3.1 High resolution mass spectra of the hybrid *pseudo*-lipopeptides used as catalyst
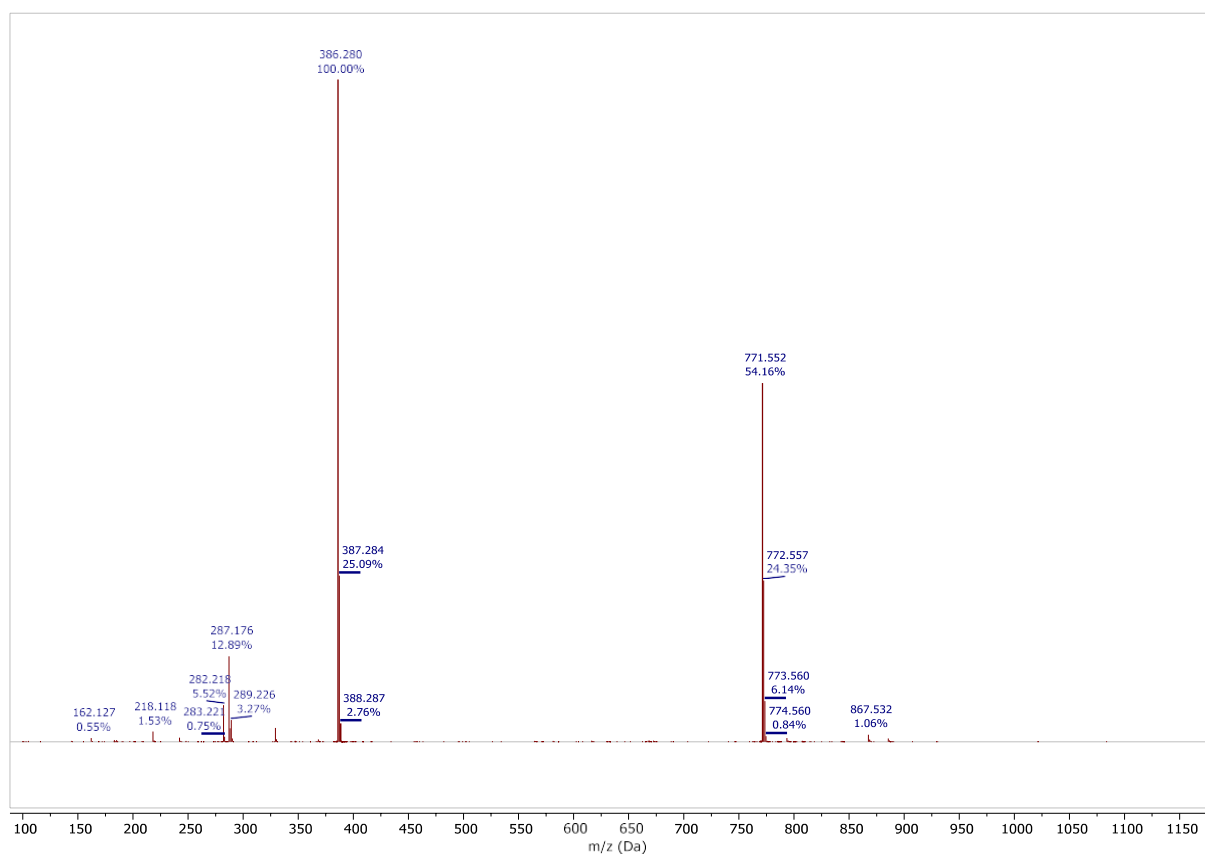
FIGURE 14. ESI-MS spectrum of compound **24** *N*-Boc deprotected.

M[$C_{23}H_{35}N_3O_2$+H]$^+$calcd: 386.2729 Da, found 386.280 Da. Non-covalent dimer M[2x($C_{23}H_{35}N_3O_2$)+H]$^+$ calcd: 771.5458 Da, found: 771.557 Da.
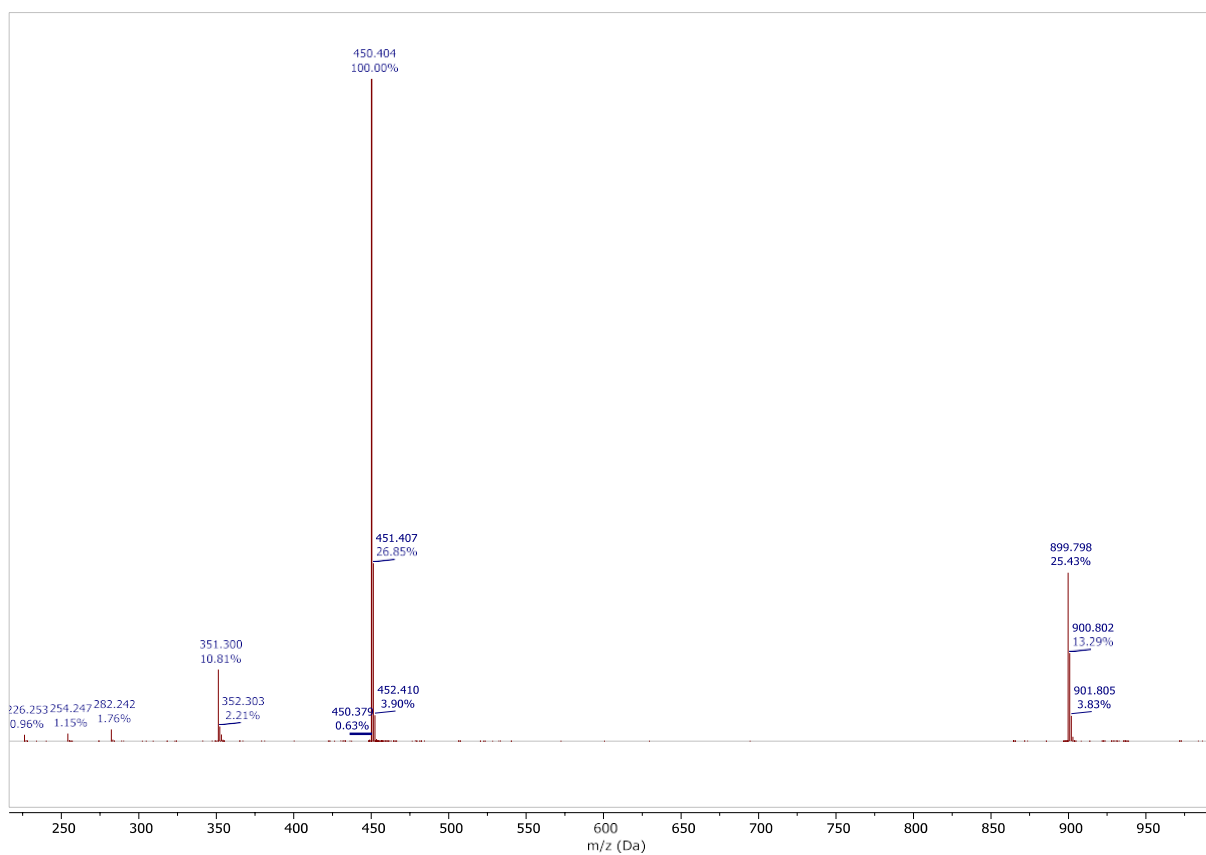
FIGURE 15. ESI-MS spectrum of compound **25** *N*-Boc deprotected.

M[$C_{27}H_{51}N_3O_2$+H]$^+$calcd: 450.3981 Da, found 450.407 Da. Non-covalent dimer M[2x($C_{27}H_{51}N_3O_2$)+H]$^+$ calcd: 899.7962 Da, found: 899.798 Da.
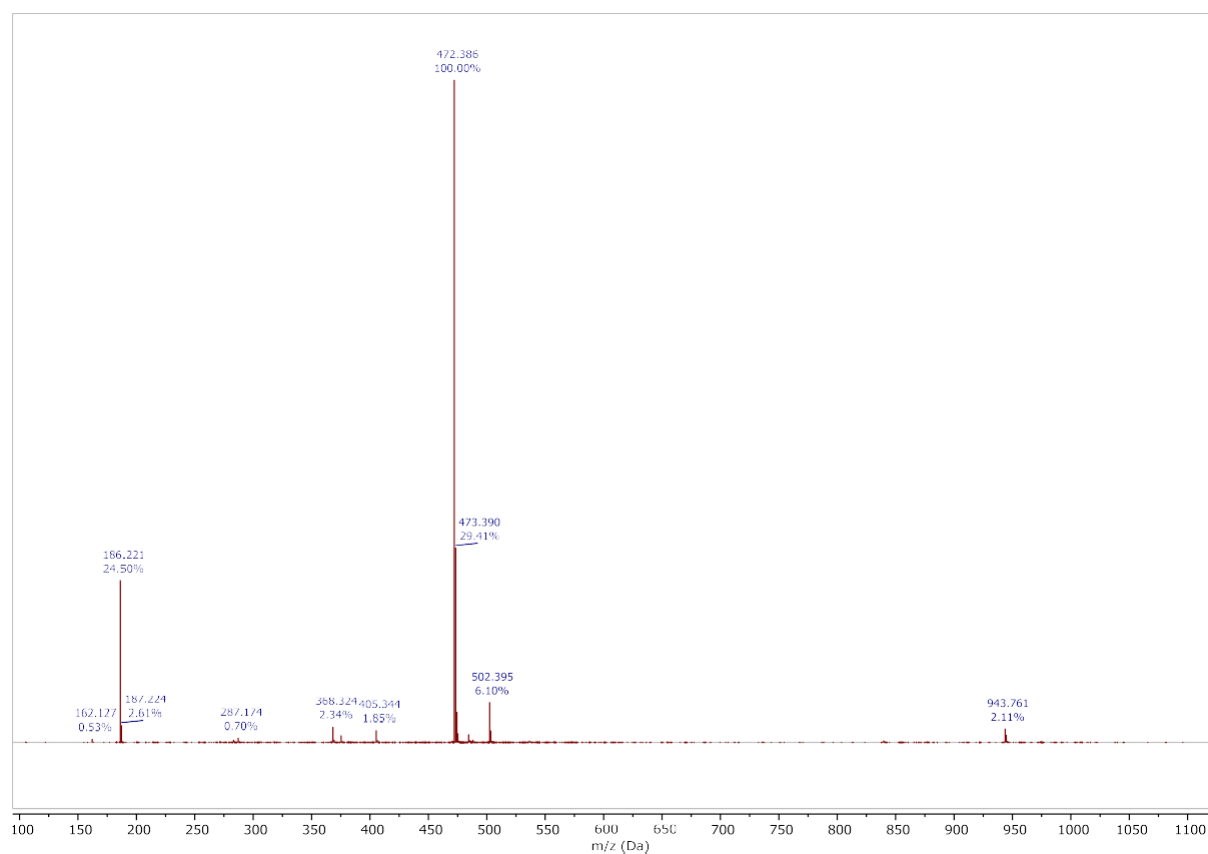
FIGURE 16. ESI-MS spectrum of compound **26** *N*-Boc deprotected.

M[$C_{29}H_{49}N_3O_2$+H]$^+$calcd: 472.3825   Da, found 472.386 Da. Non-covalent dimer M[2x($C_{29}H_{49}N_3O_2$)+H]$^+$ calcd: 943.7650 Da, found: 943.761 Da.
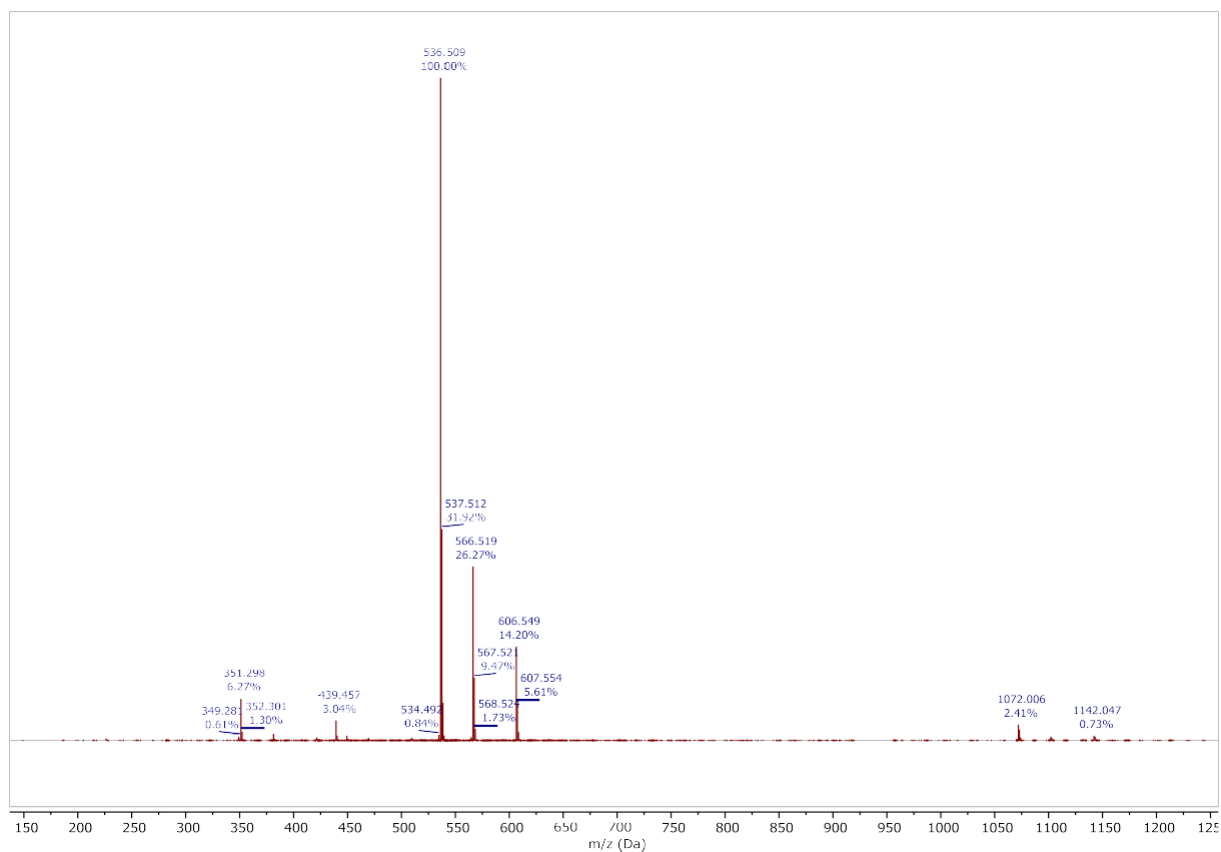
FIGURE 17. ESI-MS spectrum of compound **27** *N*-Boc deprotected.

M[$C_{33}H_{65}N_3O_2$+H]$^+$calcd: 536.5077 Da, found 536.509 Da. Non-covalent dimer M[2x($C_{33}H_{65}N_3O_2$)+H]$^+$ calcd: 1072.0154 Da, found: 1072.006 Da.
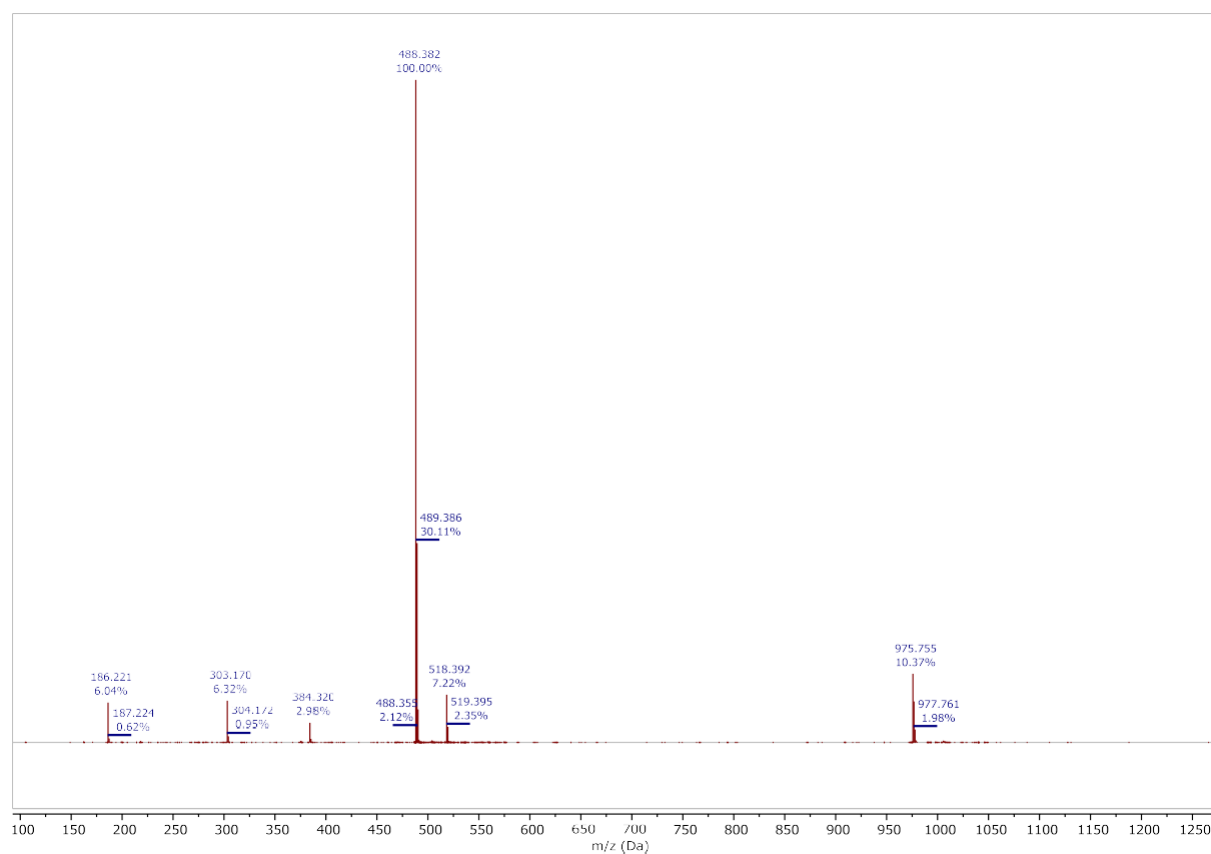
FIGURE 18. ESI-MS spectrum of compound **28** *N*-Boc deprotected.

M[$C_{29}H_{49}N_3O_3$+H]$^+$calcd: 488.3774 Da, found 488.382 Da. Non-covalent dimer M[2x($C_{29}H_{49}N_3O_3$)+H]$^+$ calcd: 975.7548 Da, found: 975.755 Da.
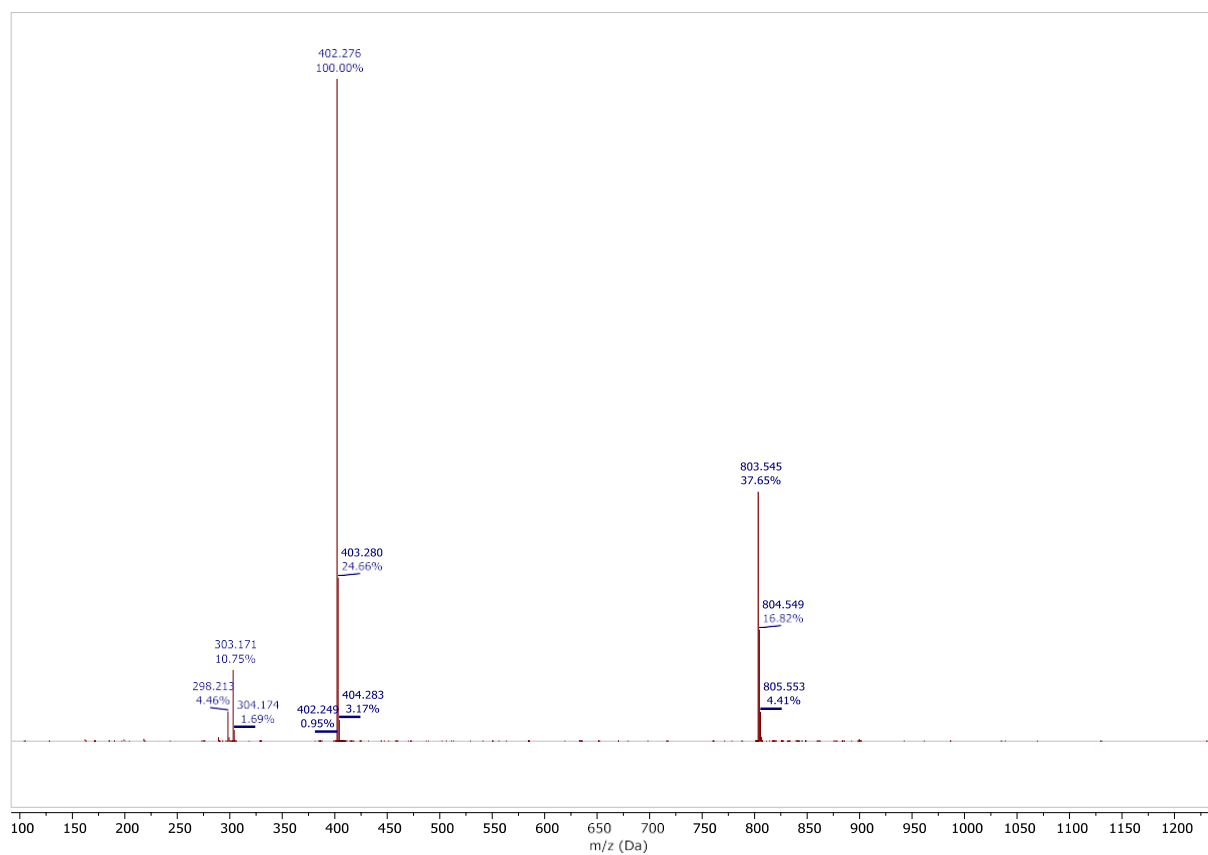
FIGURE 19. ESI-MS spectrum of compound **29** *N*-Boc deprotected.

M[$C_{23}H_{35}N_3O_3$+H]$^+$calcd: 402.2678 Da, found 402.276 Da. Non-covalent dimer M[2x($C_{23}H_{35}N_3O_3$)+H]$^+$ calcd: 803.5356 Da, found: 803.545 Da.
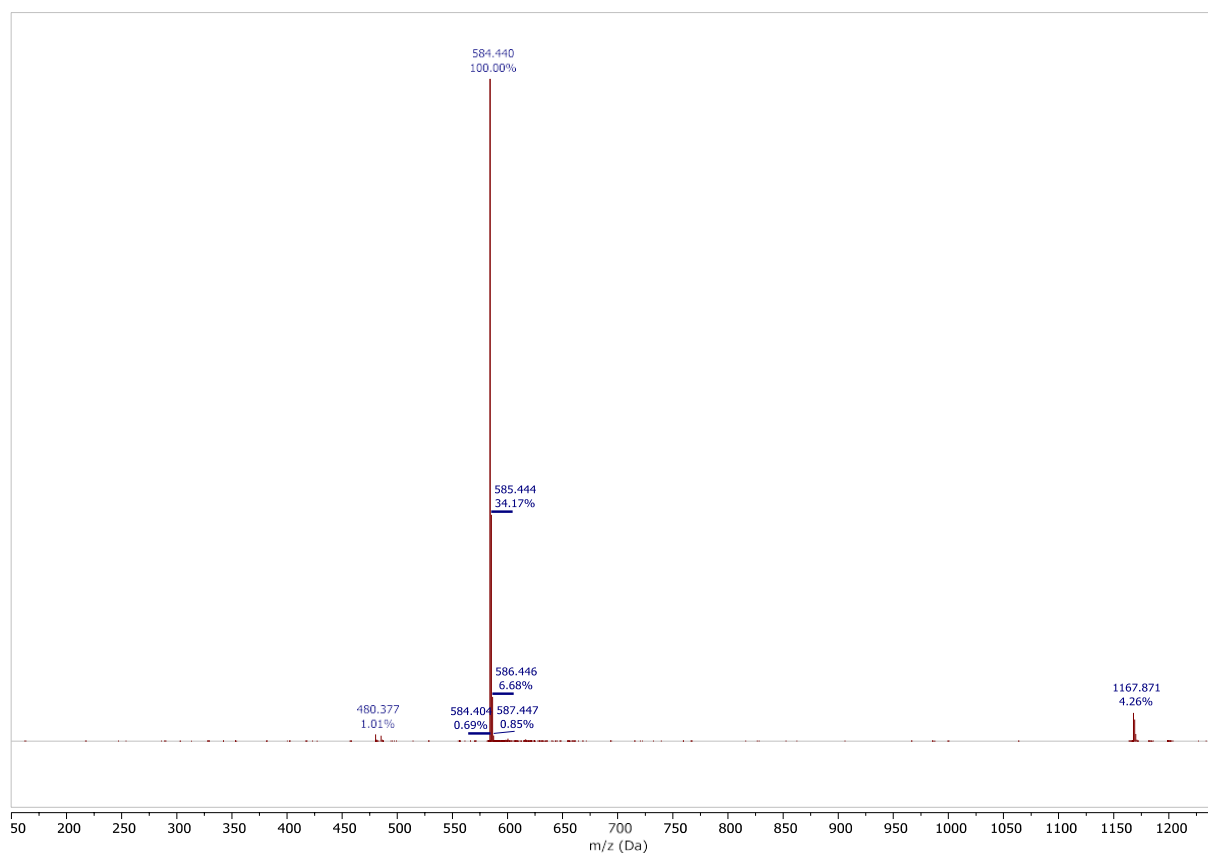
FIGURE 20. ESI-MS spectrum of compound **30** *N*-Boc deprotected.

M[$C_{35}H_{57}N_3O_4$+H]$^+$calcd: 584.4349 Da, found 584.440 Da. Non-covalent dimer M[2x($C_{35}H_{57}N_3O_4$)+H]$^+$ calcd: 1167.8698 Da, found: 1167.871 Da.
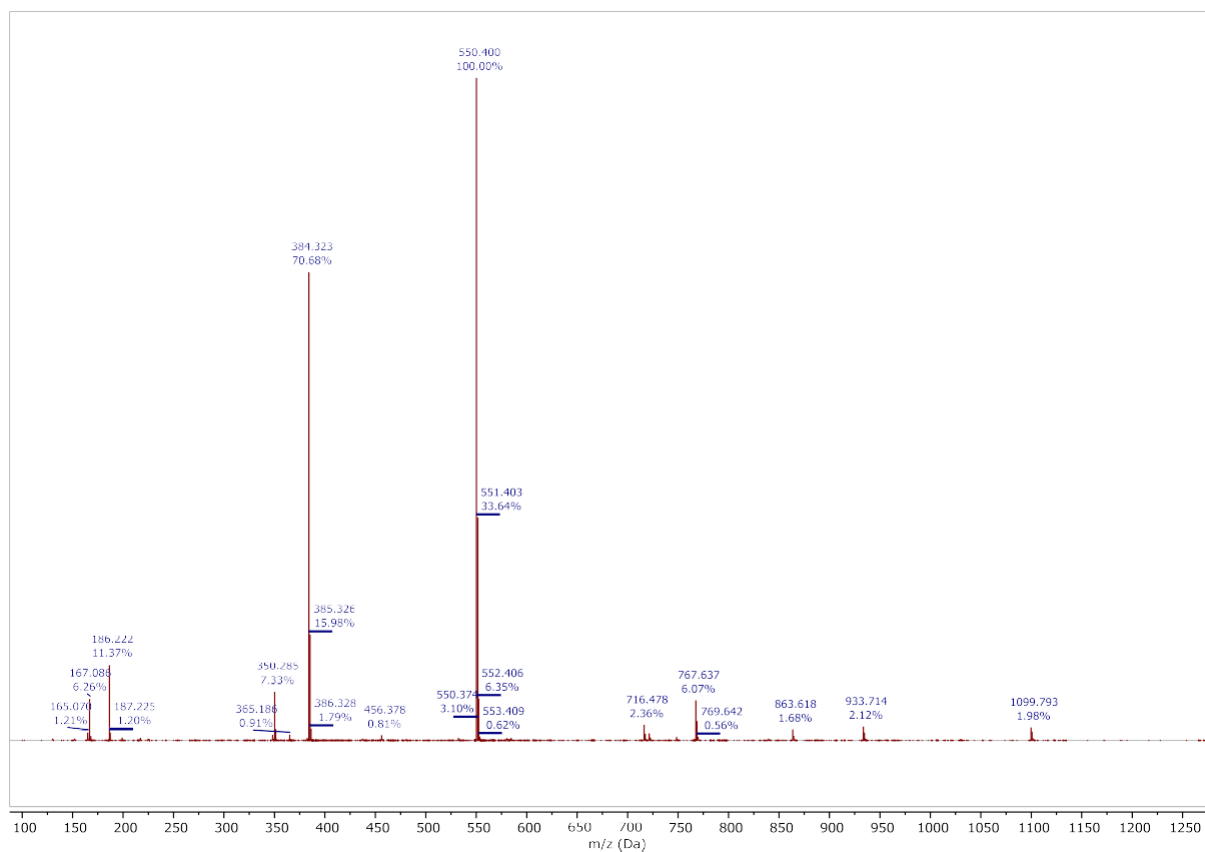
FIGURE 21. ESI-MS spectrum of compound **31** *N*-Boc deprotected.

M[$C_{34}H_{51}N_3O_3$+H]$^+$calcd: 550.3930 Da, found 550.400 Da.

6.2.4 General procedure for asymmetric 1,4-addition of aldehydes to nitrostyrenes.
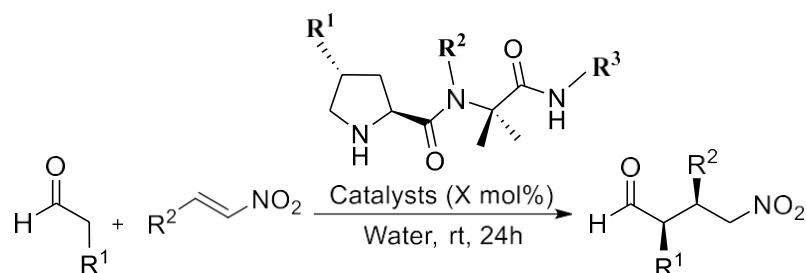
General procedure: A vial, was charged with the prolyl *pseudo*-lipopeptide **28** (X mol%), the nitroolefin (0.2 mmol, 1.0 equiv) and 0.4 mL of water. The mixture was homogenized in an ultrasound bath, treated with the aldehyde (0.40 mmol, 2.0 equiv) and was stirred for 24 h. After this period, the resulting reaction mixture was extracted with EtOAc, dried over anhydrous Na$_2$SO$_4$ and concentrated under reduced pressure. The yield was determined by ^{1}H NMR analysis of resulting crude product with 1.2.3-trimethoxybenzene (0.2 mmol, 1.0 equiv) as standard patron. The crude product was purified by flash column chromatography on silica gel using *n*-hexane/EtOAc as eluent only for the compounds that require it. The distereoisomeric ratio was determined by ^{1}H NMR analysis of crude of reaction mixture. Enantiomeric excess (*e.e.*) was determined by chiral HPLC or UPC^2 analysis through comparison with the authentic racemic material.

Spectroscopic data of compound 34: 2-ethyl-4-nitro-3-phenylbutanal
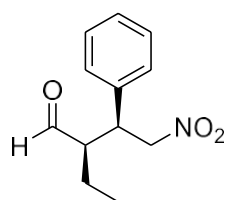
Prepared by reaction of *n*-butanal with *trans*-β-nitrostyrene according to the procedure described above. The compound was purified by flash column chromatography (*n*-Hexane/EtOAc 9:1). The enantiomeric excess was determined by chiral-stationary phase UPC^2. Trefoil CEL2, CO$_2$/EtOH 100-0% to 95-5 % in 10 min at 3 ml/min at 25°C. UV detection at 210 nm: R$_t$: (syn, major) = 4.13 min, (syn, minor) = 3.93 min.

***R*$_f$** = 0.4 (*n*-Hexane/EtOAc 9:1).

^{1}H NMR (400 MHz, CDCl$_3$) δ = 9.71, 9.48 (2xd, *J* = 2.6 Hz, 1H, CHO), 7.37 – 7.27 (m, 3H, Ph), 7.18 (d, *J* = 6.7 Hz, 2H, Ph), 4.72 (dd, *J* = 12.7, 5.0 Hz, 1H, CH$_2$NO$_2$), 4.62 (dd, *J* = 12.7, 9.7 Hz, 1H, CH$_2$NO$_2$), 3.79 (td, *J* = 9.9, 5.0 Hz, 1H, CHPh), 2.71 – 2.64 (m, 1H, CHCHO), 1.56 – 1.45 (m, 2H, CH$_2$), 0.82 (t, *J* = 7.5 Hz, 3H, CH$_3$).

^{13}C NMR (101 MHz, CDCl$_3$) δ = 203.26, 136.82, 129.11, 128.24, 128.13, 128.02, 78.57, 54.97, 42.69, 20.35, 10.65.

Spectroscopic data of compound 35: 2-(2-nitro-1-phenylethyl) hexanal
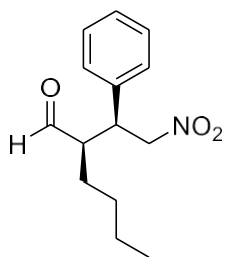
Prepared by reaction of *n*-Hexanal with *trans*-β-nitrostyrene according to the procedure described above. The compound was purified by flash column chromatography (*n*-Hexane/EtOAc 9:1). The enantiomeric excess was determined by chiral-stationary phase UPC^2. Trefoil CEL2, CO_2/EtOH 100-0% to 95-5 % in 10 min at 3 ml/min at 25°C. UV detection at 210 nm:

tR: (syn, major) = 6.95 min, (syn, minor) = 6.64 min.

R_f = 0.5 (*n*-Hexane/EtOAc 9:1).

^{1}H NMR (400 MHz, CDCl$_3$) δ = 9.70 (2xd, *J* = 2.8 Hz, 1H, CHO), 7.36 – 7.27 (m, 3H, Ph), 7.17 (d, *J* = 6.9 Hz, 2H, Ph), 4.82 – 4.60 (m, 2H, CH$_2$NO$_2$), 3.78 (td, *J* = 9.7, 5.3 Hz, 1H, CHPh), 2.74 – 2.65 (m, 1H, CHCHO), 1.43 – 1.12 (m, 6H, 3xCH$_2$), 0.78 (t, *J* = 7.0 Hz, 3H, CH$_3$).

^{13}C NMR (101 MHz, CDCl$_3$) δ = 203.30, 136.80, 129.12, 128.23, 128.15, 128.01, 78.45, 53.88, 43.13, 28.52, 27.03, 22.49, 13.65.

Spectroscopic data of compound 36: 2-Isopropyl-4-nitro-3-phenylbutanal
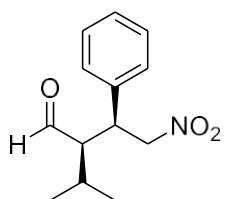
Prepared from isovaleraldehyde and *trans*-β-nitrostyrene according to the procedure described above. The compound was purified by flash column chromatography (*n*-Hexane/EtOAc 9:1). The enantiomeric excess was determined by chiral-stationary phase UPC^2. Trefoil CEL2, CO_2/EtOH 100-0% to 95-5 % in 10 min at 3 ml/min at 25°C. UV detection at 210 nm: tR: (syn, major) = 3.97 min, (syn, minor) = 3.68 min.

R_f = 0.45 (*n*-hexane/EtOAc 9:1).

^{1}H NMR (400 MHz, CDCl$_3$) δ = 9.92, 9.47 (2xd, *J* = 2.4 Hz, 1H, CHO), 7.37 – 7.28 (m, 3H, Ph), 7.19 (d, *J* = 6.8 Hz, 2H, Ph), 4.67 (dd, *J* = 12.5, 4.4 Hz, 1H, CH$_2$NO$_2$), 4.57 (dd, *J* = 12.5, 10.0 Hz, 1H, CH$_2$NO$_2$), 3.90 (td, *J* = 10.4, 4.4 Hz, 1H, CHPh), 2.78 (ddd, *J* = 10.8, 4.1, 2.4 Hz, 1H, CHCHO), 1.76 – 1.66 (m, 1H, CH), 1.09 (d, *J* = 7.2 Hz, 3H, CH$_3$), 0.88 (d, *J* = 7.0 Hz, 3H, CH$_3$).

^{13}C NMR (101 MHz, CDCl$_3$) δ = 204.40, 137.09, 129.17, 128.11, 127.97, 79.01, 58.75, 41.93, 27.92, 21.66, 16.98.

Spectroscopic data of compound 37: 3-(4-Fluorophenyl)-2-ethyl-4-nitrobutanal
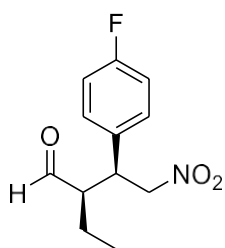
Prepared from *n*-butanal and *trans*-4-fluoro-β-nitrostyrene according to the procedure described above. The compound was purified by flash column chromatography (*n*-Hexane/EtOAc 9:1). The enantiomeric excess was determined by chiral-stationary phase UPC^2. Trefoil CEL2, Grad: CO_2/EtOH 100-0% to 95-5% in 9 min; 100-0 % in 1 min at 2 ml/min at 25°C. UV detection at 210 nm: tR: (syn, major) = 6.88 min, (syn, minor) = 6.30 min.

R_f = 0.30 (*n*-Hexane/EtOAc 9:1).

^{1}H NMR (400 MHz, CDCl$_3$) δ = 9.71, 9.48 (2xd, *J* = 2.4 Hz, 1H, CHO), 7.17 (dd, *J* = 8.7, 5.2 Hz, 2H, Ph), 7.04 (t, *J* = 8.7 Hz, 3H, Ph), 4.72 (dd, *J* = 12.7, 4.8 Hz, 1H, CH$_2$NO$_2$), 4.59 (dd, *J* = 12.7, 10.0 Hz, 1H, CH$_2$NO$_2$), 3.80 (td, *J* = 10.0, 4.8 Hz, 1H, CHPh), 2.66 (dddd, *J* = 10.3, 8.2, 4.3, 2.4 Hz, 1H, CHCHO), 1.58 – 1.45 (m, 2H, CH$_2$), 0.83 (t, *J* = 7.5 Hz, 3H, CH$_3$).

^{13}C NMR (101 MHz, CDCl$_3$) δ = 202.91, 163.57, 132.58, 129.68, 129.60, 116.24, 116.03, 78.56, 54.89, 41.92, 20.32, 10.54.

Spectroscopic data of compound 38: 3-(4-Chlorophenyl)-2-ethyl-4-nitrobutanal
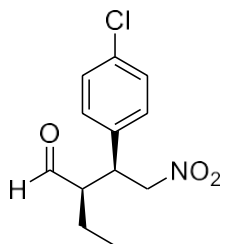
Prepared from *n*-butanal and *trans*-4-chloro-β-nitrostyrene according to the procedure described above. The compound was purified by flash column chromatography (*n*-Hexane/EtOAc 9:1). The enantiomeric excess was determined by chiral-stationary phase UPC^2. Trefoil AMY1, Grad: CO_2/MeOH 100-0% to 90-10 % in 6 min; 90-10 % in 3 min; 100-0 % in 1 min at 2 ml/min at 25°C. UV detection at 210 nm: tR: (syn, major) = 3.45 min, (syn, minor) = 3.77 min.

R_f = 0.25 (*n*-Hexane/EtOAc 9:1).

^{1}H NMR (400 MHz, CDCl$_3$) δ = 9.71, 9.48 (2xd, *J* = 2.3 Hz, 1H, CHO), 7.35 – 7.28 (m, 2H, Ph), 7.14 (d, *J* = 8.5 Hz, 2H, Ph), 4.72 (dd, *J* = 12.8, 4.8 Hz, 1H, CH$_2$NO$_2$), 4.59 (dd, *J* = 12.8, 10.0 Hz, 1H, CH$_2$NO$_2$), 3.79 (td, *J* = 9.9, 4.8 Hz, 1H, CHPh), 2.67 (dddd, *J* = 10.3, 8.2, 4.2, 2.3 Hz, 1H, CHCHO), 1.55 – 1.45 (m, 2H, CH$_2$), 0.83 (t, *J* = 7.5 Hz, 3H, CH$_3$).

^{13}C NMR (101 MHz, CDCl$_3$) δ = 202.83, 135.40, 134.01, 129.65, 129.40, 129.34, 129.27, 78.35, 54.67, 41.98, 20.29, 10.50.

Spectroscopic data of compound 39: 3-(4-Bromophenyl)-2-ethyl-4-nitrobutanal
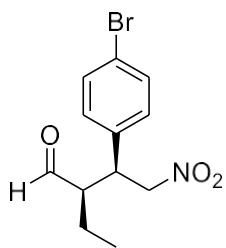
Prepared from *n*-butanal and *trans*-4-bromo-β-nitrostyrene according to the procedure described above. The compound was purified by flash column chromatography (*n*-Hexane/EtOAc 9:1). The enantiomeric excess was determined by chiral-stationary phase UPC[2]. Trefoil AMY1, Grad: CO_2/MeOH 100-0% to 90-10 % in 6 min; 90-10 % in 3 min; 100-0 % in 1 min at 2 ml/min at 25°C. UV detection at 210 nm: tR: (syn, major) = 3.98 min, (syn, minor) = 4.44 min.

*R*f = 0.30 (*n*-Hexane/EtOAc 9:1).

¹H NMR (400 MHz, CDCl₃) δ = 9.70, 9.48 (2xd, *J* = 2.3 Hz, 1H, CHO), 7.50 – 7.43 (m, 2H, Ph), 7.07 (d, *J* = 8.5 Hz, 2H, Ph), 4.72 (dd, *J* = 12.8, 4.8 Hz, 1H, CH₂NO₂), 4.59 (dd, *J* = 12.8, 10.0 Hz, 1H, CH₂NO₂), 3.77 (td, *J* = 9.9, 4.8 Hz, 1H, CHPh), 2.66 (dddd, *J* = 10.3, 8.2, 4.2, 2.3 Hz, 1H, CHCHO), 1.57 – 1.43 (m, 2H, CH₂), 0.83 (t, *J* = 7.5 Hz, 2H, CH₃).

¹³C NMR (101 MHz, CDCl₃) δ = 202.72, 135.90, 132.32, 132.26, 129.97, 129.71, 122.16, 78.26, 54.63, 42.06, 20.33, 10.53.

Spectroscopic data of compound 40: 2-Ethyl-4-nitro-3-(4-methoxyphenyl) butanal
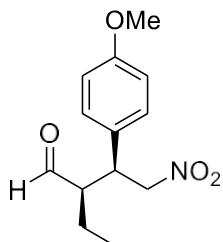
Prepared from *n*-butanal and *trans*-4-methoxy-β-nitrostyrene according to the procedure described above. The compound was purified by flash column chromatography (*n*-Hexane/EtOAc 8:2). The enantiomeric excess was determined by chiral-stationary phase UPC[2]. Trefoil CEL2, Grad: CO_2/EtOH 100-0% to 98-2 % in 19 min; 100-0 % in 1 min at 2.5 ml/min at 25°C. UV detection at 210 nm: tR: (syn, major) = 15.43 min, (syn, minor) = 14.88 min.

*R*f = 0.20 (*n*-Hexane/EtOAc 9:1).

¹H NMR (400 MHz, CDCl₃) δ = 9.70, 9.46 (2xd, *J* = 2.6 Hz, 1H, CHO), 7.09 (d, *J* = 8.7 Hz, 2H, Ph), 6.86 (d, *J* = 8.7 Hz, 2H, Ph), 4.69 (dd, *J* = 12.5, 4.8 Hz, 1H, CH₂NO₂), 4.57 (dd, *J* = 12.5, 9.9 Hz, 1H, CH₂NO₂), 3.78 (s, 3H), 3.76 – 3.69 (m, 1H, CHPh), 2.67 – 2.58 (m, 1H, CHCHO), 1.55 – 1.45 (m, 2H, CH₂), 0.82 (t, *J* = 7.5 Hz, 3H, CH₃).

¹³C NMR (101 MHz, CDCl₃) δ = 203.36, 159.27, 129.33, 129.05, 114.48, 78.79, 55.24, 55.17, 42.03, 20.34, 10.68.

Spectroscopic data of compound 41

: 2-ethyl-4-nitro-3-(4-nitrophenyl) butanal
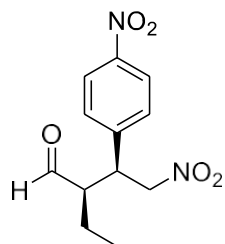
 Prepared from *n*-butanal and *trans*-4-Bromo-β-nitrostyrene according to the procedure described above. The compound was purified by flash column chromatography (*n*-Hexane/EtOAc 8:2). The enantiomeric excess was determined by chiral-stationary phase UPC^2. Trefoil AMY1, Grad: CO_2/IPA 100-0% to 90-10 % in 18 min; 90-10 % in 2 min at 2 ml/min at 25°C. UV detection at 210 nm: tR: (syn, major) = 8.84 min, (syn, minor) = 10.04 min.

R$_f$ = 0.40 (*n*-Hexane/EtOAc 8:2).

^{1}H NMR (400 MHz, CDCl$_3$) δ = 9.74, 9.53 (2xd, *J* = 2.0 Hz, 1H, CHO), 8.23 (d, *J* = 8.8 Hz, 2H, Ph), 7.43 (d, *J* = 8.7 Hz, 2H, Ph), 4.82 (dd, *J* = 13.1, 4.6 Hz, 1H, CH$_2$NO$_2$), 4.70 (dd, *J* = 13.1, 10.1 Hz, 1H, CH$_2$NO$_2$), 4.01 – 3.93 (m, 1H, CHPh), 2.84 – 2.71 (m, 1H, CHCHO), 1.63 – 1.43 (m, 2H, CH$_2$), 1.03 (t, *J* = 7.5 Hz, 3H, CH$_3$).

^{13}C NMR (101 MHz, CDCl$_3$) δ = 202.02, 147.70, 144.55, 129.43, 129.16, 124.32, 124.19, 77.80, 54.27, 42.16, 20.37, 10.42.

7 Annexes
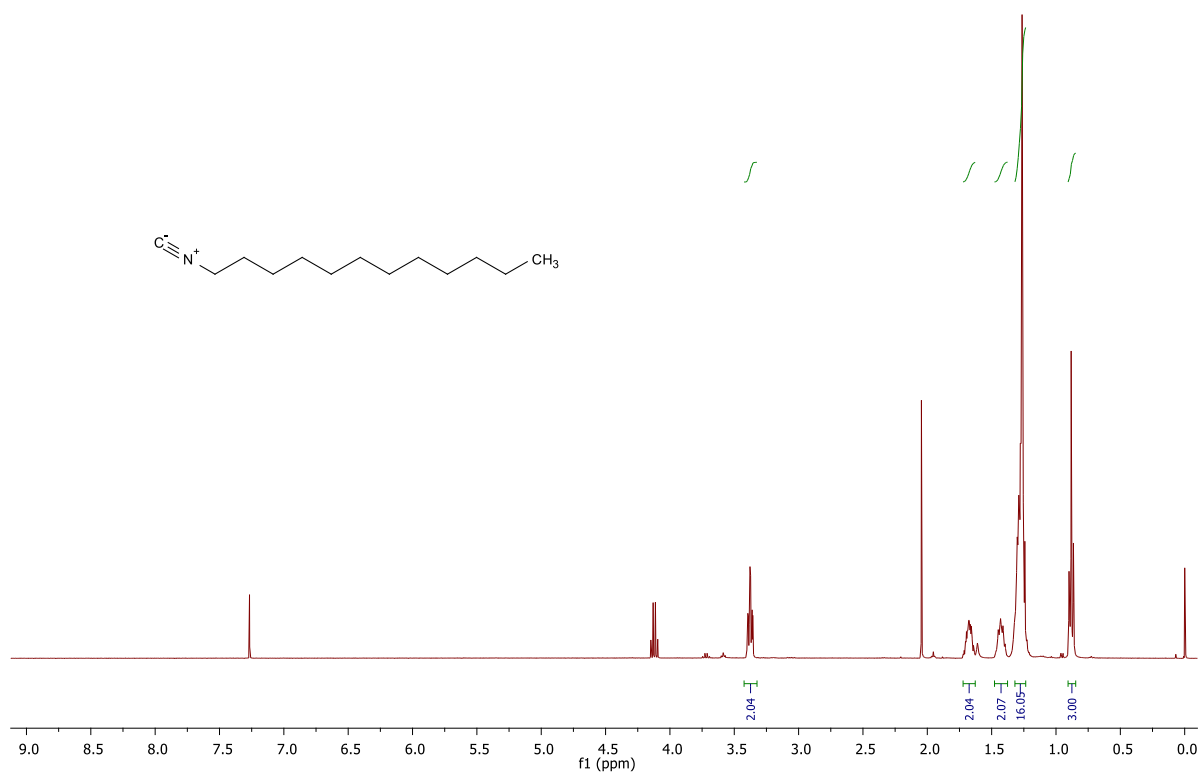
FIGURE 1. 400 MHz ^{1}H NMR spectrum in CDCl$_3$ of compound **23** (SCHEME 18).
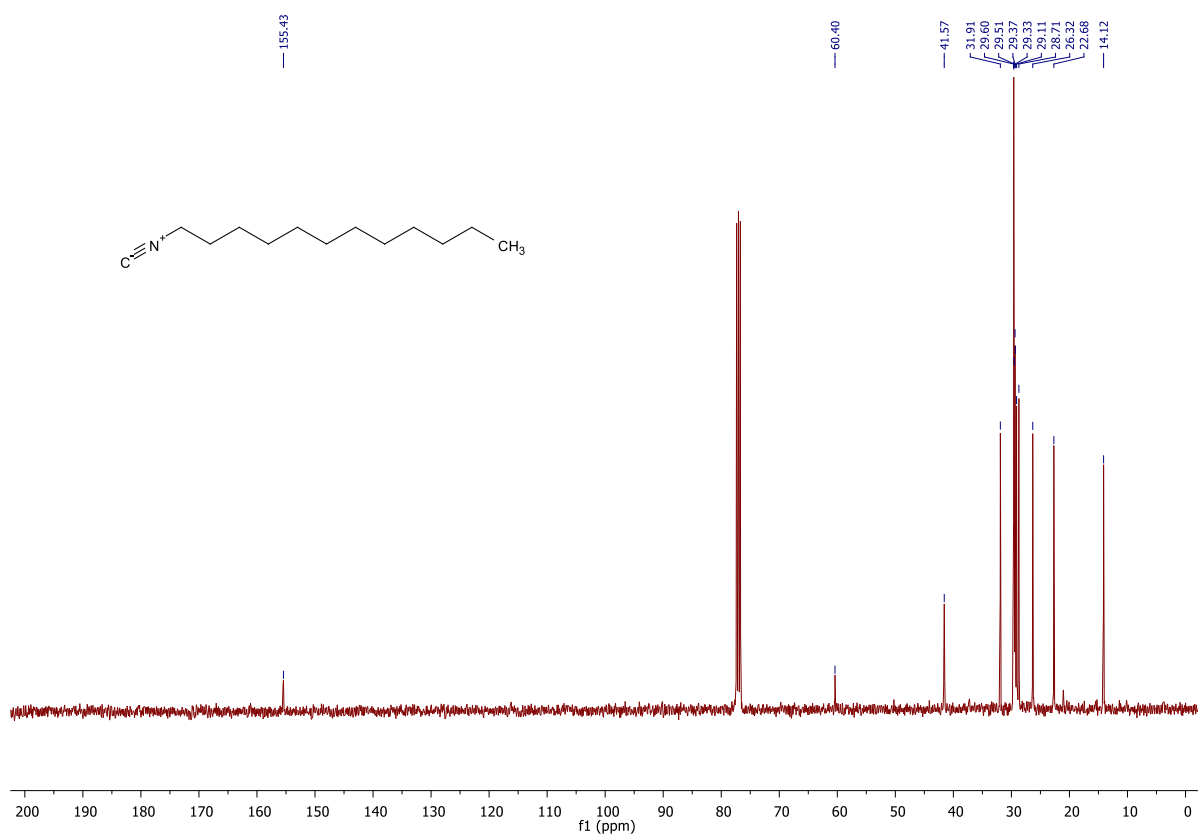
FIGURE 2. 101 MHz ^{13}C NMR spectrum in CDCl$_3$ of compound **23** (SCHEME 18).
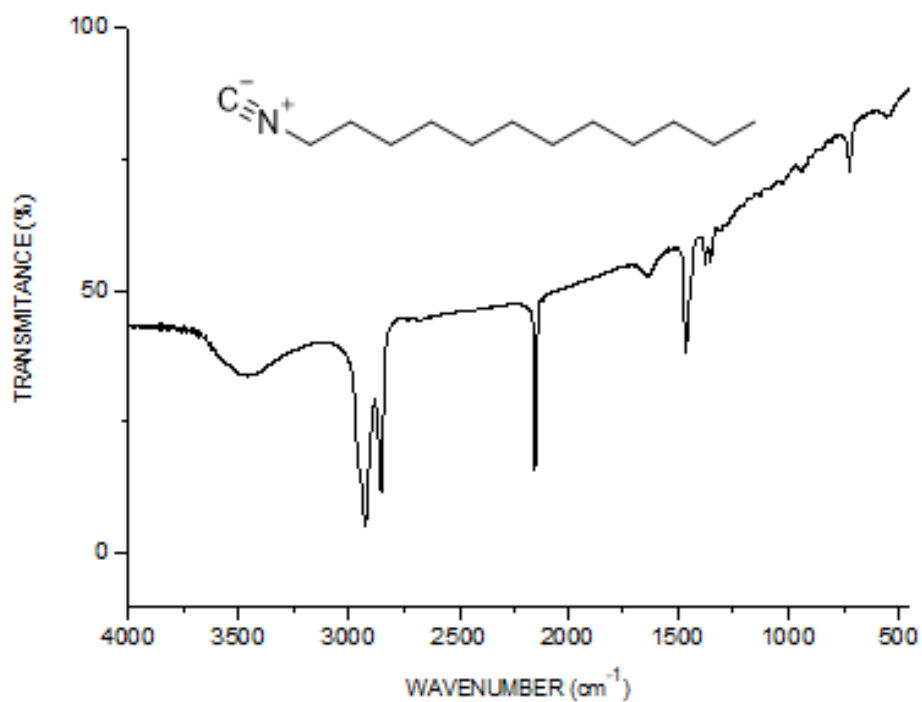
FIGURE 3. FT-IR spectrum of dodecyl isocyanide **23** (SCHEME 18). Near and below of 3000 cm^{-1} (ν_{Csp3-H}), 2145 cm^{-1} ($\nu_{C\equiv N}$), 1464 cm^{-1} (γ_{CH2}), 1375 cm^{-1} (γ_{CH3}).
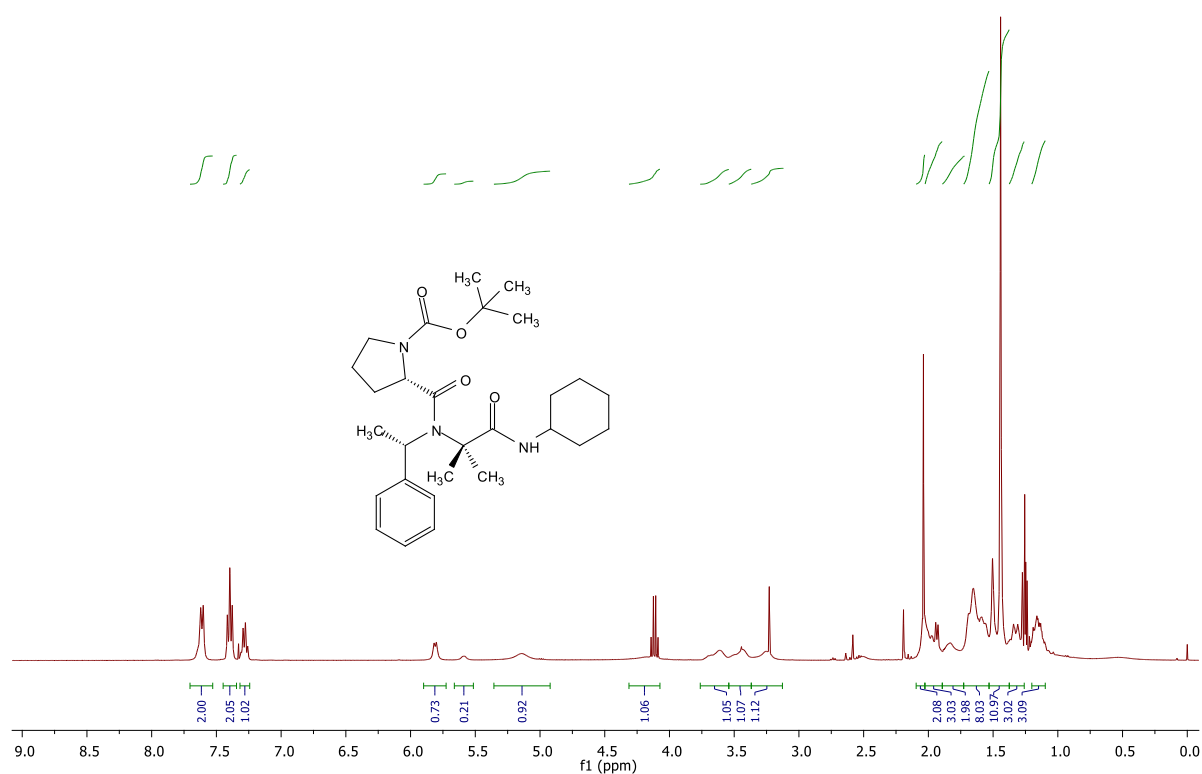
FIGURE 4. 400 MHz ^{1}H NMR spectrum in CDCl$_3$ of compound **24** (TABLE 1).
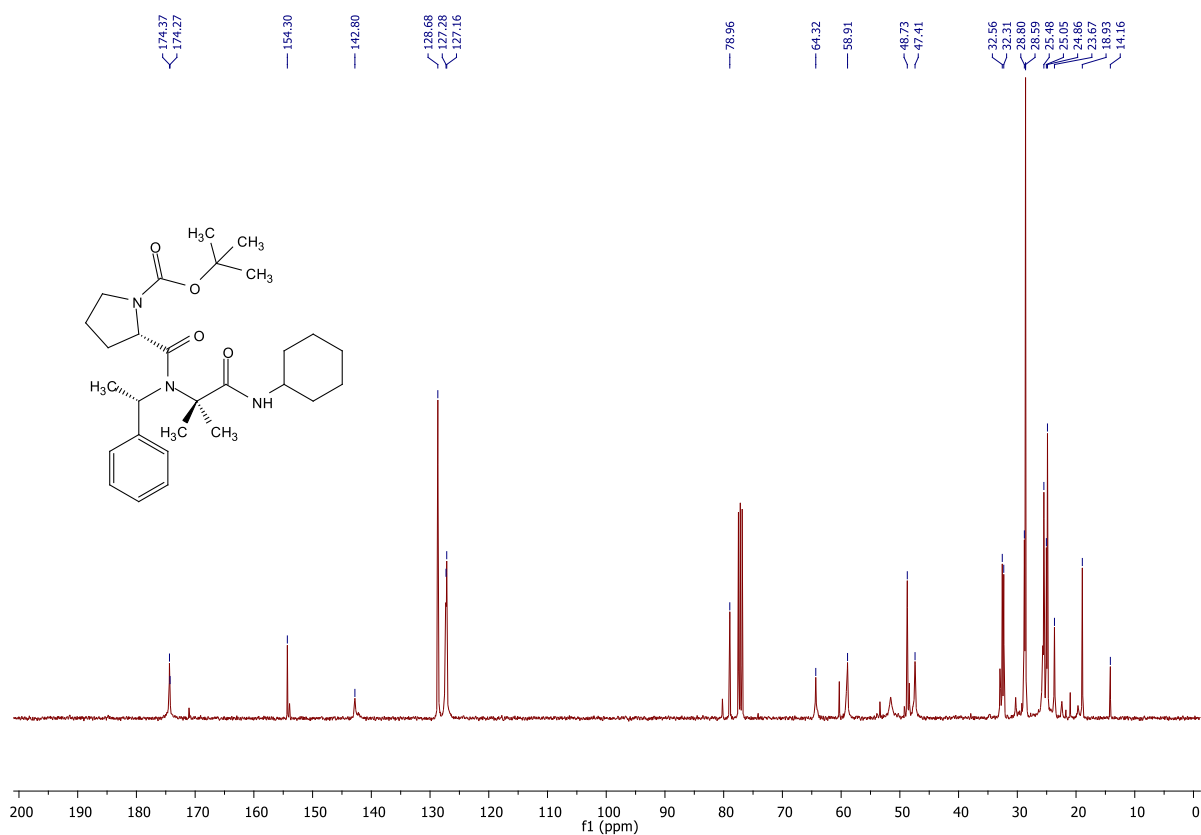
FIGURE 5. 101 MHz ^{13}C NMR spectrum in CDCl$_3$ of compound **24** (TABLE 1).
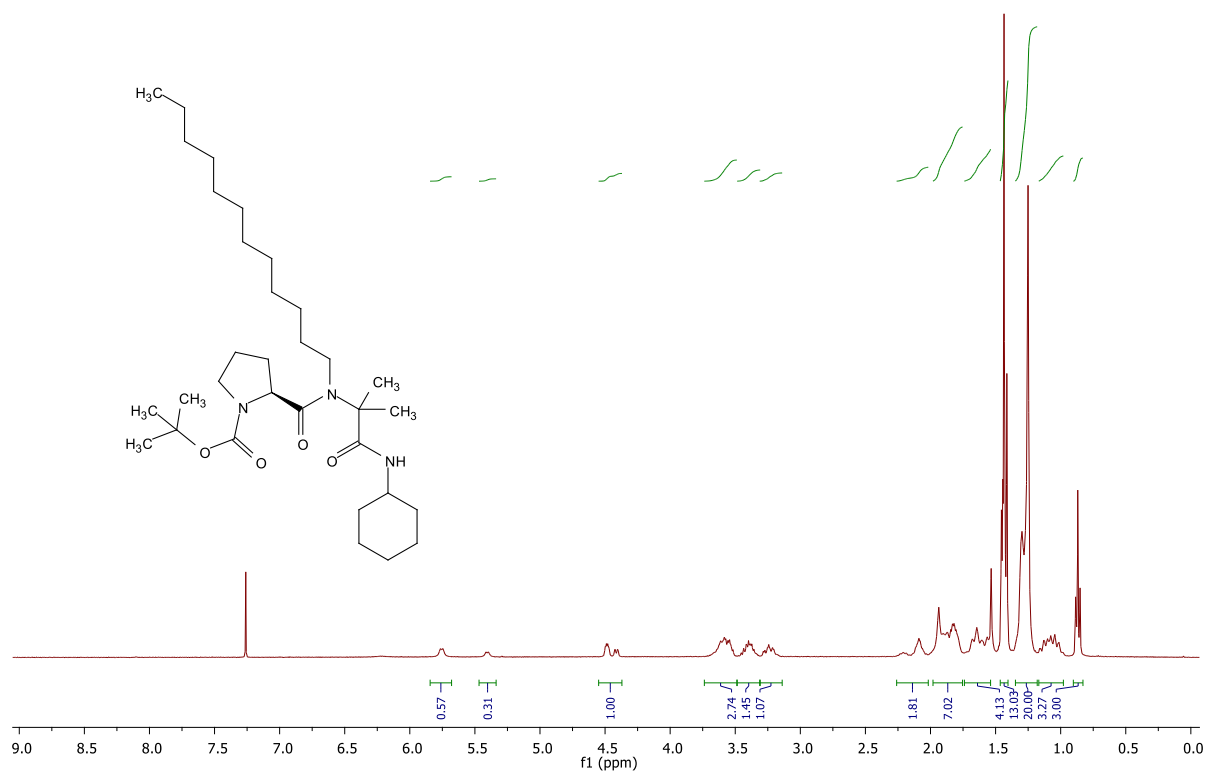
FIGURE 6. 400 MHz ^{1}H NMR spectrum in CDCl$_3$ of compound **25** (TABLE 1).
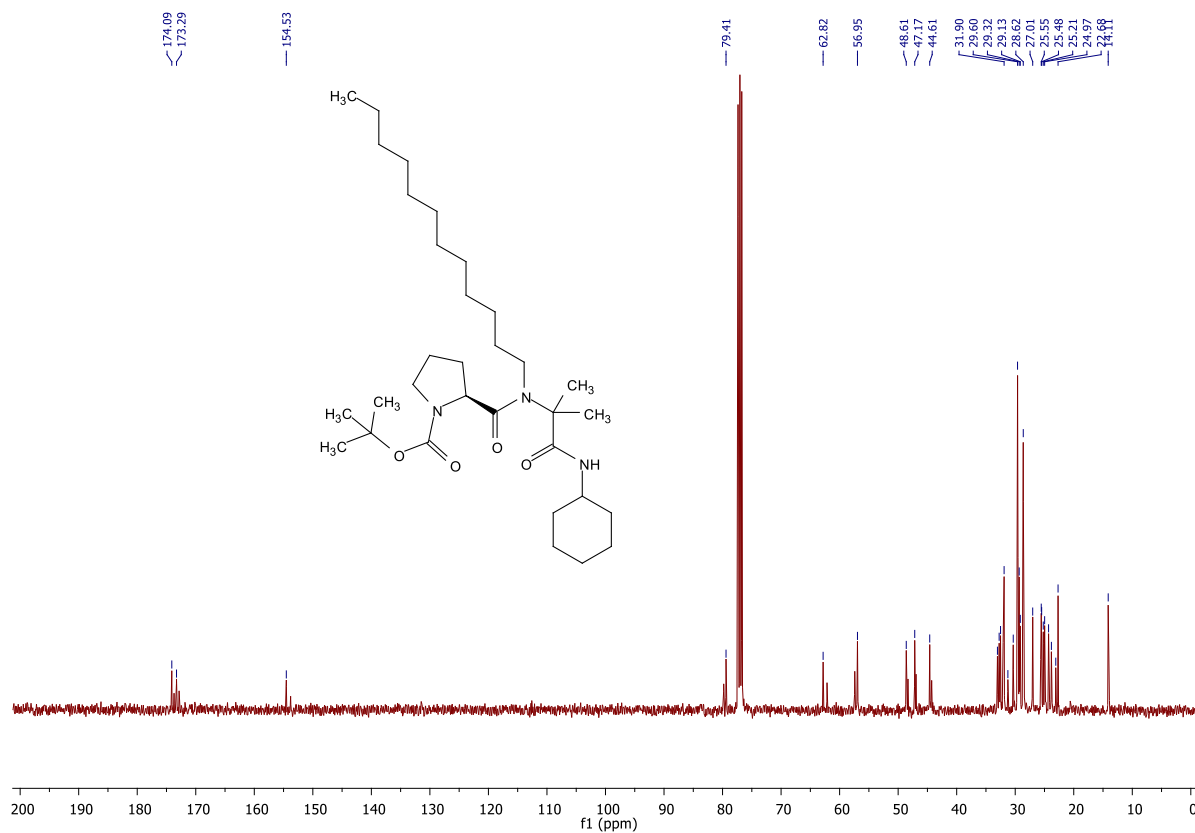
FIGURE 7. 101 MHz ^{13}C NMR spectrum in CDCl$_3$ of compound **25** (TABLE 1).
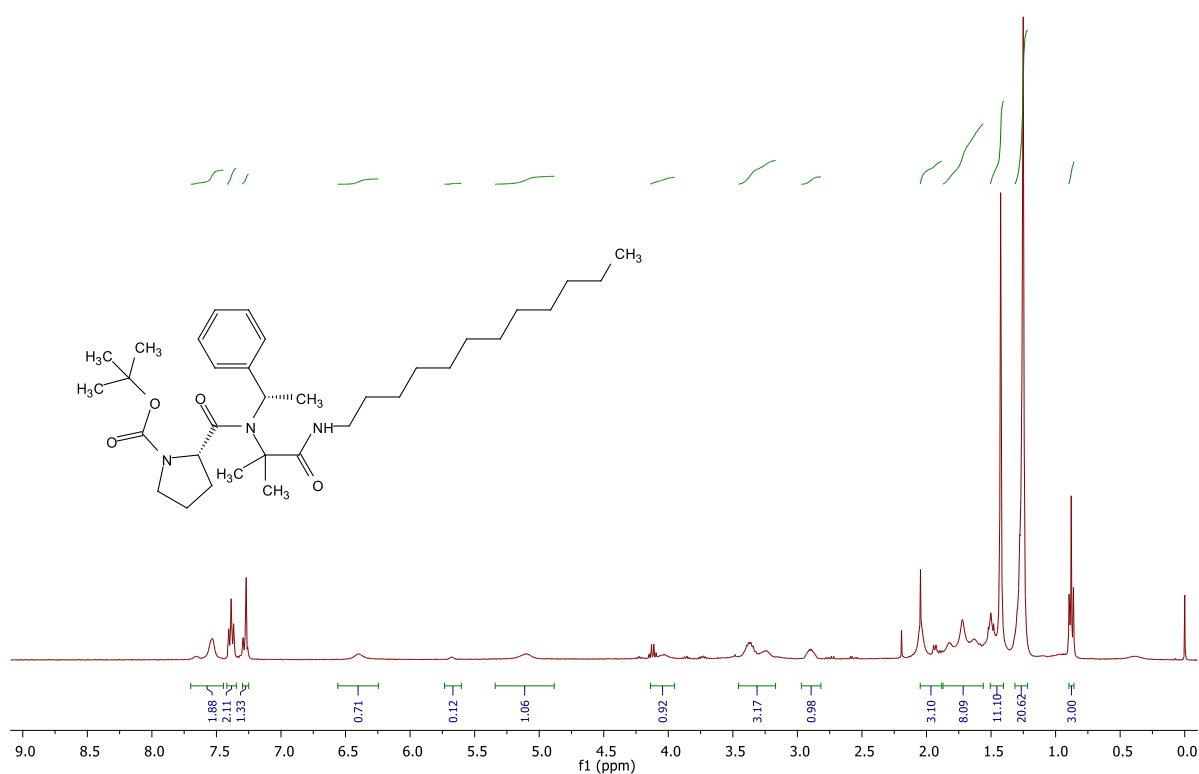
FIGURE 8. 400 MHz ^{1}H NMR spectrum in CDCl$_3$ of compound **26** (TABLE 1).
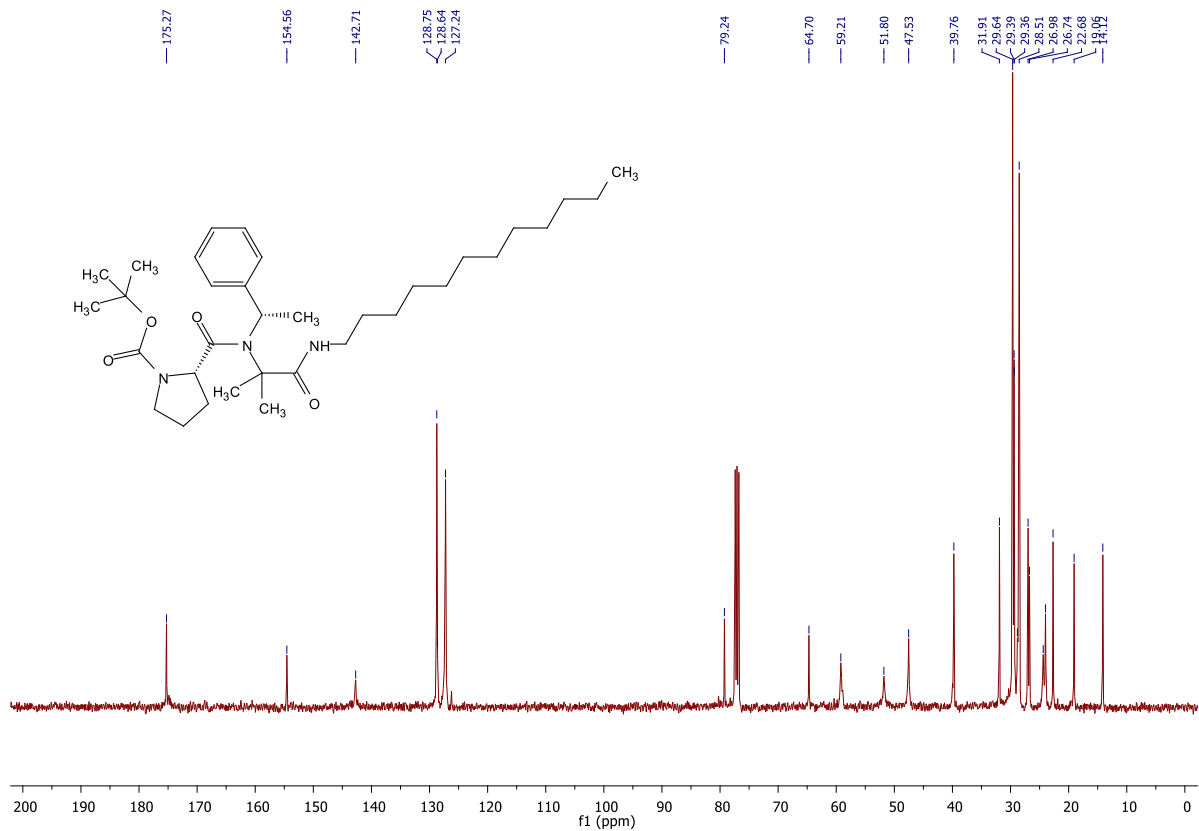
FIGURE 9. 101 MHz ^{13}C NMR spectrum in CDCl$_3$ of compound **26** (TABLE 1).
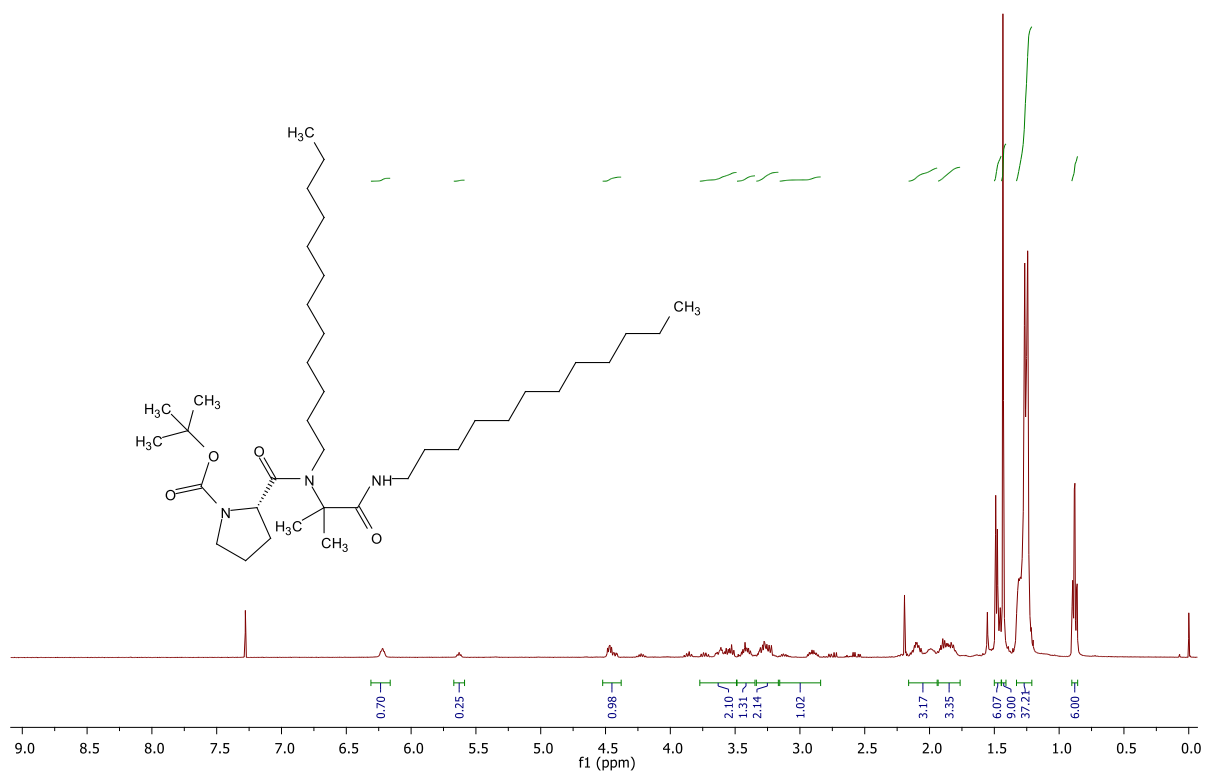
FIGURE 10. 400 MHz ^{1}H NMR spectrum in CDCl$_3$ of compound **27** (TABLE 1).
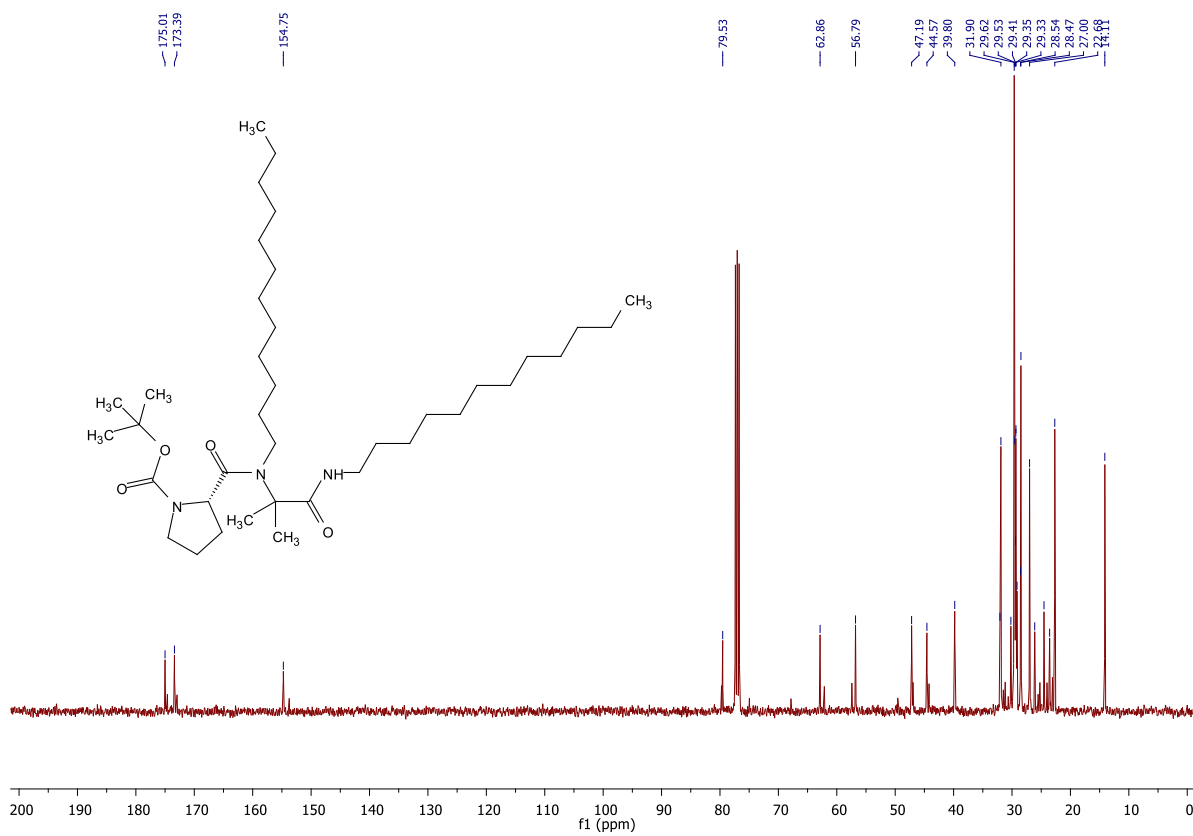
FIGURE 11. 101 MHz ^{13}C NMR spectrum in CDCl$_3$ of compound **27** (TABLE 1).
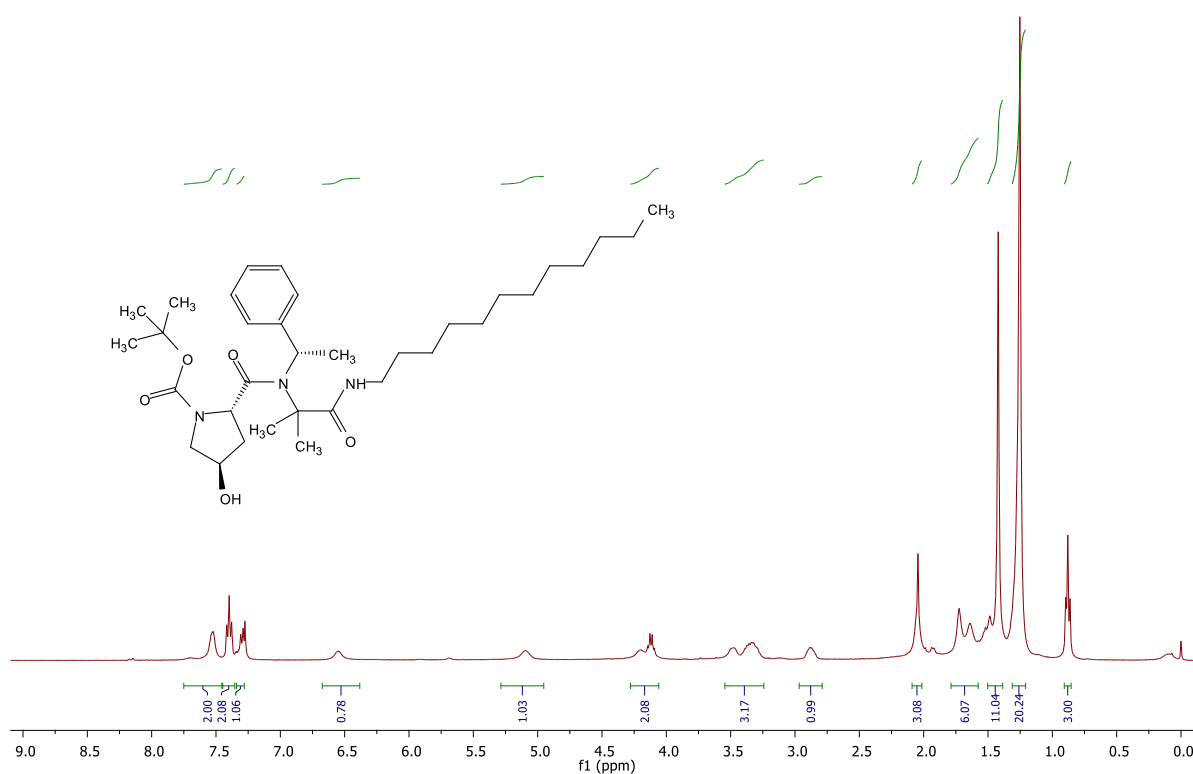
FIGURE 12. 400 MHz ^{1}H NMR spectrum in CDCl$_3$ of compound **28** (TABLE 1).
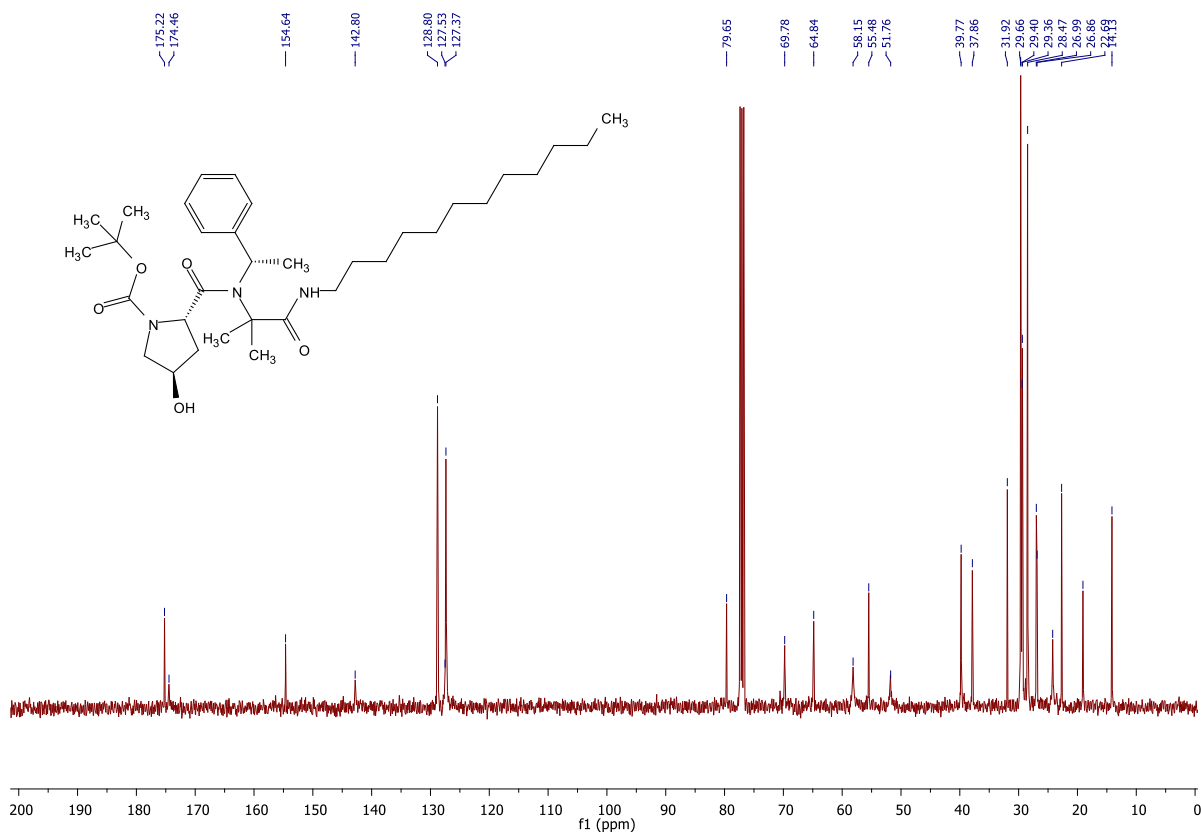
FIGURE 13. 101 MHz ^{13}C NMR spectrum in CDCl$_3$ of compound **28** (TABLE 1).
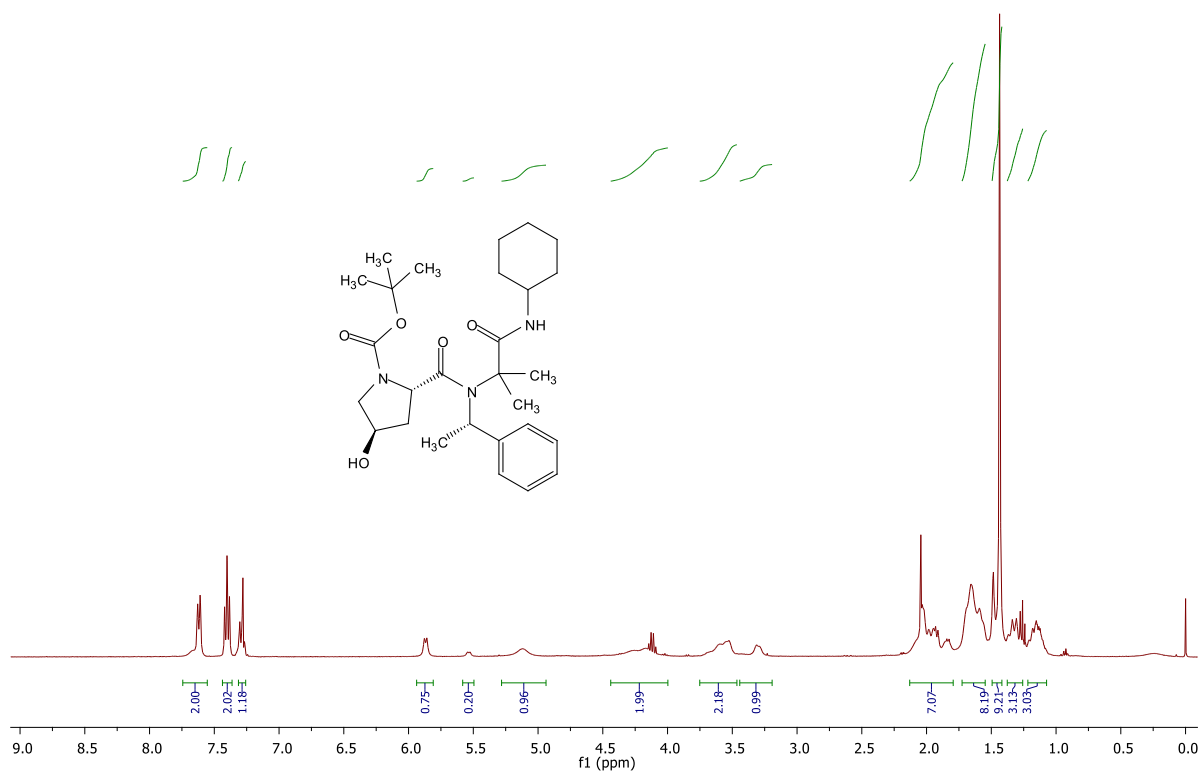
FIGURE 14. 400 MHz ^{1}H NMR spectrum in CDCl$_3$ of compound **29** (TABLE 1).
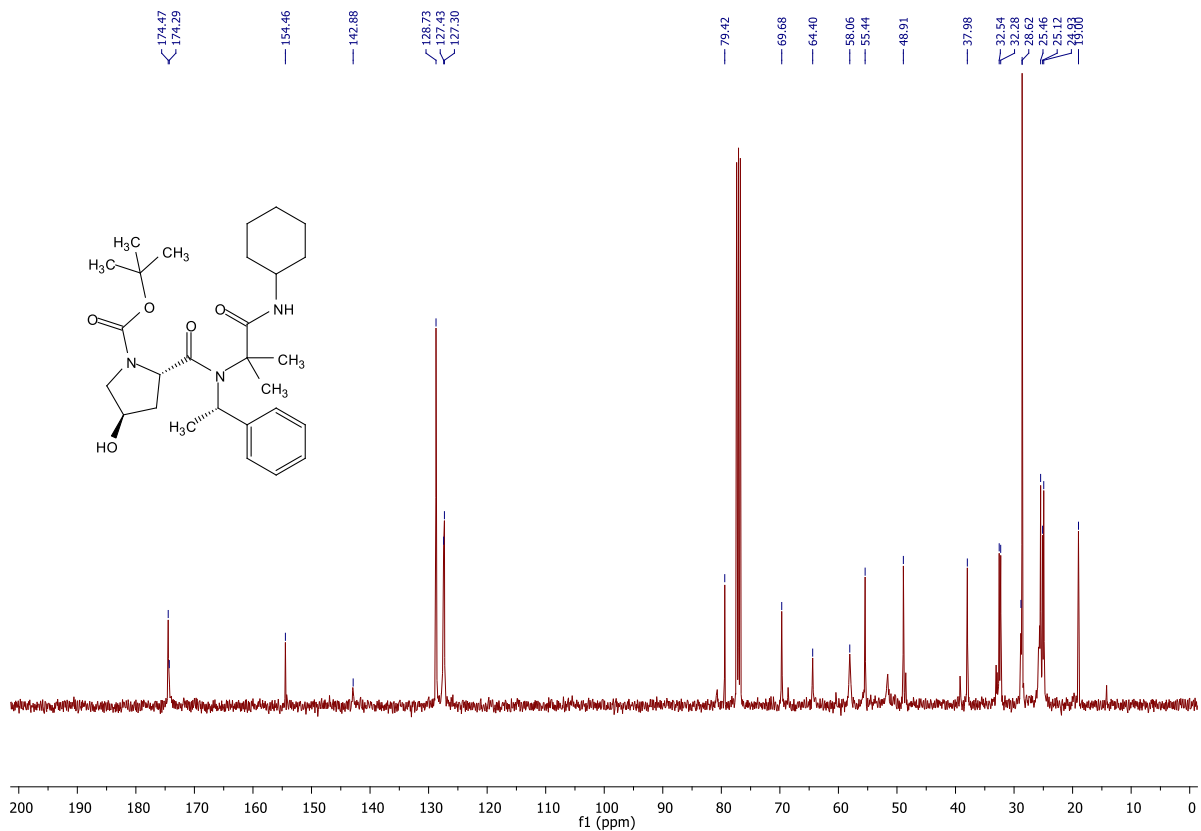
FIGURE 15. 101 MHz ^{13}C NMR spectrum in CDCl$_3$ of compound **29** (TABLE 1).
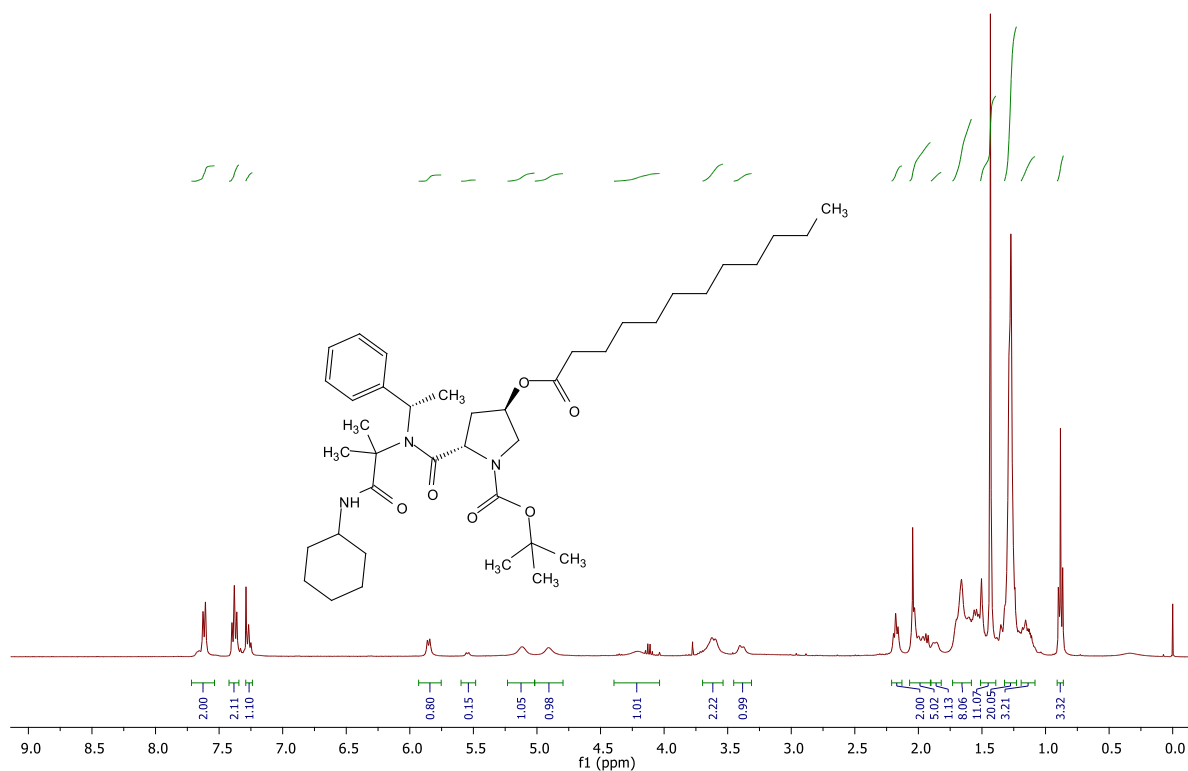
FIGURE 16. 400 MHz ^{1}H NMR spectrum in CDCl$_3$ of compound **30** (TABLE 1).
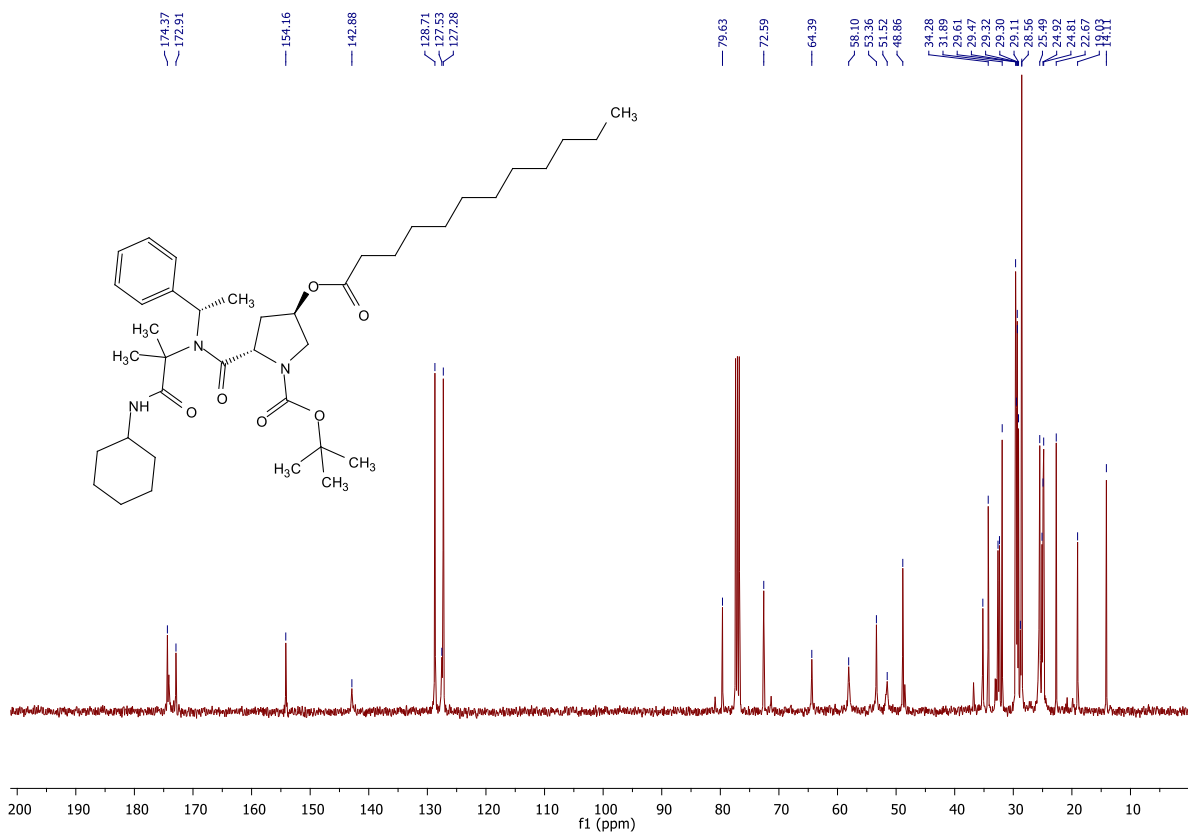
FIGURE 17. 101 MHz ^{13}C NMR spectrum in CDCl$_3$ of compound **30** (TABLE 1).
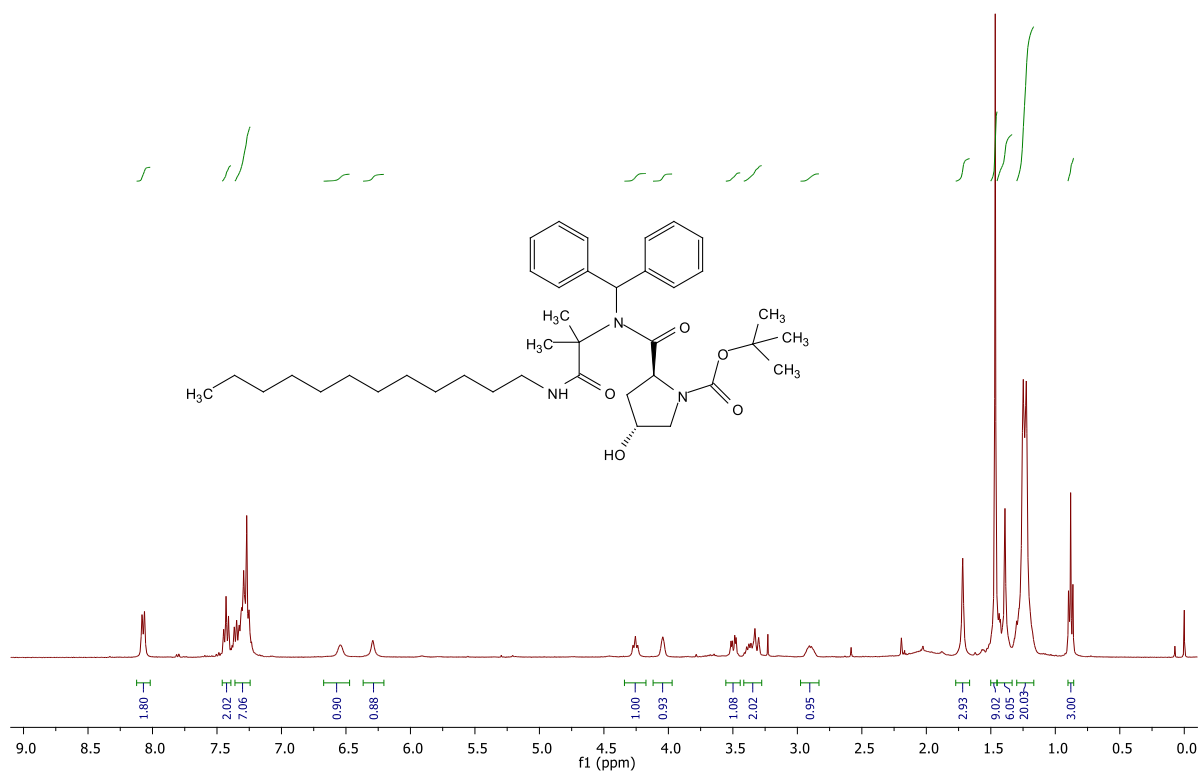
FIGURE 18. 400 MHz ¹H NMR spectrum in CDCl₃ of compound **31** (TABLE 1).
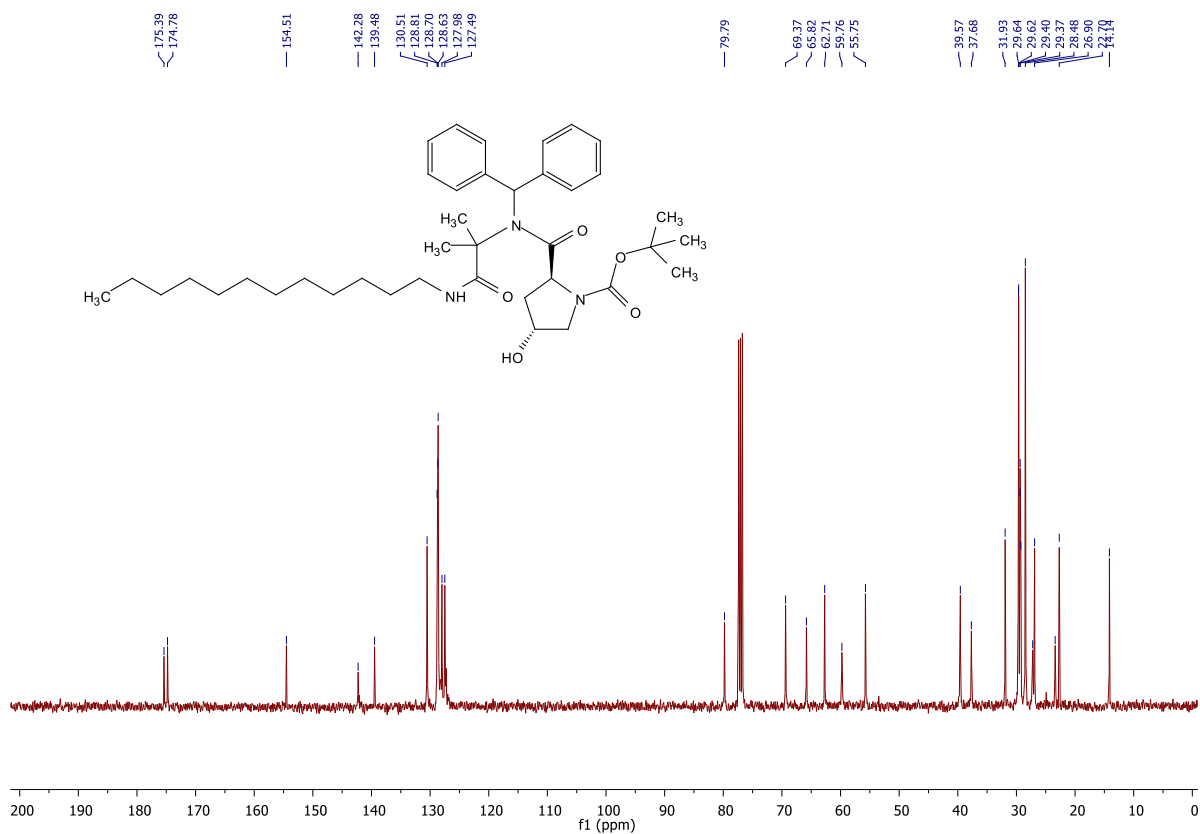
FIGURE 19. 101 MHz ¹³C NMR spectrum in CDCl₃ of compound **31** (TABLE 1).
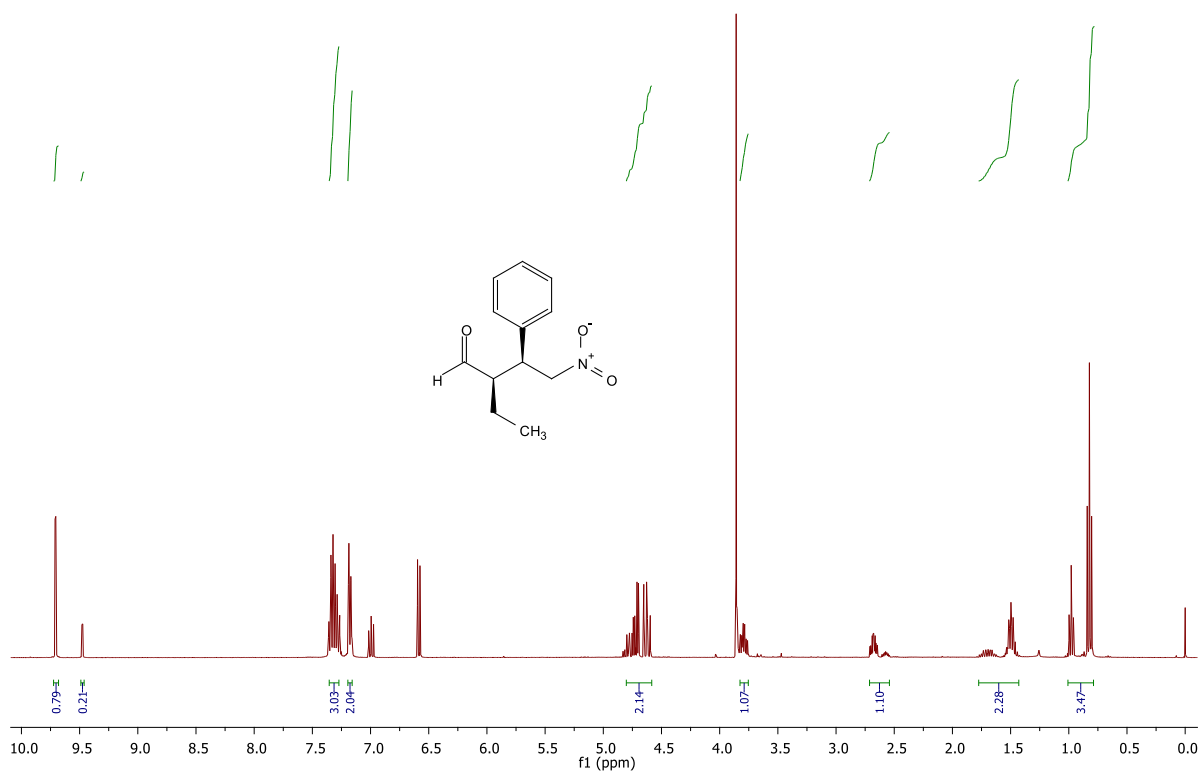
FIGURE 20. 400 MHz ^{1}H NMR spectrum in CDCl$_3$ of compound **34** (TABLE 4).
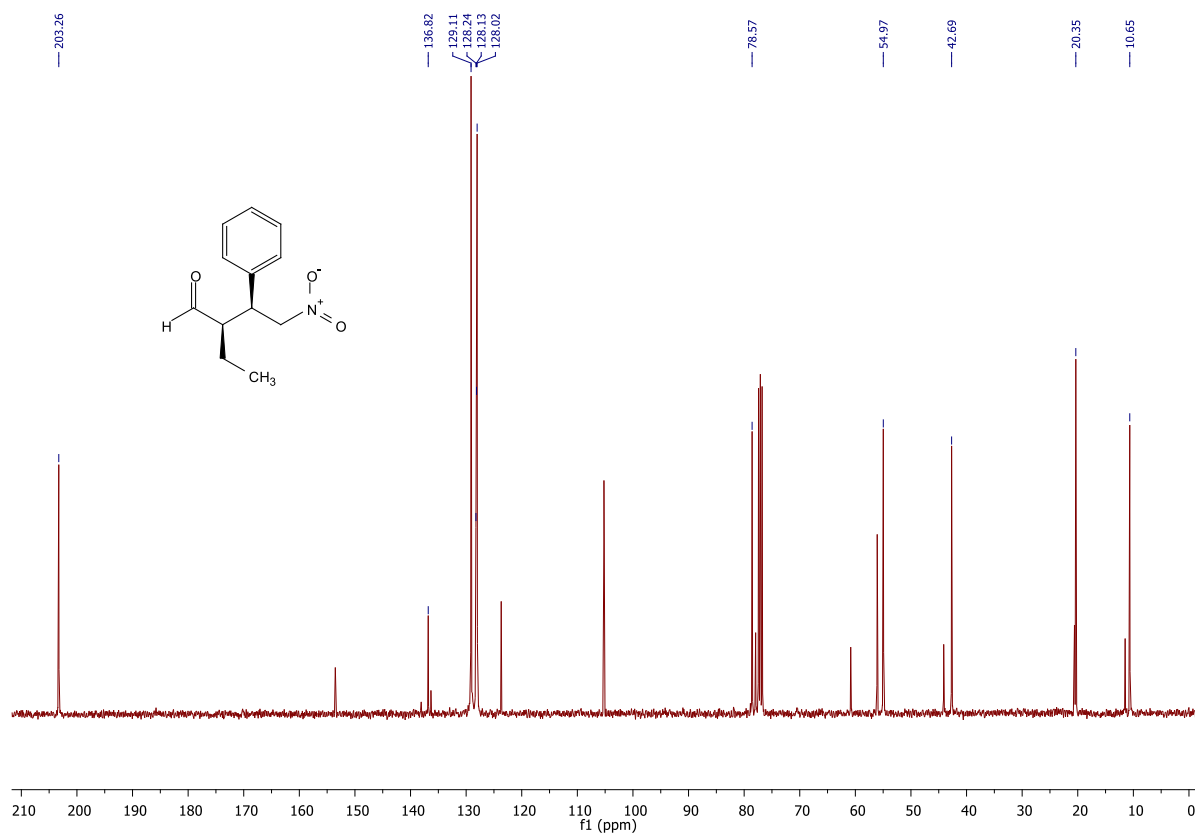
FIGURE 21. 101 MHz ^{13}C NMR spectrum in CDCl$_3$ of compound **34** (TABLE 4).
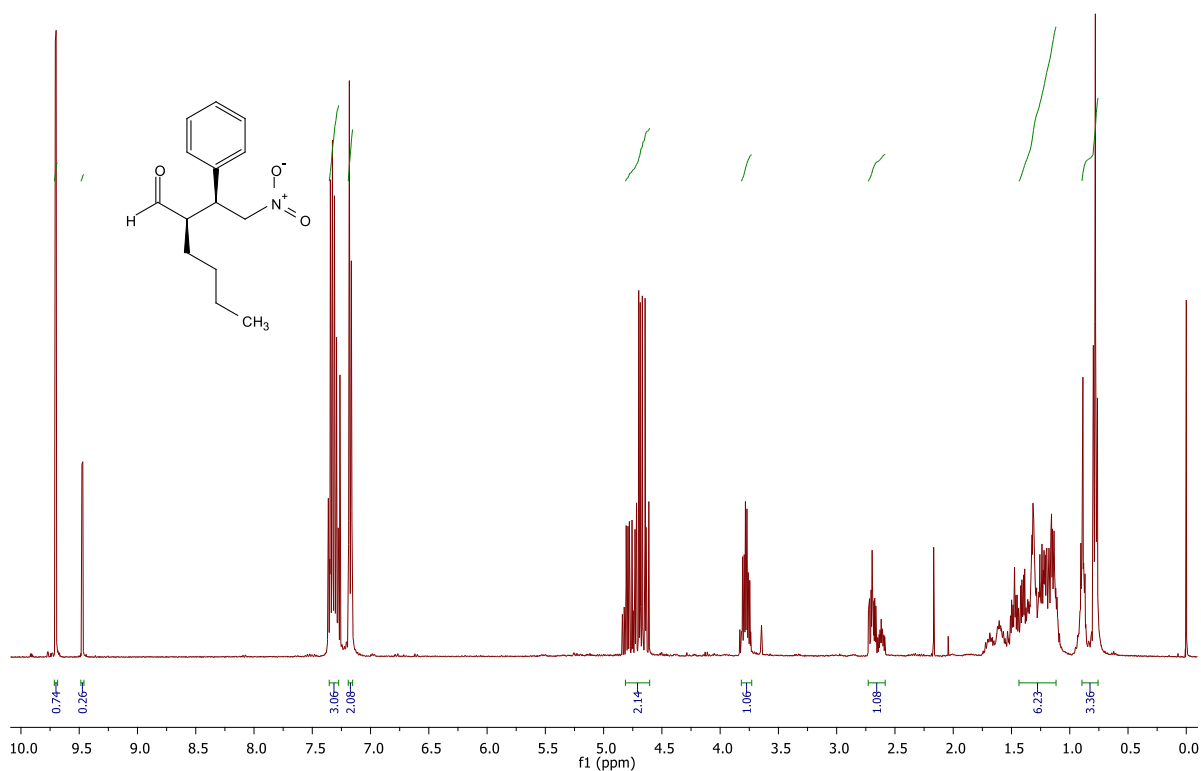
FIGURE 22. 400 MHz ^{1}H NMR spectrum in CDCl$_3$ of compound **35** (TABLE 4).
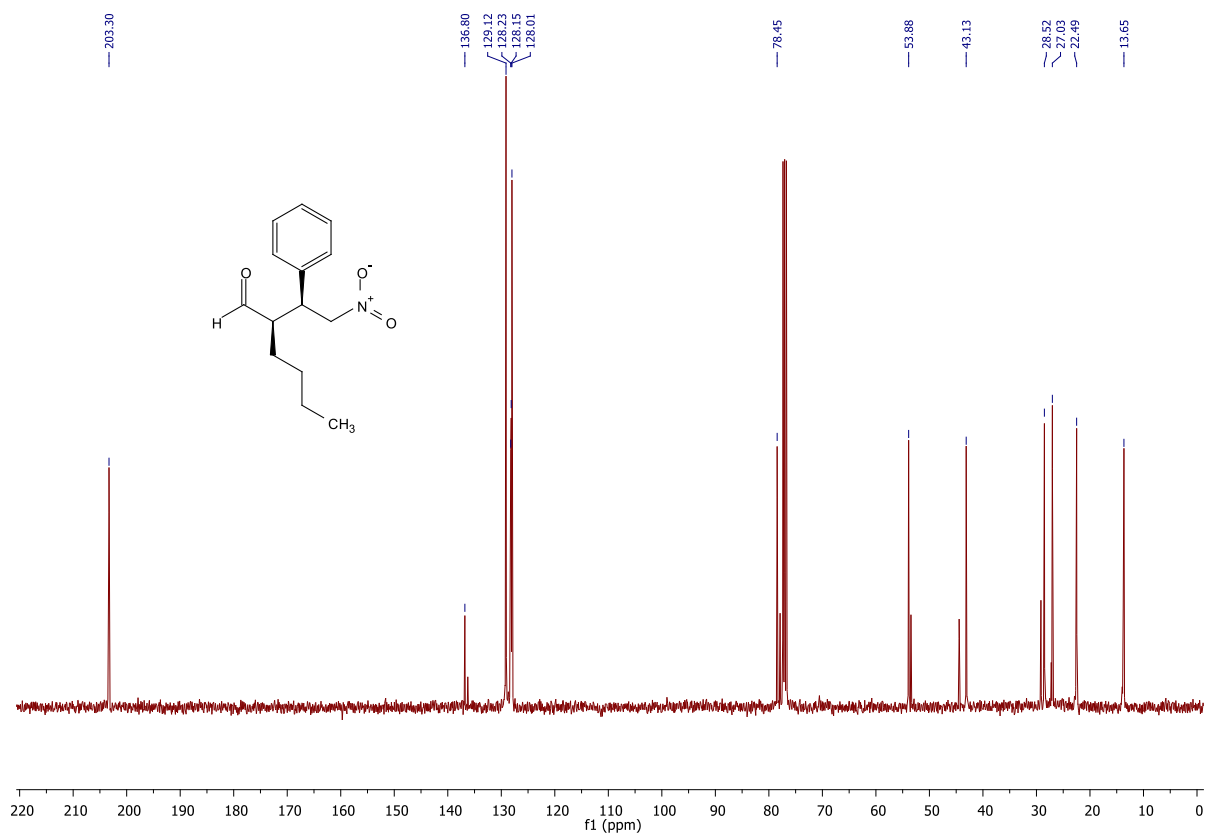
FIGURE 23. 101 MHz ^{13}C NMR spectrum in CDCl$_3$ of compound **35** (TABLE 4).
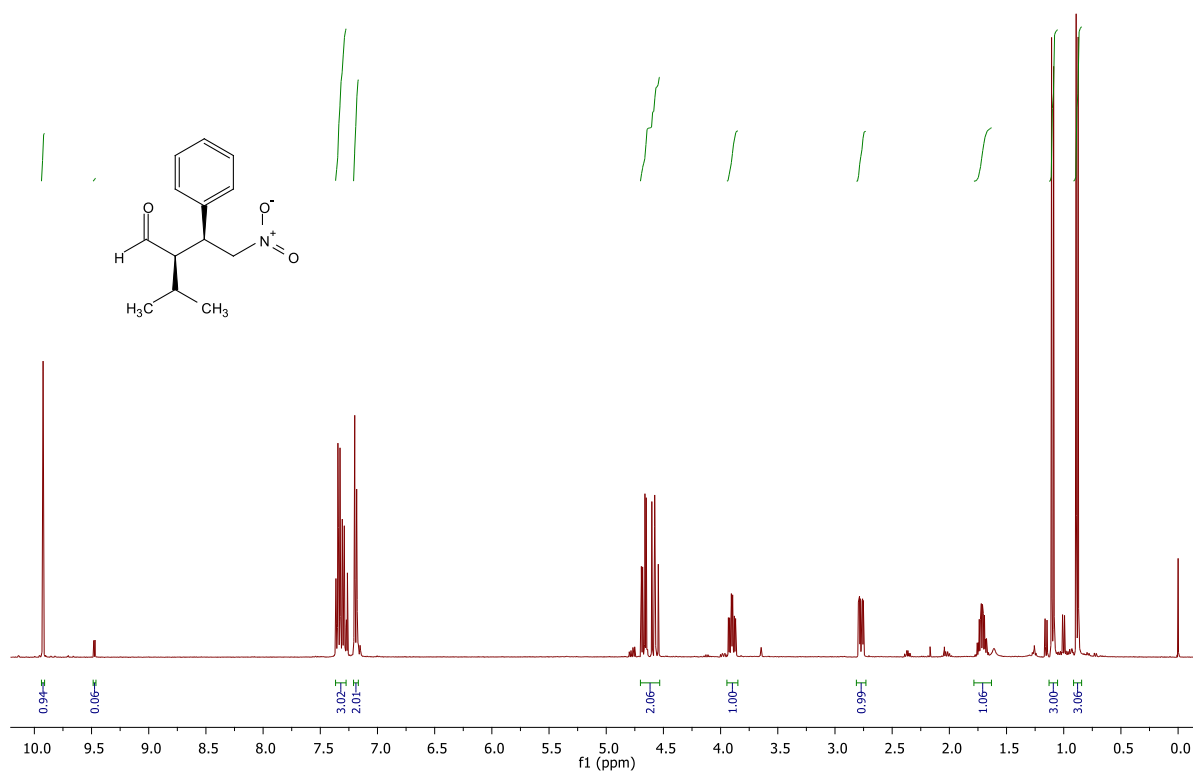
FIGURE 24. 400 MHz ^{1}H NMR spectrum in CDCl$_3$ of compound **36** (TABLE 4).
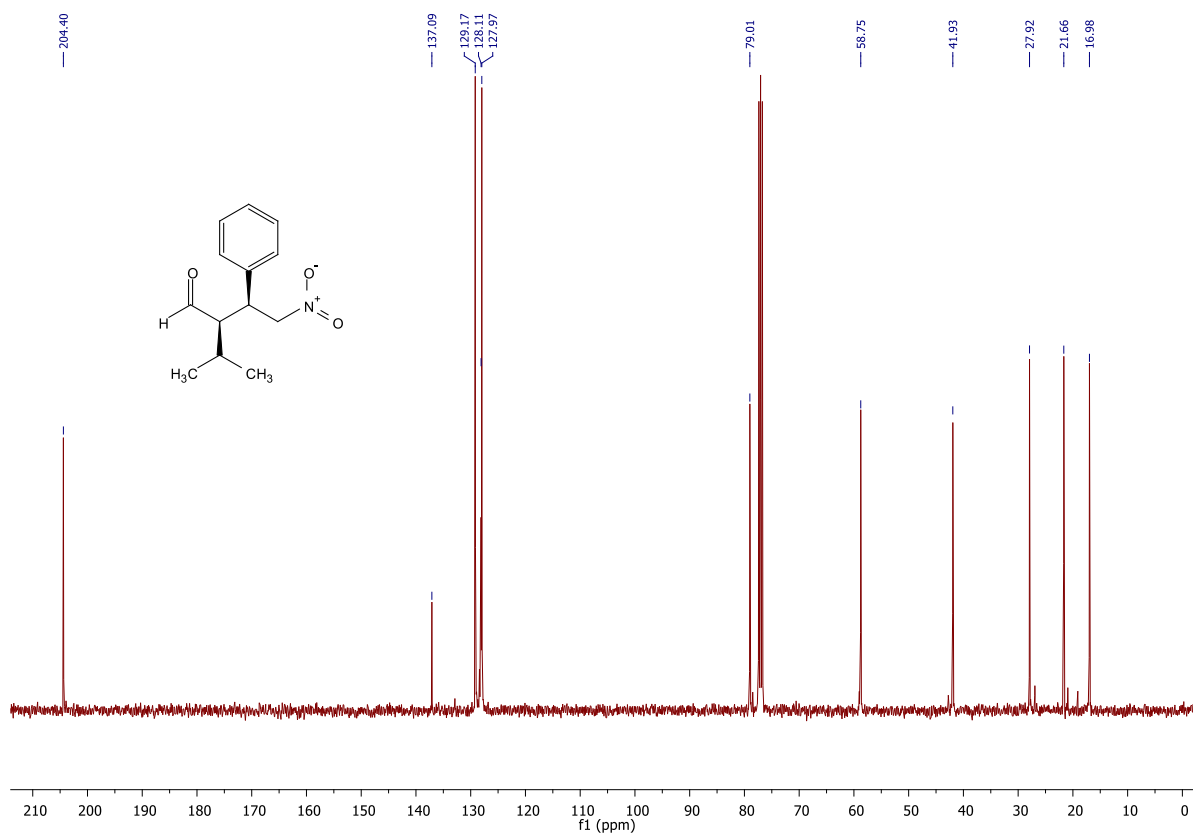
FIGURE 25. 101 MHz ^{13}C NMR spectrum in CDCl$_3$ of compound **36** (TABLE 4).
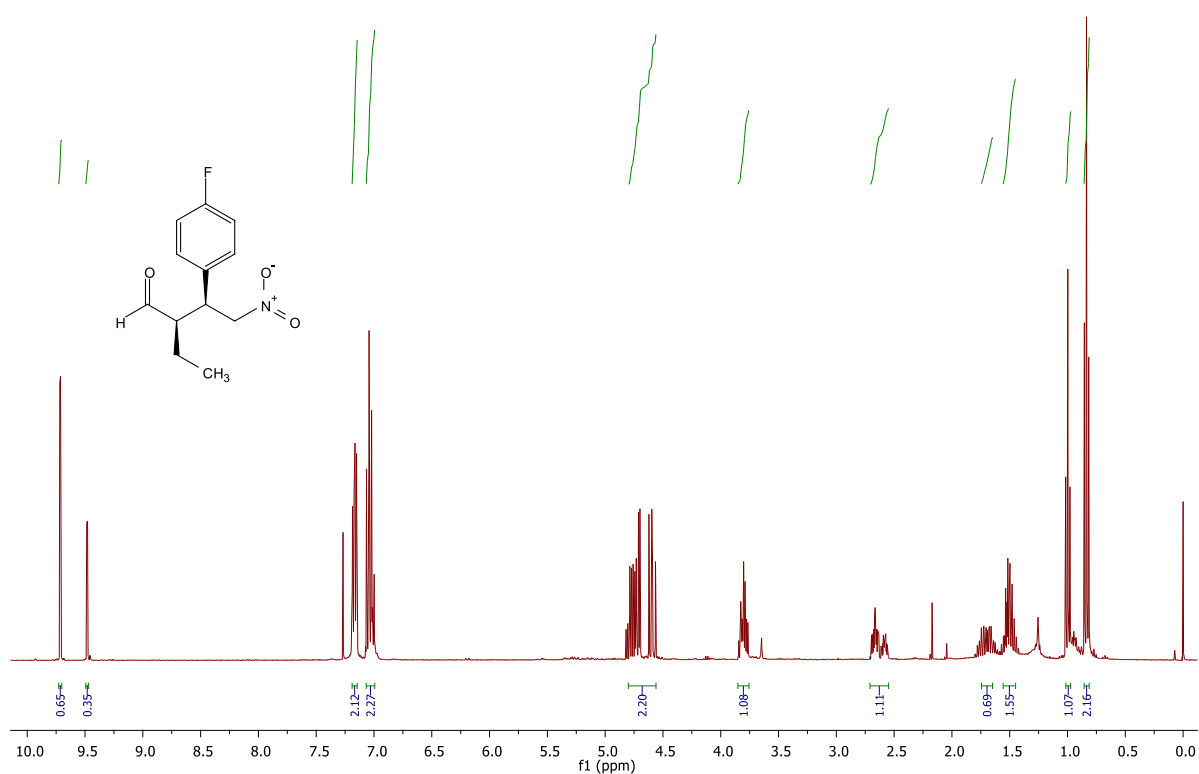
FIGURE 26. 400 MHz ^{1}H NMR spectrum in CDCl$_3$ of compound **37**(TABLE 4).
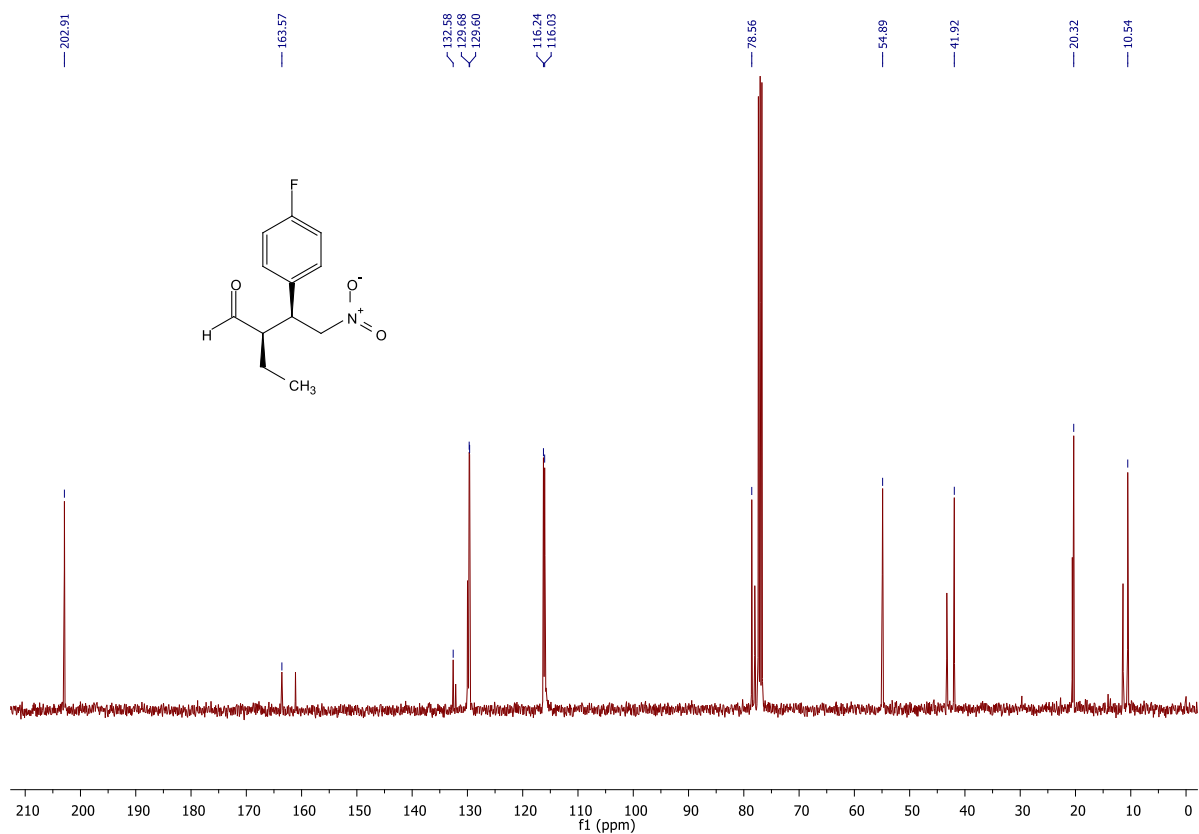
FIGURE 27. 101 MHz ^{13}C NMR spectrum in CDCl$_3$ of compound **37** (TABLE 4)..
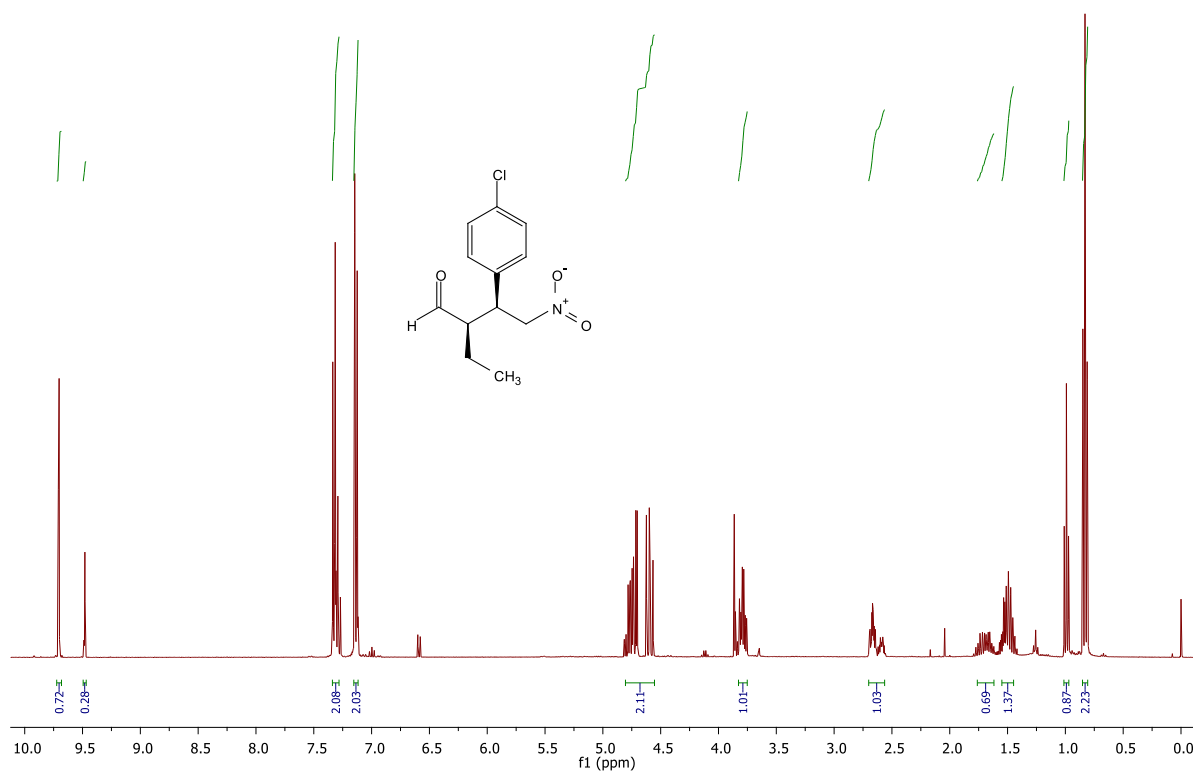
FIGURE 28. 400 MHz ^{1}H NMR spectrum in CDCl$_3$ of compound **38** (TABLE 4).
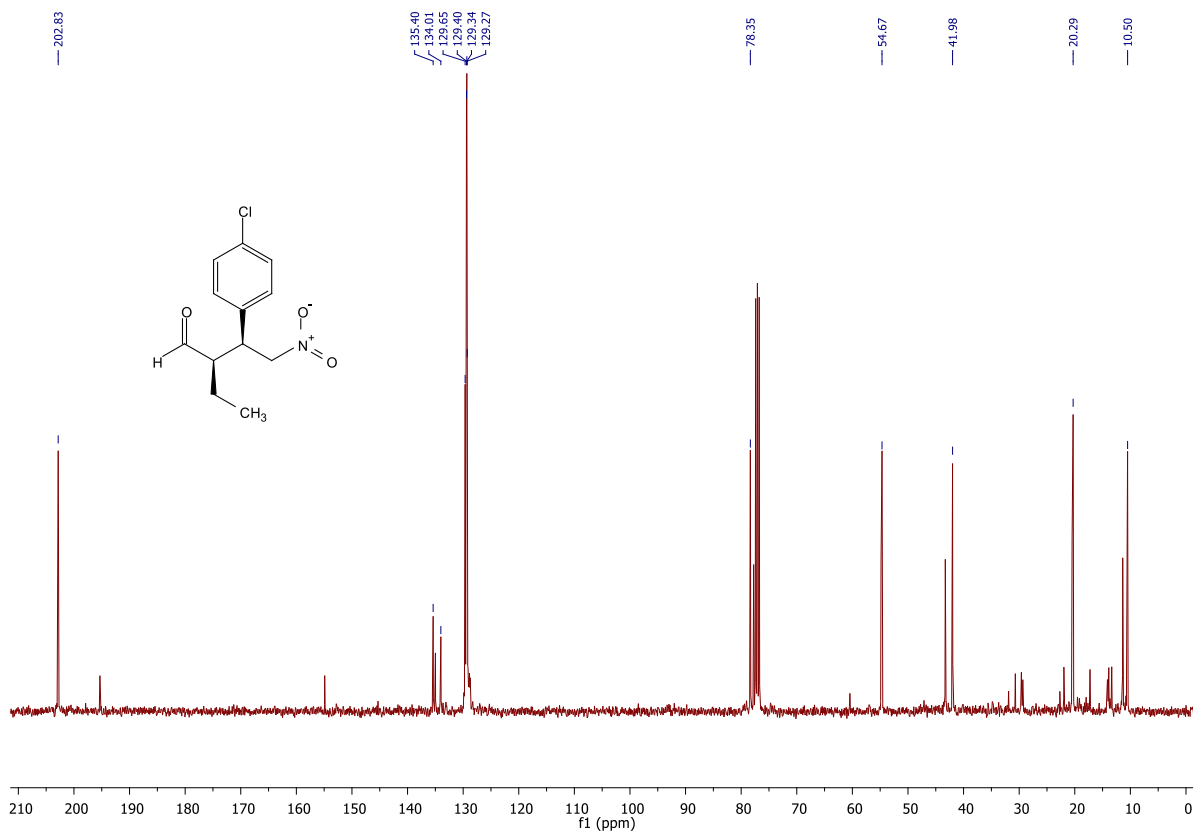
FIGURE 29. 101 MHz ^{13}C NMR spectrum in CDCl$_3$ of compound **38** (TABLE 4).
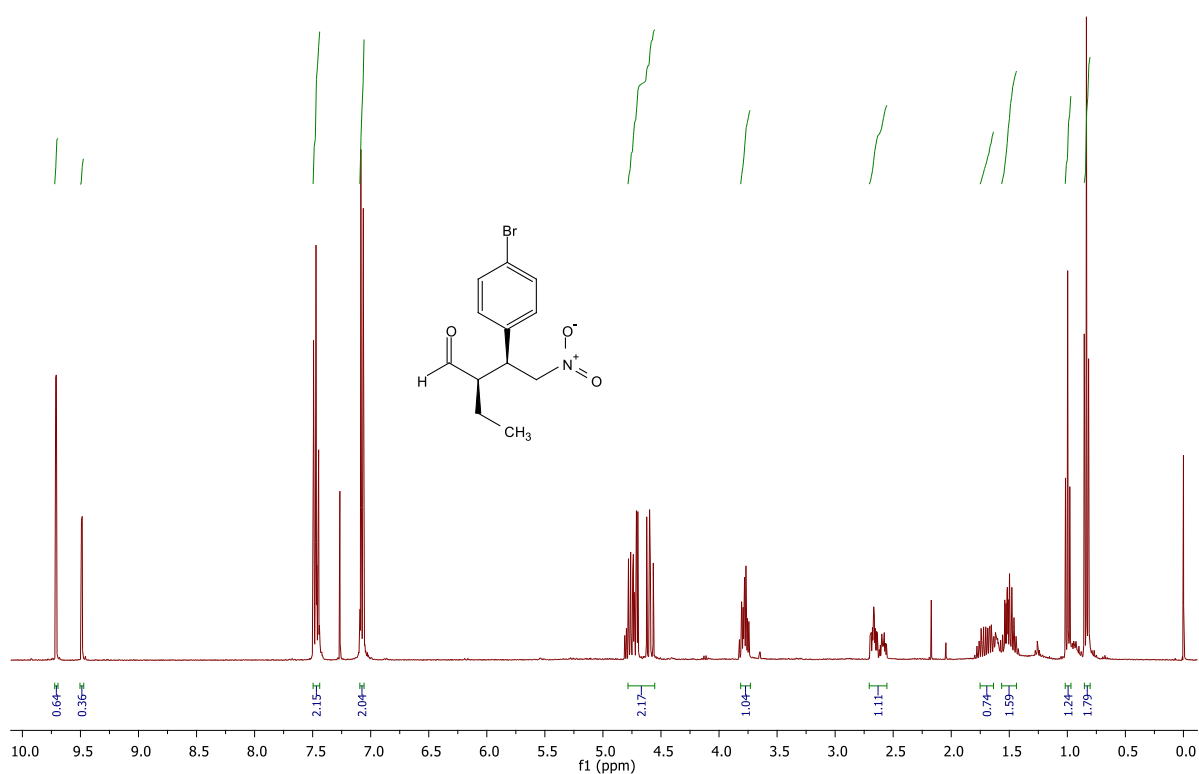
FIGURE 30. 400 MHz ¹H NMR spectrum in CDCl₃ of compound **39** (TABLE 4).
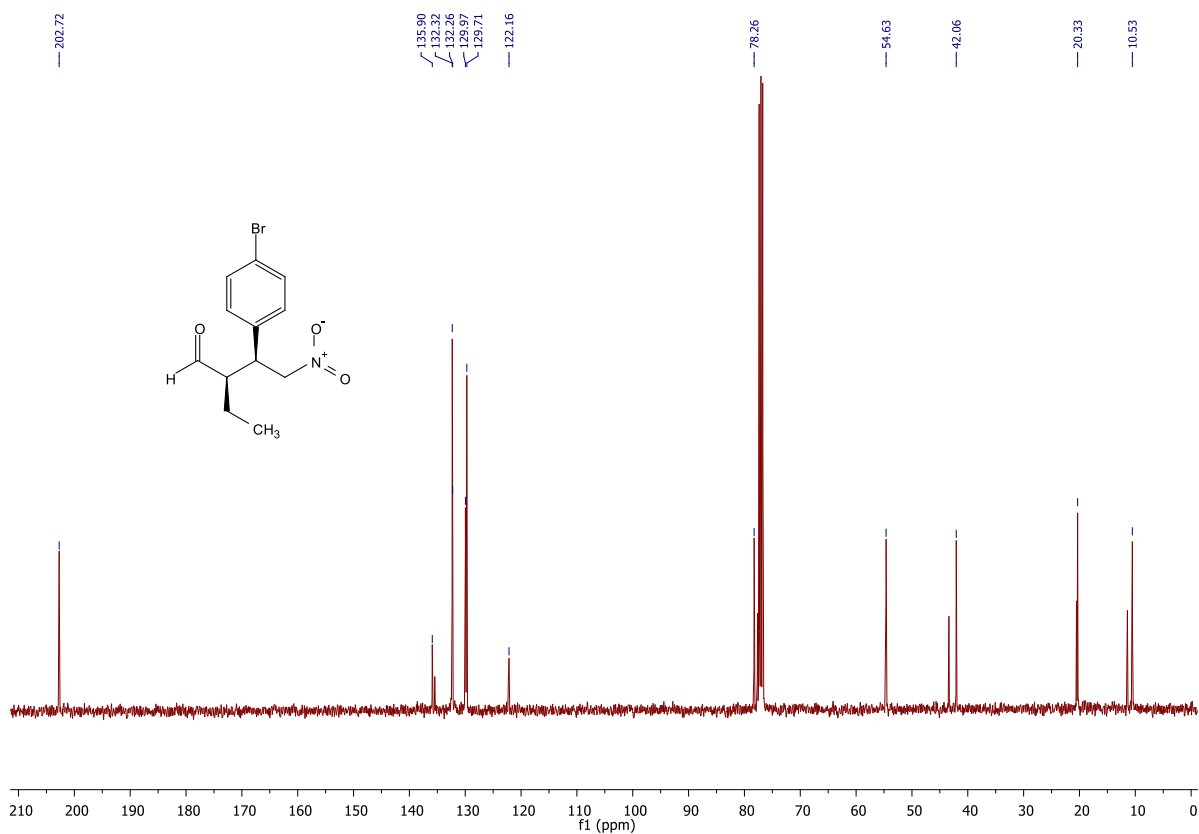
FIGURE 31. 101 MHz ¹³C NMR spectrum in CDCl₃ of compound **39** (TABLE 4).
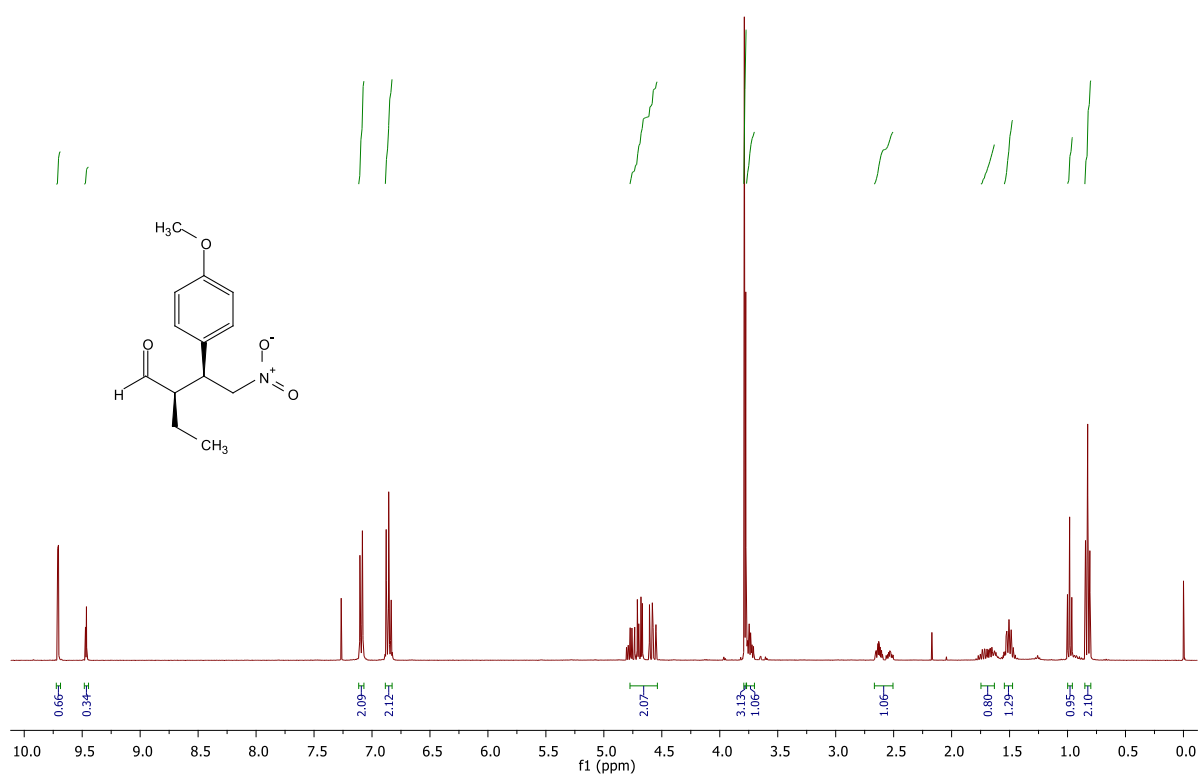
FIGURE 32. 400 MHz ^{1}H NMR spectrum in CDCl$_3$ of compound **40** (TABLE 4).
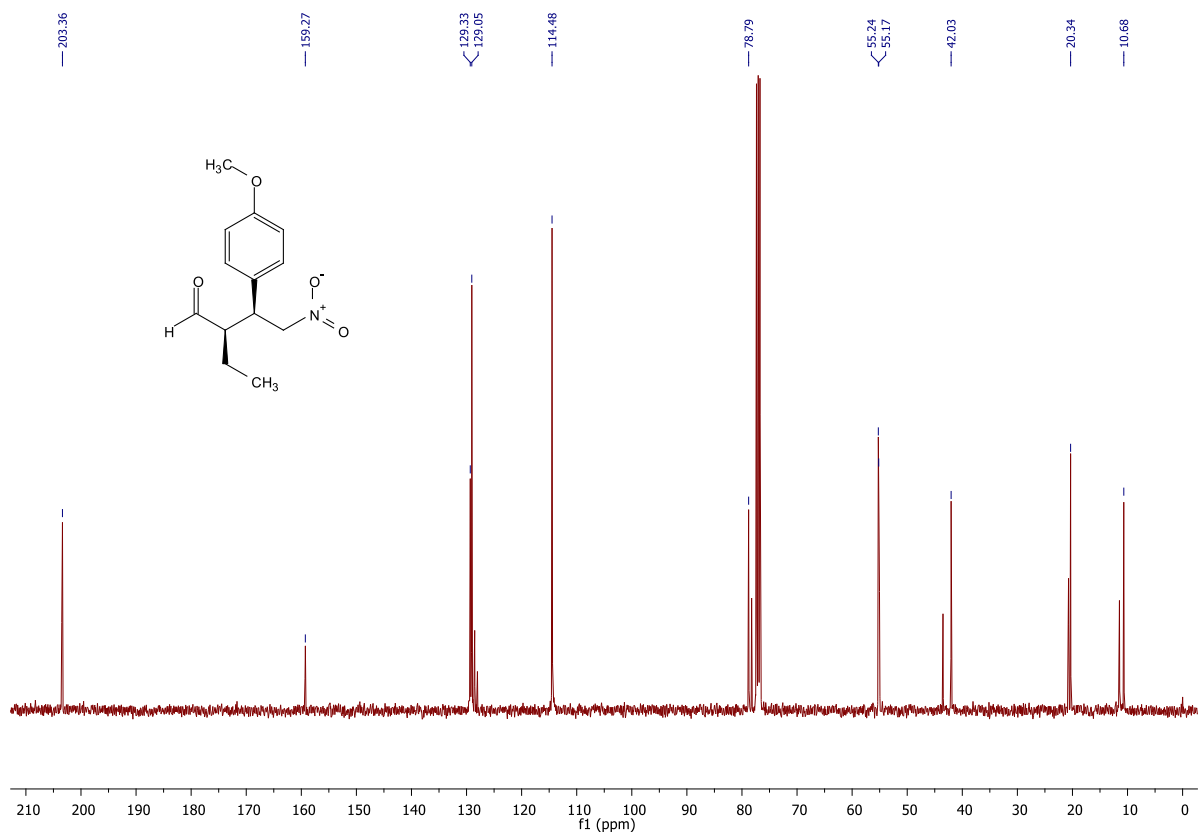
FIGURE 33. 101 MHz ^{13}C NMR spectrum in CDCl$_3$ of compound **40** (TABLE 4).
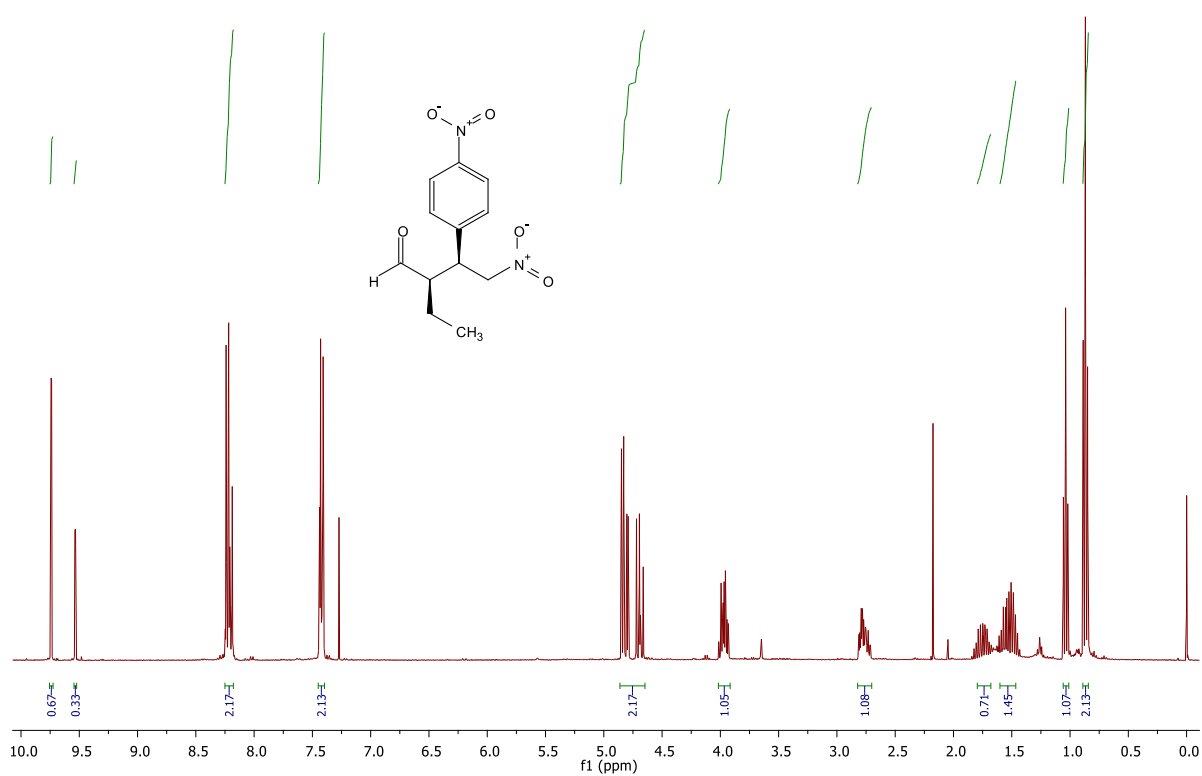
FIGURE 34. 400 MHz ^{1}H NMR spectrum in CDCl$_3$ of compound **41** (TABLE 4).
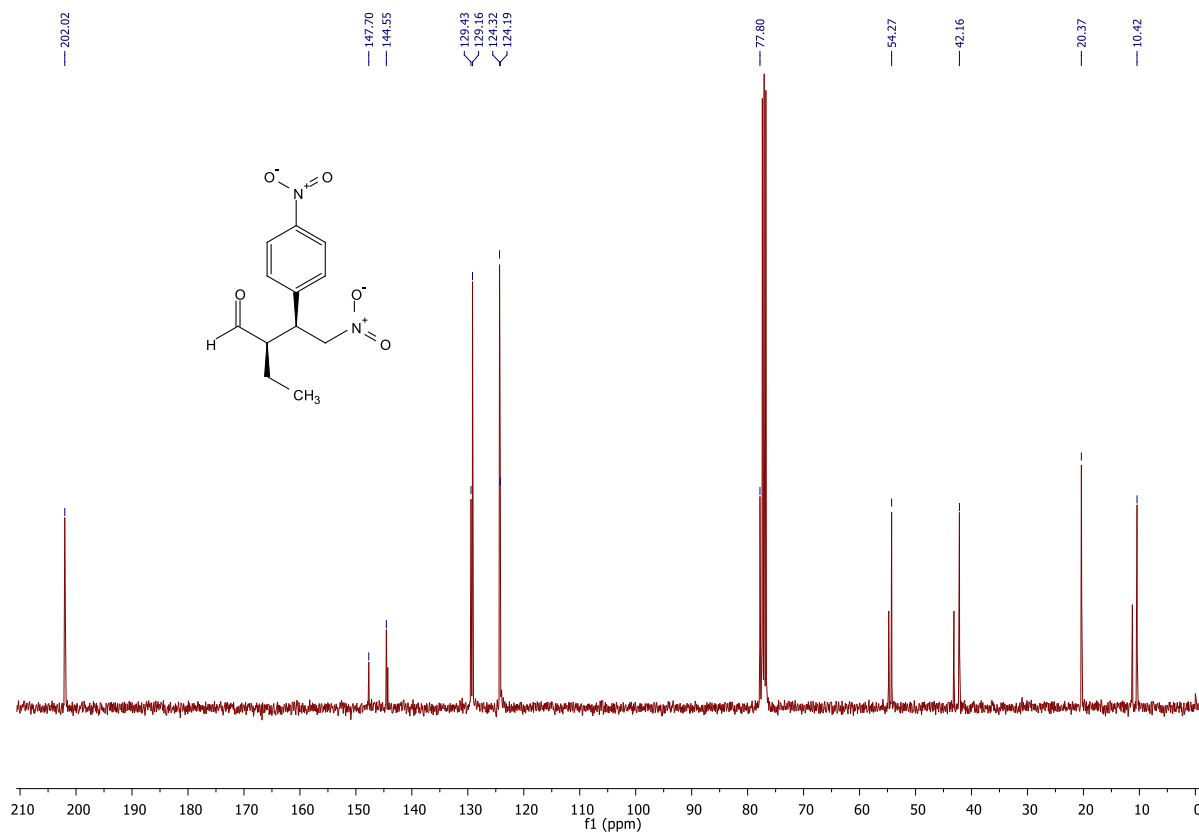
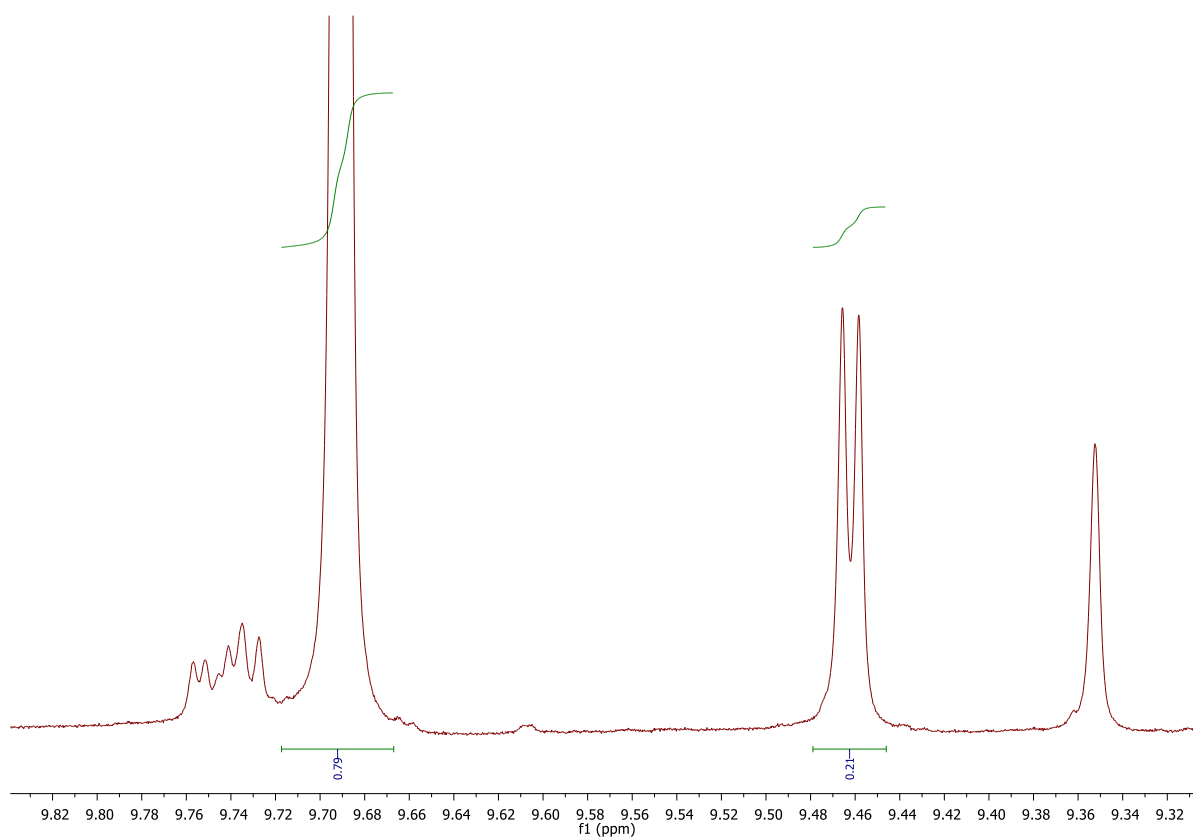**FIGURE 35.** 101 MHz ^{13}C NMR spectrum in CDCl$_3$ of compound **41** (TABLE 4).
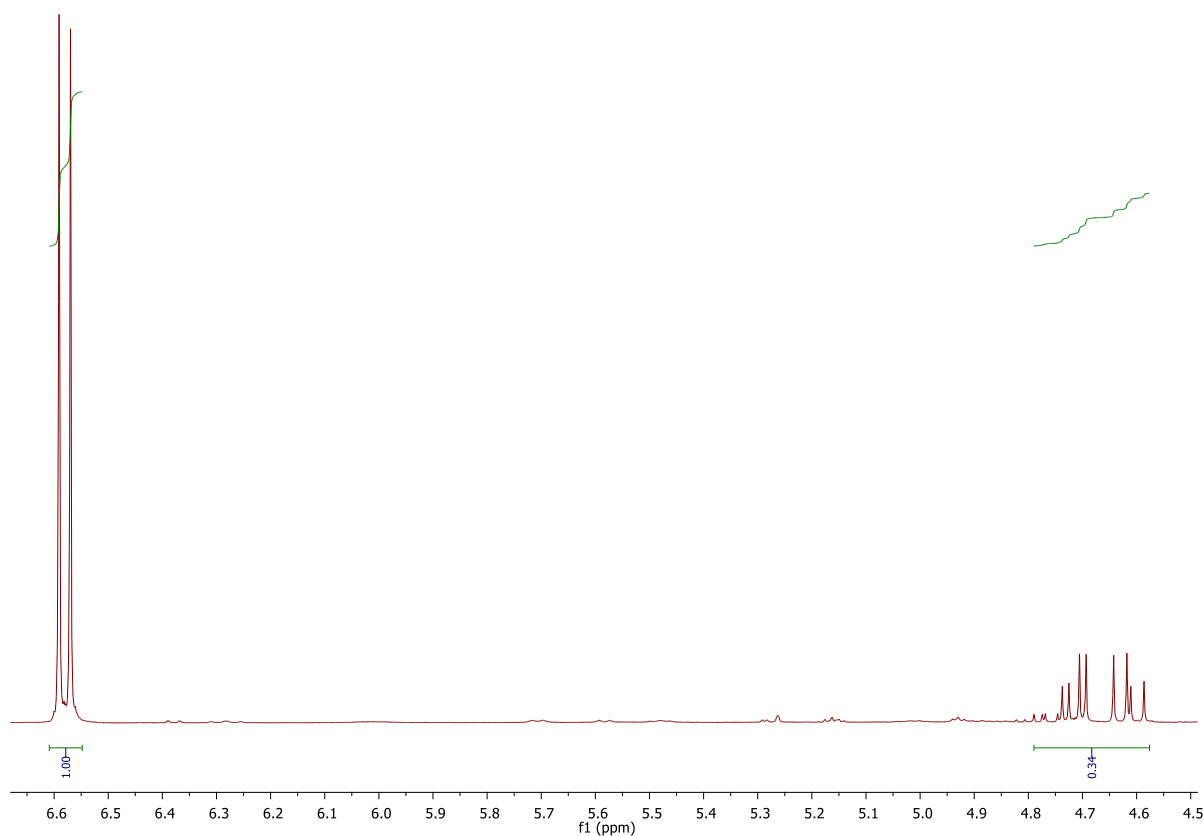
FIGURE 36. 400 MHz ^{1}H NMR spectrum in CDCl$_3$ of crude 2-ethyl-4-nitro-3-phenylbutanal obtained by the Michael reaction catalyzed by 10 mol% of compound **24** with 1,2,3-trimethoxybenzene as standard. Yield: 34%. Entry 1, TABLE 2.
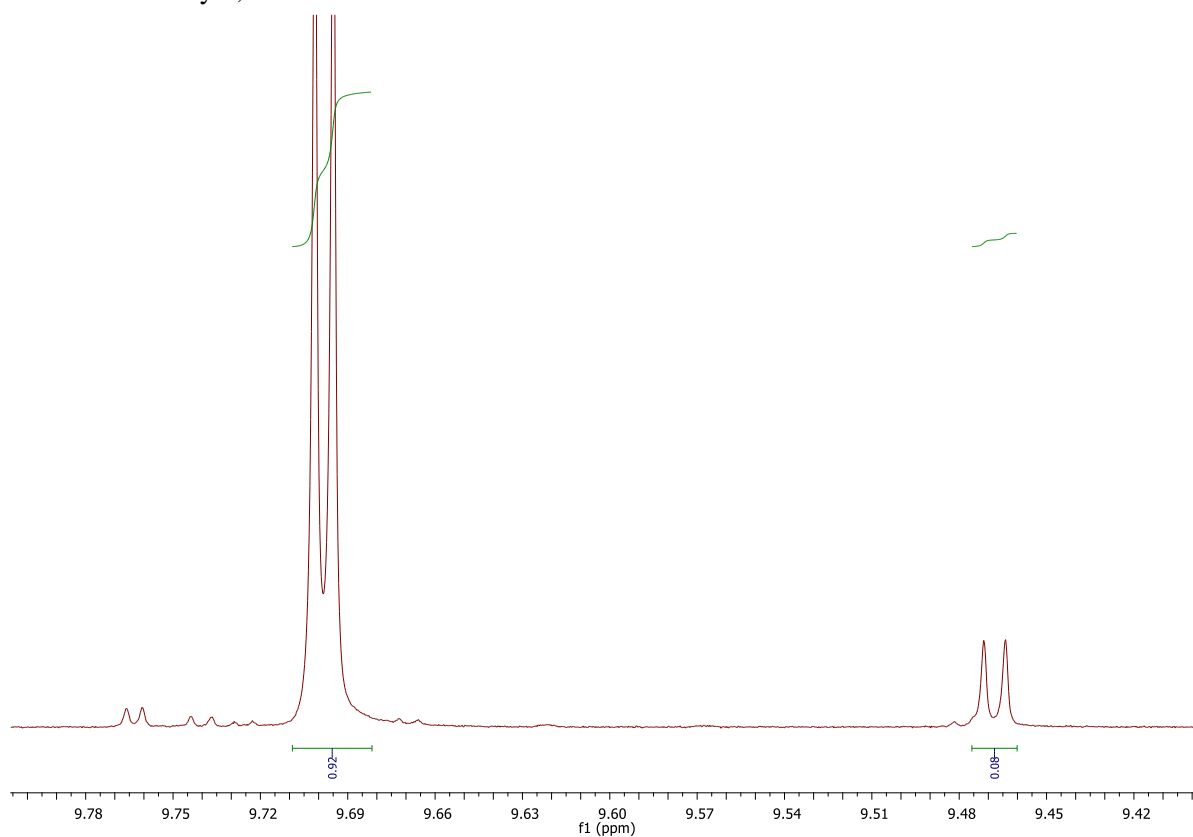
FIGURE 37. 400 MHz ^{1}H NMR spectrum in CDCl$_3$ of crude 2-ethyl-4-nitro-3-phenylbutanal obtained by the Michael reaction catalyzed by 10 mol% of compound **24**. Diastereoisomeric ratio (syn/anti): 92:08. Entry 1, TABLE 2.
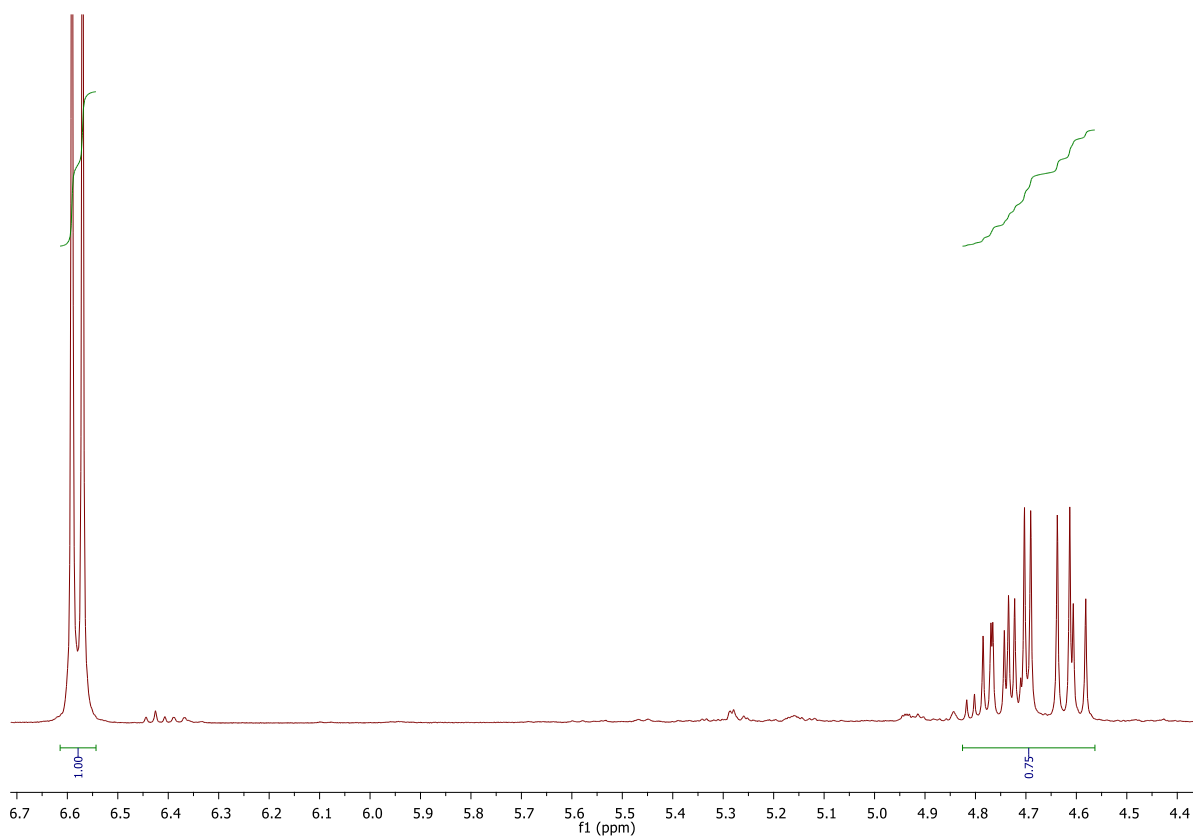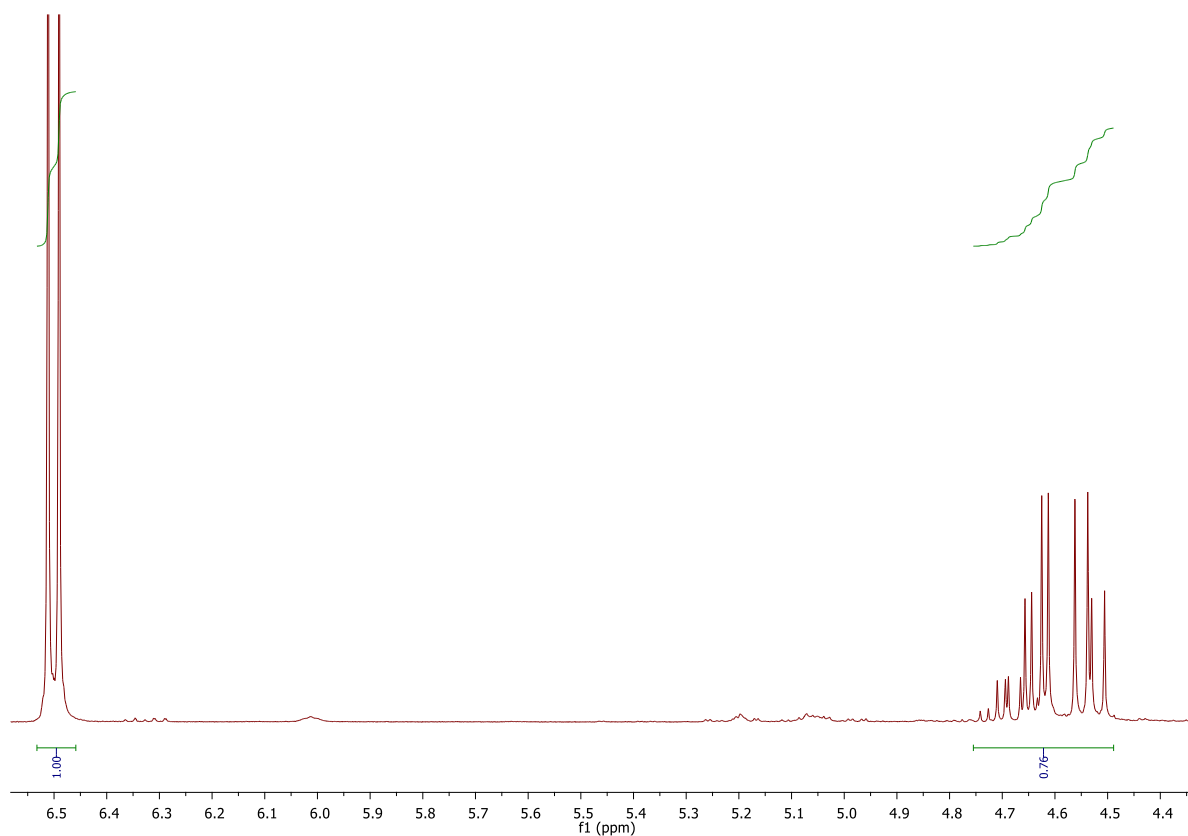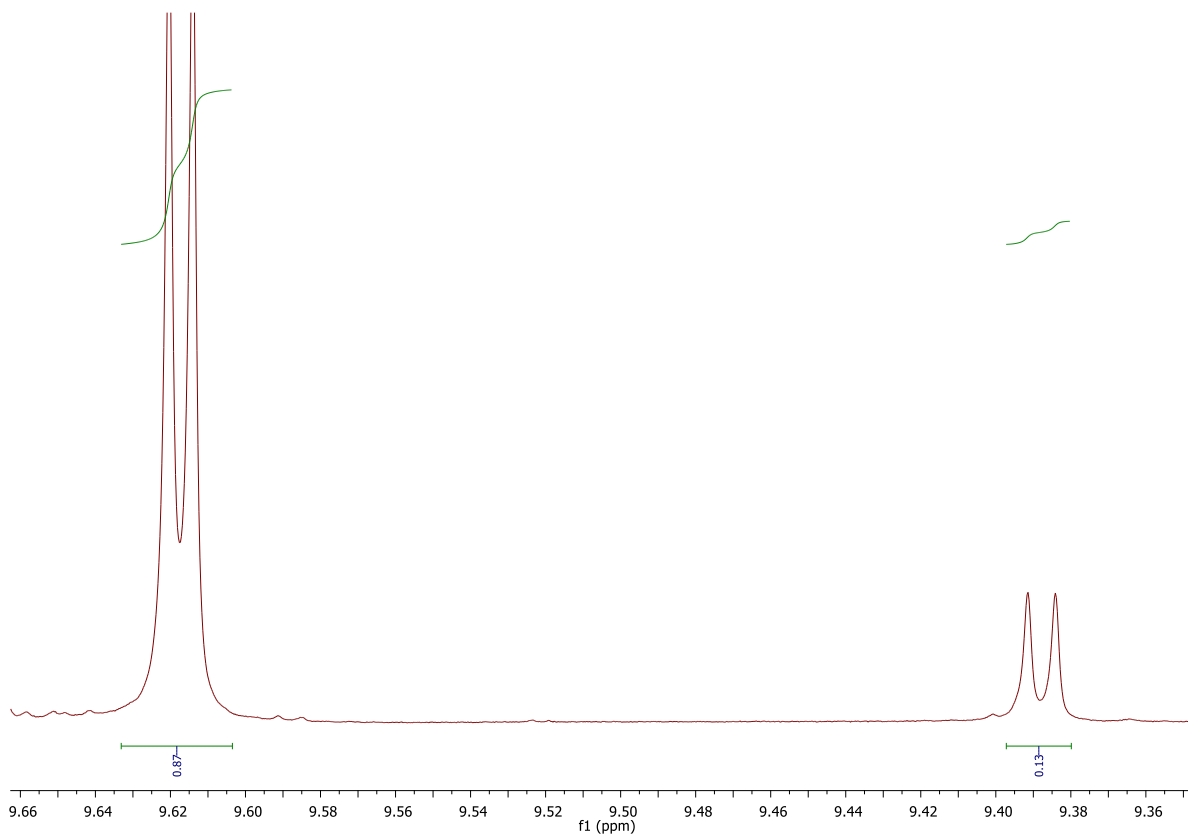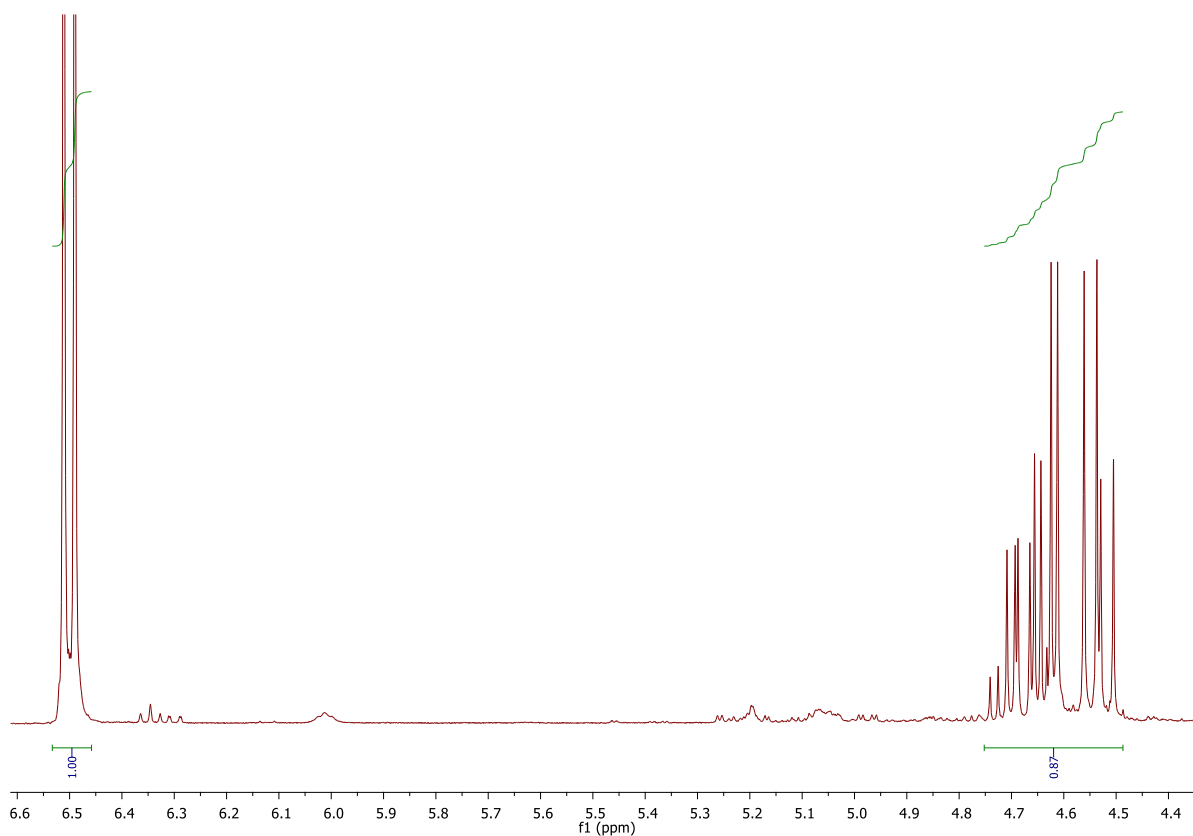
FIGURE 38. 400 MHz ^{1}H NMR spectrum in CDCl$_3$ of crude 2-ethyl-4-nitro-3-phenylbutanal obtained by the Michael reaction catalyzed by 10 mol% of compound **25** with 1,2,3-trimethoxybenzene as standard. Yield: 75%. Entry 2, TABLE 2.
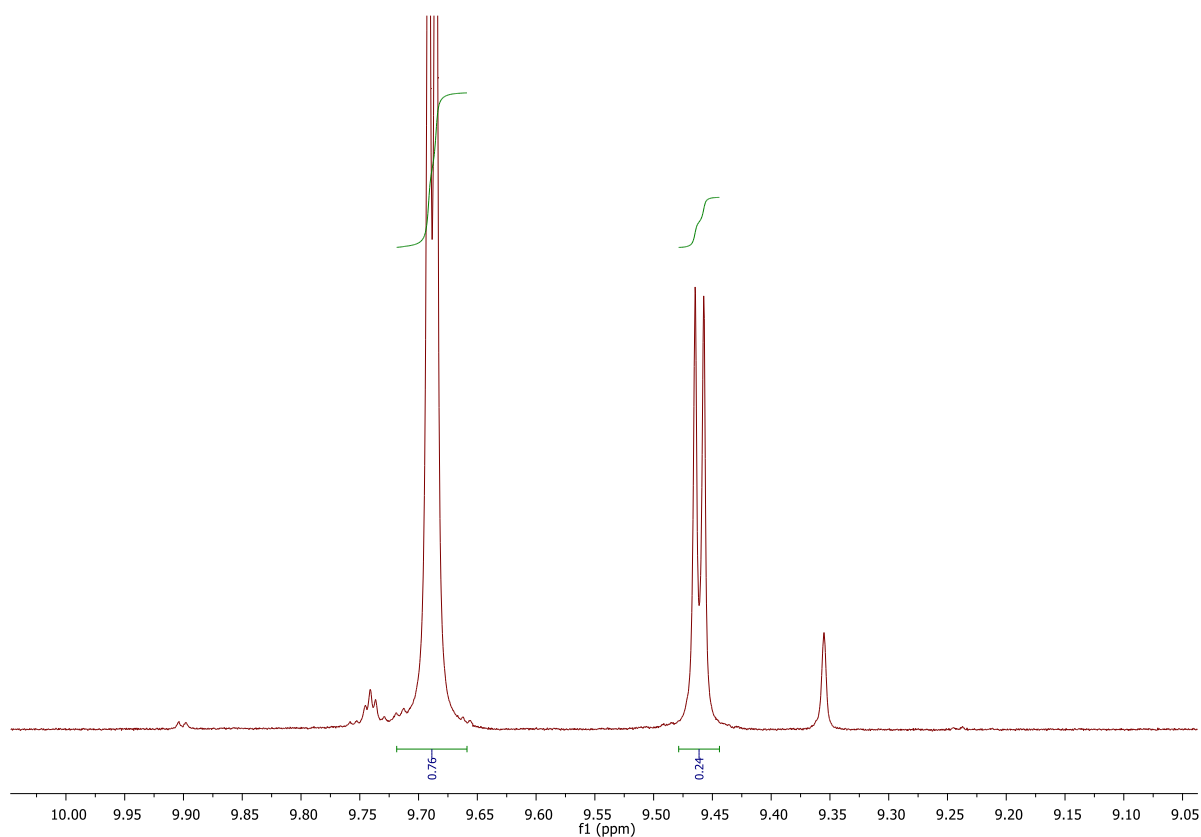
FIGURE 39. 400 MHz ^{1}H NMR spectrum in CDCl$_3$ of crude 2-ethyl-4-nitro-3-phenylbutanal obtained by the Michael reaction catalyzed by 10 mol% of compound **25**. Diastereoisomeric ratio (syn/anti): 76:24. Entry 2, TABLE 2.
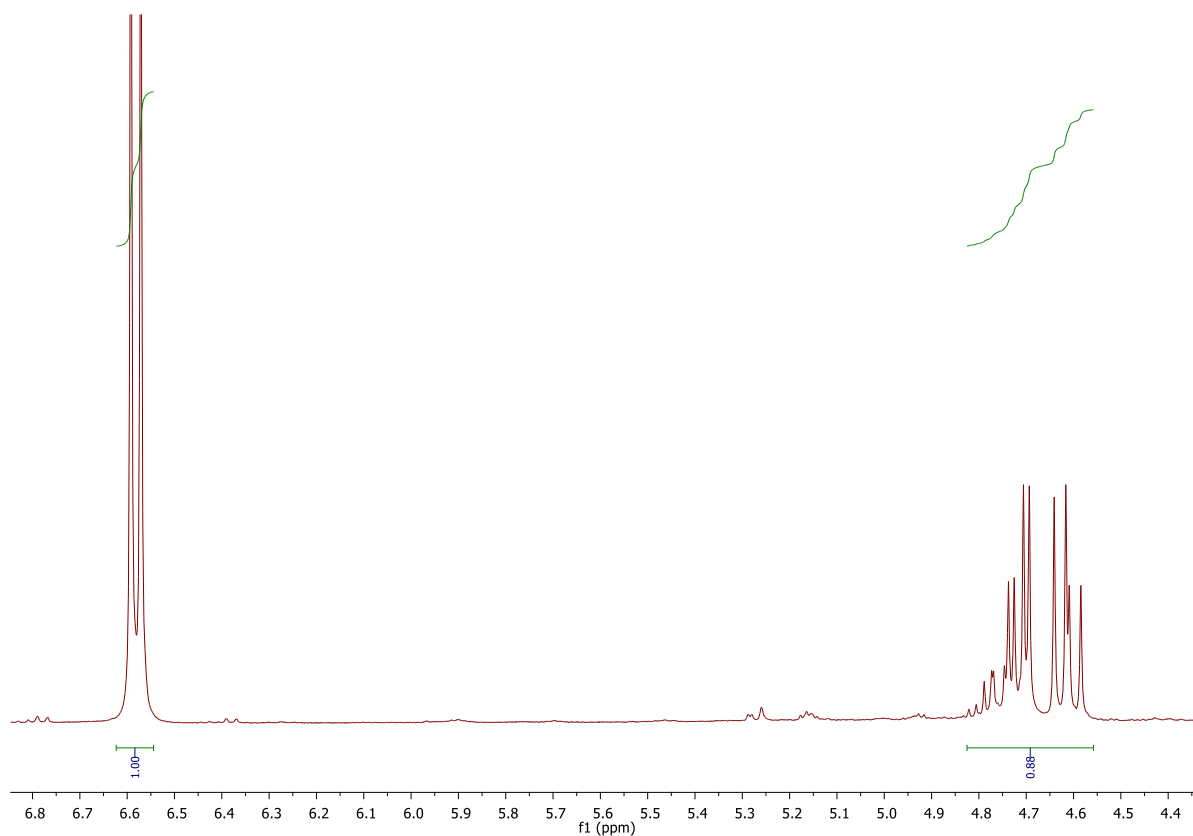
FIGURE 40. 400 MHz ^{1}H NMR spectrum in CDCl$_3$ of crude 2-ethyl-4-nitro-3-phenylbutanal obtained by the Michael reaction catalyzed by 10 mol% of compound **26**. with 1,2,3-trimethoxybenzene as standard. Yield: 88%. Entry 3, TABLE 2.
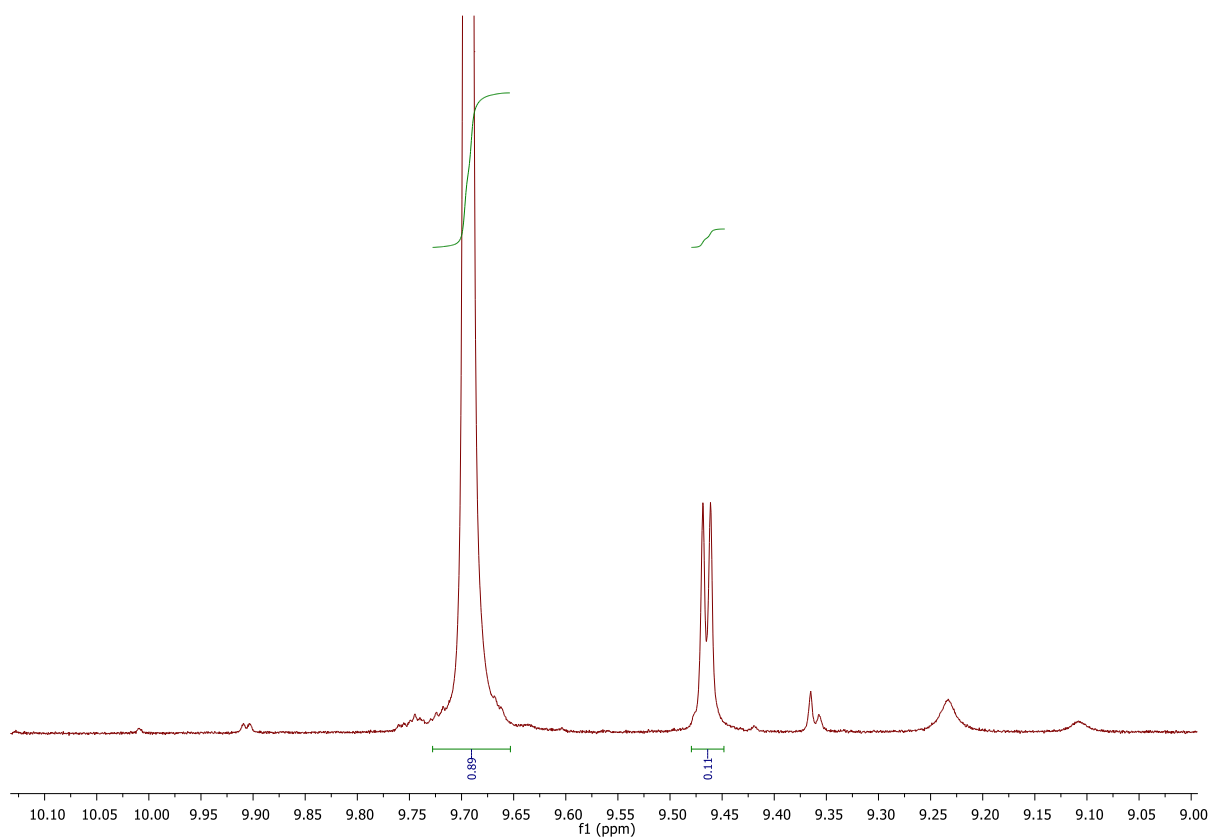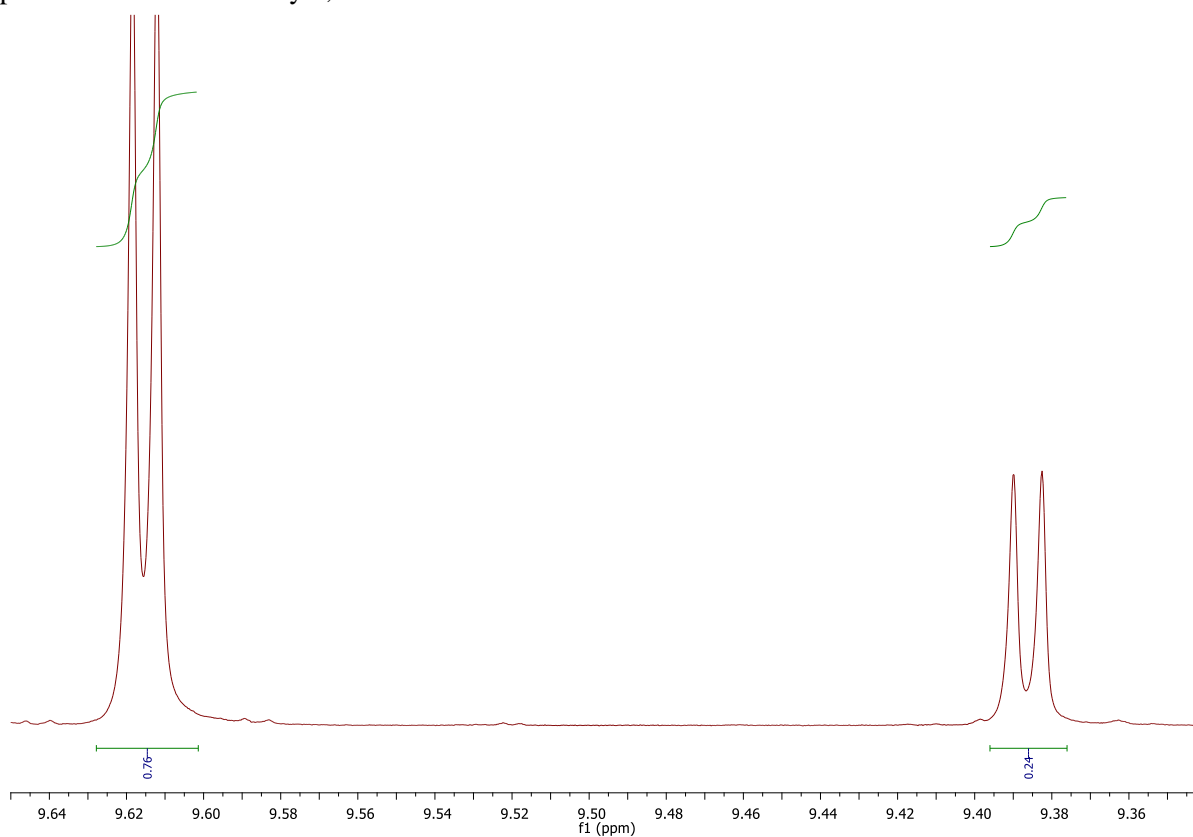

FIGURE 41. 400 MHz ^{1}H NMR spectrum in CDCl$_3$ of crude 2-ethyl-4-nitro-3-phenylbutanal obtained by the Michael reaction catalyzed by 10 mol% of compound **26**. Diastereoisomeric ratio (syn/anti): 89:11. Entry 3, TABLE 2.
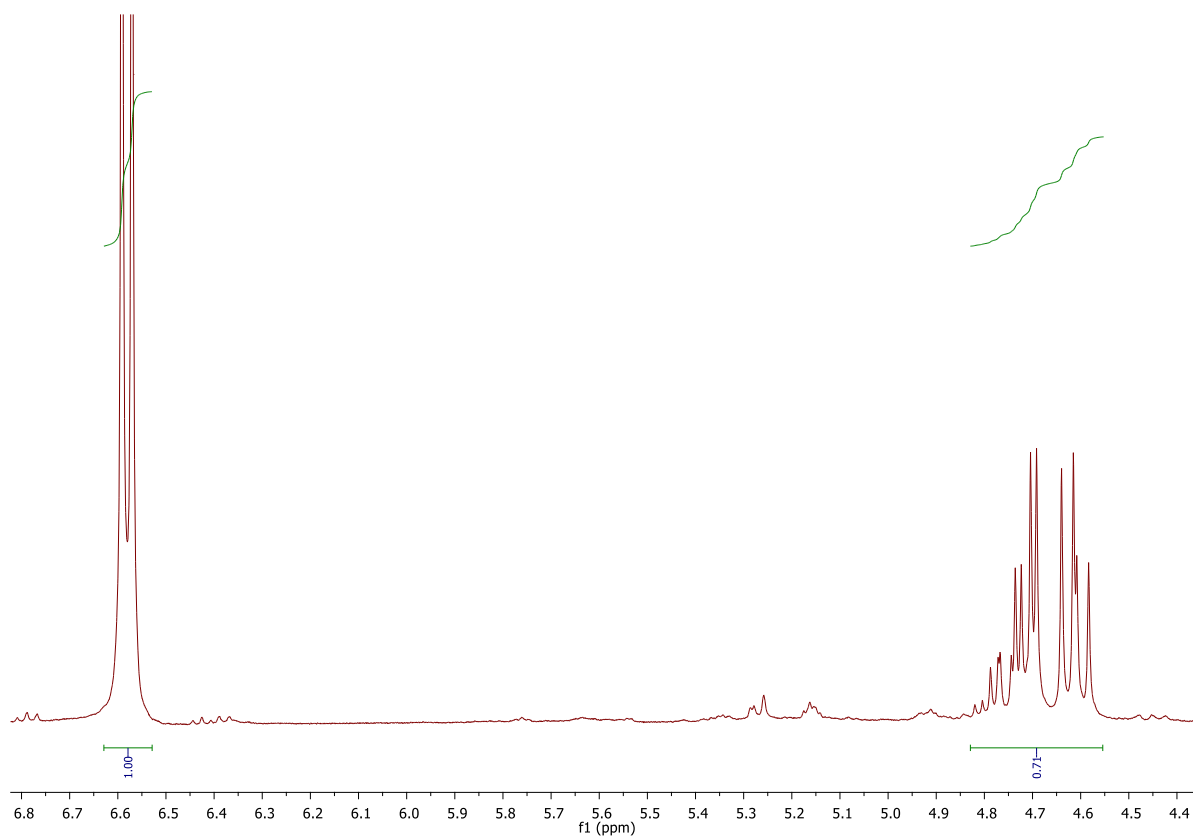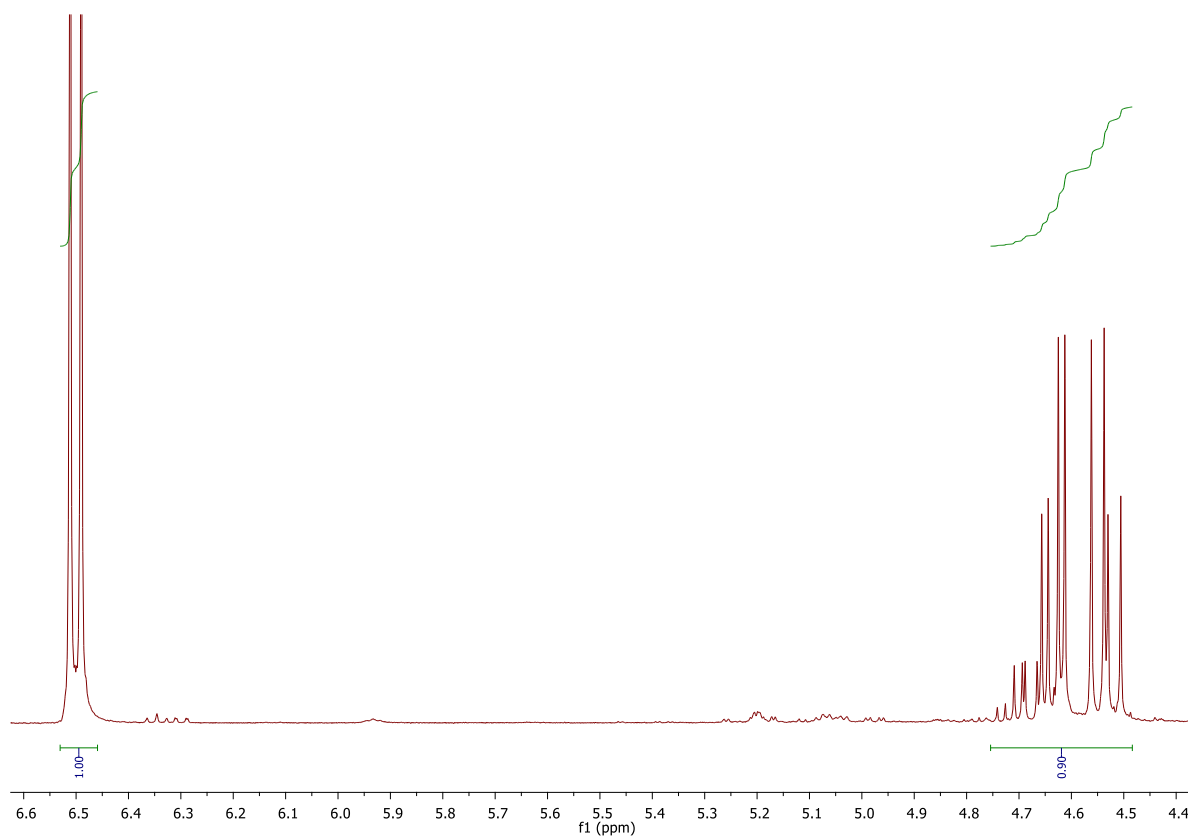
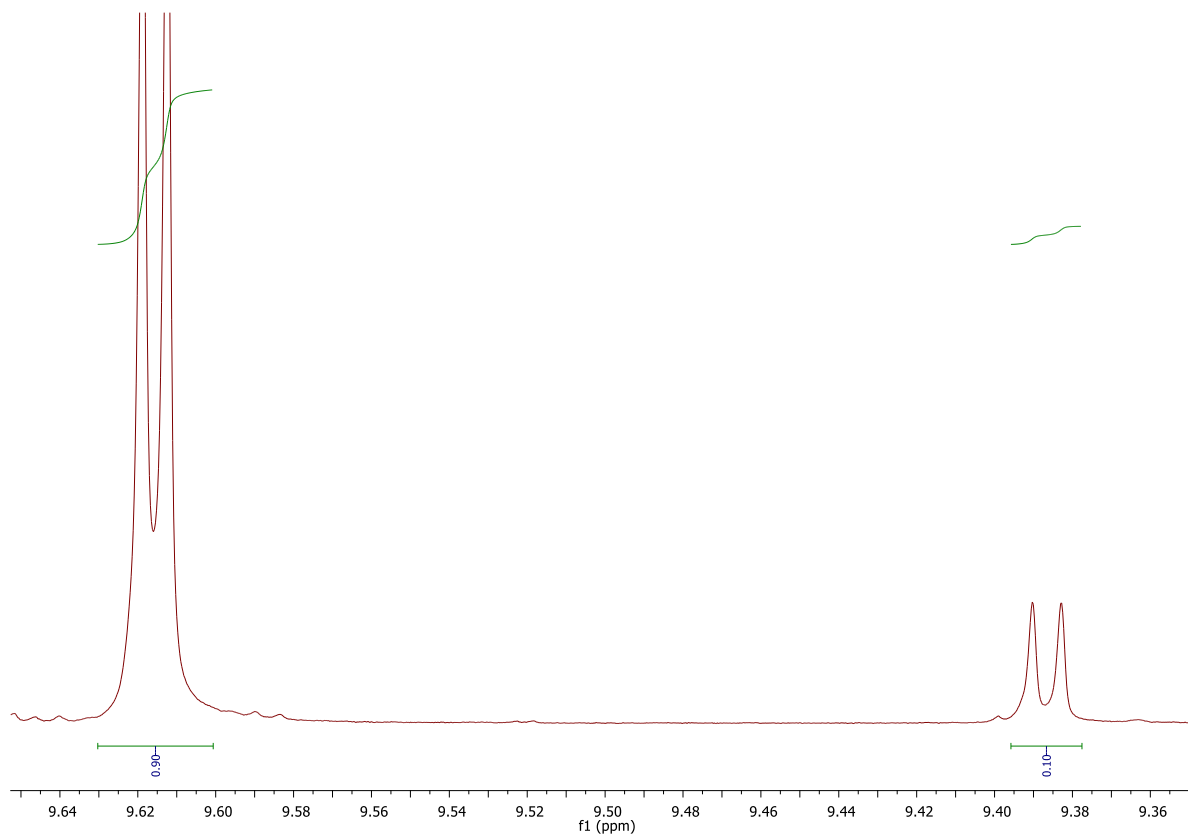**FIGURE 42.** 400 MHz ^{1}H NMR spectrum in CDCl$_3$ of crude 2-ethyl-4-nitro-3-phenylbutanal obtained by the Michael reaction catalyzed by 10 mol% of compound **27** with 1,2,3-trimethoxybenzene as standard. Yield: 71%. Entry 4, TABLE 2.
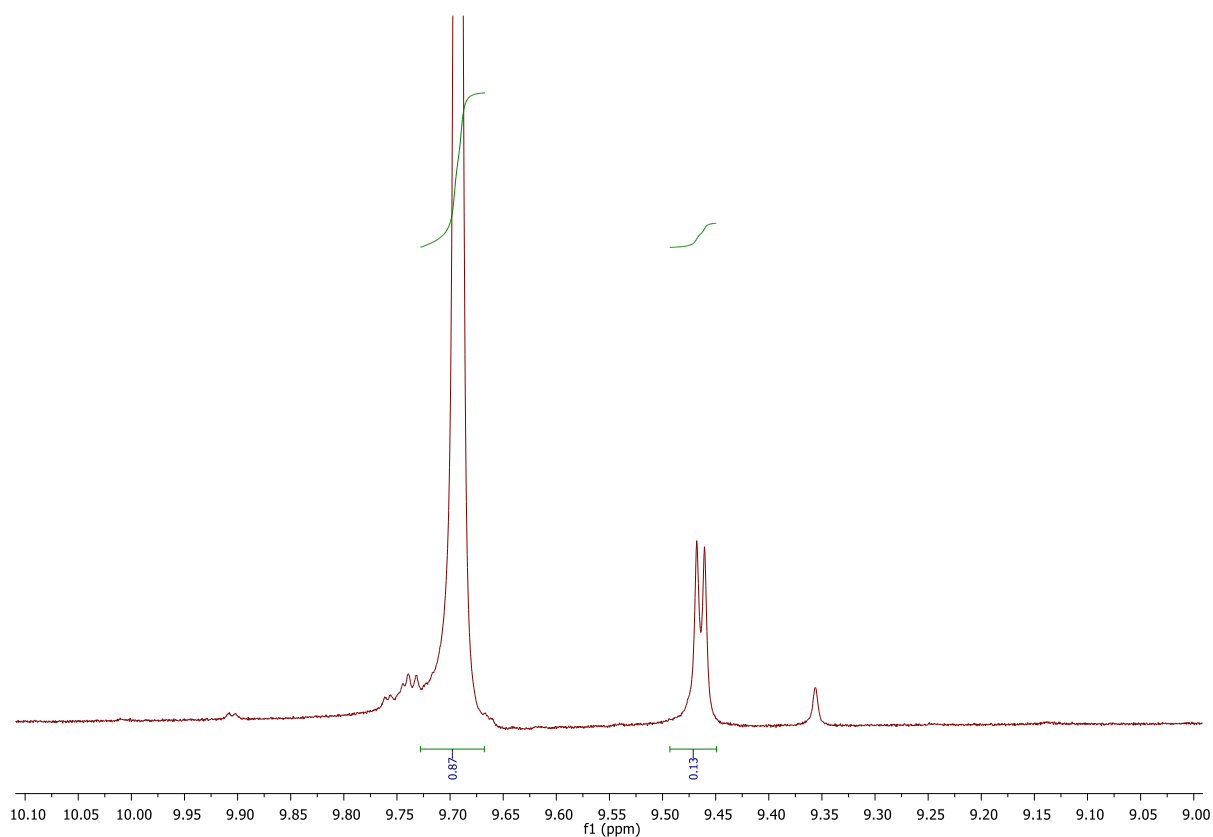
FIGURE 43. 400 MHz ^{1}H NMR spectrum in CDCl$_3$ of crude 2-ethyl-4-nitro-3-phenylbutanal obtained by the Michael reaction catalyzed by 10 mol% of compound **27**. Diastereoisomeric ratio (syn/anti): 87:13. Entry 4, TABLE 2.
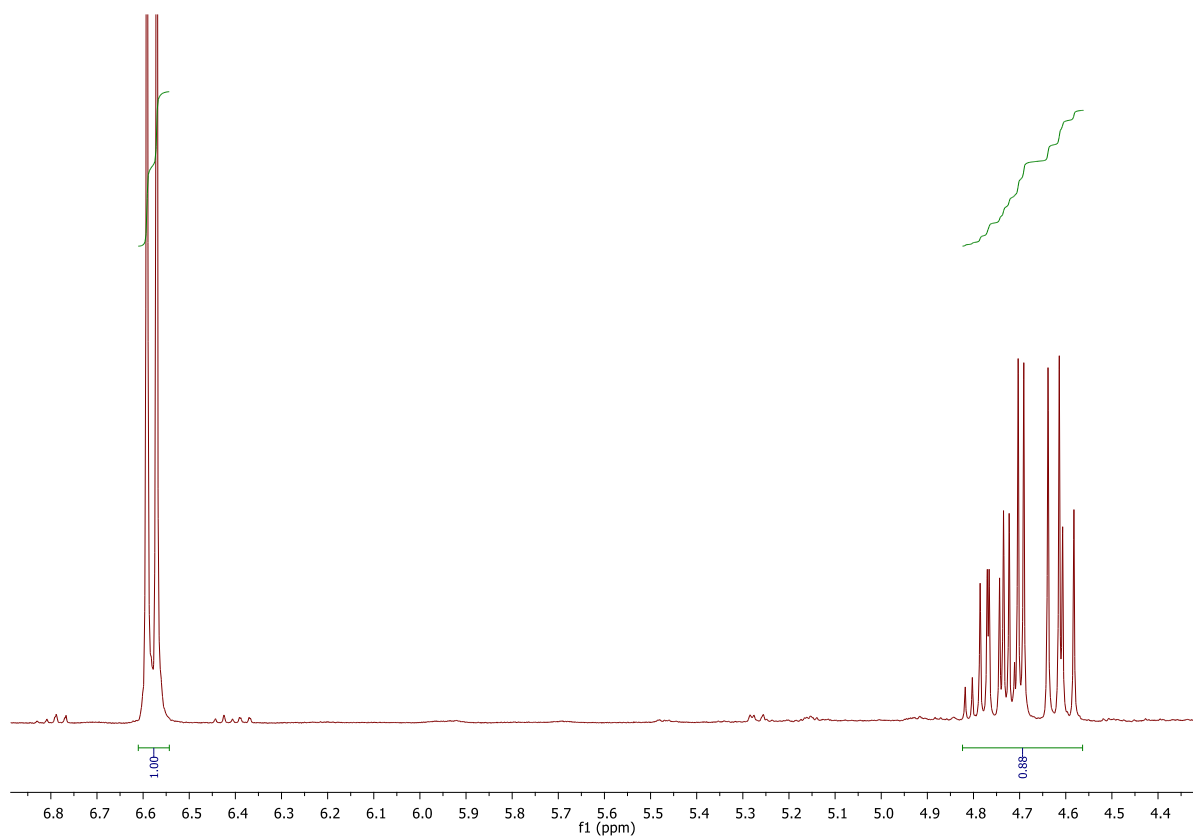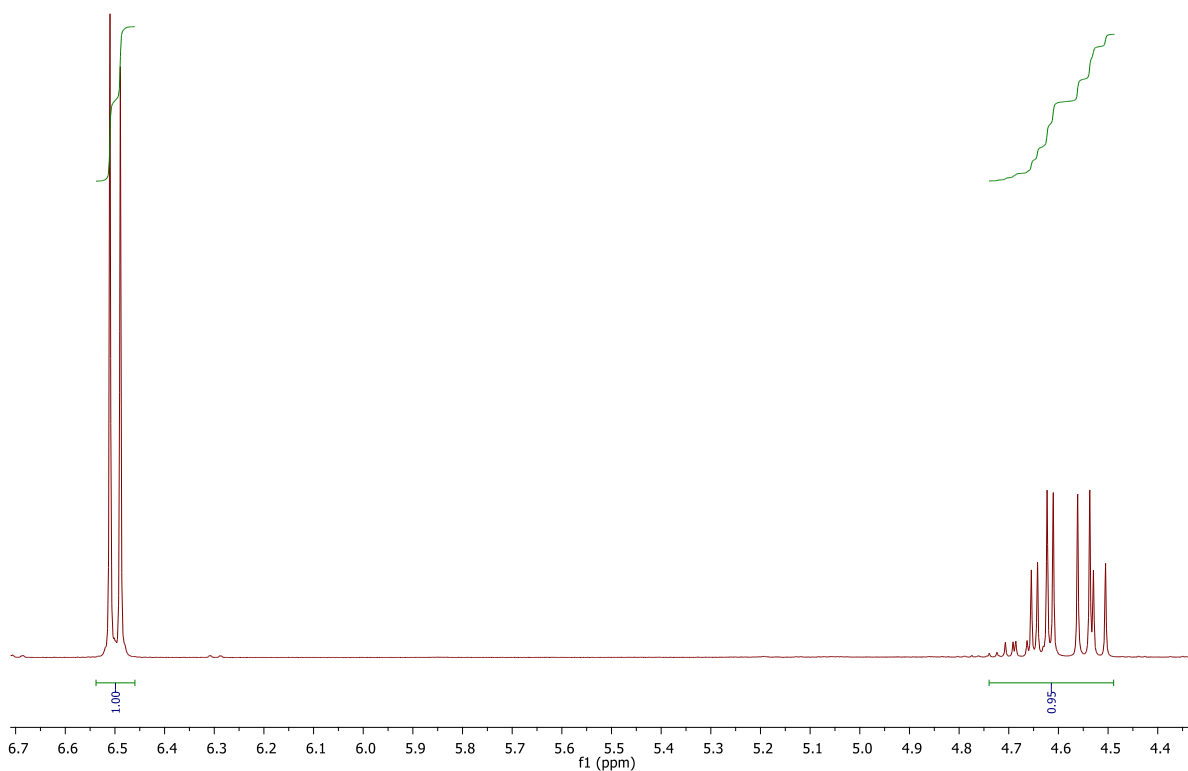
FIGURE 44. 400 MHz ^{1}H NMR spectrum in CDCl$_3$ of crude 2-ethyl-4-nitro-3-phenylbutanal obtained by the Michael reaction catalyzed by 10 mol% of compound **28** with 1,2,3-trimethoxybenzene as standard. Yield: 88%. Entry 5, TABLE 2.
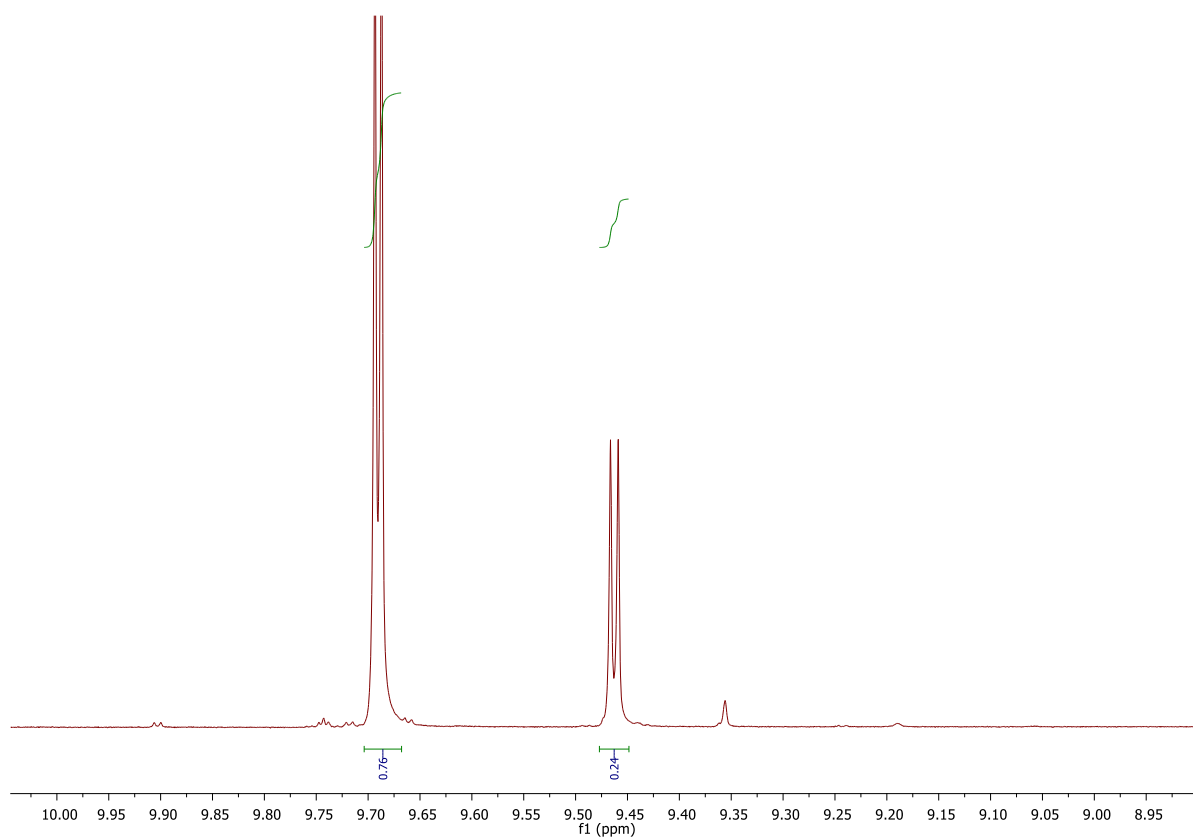
FIGURE 45. 400 MHz ^{1}H NMR spectrum in CDCl$_3$ of crude 2-ethyl-4-nitro-3-phenylbutanal obtained by the Michael reaction catalyzed by 10 mol% of compound **28**. Diastereoisomeric ratio (syn/anti): 76:24. Entry 5, TABLE 2.
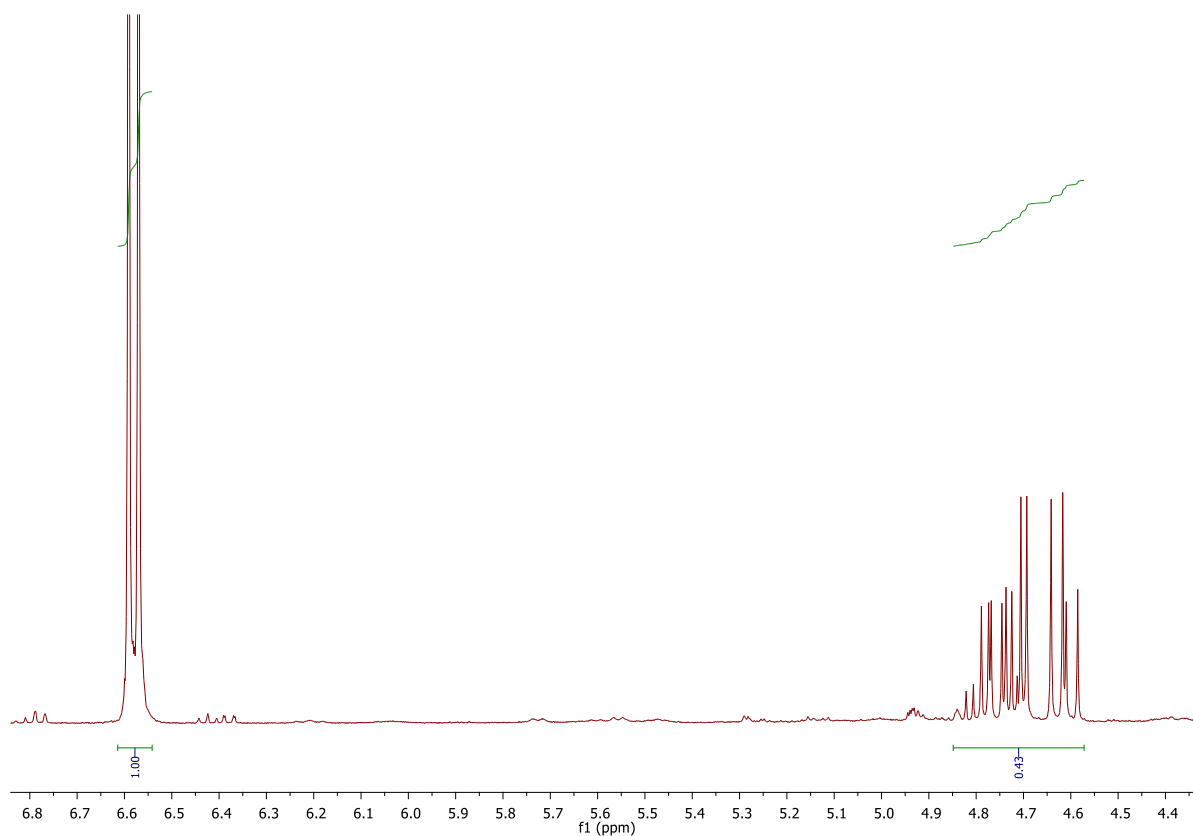
FIGURE 46. 400 MHz ^{1}H NMR spectrum in CDCl$_3$ of crude 2-ethyl-4-nitro-3-phenylbutanal obtained by the Michael reaction catalyzed by 10 mol% of compound **29** with 1,2,3-trimethoxybenzene as standard patron. Yield: 43%. Entry 6, TABLE 2.
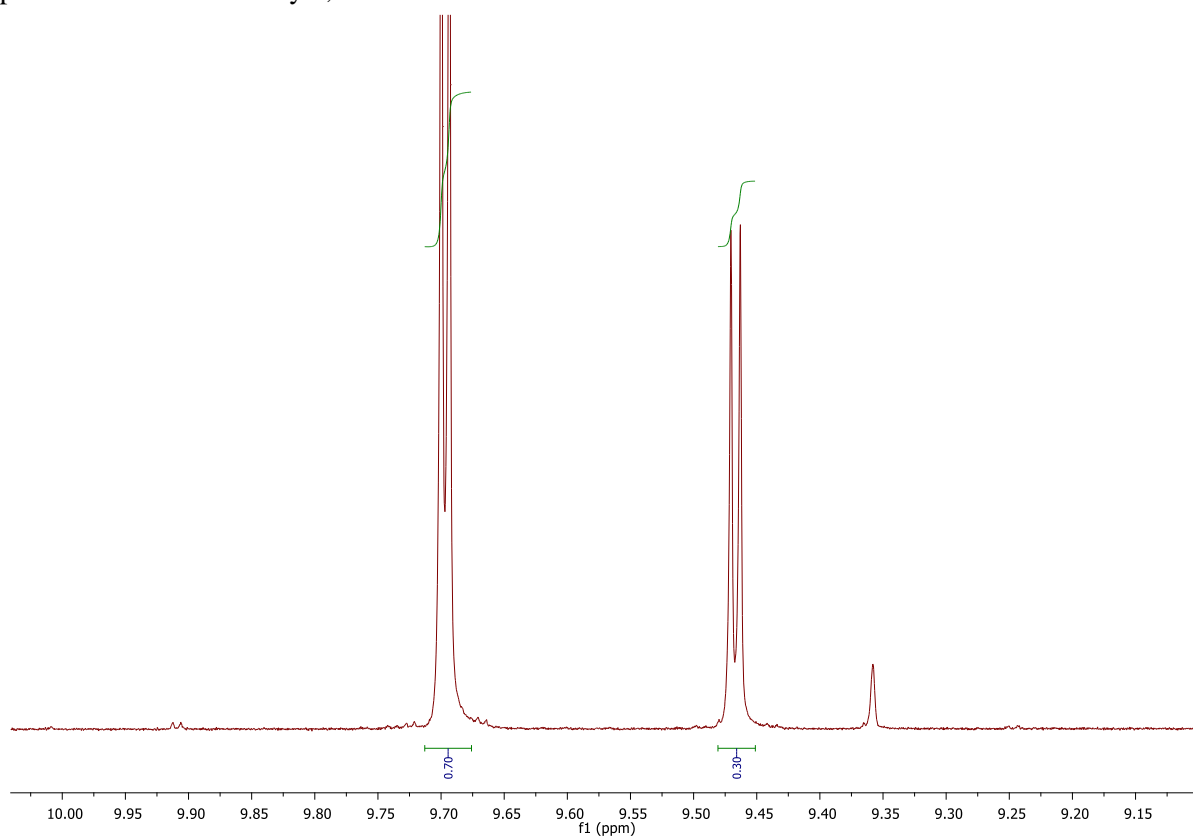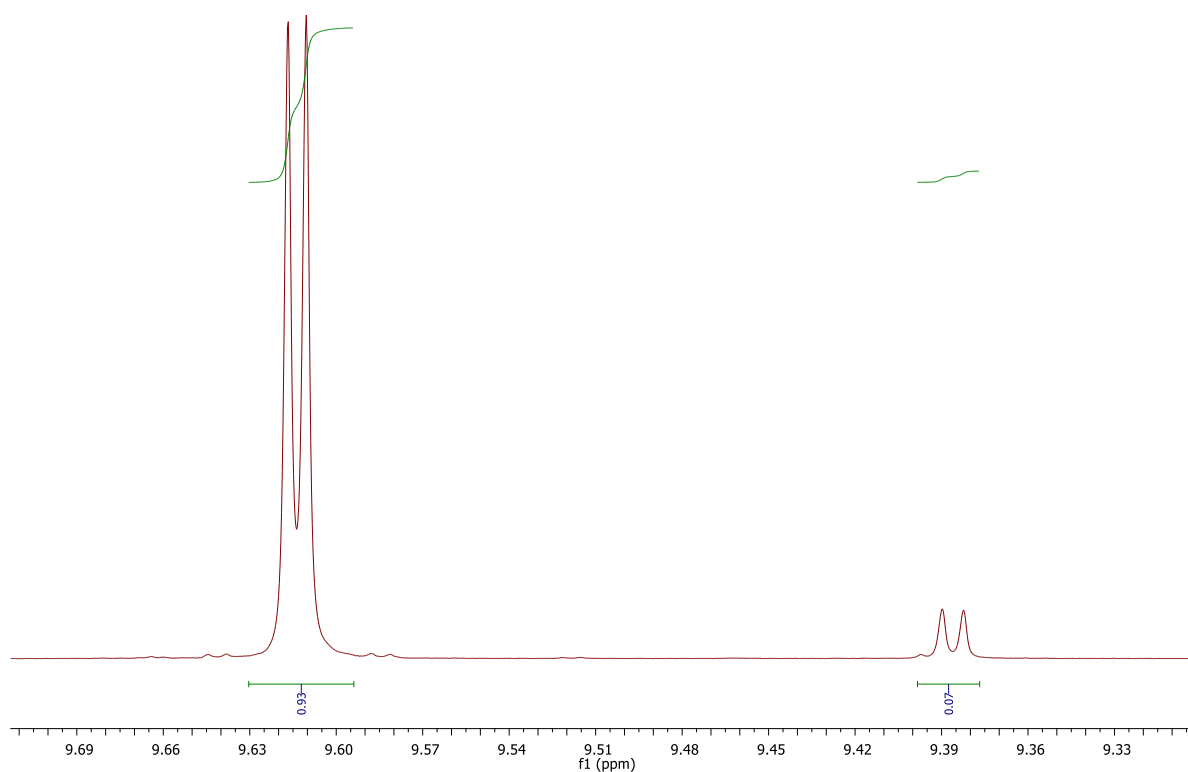

FIGURE 47. 400 MHz ^{1}H NMR spectrum in CDCl$_3$ of crude 2-ethyl-4-nitro-3-phenylbutanal obtained by the Michael reaction catalyzed by 10 mol% of compound **29**. Diastereoisomeric ratio (syn/anti): 70:30. Entry 6, TABLE 2.
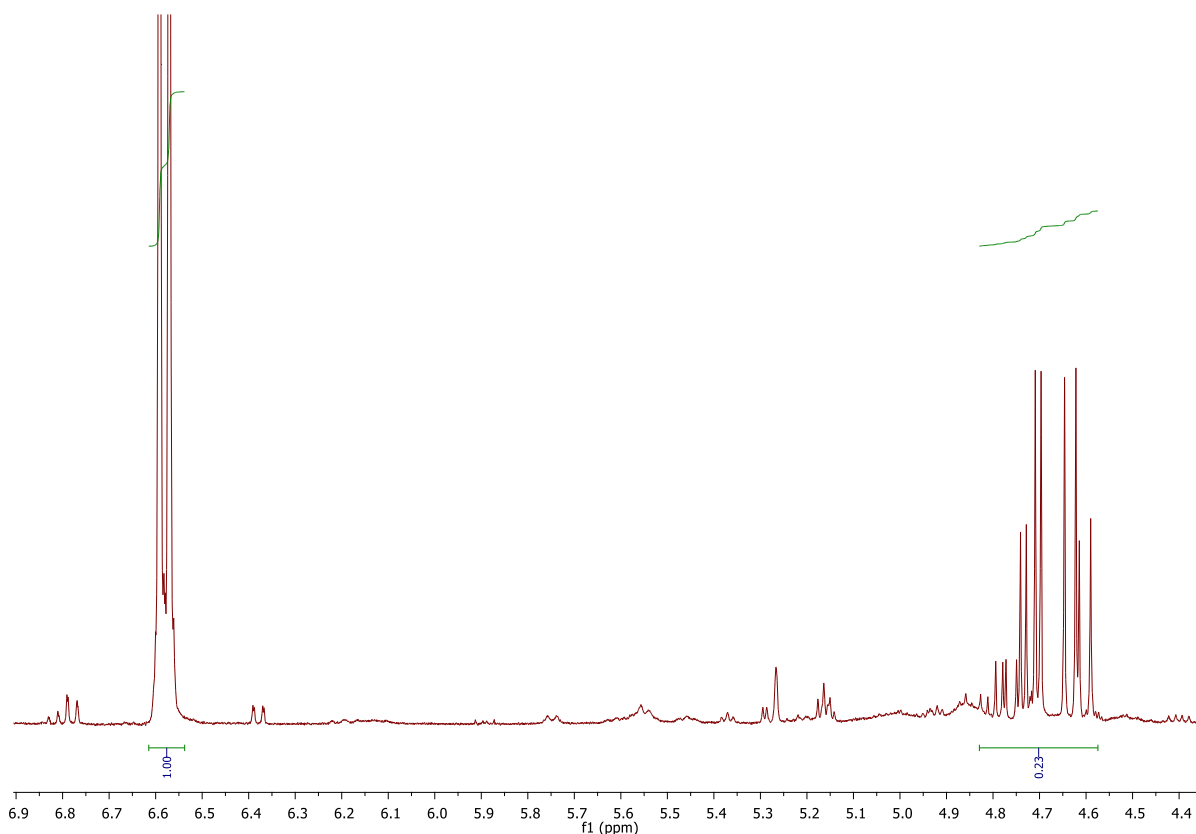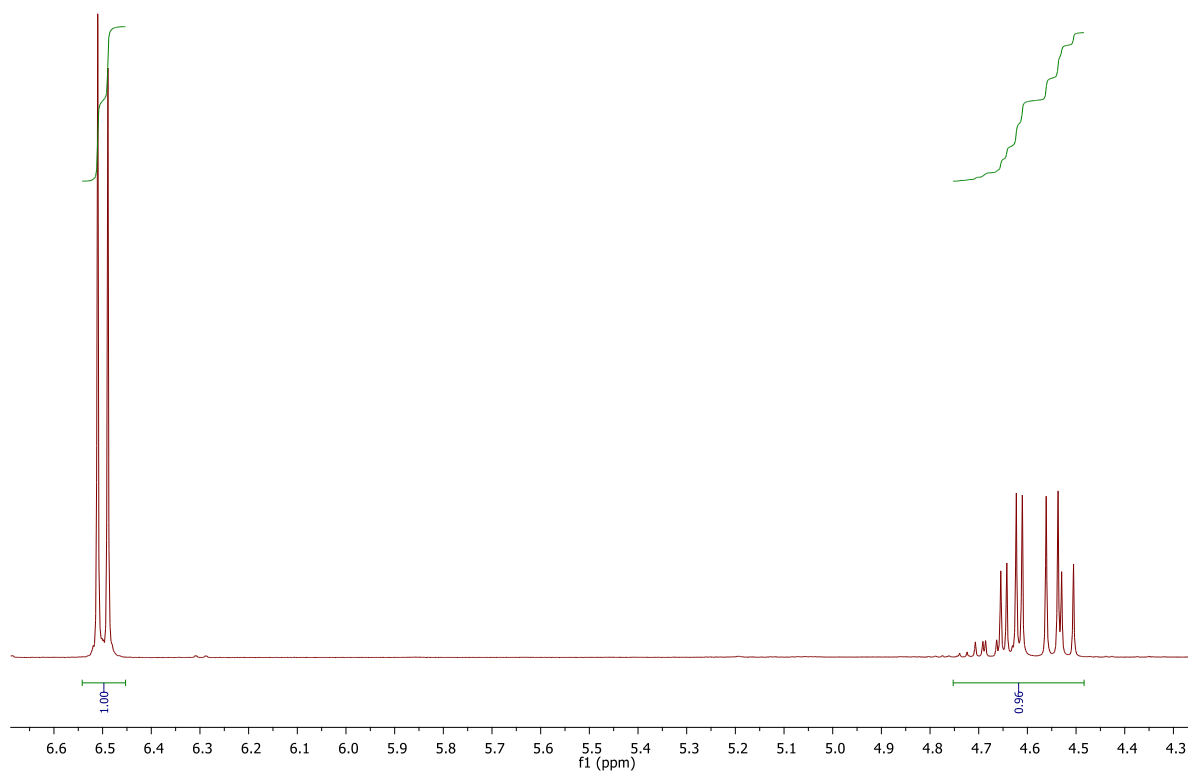
FIGURE 48. 400 MHz ^{1}H NMR spectrum in CDCl$_3$ of crude 2-ethyl-4-nitro-3-phenylbutanal obtained by the Michael reaction catalyzed by 10 mol% of compound **30** with 1,2,3-trimethoxybenzene as standard patron. Yield: 23%. Entry 7, TABLE 2.
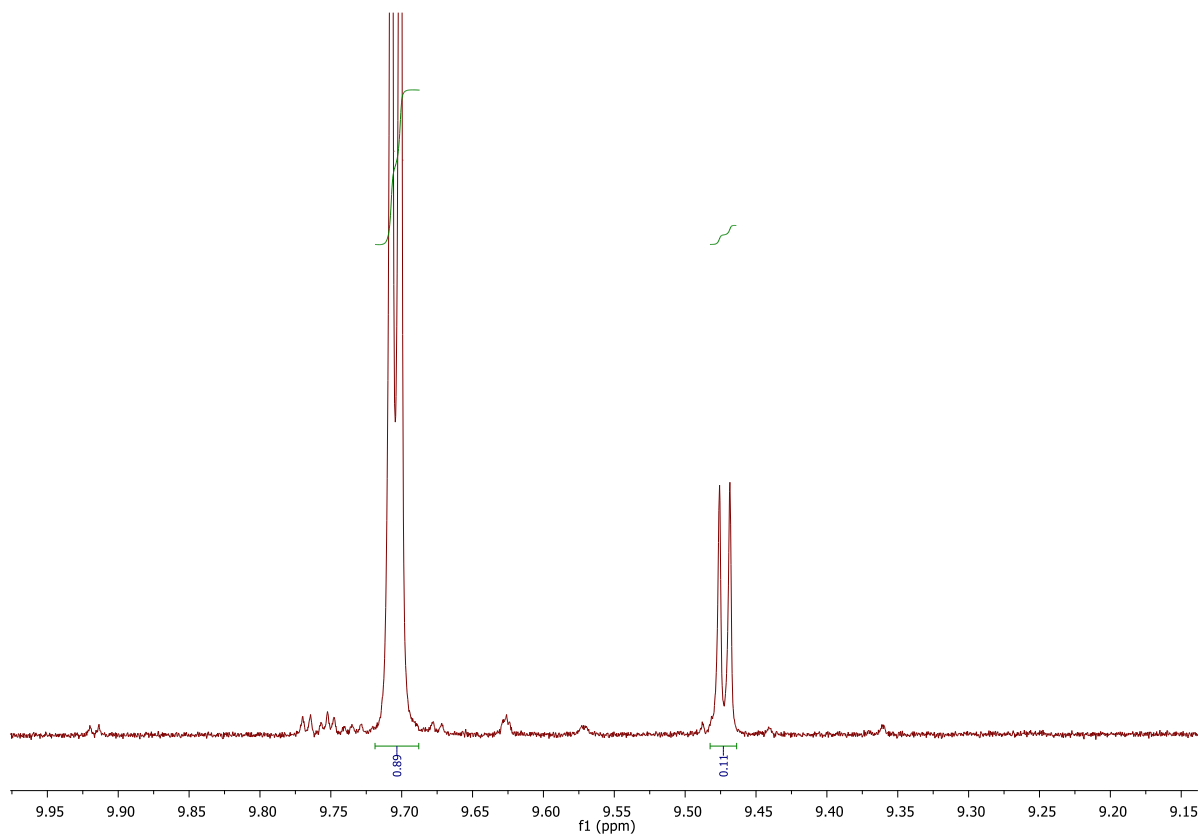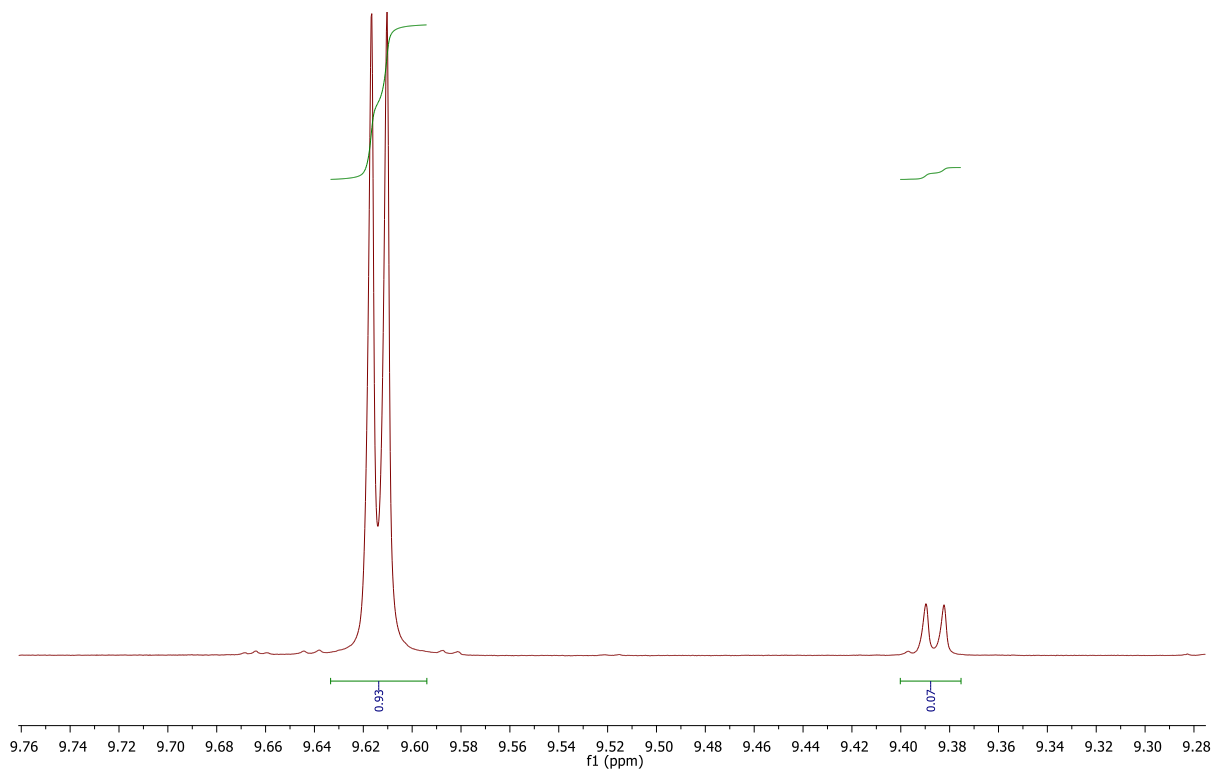

FIGURE 49. 400 MHz ^{1}H NMR spectrum in CDCl$_3$ of crude 2-ethyl-4-nitro-3-phenylbutanal obtained by the Michael reaction catalyzed by 10 mol% of compound **30**. Diastereoisomeric ratio (syn/anti): 89:11. Entry 7, TABLE 2.
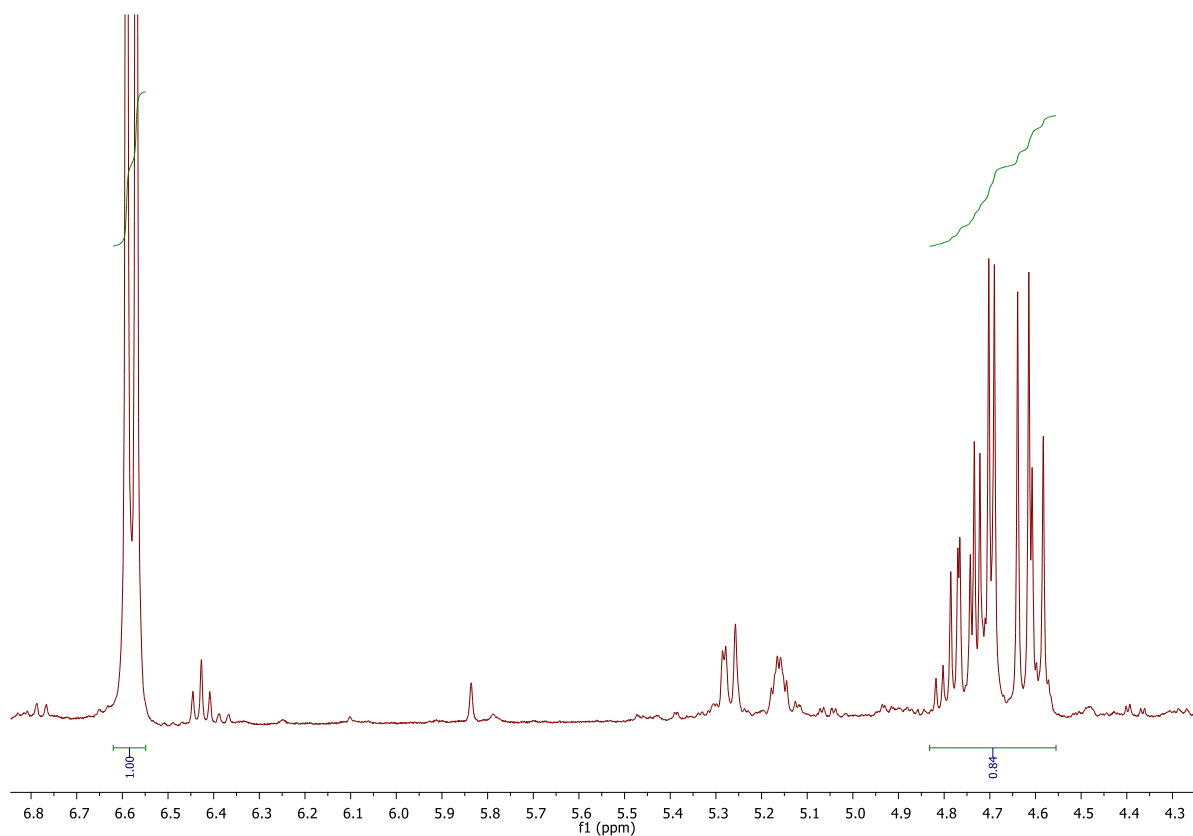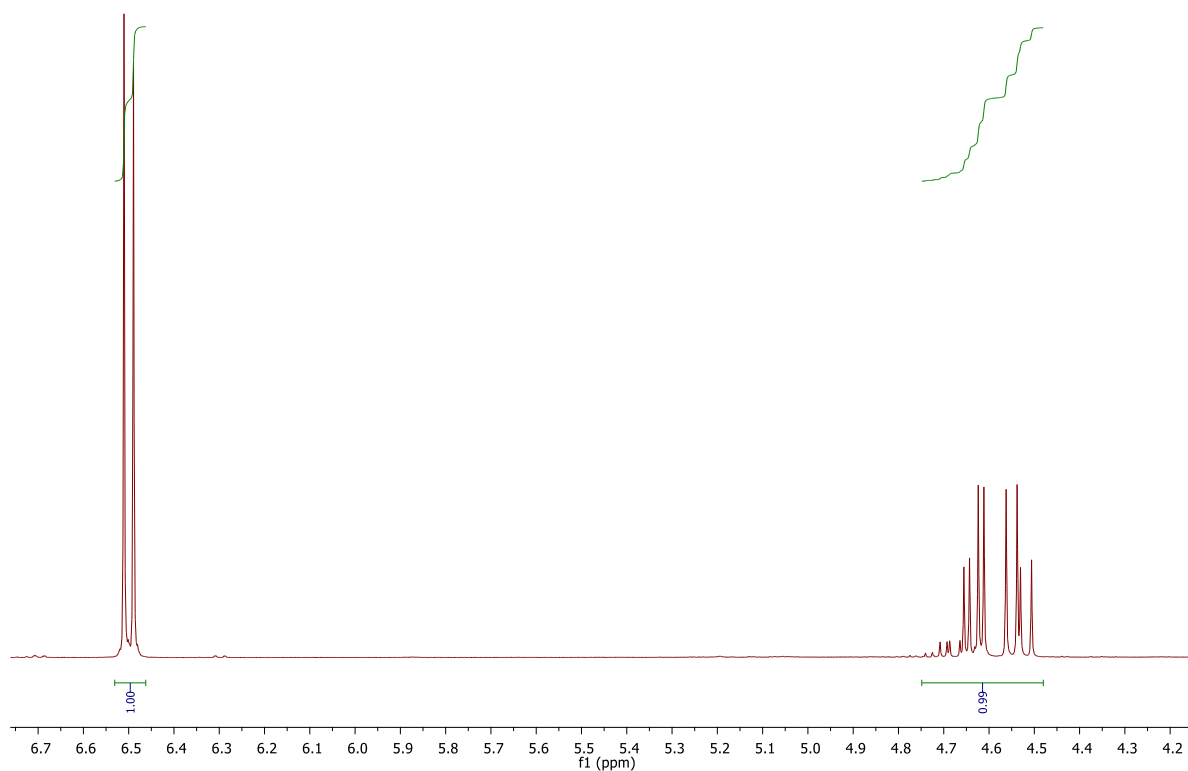
FIGURE 50. 400 MHz ^{1}H NMR spectrum in CDCl$_3$ of crude 2-ethyl-4-nitro-3-phenylbutanal obtained by the Michael reaction catalyzed by 10 mol% of compound **31** with 1,2,3-trimethoxybenzene as standard patron. Yield: 84%. Entry 8, TABLE 2.
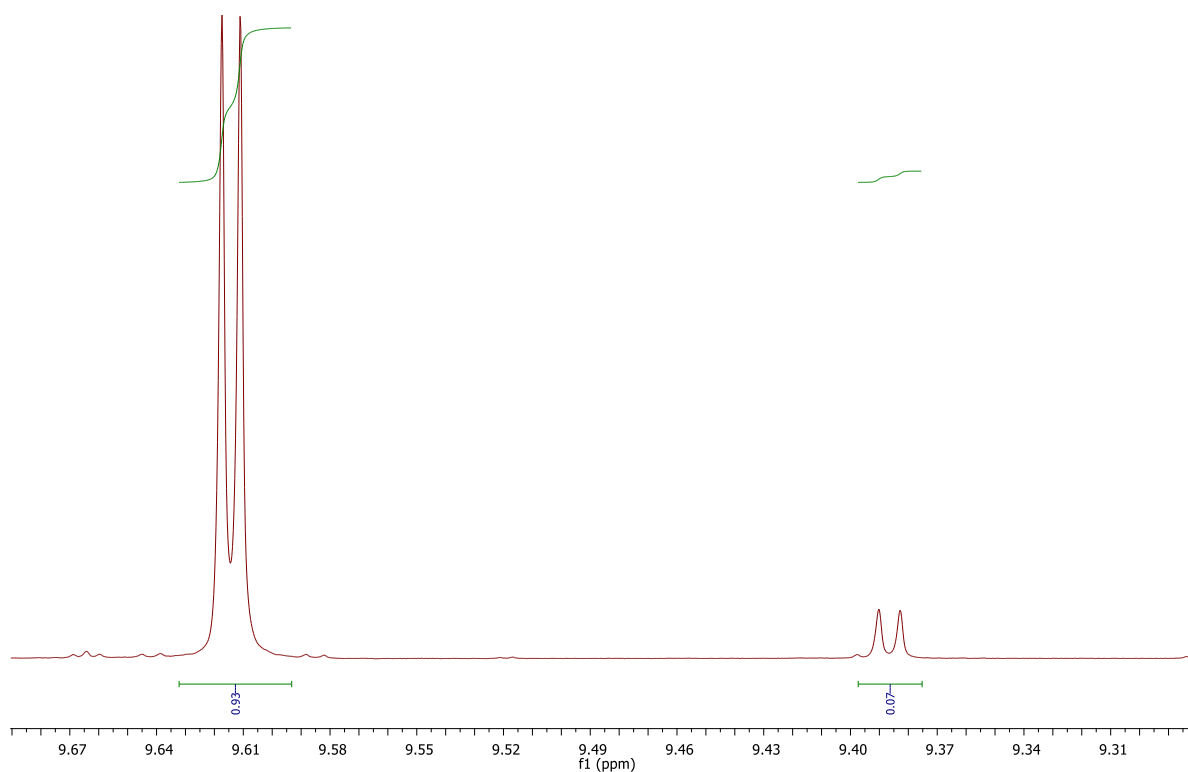

FIGURE 51. 400 MHz ^{1}H NMR spectrum in CDCl$_3$ of crude 2-ethyl-4-nitro-3-phenylbutanal obtained by the Michael reaction catalyzed by 10 mol% of compound **31**. Diastereoisomeric ratio (syn/anti): 79:21. Entry 8, TABLE 2.
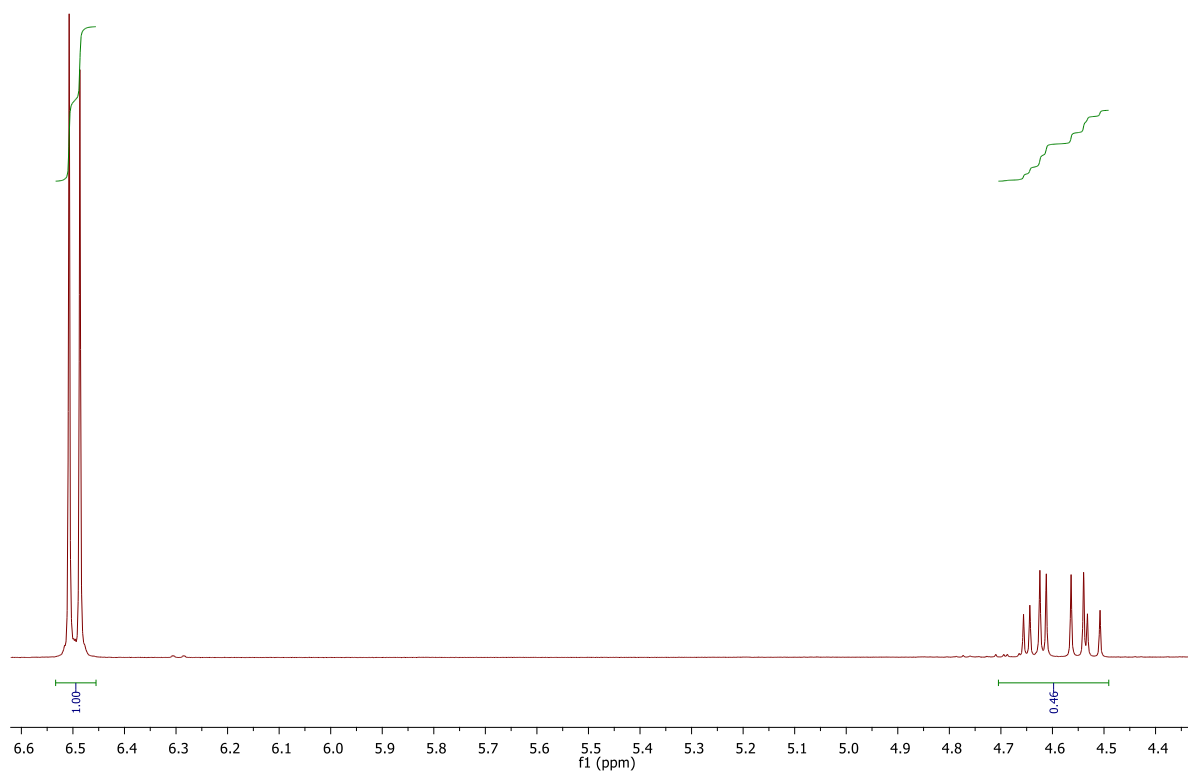
FIGURE 52. 400 MHz ^{1}H NMR spectrum in CDCl$_3$ of crude 2-ethyl-4-nitro-3-phenylbutanal obtained by the Michael reaction catalyzed by 10 mol% of compound **28** with 1,2,3-trimethoxybenzene as standard patron. Yield: 76%. Entry 1, TABLE 3.

FIGURE 53. 400 MHz ^{1}H NMR spectrum in CDCl$_3$ of crude 2-ethyl-4-nitro-3-phenylbutanal obtained by the Michael reaction catalyzed by 10 mol% of compound **28**. Diastereoisomeric ratio (syn/anti): 87:13. Entry 1, TABLE 3.

FIGURE 54. 400 MHz ^{1}H NMR spectrum in CDCl$_3$ of crude 2-ethyl-4-nitro-3-phenylbutanal obtained by the Michael reaction catalyzed by 10 mol% of compound **28** with 1,2,3-trimethoxybenzene as standard patron. Yield: 87%. Entry 2, TABLE 3.
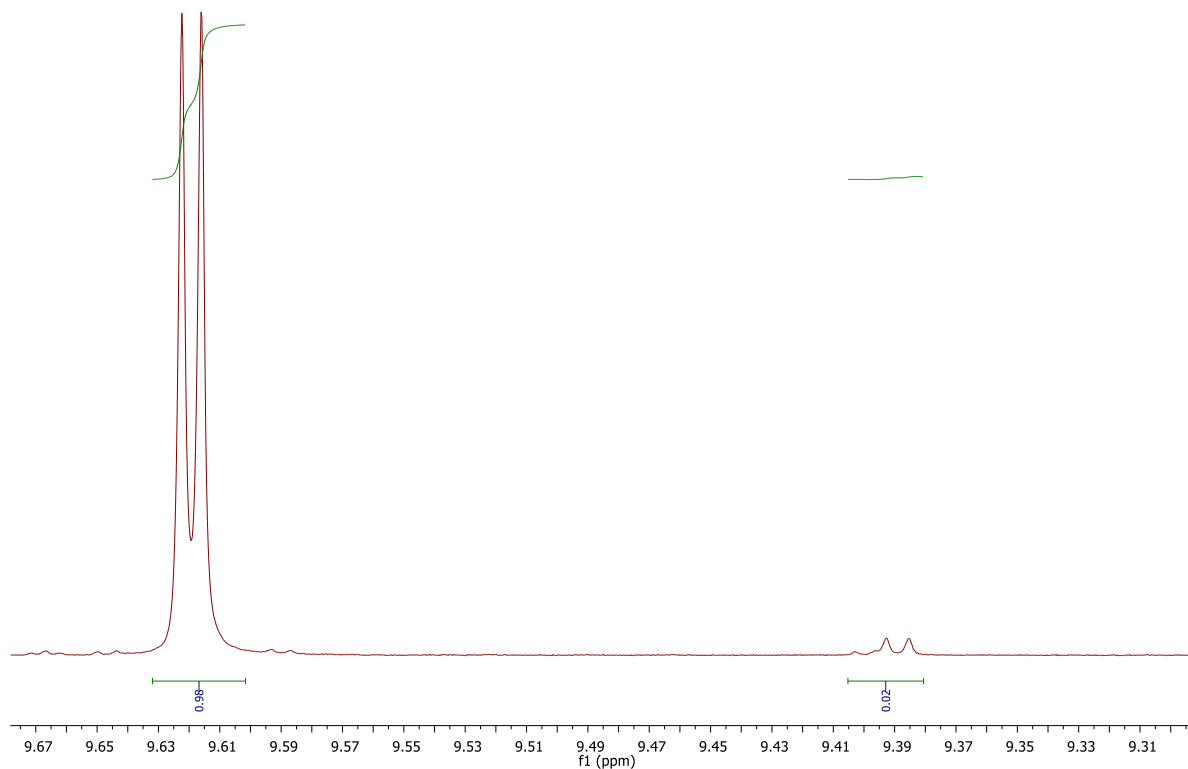

FIGURE 55. 400 MHz ^{1}H NMR spectrum in CDCl$_3$ of crude 2-ethyl-4-nitro-3-phenylbutanal obtained by the Michael reaction catalyzed by 10 mol% of compound **28**. Diastereoisomeric ratio (syn/anti): 76:24. Entry 2, TABLE 3.
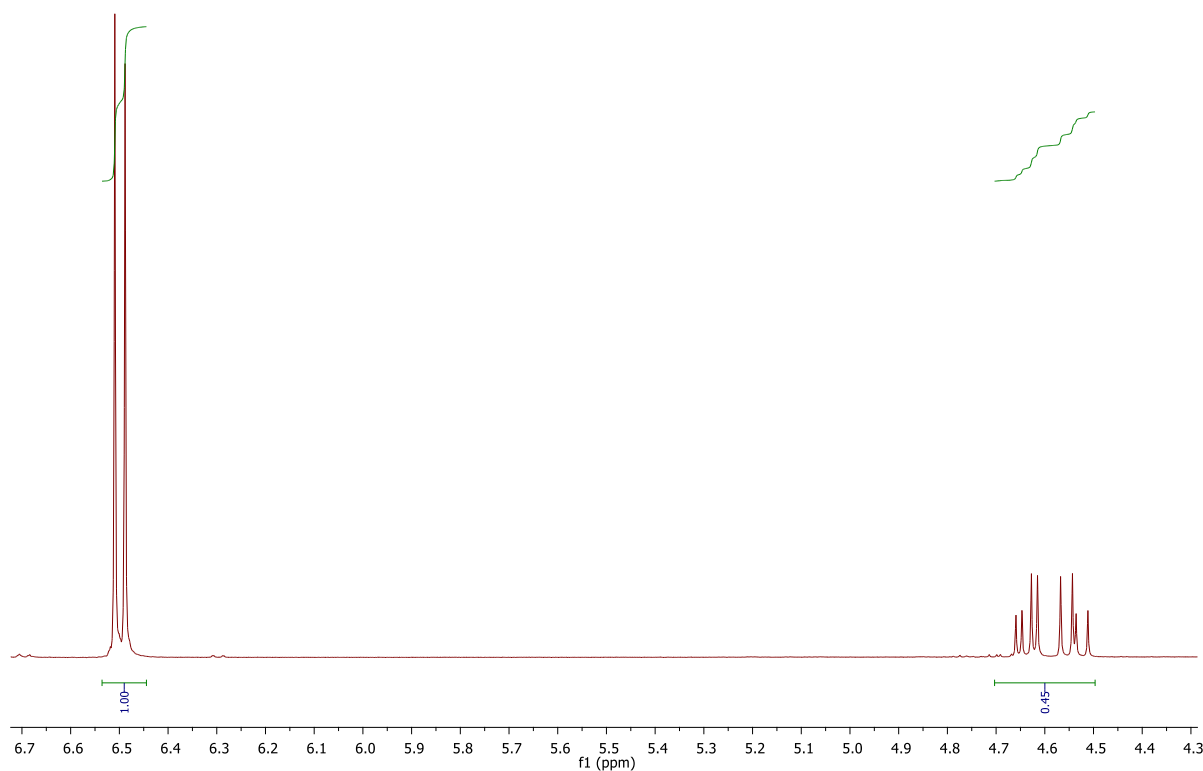
FIGURE 56. 400 MHz ^{1}H NMR spectrum in CDCl$_3$ of crude 2-ethyl-4-nitro-3-phenylbutanal obtained by the Michael reaction catalyzed by 5 mol% of compound **28** with 1,2,3-trimethoxybenzene as standard patron. Yield: 90%. Entry 3, TABLE 3.
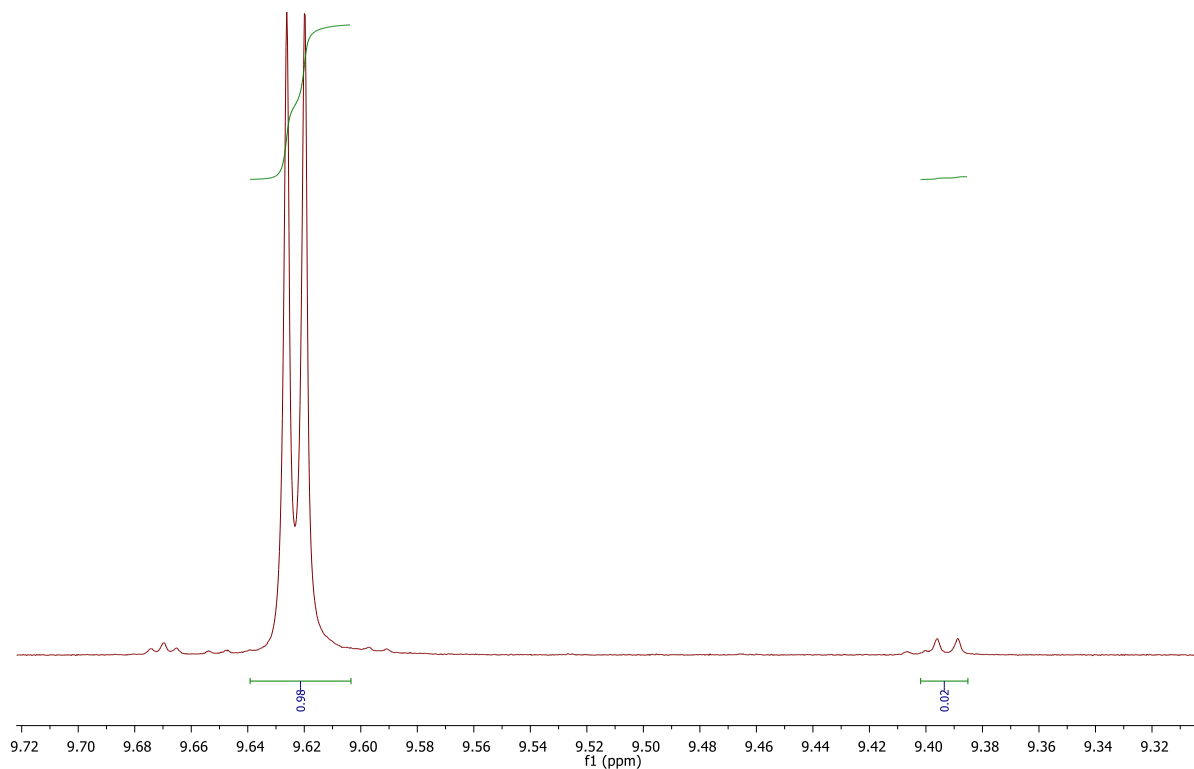

FIGURE 57. 400 MHz ^{1}H NMR spectrum in CDCl$_3$ of crude 2-ethyl-4-nitro-3-phenylbutanal obtained by the Michael reaction catalyzed by 5 mol% of compound **28**. Diastereoisomeric ratio (syn/anti): 90:10. Entry 3, TABLE 3.
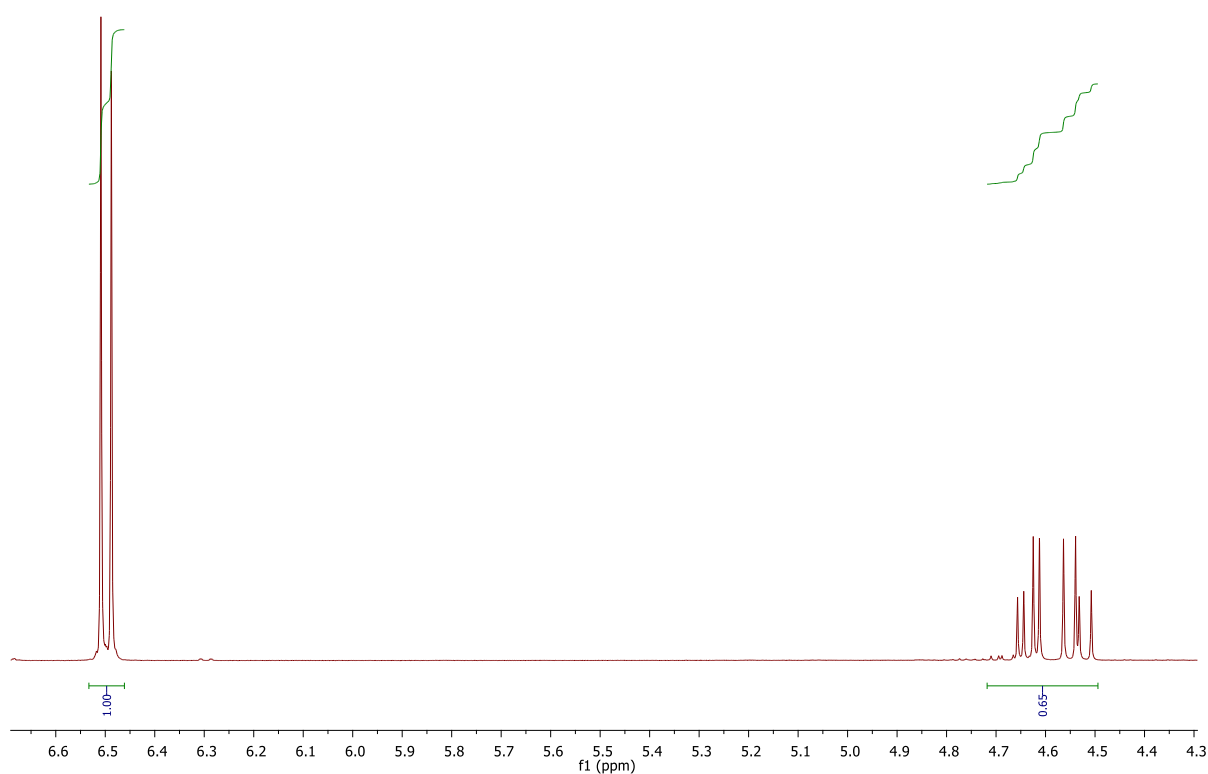
FIGURE 58. 400 MHz ^{1}H NMR spectrum in CDCl$_3$ of crude 2-ethyl-4-nitro-3-phenylbutanal obtained by the Michael reaction catalyzed by 2.5 mol% of compound **28** with 1,2,3-trimethoxybenzene as standard patron. Yield: 95%. Entry 4, TABLE 3.
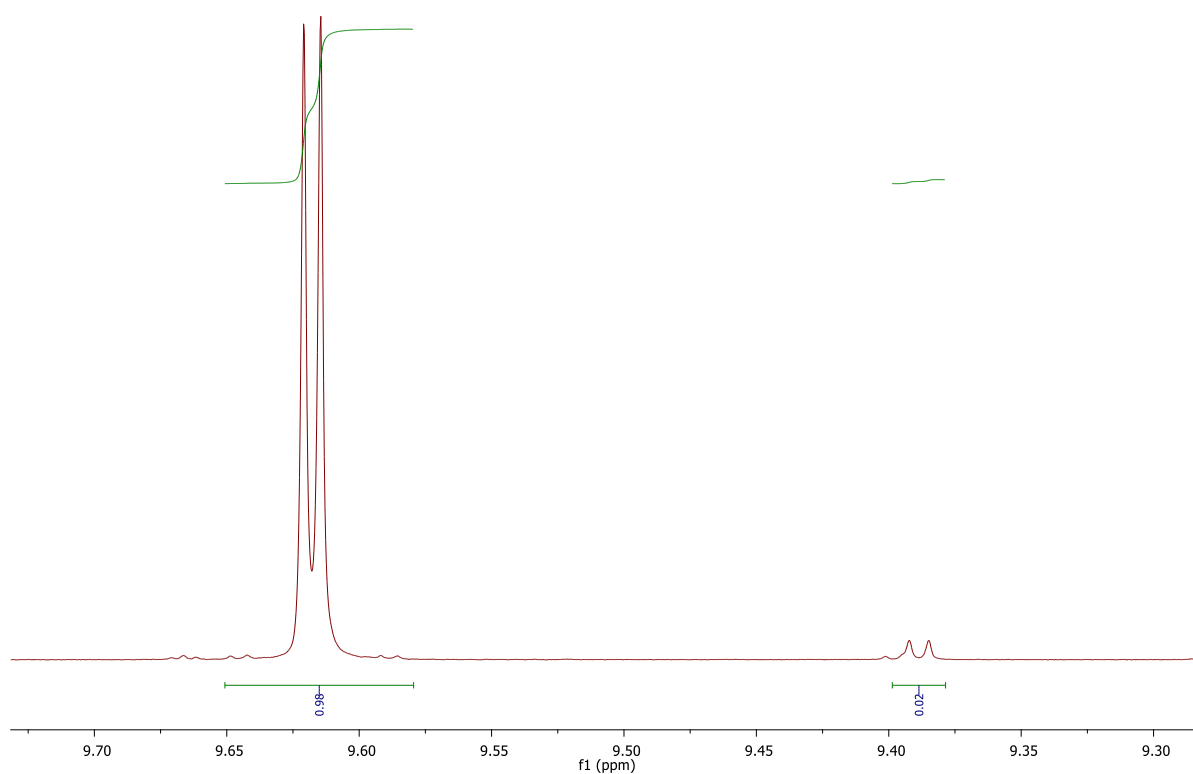

FIGURE 59. 400 MHz ^{1}H NMR spectrum in CDCl$_3$ of crude 2-ethyl-4-nitro-3-phenylbutanal obtained by the Michael reaction catalyzed by 2.5 mol% of compound **28**. Diastereoisomeric ratio (syn/anti): 93:7. Entry 4, TABLE 3.

FIGURE 60. 400 MHz ^{1}H NMR spectrum in CDCl$_3$ of crude 2-ethyl-4-nitro-3-phenylbutanal obtained by the Michael reaction catalyzed by 2.5 mol% of compound **28** with 1,2,3-trimethoxybenzene as standard patron. Yield: 96%. Entry 5, TABLE 3.

FIGURE 61. 400 MHz ^{1}H NMR spectrum in CDCl$_3$ of crude 2-ethyl-4-nitro-3-phenylbutanal obtained by the Michael reaction catalyzed by 2.5 mol% of compound **28**. Diastereoisomeric ratio (syn/anti): 93:7. Entry 5, TABLE 3.
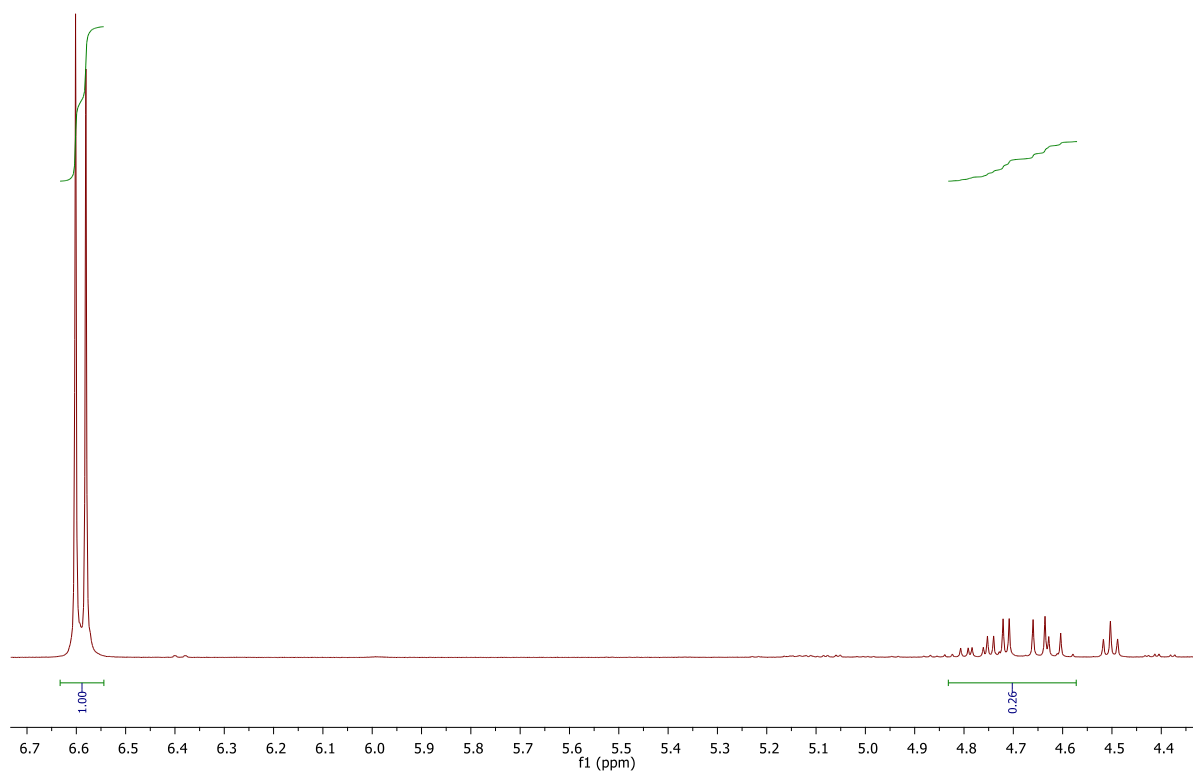
FIGURE 62. 400 MHz ^{1}H NMR spectrum in CDCl$_3$ of crude 2-ethyl-4-nitro-3-phenylbutanal obtained by the Michael reaction catalyzed by 2.5 mol% of compound **28** with 1,2,3-trimethoxybenzene as standard patron. Yield: 99%. Entry 6, TABLE 3 and TABLE 4, compound **34**.
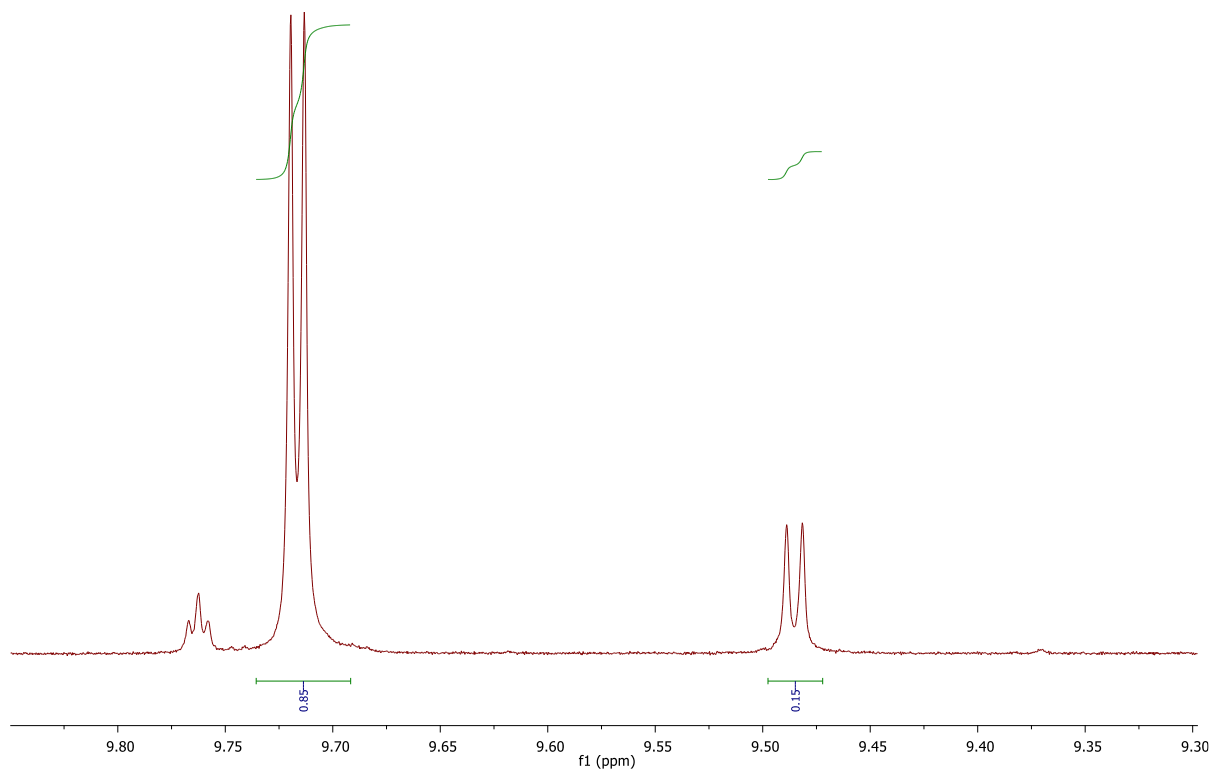

FIGURE 63. 400 MHz ^{1}H NMR spectrum in CDCl$_3$ of crude 2-ethyl-4-nitro-3-phenylbutanal obtained by the Michael reaction catalyzed by 2.5 mol% of compound **28**. Diastereoisomeric ratio (syn/anti): 93:7. Entry 6, TABLE 3 and TABLE 4, compound **34**.
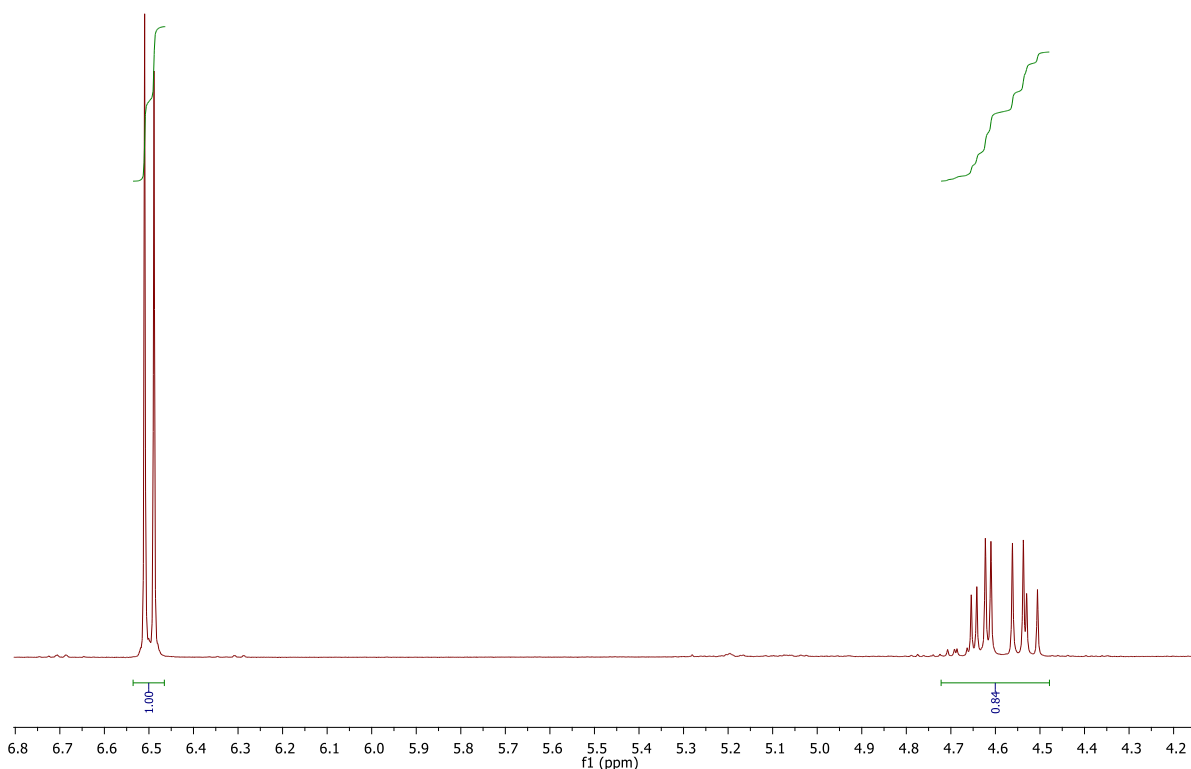
FIGURE 64. 400 MHz ^{1}H NMR spectrum in CDCl$_3$ of crude 2-ethyl-4-nitro-3-phenylbutanal obtained by the Michael reaction catalyzed by 1 mol% of compound **28** with 1,2,3-trimethoxybenzene as standard patron. Yield: 46%. Entry 7, TABLE 3.

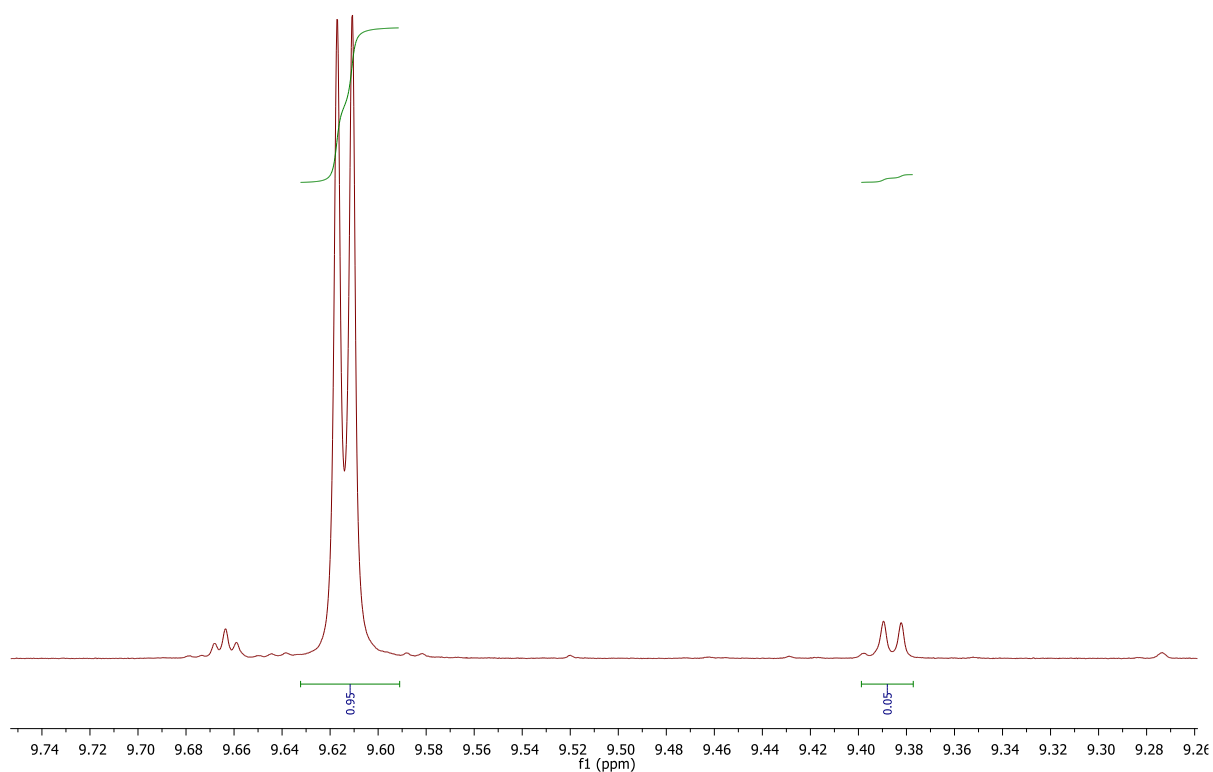**FIGURE 65.** 400 MHz ^{1}H NMR spectrum in CDCl$_3$ of crude 2-ethyl-4-nitro-3-phenylbutanal obtained by the Michael reaction catalyzed by 1 mol% of compound **28**. Diastereoisomeric ratio (syn/anti): 98:2. Entry 7, TABLE 3.
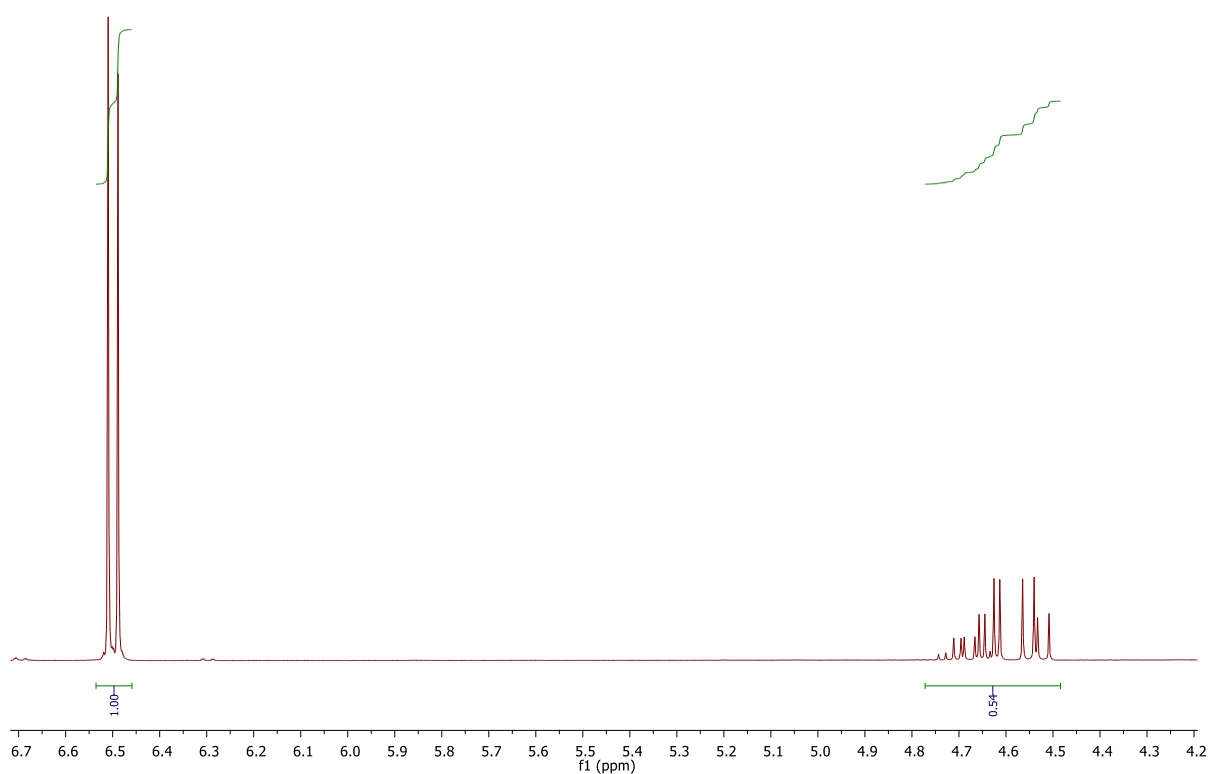
FIGURE 66. 400 MHz ^{1}H NMR spectrum in CDCl$_3$ of crude 2-ethyl-4-nitro-3-phenylbutanal obtained by the Michael reaction catalyzed by 1 mol% of compound **28** with 1,2,3-trimethoxybenzene as standard patron. Yield: 45%. Entry 8, TABLE 3.
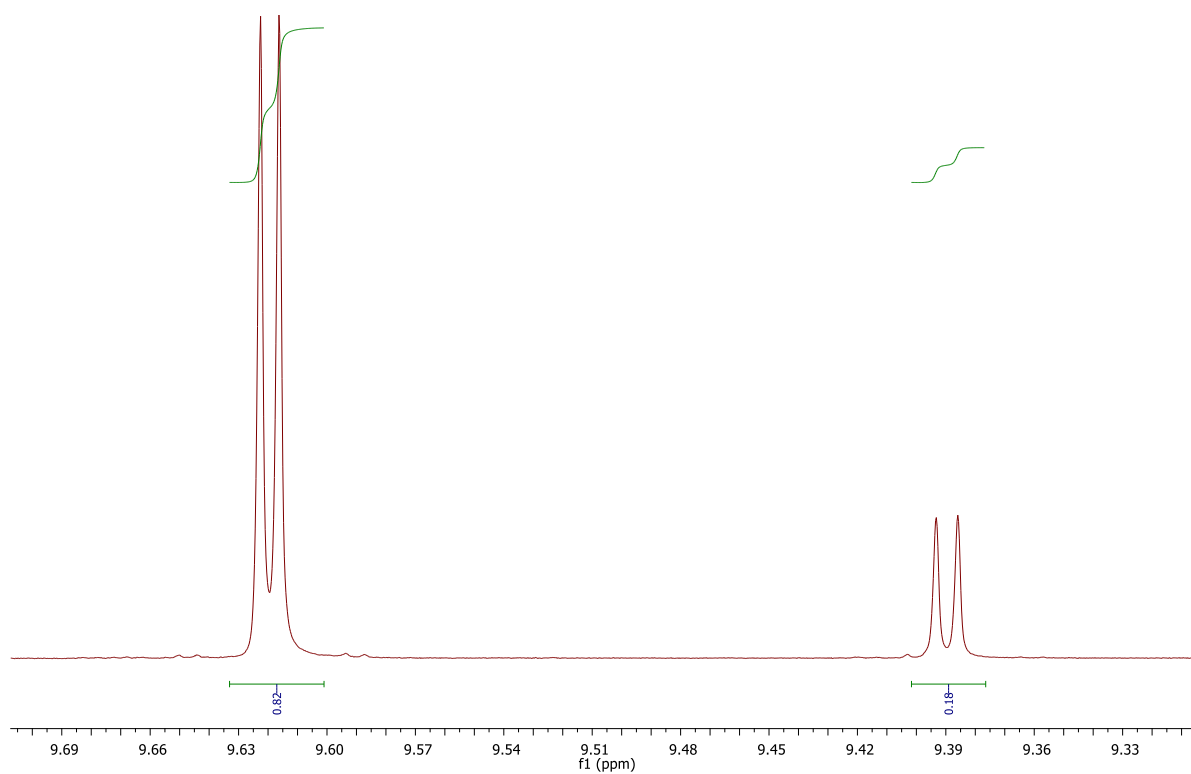

FIGURE 67. 400 MHz ^{1}H NMR spectrum in CDCl$_3$ of crude 2-ethyl-4-nitro-3-phenylbutanal obtained by the Michael reaction catalyzed by 1 mol% of compound **28**. Diastereoisomeric ratio (syn/anti): 98:2. Entry 8, TABLE 3.

FIGURE 68. 400 MHz ^{1}H NMR spectrum in CDCl$_3$ of crude 2-ethyl-4-nitro-3-phenylbutanal obtained by the Michael reaction catalyzed by 1 mol% of compound **28** with 1,2,3-trimethoxybenzene as standard patron. Yield: 65%. Entry 9, TABLE 3.

FIGURE 69. 400 MHz ^{1}H NMR spectrum in CDCl$_3$ of crude 2-ethyl-4-nitro-3-phenylbutanal obtained by the Michael reaction catalyzed by 1 mol% of compound **28**. Diastereoisomeric ratio (syn/anti): 98:2. Entry 9, TABLE 3.

FIGURE 70. 400 MHz ^{1}H NMR spectrum in CDCl$_3$ of crude 2-ethyl-4-nitro-3-phenylbutanal obtained by the Michael reaction catalyzed by 2.5 mol% of compound **28** in EtOH with 1,2,3-trimethoxybenzene as standard patron. Yield: 26%. Entry 10, TABLE 3.

FIGURE 71. 400 MHz ^{1}H NMR spectrum in CDCl$_3$ of crude 2-ethyl-4-nitro-3-phenylbutanal obtained by the Michael reaction catalyzed by 2.5 mol% of compound **28** in MeOH. Diastereoisomeric ratio (syn/anti): 85:15. Entry 10, TABLE 3.

FIGURE 72. 400 MHz ^{1}H NMR spectrum in CDCl$_3$ of crude 2-ethyl-4-nitro-3-phenylbutanal obtained by the Michael reaction catalyzed by 2.5 mol% of compound **28** in Brine with 1,2,3-trimethoxybenzene as standard patron. Yield: 84%. Entry 11, TABLE 3.

FIGURE 73. 400 MHz ^{1}H NMR spectrum in CDCl$_3$ of crude 2-ethyl-4-nitro-3-phenylbutanal obtained by the Michael reaction catalyzed by 2.5 mol% of compound **28** in Brine. Diastereoisomeric ratio (syn/anti): 95:5. Entry 11, TABLE 3.

FIGURE 74. 400 MHz ^{1}H NMR spectrum in CDCl$_3$ of crude 2-ethyl-4-nitro-3-phenylbutanal obtained by the Michael reaction catalyzed by 2.5 mol% of compound **28** in PEG-300 with 1,2,3-trimethoxybenzene as standard patron. Yield: 54%. Entry 12, TABLE 3.

FIGURE 75. 400 MHz ^{1}H NMR spectrum in CDCl$_3$ of crude 2-ethyl-4-nitro-3-phenylbutanal obtained by the Michael reaction catalyzed by 2.5 mol% of compound **28** in PEG-300. Diastereoisomeric ratio (syn/anti): 82:18. Entry 12, TABLE 3.
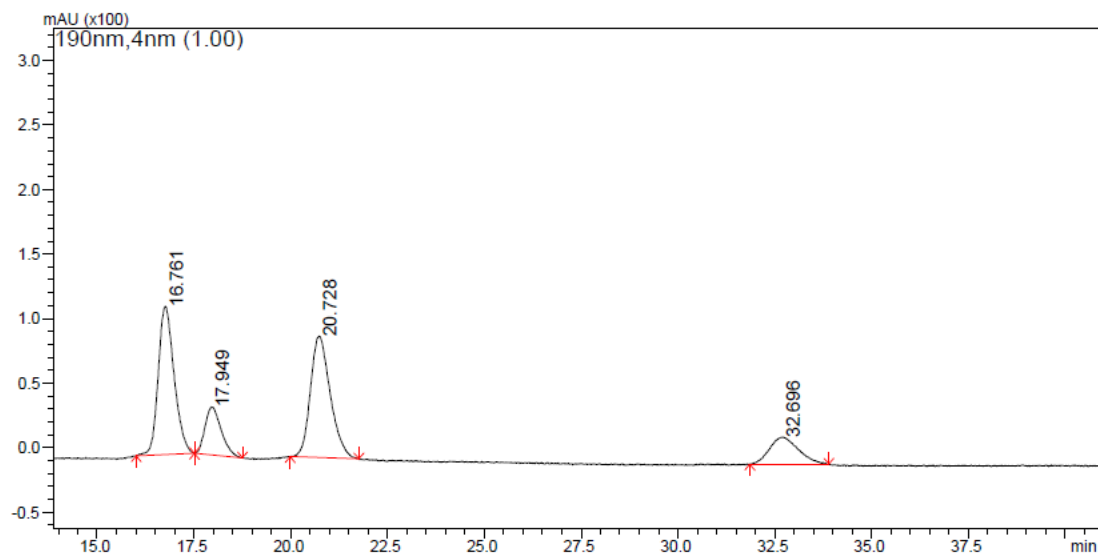
PeakTable

PDA Ch1 190nm 4nm

Peak#	Ret. Time	Area	Height	Area %	Height %
1	16.761	3284351	114890	37.327	43.054
2	17.949	1081130	37150	12.287	13.921
3	20.728	3351021	93999	38.085	35.225
4	32.696	1082358	20815	12.301	7.800
Total		8798860	266854	100.000	100.000

FIGURE 76. Chiral HPLC of racemic 2-ethyl-4-nitro-3-phenylbutanal. Chiralpak OD-H, *n*-Hexane/i-PrOH 85:15, 25°C) at 0.9 ml/min. UV detection at 190 nm.
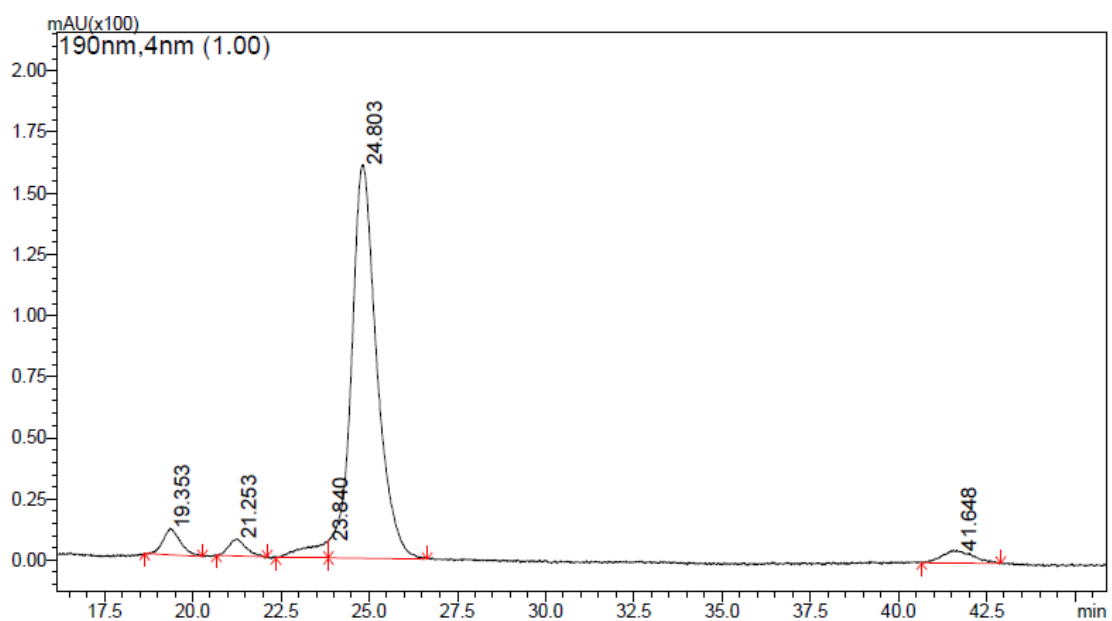
PeakTable

PDA Ch1 190nm 4nm

Peak#	Ret. Time	Area	Height	Area %	Height %
1	19.353	364981	10841	3.958	5.677
2	21.253	234312	7054	2.541	3.694
3	23.840	306958	6806	3.329	3.564
4	24.803	7999848	160922	86.760	84.267
5	41.648	314599	5344	3.412	2.799
Total		9220697	190967	100.000	100.000

FIGURE 77. Chiral HPLC of 2-ethyl-4-nitro-3-phenylbutanal obtained by the Michael reaction catalyzed by 10 mol% of compound **24**. Chiralpak OD-H, *n*-Hexane/i-PrOH 85:15, 25°C) at 0.9 ml/min. UV detection at 190 nm: tR: (syn, minor) = 19.4 min, (syn, major) = 24.8 min. TABLE 2, Entry 1.
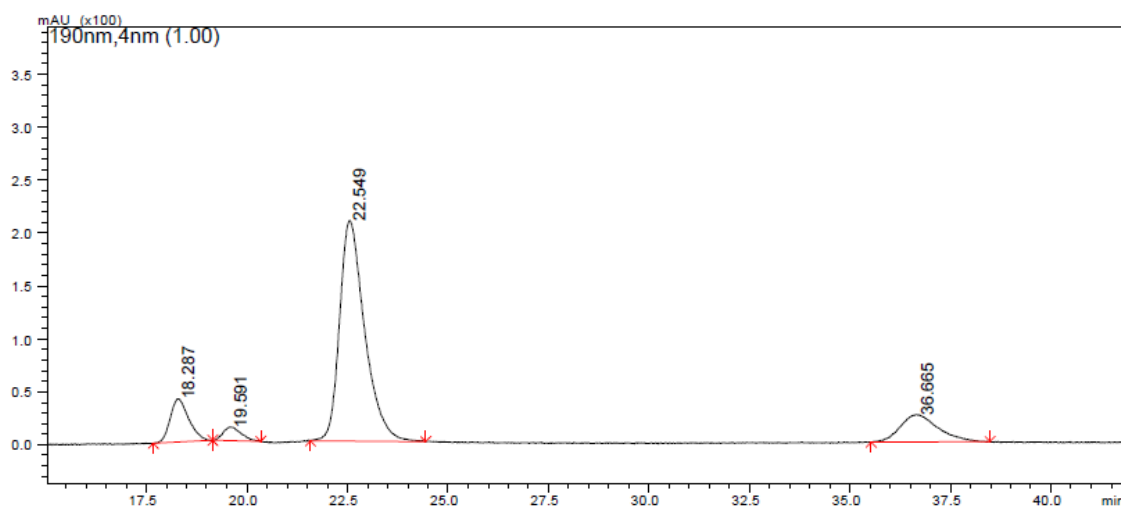

PeakTable

PDA Ch1 190nm 4nm

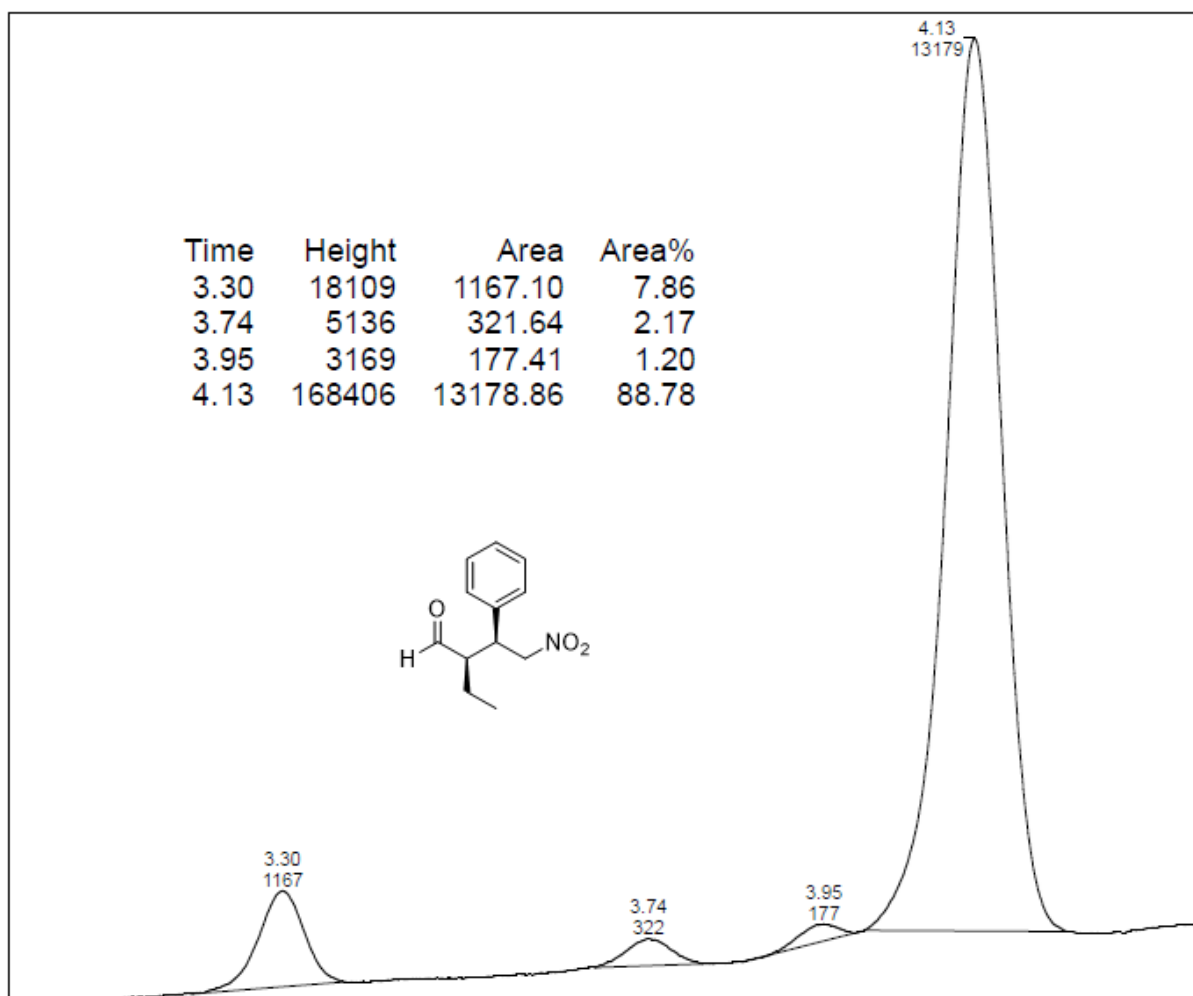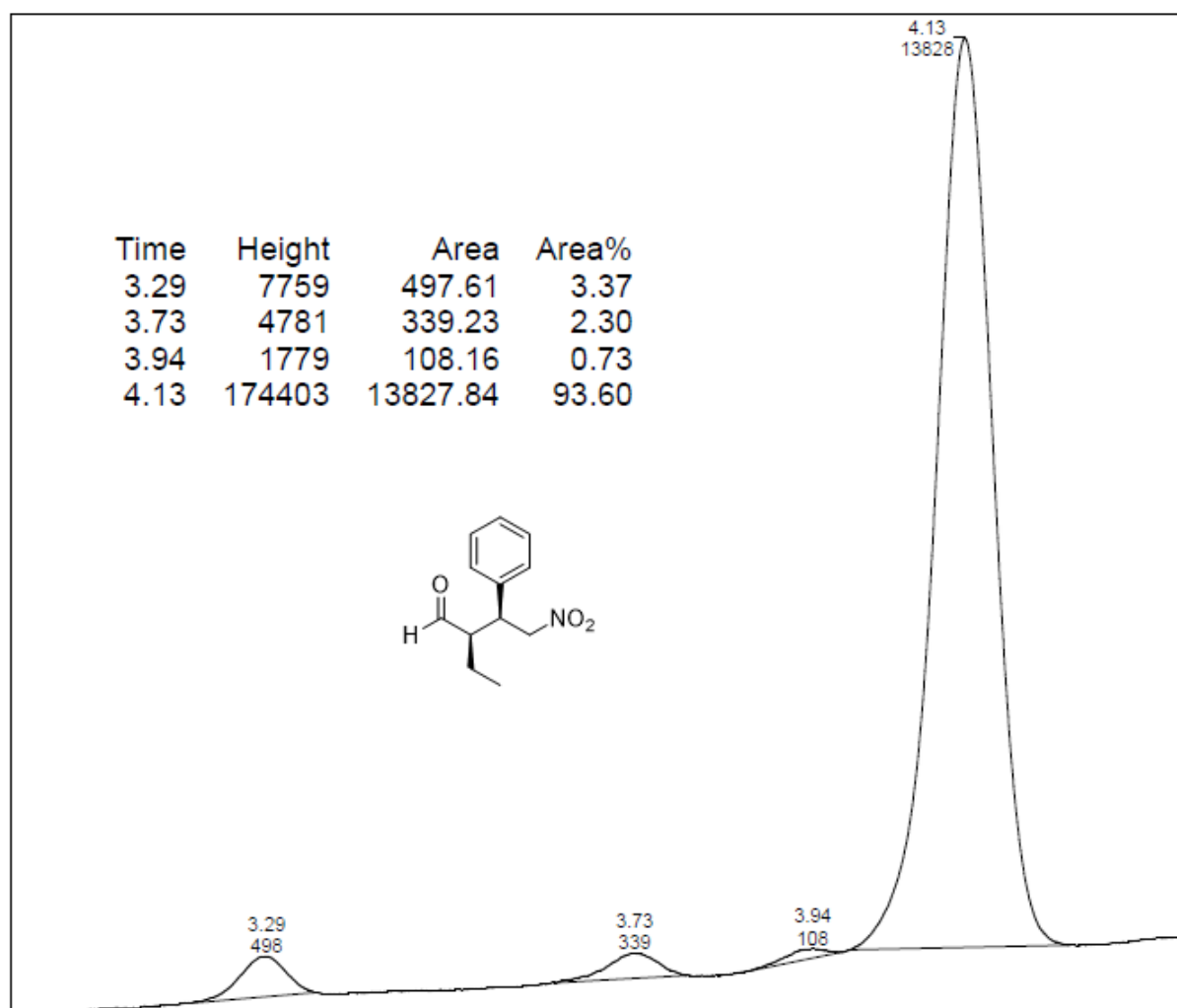| Peak#	Ret. Time	Area	Height	Area %	Height %
1	18.287	1297924	40704	10.437	14.134
2	19.591	402348	12930	3.235	4.490
3	22.549	9057294	208475	72.830	72.392
4	36.665	1678633	25872	13.498	8.984
Total		12436199	287981	100.000	100.000

FIGURE 78. Chiral HPLC of 2-ethyl-4-nitro-3-phenylbutanal obtained by the Michael reaction catalyzed by 10 mol% of compound **25**. Chiralpak OD-H, *n*-Hexane/i-PrOH 85:15, 25°C) at 0.9 ml/min. UV detection at 190 nm: tR: (syn, minor) = 18.3 min, (syn, major) = 22.5 min. TABLE 2, Entry 2.
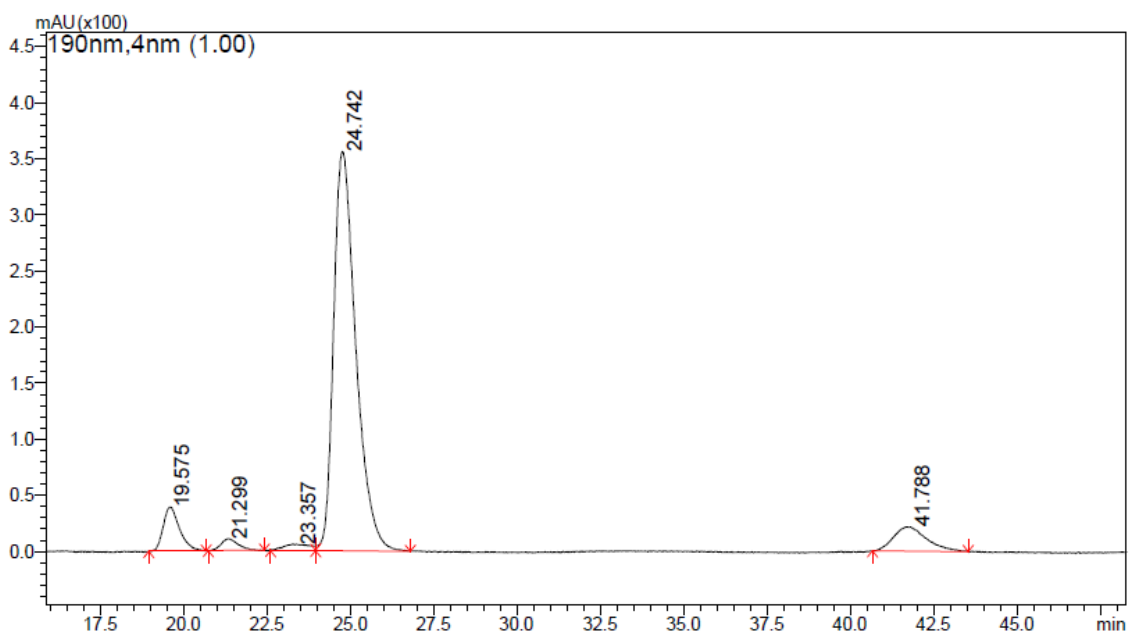
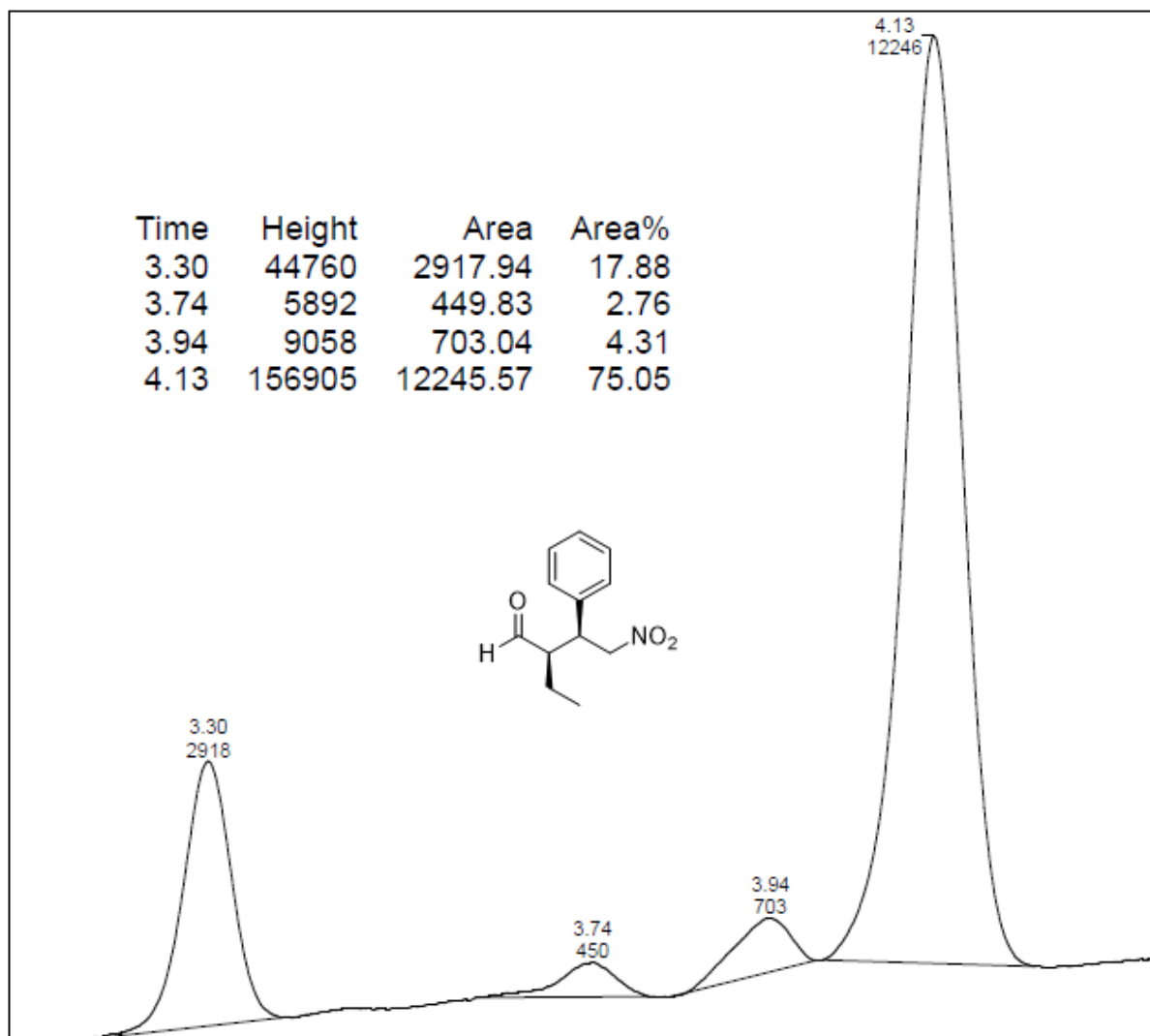| Peak#	Ret. Time	Area	Height	Area %	Height %
1	19.575	1358570	39463	6.787	9.107
2	21.299	355371	10376	1.775	2.395
3	23.357	314882	5755	1.573	1.328
4	24.742	16494758	356118	82.400	82.184
5	41.788	1494389	21605	7.465	4.986
Total		20017970	433317	100.000	100.000

FIGURE 79. Chiral HPLC of 2-ethyl-4-nitro-3-phenylbutanal obtained by the Michael reaction catalyzed by 10 mol% of compound **26**. Chiralpak OD-H, *n*-Hexane/i-PrOH 85:15, 25°C) at 0.9 ml/min. UV detection at 190 nm: tR: (syn, minor) = 19.6 min, (syn, major) = 24.7 min. TABLE 2, Entry 3.
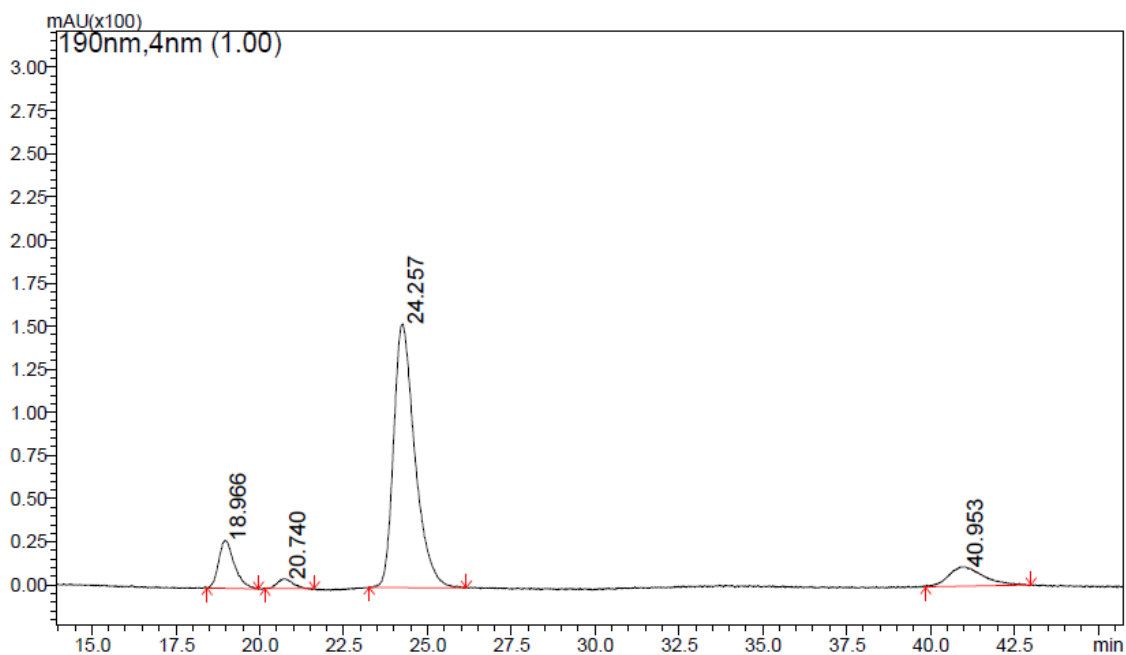
PeakTable

PDA Ch1 190nm 4nm

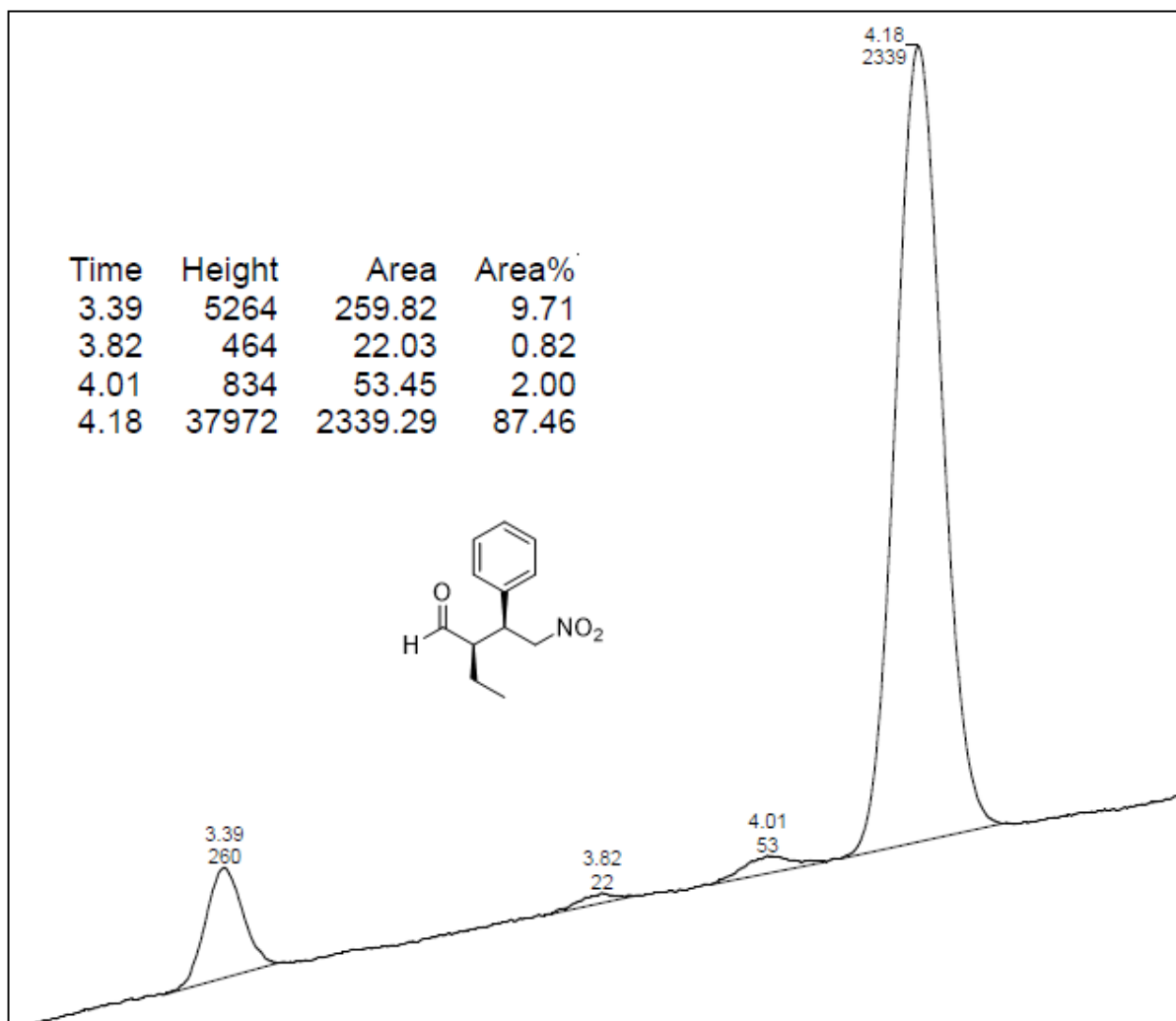| Peak#	Ret. Time	Area	Height	Area %	Height %
1	18.966	905344	27656	10.488	14.024
2	20.740	175717	5591	2.036	2.835
3	24.257	6747042	152748	78.161	77.458
4	40.953	804159	11206	9.316	5.683
Total		8632263	197201	100.000	100.000

FIGURE 80. Chiral HPLC of 2-ethyl-4-nitro-3-phenylbutanal obtained by the Michael reaction catalyzed by 10 mol% of compound **27**. Chiralpak OD-H, *n*-Hexane/i-PrOH 85:15, 25°C) at 0.9 ml/min. UV detection at 190 nm: tR: (syn, minor) = 19.0 min, (syn, major) = 24.3 min. TABLE 2, Entry 4.
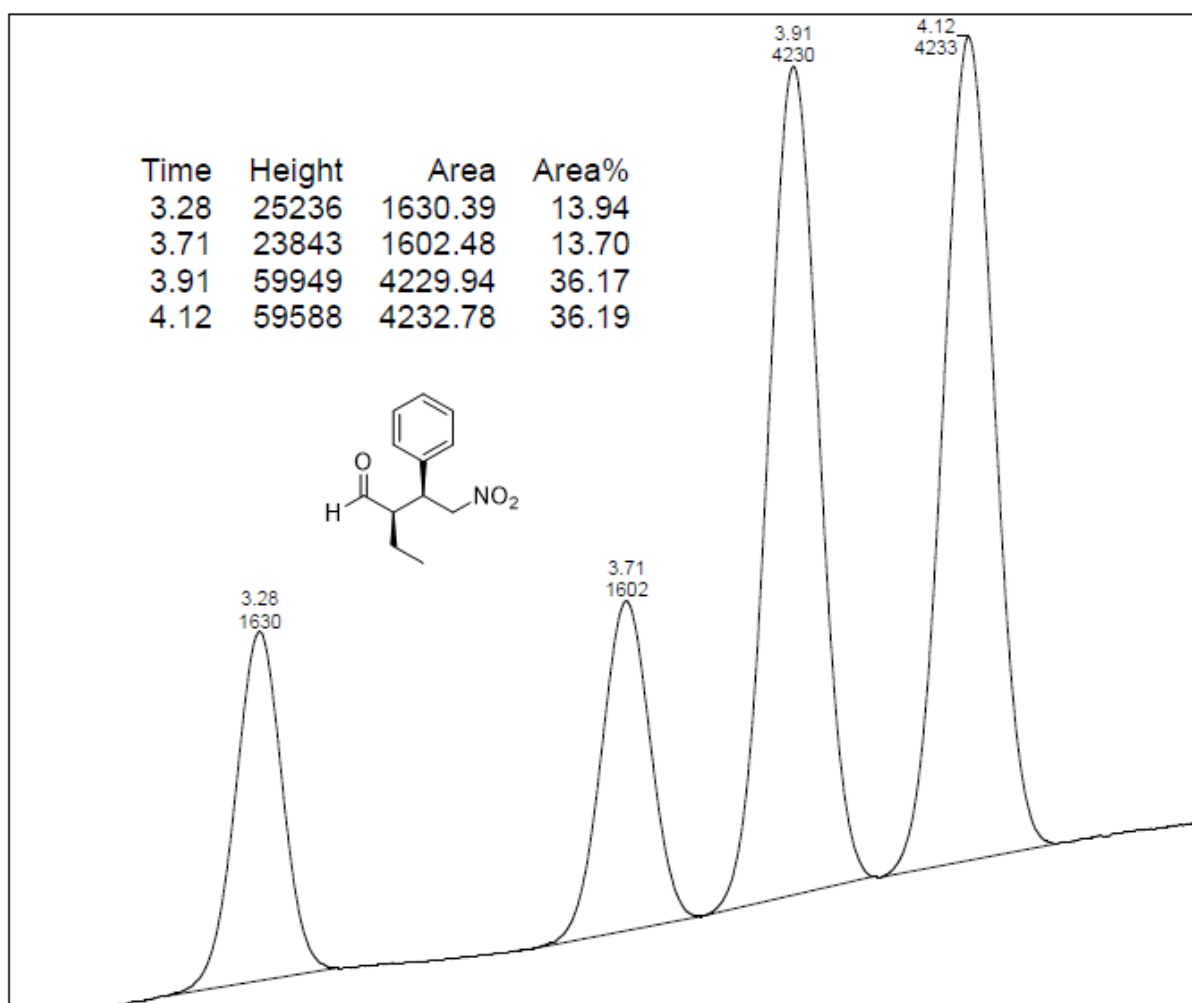
FIGURE 81. Chiral UPC^2 of racemic 2-ethyl-4-nitro-3-phenylbutanal. Trefoil CEL2, CO_2/EtOH 100-0% to 95-5 % in 10 min at 3 ml/min at 25°C. UV detection at 210 nm.

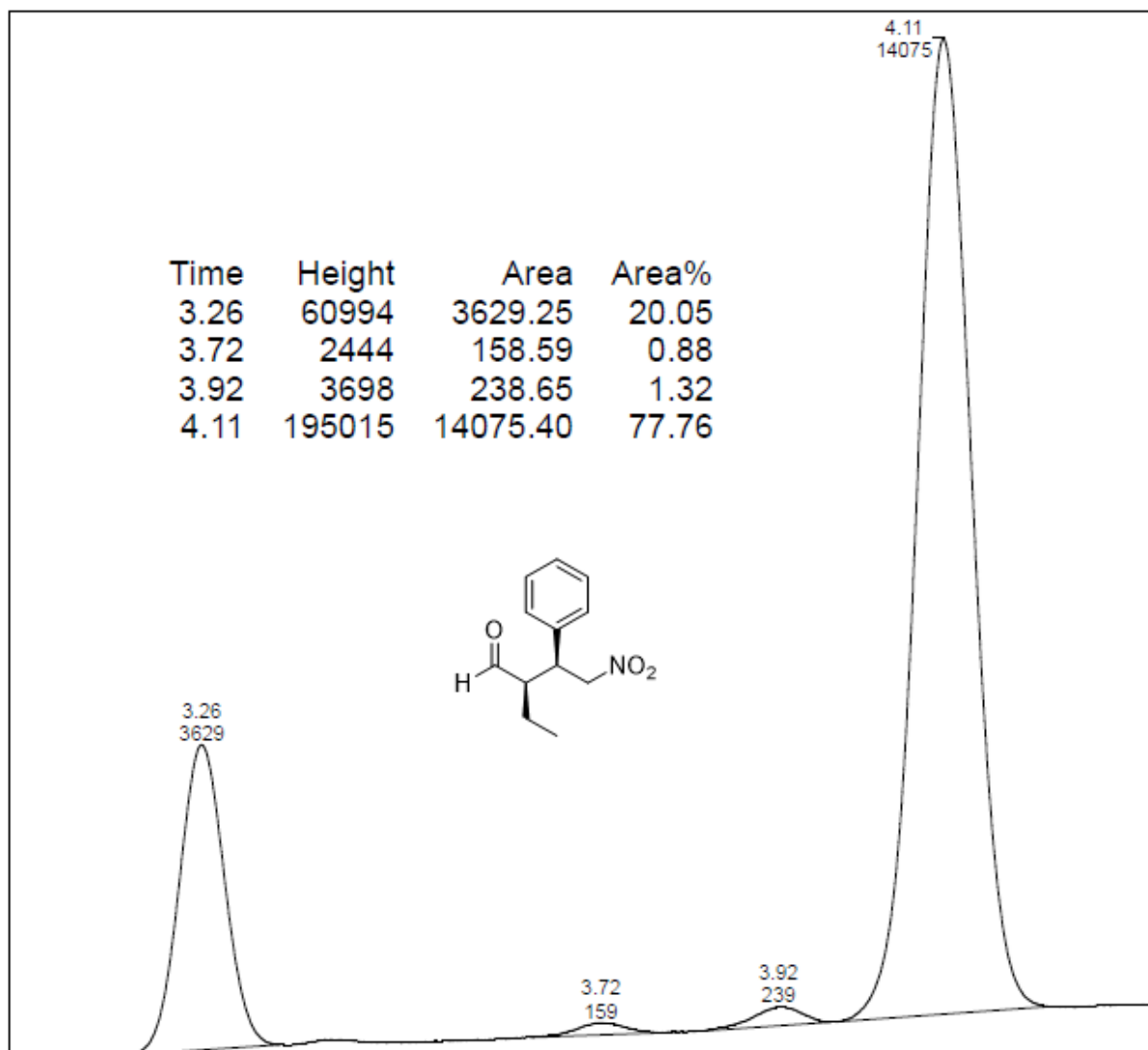| Time	Height	Area	Area%
3.30	18109	1167.10	7.86
3.74	5136	321.64	2.17
3.95	3169	177.41	1.20
4.13	168406	13178.86	88.78

FIGURE 82. Chiral UPC^2 of 2-ethyl-4-nitro-3-phenylbutanal obtained by the Michael reaction catalyzed by 10 mol% of compound **28**. Trefoil CEL2, CO_2/EtOH 100-0% to 95-5 % in 10 min at 3 ml/min at 25°C. UV detection at 210 nm: tR: (syn, minor) = 3.95 min, (syn, major) = 4.13 min. TABLE 2, Entry 5.
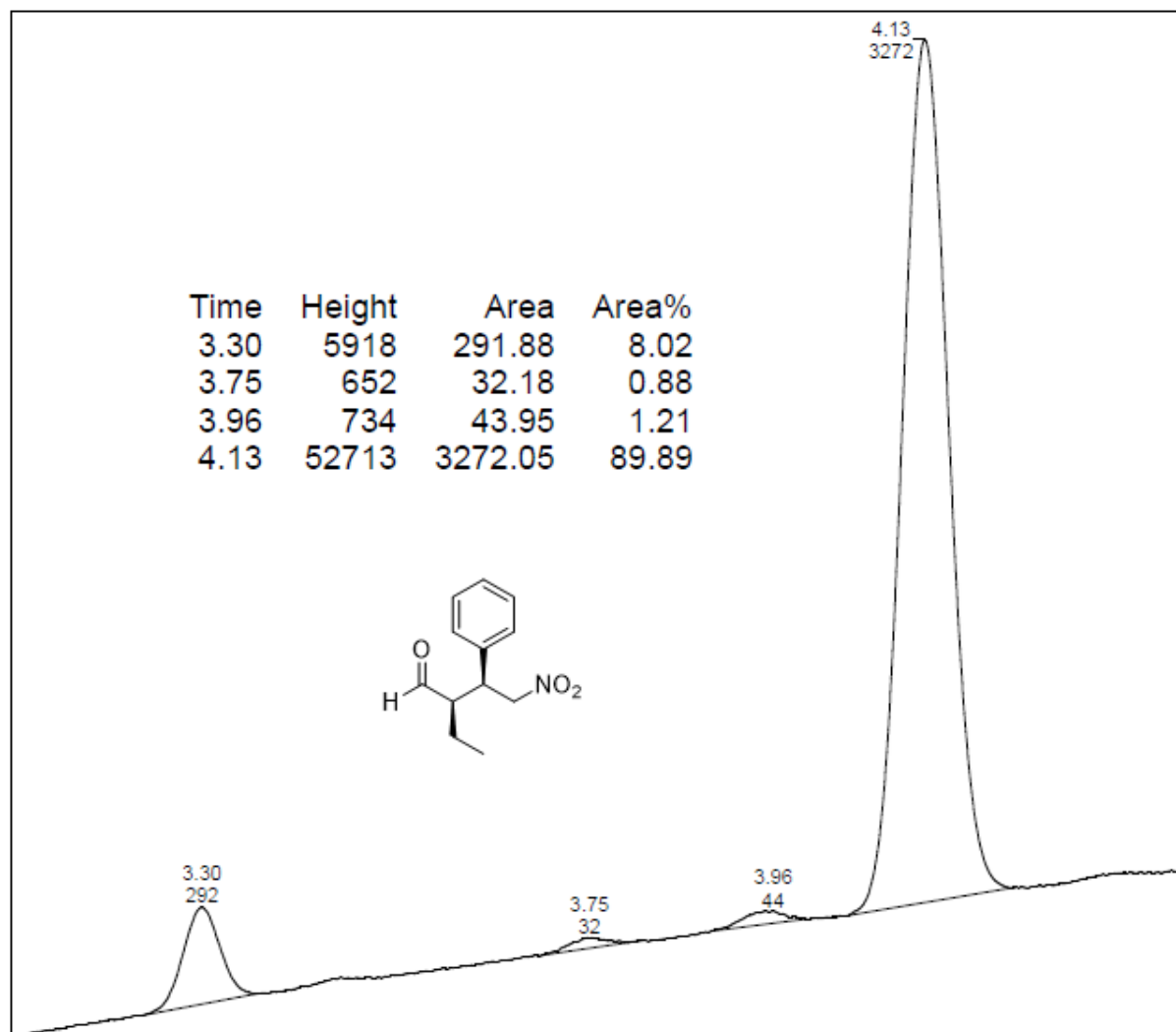
Time	Height	Area	Area%
3.29	7759	497.61	3.37
3.73	4781	339.23	2.30
3.94	1779	108.16	0.73
4.13	174403	13827.84	93.60

FIGURE 83. Chiral UPC^2 of 2-ethyl-4-nitro-3-phenylbutanal obtained by the Michael reaction catalyzed by 10 mol% of compound **29**. Trefoil CEL2, CO$_2$/EtOH 100-0% to 95-5 % in 10 min at 3 ml/min at 25°C. UV detection at 210 nm: tR: (syn, minor) = 3.94 min, (syn, major) = 4.13 min. TABLE 2, Entry 6.
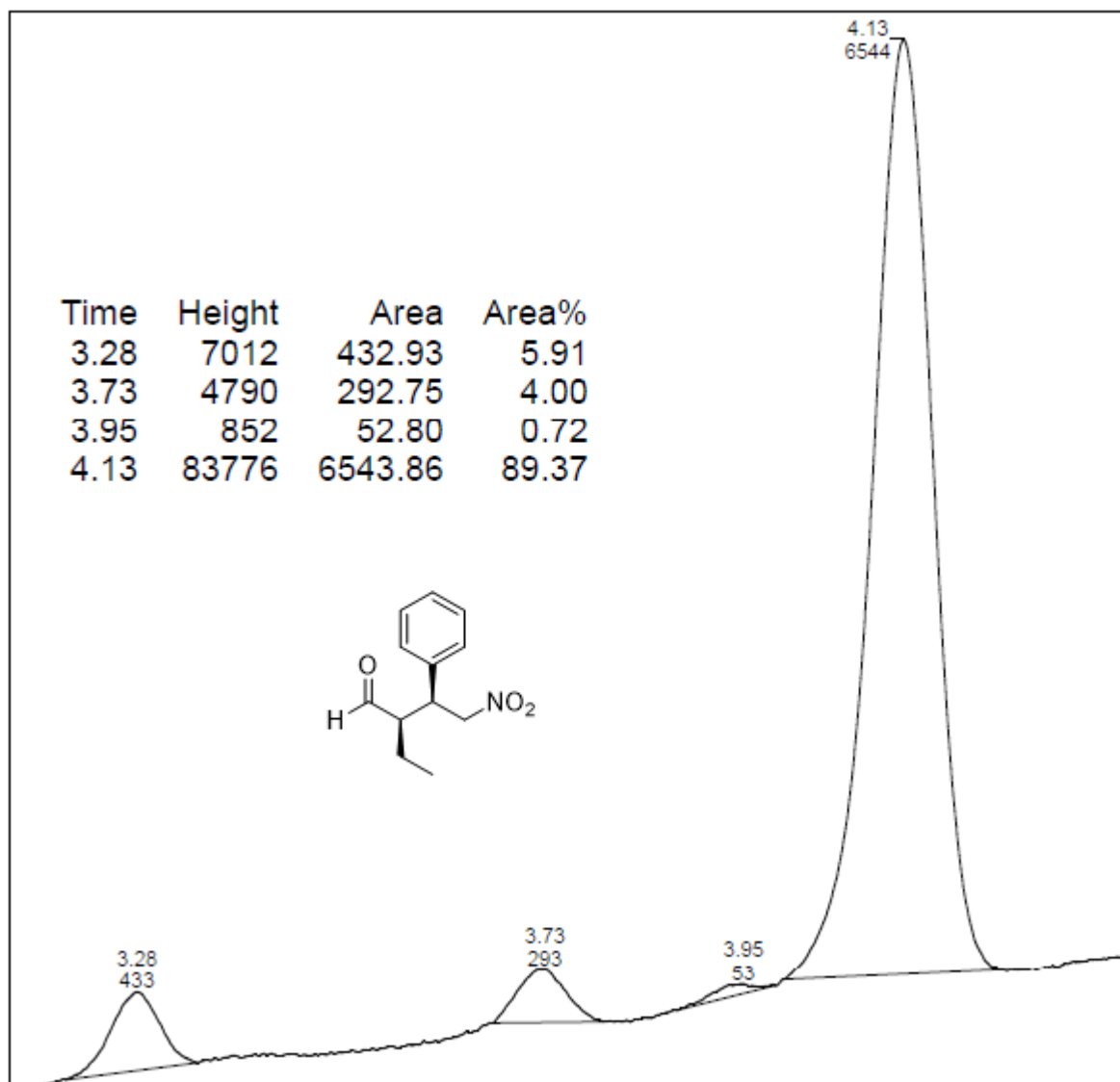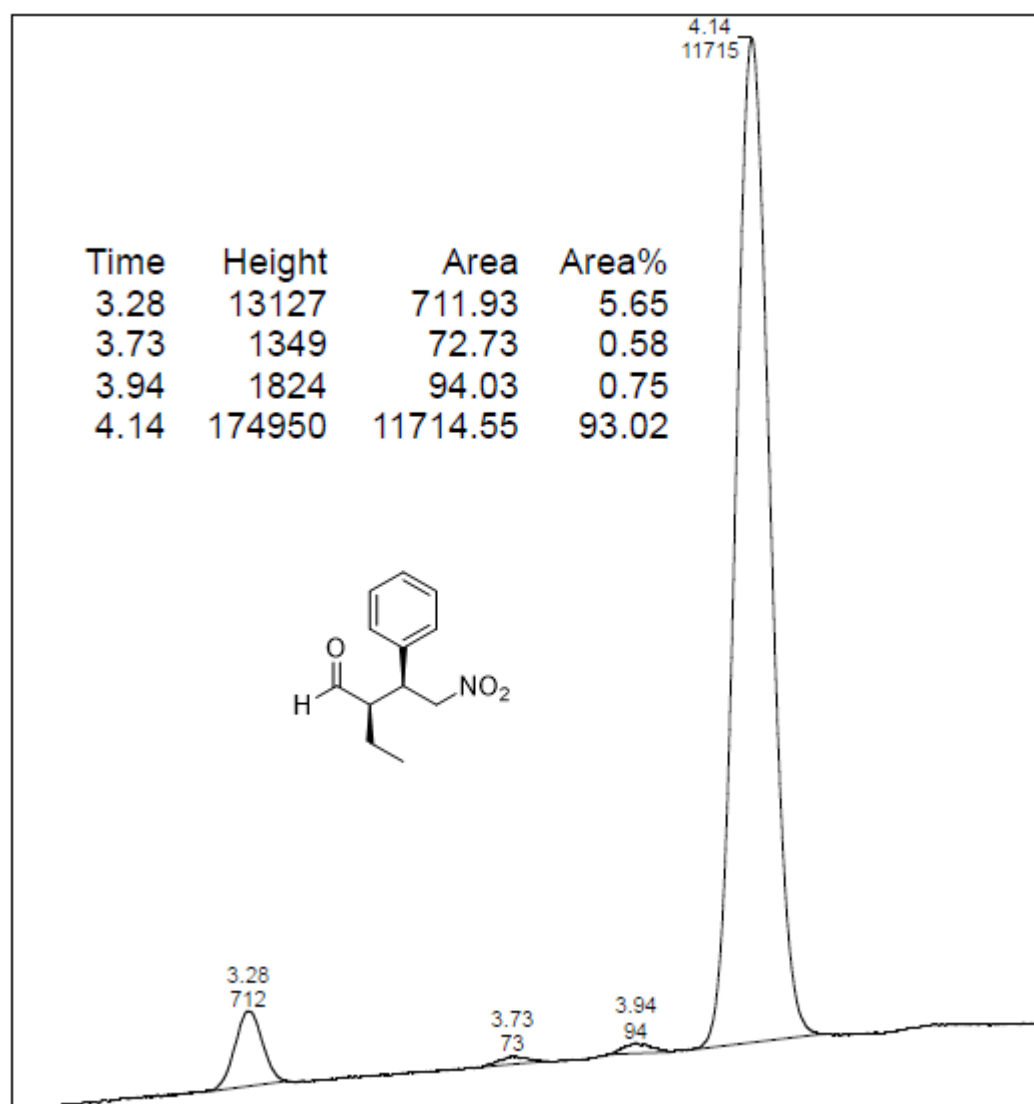
FIGURE 84. Chiral UPC^2 of 2-ethyl-4-nitro-3-phenylbutanal obtained by the Michael reaction catalyzed by 10 mol% of compound **30**. Trefoil CEL2, CO$_2$/EtOH 100-0% to 95-5 % in 10 min at 3 ml/min at 25°C. UV detection at 210 nm: tR: (syn, minor) = 3.95 min, (syn, major) = 4.13 min. TABLE 2, Entry 7.

Time	Height	Area	Area%
3.30	44760	2917.94	17.88
3.74	5892	449.83	2.76
3.94	9058	703.04	4.31
4.13	156905	12245.57	75.05

FIGURE 85. Chiral UPC^2 of 2-ethyl-4-nitro-3-phenylbutanal obtained by the Michael reaction catalyzed by 10 mol% of compound **31**. Trefoil CEL2, CO_2/EtOH 100-0% to 95-5 % in 10 min at 3 ml/min at 25°C. UV detection at 210 nm: tR: (syn, minor) = 3.94 min, (syn, major) = 4.13 min. TABLE 2, Entry 8.

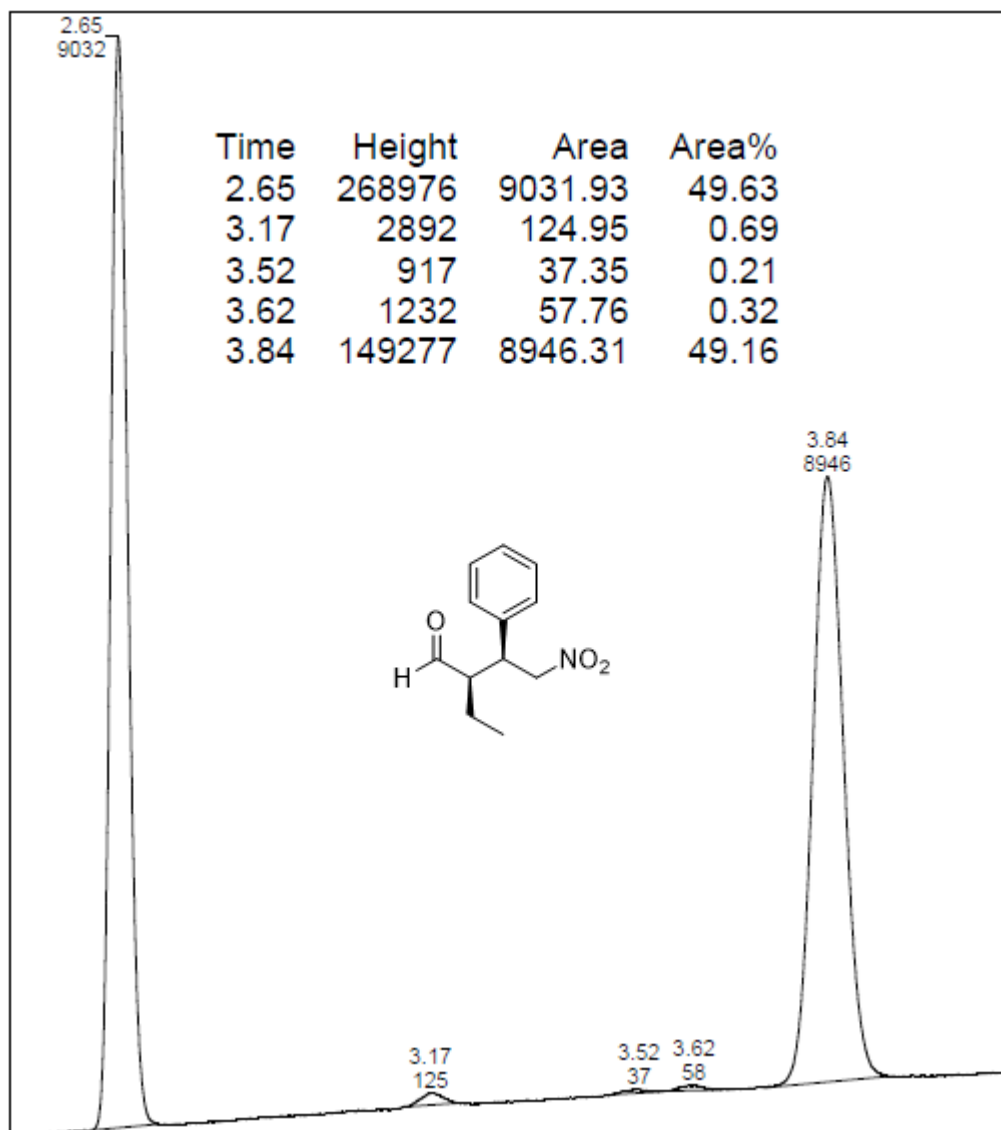| Time	Height	Area	Area%
3.39	5264	259.82	9.71
3.82	464	22.03	0.82
4.01	834	53.45	2.00
4.18	37972	2339.29	87.46

FIGURE 86. Chiral UPC^2 of 2-ethyl-4-nitro-3-phenylbutanal obtained by the Michael reaction catalyzed by 10 mol% of compound **28**. Trefoil CEL2, CO_2/EtOH 100-0% to 95-5 % in 10 min at 3 ml/min at 25°C. UV detection at 210 nm: tR: (syn, minor) = 4.01 min, (syn, major) = 4.18 min. TABLE 3, Entry 1.

Time	Height	Area	Area%
3.26	60994	3629.25	20.05
3.72	2444	158.59	0.88
3.92	3698	238.65	1.32
4.11	195015	14075.40	77.76

FIGURE 87. Chiral UPC^2 of 2-ethyl-4-nitro-3-phenylbutanal obtained by the Michael reaction catalyzed by 10 mol% of compound **28**. Trefoil CEL2, CO_2/EtOH 100-0% to 95-5 % in 10 min at 3 ml/min at 25°C. UV detection at 210 nm: tR: (syn, minor) = 3.92 min, (syn, major) = 4.11 min. TABLE 3, Entry 2.
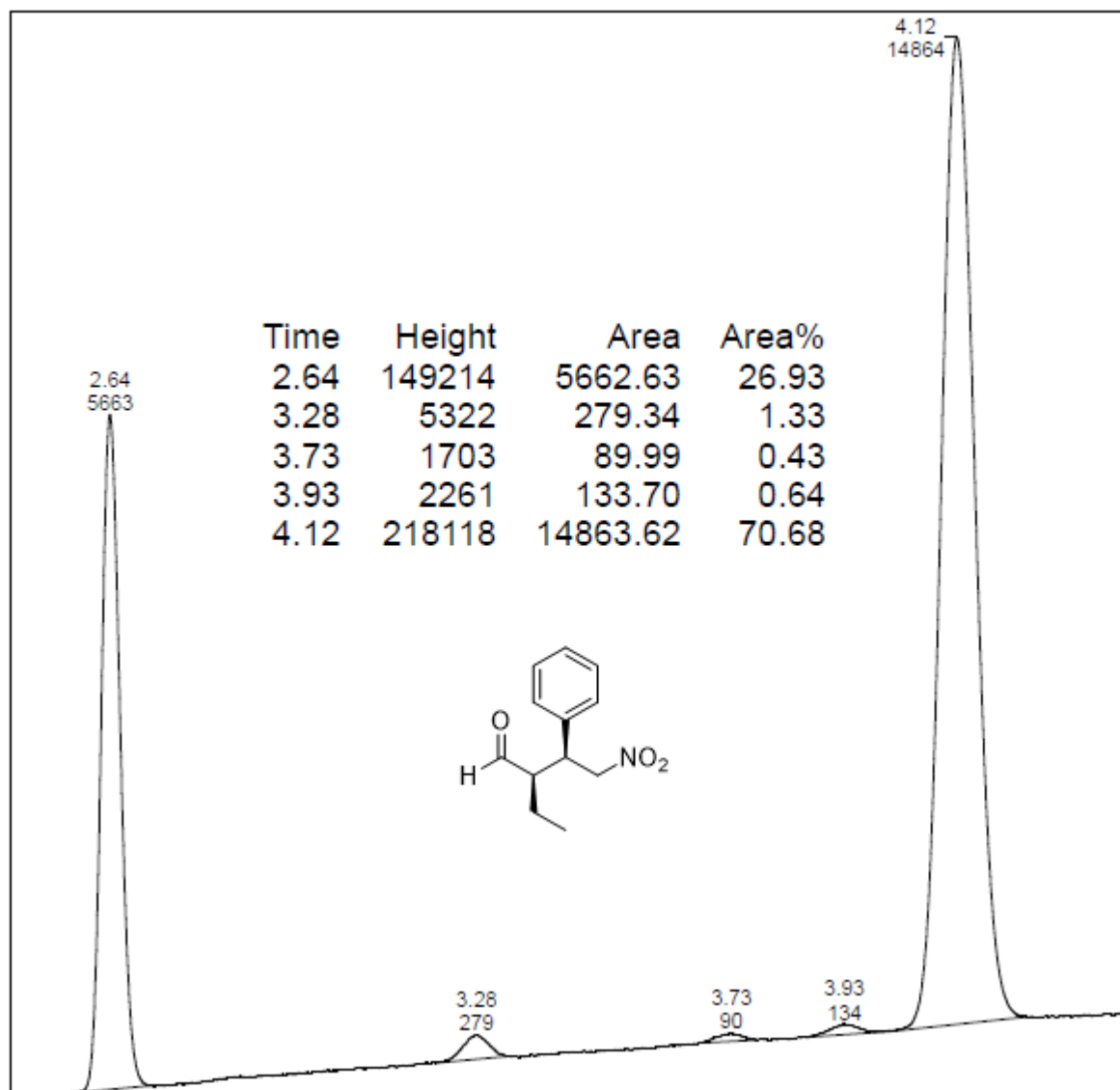
Time	Height	Area	Area%
3.30	5918	291.88	8.02
3.75	652	32.18	0.88
3.96	734	43.95	1.21
4.13	52713	3272.05	89.89

FIGURE 88. Chiral UPC^2 of 2-ethyl-4-nitro-3-phenylbutanal obtained by the Michael reaction catalyzed by 5 mol% of compound **28**. Trefoil CEL2, CO_2/EtOH 100-0% to 95-5 % in 10 min at 3 ml/min at 25°C. UV detection at 210 nm: tR: (syn, minor) = 3.96 min, (syn, major) = 4.13 min. TABLE 3, Entry 3.
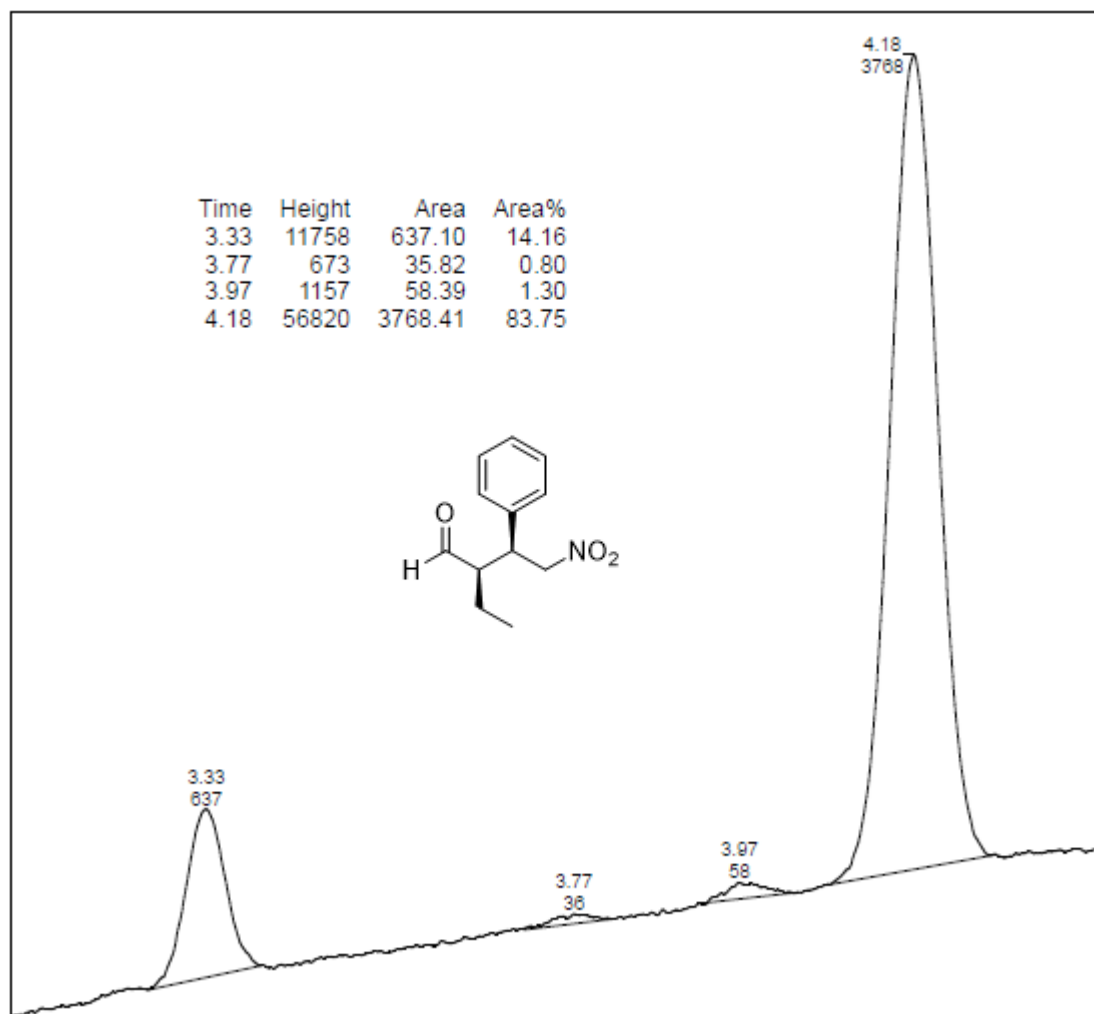
FIGURE 89. Chiral UPC^2 of 2-ethyl-4-nitro-3-phenylbutanal obtained by the Michael reaction catalyzed by 2.5 mol% of compound **28**. Trefoil CEL2, CO_2/EtOH 100-0% to 95-5 % in 10 min at 3 ml/min at 25°C. UV detection at 210 nm: tR: (syn, minor) = 3.94 min, (syn, major) = 4.14 min. TABLE 3, Entry 4.
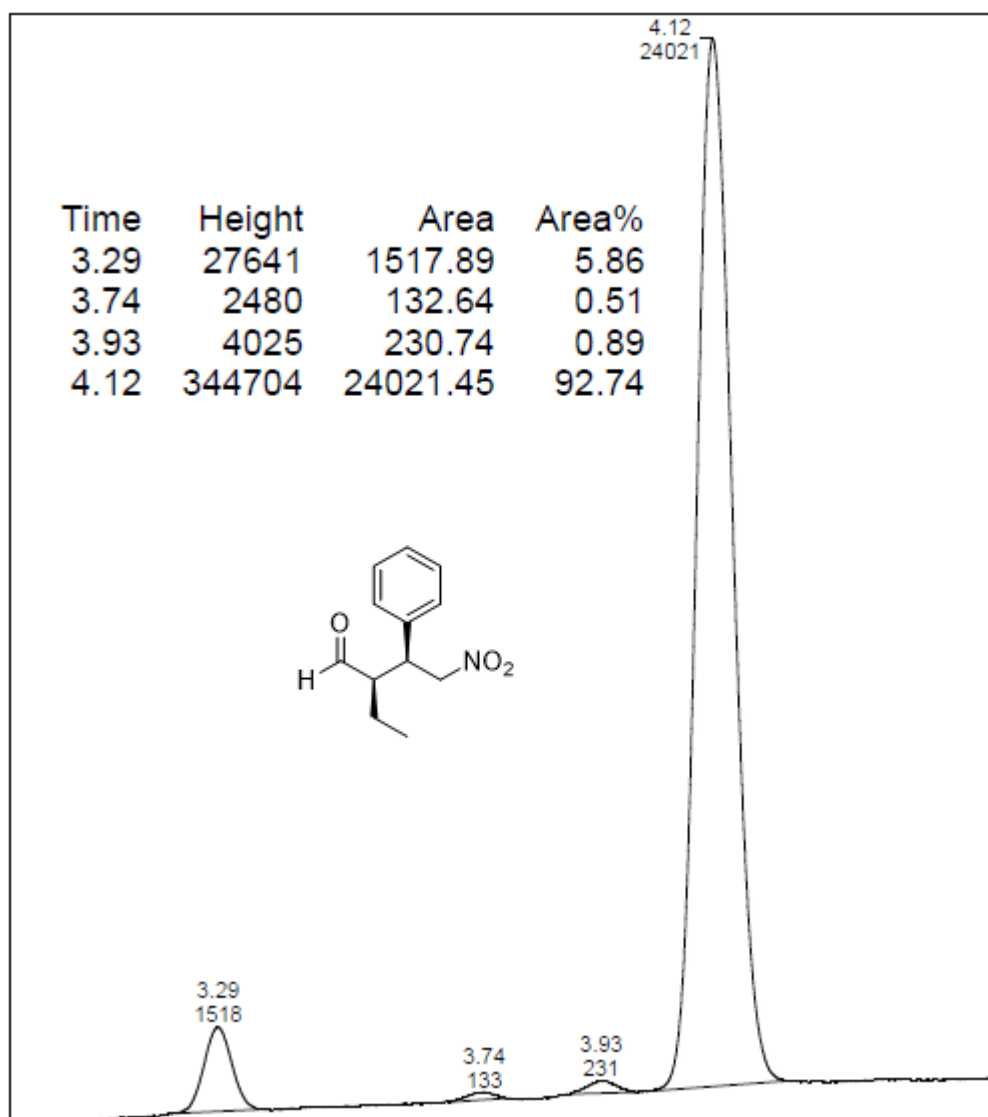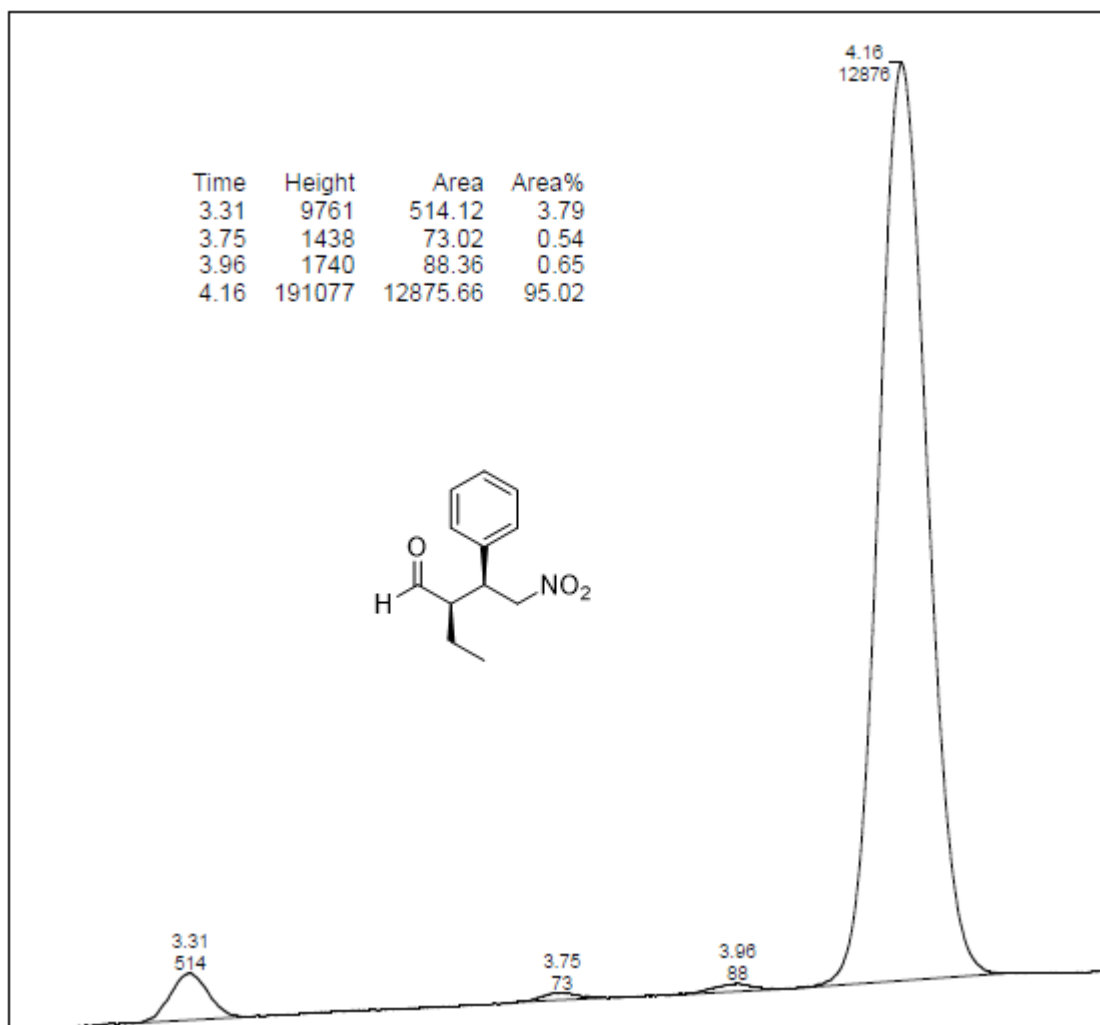
FIGURE 90. Chiral UPC^2 of 2-ethyl-4-nitro-3-phenylbutanal obtained by the Michael reaction catalyzed by 2.5 mol% of compound **28**. Trefoil CEL2, CO$_2$/EtOH 100-0% to 95-5 % in 10 min at 3 ml/min at 25°C. UV detection at 210 nm: tR: (syn, minor) = 3.93 min, (syn, major) = 4.12 min. TABLE 3, Entry 5.
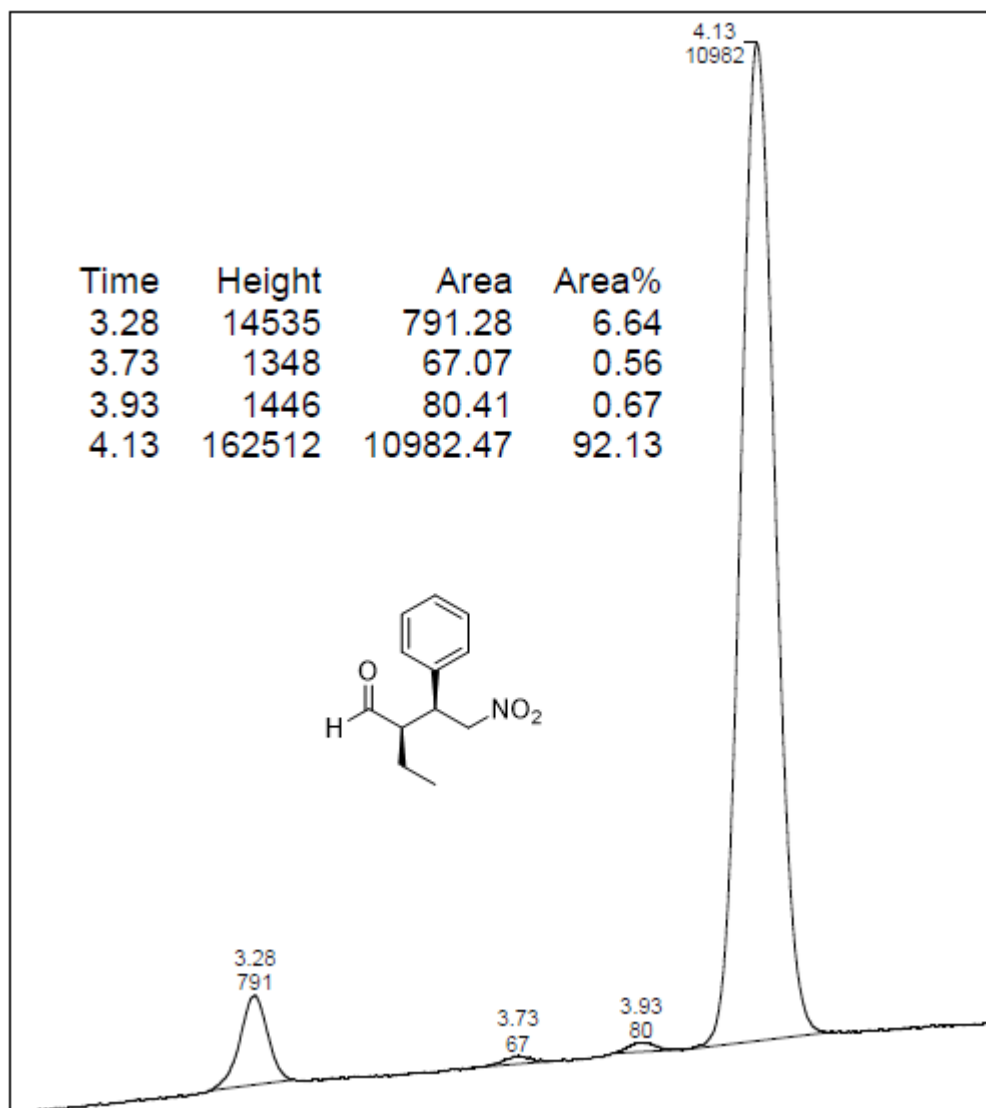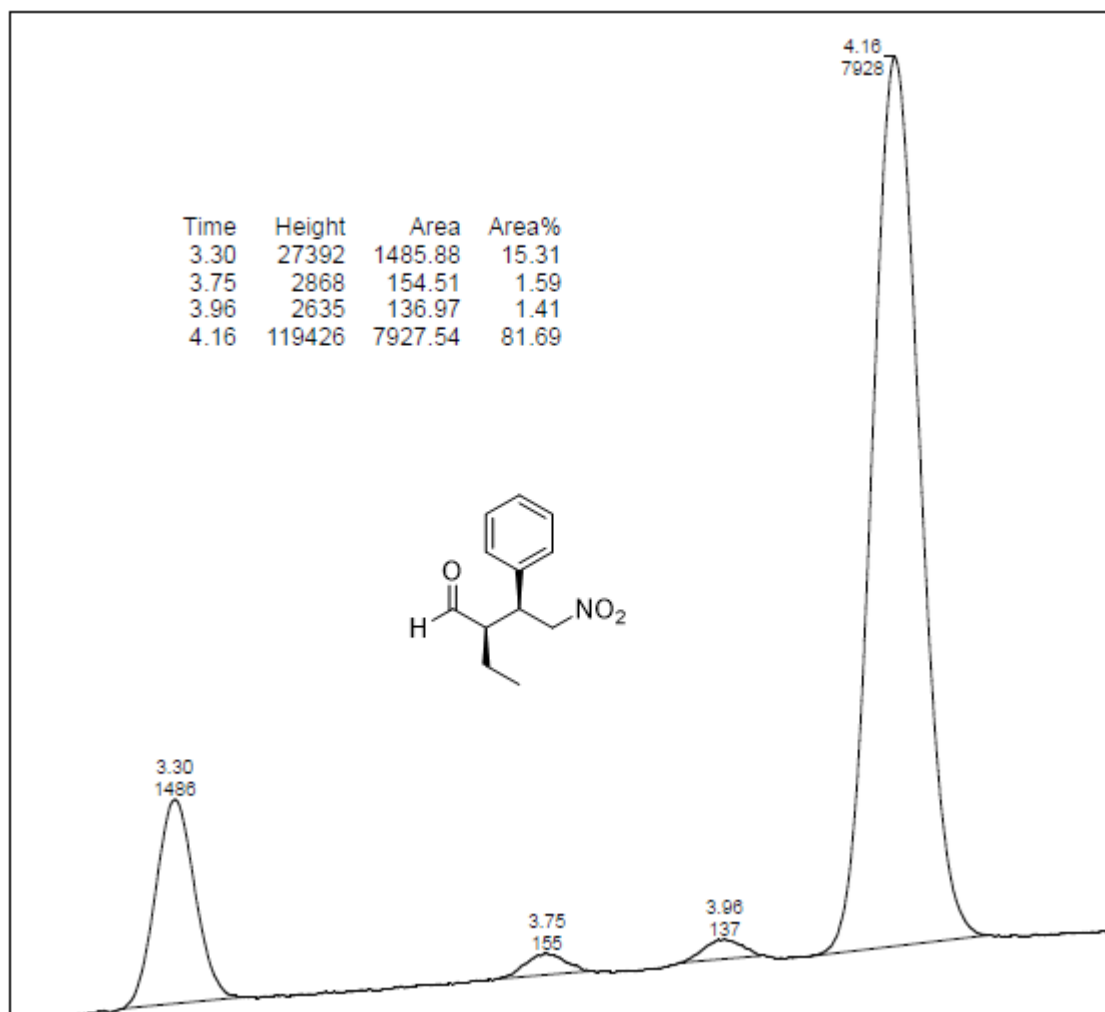
FIGURE 91. Chiral UPC^2 of 2-ethyl-4-nitro-3-phenylbutanal obtained by the Michael reaction catalyzed by 2.5 mol% of compound **28**. Trefoil CEL2, CO$_2$/EtOH 100-0% to 95-5 % in 10 min at 3 ml/min at 25°C. UV detection at 210 nm: tR: (syn, minor) = 3.93 min, (syn, minor) = 4.13 min. TABLE 3, Entry 6 and TABLE 4, compound **34**.

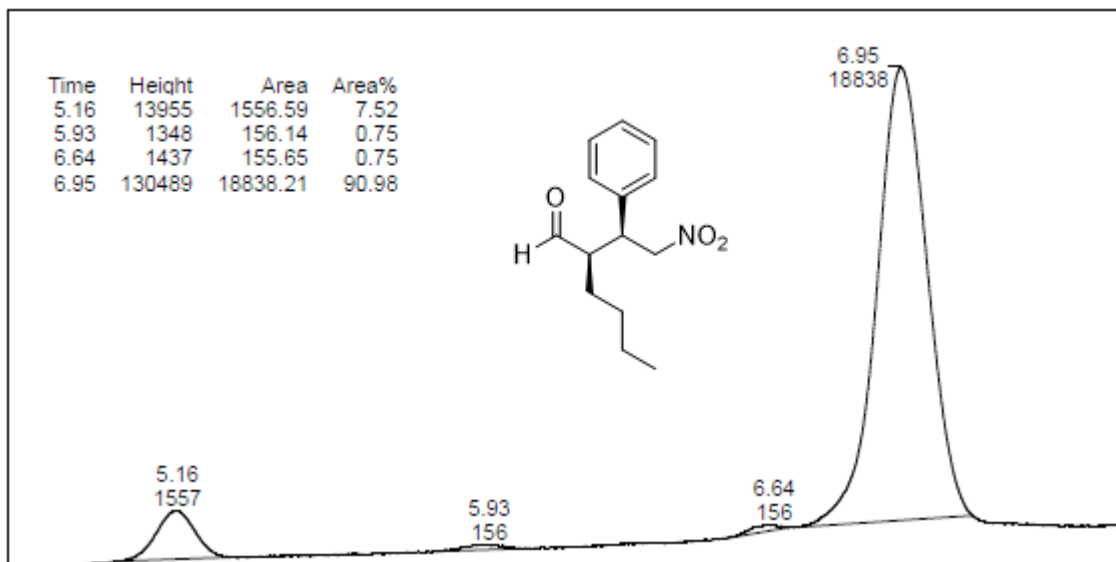| Time	Height	Area	Area%
2.65	268976	9031.93	49.63
3.17	2892	124.95	0.69
3.52	917	37.35	0.21
3.62	1232	57.76	0.32
3.84	149277	8946.31	49.16

FIGURE 92. Chiral UPC^2 of 2-ethyl-4-nitro-3-phenylbutanal obtained by the Michael reaction catalyzed by 1 mol% of compound **28**. Trefoil CEL2, CO_2/EtOH 100-0% to 95-5 % in 10 min at 3 ml/min at 25°C. UV detection at 210 nm: tR: (syn, minor) = 3.62 min, (syn, major) = 3.84 min. TABLE 3, Entry 7.
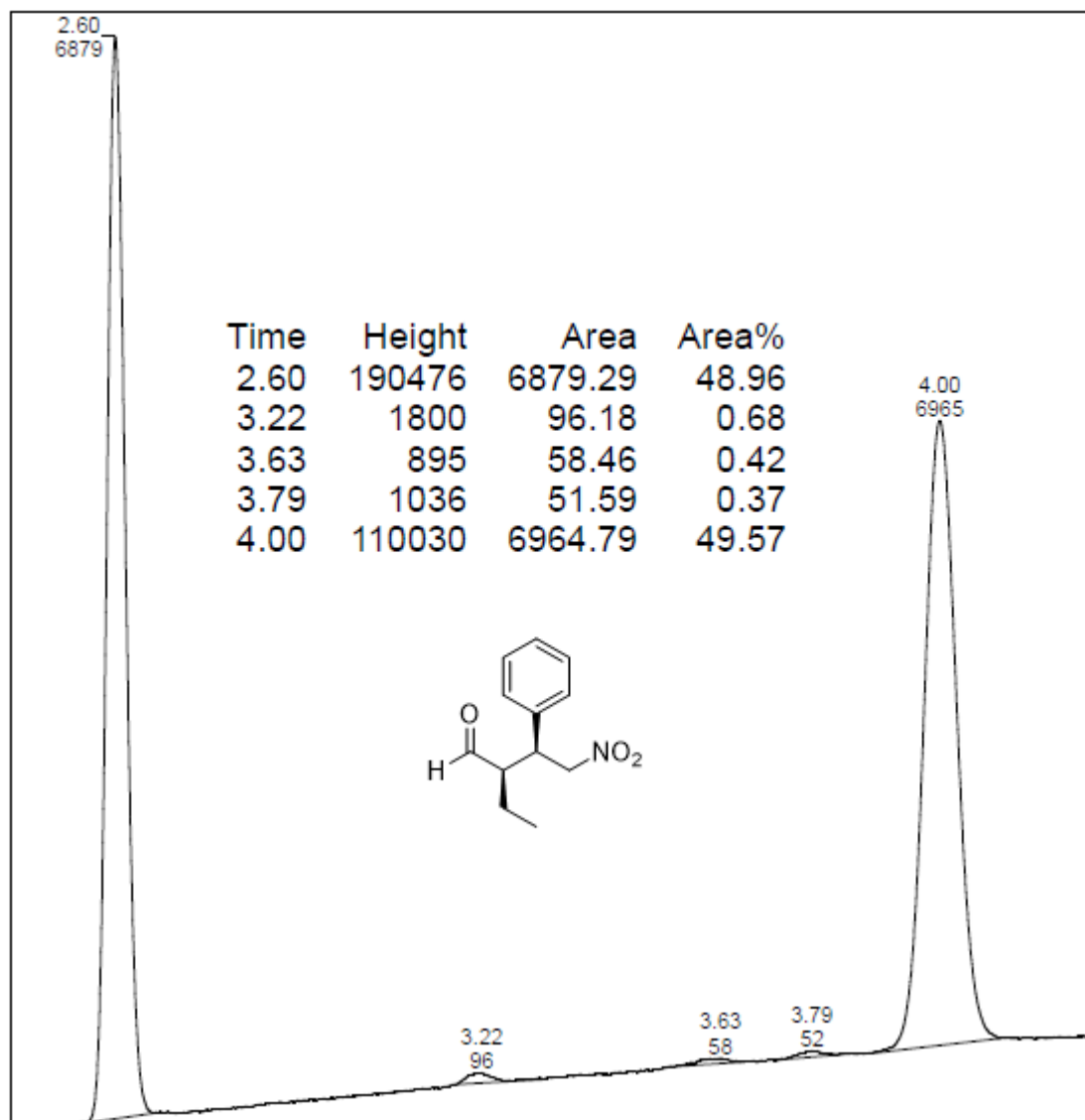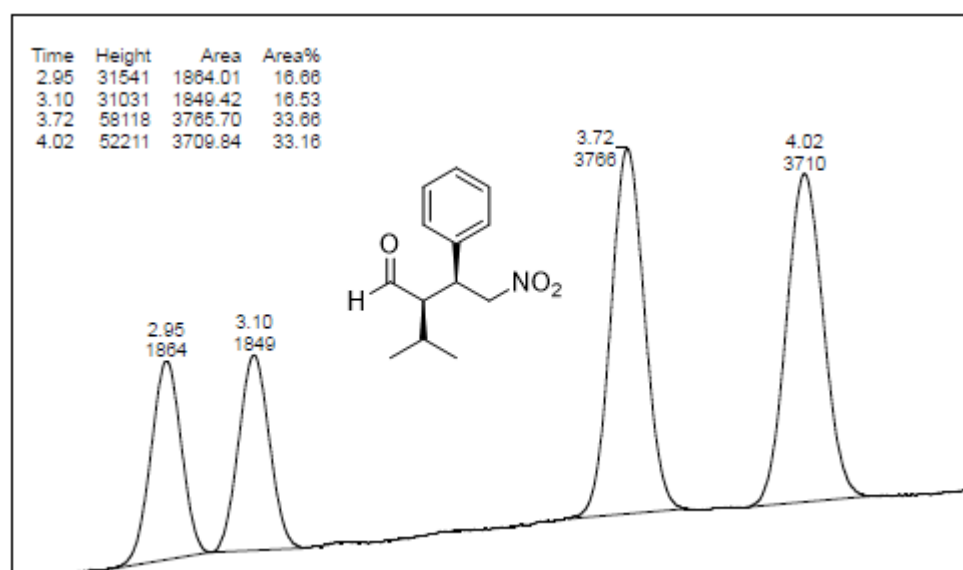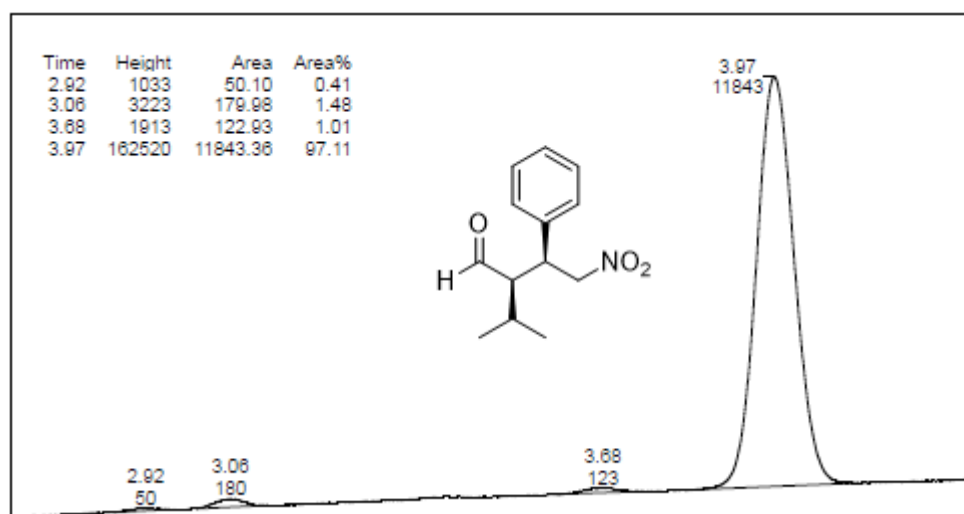
FIGURE 93. Chiral UPC^2 of 2-ethyl-4-nitro-3-phenylbutanal obtained by the Michael reaction catalyzed by 1 mol% of compound **28**. Trefoil CEL2, CO$_2$/EtOH 100-0% to 95-5 % in 10 min at 3 ml/min at 25°C. UV detection at 210 nm: tR: (syn, minor) = 3.79 min, (syn, major) = 4.00 min. TABLE 3, Entry 8.

Time	Height	Area	Area%
2.64	149214	5662.63	26.93
3.28	5322	279.34	1.33
3.73	1703	89.99	0.43
3.93	2261	133.70	0.64
4.12	218118	14863.62	70.68

FIGURE 94. Chiral UPC^2 of 2-ethyl-4-nitro-3-phenylbutanal obtained by the Michael reaction catalyzed by 1 mol% of compound **28**. Trefoil CEL2, CO_2/EtOH 100-0% to 95-5 % in 10 min at 3 ml/min at 25°C. UV detection at 210 nm: tR: (syn, minor) = 3.93 min, (syn, major) = 4.12 min. TABLE 3, Entry 9.
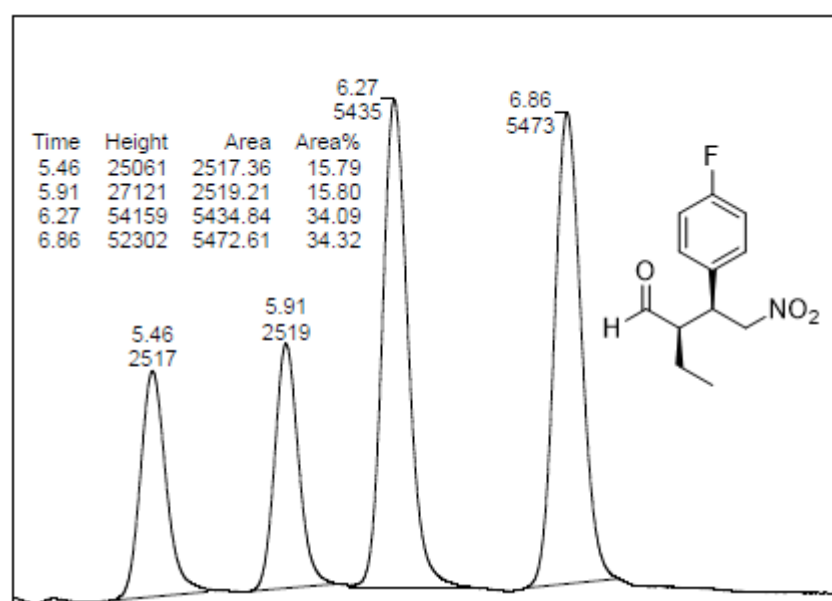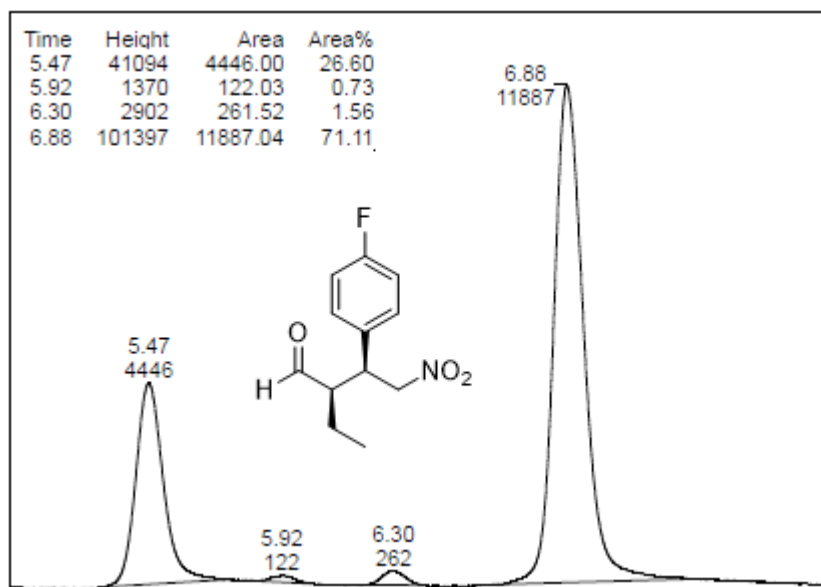
FIGURE 95. Chiral UPC^2 of 2-ethyl-4-nitro-3-phenylbutanal obtained by the Michael reaction catalyzed by 2.5 mol% of compound **28** in EtOH as a solvent. Trefoil CEL2, CO$_2$/EtOH 100-0% to 95-5 % in 10 min at 3 ml/min at 25°C. UV detection at 210 nm: tR: (syn, minor) = 3.97 min, (syn, major) = 4.18 min. TABLE 3, Entry 10.

FIGURE 96. Chiral UPC^2 of 2-ethyl-4-nitro-3-phenylbutanal obtained by the Michael reaction catalyzed by 2.5 mol% of compound **28** in brine as a solvent. Trefoil CEL2, CO_2/EtOH 100-0% to 95-5 % in 10 min at 3 ml/min at 25°C. UV detection at 210 nm: tR: (syn, minor) = 3.96 min, (syn, major) = 4.16 min. TABLE 3, Entry 11.

FIGURE 97. Chiral UPC^2 of 2-ethyl-4-nitro-3-phenylbutanal obtained by the Michael reaction catalyzed by 2.5 mol% of compound **28** in PEG-300 as a solvent. Trefoil CEL2, CO$_2$/EtOH 100-0% to 95-5 % in 10 min at 3 ml/min at 25°C. UV detection at 210 nm: tR: (syn, minor) = 3.96 min, (syn, major) = 4.16 min. TABLE 3, Entry 12.
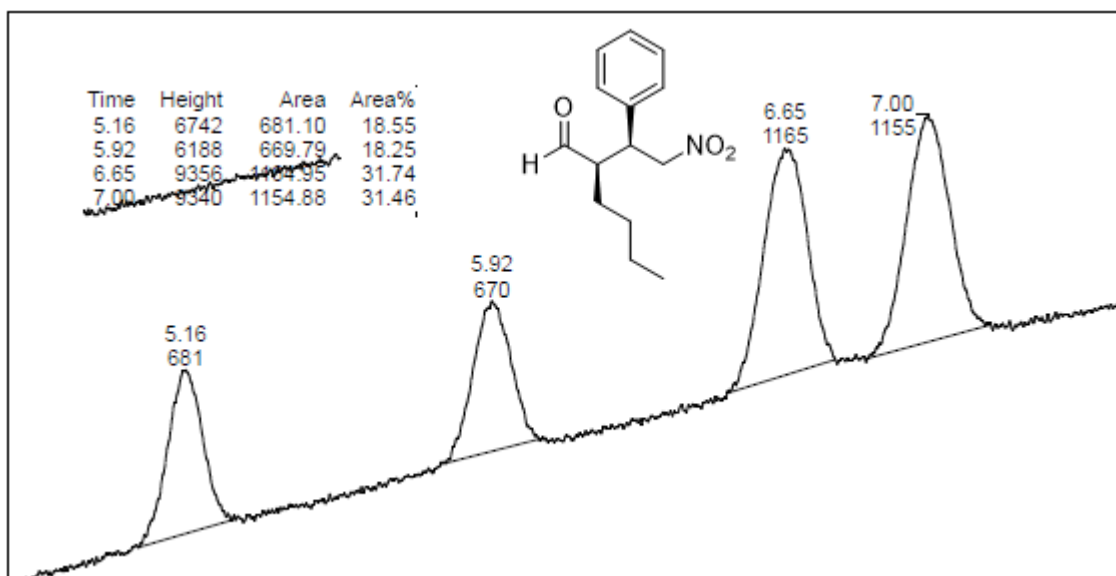
FIGURE 98. Chiral UPC^2 of racemic 2-(2-nitro-1-phenylethyl) hexanal. Trefoil CEL2, CO$_2$/EtOH 100-0% to 95-5 % in 10 min at 3 ml/min at 25°C. UV detection at 210 nm.

Time	Height	Area	Area%
5.16	13955	1556.59	7.52
5.93	1348	156.14	0.75
6.64	1437	155.65	0.75
6.95	130489	18838.21	90.98

FIGURE 99. Chiral UPC^2 of 2-(2-nitro-1-phenylethyl) hexanal obtained by the Michael reaction catalyzed by 2.5 mol% of compound **28**. Trefoil CEL2, CO$_2$/EtOH 100-0% to 95-5 % in 10 min at 3 ml/min at 25°C. UV detection at 210 nm: tR: (syn, minor) = 6.64 min, (syn, major) = 6.95 min. TABLE 4, compound **35**.

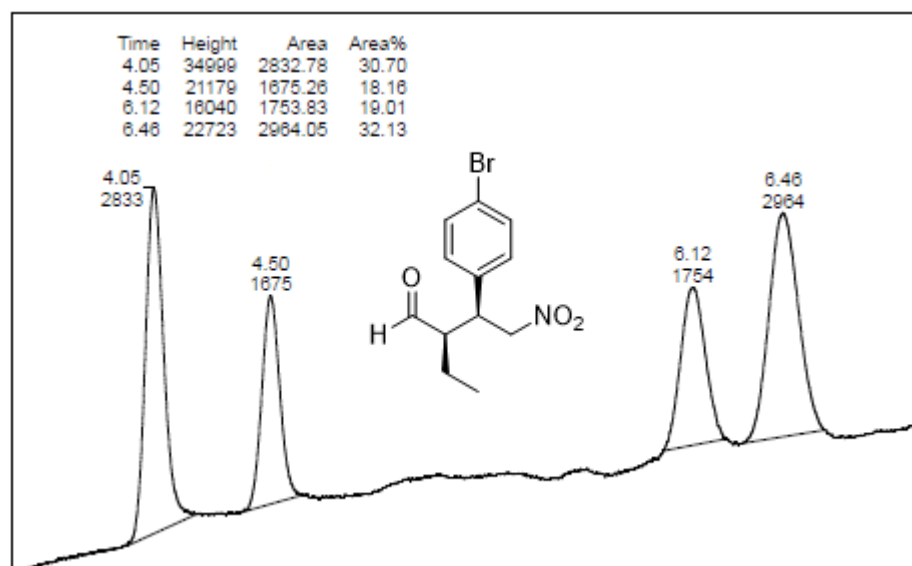| Time	Height	Area	Area%
2.95	31541	1864.01	16.66
3.10	31031	1849.42	16.53
3.72	58118	3765.70	33.66
4.02	52211	3709.84	33.16

FIGURE 100. Chiral UPC^2 of racemic 2-isopropyl-4-nitro-3-phenylbutanal. Trefoil CEL2, CO$_2$/EtOH 100-0% to 95-5 % in 10 min at 3 ml/min at 25°C. UV detection at 210 nm.

Time	Height	Area	Area%
2.92	1033	50.10	0.41
3.06	3223	179.98	1.48
3.68	1913	122.93	1.01
3.97	162520	11843.36	97.11

FIGURE 101. Chiral UPC^2 of 2-isopropyl-4-nitro-3-phenylbutanal obtained by the Michael reaction catalyzed by 2.5 mol% of compound **28**. Trefoil CEL2, CO$_2$/EtOH 100-0% to 95-5 % in 10 min at 3 ml/min at 25°C. UV detection at 210 nm: tR: (syn, minor) = 3.68 min, (syn, minor) = 3.97 min. TABLE 4, compound **36**.

Time	Height	Area	Area%
5.46	25061	2517.36	15.79
5.91	27121	2519.21	15.80
6.27	54159	5434.84	34.09
6.86	52302	5472.61	34.32

FIGURE 102. Chiral UPC^2 of racemic 2-ethyl-3-(4-fluorophenyl)-4-nitrobutanal. Trefoil CEL2, Grad: CO$_2$/EtOH 100-0% to 95-5% in 9 min; 100-0 % in 1 min at 2 ml/min at 25°C. UV detection at 210 nm.
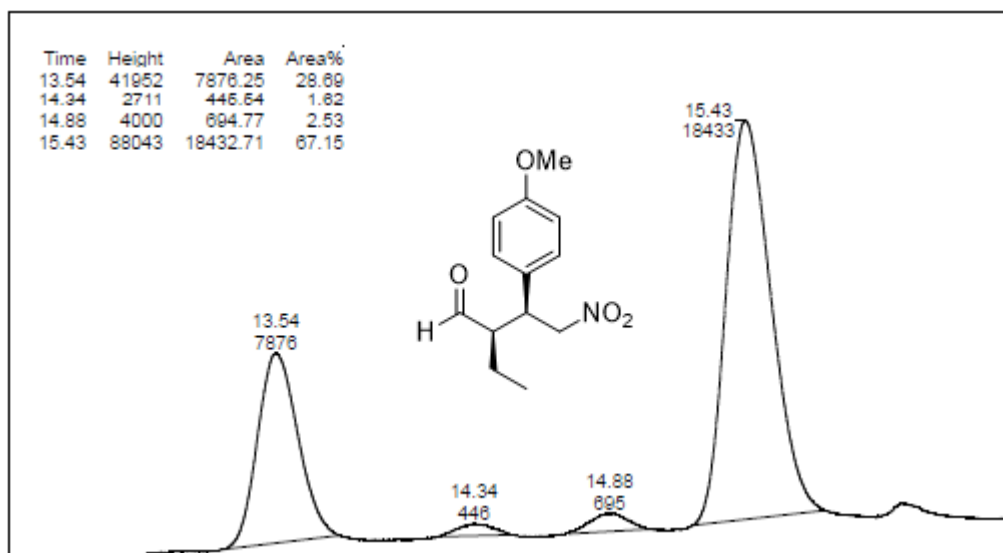
FIGURE 103. Chiral UPC^2 of 2-ethyl-3-(4-fluorophenyl)-4-nitrobutanal obtained by the Michael reaction catalyzed by 2.5 mol% of compound **28**. Trefoil CEL2, Grad: CO$_2$/EtOH 100-0% to 95-5% in 9 min; 100-0 % in 1 min at 2 ml/min at 25°C. UV detection at 210 nm: tR: (syn, minor) = 6.30 min, (syn, major) = 6.88 min. TABLE 4, compound **37**.
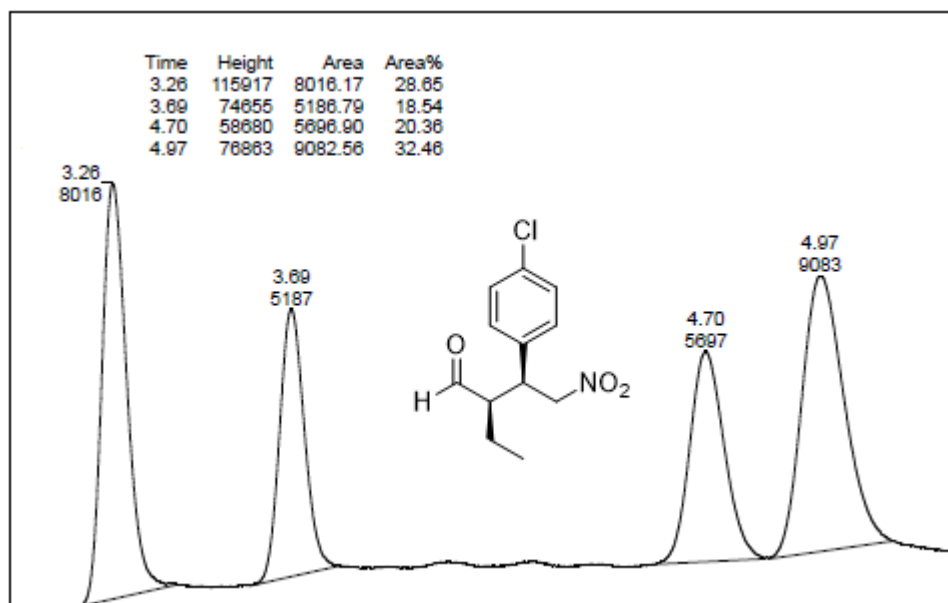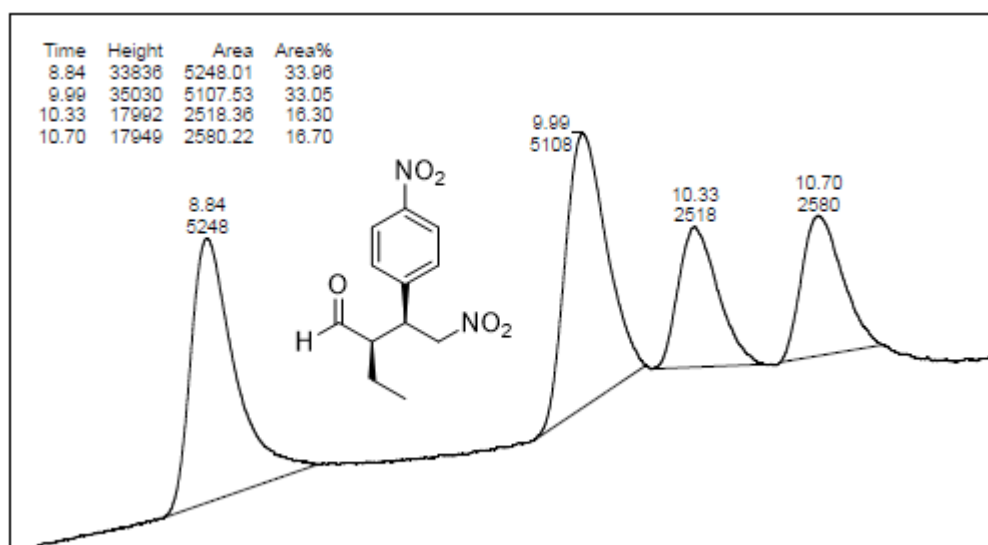

FIGURE 104. Chiral UPC^2 of racemic 3-(4-chlorophenyl)-2-ethyl-4-nitrobutanal. Trefoil AMY1, Grad: CO$_2$/MeOH 100-0% to 90-10 % in 6 min; 90-10 % in 3 min; 100-0 % in 1 min at 2 ml/min at 25°C. UV detection at 210 nm.

Time	Height	Area	Area%
3.45	347095	22318.43	90.57
3.77	34098	1837.18	7.46
4.05	3951	210.67	0.85
4.21	4623	277.06	1.12
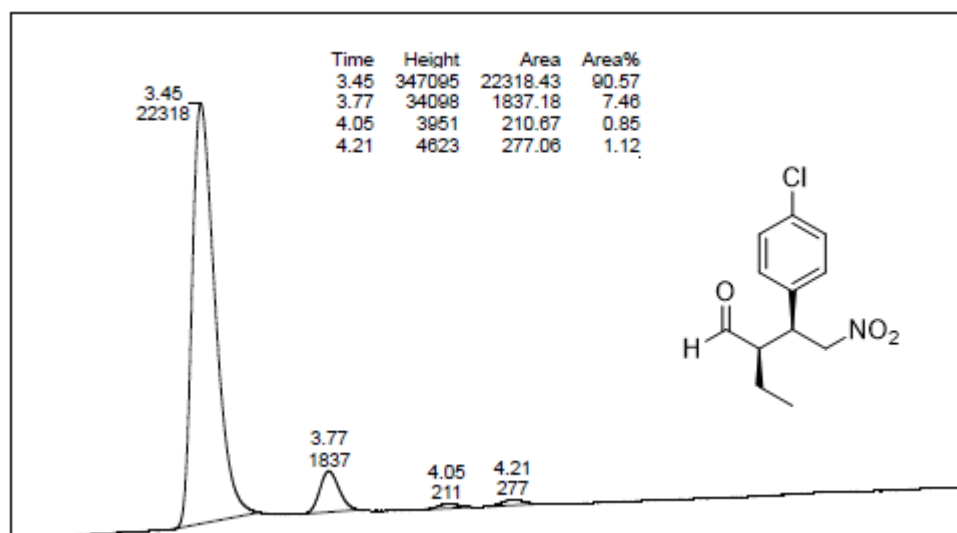
FIGURE 105. Chiral UPC^2 of 3-(4-chlorophenyl)-2-ethyl-4-nitrobutanal obtained by the Michael reaction catalyzed by 2.5 mol% of compound **28**. Trefoil AMY1, Grad: CO_2/MeOH 100-0% to 90-10 % in 6 min; 90-10 % in 3 min; 100-0 % in 1 min at 2 ml/min at 25°C. UV detection at 210 nm: tR: (syn, major) = 3.45 min, (syn, minor) = 3.77 min. TABLE 4, compound **38**.

Time	Height	Area	Area%
4.05	34999	2832.78	30.70
4.50	21179	1675.26	18.16
6.12	16040	1753.83	19.01
6.46	22723	2964.05	32.13

FIGURE 106. Chiral UPC^2 of racemic 3-(4-bromophenyl)-2-ethyl-4-nitrobutanal. Trefoil AMY1, Grad: CO_2/MeOH 100-0% to 90-10 % in 6 min; 90-10 % in 3 min; 100-0 % in 1 min at 2 ml/min at 25°C. UV detection at 210 nm.
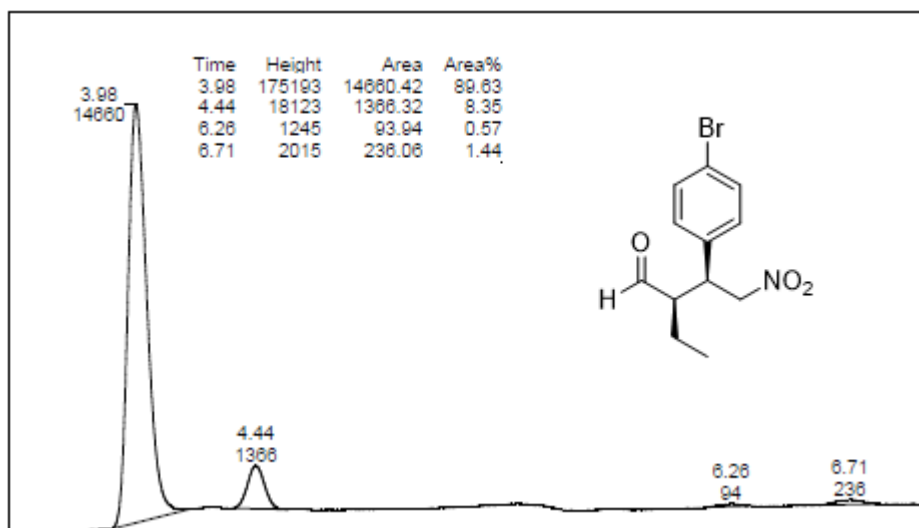
FIGURE 107. Chiral UPC^2 of 3-(4-bromophenyl)-2-ethyl-4-nitrobutanal obtained by the Michael reaction catalyzed by 2.5 mol% of compound **28**. Trefoil AMY1, Grad: CO$_2$/MeOH 100-0% to 90-10 % in 6 min; 90-10 % in 3 min; 100-0 % in 1 min at 2 ml/min at 25°C. UV detection at 210 nm: tR: (syn, major) = 3.98 min, (syn, minor) = 4.44 min. TABLE 4, compound **39**.
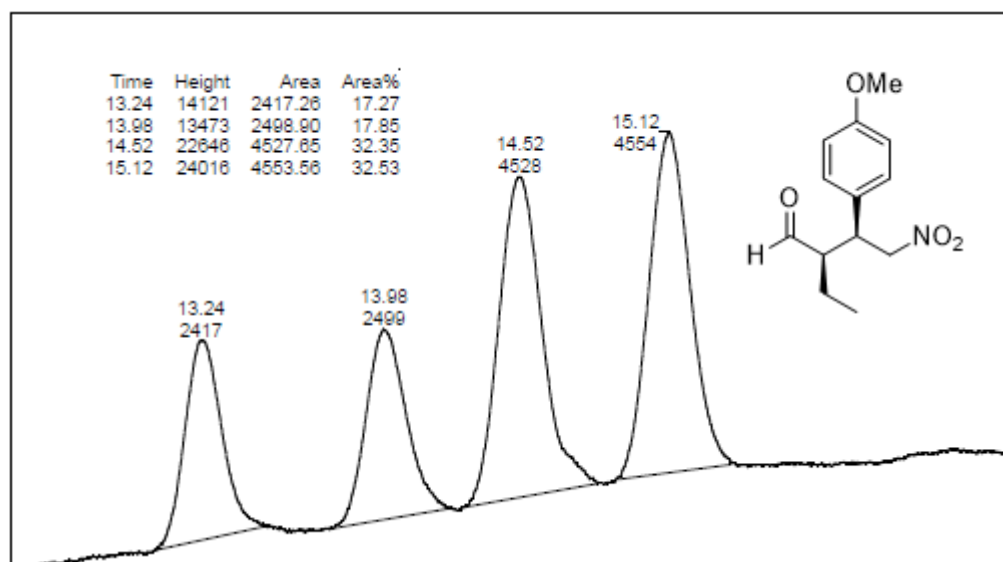
FIGURE 108. Chiral UPC^2 of racemic 2-ethyl-3-(4-methoxyphenyl)-4-nitrobutanal. Trefoil CEL2, Grad: CO$_2$/EtOH 100-0% to 98-2 % in 19 min; 100-0 % in 1 min at 2.5 ml/min at 25°C. UV detection at 210 nm.

FIGURE 109. Chiral UPC^2 of 2-ethyl-3-(4-methoxyphenyl)-4-nitrobutanal obtained by the Michael reaction catalyzed by 2.5 mol% of compound **28**. Trefoil CEL2, Grad: CO$_2$/EtOH 100-0% to 98-2 % in 19 min; 100-0 % in 1 min at 2.5 ml/min at 25°C. UV detection at 210 nm: tR: (syn, minor) = 14.88 min, (syn, major) = 15.43 min. TABLE 4, compound **40**.

FIGURE 110. Chiral UPC^2 of racemic 2-ethyl-4-nitro-3-(4-nitrophenyl) butanal. Trefoil AMY1, Grad: CO$_2$/IPA 100-0% to 90-10 % in 18 min; 90-10 % in 2 min at 2 ml/min at 25°C. UV detection at 210 nm.
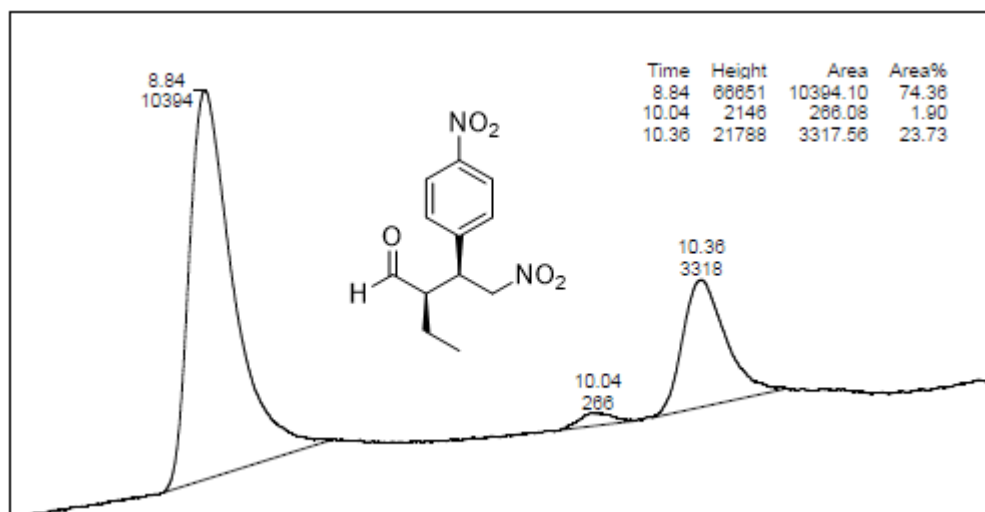
FIGURE 111. Chiral UPC² of 2-ethyl-4-nitro-3-(4-nitrophenyl) butanal obtained by the Michael reaction catalyzed by 2.5 mol% of compound **28**. Trefoil AMY1, Grad: CO₂/IPA 100-0% to 90-10 % in 18 min; 90-10 % in 2 min at 2 ml/min at 25°C. UV detection at 210 nm: tR: (syn, major) = 8.84 min, (syn, minor) = 10.04 min. TABLE 4, compound **41**.

NJC

Check for updates

Synthesis of *N*-alkylated lipopeptides and their application as organocatalysts in asymmetric Michael addition in aqueous environments†

José A. C. Delgado, [ID] [a] Fidel E. M. Vicente,[ab] Alexander F. de la Torre,[c] Vitor A. Fernandes, [ID] [a] Arlene G. Corrêa [ID] [a] and Márcio W. Paixão [ID] *[a]

A library of *N*-alkylated lipopeptide organocatalysts were synthesized through an isocyanide-based multicomponent reaction. Various structural motifs were tunably introduced on the catalyst backbone with the aim of incorporating amphiphilic features. Consequently, they have further been evaluated in the 1,4-addition of aldehydes to *trans*-β-nitrostyrene having water as the sole solvent. Under sustainable reaction conditions, Michael adducts were obtained in excellent yields, diastereoselectivities, and enantioselectivities using low catalyst loadings and without additives.

Introduction

The construction of carbon–carbon bonds is one of the leading chemical transformations in organic synthesis, especially in a stereoselective fashion.[1] Amongst a plethora of strategies already developed, asymmetric aminocatalysis, since its conception, has posed as one of the most important tools for forging C–C and C–X bonds.[2] Consequently, many proline-based organocatalysts have been successfully developed and further applied to a variety of synthetic transformations in the presence of traditional organic solvents.[3] However, environmental concerns associated with synthetic organic chemistry have posed stringent and compelling demands for greener processes. Over the past few years, the replacement of organic solvents for an environmentally benign reaction medium has been pursued by the synthetic community in a quest for the improvement of green metrics.[4]

In this regard, amphiphilic or water-compatible organic molecules which successfully catalyzed asymmetric chemical transformations "in-water", "on-water" or in the presence of a small amount of water have been widely used as an excellent environmentally benign alternative.[5] These molecules hold both hydrophilic and hydrophobic portions in their chemical architecture, which allow them to act at the water–oil interface by decreasing superficial tension.[6] Due to its intrinsic characteristics, amphiphilic molecules have widespread applications, mainly as surfactants,[7] and more recently in catalytic transformations in aqueous environments.[8]

Moreover, when an amphiphilic catalyst is employed under aqueous conditions, two systems with different physical–chemical features – micelles or self-assembly emulsions – are expected to be formed, and therefore the catalysis could be performed either inside the micelle[9] or at the water–oil interface.[10]

In this way, there are numerous reports in the literature that have explored either the catalytic properties of micelles or the amphiphilic properties of appropriate organocatalysts in challenging asymmetric transformations.[11]

Wennemers and co-workers took advantage of the hydrophilic nature of peptides developed through an efficient lipopeptide-based organocatalyst by introducing on the C-terminus a long alkyl chain in the known catalytic structural motif (H-(*D*)Pro-Pro-Glu-NH$_2$).[12] This lipopeptide displayed both high activity and stereocontrol upon the Michael addition of aldehydes to nitrostyrene under aqueous conditions through emulsion formation (Scheme 1A). Moreover, Alves and co-workers designed a new lipopeptide-catalyzed stereoselective aldol reaction in an aqueous microstructured environment (micellar catalysis).[13]

Likewise, we have also been involved in the design of new catalytic structural motifs by exploiting the synthetic ability of isocyanide-based multicomponent reactions (I-MCRs) to generate structural diversity (Scheme 1B).[14] Therefore, we planned to introduce a long alkyl chain onto the chemical architecture

[a] Centre of Excellence for Research in Sustainable Chemistry (CERSusChem), Department of Chemistry, Federal University of São Carlos – UFSCar, Rodovia Washington Luís, km 235 - SP-310, São Carlos, São Paulo-13565-905, Brazil. E-mail: mwpaixao@ufscar.br

[b] General Chemistry Department, Faculty of Chemistry, University of Havana, La Habana, Cuba

[c] Departamento de Química Orgánica, Facultad de Ciencias Químicas, Universidad de Concepción, Concepción, Chile

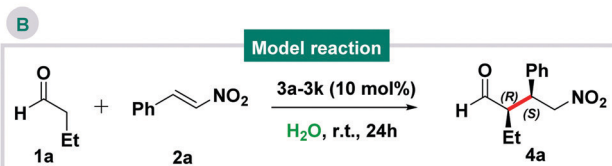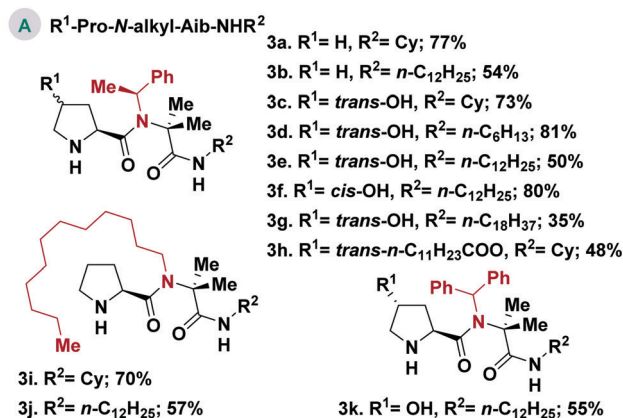† Electronic supplementary information (ESI) available. See DOI: 10.1039/d1nj01112j

A Wennemers Group

B Our Group

C This work
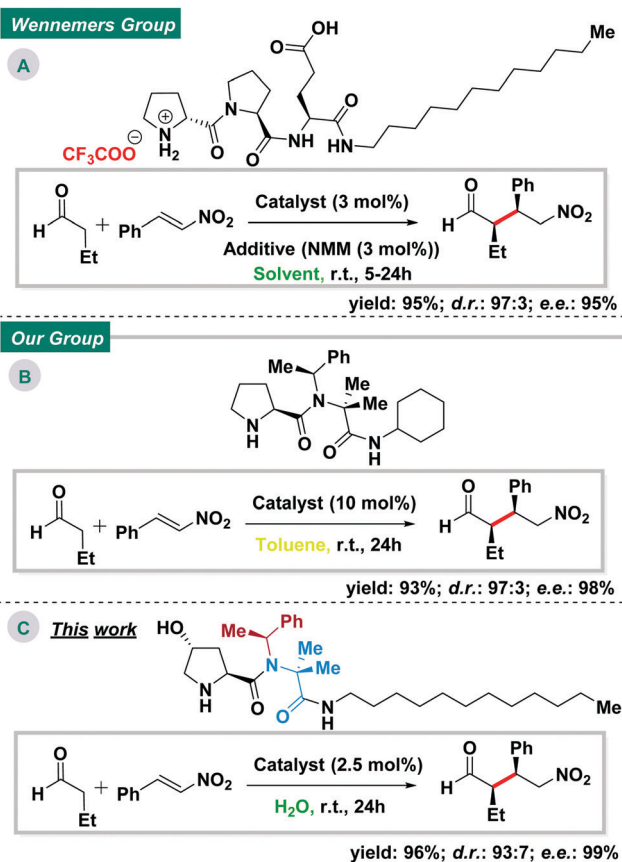
Scheme 1 (**A**) Amphiphilic lipopeptide organocatalyst having a H-(*D*)Pro-Pro-Glu-NHC$_{12}$H$_{25}$ sequence. (**B**) Prolyl peptide–peptoid hybrid catalyst assembly by Ugi-4CR having a Pro-*N*((*S*)-MeBn)-Aib-NHCy structural motif. (**C**) Merged *N*-alkylated lipopeptide organocatalyst *trans*-OH-Pro-*N*((*S*)-MeBn)-Aib-NHC$_{12}$H$_{25}$.

A R^1-Pro-*N*-alkyl-Aib-NHR^2

3a. R^1= H, R^2= Cy; 77%
3b. R^1= H, R^2= *n*-C$_{12}$H$_{25}$; 54%
3c. R^1= *trans*-OH, R^2= Cy; 73%
3d. R^1= *trans*-OH, R^2= *n*-C$_6$H$_{13}$; 81%
3e. R^1= *trans*-OH, R^2= *n*-C$_{12}$H$_{25}$; 50%
3f. R^1= *cis*-OH, R^2= *n*-C$_{12}$H$_{25}$; 80%
3g. R^1= *trans*-OH, R^2= *n*-C$_{18}$H$_{37}$; 35%
3h. R^1= *trans*-*n*-C$_{11}$H$_{23}$COO, R^2= Cy; 48%

3i. R^2= Cy; 70%
3j. R^2= *n*-C$_{12}$H$_{25}$; 57%

3k. R^1= OH, R^2= *n*-C$_{12}$H$_{25}$; 55%

B Model reaction

Catalyst	Yield (4a%)	d.r. (syn/anti)	e.e. (4a%)
3a	57	94:06	96
3b	90	89:11	94
3c	43	70:30	99
3d	72	81:19	97
3e	**88**	**76:24**	**99**
3f	78	79:21	94
3g	35	87:13	92
3h	23	89:11	99
3i	75	76:24	88
3j	87	88:12	83
3k	84	79:21	89

Scheme 2 (**A**) Structures and yields of *N*-alkylated lipopeptides synthesized in this work. (**B**) Screening of organocatalysts **3a–3k** upon the addition of butyraldehyde to *trans*-β-nitrostyrene. All reactions were carried out using 2 equivalents of butanal and 0.2 mmol of β-nitrostyrene in 0.4 mL of solvent. The yield was determined by ^{1}H NMR spectroscopic analysis of the crude reaction mixture with 1,2,3-trimethoxybenzene as the internal standard. The *syn/anti* ratio was determined by ^{1}H NMR and the enantiomeric excess was determined *via* chiral-stationary phase UPC^2 analysis.

of the organocatalyst previously developed by our group to generate an amphiphilic system (Scheme 1C).

Results and discussion

Herein, we describe a new amphiphilic organocatalyst which is capable of performing a stereoselective carbon–carbon bond forming reaction in an aqueous environment. We started our investigation by synthesizing a library of *N*-alkylated lipopeptides through a widely employed isocyanide-based multicomponent approach, the Ugi-4CR (Ugi-4-component reaction). Under this environmentally benign reaction protocol, prolyl *pseudo*-lipopeptides were obtained in moderate to excellent yields (35–81%), having the generic sequence of R^1-Pro-*N*-alkyl-Aib-NHR^2 (Scheme 2A). With the library of *N*-alkylated lipopeptide organocatalysts in hand, we turned to the evaluation of their catalytic performance in the Michael reaction, which is one of the most employed methods for both carbon–carbon and carbon–heteroatom bond formation. For the initial catalyst screening, butyraldehyde and *trans*-β-nitrostyrene were chosen as model substrates (Scheme 2B). These reactions were carried out using a catalyst loading of 10 mol%, and water as the solvent at room temperature. In all cases, the

stereoselectivity is influenced by the proline-core and conformational rigidity of the catalyst, thereby leading to the formation of the Michael adduct predominantly with the *syn* relationship and (*R*,*S*)-absolute configuration.[15]

Moreover, many of the evaluated organocatalysts – specifically **3a–h** – delivered the desired product **4a** with moderate to excellent diastereo- and enantioselectivities. These results are in agreement with a previous observation by our group,[14,16] where the *beta*-turn structural motif -*N*((*S*)-MeBn)-Aib- is required to achieve high levels of stereoinduction (compare **3a–h** *vs.* **3i–k**). Besides, no considerable difference in terms of enantioselectivity was observed among the organocatalysts of this series.

Notwithstanding the relative water-solubility of these *N*-alkylated lipopeptides and due to the nonsoluble nature of

organic compounds, the reaction mixtures were a heterogeneous slurry or a biphasic water–oil system of the substrates in the aqueous medium. In this sense, the introduction of a long alkyl chain – of twelve carbon atoms – at the R^2 position improves the reaction performance, and hence the catalysts bearing the sequence R^1-Pro-N((S)-MeBn)-Aib-NHC$_{12}$H$_{25}$ (*i.e.*, **3b**, **3e–f**, and **3j–k**) render the products in a higher chemical yield. On the other hand, the organocatalyst **3a**, previously developed by our group, afforded **4a** in a moderate chemical yield (57%). Based on these observations, we assume that the hydrophobic effect is the main factor that causes the improvement in terms of efficiency of the Michael reaction in an aqueous environment. Additionally, the insertion of a lipidic side chain at the R^1 position[17] triggered an erosion in terms of yield (**3h**). The hydroxyl group remains as a hydrophilic part or head whereas the long alkyl chain acts as a hydrophobic part or tail, reinforcing its amphiphilic features and allowing it to act as a tenside. Besides, neither the incorporation of the hydrophobic chain nor the achiral bulky (N-α-diphenylmethane) as an N-alkyl substituent into the catalyst backbone gave better results for the asymmetric organic transformation than previously discussed catalysts (*i.e.*, **3i–j** and **3k**). The fine-tuning of the R^1 and R^2 substituents incorporating the three-dimensional *beta*-turn structural motif led to the organocatalyst *trans*-OH-Pro-N((S)-MeBn)-Aib-NHC$_{12}$H$_{25}$ (**3e**), which afforded the desired Michael adduct in 88% yield, 76:14 *d.r.* and 99% *e.e.*

Once a suitable catalyst was identified, we continued the optimization study by evaluating the catalyst loading of **3e**, and the influence of other environmentally friendly solvents (Table 1).

As shown in Table 1, by decreasing the catalyst loading to 5 mol%, the chemical yield was slightly improved and the enantioselectivity of the Michael adduct **4a** remained at the same level – albeit, a great improvement was observed in the diastereoselectivity ratio (Table 1, entry 1). To our delight, with a catalyst loading of 2.5 mol%, compound **4a** was obtained in quantitative yield and with excellent levels of stereoselectivity (Table 1, entry 2). Notwithstanding, upon decreasing the catalyst loading to 1 mol%, the reaction underwent an erosion in terms of chemical efficiency (Table 1, entry 3), although non-substantial changes in diastereoselectivity and enantioselectivity could be observed. Then, we turned our attention to evaluate the

influence of other greener solvents on the catalytic activity. When brine is used instead of water, the reaction undergoes a slight change in the chemical efficiency (Table 1, entry 4). Moreover, both ethanol and polyethylene glycol (PEG-300) delivered the Michael adduct in low chemical yield, however, with moderate diastereoselectivity and high enantioselectivity (Table 1, entry 5 and 6). A visual schematic representation of the optimized condition in different stages is depicted in Fig. 1 showing the emulsion formation upon the addition of all substrates to the amphiphilic organocatalyst **3e** in water.

With these notably improved reaction conditions in hand, we explored the scope of the Michael addition between different aldehydes and *trans*-β-nitrostyrene mediated by the organocatalyst **3e** in an aqueous environment (Scheme 3).

Gratifyingly, the extension of this sustainable transformation to hexanal, under the previously established optimized reaction conditions, resulted in the formation of product **4b** in 91% yield, with 99% *e.e.* and 92:8 *d.r.* When isovaleraldehyde was used as the donor, the reaction proceeded efficiently, affording the corresponding product **4c** in 79% yield, with high levels of stereoselectivities (*d.r.*: 99:1, *e.e.*: 99%). Additionally, (R)-(+)-Citronellal was also compatible with the reaction, which led to the desired Michael adduct **4d** with moderate yield, good diastereoselectivity and high enantioselectivity.

Moreover, a representative selection of *trans*-β-nitrostyrenes was evaluated to establish the generality of this asymmetric catalytic system. Of particular note, nitrostyrene bearing distinct substituents, either electron-withdrawing groups (*i.e.*, F, Cl, Br, NO$_2$ and CF$_3$) (**4e–i**, **4m**) or electron-donating groups (*i.e.*, OMe, Me and *t*-Bu) (**4j–l**, **4n**) gave the desired Michael adducts in moderate to excellent yields as well as diastereoselectivities and maintained enantioselectivity ranges of 96–99%. Interestingly, modification of the aromatic ring to introduce heterocycles such as furan was also well tolerated (compound **4o**, 83% yield, 99% *e.e.* and 82:18 *d.r.*). Moreover, alteration to alkyl-substituted nitroolefins also afforded the corresponding products in good yield and excellent stereoselectivity (**4p** and **4q**).

Performing the reaction on a 2 mmol scale under a prolonged reaction time of 72 hours afforded **4a** in a similar yield and enantioselectivity, albeit with a drop in the diastereoisomeric

Table 1 Optimization of the system. All reactions were carried out using 2 equivalents of butanal and 0.2 mmol of *trans*-β-nitrostyrene in 0.4 mL of solvent for 24 h. The yield was determined by ^{1}H NMR spectroscopic analysis of the crude reaction mixture with 1,2,3-trimethoxybenzene as the internal standard (yield of the isolated product). The *syn/anti* ratio was determined by ^{1}H NMR and the enantiomeric excess was determined by chiral-stationary phase UPC^2 analysis

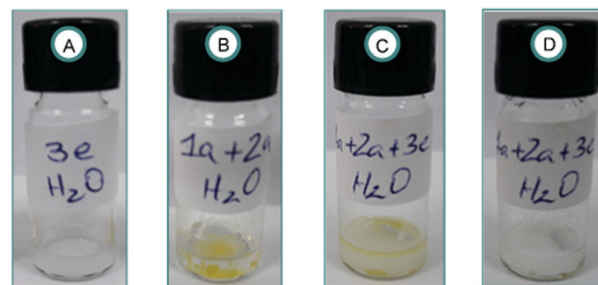| Entry	Deviation from initial conditions	Yield (%)	*d.r.* syn:anti	*e.e.* (%)
1	Using 5 mol% of catalyst loading	90	90:10	99
2	Using 2.5 mol% of catalyst loading	99 (96)	93:7	99
3	Using 1 mol% of catalyst loading	52	98:2	99
4	Brine instead water	84	95:5	99
5	Ethanol instead water	26	85:15	99
6	PEG-300 instead water	54	82:18	99

Fig. 1 (**A**) catalyst **3e** in water; (**B**) mixture of butyraldehyde and *trans*-β-nitrostyrene in water; (**C**) mixture of butyraldehyde, *trans*-β-nitrostyrene and catalyst **3e** in water; and (**D**) mixture of butyraldehyde, *trans*-β-nitrostyrene and catalyst **3e** in water after being stirred for 24 h.
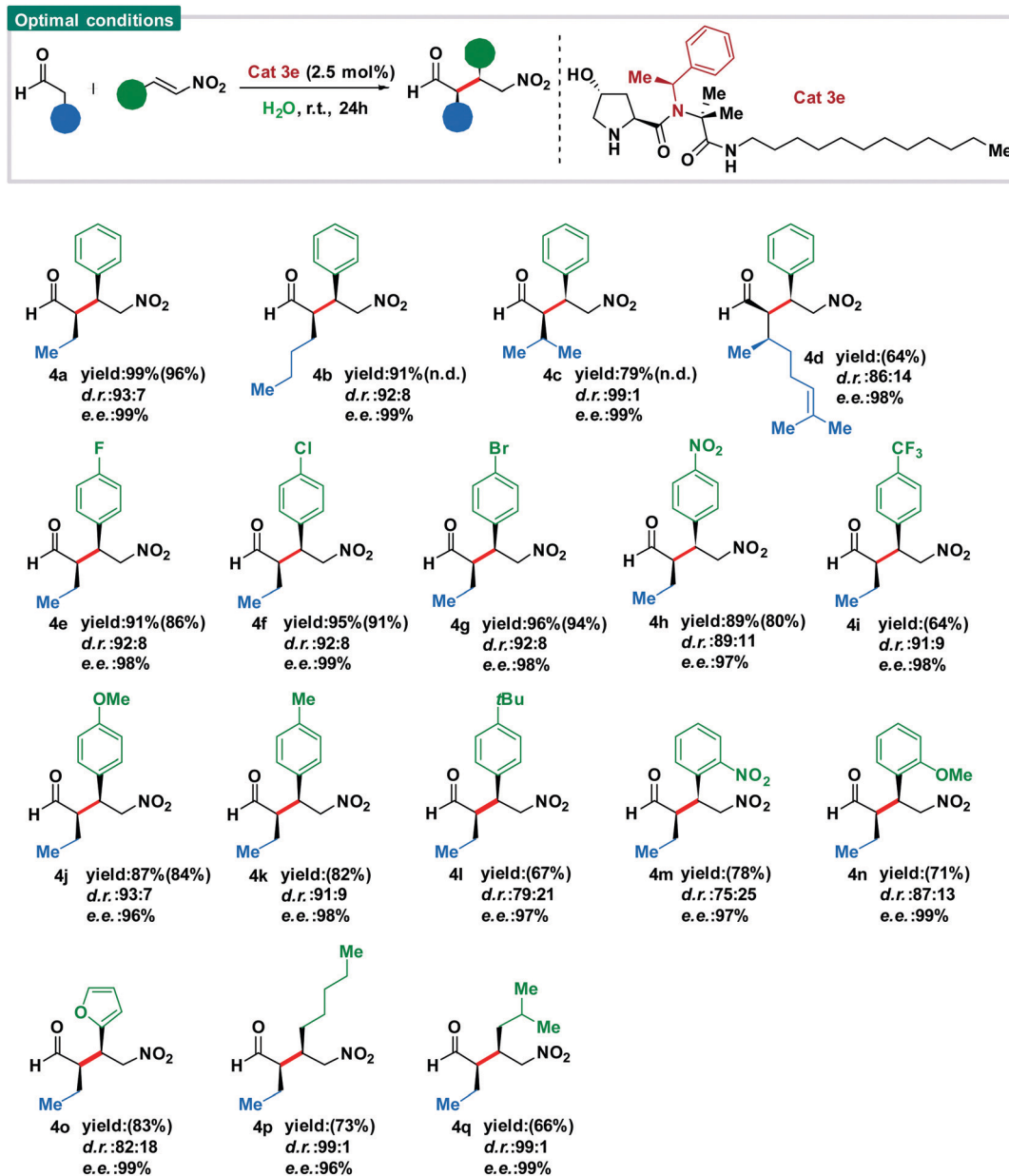
Scheme 3 Scope of reaction with catalyst **3e**. All reactions were conducted using 2 equivalents of the aldehyde and 0.2 mmol of β-nitrostyrene in 0.4 mL of water. The yield was determined by ^{1}H NMR spectroscopic analysis of the crude reaction mixture with 1,2,3-trimethoxybenzene as the internal standard (yield of the isolated product). The diastereoisomeric ratio was determined by ^{1}H NMR of the crude reaction mixture and the enantiomeric excess was determined by chiral-stationary phase UPC^2 analysis. Note: The diastereoisomeric ratio for isolated products changes upon purification and the values are reported in the ESI,† Section 17.

ratio (see the ESI† for further details, 90% yield, 72:28 *d.r.* and 99% *e.e.*). To our delight, catalyst recycling was easily achieved after filtration over a pad of silica flash using ethyl acetate as the mobile phase for eluting the crude product with the organocatalyst being trapped on the silica. Afterwards, the organocatalyst could be recovered by passing methanol through the silica and evaporating the solvent. Moreover, under the optimized reaction conditions, the recovered organocatalyst **3e** was successfully subjected to four cycles delivering the desired product **4a** with a stable tendency for reproducibility over each cycle (see the ESI† for further information).

Conclusions

In summary, we have developed an amphiphilic *N*-alkylated lipopeptide (**3e**) which presented extraordinary catalytic activity in the asymmetric Michael addition of aldehydes to *trans*-β-nitrostyrene in water – neither organic solvent nor additional additives were found to be necessary in this sustainable reaction protocol. This new catalytic system is appropriate for functionalization of an array of *trans*-β-nitroolefins, including aromatic and aliphatic, in good to excellent yields and stereoselectivities under low catalyst loadings. Furthermore, the

reaction could be easily scaled-up and the catalyst could be recycled, delivering the Michael adduct with similar results in both cases. Hence, these remarkable advantages make this catalytic system suitable for future pharmaceutical developments and opens new perspectives in stereoselective organic synthesis in water.

Experimental

Materials and methods

All solvents were dried and distilled before use using standard procedures and the reagents were of the highest commercially available grade purchased from Sigma-Aldrich, Oakwood Chemicals, and Strem Chemicals and used as received or purified according to the procedures outlined in Purification of Common Laboratory Chemicals.[18] Glassware used was dried in an oven or flame dried under a vacuum and cooled under an inert atmosphere. Column flash chromatography was performed using silica gel 60 (230–400 mesh), and thin-layer chromatography (TLC) analysis was performed using silica gel aluminum sheets. Compounds were visualized on TLC by UV-light, $KMnO_4$, I_2, $H_3[P(Mo_3O_{10})_4]$ x H_2O (PMA) and Vanillin. Yields refer to chromatographically and spectroscopically pure compounds unless otherwise noted. ^1H NMR and ^{13}C NMR spectra were recorded at 400 and 100 MHz, respectively. Chemical shifts (δ) are reported in parts per million relative to the residual solvent signals,[19] and coupling constants (J) are reported in hertz. The following abbreviations indicate the multiplicity of each signal: (s), singlet; (bs), broad singlet; (d), doublet; (t), triplet; (q), quartet; (p), pentet; (m), multiplet; (dd), doublet of doublets; (dt), doublet of triplets; (dq), doublet of quartet; (dp), doublet of pentet; (td), triplet of doublets; (ddt), doublet of doublet of triplets; (dtd), doublet of triplet of doublets; (ddd), doublet of doublet of doublets; (dddd), doublet of doublet of doublet of doublets; (heptd), heptet of doublets. High-resolution ESI mass spectra were obtained using a Waters Acquity UPLC H-class liquid chromatograph coupled with a Waters Xevo G2-XS QToF mass spectrometer with an electrospray interface (ESI). HPLC analysis was carried out on an analytical HPLC using a diode array detector SPD-M20A from Shimadzu using a Chiralpak column OD-H (250 mm × 4.6 mm) from Daicel Chemical Ind. LTD. UPLC analysis was carried out on an Acquity UPC^2 system from Waters using a 2998 photodiode array (PDA) and Xevo TQD triple quadrupole mass spectrometer as detectors using Trefoil columns CEL2 and AMY1 (2.1 mm × 50 mm) from Waters. Optical rotations were measured on a PerkinElmer polarimeter.

General procedures for the synthesis of prolyl *pseudo*-lipopeptides by Ugi-4CR:

General procedure A. A solution containing acetone (3 equiv.), amine (1.5 equiv.) and anhydrous sodium sulfate (3 equiv.) in MeOH was stirred at room temperature for 2 hours. After the addition of carboxylic acid (1.2 equiv.) and isocyanide

(1 equiv.), the resulting mixture was allowed to stir at room temperature for 24 h. Finally, the solvent was removed under reduced pressure and the residue was subjected to a deprotection procedure and purified using column chromatography.

General procedure B. A solution containing acetone (3 equiv.) and amine (1.5 equiv.) and anhydrous sodium sulfate (3 equiv.) in MeOH/THF (2 : 1 v/v) was stirred under microwave irradiation at 70 °C for 10 min. After the carboxylic acid (1.2 equiv.) and isocyanide (1 equiv.) were added, the resulting mixture was stirred under microwave irradiation (at 70 °C) for 30 min. Finally, the solvent was removed under reduced pressure and the residue was subjected to a deprotection procedure and purified using column chromatography.

General procedure C. A solution containing acetone (3 equiv.), amine (1.5 equiv.) and anhydrous sodium sulfate (3 equiv.) in MeOH/THF (2 : 1 v/v) was stirred under microwave irradiation at (70 °C) during 10 min to preform the imine. After carboxylic acid (1.2 equiv.) and isocyanide (1 equiv.) were added, the resulting mixture was allowed to stir at room temperature for 24–48 h. Finally, the solvent was removed under reduced pressure and the residue was subjected to the deprotection procedure and purified using column chromatography.

N-Boc deprotection procedure of prolyl *pseudo*-lipopeptides:

The crude *N*-Boc product of the Ugi-4CR was dissolved in 1 mL of a mixture of TFA/DCM 9 : 1 v/v at 0 °C. The reaction mixture was allowed to stir for 30 min and then concentrated under reduced pressure (TFA was entirely removed by repetitive addition and evaporation of further DCM). The crude product was dissolved in 10 mL of DCM and neutralized over anhydrous K_2CO_3, filtered and evaporated under reduced pressure afford the crude product.

Peptide–lipopeptoid hybrid 3a. ^1H NMR (400 MHz, Methanol-d_4) δ 7.64 (d, J = 7.7 Hz, 2H, CH), 7.42 (t, J = 7.6 Hz, 2H, CH), 7.31 (t, J = 7.4 Hz, 1H, CH), 5.23 (q, J = 7.1 Hz, 1H, CH), 3.91 (s, 1H, NH), 3.62 (ddt, J = 9.8, 7.3, 3.6 Hz, 1H, CH), 3.20 (dt, J = 11.2, 6.7 Hz, 1H, CH_2), 2.92 (dt, J = 11.5, 7.3 Hz, 1H, CH_2), 1.90 (d, J = 7.1 Hz, 3H, CH_3), 1.87–1.70 (m, 5H, CH_2), 1.69–1.42 (m, 9H, CH_2, CH_3), 1.38–1.13 (m, 6H, CH_2). ^{13}C NMR (100 MHz, Methanol-d_4) δ 176.3 (2 x C=O), 143.5 (C), 129.9 (CH), 128.5 (CH), 128.2 (CH), 65.9 (C), 61.4 (CH), 53.1 (CH), 50.4 (CH_2), 48.0 (CH), 33.49 (CH_2), 33.46 (CH_2), 30.5 (CH_2), 26.7 (CH_2), 26.4 (CH_3), 26.0 (CH_2), 25.6 (CH_2), 24.8 (CH_2), 20.2 (CH_3). HRMS (ESI-Q-TOF): *m/z*: 386.2808. Calcd. for [M + H]$^+$:386.2802.

Peptide–Lipopeptoid Hybrid 3b. ^1H NMR (400 MHz, Methanol-d_4) δ 7.65 (d, J = 7.7 Hz, 2H, CH), 7.43 (t, J = 7.5 Hz, 2H, CH), 7.33 (t, J = 7.4 Hz, 1H, CH), 5.25 (q, J = 7.1 Hz, 1H, CH), 4.22 (s, 1H, CH), 3.36–3.31 (m, 1H, CH_2), 3.25–3.09 (m, 3H, CH_2), 1.90 (d, J = 7.1 Hz, 3H, CH_3), 1.69–1.48 (m, 10H, CH_2, CH_3), 1.28 (s, 20H, CH_2), 0.89 (t, J = 6.5 Hz, 3H, CH_3). ^{13}C NMR (100 MHz, Methanol-d_4) δ 177.0 (C=O), 171.4 (C=O), 142.9 (C), 130.0 (CH), 128.7 (CH), 128.4 (CH), 66.2 (CH), 61.2 (CH), 53.3 (C), 47.6 (CH_2), 40.9 (CH_2), 33.1 (CH_2), 30.7 (CH_2), 30.5 (CH_2), 30.3 (CH_2), 30.0 (CH_2), 28.1 (CH_3), 25.6 (CH_2), 25.1 (CH_2), 24.9 (CH_2), 23.7 (CH_3), 20.0 (CH_2), 14.4 (CH_3). HRMS (ESI-Q-TOF): *m/z*: 472.3876. Calcd. for [M + H]$^+$: 472.3898.

Peptide–lipopeptoid hybrid 3c. ^{1}H NMR (400 MHz, Methanol-d$_4$) δ 7.60 (d, J = 7.7 Hz, 2H, CH), 7.41 (t, J = 7.6 Hz, 2H, CH), 7.30 (t, J = 7.4 Hz, 1H, CH), 5.20 (q, J = 7.2 Hz, 1H, CH), 4.28 (s, 1H, CH), 3.59 (dp, J = 11.6, 4.1 Hz, 1H, CH), 3.27 (ddd, J = 6.8, 5.3, 3.8 Hz, 2H, CH$_2$), 3.15–3.08 (m, 1H, CH), 1.88 (d, J = 7.1 Hz, 3H, CH$_3$), 1.85–1.70 (m, 4H, CH$_2$), 1.69–1.46 (m, 8H, CH$_2$, CH$_3$), 1.37–1.09 (m, 6H, CH$_2$). ^{13}C NMR (100 MHz, Methanol-d$_4$) δ 174.8 (C=O), 170.8 (C=O), 141.7 (C), 128.7 (CH), 127.4 (CH), 126.8 (CH), 69.6 (CH), 64.8 (C), 58.6 (CH), 54.1 (CH), 49.1 (CH), 38.4 (CH$_2$), 32.1 (CH$_2$), 25.2 (CH$_2$), 25.1 (CH$_3$), 24.1 (CH$_2$), 23.4 (CH$_2$), 18.8 (CH$_3$). HRMS (ESI-Q-TOF): m/z: 402.2757. Calcd. for [M + H]$^+$: 402.2751.

Peptide–lipopeptoid hybrid 3d. ^{1}H NMR (400 MHz, Methanol-d$_4$) δ 7.63 (d, J = 7.7 Hz, 2H, CH), 7.42 (t, J = 7.6 Hz, 2H, CH), 7.31 (t, J = 7.4 Hz, 1H, CH), 5.20 (q, J = 7.1 Hz, 1H, CH), 4.26 (s, 1H, CH), 4.18 (s, 1H, NH), 3.24 (dd, J = 11.9, 3.9 Hz, 1H, CH$_2$), 3.16 (q, J = 6.7 Hz, 2H, CH$_2$), 3.00 (d, J = 11.8 Hz, 1H, CH$_2$), 1.90 (d, J = 7.0 Hz, 3H, CH$_3$), 1.69–1.46 (m, 9H, CH$_2$, CH$_3$), 1.38–1.26 (m, 6H, CH$_2$), 0.88 (t, 3H, CH$_3$). ^{13}C NMR (100 MHz, Methanol-d$_4$) δ 177.1 (C=O), 173.5 (C=O), 143.4 (C), 130.0 (CH), 128.6 (CH), 128.1 (CH), 71.5 (CH), 65.9 (CH), 60.0 (CH), 55.6 (CH$_2$), 53.0 (C), 40.9 (CH$_2$), 40.0 (CH$_2$), 32.7 (CH$_2$), 30.3 (CH$_2$), 27.8 (CH$_3$), 25.6 (CH$_2$), 24.8 (CH$_2$), 23.7 (CH$_3$), 20.4 (CH$_2$), 14.4 (CH$_3$). HRMS (ESI-Q-TOF): m/z: 404.2906. Calcd. for [M + H]$^+$: 404.2908.

Peptide–lipopeptoid hybrid 3e. ^{1}H NMR (400 MHz, Methanol-d$_4$) δ 7.65 (d, J = 7.7 Hz, 2H, CH), 7.45 (t, J = 7.5 Hz, 2H, CH), 7.35 (t, J = 7.4 Hz, 1H, CH), 5.24 (q, J = 7.1 Hz, 1H, CH), 4.32 (s, 1H, CH), 3.31–3.28 (m, 2H, CH$_2$), 3.18 (dd, J = 8.9, 5.7 Hz, 2H, CH$_2$), 1.92 (d, J = 7.0 Hz, 3H, CH$_3$), 1.70–1.58 (m, 6H, CH$_3$), 1.57–1.50 (m, 2H, CH$_2$), 1.29 (s, 20H. CH$_2$), 0.92–0.87 (m, 4H, CH$_2$, CH$_3$). ^{13}C NMR (100 MHz, Methanol-d$_4$) δ 177.0 (C=O), 171.9 (C=O), 143.0 (C), 130.1 (CH), 128.8 (CH), 128.2 (CH), 70.8 (CH), 66.2 (CH), 60.0 (CH), 55.5 (CH$_2$), 53.2 (C), 41.0 (CH$_2$), 39.8 (CH$_2$), 33.1 (CH$_2$), 30.7 (CH$_2$), 30.5 (CH$_2$), 30.4 (CH$_2$), 28.1 (CH$_3$), 25.4 (CH$_2$), 24.9 (CH$_2$), 23.7 (CH$_3$), 20.2 (CH$_2$), 14.4 (CH$_3$). HRMS (ESI-Q-TOF): m/z: 488.3827. Calcd. for [M + H]$^+$: 488.3847.

Peptide–lipopeptoid hybrid 3f. ^{1}H NMR (400 MHz, Methanol-d$_4$) δ 7.65 (d, J = 7.7 Hz, 2H, CH), 7.40 (t, J = 7.7 Hz, 2H, CH), 7.28 (t, J = 7.6 Hz, 1H, CH), 5.17 (q, J = 7.2 Hz, 1H, CH), 4.00 (s, 1H, CH), 3.62 (s, 1H, OH), 3.17 (td, J = 7.0, 3.9 Hz, 2H, CH$_2$), 2.95 (d, J = 12.0 Hz, 1H, CH$_2$), 2.60 (dd, J = 12.4, 4.2 Hz, 1H, CH$_2$), 1.89 (d, J = 7.0 Hz, 3H, CH$_3$), 1.62–1.49 (m, 8H, CH$_2$, CH$_3$), 1.28 (s, 20H, CH$_2$), 0.89 (t, J = 6.7 Hz, 3H, CH$_3$). ^{13}C NMR (100 MHz, Methanol-d$_4$) δ 177.3 (2 x C=O), 144.3 (C), 129.8 (CH), 128.2 (CH), 127.8 (CH), 73.2 (CH), 65.5 (CH), 60.8 (CH), 56.9 (CH$_2$), 52.8 (C), 40.9 (CH$_2$), 39.8 (CH$_2$), 33.1 (CH$_2$), 30.8 (CH$_2$), 30.7 (CH$_2$), 30.50 (CH$_2$), 30.48 (CH$_2$), 30.4 (CH$_2$), 28.1 (CH$_3$), 25.9 (CH$_2$), 24.6 (CH$_2$), 23.7 (CH$_3$), 20.9 (CH$_2$), 14.5 (CH$_3$). HRMS (ESI-Q-TOF): m/z: 488.3863. Calcd. for [M + H]$^+$: 488.3847.

Peptide–lipopeptoid hybrid 3g. ^{1}H NMR (400 MHz, Methanol-d$_4$) δ 7.52–7.26 (m, 5H, CH), 5.29–5.12 (m, 1H, CH), 4.64 (s, 1H, OH), 4.04–3.63 (m, 1H, CH), 3.54–3.31 (m, 2H, CH$_2$), 3.20–3.13 (m, 2H, CH$_2$), 2.58–1.82 (m, 3H, CH$_2$), 1.78–1.39 (m, 6H, CH$_2$, CH$_3$), 1.27 (s, 30H, CH$_2$, CH$_3$), 1.16–0.71 (m, 5H, CH$_2$, CH$_3$). ^{13}C NMR (100 MHz, Methanol-d$_4$) δ 172.7 (C=O), 169.6 (C=O), 140.0 (C), 129.9 (CH), 129.8 (CH), 129.5 (CH), 129.3 (CH), 129.2 (CH), 71.4 (CH), 61.8 (CH), 60.6 (CH), 59.8 (CH$_2$), 56.8 (CH$_2$), 55.0 (C), 40.9 (CH$_2$), 40.8 (CH$_2$), 39.5 (CH$_2$), 33.1 (CH$_2$), 30.8 (CH$_2$), 30.5 (CH$_2$), 30.46 (CH$_2$), 30.43 (CH$_2$), 28.7 (CH$_2$), 28.1 (CH$_3$), 23.7 (CH$_3$), 17.1 (CH$_2$), 14.5 (CH$_3$). HRMS (ESI-Q-TOF): m/z: 603.5006. Calcd. for [M + CH3OH]$^+$: 603.4975.

Peptide–lipopeptoid hybrid 3h. ^{1}H NMR (400 MHz, Methanol-d$_4$) δ 7.68 (d, J = 7.7 Hz, 2H, CH), 7.47 (t, J = 7.7 Hz, 2H, CH), 7.35 (t, J = 7.7 Hz, 1H, CH), 5.27 (q, J = 7.1 Hz, 1H, CH), 3.74–3.61 (m, 1H, CH), 3.59 (dd, J = 12.9, 4.7 Hz, 2H, CH$_2$), 3.40–3.31 (m, 1H, CH), 2.34–2.19 (m, 2H, CH$_2$), 1.94 (d, J = 7.0 Hz, 3H, CH$_3$), 1.92–1.55 (m, 13H, CH$_2$, CH$_3$), 1.44–1.14 (m, 25H, CH$_2$), 0.92 (t, J = 6.6 Hz, 3H, CH$_3$). ^{13}C NMR (100 MHz, Methanol-d$_4$) δ 176.1 (C=O), 173.7 (C=O), 170.8 (C=O), 143.2 (C), 130.2 (CH), 128.9 (CH), 128.4 (CH), 73.8 (CH), 66.3 (CH), 60.3 (CH), 53.0 (C), 52.7 (CH$_2$), 50.6 (CH), 37.1 (CH$_2$), 34.8 (CH$_2$), 33.5 (CH$_2$), 33.1 (CH$_2$), 30.7 (CH$_2$), 30.6 (CH$_2$), 30.5 (CH$_2$), 30.2 (CH$_2$), 26.6 (CH$_3$), 26.5 (CH$_3$), 25.9 (CH$_2$), 25.7 (CH$_2$), 25.5 (CH$_2$), 24.8 (CH$_2$), 23.7 (CH$_2$), 20.1 (CH$_3$), 14.4 (CH$_3$). HRMS (ESI-Q-TOF): m/z: 584.4412. Calcd. for [M + H]$^+$: 584.4422.

Peptide–lipopeptoid hybrid 3i. ^{1}H NMR (400 MHz, Chloroform-d$_3$) δ 5.97 (d, J = 8.2 Hz, 1H, NH), 4.66 (t, J = 7.6 Hz, 1H, CH), 3.67–3.57 (m, 1H, CH$_2$), 3.53–3.39 (m, 3H, CH$_2$), 3.31 (ddd, J = 16.3, 11.7, 5.3 Hz, 1H, CH), 2.44–2.33 (m, 1H, CH$_2$), 2.17–1.93 (m, 3H, CH$_2$), 1.83 (dt, J = 14.4, 7.2 Hz, 2H, CH$_2$), 1.75–1.63 (m, 3H, CH$_2$), 1.61–1.42 (m, 6H, CH$_2$, CH$_3$), 1.33–1.09 (m, 24H, CH$_2$), 0.89–0.82 (m, 3H, CH$_2$, CH$_3$). ^{13}C NMR (100 MHz, Chloroform-d$_3$) δ 173.1 (C=O), 168.8 (C=O), 63.3 (CH), 58.9 (C), 48.9 (CH), 46.5 (CH$_2$), 45.1 (CH$_2$), 32.9 (CH$_2$), 32.9 (CH$_2$), 32.0 (CH$_2$), 31.9 (CH$_2$), 29.8 (CH$_2$), 29.7 (CH$_2$), 29.67 (CH$_2$), 29.65 (CH$_2$), 29.4 (CH$_2$), 29.3 (CH$_2$), 27.2 (CH$_3$), 25.6 (CH$_2$), 25.2 (CH$_2$), 25.2 (CH$_2$), 25.0 (CH$_2$), 24.6 (CH$_2$), 24.5 (CH$_2$), 22.8 (CH$_2$), 14.2 (CH$_3$). HRMS (ESI-Q-TOF): m/z: 450.4043. Calcd. for [M + H]$^+$: 450.4054.

Peptide–lipopeptoid hybrid 3j. ^{1}H NMR (400 MHz, Methanol-d$_4$) δ 4.50–4.42 (m, 1H, CH), 3.50–3.32 (m, 3H, CH$_2$), 3.27–3.01 (m, 3H, CH$_2$), 2.48 (dq, J = 13.0, 6.9, 5.4 Hz, 1H, CH$_2$), 2.11–1.91 (m, 3H, CH$_2$), 1.74–1.59 (m, 2H, CH$_2$), 1.52 (s, 3H, CH$_3$), 1.47 (s, 3H, CH$_3$), 1.39–1.22 (m, 38H, CH$_2$), 0.88 (t, J = 6.6 Hz, 6H. CH$_3$). ^{13}C NMR (100 MHz, Methanol-d$_4$) δ 176.9 (C=O), 169.8 (C=O), 64.2 (C), 60.4 (CH), 47.5 (CH$_2$), 45.6 (CH$_2$), 40.9 (CH$_2$), 33.1 (CH$_2$), 32.6 (CH$_2$), 30.8 (CH$_2$), 30.5 (CH$_2$), 30.4 (CH$_2$), 28.1 (CH$_3$), 27.9 (CH$_2$), 25.4 (CH$_2$), 24.8 (CH$_2$), 24.3 (CH$_2$), 23.7 (CH$_2$), 14.4 (CH$_3$). HRMS (ESI-Q-TOF): m/z: 536.5145. Calcd. for [M + H]$^+$: 536.5150.

Peptide–lipopeptoid hybrid 3k. ^{1}H NMR (400 MHz, Methanol-d$_4$) δ 7.52–7.41 (m, 4H, CH), 7.43–7.34 (m, 4H, CH), 7.34–7.24 (m, 2H, CH), 6.45 (bs, 1H, CH), 4.12 (s, 1H, CH), 3.88 (t, J = 7.8 Hz, 1H, CH), 3.26–3.15 (m, 2H, CH$_2$), 3.12 (dd, J = 11.8, 4.7 Hz, 1H, CH$_2$), 2.63 (d, J = 11.8 Hz, 1H, CH$_2$), 1.72–1.59 (m, 3H, CH$_3$), 1.57–1.45 (m, 5H, CH$_2$, CH$_3$), 1.38–1.24 (m, 20H, CH$_2$), 0.89 (t, J = 6.6 Hz, 3H, CH$_3$). ^{13}C NMR (100 MHz, Methanol-d$_4$) δ 177.5 (C=O), 177.1 (C=O), 143.1 (C), 139.9 (C), 130.1 (CH), 130.0 (CH), 129.9 (CH), 129.5 (CH), 128.9 (CH),

128.8 (CH), 72.5 (CH), 66.0 (C), 62.2 (CH), 61.6 (CH), 56.1 (CH$_2$), 40.9 (CH$_2$), 39.7 (CH$_2$), 33.1 (CH$_2$), 30.8 (CH$_2$), 30.7 (CH$_2$), 30.50 (CH$_2$), 30.47 (CH$_2$), 30.4 (CH$_2$), 28.1 (CH$_3$), 25.7 (CH$_2$), 24.5 (CH$_2$), 23.7 (CH$_2$), 14.5 (CH$_3$). HRMS (ESI-Q-TOF): m/z: 550.4002. Calcd. for [M + H]$^+$: 550.4003.

General procedure for asymmetric 1,4-addition of aldehydes to nitrostyrenes

A vial was charged with the prolyl pseudo-lipopeptide hybrid catalyst **3e** (2.5 mol%), the nitrostyrene (0.2 mmol, 1.0 equiv.) and 0.4 mL of water. The mixture was homogenized in an ultrasound bath, the aldehyde (0.40 mmol, 2.0 equiv.) was added and this mixture was stirred for 24 h. After this period, the resulting reaction mixture was extracted with EtOAc, dried over anhydrous Na$_2$SO$_4$ and concentrated under reduced pressure. The crude product was purified by flash column chromatography on silica gel using n-hexane/EtOAc as the eluent. The diastereoisomeric ratio was determined by ^{1}H NMR analysis of the crude reaction mixture. Enantiomeric excess (*e.e.*) was determined by chiral HPLC or UPC^2 analysis through comparison with the authentic racemic material. Assignment of the stereoisomers was performed by comparison with literature data.[3f]

Conflicts of interest

There are no conflicts to declare.

Acknowledgements

Notes and references

1 (a) R. Mahrwald, *Drug Discovery Today: Technol.*, 2013, **10**, e29–e36; (b) U. Scheffler and R. Mahrwald, *Chem. – Eur. J.*, 2013, **19**, 14346–14396.

2 (a) B. List, *Chem. Rev.*, 2007, **107**, 5413–5415; (b) D. W. C. MacMillan, *Nature*, 2008, **455**, 304–308; (c) B. List, R. A. Lerner and C. F. Barbas, *J. Am. Chem. Soc.*, 2000, **122**, 2395–2396.

3 (a) A. Znabet, E. Ruijter, F. J. J. De Kanter, V. Köhler, M. Helliwell, N. J. Turner and R. V. A. Orru, *Angew. Chem., Int. Ed.*, 2010, **49**, 5289–5292; (b) M. Raj, V. Bisai, S. K. Ginotra and V. K. Singh, *Org. Lett.*, 2006, **8**, 4097–4099; (c) P. Melchiorre and K. A. Jørgensen, *J. Org. Chem.*, 2003, **68**, 4151–4157; (d) H. Wennemers, *CHIMA Int. J. Chem.*, 2007, **61**, 276–278; (e) N. Mase, Y. Nakai, N. Ohara, H. Yoda, K. Takabe, F. Tanaka and C. F. Barbas, *J. Am. Chem. Soc.*, 2006, **128**, 734–735; (f) Y. Hayashi, H. Gotoh, T. Hayashi and M. Shoji, *Angew. Chem., Int. Ed.*, 2005, **44**,

4212–4215; (g) N. Halland, P. S. Aburel and K. A. Jørgensen, *Angew. Chem., Int. Ed.*, 2003, **42**, 661–665.

4 (a) J. L. Tucker and M. M. Faul, *Nature*, 2016, **534**, 27–29; (b) K. Sanderson, *Nature*, 2011, **469**, 18–20.

5 (a) M. Raj and V. K. Singh, *Chem. Commun.*, 2009, 6687–6703; (b) M. Gruttadauria, F. Giacalone and R. Noto, *Adv. Synth. Catal.*, 2009, **351**, 33–57; (c) N. Mase and C. F. Barbas, *Org. Biomol. Chem.*, 2010, **8**, 4043–4050; (d) T. Kitanosono, K. Masuda, P. Xu and S. Kobayashi, *Chem. Rev.*, 2018, **118**, 679–746; (e) M. P. van der Helm, B. Klemm and R. Eelkema, *Nat. Rev. Chem.*, 2019, **3**, 491–508.

6 M. Kjellin, A. Surfactants and S. Stenungsund, *Surfactants from Renewable Resources*, John Wiley & Sons, Ltd, Chichester, UK, 2010.

7 M. Shiri and M. A. Zolfigol, *Tetrahedron*, 2009, **65**, 587–598.

8 (a) M. P. van der Helm, B. Klemm and R. Eelkema, *Nat. Rev. Chem.*, 2019, **3**, 491–508; (b) T. Lorenzetto, G. Berton, F. Fabris and A. Scarso, *Catal. Sci. Technol.*, 2020, **10**, 4492–4502.

9 G. La Sorella, G. Strukul and A. Scarso, *Green Chem.*, 2015, **17**, 644–683.

10 W. Guo, X. Liu, Y. Liu and C. Li, *ACS Catal.*, 2018, **8**, 328–341.

11 (a) B. H. Lipshutz and S. Ghorai, *Org. Lett.*, 2012, **14**, 422–425; (b) L. Zhong, Q. Gao, J. Gao, J. Xiao and C. Li, *J. Catal.*, 2007, **250**, 360–364; (c) B. Zhang, Z. Jiang, X. Zhou, S. Lu, J. Li, Y. Liu and C. Li, *Angew. Chem., Int. Ed.*, 2012, **51**, 13159–13162; (d) W. Guo, B. Wu, X. Zhou, P. Chen, X. Wang, Y.-G. Zhou, Y. Liu and C. Li, *Angew. Chem., Int. Ed.*, 2015, **54**, 4522–4526; (e) D. Sarkar, R. Bhattarai, A. D. Headley and B. Ni, *Synthesis*, 2011, 1993–1997; (f) N. Mase, K. Watanabe, H. Yoda, K. Takabe, F. Tanaka and C. F. Barbas, *J. Am. Chem. Soc.*, 2006, **128**, 4966–4967; (g) S. Zhu, S. Yu and D. Ma, *Angew. Chem., Int. Ed.*, 2008, **47**, 545–548; (h) M. Lombardo, M. Chiarucci, A. Quintavalla and C. Trombini, *Adv. Synth. Catal.*, 2009, **351**, 2801–2806; (i) Y.-J. Cao, Y.-Y. Lai, X. Wang, Y.-J. Li and W.-J. Xiao, *Tetrahedron Lett.*, 2007, **48**, 21–24; (j) C. Palomo, S. Vera, A. Mielgo and E. Gómez-Bengoa, *Angew. Chem., Int. Ed.*, 2006, **45**, 5984–5987; (k) Z. Zheng, B. L. Perkins and B. Ni, *J. Am. Chem. Soc.*, 2010, **132**, 50–51; (l) L. Zu, J. Wang, H. Li and W. Wang, *Org. Lett.*, 2006, **8**, 3077–3079; (m) B. H. Lipshutz, S. Ghorai, A. R. Abela, R. Moser, T. Nishikata, C. Duplais, A. Krasovskiy, R. D. Gaston and R. C. Gadwood, *J. Org. Chem.*, 2011, **76**, 4379–4391; (n) B. H. Lipshutz, S. Ghorai and M. Cortes-Clerget, *Chem. – Eur. J.*, 2018, **24**, 6672–6695; (o) K. S. Feu, A. F. De La Torre, S. Silva, M. A. F. De Moraes Junior, A. G. Corrêa and M. W. Paixão, *Green Chem.*, 2014, **16**, 3169–3174; (p) K. S. Feu, A. M. Deobald, S. Narayanaperumal, A. G. Corrêa and M. Weber Paixão, *Eur. J. Org. Chem.*, 2013, 5917–5922; (q) A. M. Deobald, A. G. Corrêa, D. G. Rivera and M. W. Paixão, *Org. Biomol. Chem.*, 2012, **10**, 7681–7684; (r) L.-W. Xu, L. Li and Z.-H. Shi, *Adv. Synth. Catal.*, 2010, **352**, 243–279; (s) S.-P. Zhang, X.-K. Fu and S.-D. Fu, *Tetrahedron Lett.*, 2009, **50**, 1173–1176; (t) A. Kumar, S. Singh, V. Kumar and S. S. Chimni, *Org. Biomol. Chem.*, 2011, **9**, 2731–2742; (u) C. Wu,

X. Fu, X. Ma and S. Li, *Tetrahedron: Asymmetry*, 2010, **21**, 2465–2470; (*v*) L. Zhang, S. Luo and J. P. Cheng, *Catal. Sci. Technol.*, 2011, **1**, 507–516; (*w*) Q. Zhao, Y.-H. Lam, M. Kheirabadi, C. Xu, K. N. Houk and C. E. Schafmeister, *J. Org. Chem.*, 2012, **77**, 4784–4792; (*x*) S. V. Kochetkov, A. S. Kucherenko and S. G. Zlotin, *Eur. J. Org. Chem.*, 2011, 6128–6133; (*y*) E. G. Doyagüez, G. Corrales, L. Garrido, J. Rodríguez-Hernández, A. Gallardo and A. Fernández-Mayoralas, *Macromolecules*, 2011, **44**, 6268–6276.

12 J. Duschmalé, S. Kohrt and H. Wennemers, *Chem. Commun.*, 2014, **50**, 8109–8112.

13 B. M. Soares, A. M. Aguilar, E. R. Silva, M. D. Coutinho-Neto, I. W. Hamley, M. Reza, J. Ruokolainen and W. A. Alves, *Phys. Chem. Chem. Phys.*, 2017, **19**, 1181–1189.

14 A. F. De La Torre, D. G. Rivera, M. A. B. Ferreira, A. G. Corrêa and M. W. Paixão, *J. Org. Chem.*, 2013, **78**, 10221–10232.

15 The assignment of absolute configuration was done by comparison of $[\alpha]_D$ values with reference 3f.

16 (*a*) G. S. Scatena, A. F. De La Torre, Q. B. Cass, D. G. Rivera and M. W. Paixão, *ChemCatChem*, 2014, **6**, 3208–3214; (*b*) A. F. De La Torre, G. S. Scatena, O. Valdés, D. G. Rivera and M. W. Paixão, *Beilstein J. Org. Chem.*, 2019, **15**, 1210–1216.

17 T. Schnitzer and H. Wennemers, *Synthesis*, 2018, 4377–4382.

18 W. L. E. Armarego and C. L. L. Chai, *Purification of laboratory chemicals (Fifth Edition)*, 2003.

19 G. R. Fulmer, A. J. M. Miller, N. H. Sherden, H. E. Gottlieb, A. Nudelman, B. M. Stoltz, J. E. Bercaw and K. I. Goldberg, *Organometallics*, 2010, **29**, 2176–2179.

Synthesis of *N*-alkylated lipopeptides and their application as organocatalyst in asymmetric Michael addition under aqueous environment

José A. C. Delgado,[a] Fidel E. Morales,[b] Alexander F. de la Torre,[c] Vitor A. Fernandes,[a] Arlene G. Corrêa,[a] and Márcio W. Paixão.[a]

[a.] *Center of Excellence for Research in Sustainable Chemistry (CERSusChem), Department of Chemistry, Federal University of São Carlos – UFSCar, São Carlos, São Paulo, Brazil.*
E-mail: mwpaixao@ufscar.br
[b.] *General Chemistry Department, Faculty of Chemistry, University of Havana, La Habana, Cuba.*
[c.] *Departamento de Química Orgánica, Facultad de Ciencias Químicas, Universidad de Concepción, Concepción, Chile.*

Contents

1. General Information

All solvents were dried and distilled before use by standard procedures and reagents were of the highest commercially available grade purchased from Sigma-Aldrich, Oakwood Chemicals, and Strem Chemicals and used as received or purified according to the procedures outlined in *Purification of Common Laboratory Chemicals.*[1] Glassware used was dried in oven or flame dried under vacuum and cooled under an inert atmosphere. Column flash chromatography was performed using silica gel 60 (230−400 mesh), and analytical thin-layer chromatography (TLC) was performed using silica gel aluminum sheets. Compounds were visualized on TLC by UV-light, $KMnO_4$, I_2, $H_3[P(Mo_3O_{10})_4]$ x H_2O (PMA) and Vanillin. Yields refer to chromatographically and spectroscopically pure compounds unless otherwise noted. ^{1}H NMR and ^{13}C NMR spectra were recorded at 400 and 100 MHz, respectively. Chemical shifts (δ) are reported in parts per million relative to the residual solvent signals,[2] and coupling constants (J) are reported in hertz. the following abbreviations indicate the multiplicity of each signal: (s), singlet; (bs), broad singlet; (d), doublet; (t), triplet; (q), quartet; (p), pentet; (m), multiplet; (dd), doublet of doublets; (dt), doublet of triplets; (dq), doublet of quartet; (dp), doublet of pentet; (td), triplet of doublets; (ddt), doublet of doublet of triplets; (dtd), doublet of triplet of doublets; (ddd), doublet of doublet of doublets; (dddd), doublet of doublet of doublet of doublets; (heptd), heptet of doublets. High-resolution ESI mass spectra were obtained from a Fourier transform ion cyclotron resonance (FT-ICR) mass spectrometer, an RF-only hexapole ion guide and an external electrospray ion source. HPLC analysis were carried out on an analytical HPLC with a diode array detector SPD-M20A from Shimadzu using Chiralpak column OD-H (250 mm x 4.6 mm) from Daicel Chemical Ind. LTD. UPLC analysis was carried out on Acquity UPC[2] system from Waters with 2998 photodiode array (PDA) and Xevo TQD triple quadrupole mass spectrometry as detectors using Trefoil columns CEL2 and AMY1 (2.1 mm x 50 mm) from Waters. Optical rotations were measured on a Perkin Elmer Polarimeter.

2. Synthesis of lipidic isocyanides

General procedure A

$$R-NH_2 \xrightarrow[\text{60 °C, 24h}]{\overset{O}{\underset{O}{\parallel}}\text{EtO}-\text{C}-\text{H}} R-NHCHO \xrightarrow[\text{NEt}_3]{\text{POCl}_3} \overset{\oplus}{R-N}\overset{\ominus}{\equiv}C$$

1
1a, R= n-$C_{12}H_{25}$
1b, R= n-C_6H_{13}
1c, R= n-$C_{18}H_{37}$

2
2a, R= n-$C_{12}H_{25}$
2b, R= n-C_6H_{13}
2c, R= n-$C_{18}H_{37}$
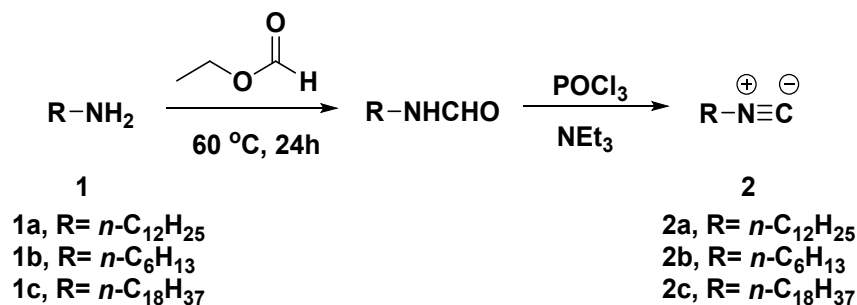
In a 50 mL bottom flask, aliphatic amine **1a-c** (11 mmol) was dissolved in HCOOEt (20 mL). The resulting solution was refluxed at 60 °C for 24 h in a silicone bath and the quantitative formation of formamide was verified by TLC (hexanes/EtOAc 1:1). The reaction was concentrated to dryness, the crude mixture was dissolved in NEt$_3$ (30 mL) and cooled to -70 °C. Then POCl$_3$ (3 mL, 33 mmol, 3 equiv.) was added dropwise during 15 min under argon atmosphere. The reaction mixture was stirred at room temperature for 48h. The resulting mixture was decanted; the solvent removed by reduced pressure and the resulting very viscous oil was directly purified by column chromatography (hexanes, until 10% of EtOAc). The fractions containing the product were combined and evaporated under reduced pressure to give the corresponding isocyanides **2a-c**.

3. Characterization data of compounds 2a-c
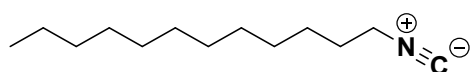
1-isocyanododecane (**2a**)[3]:The title compound was synthesized according to the general procedure A in 71% (1.50 g) isolated yield as a light yellow oil. R_f = 0.83 (hexanes/EtOAc 10:1). **NMR ^{1}H (400 MHz, CDCl$_3$)** δ 3.41 – 3.35 (m, 2H), 1.72 – 1.63 (m, 2H), 1.48 – 1.38 (m, 2H), 1.32 – 1.24 (m, 16H), 0.88 (t, J = 6.9 Hz, 3H). **NMR ^{13}C (100 MHz, CDCl$_3$)** δ 155.6, 60.5, 41.7, 32.0, 29.7, 29.6, 29.5, 29.5, 29.2, 28.8, 26.5, 22.8, 14.3.
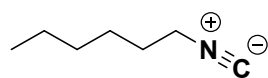
1-isocyanohexane (**2b**)[4]: The title compound was synthesized according to the general procedure A in 65% (795 mg) isolated yield as a light yellow oil. R_f= 0.90 (hexanes/EtOAc 10:1). **NMR ^{1}H (400 MHz, CDCl$_3$)** δ 3.38 (td, J = 6.7, 2.1 Hz, 2H), 1.73 – 1.62 (m, 2H), 1.44 (p, J = 7.2 Hz, 2H), 1.37 –

1.27 (m, 4H), 0.90 (t, J = 6.7 Hz, 2H). **NMR ^{13}C (100 MHz, CDCl$_3$)** δ 155.6, 41.7, 31.0, 29.2, 26.1, 22.6, 14.1.
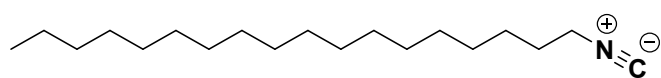
1-isocyanooctadecane (2c)[3]: The title compound was synthesized according to the general procedure A in 76% (2.34 g) isolated yield as a light yellow solid. R_f = 0.65 (hexanes). **NMR ^{1}H (400 MHz, CDCl$_3$)** δ 3.40 – 3.34 (m, 2H), 1.71 – 1.62 (m, 2H), 1.48 – 1.37 (m, 1H), 1.32 – 1.21 (m, 29H), 0.88 (t, J = 6.6 Hz, 3H). **NMR ^{13}C (100 MHz, CDCl$_3$)** δ 155.7, 41.7, 32.1, 29.8, 29.7, 29.5, 29.3, 28.9, 26.5, 22.8, 14.3.

4. General procedures for the synthesis of prolyl pseudo-lipopeptides by Ugi-4CR

General Procedure B: A solution containing acetone (3 equiv.), amine (1.5 equiv.) and anhydrous sodium sulfate (3 equiv.) in MeOH was stirred at room temperature for 2 hours. After the addition of carboxylic acid (1.2 equiv.) and isocyanide (1 equiv.), the resulting mixture was allowed to stir at room temperature for 24 h. Finally, the solvent was removed under reduced pressure and the residue was subjected to deprotection procedure E and purified by column chromatography.

General Procedure C: A solution containing acetone (3 equiv.) and amine (1.5 equiv.) and anhydrous sodium sulfate (3 equiv.) in MeOH/THF (2:1 v/v) was stirred under microwave irradiation at 70 °C during 10 min. After the carboxylic acid (1.2 equiv.) and isocyanide (1 equiv.) were added, the resulting mixture was stirred under microwave irradiation (at 70 °C) for 30 min. Finally, the solvent was removed under reduced pressure and the residue was subjected to deprotection procedure E and purified by column chromatography.

General Procedure D: A solution containing acetone (3 equiv.), amine (1.5 equiv.) and anhydrous sodium sulfate (3 equiv.) in MeOH/THF (2:1 v/v) was stirred under microwave irradiation at (70 °C) during 10 min to preform the imine. After carboxylic acid (1.2 equiv.) and isocyanide (1 equiv.) were added, the resulting mixture was allowed to stir at room temperature for 24-48 h. Finally, the solvent was removed under

reduced pressure and the residue was subjected to deprotection procedure E and purified by column chromatography.

5. *N*-Boc deprotection of prolyl *pseudo*-lipopeptides

General procedure E: The crude *N*-Boc product of the Ugi-4CR was dissolved in 1 mL of a mixture of TFA/DCM 9:1 v/v at 0 °C. The reaction mixture was allowed to stir for 30 min and then concentrated to reduced pressure (TFA was entirely removed by repetitive addition and evaporation of further DCM). The crude was dissolved in 10 mL of DCM and neutralized over anhydrous K_2CO_3, filtered and evaporated under reduced pressure afforded to the crude product.

TABLE 1. Synthesis of prolyl *pseudo*-lipopeptides by Ugi-4CR.

3a-k
prolyl *pseudo*-lipopeptides
hybrid catalysts
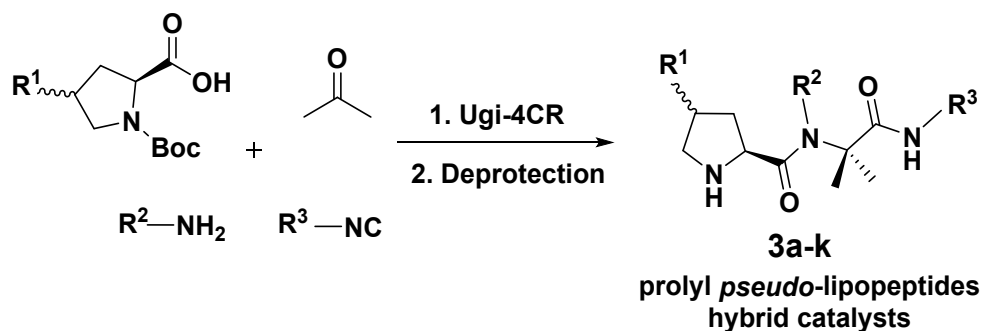
Entry	R^1/ R^2/ R^3	Catalyst	Yield (%)^a
1	H/ (*S*)-α-MeBn/ Cy	**3a**	77
2	H/ (*S*)-α-MeBn/ *n*-C$_{12}$H$_{25}$	**3b**	54
3	*trans*-OH/ (*S*)-α-MeBn/ Cy	**3c**	73
4	*trans*-OH/ (*S*)-α-MeBn/ *n*-C$_6$H$_{13}$	**3d**	81
5	*trans*-OH/ (*S*)-α-MeBn/ *n*-C$_{12}$H$_{25}$	**3e**	50
6	*cis*-OH/ (*S*)-α-MeBn/ *n*-C$_{12}$H$_{25}$	**3f**	80
7	*trans*-OH/ (*S*)-α-MeBn/ *n*-C$_{18}$H$_{35}$	**3g**	35
8	*trans*-*n*-C$_{11}$H$_{23}$COO/ (*S*)-α-MeBn/ Cy	**3h**	48
9	H/ *n*-C$_{12}$H$_{25}$/ Cy	**3i**	70
10	H/ *n*-C$_{12}$H$_{25}$/ *n*-C$_{12}$H$_{25}$	**3j**	57
11	*trans*-OH/ α-PhBn / *n*-C$_{12}$H$_{25}$	**3k**	55

^{a} Isolated yields after two step.

6. Characterization data of compounds 3a-k
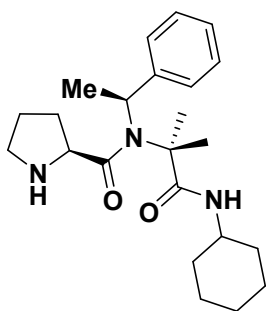
(*S*)-*N*-(1-(cyclohexylamino)-2-methyl-1-oxopropan-2-yl)-*N*-((*S*)-1-phenylethyl)pyrrolidine-2-carboxamide (**3a**)[5]: (*S*)-α-methylbenzylamine (39 μL, 0.3 mmol), acetone (44 μL, 0.6 mmol), *N*-Boc-proline (52 mg, 0.24 mmol), cyclohexyl isocyanide (25 μL, 0.2 mmol) and anhydrous sodium sulfate (85 mg, 0.6 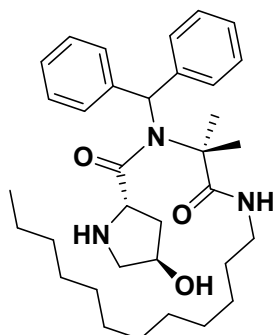mmol) were reacted in MeOH (200 μL) according to the general procedure C. Flash column chromatography purification 0-10% of MeOH in DCM afforded the peptide-peptoid hybrid **3a** in 77% (59 mg) as a colorless oil. R_f = 0.5 (DCM/MeOH 95:5). $[α]_D^{23}$ = -5.0 (c 0.1, MeOH, 23 °C). **NMR ¹H (400 MHz, Methanol-d₄)** δ 7.64 (d, J = 7.7 Hz, 2H), 7.42 (t, J = 7.6 Hz, 2H), 7.31 (t, J = 7.4 Hz, 1H), 5.23 (q, J = 7.1 Hz, 1H), 3.91 (s, 1H), 3.62 (ddt, J = 9.8, 7.3, 3.6 Hz, 1H), 3.31 – 3.29 (m, 1H), 3.20 (dt, J = 11.2, 6.7 Hz, 1H), 2.92 (dt, J = 11.5, 7.3 Hz, 1H), 1.90 (d, J = 7.1 Hz, 3H), 1.87 – 1.70 (m, 5H), 1.69 – 1.42 (m, 9H), 1.38 – 1.13 (m, 6H). **NMR ¹³C (100 MHz, Methanol-d₄)** δ 176.31, 173.88, 143.48, 129.92, 128.54, 128.18, 65.88, 61.37, 53.09, 50.35, 48.00, 33.49, 33.46, 30.52, 26.66, 26.40, 25.98, 25.64, 24.76, 20.22. **HRMS (ESI-Q-TOF)**: m/z: 386.2808. Calcd. for [M+H]⁺:386.2802.
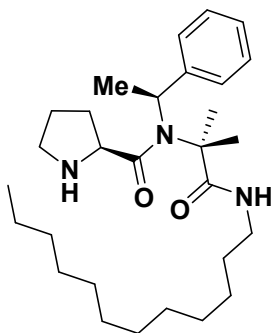
(*S*)-*N*-(1-(dodecylamino)-2-methyl-1-oxopropan-2-yl)-*N*-((*S*)-1-phenylethyl)pyrrolidine-2-carboxamide (**3b**): (*S*)-α-methylbenzylamine (39 μL, 0.3 mmol), acetone (44 μL, 0.6 mmol), *N*-Boc-proline (52 mg, 0.24 mmol), *n*-dodecyl isocyanide (45 μL, 0.2 mmol) and anhydrous sodium sulfate (85 mg, 0.6 mmol) were reacted in MeOH/THF (300 μL) according to the general procedure C. Flash column chromatography purification 0-10% of MeOH in DCM afforded the peptide-lipopeptoid hybrid **3b** in 54% (51 mg) as a colorless oil. R_f = 0.30 (EtOAc/MeOH 10:1). $[α]_D^{23}$ = -1.2 (c 0.1, MeOH, 23 °C). **NMR ¹H (400 MHz, Methanol-d₄)** δ 7.65 (d, J = 7.7 Hz, 2H), 7.43 (t, J = 7.6 Hz, 2H), 7.33 (t, J = 7.4 Hz, 1H), 5.25 (q, J = 7.2 Hz, 1H), 4.22 (s, 1H), 3.35 – 3.27 (m, 2H), 3.24 – 3.10 (m, 3H), 1.92 – 1.83 (m, 4H), 1.76 – 1.58 (m, 6H), 1.57 – 1.43 (m, 5H), 1.32 – 1.28 (m, 18H), 0.89 (t, J = 6.5 Hz, 3H). **NMR ¹³C (100 MHz, Methanol-d₄)** δ 177.0, 171.4, 142.9, 130.0, 128.7, 128.4, 66.2, 61.2, 53.3, 47.6, 40.9, 33.1, 30.7, 30.5, 30.3, 30.0, 28.1,

25.6, 25.1, 24.9, 23.7, 20.0, 14.4. **HRMS (ESI-Q-TOF)**: m/z: 472.3876. Calcd. for [M+H]⁺: 472.3898.
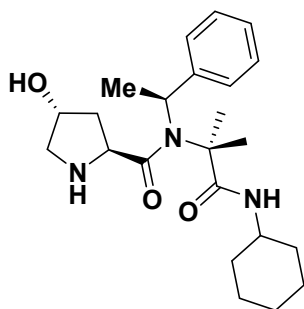
(2*S*,4*R*)-*N*-(1-(cyclohexylamino)-2-methyl-1-oxopropan-2-yl)-4-hydroxy-*N*-((*S*)-1-phenylethyl)pyrrolidine-2-carboxamide (**3c**): (*S*)-α-methylbenzylamine (39 μL, 0.3 mmol), acetone (44 μL, 0.6 mmol), *N*-Boc-*trans*-4-hydroxy-proline (56 mg, 0.24 mmol), cyclohexyl isocyanide (25 μL, 0.2 mmol) and anhydrous sodium sulfate (85 mg, 0.6 mmol) were reacted in MeOH/THF (300 μL) according to the general procedure D. Flash column chromatography purification 0-10% of MeOH in DCM afforded the peptide-peptoid hybrid **3c** in 73% (59 mg) as a colorless oil. *R*$_f$ = 0.3 (DCM/MeOH 95:5). [α]$_D^{23}$ = 3.0 (c 0.1, MeOH, 23 °C). **NMR ¹H (400 MHz, Methanol-d₄)** δ 7.60 (d, J = 7.7 Hz, 2H), 7.41 (t, J = 7.6 Hz, 2H), 7.30 (t, J = 7.4 Hz, 1H), 5.20 (q, J = 7.2 Hz, 1H), 4.28 (bs, 2H), 3.59 (dp, J = 11.5, 4.1 Hz, 1H), 3.31 – 3.23 (m, 2H), 3.20 – 3.08 (m, 1H), 1.88 (d, J = 7.1 Hz, 3H), 1.85 – 1.70 (m, 4H), 1.69 – 1.49 (m, 8H), 1.37 – 1.09 (m, 6H). **NMR ¹³C (100 MHz, Methanol-d₄)** δ 174.8, 170.8, 141.7, 128.7, 127.4, 126.8, 69.6, 64.8, 58.6, 54.1, 49.1, 38.4, 32.1, 25.2, 25.1, 24.1, 23.4, 18.8. **HRMS (ESI-Q-TOF)**: m/z: 402.2757. Calcd. for [M+H]⁺: 402.2751.
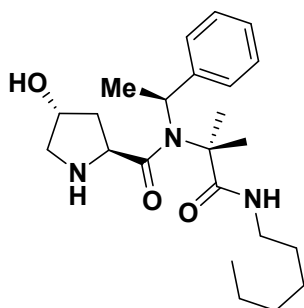
(2*S*,4*R*)-*N*-(1-(hexylamino)-2-methyl-1-oxopropan-2-yl)-4-hydroxy-*N*-((*S*)-1-phenylethyl)pyrrolidine-2-carboxamide (**3d**): (*S*)-α-methylbenzylamine (39 μL, 0.3 mmol), acetone (44 μL, 0.6 mmol), *N*-Boc-*trans*-4-hydroxy-proline (56 mg, 0.24 mmol), *n*-hexyl isocyanide (27 μL, 0.2 mmol) and anhydrous sodium sulfate (85 mg, 0.6 mmol) were reacted in MeOH/THF (300 μL) according to the general procedure D. Flash column chromatography purification 0-10% of MeOH in DCM afforded the peptide-peptoid hybrid **3d** in 81% (66 mg) as a colorless oil. *R*$_f$ = 0.3 (DCM/MeOH 95:5). [α]$_D^{23}$ = -9.8 (c 0.1, MeOH, 23 °C). **NMR ¹H (400 MHz, Methanol-d₄)** δ 7.63 (d, *J* = 7.7 Hz, 2H), 7.42 (t, J = 7.6 Hz, 2H), 7.31 (t, *J* = 7.4 Hz, 1H), 5.20 (q, *J* = 7.1 Hz, 1H), 4.26 (s, 1H), 4.18 (s, 1H), 3.24 (dd, J = 11.9, 3.9 Hz, 1H), 3.16 (q, *J* = 6.7 Hz, 2H), 3.00 (d, *J* = 11.8 Hz, 1H), 1.90 (d, *J* = 7.0 Hz, 3H), 1.69 – 1.46 (m, 9H), 1.38 – 1.26 (m, 6H), 0.88 (t, 3H). **NMR ¹³C (100 MHz, Methanol-d₄)** δ 177.1, 173.5, 143.4, 130.0, 128.6, 128.1, 71.5, 65.9, 60.0, 55.6, 53.0,

40.9, 40.0, 32.7, 30.3, 27.8, 25.6, 24.8, 23.7, 20.4, 14.4. **HRMS (ESI-Q-TOF)**: m/z: 404.2906. Calcd. for [M+H]⁺: 404.2908.
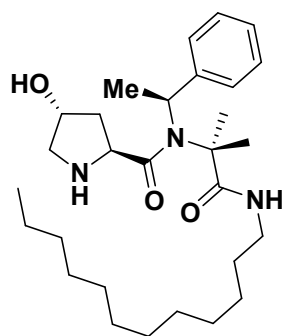
(2S,4R)-N-(1-(dodecylamino)-2-methyl-1-oxopropan-2-yl)-4-hydroxy-N-((S)-1-phenylethyl)pyrrolidine-2-carboxamide (**3e**): (S)-α-methylbenzylamine (39 μL, 0.3 mmol), acetone (44 μL, 0.6 mmol), N-Boc-trans-4-hydroxy-proline (56 mg, 0.24 mmol), n-dodecyl isocyanide (45 μL, 0.2 mmol) and anhydrous sodium sulfate (85 mg, 0.6 mmol) were reacted in MeOH/THF (300 μL) according to the general Ugi-4CR-based procedure D.

Flash column chromatography purification 0-10% of MeOH in DCM afforded the peptide-lipopeptoid hybrid **3e** in 50% (49 mg) as a colorless oil. R_f = 0.4 (DCM/MeOH 95:5). $[α]_D^{23}$ = 3.2 (c 0.1, MeOH, 23 °C). **NMR ¹H (400 MHz, Methanol-d₄)** δ 7.65 (d, J = 7.7 Hz, 2H), 7.45 (t, J = 7.5 Hz, 2H), 7.35 (t, J = 7.4 Hz, 1H), 5.24 (q, J = 7.1 Hz, 1H), 4.32 (s, 1H), 3.31 – 3.28 (m, 2H), 3.18 (dd, J = 8.9, 5.7 Hz, 2H), 1.92 (d, J = 7.0 Hz, 3H), 1.70 – 1.58 (m, 6H), 1.57 – 1.50 (m, 2H), 1.29 (s, 20H), 0.92 – 0.87 (m, 4H). **NMR ¹³C (100 MHz, Methanol-d₄)** δ 177.0, 171.9, 143.0, 130.1, 128.8, 128.2, 70.8, 66.2, 60.0, 55.5, 53.2, 41.0, 39.8, 33.1, 30.7, 30.5, 30.4, 28.1, 25.4, 24.9, 23.7, 20.2, 14.4. **HRMS (ESI-Q-TOF)**: m/z: 488.3827. Calcd. for [M+H]⁺: 488.3847.
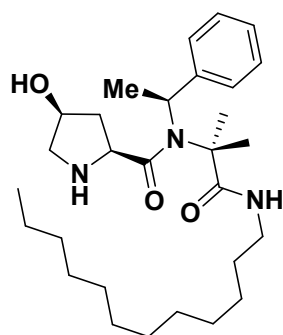
(2S,4S)-N-(1-(dodecylamino)-2-methyl-1-oxopropan-2-yl)-4-hydroxy-N-((S)-1-phenylethyl)pyrrolidine-2-carboxamide (**3f**): (S)-α-methylbenzylamine (39 μL, 0.3 mmol), acetone (44 μL, 0.6 mmol), N-Boc-cis-4-hydroxy-proline (56 mg, 0.24 mmol), n-dodecyl isocyanide (45 μL, 0.2 mmol) and anhydrous sodium sulfate (85 mg, 0.6 mmol) were reacted in MeOH/THF (300 μL) according to the general procedure D. Flash column chromatography purification 0-10% of MeOH in DCM afforded the peptide-lipopeptoid hybrid **3f** in 80% (78 mg) as a colorless oil. R_f = 0.45 (DCM/MeOH 95:5). $[α]_D^{23}$ = -21.2 (c 0.1, MeOH, 23 °C). **NMR ¹H (400 MHz, Methanol-d₄)** δ 7.65 (d, J = 7.7 Hz, 2H), 7.40 (t, J = 7.7 Hz, 2H), 7.28 (t, J = 7.6 Hz, 1H), 5.17 (q, J = 7.2 Hz, 1H), 4.00 (s, 1H), 3.62 (s, 1H), 3.17 (td, J = 7.0, 3.9 Hz, 2H), 2.95 (d, J = 12.0 Hz, 1H), 2.60 (dd, J = 12.4, 4.2 Hz, 1H), 1.89 (d, J = 7.0 Hz, 3H), 1.62 – 1.49 (m, 8H), 1.28 (s, 20H), 0.89 (t, J = 6.7 Hz, 3H). **NMR ¹³C (100 MHz, Methanol-d₄)** δ 177.3, 144.3, 129.8, 128.2, 127.8,

73.2, 65.5, 60.8, 56.9, 52.8, 40.9, 39.8, 33.1, 30.8, 30.7, 30.50, 30.48, 30.4, 28.1, 25.9, 24.6, 23.7, 20.9, 14.5. **HRMS (ESI-Q-TOF)**: m/z: 488.3863. Calcd. for [M+H]$^+$: 488.3847.
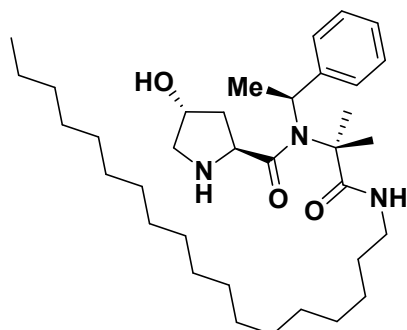
(2*S*,4*R*)-4-hydroxy-*N*-(2-methyl-1-(octadecylamino)-1-oxopropan-2-yl)-*N*-((*S*)-1-phenylethyl)pyrrolidine-2-carboxamide (**3g**): (*S*)-α-methylbenzylamine (39 μL, 0.3 mmol), acetone (44 μL, 0.6 mmol), *N*-Boc-*trans*-4-hydroxy-proline (56 mg, 0.24 mmol), *n*-octadecyl isocyanide (56 mg, 0.2 mmol) and anhydrous sodium sulfate (85 mg, 0.6 mmol) were reacted in MeOH/THF (300 μL) according to the general Ugi-4CR-based procedure D. Flash column chromatography purification 0-10% of MeOH in DCM afforded the peptide-lipopeptoid hybrid **3g** in 35% (40 mg) as a colorless oil. *R$_f$* = 0.2 (DCM/MeOH 95:5). **[α]$_D$^{23}** = -38.4 (c 0.1, MeOH, 23 °C). **NMR ^{1}H (400 MHz, Methanol-d$_4$)** δ 7.52 – 7.26 (m, 5H), 5.29 – 5.12 (m, 1H), 4.64 (s, 1H), 4.04 – 3.63 (m, 1H), 3.54 – 3.31 (m, 2H), 3.20 – 3.13 (m, 2H), 2.58 – 1.82 (m, 3H), 1.78 – 1.39 (m, 6H), 1.27 (s, 30H), 1.16 – 0.71 (m, 5H). **NMR ^{13}C (100 MHz, Methanol-d$_4$)** δ 172.7, 169.6, 140.0, 129.9, 129.8, 129.5, 129.3, 129.2, 71.4, 61.8, 60.6, 59.8, 56.8, 55.0, 40.9, 40.8, 39.5, 33.1, 30.8, 30.5, 30.46, 30.43, 28.7, 28.1, 23.7, 17.1, 14.5. **HRMS (ESI-Q-TOF)**: m/z: 603.5006. Calcd. for [M+CH$_3$OH]$^+$: 603.4975.
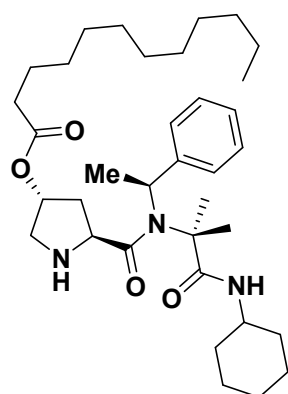
(3*R*,5*S*)-5-((1-(cyclohexylamino)-2-methyl-1-oxopropan-2-yl)((*S*)-1-phenylethyl)carbamoyl)pyrrolidin-3-yl dodecanoate (**3h**): (*S*)-α-methylbenzylamine (97 μL, 0.75 mmol), acetone (110 μL, 0.6 mmol), (2*S*,4*R*)-4-(dodecanoyloxy)pyrrolidine-2-carboxylic acid[6] (248 mg, 0.6 mmol), cyclohexyl isocyanide (62 μL, 0.5 mmol) and anhydrous sodium sulfate (213 mg, 1.5 mmol) were reacted in MeOH/THF (600 μL) according to the general procedure D. Flash column chromatography purification 0-10% of MeOH in DCM afforded the peptide-lipopeptoid hybrid **3h** in 48% (140 mg) as a colorless oil. *R$_f$* = 0.50 (hexanes/EtOAc 7:3). **[α]$_D$^{23}** = 8.6 (c 0.1, MeOH, 23 °C). **NMR ^{1}H (400 MHz, Methanol-d$_4$)** δ 7.68 (d, *J* = 7.7 Hz, 2H), 7.47 (t, *J* = 7.7 Hz, 2H), 7.35 (t, *J* = 7.7 Hz, 1H), 5.27 (q, *J* = 7.1 Hz, 1H), 3.74 – 3.61 (m, 1H), 3.59 (dd, *J* = 12.9, 4.7

Hz, 2H), 3.40 – 3.31 (m, 1H), 2.34 – 2.19 (m, 2H), 1.94 (d, J = 7.0 Hz, 3H), 1.92 – 1.55 (m, 13H), 1.44 – 1.14 (m, 25H), 0.92 (t, J = 6.6 Hz, 3H). **NMR ^{13}C (100 MHz, Methanol-d$_4$)** δ 176.1, 173.7, 170.8, 143.2, 130.2, 128.9, 128.4, 73.8, 66.3, 60.3, 53.0, 52.7, 50.6, 37.1, 34.8, 33.5, 33.1, 30.7, 30.6, 30.5, 30.2, 26.6, 26.5, 25.9, 25.7, 25.5, 24.8, 23.7, 20.1, 14.4. **HRMS (ESI-Q-TOF)**: m/z: 584.4412. Calcd. for [M+H]$^+$: 584.4422.
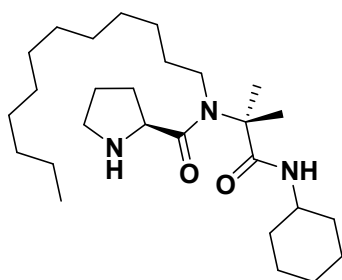
(*S*)-*N*-(1-(cyclohexylamino)-2-methyl-1-oxopropan-2-yl)-*N*-dodecylpyrrolidine-2-carboxamide (**3i**): *N*-dodecyl amine (56 mg, 0.3 mmol), acetone (44 µL, 0.6 mmol), *N*-Boc-proline (52 mg, 0.24 mmol), cyclohexyl isocyanide (25 µL, 0.2 mmol) and anhydrous sodium sulfate (85 mg, 0.6 mmol) were reacted in MeOH (200 µL) according to the general procedure B. Flash column chromatography purification 0-10% of MeOH in DCM afforded the peptide-lipopeptoid hybrid **3i** in 70% (63 mg) as a colorless oil. R_f = 0.6 (DCM/MeOH 95:5). **[α]$_D^{23}$** = -11.2 (c 0.1, MeOH, 23 °C). **NMR ^{1}H (400 MHz, Chloroform-d$_3$)** δ 5.97 (d, J = 8.2 Hz, 1H), 4.66 (t, J = 7.6 Hz, 1H), 3.67 – 3.57 (m, 1H), 3.53 – 3.39 (m, 3H), 3.31 (ddd, J = 16.3, 11.7, 5.3 Hz, 1H), 2.44 – 2.33 (m, 1H), 2.17 – 1.93 (m, 3H), 1.83 (dt, J = 14.4, 7.2 Hz, 2H), 1.75 – 1.63 (m, 3H), 1.61 – 1.42 (m, 6H), 1.33 – 1.09 (m, 24H), 0.89 – 0.82 (m, 4H). **NMR ^{13}C (100 MHz, Chloroform-d$_3$)** δ 173.1, 168.8, 63.3, 58.9, 48.9, 46.5, 45.1, 32.9, 32.9, 32.0, 31.9, 29.8, 29.7, 29.67, 29.65, 29.4, 29.3, 27.2, 25.6, 25.2, 25.2, 25.0, 24.6, 24.5, 22.8, 14.2. **HRMS (ESI-Q-TOF)**: m/z: 450.4043. Calcd. for [M+H]$^+$: 450.4054.
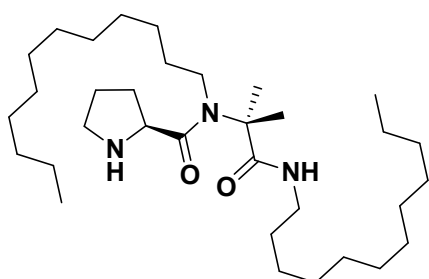
(*S*)-*N*-dodecyl-*N*-(1-(dodecylamino)-2-methyl-1-oxopropan-2-yl)pyrrolidine-2-carboxamide (**3j**): *N*-dodecyl amine (56 mg, 0.3 mmol), acetone (44 µL, 0.6 mmol), *N*-Boc-proline (52 mg, 0.24 mmol), *n*-dodecyl isocyanide (45 µL, 0.2 mmol) and anhydrous sodium sulfate (85 mg, 0.6 mmol) were reacted in MeOH/THF (300 µL) according to the general procedure C. Flash column chromatography purification 0-10% of MeOH in DCM afforded the peptide-lipopeptoid hybrid **3j** in 57% (61 mg) as a colorless oil. R_f = 0.5-0.6 (DCM/MeOH 95:5). **[α]$_D^{23}$** = -14.2 (c 0.1, MeOH, 23 °C). **NMR ^{1}H (400 MHz, Methanol-d$_4$)** δ 4.50 – 4.42 (m, 1H), 3.50 – 3.32 (m, 3H), 3.27 – 3.01 (m, 3H), 2.48 (dq, J = 13.0, 6.9, 5.4 Hz, 1H), 2.11 – 1.91 (m, 3H), 1.74 –

1.59 (m, 2H), 1.52 (s, 3H), 1.47 (s, 3H), 1.39 – 1.22 (m, 38H), 0.88 (t, *J* = 6.6 Hz, 6H). **NMR ¹³C (100 MHz, Methanol-d₄)** δ 176.9, 169.8, 64.2, 60.4, 47.5, 45.6, 40.9, 33.1, 32.6, 30.8, 30.5, 30.4, 28.1, 27.9, 25.4, 24.8, 24.3, 23.7, 14.4. **HRMS (ESI-Q-TOF)**: m/z: 536.5145. Calcd. for [M+H]⁺: 536.5150.

(2*S*,4*R*)-*N*-benzhydryl-*N*-(1-(dodecylamino)-2-methyl-1-oxopropan-2-yl)-4-hydroxypyrrolidine-2-carboxamide (**3k**): 2,2-diphenylglycine methyl ester hydrochloride (241 mg, 1 mmol), DIPEA (174 *μ*L, 1 mmol), acetone (110 *μ*L, 1.5 mmol), *N*-Boc-*trans*-4-hydroxy-proline (139 mg, 0.6 mmol), *n*-dodecyl isocyanide (98 *μ*L, 0.5 mmol) and anhydrous sodium sulfate (213 mg, 1.5 mmol) were reacted in MeOH/THF (600 μL) according to the general procedure D. Flash column chromatography purification 0-10% of MeOH in DCM afforded the peptide-lipopeptoid hybrid **3k** in 55% (151 mg) as a colorless oil. *R*$_f$ = 0.5 (DCM/MeOH 95:5). **[α]$_D$²³** = 2.6 (c 0.1, MeOH, 23 °C). **NMR ¹H (400 MHz, Methanol-d₄)** δ 7.52 – 7.41 (m, 4H), 7.43 – 7.34 (m, 4H), 7.34 – 7.24 (m, 2H), 6.45 (bs, 1H), 4.12 (s, 1H), 3.88 (t, *J* = 7.8 Hz, 1H), 3.26 – 3.15 (m, 2H), 3.12 (dd, *J* = 11.8, 4.7 Hz, 1H), 2.63 (d, *J* = 11.8 Hz, 1H), 1.72 – 1.59 (m, 3H), 1.57 – 1.45 (m, 5H), 1.38 – 1.24 (m, 20H), 0.89 (t, *J* = 6.6 Hz, 3H). **NMR ¹³C (100 MHz, Methanol-d₄)** δ 177.5, 177.1, 143.1, 139.9, 130.1, 130.0, 129.9, 129.5, 128.9, 128.8, 72.5, 66.0, 62.2, 61.6, 56.1, 40.9, 39.7, 33.1, 30.8, 30.7, 30.50, 30.47, 30.4, 28.1, 25.7, 24.5, 23.7, 14.5. **HRMS (ESI-Q-TOF)**: m/z: 550.4002. Calcd. for [M+H]⁺: 550.4003.

7. General procedure for asymmetric 1,4-addition of butanal to *trans-β*-nitrostyrene: Catalyst Screening

General procedure F: A vial was charged with the prolyl *pseudo*-lipopeptides hybrid catalyst **3a-k** (10 mol%), *trans-β*-nitrostyrene[7] (0.2 mmol, 1.0 equiv.) and 0.4 mL of water. The mixture was homogenized in an ultrasound bath, butanal (0.40 mmol, 2.0 equiv.) was added and this mixture was stirred for 24 h. After this period, the resulting reaction mixture was extracted with EtOAc, dried over anhydrous Na₂SO₄ and concentrated under reduced pressure. The yield was determined by ¹H NMR analysis of crude product with 1.2.3-trimethoxybenzene (0.2 mmol, 1.0 equiv.) as internal standard. The crude product was purified by flash column chromatography on silica gel using hexanes/EtOAc (9:1 v/v) as eluent. The diastereoisomeric ratio was

determined by ^{1}H NMR analysis of crude of the reaction mixture. Enantiomeric excess (*e.e.*) was determined by chiral HPLC or UPC[2] analysis through comparison with the authentic racemic material.

TABLE 2. Catalysts Screening.

3a-k

4a
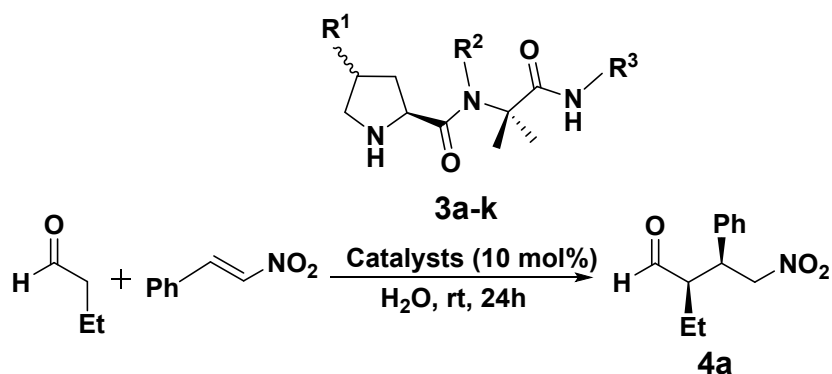
Entry	Catalyst	Yield (%)[a]	d.r. (*syn/anti*)[c]	e.e. (%)[d]
1	**3a**	57	94:06	96
2	**3b**	90	89:11	94
3	**3c**	43	70:30	99
4	**3d**	72[b]	81:19	97
5	**3e**	**88**	**76:24**	**99**
6	**3f**	78[b]	79:21	94
7	**3g**	35[b]	87:13	92
8	**3h**	23	89:11	99
9	**3i**	75	76:24	88
10	**3j**	87	88:12	83
11	**3k**	84	79:21	89

[a] Yield determined by ^{1}H NMR spectroscopy analysis of crude of the reaction mixture with 1,2,3-trimethoxybenzene as standard; [b] Isolated yield; [c] *syn/trans* ratio determined by ^{1}H NMR; [d] Determined by chiral-stationary phase HPLC or UPC[2] analysis.

8. Optimization of asymmetric Michael reaction of butanal and *trans-β*-nitrostyrene catalyzed by compound 3e

TABLE 3. Optimization of the system.
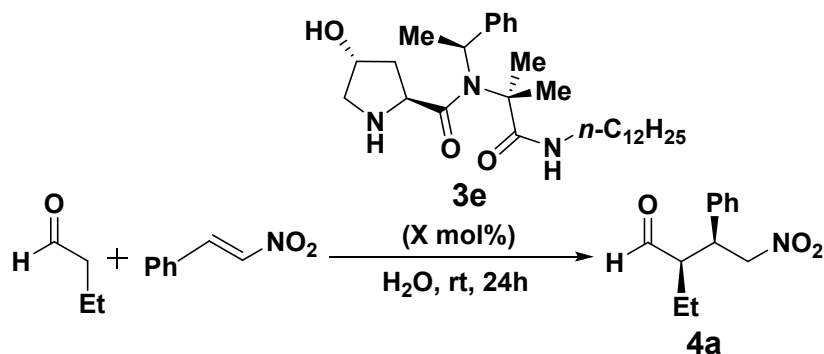
Entry [a]	Catalyst (mol%)	Solvent	Yield (%) [b]	d.r. (*syn/anti*) [c]	e.e. (%) [d]
1	10	H_2O	88	76:24	99
2	5	H_2O	90	90:10	99
3	**2.5**	**H_2O**	**99(96)**	**93:7**	**99**
4	1	H_2O	65	98:2	99
5	2.5	Ethanol	26	85:15	98
6	2.5	Brine	84	95:5	99
7	2.5	PEG-300	54	82:18	98

[a] Reactions using 2 equivalents of butanal and 0.2 mmol of β-nitrostyrene in 0.4 mL of solvent; [b] Yield determined by ^{1}H NMR spectroscopy analysis of crude of the reaction mixture (yield of isolated product); [c] *syn/anti* ratio determined by ^{1}H NMR; [d] Determined by chiral-stationary phase HPLC or UPC2 analysis.
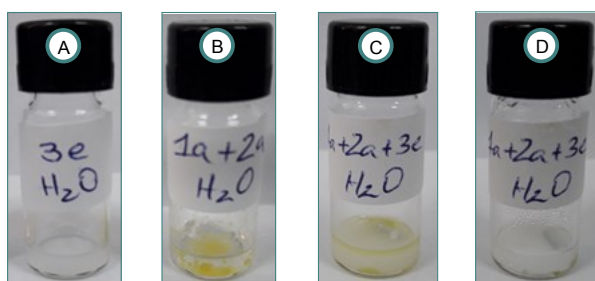
FIGURE 1. Visual schematic representation of the optimized condition in different stages. (**A**) Catalyst 3e in water; (**B**) mixture of butyraldehyde and trans-β-nitrostyrene in water; (**C**) mixture of butyraldehyde, trans-β-nitrostyrene and catalyst 3e in water; (**D**) mixture of butyraldehyde, trans-β-nitrostyrene and catalyst 3e in water after stirred for 24h.

9. General procedure for asymmetric 1,4-addition of aldehydes to nitrostyrenes

General procedure G: A vial was charged with the prolyl pseudo-lipopeptide hybrid catalyst **3e** (2.5 mol%), the nitrostyrene[7] (0.2 mmol, 1.0 equiv) and 0.4 mL of water. The mixture was homogenized in an ultrasound bath, the aldehyde (0.40 mmol, 2.0 equiv) was added and this mixture was stirred for 24 h. After this period, the resulting reaction mixture was extracted with EtOAc, dried over anhydrous Na_2SO_4 and

concentrated under reduced pressure. The crude product was purified by flash column chromatography on silica gel using hexanes/EtOAc as eluent. The diastereoisomeric ratio was determined by ^{1}H NMR analysis of crude of the reaction mixture. Enantiomeric excess (*e.e.*) was determined by chiral HPLC or UPC[2] analysis through comparison with the authentic racemic material.

TABLE 4. Scope of catalyst **3e** in the asymmetric Michael reaction between different aldehydes and *trans-β*-nitrostyrenes.
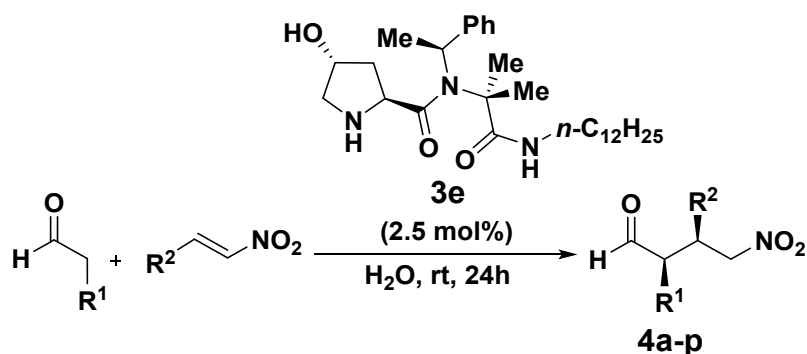
Entry[a]	R[1]	R[2]	Compound	Yield (%)[b]	d.r. (syn/anti)[c]	e.e. (%)[d]
1	Ethyl	Phenyl	**4a**	99(96)	93:07	99
2	*n*-Butyl	Phenyl	**4b**	91(n.d.)	92:08	99
3	*i*-Propyl	Phenyl	**4c**	79(n.d.)	99:01	99
4	6-(2-methylhept-2-ene)	Phenyl	**4d**	(64)	86:14	98
5	Ethyl	4-FC$_6$H$_4$	**4e**	91(86)	92:08	98
6	Ethyl	4-ClC$_6$H$_4$	**4f**	95(91)	92:08	99
7	Ethyl	4-BrC$_6$H$_4$	**4g**	96(94)	92:08	98
8	Ethyl	4-NO$_2$C$_6$H$_4$	**4h**	89(80)	89:11	97
9	Ethyl	4-CF$_3$C$_6$H$_4$	**4i**	(64)	91:09	98
10	Ethyl	4-MeOC$_6$H$_4$	**4j**	87(84)	93:07	96
11	Ethyl	4-MeC$_6$H$_4$	**4k**	(82)	91:09	98
12	Ethyl	4-*t*-BuC$_6$H$_4$	**4l**	(67)	79:21	97
13	Ethyl	2-NO$_2$C$_6$H$_4$	**4m**	(78)	75:25	97
14	Ethyl	2-MeOC$_6$H$_4$	**4n**	(71)	87:13	99
15	Ethyl	2-Furyl	**4o**	(83)	82:18	99
16	Ethyl	*n*-Pentyl	**4p**	(73)	99:01	96
17	Ethyl	*i*-Butyl	**4q**	(66)	99:01	99

[a] All reactions were conducted using 2 equivalents of the aldehyde and 0.2 mmol of *β*-nitrostyrene in 0.4 mL of water; [b] Yield determined by ^{1}H-NMR analysis with 1,2,3-trimethoxybenzene as internal patron and (isolated product); [c] Determined by ^{1}H NMR of crude of the reaction mixture; [d] Determined by chiral-stationary phase HPLC or UPC[2] analysis.

10. Scale-up

A vial was charged with the prolyl *pseudo*-lipopeptide hybrid catalyst **3e** (2.5 mol%, 24 mg), the nitrostyrene[7] (2 mmol, 298 mg, 1.0 equiv,) and 4 mL of water. The mixture was homogenized in an ultrasound bath, the butanal (4 mmol, 361 μL, 2.0 equiv) was added and this mixture was stirred for 72 h. After this period, the

resulting reaction mixture was extracted with EtOAc, dried over anhydrous Na$_2$SO$_4$ and concentrated under reduced pressure. The crude product was purified by flash column chromatography on silica gel using (hexanes/EtOAc 9:1) to afford **4a** in 90% (400.4 mg) as a colorless oil. The diastereoisomeric ratio was determined by ^{1}H NMR analysis of crude of the reaction mixture. Enantiomeric excess (*e.e.*) was determined by chiral UPC[2] analysis through comparison with the authentic racemic material.
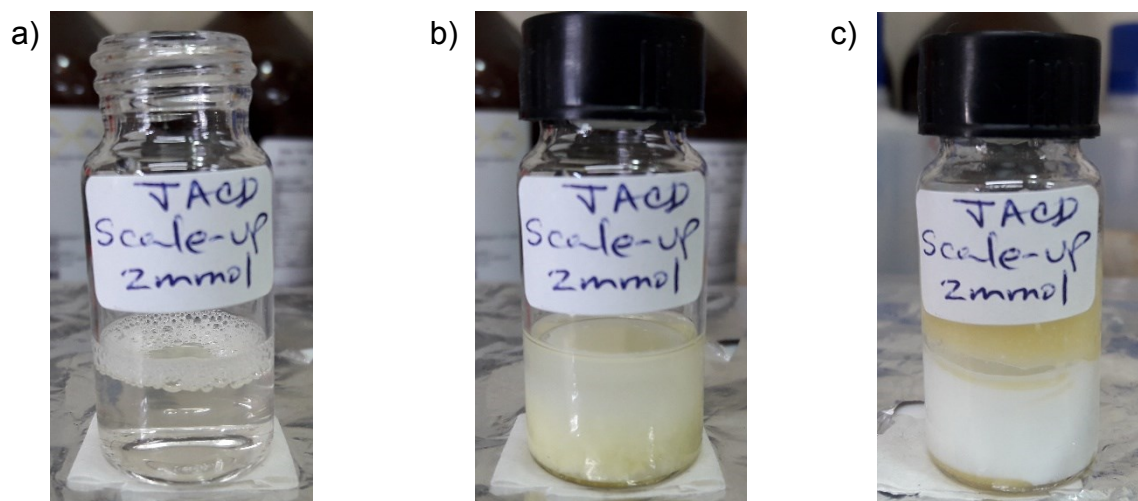
a) Catalyst **3e** in water; b) After the addition of nitrostyrene and butanal; c) After 72h of reaction.

11. Catalyst recycle

A vial was charged with the prolyl pseudo-lipopeptide hybrid catalyst **3e** (10 mol%), the nitrostyrene[7] (0.2 mmol, 1.0 equiv), and 0.4 mL of water. The mixture was homogenized in an ultrasound bath, the aldehyde (0.40 mmol, 2.0 equiv) was added and this mixture was stirred for 24 h. After this period, the resulting reaction mixture was extracted with EtOAc, dried over anhydrous Na$_2$SO$_4$, and concentrated under reduced pressure. The crude product was filtered by a small amount of silica flash using ethyl acetate to afford **4a** in as follows in Table 2, entry 5. After that, the catalyst remains in the silica, and it is recovered by passing 50 ml of methanol through the silica. Then, the solvent was removed by reduced pressure on rotovapory and transferred to the 5 ml vial, and dried under a high vacuum for 2 h. After this period, the nitrostyrene[7] (0.2 mmol, 1.0 equiv) and 0.4 mL of water were added into the vial containing the catalyst. The mixture was homogenized in an ultrasound bath, the aldehyde (0.40 mmol, 2.0 equiv) was added and this mixture was stirred for 24 h. The procedure was carried out over four times and the results

are depicted in Figure 2. The yield was determined by ^1H NMR analysis of the crude product with 1.2.3-trimethoxybenzene (0.2 mmol, 1.0 equiv.) as an internal standard. The diastereoisomeric ratio was determined by 1H NMR analysis of crude of the reaction mixture. Enantiomeric excess (*e.e.*) was determined by chiral UPC^2 analysis through comparison with the authentic racemic material.

Recycle [a]	Yield (%) [b]	d.r. (*syn/anti*) [c]	e.e. (%) [d]
1	90	80:20	99
2	87	91:9	99
3	88	92:8	99
4	88	93:2	99

[a] Reactions using 2 equivalents of butanal and 0.2 mmol of β-nitrostyrene in 0.4 mL of solvent; [b] Yield determined by ^1H NMR spectroscopy analysis of crude of the reaction mixture; [c] *syn/anti* ratio determined by ^1H NMR; [d] Determined by chiral-stationary phase HPLC or UPC2 analysis.
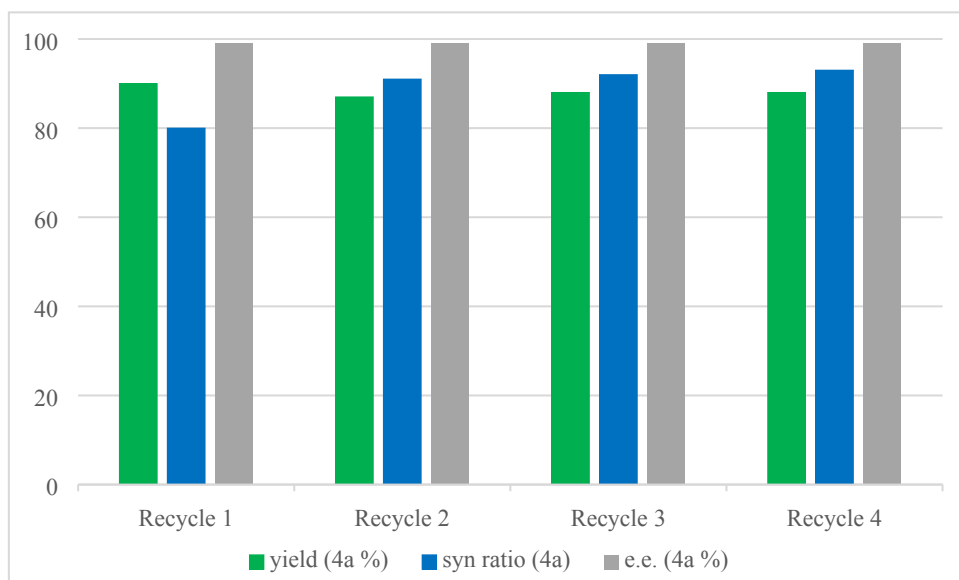
FIGURE 2. Catalyst recycled over four-times.

12. Characterization data of compounds 4a-q
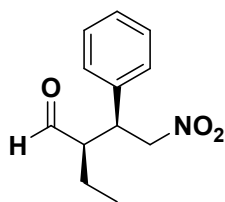
(2*R*,3*S*)-2-ethyl-4-nitro-3-phenylbutanal (**4a**)[8]: Prepared by reaction of butanal with *trans-β*-nitrostyrene according to the procedure G. Flash chromatography (hexanes/EtOAc 9:1) afforded **4a** in 96% (42 mg) as a colorless oil. The enantiomeric excess was determined by chiral-stationary phase UPC^2. Trefoil CEL2, **Grad:** CO_2/EtOH 100-0% to 95-5% in 9 min; 100-0 % in 1 min at 3 ml/min at 25°C. UV detection at 210 nm: **R$_t$**: (syn, major) = 4.13 min, (syn, minor) = 3.93 min. **R$_f$** = 0.4 (hexanes/EtOAc 9:1). **NMR ^1H (400 MHz,**

CDCl₃) δ 9.65 (s, 1H), 7.30 – 7.20 (m, 3H), 7.11 (d, *J* = 7.6 Hz, 2H), 4.77 – 4.52 (m, 2H), 3.72 (td, *J* = 10.1, 5.3 Hz, 1H), 2.61 (dddd, *J* = 10.1, 7.5, 4.7, 2.2 Hz, 1H), 1.48 – 1.39 (m, 2H), 0.76 (t, *J* = 7.3 Hz, 3H). **NMR ¹³C (100 MHz, CDCl₃)** δ 203.4, 136.9, 129.3, 128.3, 128.1, 78.7, 55.1, 42.9, 20.5, 10.8.
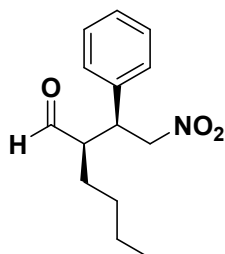
(*R*)-2-((*S*)-2-nitro-1-phenylethyl)hexanal (**4b**)[9]: Prepared by reaction of hexanal with *trans-β*-nitrostyrene according to the procedure G. Flash chromatography (hexanes/EtOAc 9:1) afforded **4b** in 91%. The enantiomeric excess was determined by chiral-stationary phase UPC². Trefoil CEL2, **Grad:** CO₂/EtOH 100-0% to 95-5% in 9 min; 100-0 % in 1 min at 3 ml/min at 25°C. UV detection at 210 nm: **R$_t$**: (syn, major) = 6.95 min, (syn, minor) = 6.64 min. **R$_f$** = 0.5 (hexanes/EtOAc 9:1). **NMR ¹H (400 MHz, CDCl₃)** δ 9.70 (d, *J* = 2.8 Hz, 1H), 7.37 – 7.27 (m, 3H), 7.19 – 7.15 (m, 2H), 4.85 – 4.60 (m, 2H), 3.84 – 3.73 (m, 1H), 2.70 (dddd, *J* = 9.8, 8.9, 4.0, 2.8 Hz, 1H), 1.51 – 1.35 (m, 2H), 1.34 – 1.24 (m, 2H), 1.22 – 1.12 (m, 2H), 0.79 (t, 3H). **NMR ¹³C (100 MHz, CDCl₃)** δ 203.4, 136.9, 129.2, 128.3, 128.1, 78.6, 54.0, 43.2, 28.6, 27.1, 22.6, 13.8.
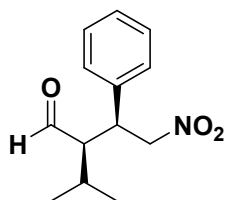
(2*R*,3*S*)-2-isopropyl-4-nitro-3-phenylbutanal (**4c**)[5]: Prepared by reaction of isovaleraldehyde with *trans-β*-nitrostyrene according to the procedure G. Flash chromatography (hexanes/EtOAc 9:1) afforded **4c** in 79%. The enantiomeric excess was determined by chiral-stationary phase UPC². Trefoil CEL2, **Grad:** CO₂/EtOH 100-0% to 95-5% in 9 min; 100-0 % in 1 min at 3 ml/min at 25°C. UV detection at 210 nm: **R$_t$**: (syn, major) = 3.97 min, (syn, minor) = 3.68 min. **R$_f$** = 0.45 (hexanes/EtOAc 9:1). **NMR ¹H (400 MHz, CDCl₃)** δ 9.93 (d, *J* = 2.4 Hz, 1H), 7.37 – 7.27 (m, 3H), 7.21 – 7.17 (m, 2H), 4.71 – 4.53 (m, 2H), 3.90 (td, *J* = 10.3, 4.4 Hz, 1H), 2.77 (ddd, *J* = 10.8, 4.1, 2.4 Hz, 1H), 1.72 (heptd, *J* = 7.1, 4.1 Hz, 1H), 1.10 (d, *J* = 7.2 Hz, 3H), 0.88 (d, *J* = 7.0 Hz, 3H). **NMR ¹³C (100 MHz, CDCl₃)** δ 204.4, 137.1, 129.2, 128.1, 128.0, 79.0, 58.8, 41.9, 27.9, 21.7, 17.0.
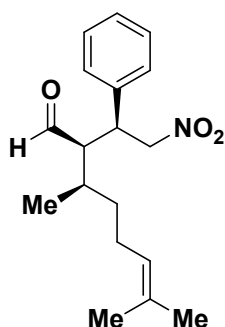
(2*R*,3*R*)-3,7-dimethyl-2-((*S*)-2-nitro-1-phenylethyl)oct-6-enal (**4d**): Prepared by reaction of (*R*)-(+)-Citronellal with *trans-β*-nitrostyrene according to the procedure G. Flash chromatography (hexanes/EtOAc 9:1) afforded **4d** in 64% (38.6 mg) as a colorless oil.

The enantiomeric excess was determined by chiral-stationary phase UPC^2. Trefoil CEL1, **Grad:** CO_2/ACN 100-0% to 98-2% in 9 min; 100-0 % in 1 min at 3 ml/min at 25°C. UV detection at 210 nm: **R$_t$**: (syn, major) = 4.09 min, (syn, minor) = 3.70 min. **R$_f$** = 0.6-0.7 (hexanes/EtOAc 9:1). **NMR ^{1}H (400 MHz, CDCl$_3$)** δ 9.84 – 9.79 (m, 1H), 7.30 – 7.20 (m, 3H), 7.10 (d, J = 8.2 Hz, 2H), 4.72 (t, J = 6.5 Hz, 1H), 4.64 – 4.46 (m, 2H), 3.87 (td, J = 10.4, 4.4 Hz, 1H), 2.68 (dt, J = 10.7, 3.1 Hz, 1H), 1.90 – 1.79 (m, 1H), 1.64 – 1.52 (m, 2H), 1.51 (s, 3H), 1.48 – 1.43 (m, 2H), 1.42 (s, 3H), 1.00 (d, J = 7.1 Hz, 3H). **NMR ^{13}C (100 MHz, CDCl$_3$)** δ 204.14, 137.23, 132.29, 129.21, 128.19, 123.30, 79.22, 59.20, 41.70, 32.13, 31.48, 25.72, 25.70, 18.66, 17.67.
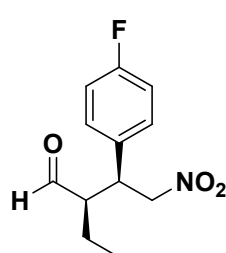
(2*R*,3*S*)-2-ethyl-3-(4-fluorophenyl)-4-nitrobutanal (**4e**)[8]: Prepared by reaction of butanal with *trans*-4-fluoro-*β*-nitrostyrene according to the procedure G. Flash chromatography (hexanes/EtOAc 9:1) afforded **4f** in 86% (41 mg) as a colorless oil. The enantiomeric excess was determined by chiral-stationary phase UPC^2. Trefoil CEL2, **Grad:** CO_2/EtOH 100-0% to 95-5% in 9 min; 100-0 % in 1 min at 2 ml/min at 25°C. UV detection at 210 nm: **R$_t$**: (syn, major) = 6.88 min, (syn, minor) = 6.30 min. **R$_f$** = 0.3 (hexanes/EtOAc 9:1). **NMR ^{1}H (400 MHz, CDCl$_3$)** δ 9.72 (d, J = 2.4 Hz, 1H), 7.19 – 7.15 (m, 2H), 7.07 – 7.00 (m, 2H), 4.83 – 4.56 (m, 2H), 3.85 – 3.75 (m, 1H), 2.66 (dddd, J = 10.3, 8.1, 4.3, 2.4 Hz, 1H), 1.54 – 1.47 (m, 2H), 0.84 (t, J = 7.5 Hz, 3H). **NMR ^{13}C (100 MHz, CDCl$_3$)** δ 202.9, 163.6, 161.1 (d, $^1J_{C-F}$ = 247.2 Hz), 132.58, 132.55 (d, $^4J_{C-F}$ = 3.1 Hz), 129.7, 129.6 (d, $^3J_{C-F}$ = 8.1 Hz), 116.3, 116.0 (d, $^2J_{C-F}$ = 21.6 Hz), 78.6, 54.9, 42.0, 20.3, 10.6. **^{19}F NMR (377 MHz, CDCl$_3$)** δ -113.42 – -113.76 (m).
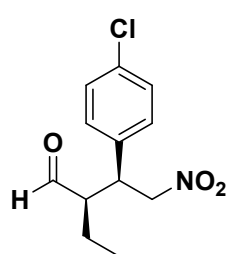
(2*R*,3*S*)-3-(4-chlorophenyl)-2-ethyl-4-nitrobutanal (**4f**)[8]: Prepared by reaction of butanal with *trans*-4-chloro-*β*-nitrostyrene according to the procedure G. Flash chromatography (hexanes/EtOAc 9:1) afforded **4g** in 91% (46 mg) as a colorless oil. The enantiomeric excess was determined by chiral-stationary phase UPC^2. Trefoil AMY1, **Grad:** CO_2/MeOH 100-0% to 90-10 % in 6 min; 90-10 % in 3 min; 100-0 % in 1 min at 2 ml/min at 25°C. UV detection at 210 nm: **R$_t$**: (syn, major) = 3.45 min, (syn, minor) = 4.21 min. **R$_f$** = 0.25 (hexanes/EtOAc 9:1). **NMR ^{1}H (400 MHz, CDCl$_3$)** δ 9.71 (d, J = 2.3 Hz, 1H), 7.35 – 7.28 (m, 2H), 7.16 – 7.11 (m, 2H), 4.82 – 4.55 (m, 2H), 3.79 (td, J = 9.9, 4.9 Hz, 2H), 2.67 (dddd, J = 10.3, 8.2, 4.2, 2.3 Hz, 1H), 1.55 – 1.45 (m,

2H), 0.83 (t, J = 7.5 Hz, 3H). **NMR ^{13}C (100 MHz, CDCl$_3$)** δ 202.9, 135.5, 129.6, 129.5, 129.4, 78.5, 54.8, 42.1, 20.4, 10.7.
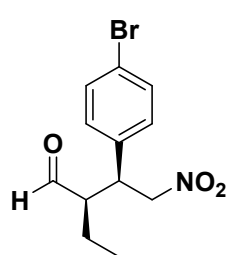
(2R,3S)-3-(4-bromophenyl)-2-ethyl-4-nitrobutanal (**4g**)[8]: Prepared by reaction of butanal with *trans*-4-bromo-β-nitrostyrene according to the procedure G. Flash chromatography (hexanes/EtOAc 9:1) afforded **4h** in 94% (57 mg) as a light yellow oil. The enantiomeric excess was determined by chiral-stationary phase UPC^2. Trefoil AMY1, **Grad:** CO$_2$/MeOH 100-0% to 90-10 % in 6 min; 90-10 % in 3 min; 100-0 % in 1 min at 2 ml/min at 25°C. UV detection at 210 nm: **R$_t$**: (syn, major) = 3.98 min, (syn, minor) = 6.71min. **R$_f$** = 0.3 (hexanes/EtOAc 9:1). **NMR ^{1}H (400 MHz, CDCl$_3$)** δ 9.71 (d, J = 2.3 Hz, 1H), 7.50 – 7.44 (m, 2H), 7.10 – 7.05 (m, 2H), 4.82 – 4.55 (m, 2H), 3.83 – 3.74 (m, 1H), 2.67 (dddd, J = 10.3, 8.2, 4.2, 2.3 Hz, 1H), 1.54 – 1.47 (m, 2H), 0.84 (t, J = 7.5 Hz, 2H). **NMR ^{13}C (100 MHz, CDCl$_3$)** δ 202.8, 136.0, 132.4, 129.8, 122.3, 78.4, 54.8, 42.2, 20.5, 10.7.
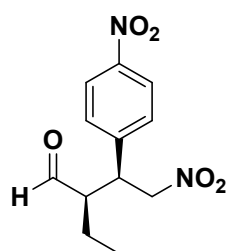
(2R,3S)-2-ethyl-4-nitro-3-(4-nitrophenyl)butanal (**4h**): Prepared by reaction of butanal with *trans*-4-nitro-β-nitrostyrene according to the procedure G. Flash chromatography (hexanes/EtOAc 8:2) afforded **4i** in 80% (43 mg) as a light yellow oil. The enantiomeric excess was determined by chiral-stationary phase UPC^2. Trefoil AMY1, **Grad:** CO$_2$/IPA 100-0% to 90-10 % in 18 min; 90-10 % in 2 min at 2 ml/min at 25°C. UV detection at 210 nm: **R$_t$**: (syn, major) = 8.84 min, (syn, minor) = 10.04 min. **R$_f$** = 0.4 (hexanes/EtOAc 8:2). **NMR ^{1}H (400 MHz, CDCl$_3$)** δ 9.74 (d, J = 1.9 Hz, 1H), 8.26 – 8.18 (m, 2H), 7.45 – 7.39 (m, 2H), 4.86 – 4.65 (m, 2H), 4.02 – 3.92 (m, 1H), 2.82 – 2.70 (m, 1H), 1.61 – 1.44 (m, 2H), 0.87 (t, J = 7.5 Hz, 3H). **NMR ^{13}C (100 MHz, CDCl$_3$)** δ 202.1, 147.8, 144.7, 129.3, 124.4, 77.9, 54.4, 42.3, 20.5, 10.5.
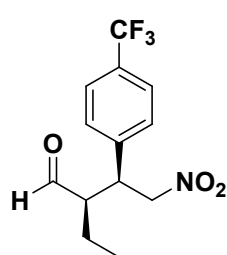
(2R,3S)-2-ethyl-4-nitro-3-(4-(trifluoromethyl)phenyl)butanal (**4i**): Prepared by reaction of butanal with *trans*-4-trifluoromethyl-β-nitrostyrene according to the procedure G. Flash chromatography (hexanes/EtOAc 9:1) afforded **4j** in 64% (37 mg) as a light yellow oil. The enantiomeric excess was determined by chiral-stationary phase UPC^2. Trefoil CEL2, **Grad:** CO$_2$/IPA 100- 0% to 95-05 % in 14 min; 100-0 % in 1 min

at 1.5 ml/min at 25°C. UV detection at 210 nm: R_t: (syn, minor) = 10.69 min, (syn, major) = 11.18 min. R_f = 0.3 (hexanes/EtOAc 9:1). **NMR ^{1}H (400 MHz, CDCl$_3$)** δ = 9.73 (d, J = 2.0 Hz, 1H), 7.62 (d, J = 8.1 Hz, 2H), 7.34 (d, J = 8.0 Hz, 2H), 4.83 – 4.63 (m, 2H), 3.89 (td, J = 10.0, 4.8 Hz, 1H), 2.78 – 2.69 (m, 1H), 1.57 – 1.44 (m, 2H), 0.85 (t, J = 7.5 Hz, 3H). **NMR ^{13}C (100 MHz, CDCl$_3$)** δ 202.6, 141.3, 131.1, 130.8, 130.4, 130.1 (q, $^2J_{C-F}$ = 32.4 Hz), 128.7, 128.0, 126.30, 126.26, 126.22, 126.18 (q, $^3J_{C-F}$ = 4.0 Hz), 125.3, 122.6, 119.9 (q, $^1J_{C-F}$ = 272.2 Hz)., 78.2, 54.7, 42.4, 20.5, 10.6. **^{19}F NMR (377 MHz, CDCl$_3$)** δ -62.52 – -62.90 (m).
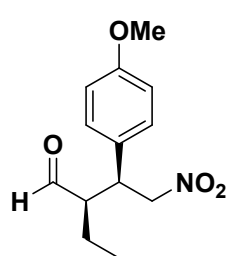
(2R,3S)-2-ethyl-3-(4-methoxyphenyl)-4-nitrobutanal (**4j**)[8]: Prepared by reaction of butanal with *trans*-4-methoxy-*β*-nitrostyrene according to the procedure G. Flash chromatography (hexanes/EtOAc 8:2) afforded **4k** in 84% (42 mg) as a light yellow oil. The enantiomeric excess was determined by chiral-stationary phase UPC^2. Trefoil CEL2, **Grad:** CO$_2$/EtOH 100-0% to 98-2 % in 19 min; 100-0 % in 1 min at 2.5 ml/min at 25°C. UV detection at 210 nm: R_t: (syn, major) = 15.43 min, (syn, minor) = 14.88 min. R_f = 0.2 (hexanes/EtOAc 9:1). **NMR ^{1}H (400 MHz, CDCl$_3$)** δ 9.71 (d, J = 2.7 Hz, 1H), 7.11 – 7.07 (m, 2H), 6.89 – 6.83 (m, 2H), 4.81 – 4.54 (m, 2H), 3.79 (s, 3H), 3.73 (dt, J = 10.0, 5.1 Hz, 1H), 2.67 – 2.59 (m, 1H), 1.56 – 1.46 (m, 2H), 0.83 (t, J = 7.5 Hz, 3H). **NMR ^{13}C (100 MHz, CDCl$_3$)** δ 203.5, 159.4, 129.4, 129.2, 114.6, 78.9, 55.4, 42.1, 20.5, 10.8.
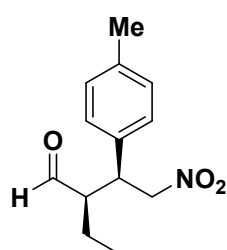
(2R,3S)-2-ethyl-4-nitro-3-(p-tolyl)butanal (**4k**): Prepared by reaction of butanal with *trans*-4-methyl-*β*-nitrostyrene according to the procedure G. Flash chromatography (hexanes/EtOAc 9:1) afforded **4l** in 82% (39 mg) as a colorless oil. The enantiomeric excess was determined by chiral-stationary phase UPC^2. Trefoil CEL2, **Grad:** CO$_2$/ACN 100- 0% to 90-10 % in 5 min; 90-10 % in 4 min; 100-0 % in 1 min at 1 ml/min at 25°C. UV detection at 210 nm: R_t: (syn, minor) = 5.85 min, (syn, major) = 6.17 min. R_f = 0.45-0.50 (hexanes/EtOAc 9:1). **NMR ^{1}H (400 MHz, CDCl$_3$)** δ 9.70 (d, J = 2.3 Hz, 1H), 7.14 (d, J = 7.8 Hz, 2H), 7.06 (d, J = 8.0 Hz, 2H), 4.81 – 4.56 (m, 2H), 3.75 (td, J = 9.8, 5.1 Hz, 1H), 2.65 (dddd, J = 10.2, 7.7, 4.5, 2.4 Hz, 1H), 2.32 (s, 3H), 1.57 – 1.44 (m, 2H), 0.82 (t, J = 7.5 Hz, 4H). **NMR ^{13}C (100 MHz, CDCl$_3$)** δ 203.5, 138.0, 133.8, 129.9, 128.0, 78.8, 55.2, 42.5, 21.2, 20.5, 10.8.
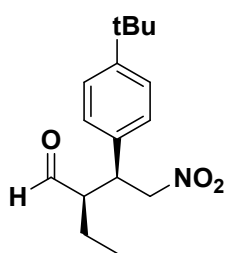
(2R,3S)-3-(4-(tert-butyl)phenyl)-2-ethyl-4-nitrobutanal (4l): Prepared by reaction of butanal with *trans*-4-*tert*-butyl-β-nitrostyrene according to the procedure G. Flash chromatography (hexanes/EtOAc 9:1) afforded **4m** in 67% (37 mg) as a light yellow oil. The enantiomeric excess was determined by chiral-stationary phase UPC^2. Trefoil CEL2, **Grad:** CO_2/EtOH 100-0% to 98-02 % in 19 min; 100-0 % in 1 min at 3 ml/min at 40°C. UV detection at 210 nm: **R$_t$:** (syn, minor) = 9.30 min, (syn, major) = 9.65 min. **R$_f$** = 0.5 (hexanes/EtOAc 9:1). **NMR ^{1}H (400 MHz, CDCl$_3$)** δ 9.71 (d, *J* = 2.6 Hz, 1H), 7.35 – 7.29 (m, 2H), 7.14 – 7.05 (m, 2H), 4.84 – 4.58 (m, 2H), 3.77 (td, J = 9.6, 5.3 Hz, 1H), 2.65 (dtd, *J* = 9.3, 6.4, 2.7 Hz, 1H), 1.51 (p, *J* = 7.2 Hz, 2H), 1.29 (s, 9H), 0.84 (t, *J* = 7.5 Hz, 3H). **NMR ^{13}C (100 MHz, CDCl$_3$)** δ 203.6, 151.1, 133.7, 127.7, 126.1, 78.6, 55.4, 42.4, 34.6, 31.4, 20.5, 11.0.
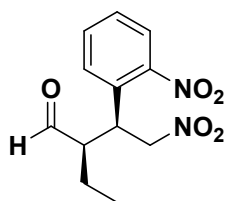
(2R,3S)-2-ethyl-4-nitro-3-(2-nitrophenyl)butanal (4m): Prepared by reaction of butanal with *trans*-2-nitro-β-nitrostyrene according to the procedure G. Flash chromatography (hexanes/EtOAc 7:3) afforded **4n** in 78% (42 mg) as a light yellow oil. The enantiomeric excess was determined by chiral-stationary phase UPC^2. Trefoil CEL2, **Grad:** CO_2/ACN 100-0% to 90-10 % in 5 min; 90-10 % in 4 min; 100-0 % in 1 min at 2 ml/min at 25°C. UV detection at 210 nm: **R$_t$:** (syn, minor) = 5.77 min, (syn, major) = 7.14 min. **R$_f$** = 0.6 (hexanes/EtOAc 7:3). **NMR ^{1}H (400 MHz, CDCl$_3$)** δ = 9.73 (d, *J* = 2.2 Hz, 1H), 7.90 – 7.86 (m, 1H), 7.64 – 7.58 (m, 1H), 7.50 – 7.36 (m, 2H), 4.92 – 4.70 (m, 2H), 4.42 (td, *J* = 9.2, 4.2 Hz, 1H), 3.00 – 2.84 (m, 1H), 1.74 – 1.44 (m, 2H), 0.88 (t, *J* = 7.5 Hz, 3H). **NMR ^{13}C (100 MHz, CDCl$_3$)** δ = 202.6, 150.7, 133.4, 132.0, 129.1, 125.4, 77.4, 54.4, 37.2, 21.1, 11.1.
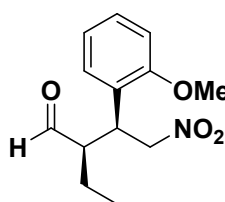
(2R,3S)-2-ethyl-3-(2-methoxyphenyl)-4-nitrobutanal (4n)[8]: Prepared by reaction of butanal with *trans*-2-methoxy-β-nitrostyrene according to the procedure G. Flash chromatography (hexanes/EtOAc 9:1) afforded **4o** in 71% (36 mg) as a light yellow oil. The enantiomeric excess was determined by chiral-stationary phase UPC^2. Trefoil CEL2, **Grad:** CO_2/EtOH 100- 0% to 98-02 % in 19 min; 100-0 % in 1 min at 2 ml/min at 25°C. UV detection at 210 nm: **R$_t$:** (syn, minor) = 11.37 min, (syn, major) = 12.03 min. **R$_f$** = 0.4

(hexanes/EtOAc 9:1). **NMR [1]H (400 MHz, CDCl$_3$)** δ 9.63 (d, J = 2.6 Hz, 1H), 7.24 – 7.15 (m, 1H), 7.02 (d, J = 7.5 Hz, 1H), 6.86 – 6.80 (m, 2H), 4.80 – 4.55 (m, 2H), 3.95 (td, J = 9.7, 4.9 Hz, 1H), 2.95 – 2.82 (m, 1H), 1.45 – 1.35 (m, 2H), 0.73 (t, J = 7.5 Hz, 3H). **NMR [13]C (100 MHz, CDCl$_3$)** δ 203.9, 157.6, 130.6, 129.4, 121.1, 111.3, 55.5, 53.6, 39.6, 20.6, 10.9.
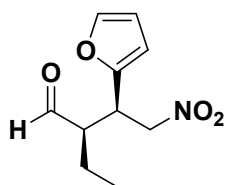
(2R,3R)-2-ethyl-3-(furan-2-yl)-4-nitrobutanal (**4o**)[5]: Prepared by reaction of butanal with *trans-β*-nitrovinylfuran according to the procedure G. Flash chromatography (hexanes/EtOAc 9:1) afforded **4p** in 83% (35 mg) as a light yellow oil. The enantiomeric excess was determined by chiral-stationary phase UPC[2]. Trefoil CEL2, CO$_2$/MeOH 98.5-1.5 in 8 min at 1 ml/min at 35°C. UV detection at 210 nm: **R$_t$**: (syn, minor) = 5.53 min, (syn, major) = 5.78 min. **R$_f$** = 0.5 (hexanes/EtOAc 9:1). **NMR [1]H (400 MHz, CDCl$_3$)** δ = 9.71 (s, 1H), 7.37 (d, J = 0.9 Hz, 1H), 6.34 – 6.28 (m, 1H), 6.20 (d, J = 3.3 Hz, 1H), 4.76 – 4.63 (m, 2H), 4.05 – 3.95 (m, 1H), 2.76 (dtd, J = 8.6, 6.9, 1.5 Hz, 1H), 1.62 – 1.52 (m, 2H), 0.90 (t, J = 7.5 Hz, 3H). **NMR [13]C (100 MHz, CDCl$_3$)** δ 202.5, 150.2, 142.8, 110.6, 108.9, 76.3, 53.5, 36.7, 20.1, 11.0.
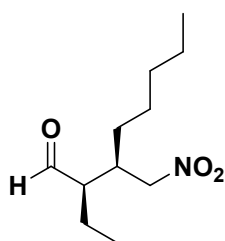
(2R,3R)-2-ethyl-3-(nitromethyl)octanal (**4p**): Prepared by reaction of butanal with (*E*)-1-nitrohept-1-ene according to the procedure G. Flash chromatography (hexanes/EtOAc 9:1) afforded **4q** in 73% (31 mg) as a colorless oil. The enantiomeric excess was determined by chiral-stationary phase UPC[2]. Trefoil CEL2, CO$_2$/IPA 99-1 in 8 min at 1 ml/min at 35°C. UV detection at 210 nm: **R$_t$**: (syn, minor) = 5.71 min, (syn, major) = 6.71 min. **R$_f$** = 0.8 (hexanes/EtOAc 9:1). **NMR [1]H (400 MHz, CDCl$_3$)** δ 9.69 (s, 1H), 4.49 – 4.31 (m, 2H), 2.68 – 2.53 (m, 1H), 2.43 – 2.31 (m, 1H), 1.84 – 1.70 (m, 1H), 1.59 – 1.43 (m, 1H), 1.42 – 1.20 (m, 8H), 1.03 – 0.94 (m, 3H), 0.90 – 0.84 (m, 3H). **NMR [13]C (100 MHz, CDCl$_3$)** δ 203.3, 54.0, 36.9, 31.7, 29.2, 26.5, 22.5, 18.7, 14.1, 12.2.
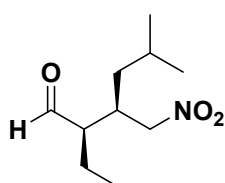
(2R,3R)-2-ethyl-5-methyl-3-(nitromethyl)hexanal (**4q**)[8]: Prepared by reaction of butanal with (E)-4-methyl-1-nitropent-1-ene according to the procedure G. Flash chromatography (hexanes/EtOAc 9:1) afforded **4r** in 66% (27 mg) as a colorless oil. The enantiomeric

excess was determined by chiral-stationary phase UPC^2. Trefoil CEL2, CO_2/MeOH 99-1 in 8 min at 1 ml/min at 35°C. UV detection at 210 nm: **R$_t$**: (syn, major) = 5.34 min. ***R$_f$*** = 0.75 (hexanes/EtOAc 9:1). **NMR ^{1}H (400 MHz, CDCl$_3$)** δ 9.70 (s, 1H), 4.50 – 4.29 (m, 2H), 2.76 – 2.61 (m, 1H), 2.41 (dt, *J* = 9.0, 4.7 Hz, 1H), 1.85 – 1.72 (m, 1H), 1.64 – 1.44 (m, 2H), 1.30 – 1.17 (m, 2H), 1.04 – 0.95 (m, 3H), 0.89 (dt, *J* = 5.8 Hz, 6H). **NMR ^{13}C (100 MHz, CDCl$_3$)** δ 203.2, 77.2, 54.2, 38.4, 34.8, 25.3, 22.8, 22.2, 18.6, 12.3.

13. NMR Spectra: Isocyanides
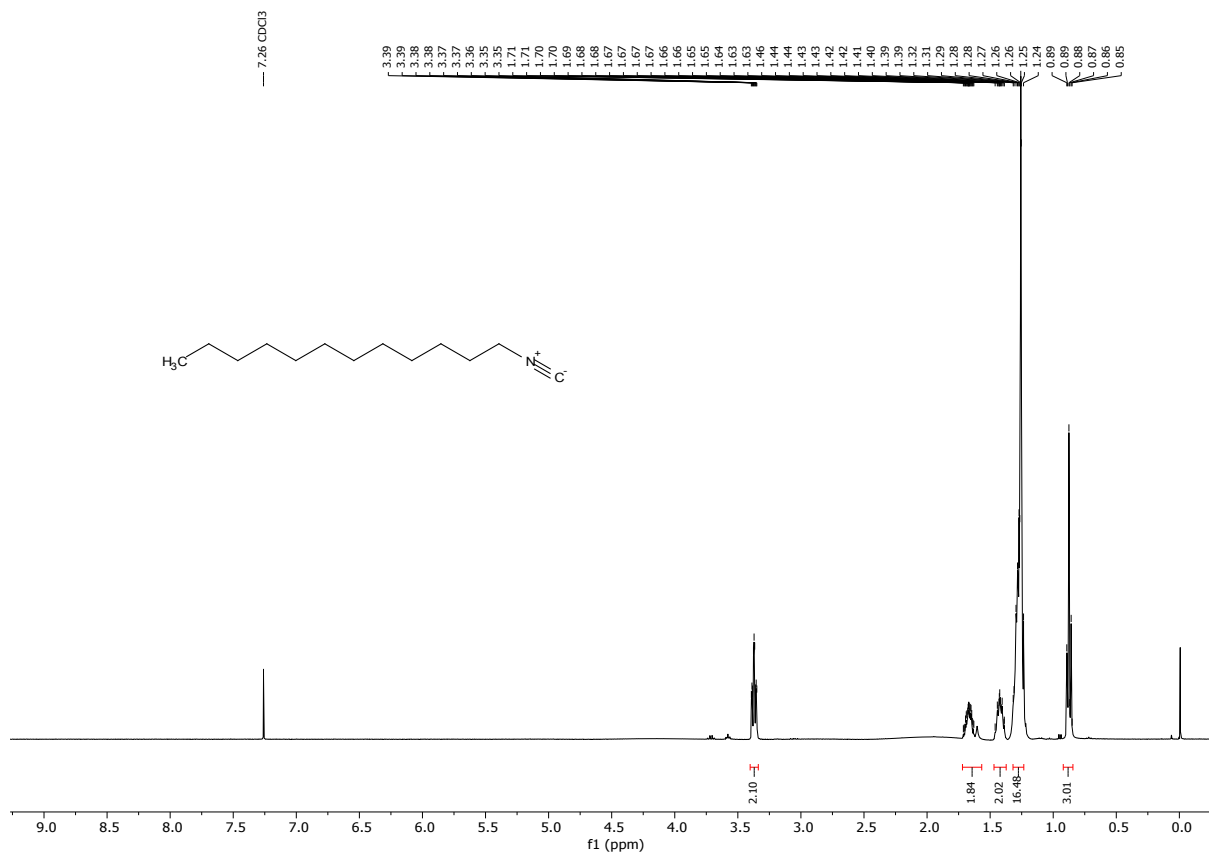
FIGURE 3. ^{1}H NMR of compound **2a** (400 MHz, CDCl$_3$).
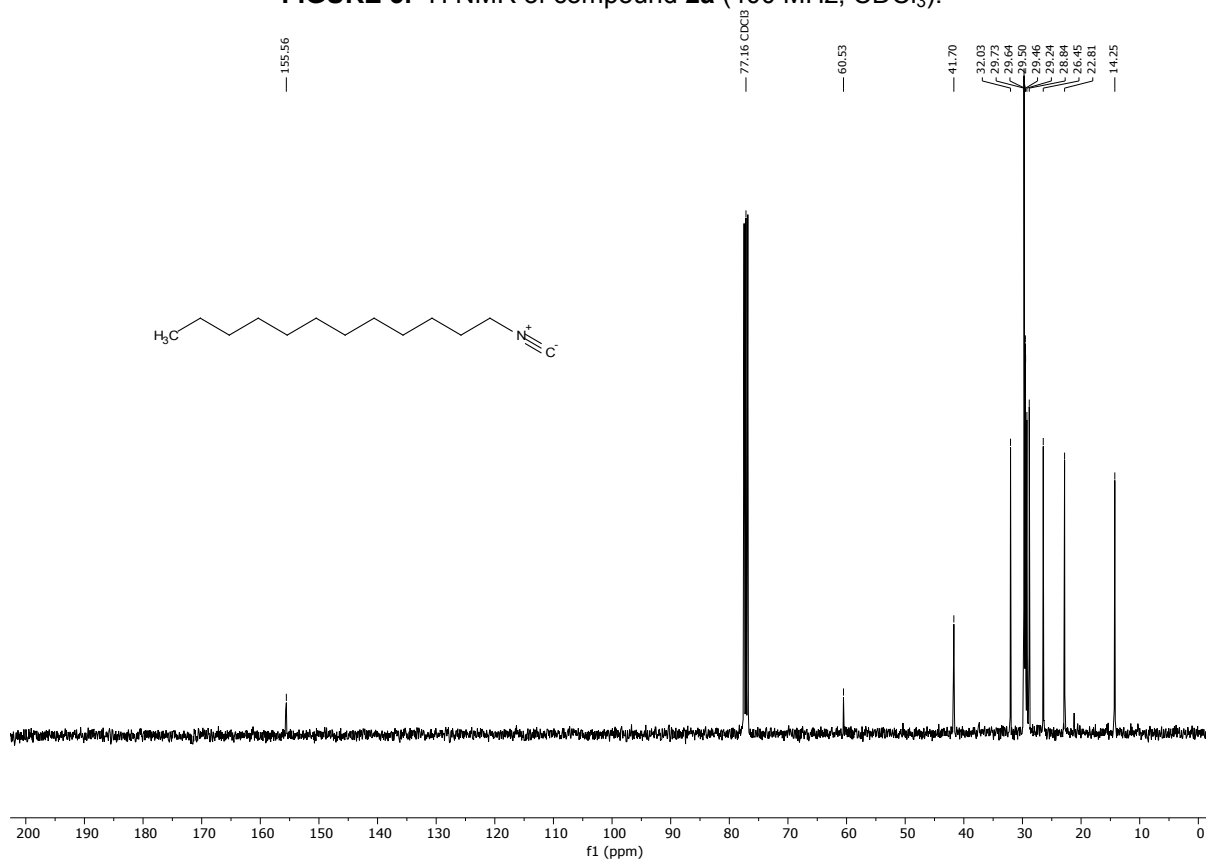
FIGURE 4. ^{13}C NMR of compound **2a** (100 MHz, CDCl$_3$).
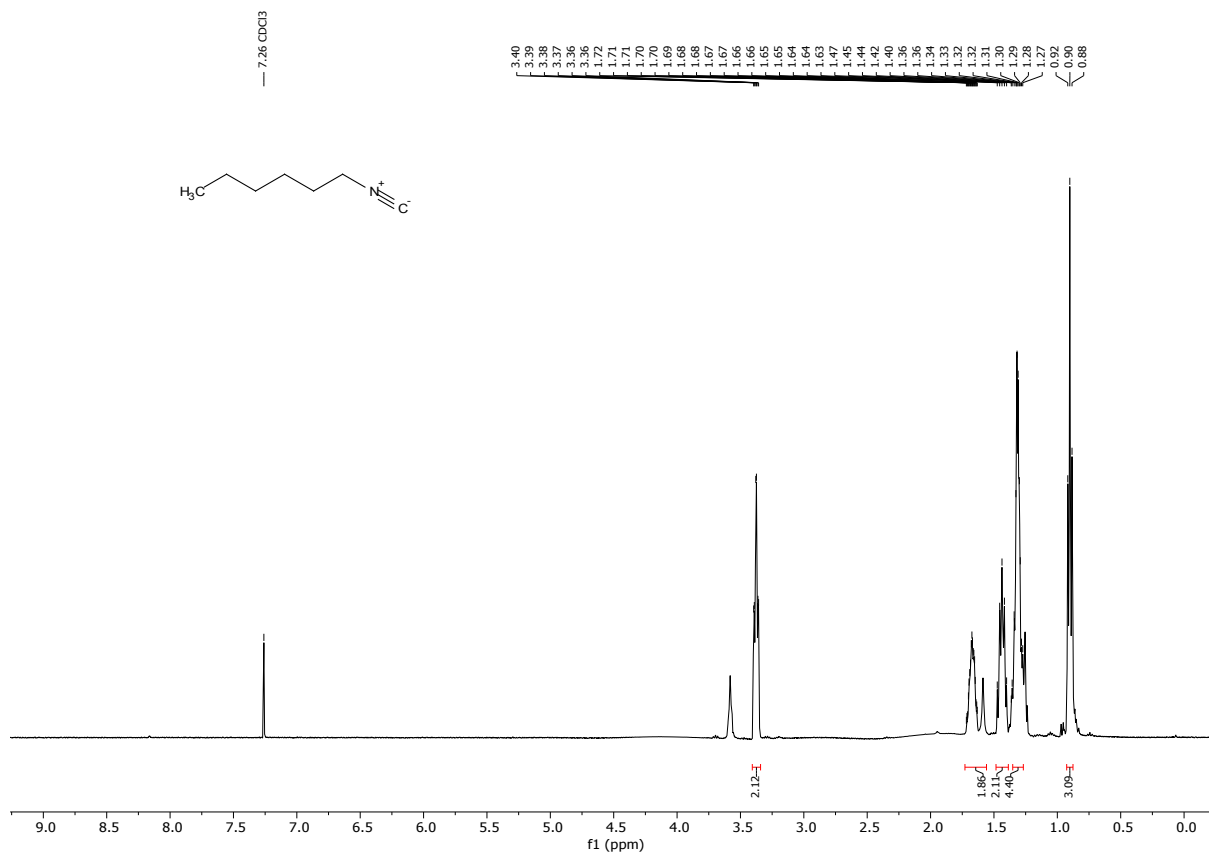
FIGURE 5. ^{1}H NMR of compound **2b** (400 MHz, CDCl$_3$).
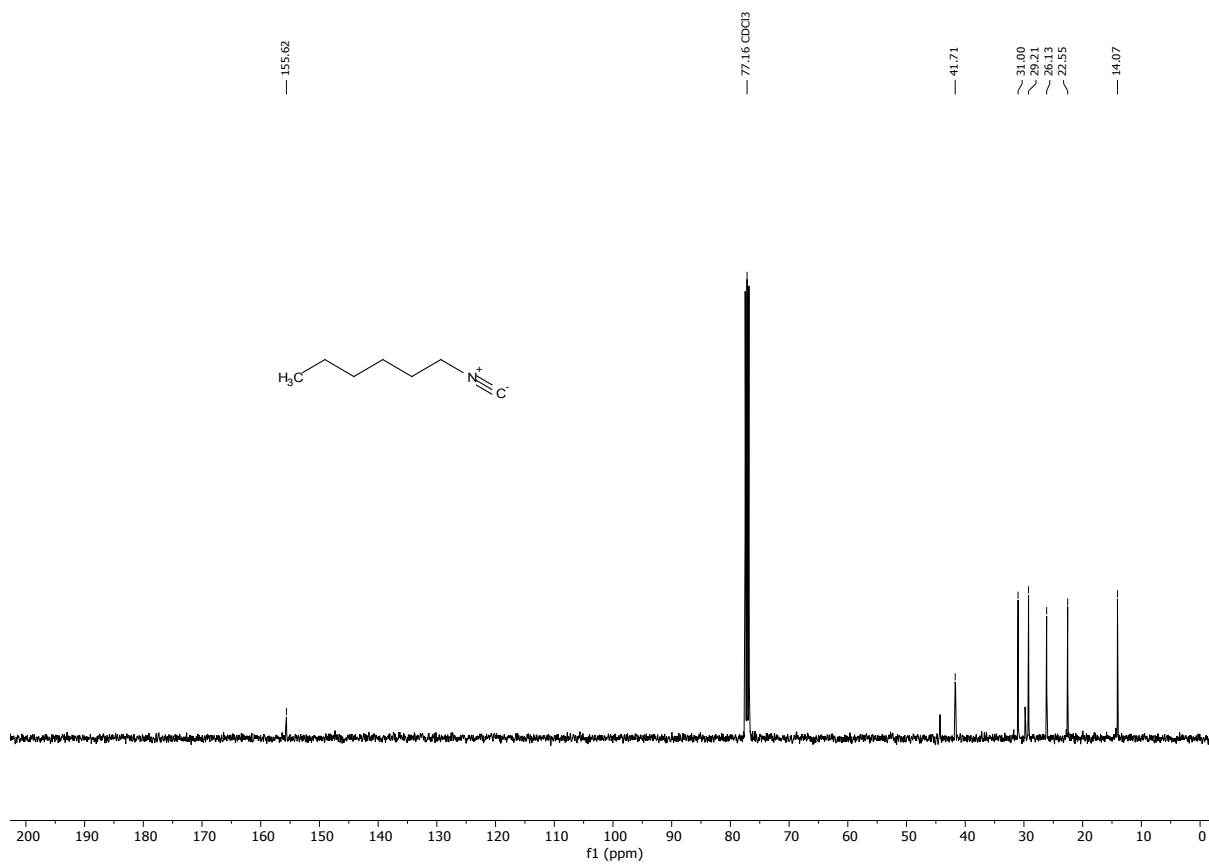
FIGURE 6. ^{13}C NMR of compound **2b** (100 MHz, CDCl$_3$).

S25
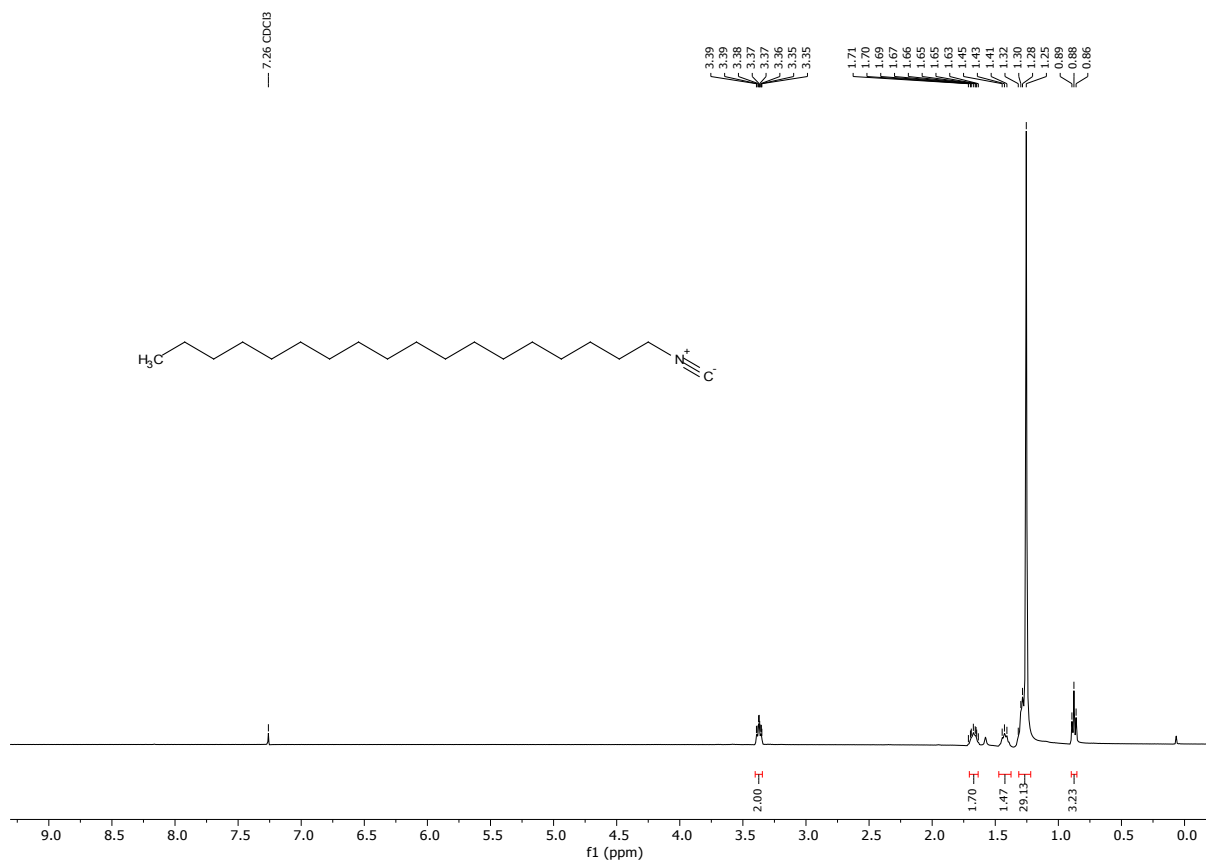
FIGURE 7. ^{1}H NMR of compound **2c** (400 MHz, CDCl$_3$).
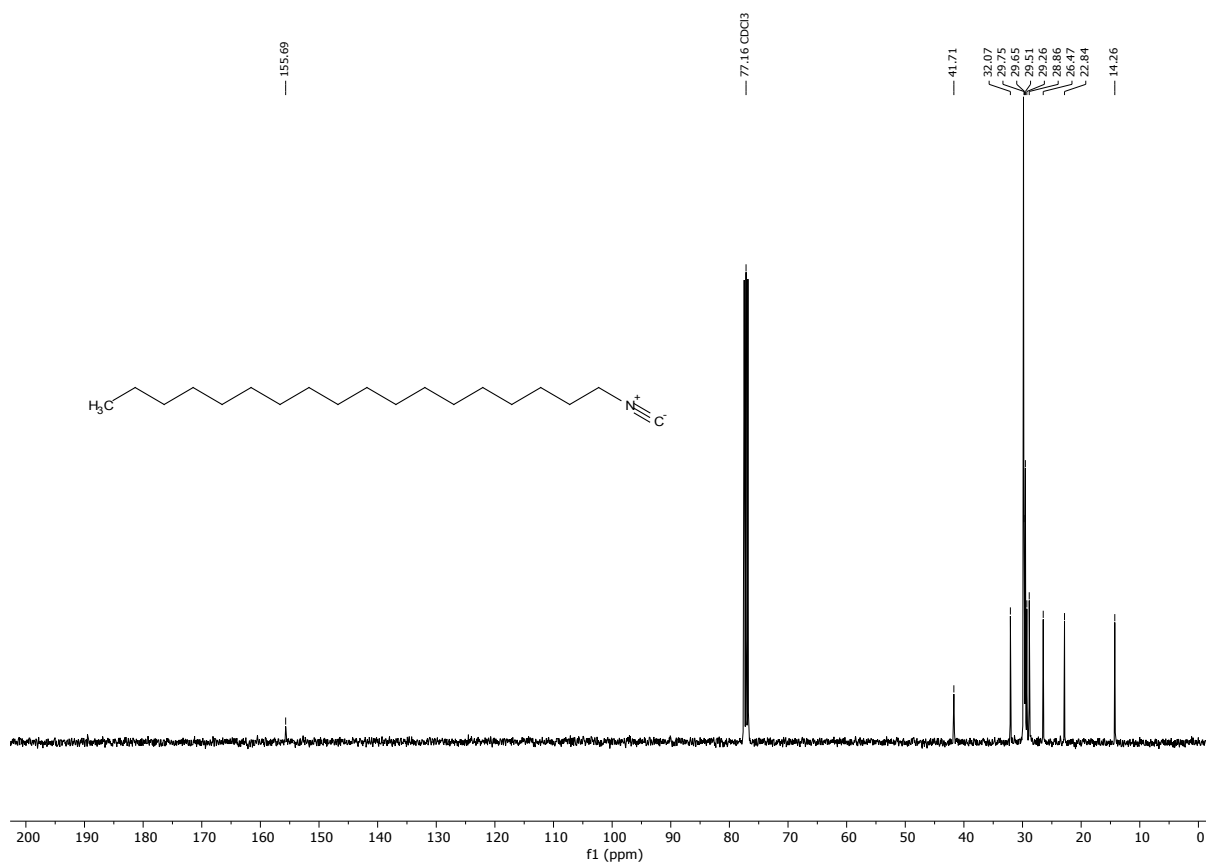
FIGURE 8. ^{13}C NMR of compound **2c** (100 MHz, CDCl$_3$).

14. NMR Spectra: Catalysts
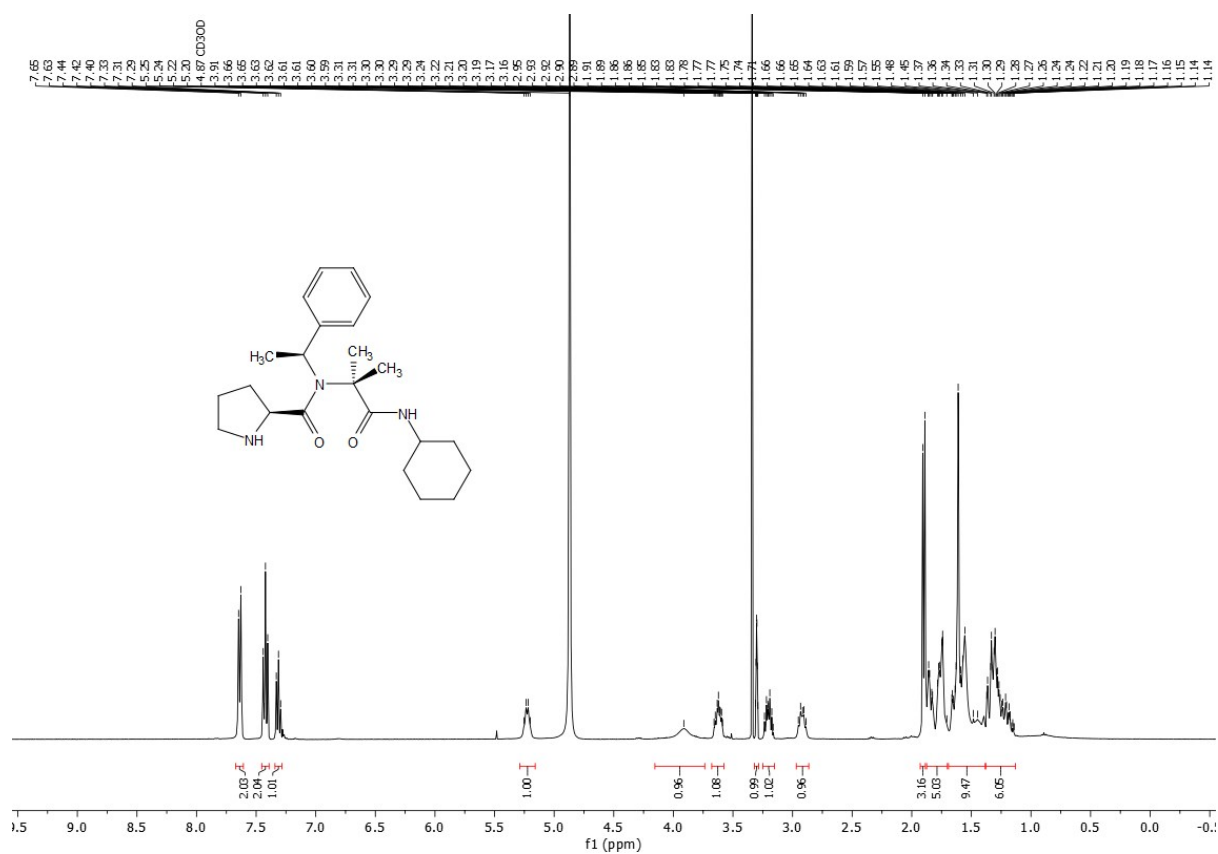
FIGURE 9. ^{1}H NMR of compound **3a** (400 MHz, CD$_3$OD).
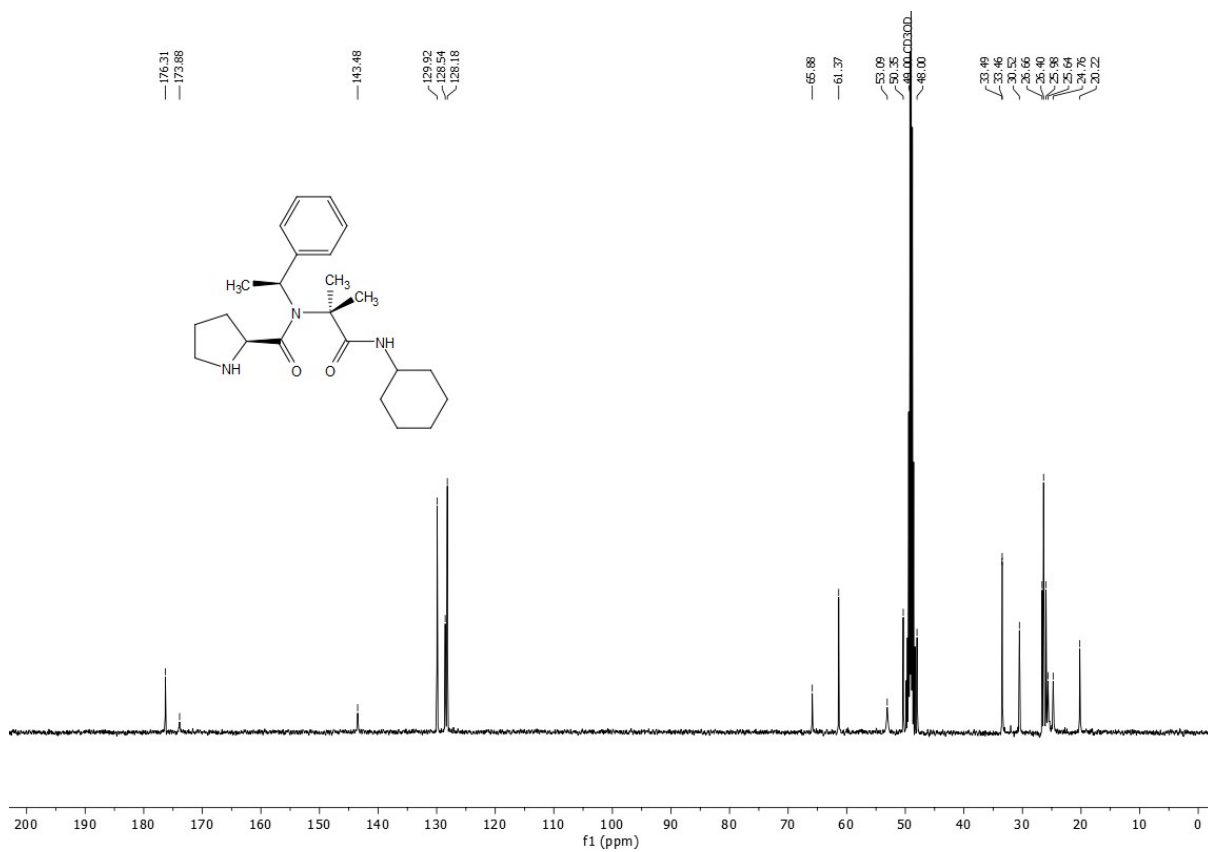
FIGURE 10. ^{13}C NMR of compound **3a** (100 MHz, CD$_3$OD).
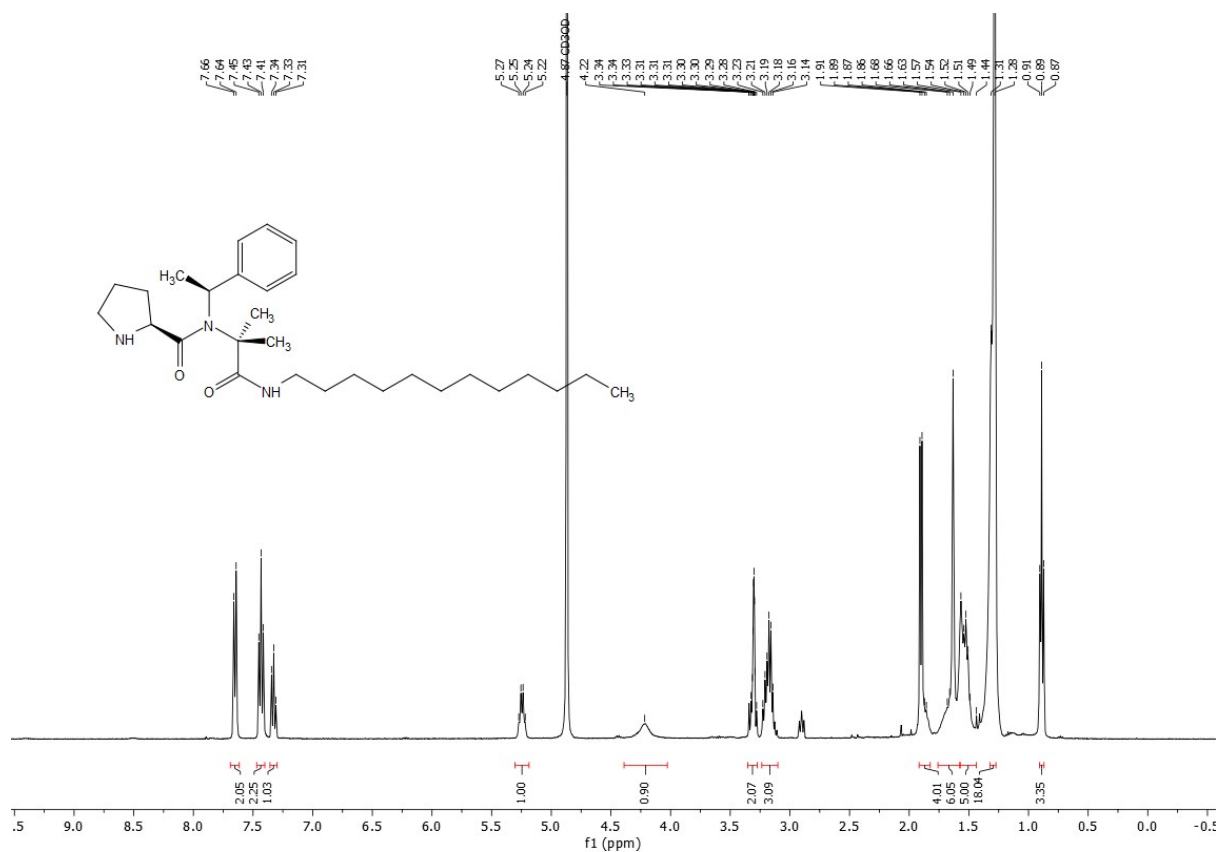
FIGURE 11. ^{1}H NMR of compound **3b** (400 MHz, CD$_3$OD).
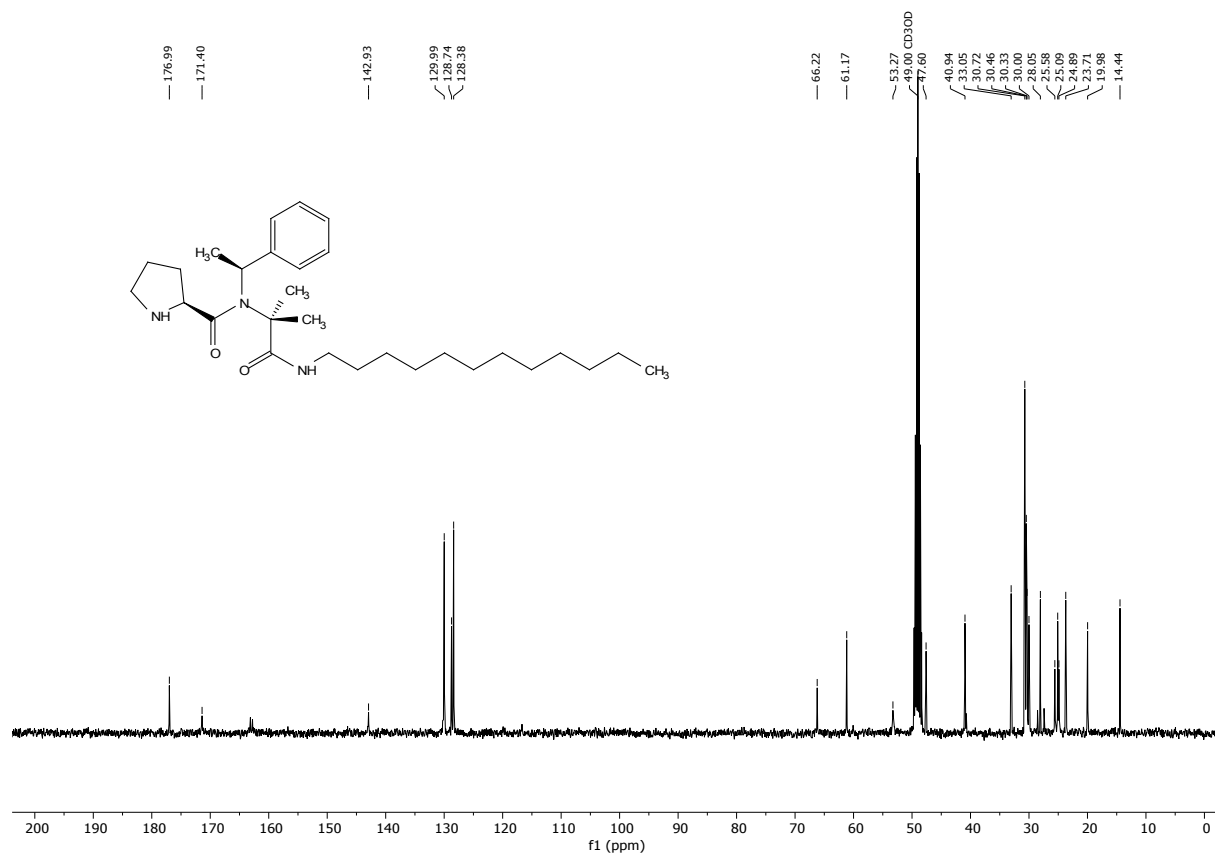
FIGURE 12. ^{13}C NMR of compound **3b** (100 MHz, CD$_3$OD).

S28
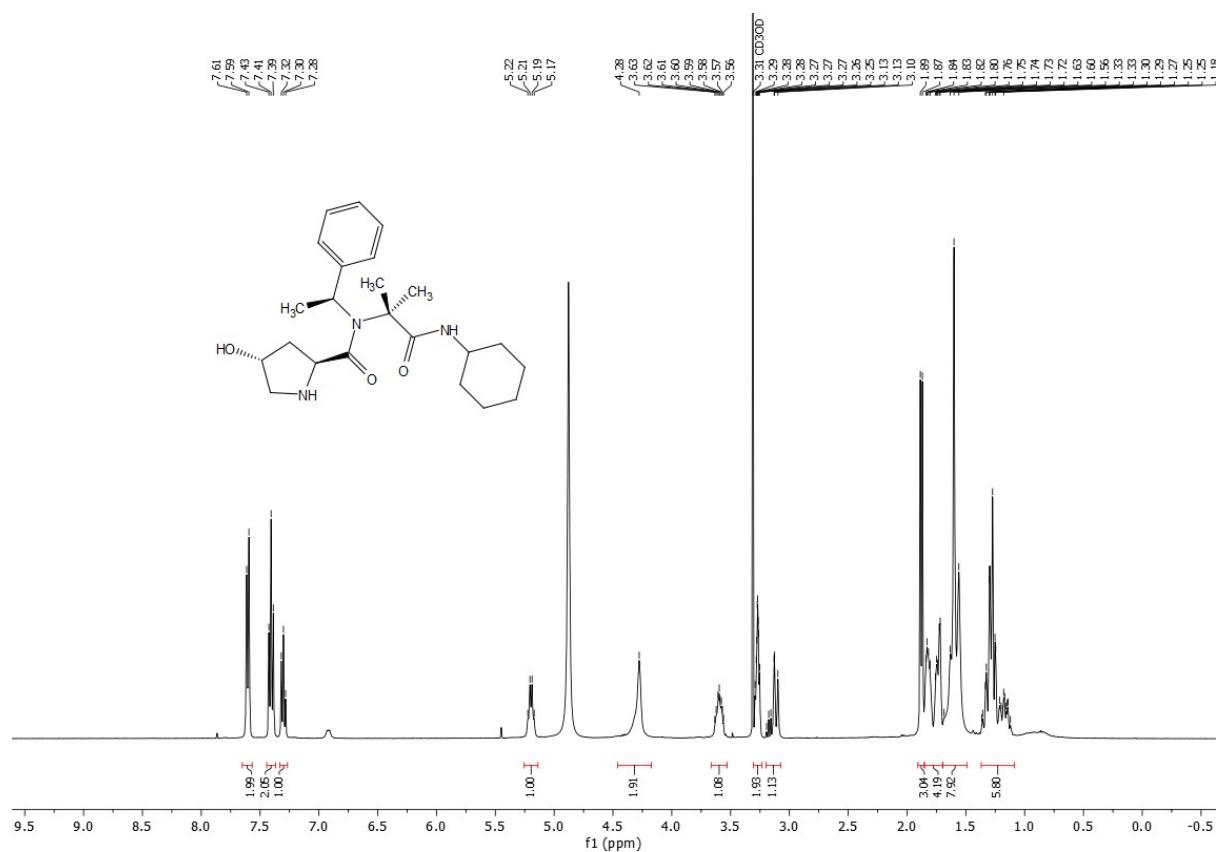
FIGURE 13. ^{1}H NMR of compound **3c** (400 MHz, CD$_3$OD).
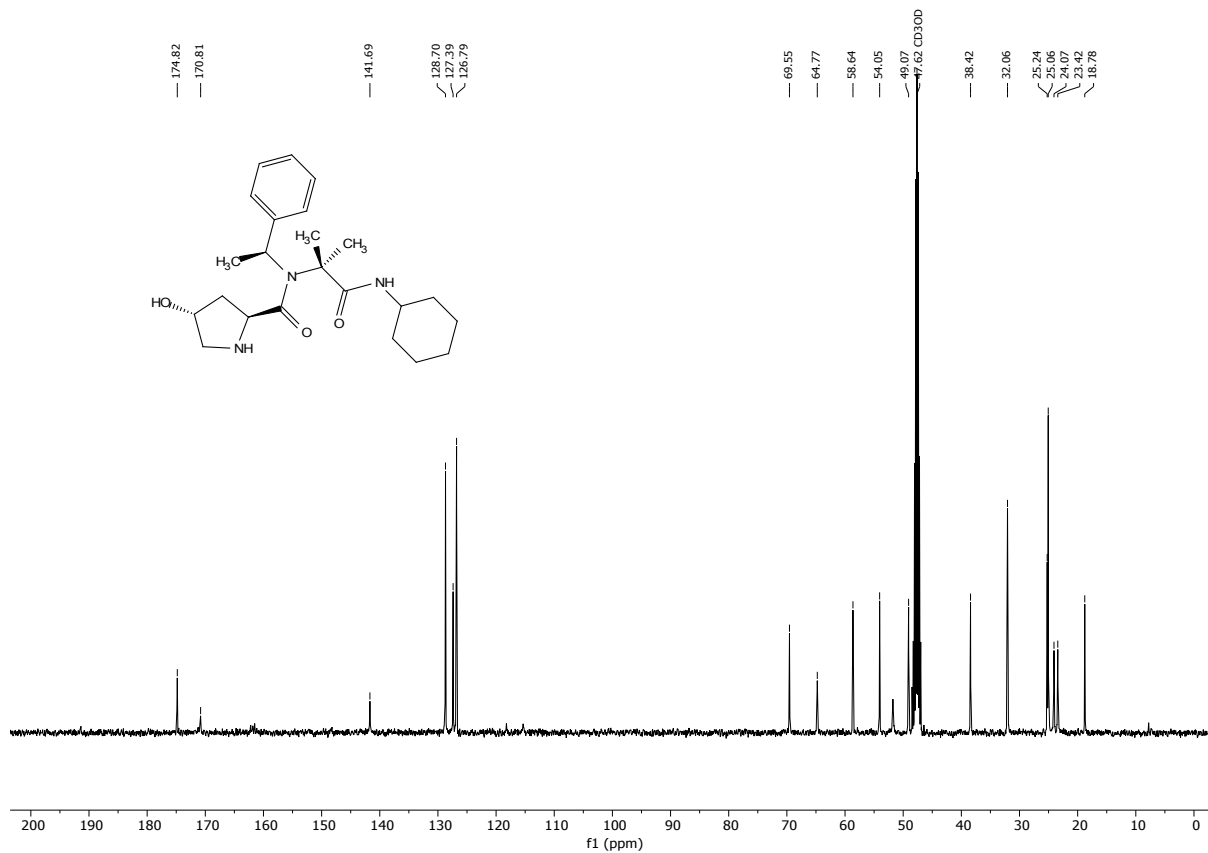
FIGURE 14. ^{13}C NMR of compound **3c** (100 MHz, CD$_3$OD).

S29
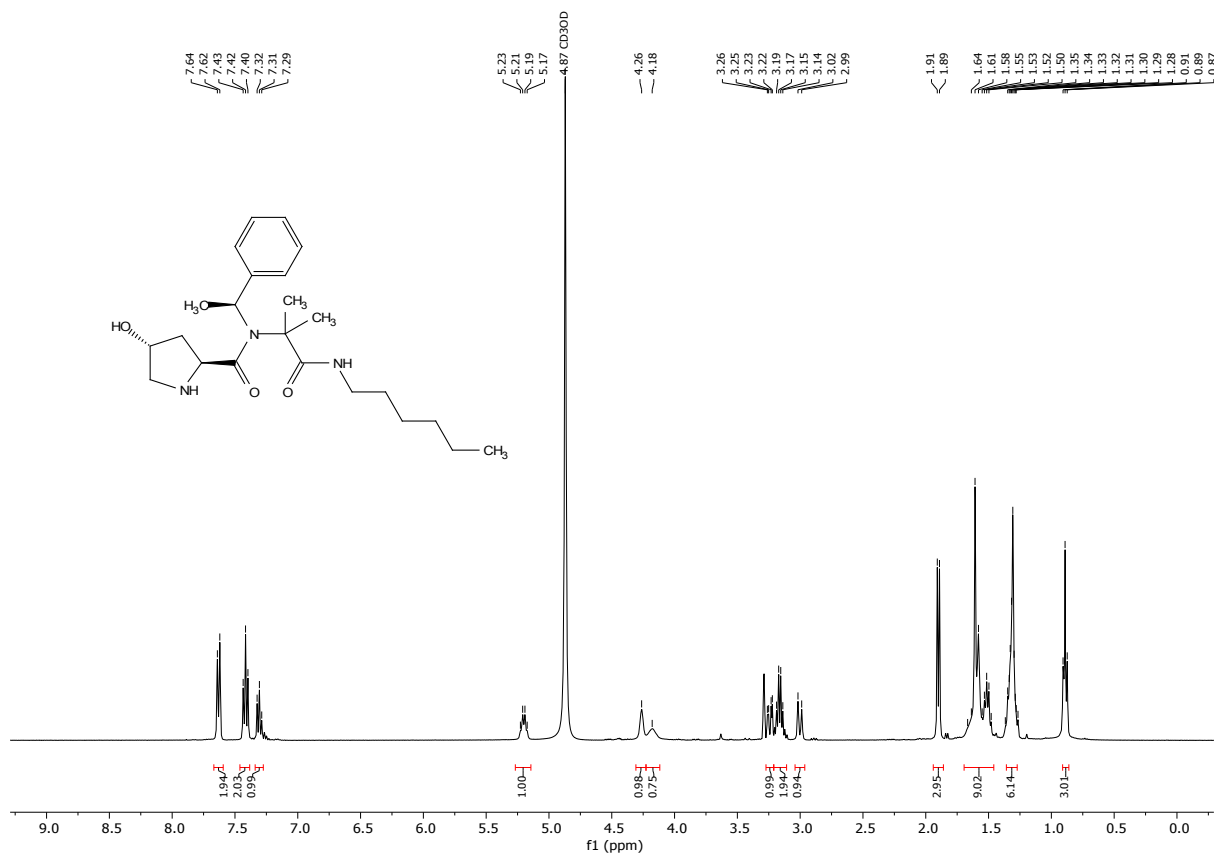
FIGURE 15. ^{1}H NMR of compound **3d** (400 MHz, CD$_3$OD).
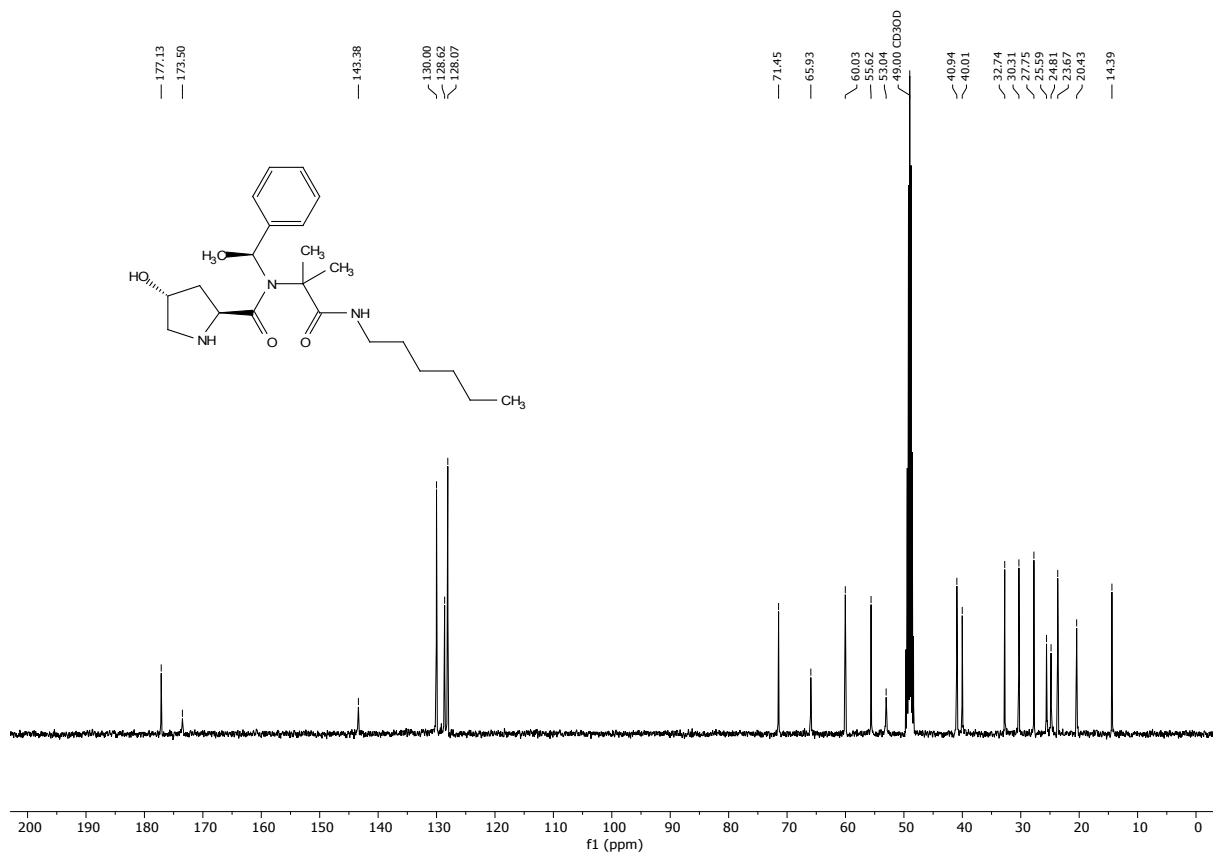
FIGURE 16. ^{13}C NMR of compound **3d** (100 MHz, CD$_3$OD).

S30
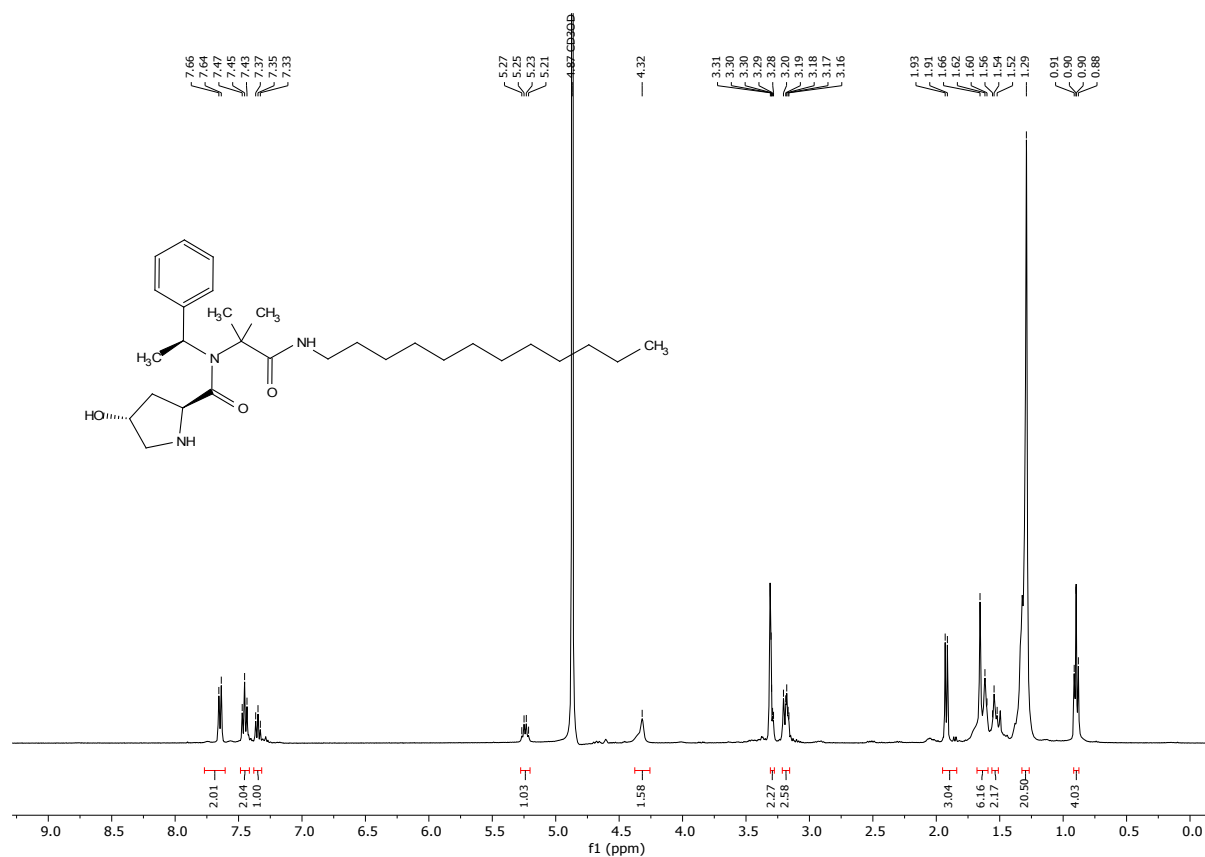
FIGURE 17. ^{1}H NMR of compound **3e** (400 MHz, CD$_3$OD).
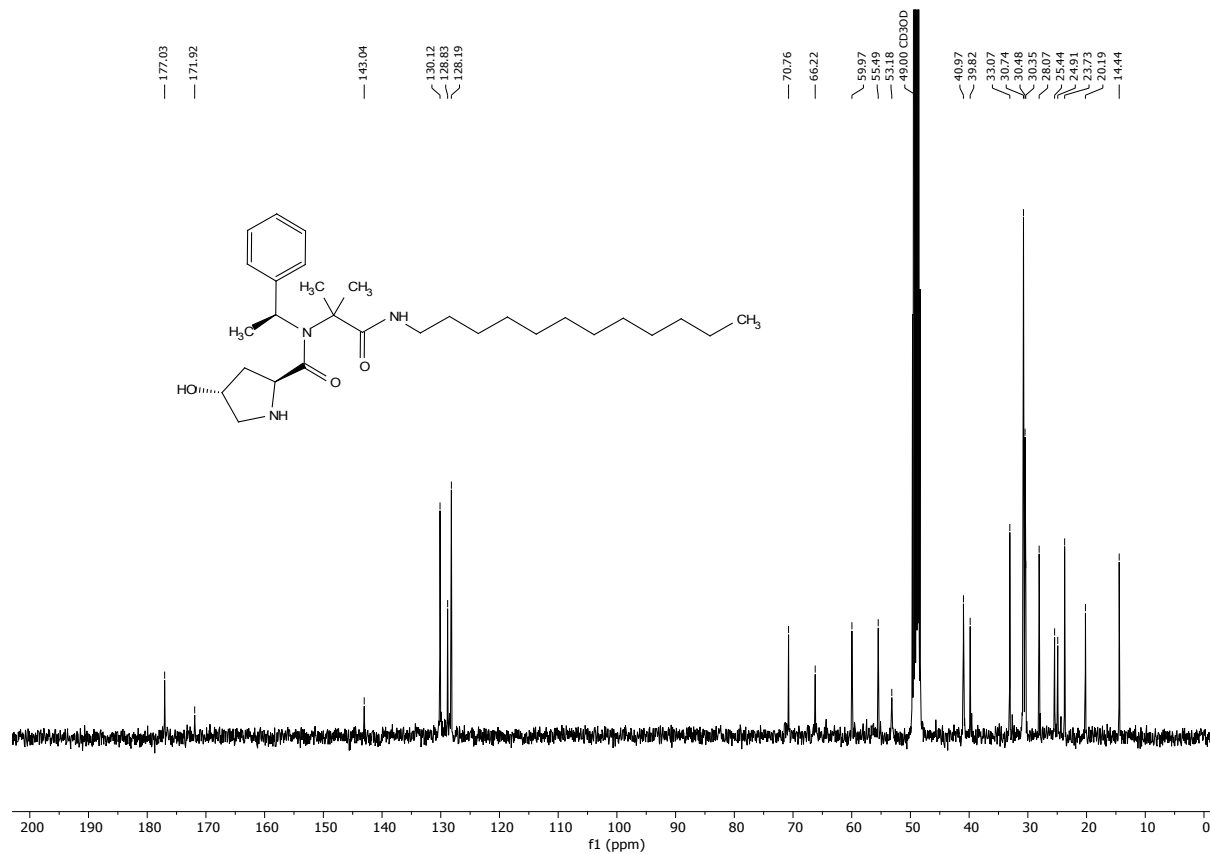
FIGURE 18. ^{13}C NMR of compound **3e** (100 MHz, CD$_3$OD).
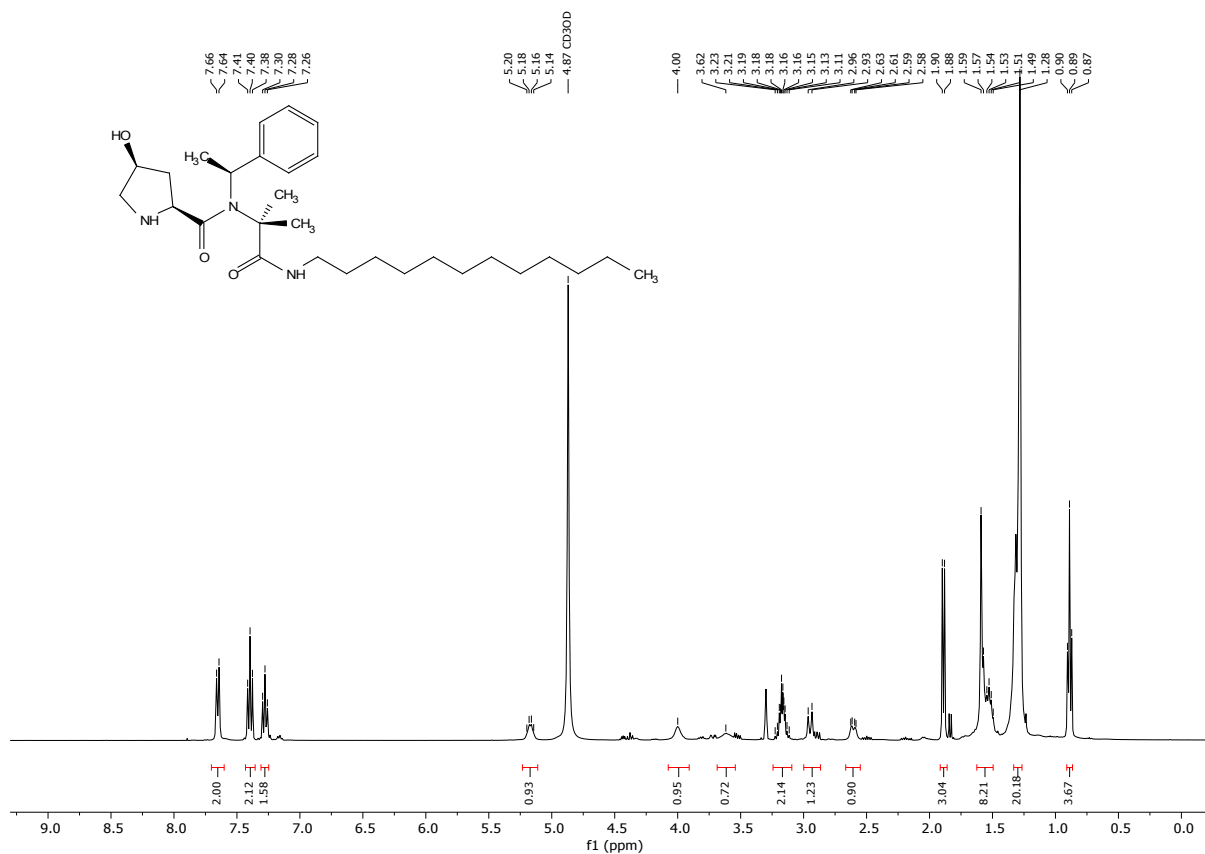
FIGURE 19. ¹H NMR of compound **3f** (400 MHz, CD₃OD).
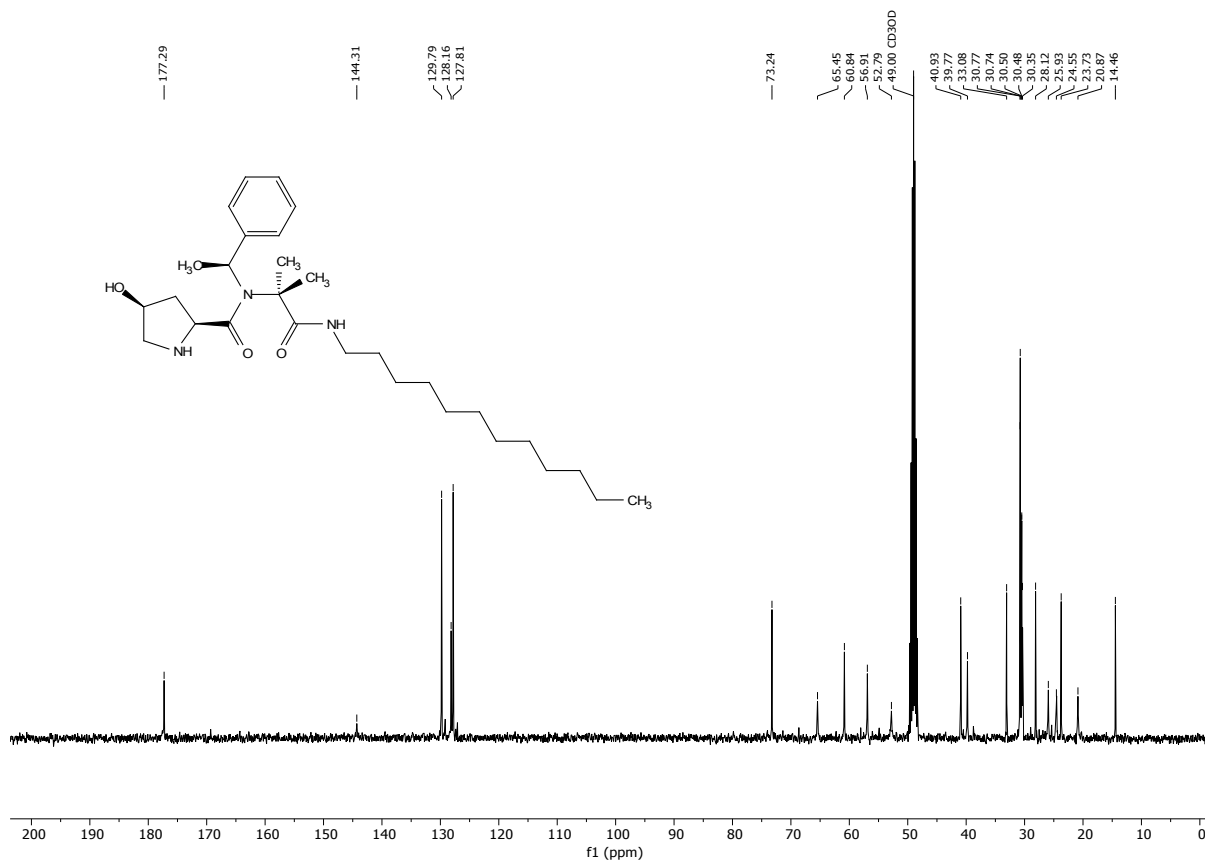
FIGURE 20. ¹³C NMR of compound **3f** (100 MHz, CD₃OD).
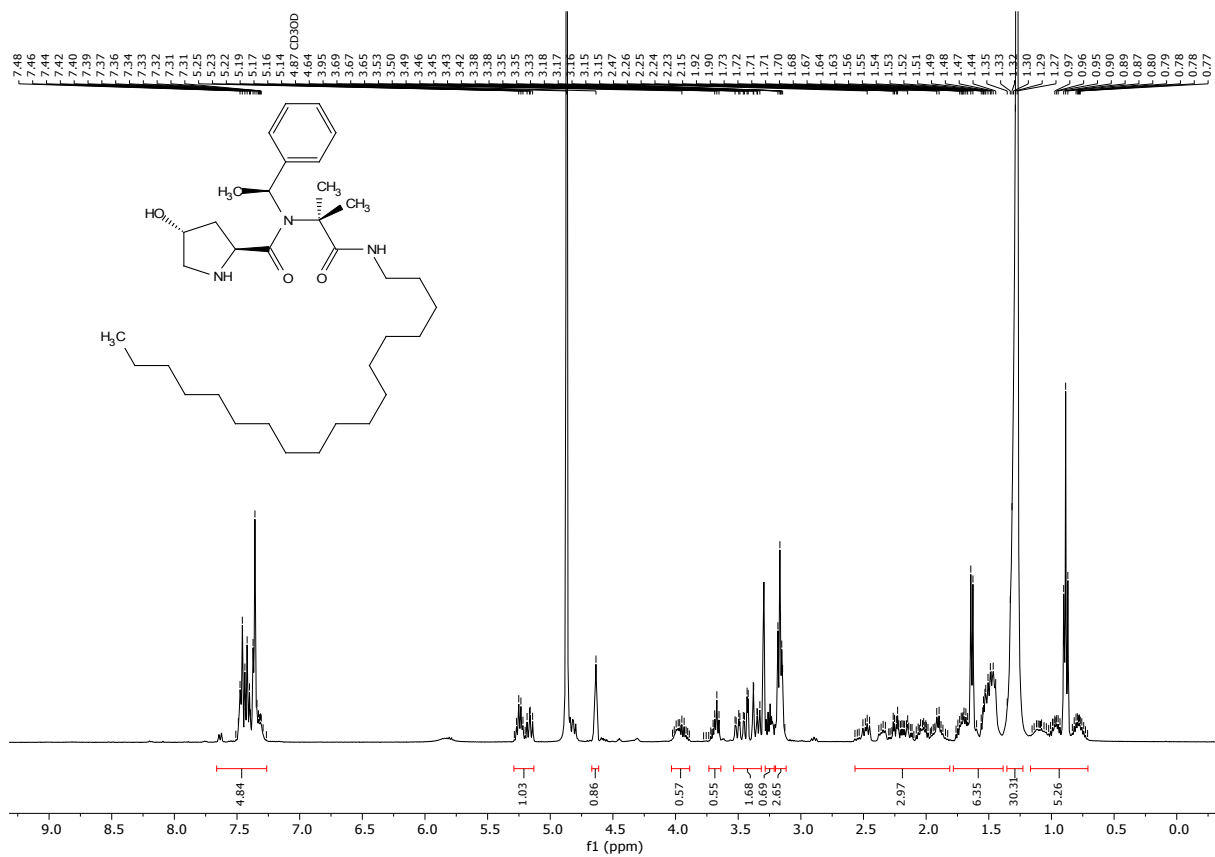
FIGURE 21. ^{1}H NMR of compound **3g** (400 MHz, CD$_3$OD).
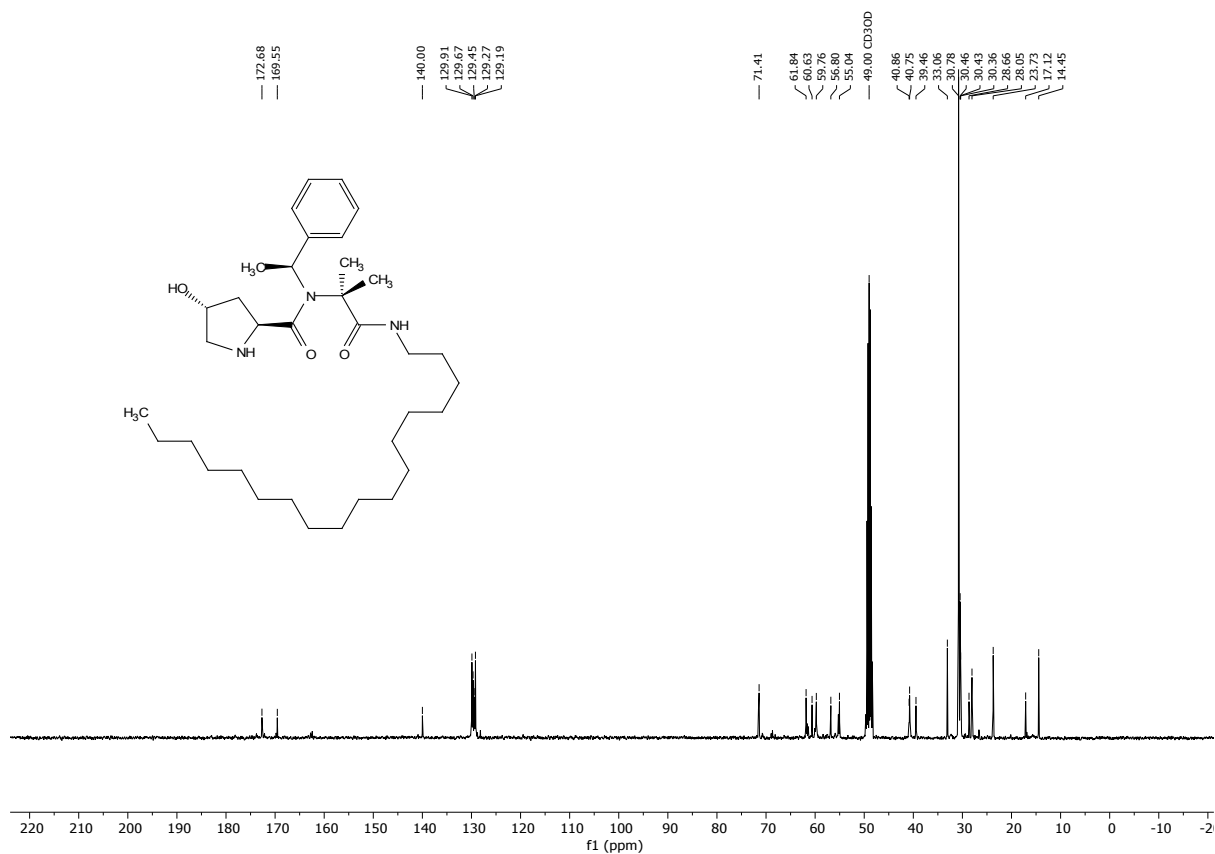
FIGURE 22. ^{13}C NMR of compound **3g** (100 MHz, CD$_3$OD).
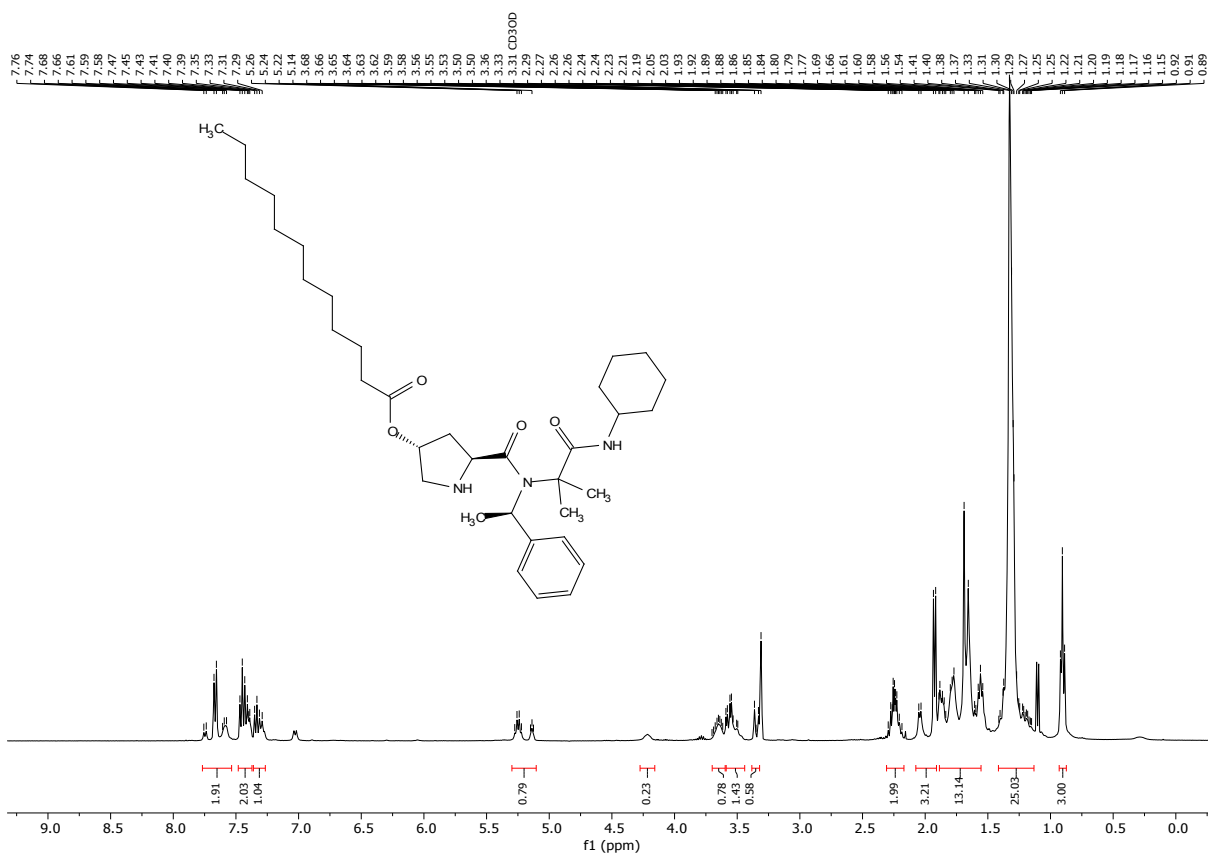
FIGURE 23. ^{1}H NMR of compound **3h** (400 MHz, CD$_3$OD).

S34
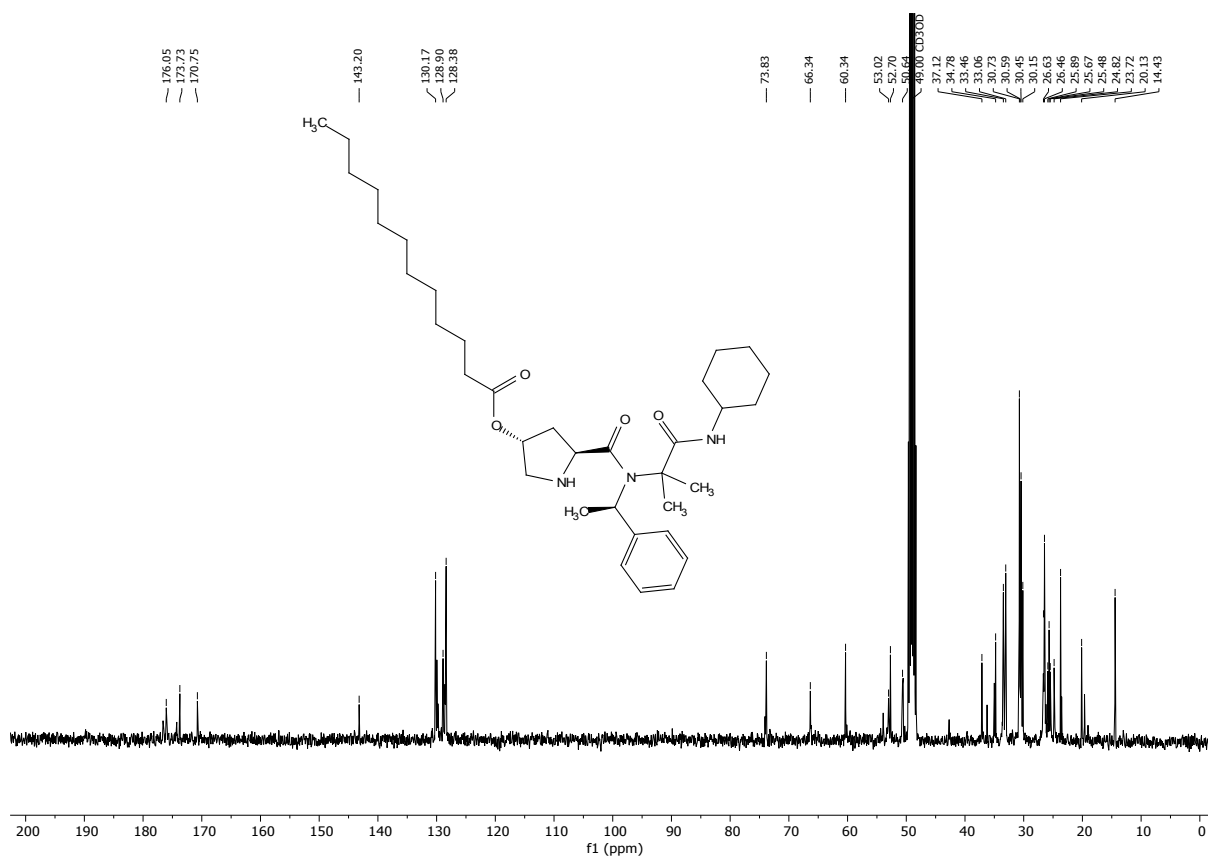
FIGURE 24. ^{13}C NMR of compound **3h** (100 MHz, CD$_3$OD).
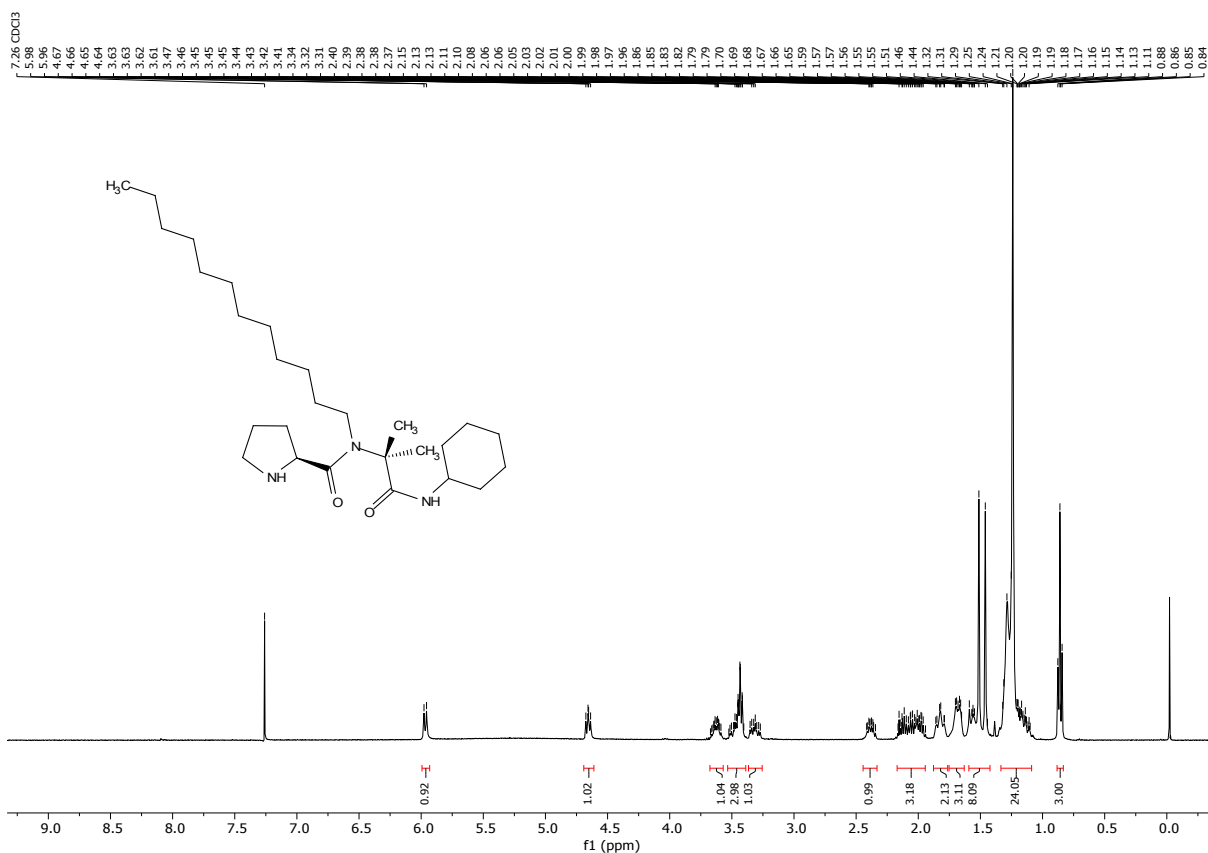
FIGURE 25. ^{1}H NMR of compound **3i** (400 MHz, CDCl$_3$).
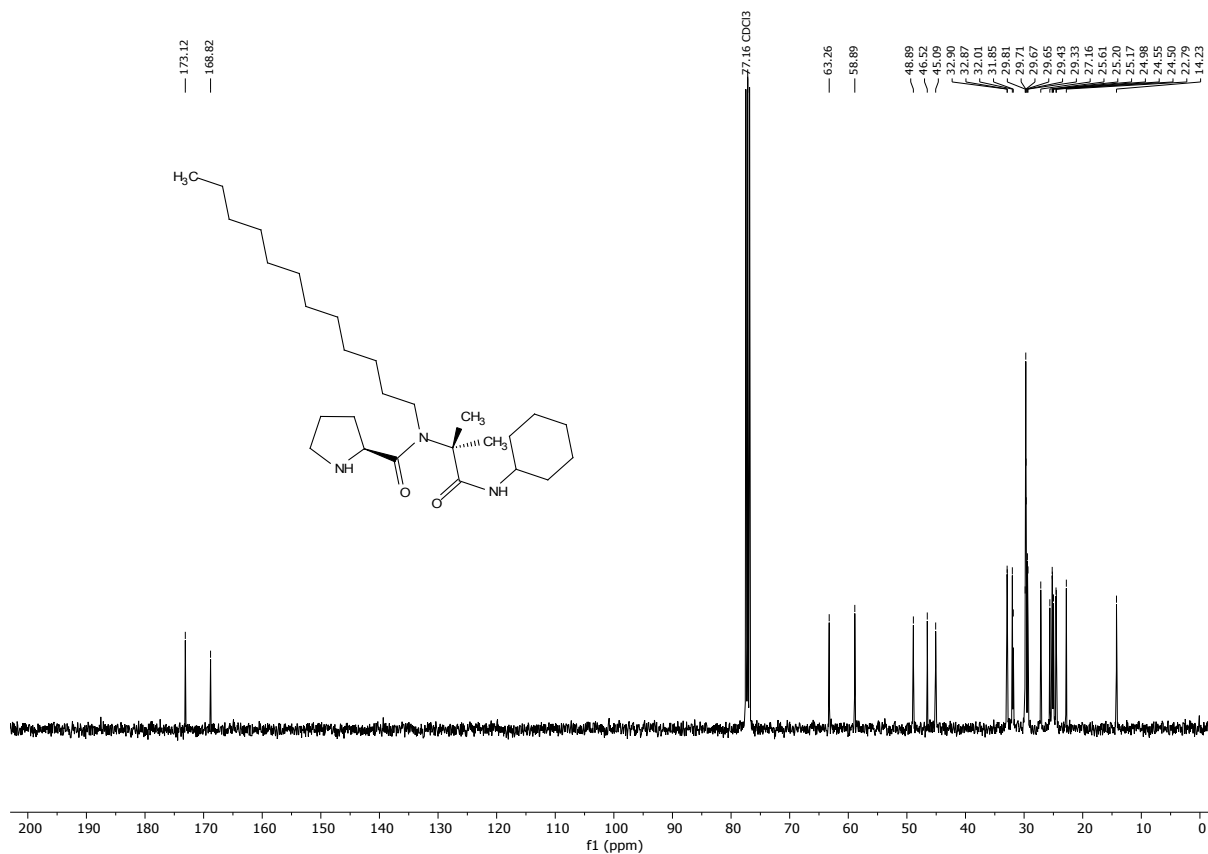
FIGURE 26. ^{13}C NMR of compound **3i** (100 MHz, CDCl$_3$).
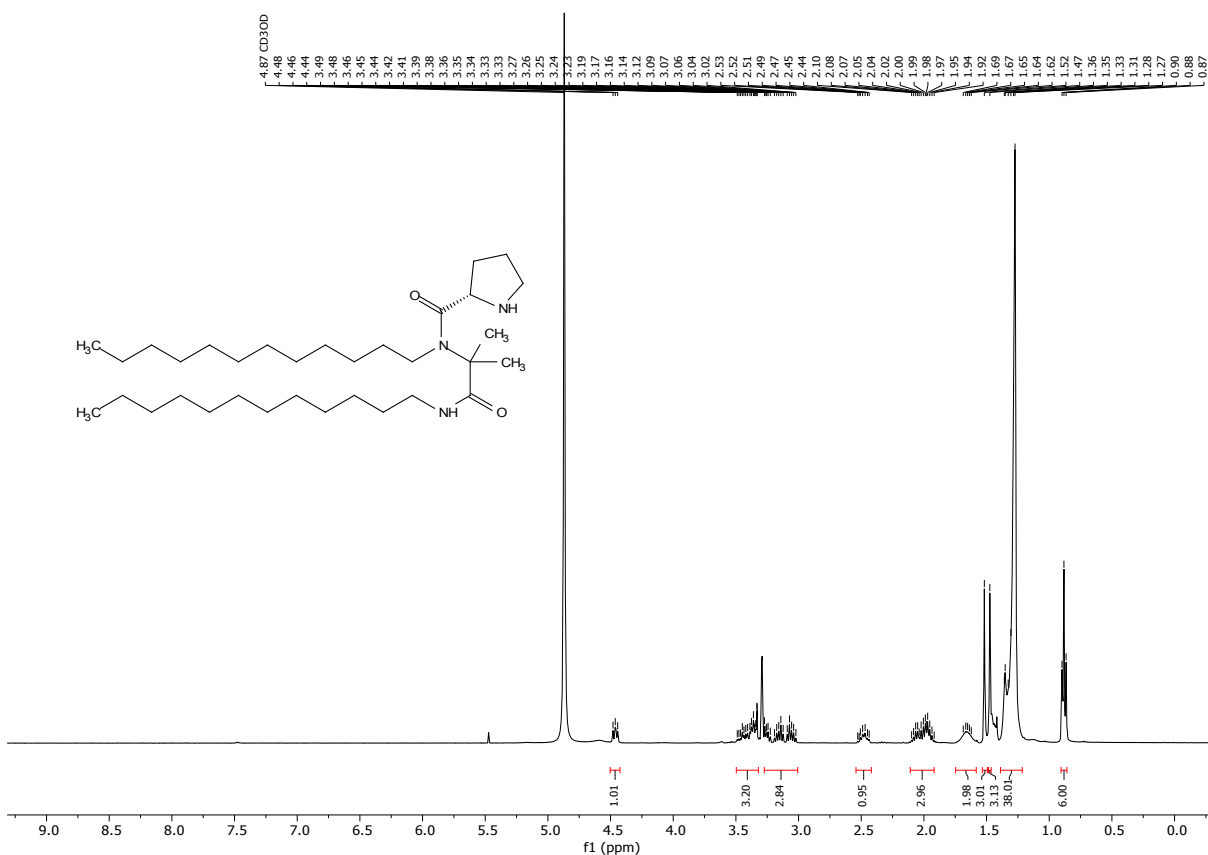
FIGURE 27. ^{1}H NMR of compound **3j** (400 MHz, CD$_3$OD).
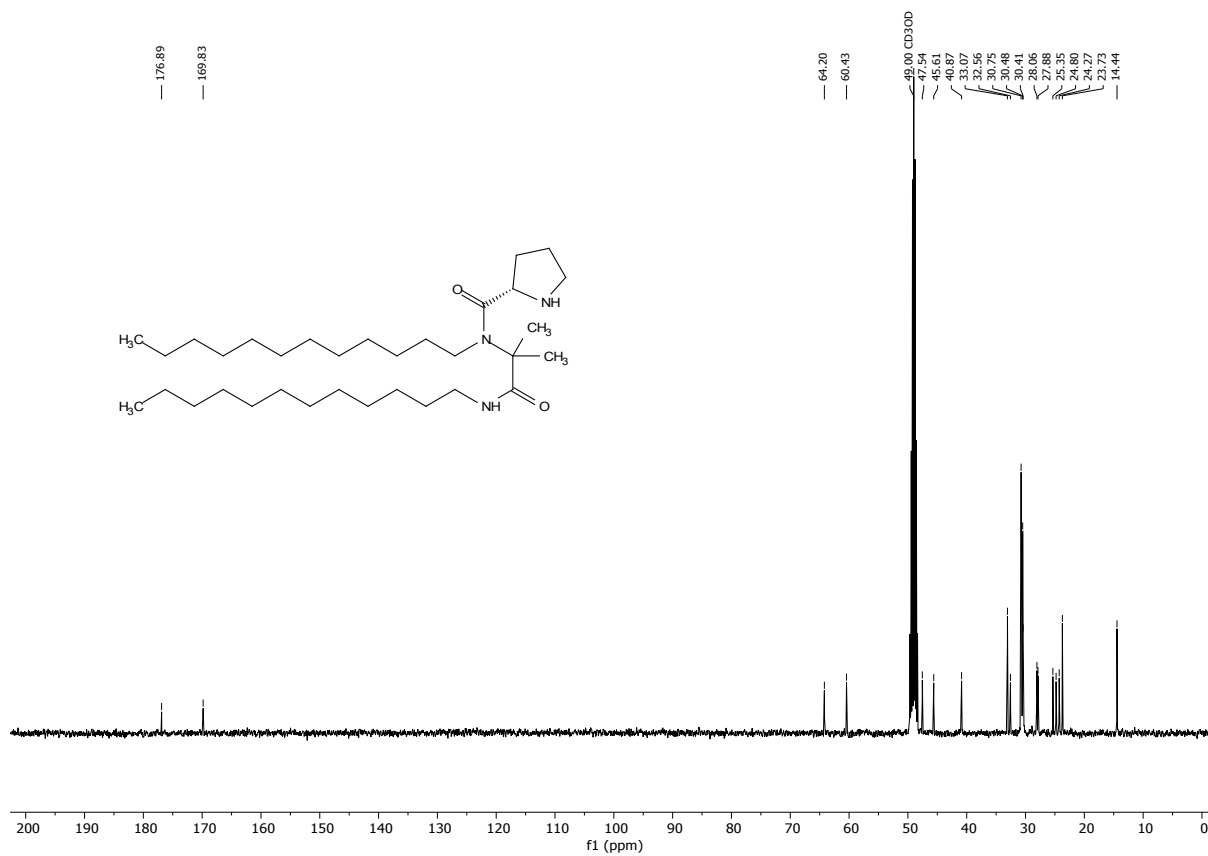
FIGURE 28. ^{13}C NMR of compound **3j** (100 MHz, CD$_3$OD).
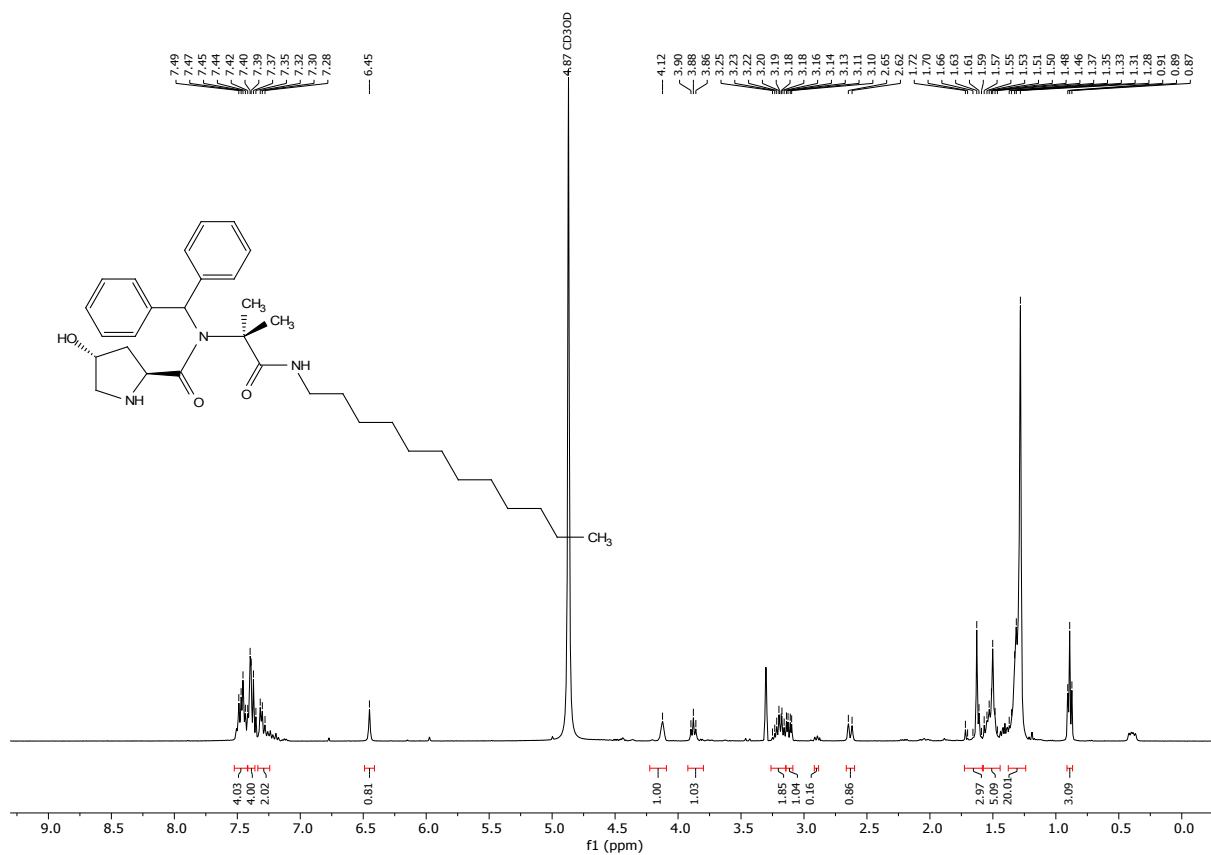
FIGURE 29. ^1H NMR of compound **3k** (400 MHz, CD$_3$OD).
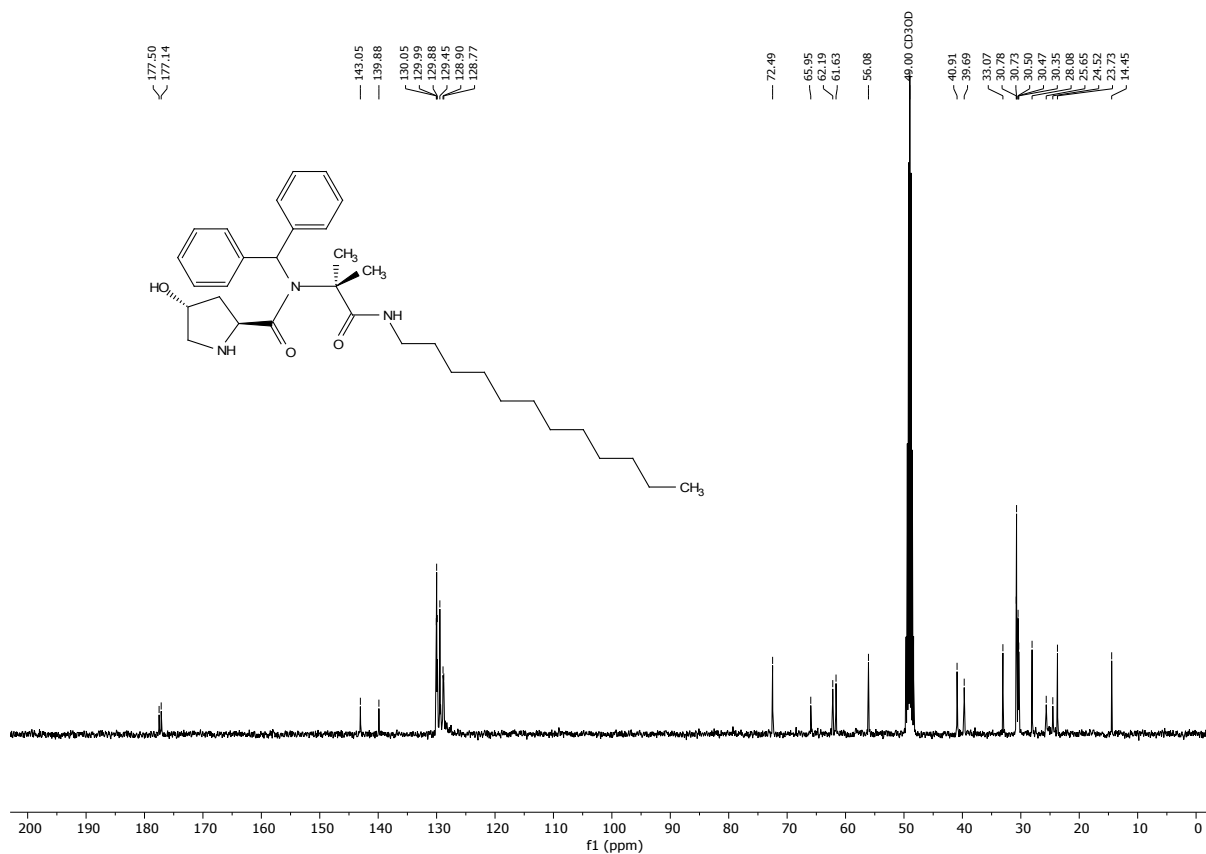
FIGURE 30. ^{13}C NMR of compound **3k** (100 MHz, CD$_3$OD).

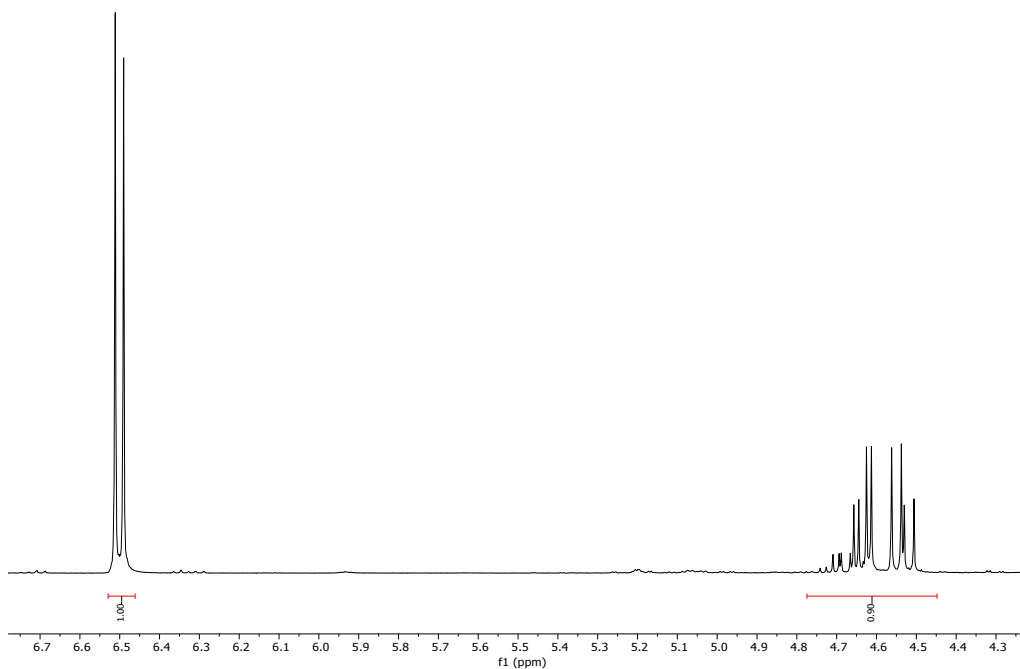## 15. NMR Spectra and Chromatograms: Catalyst Screening
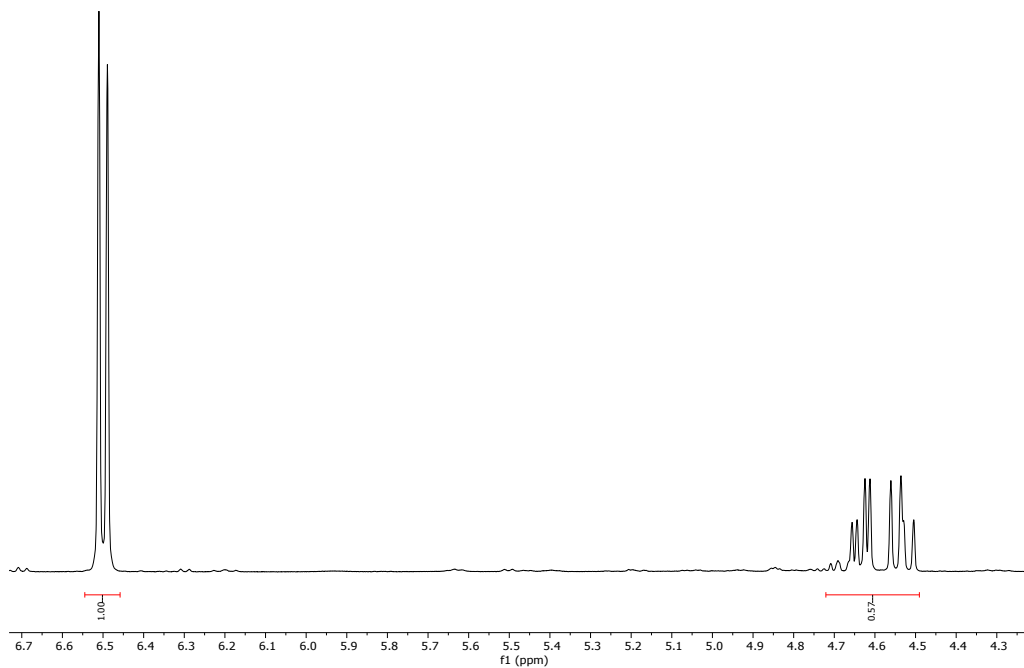
FIGURE 31. ^{1}H NMR of crude compound **4a** (400 MHz, CDCl$_3$) obtained by the Michael reaction catalyzed by 10 mol% of compound **3a** with 1, 2, 3-trimethoxybenzene as standard. Yield: 57%. TABLE 2, Entry 1.
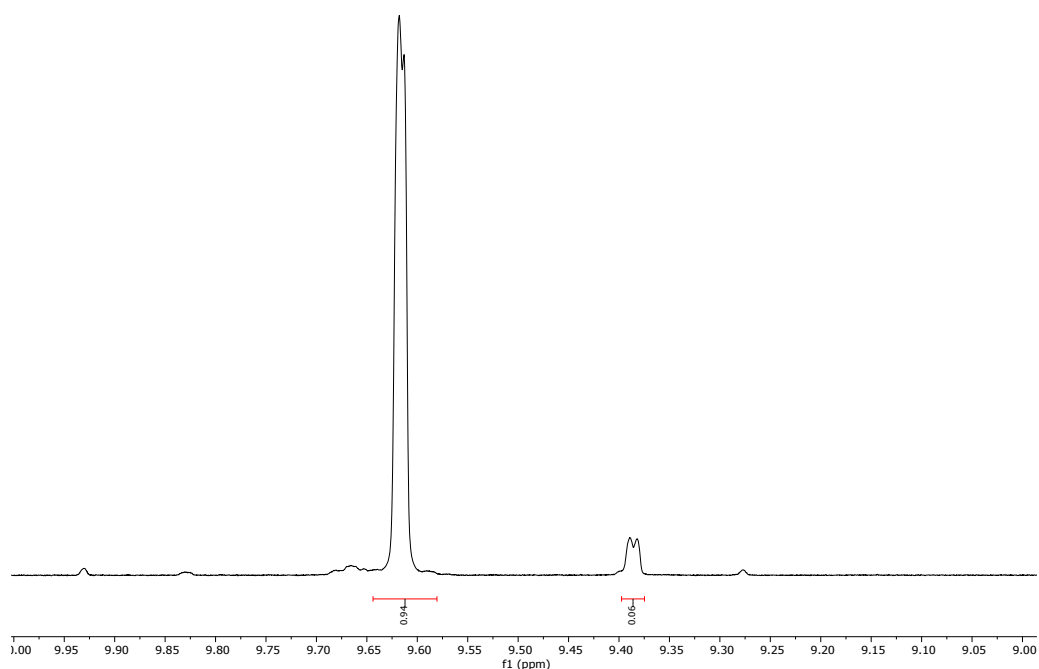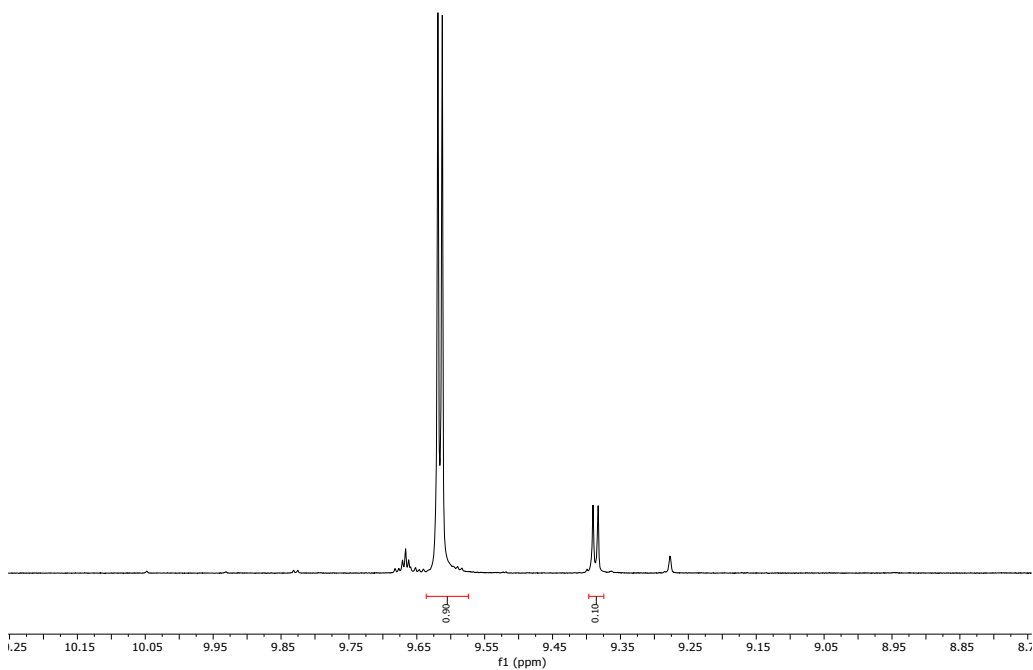
FIGURE 32. ^{1}H NMR of crude compound **4a** (400 MHz, CDCl$_3$) obtained by the Michael reaction catalyzed by 10 mol% of compound **3a**. Diastereoisomeric ratio (*syn/anti*): 94:06. TABLE 2, Entry 1.
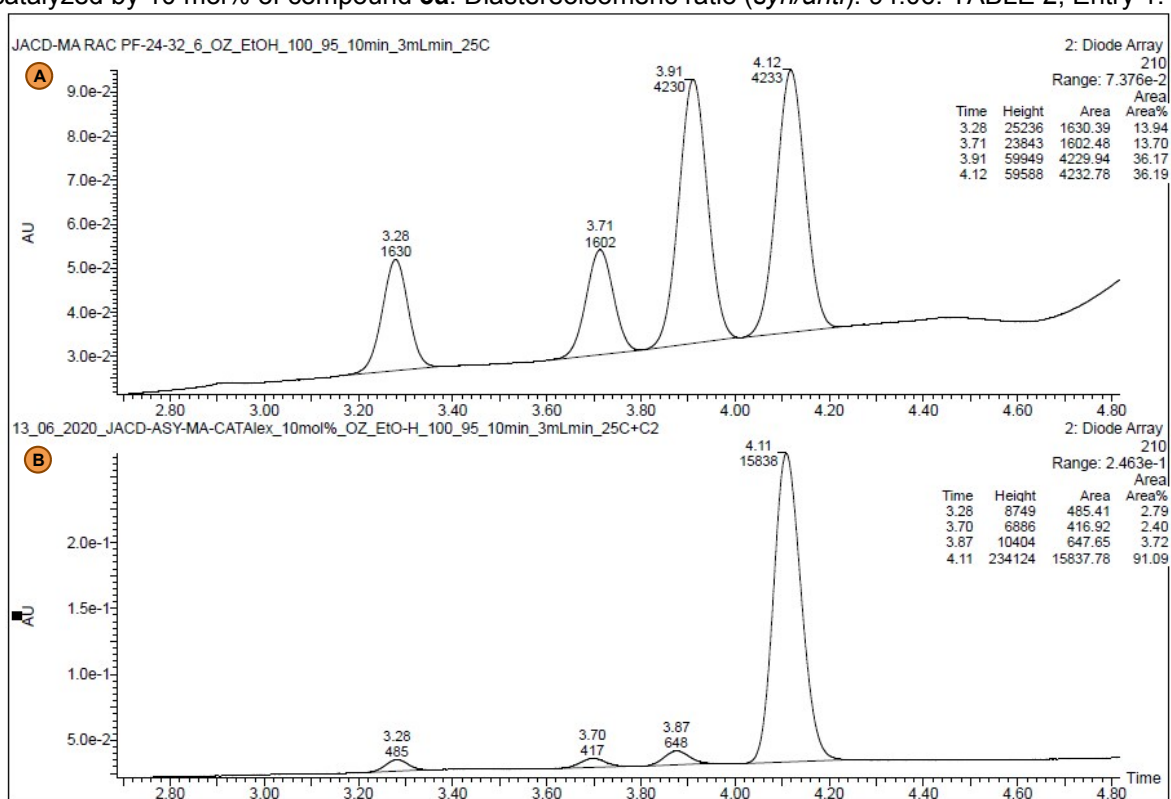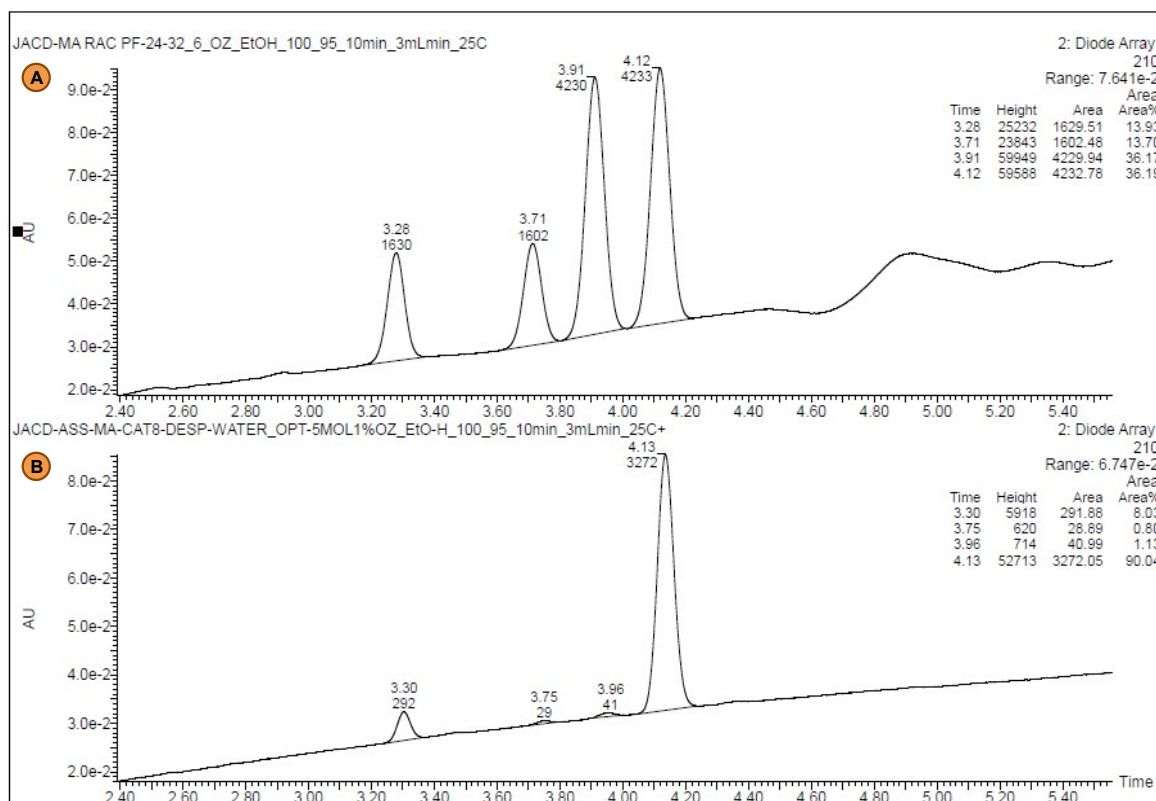

FIGURE 33. (a) Chiral UPC[2] of racemic 2-ethyl-4-nitro-3-phenylbutanal (**4a**); (b) Chiral UPC[2] of 2-ethyl-4-nitro-3-phenylbutanal (**4a**) obtained by the Michael reaction catalyzed by 10 mol% of compound **3a**. Trefoil CEL2, Grad: CO$_2$/EtOH 100-0% to 95-5 % in 10 min at 3 ml/min at 25°C. UV detection at 210 nm: **R$_t$**: (syn, minor) = 3.87 min, (syn, major) = 4.11 min. TABLE 2, Entry 1
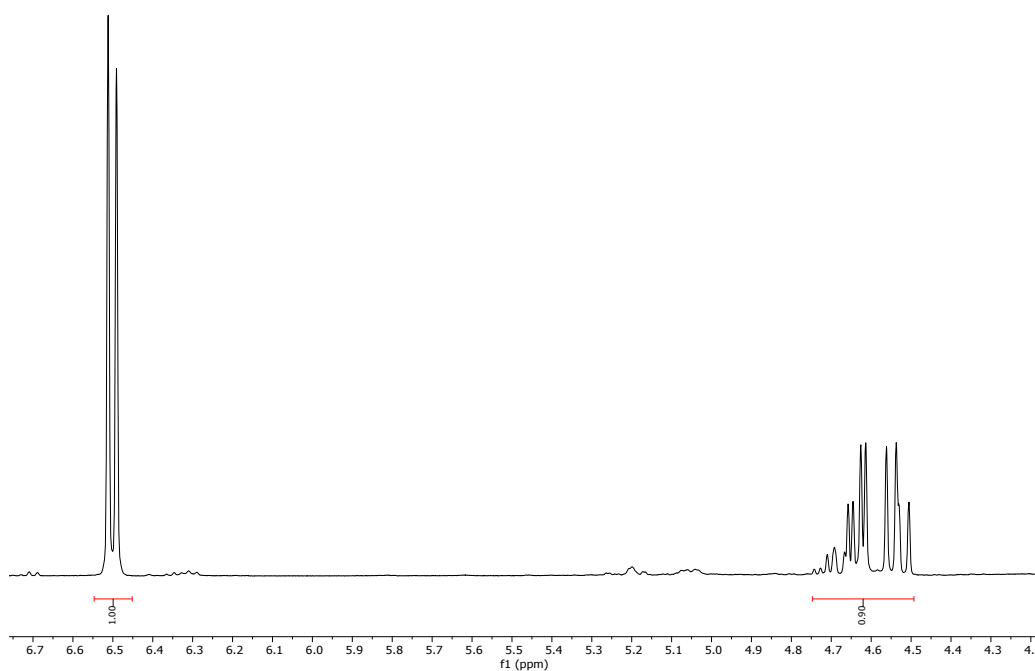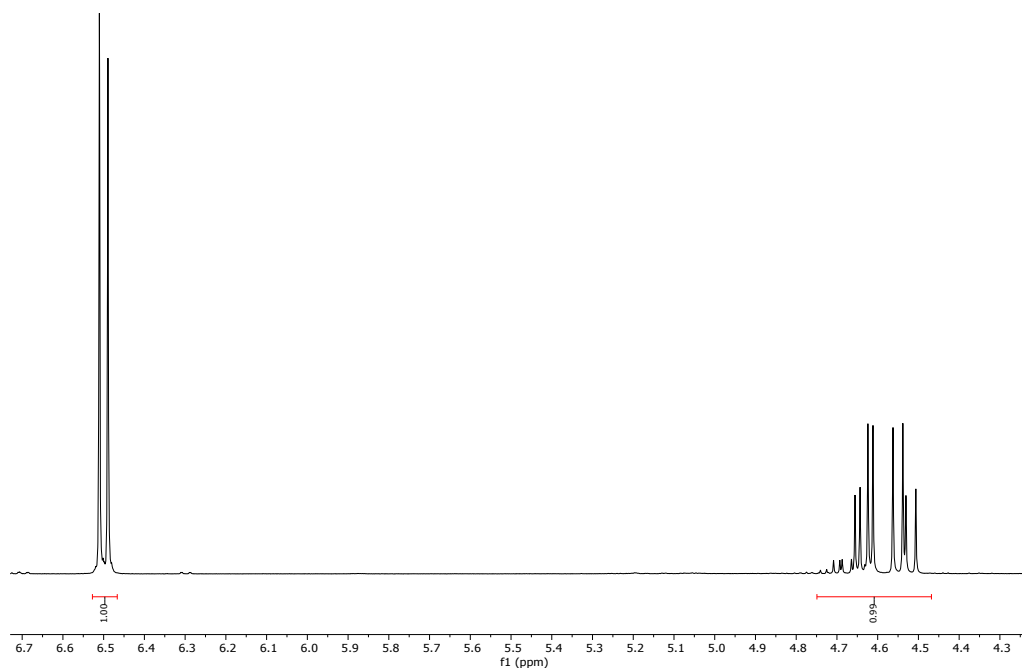
FIGURE 34. ^{1}H NMR of crude compound **4a** (400 MHz, CDCl3) obtained by the Michael reaction catalyzed by 10 mol% of compound **3b** with 1, 2, 3-trimethoxybenzene as standard. Yield: 90%. TABLE 2, Entry 2.
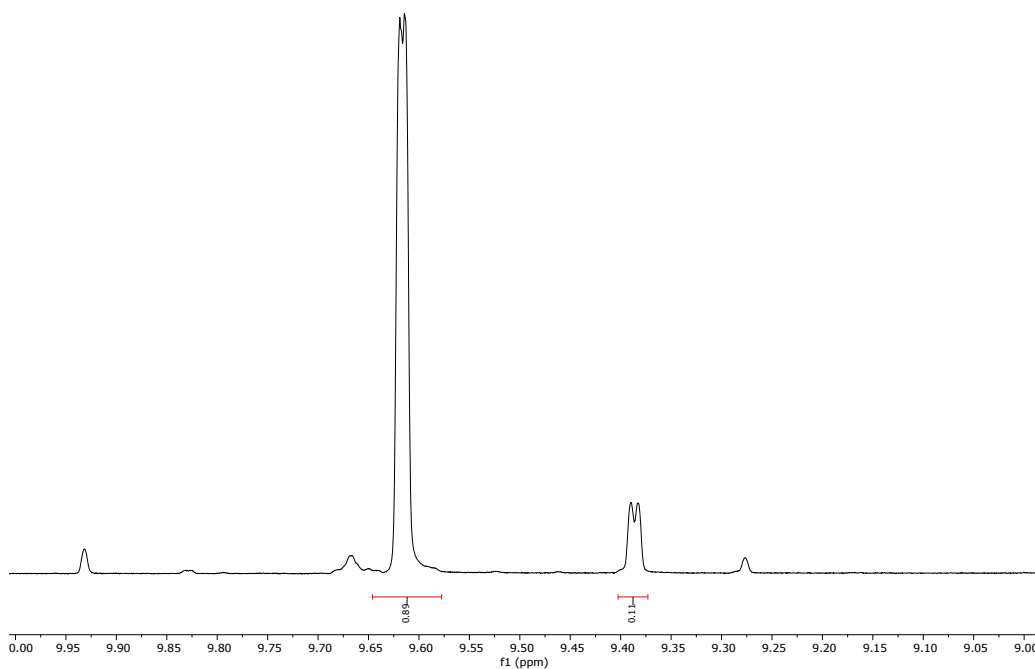
FIGURE 35. ^{1}H NMR of crude compound **4a** (400 MHz, CDCl$_3$) obtained by the Michael reaction catalyzed by 10 mol% of compound **3b**. Diastereoisomeric ratio (*syn/anti*): 89:11. TABLE 2, Entry 2.
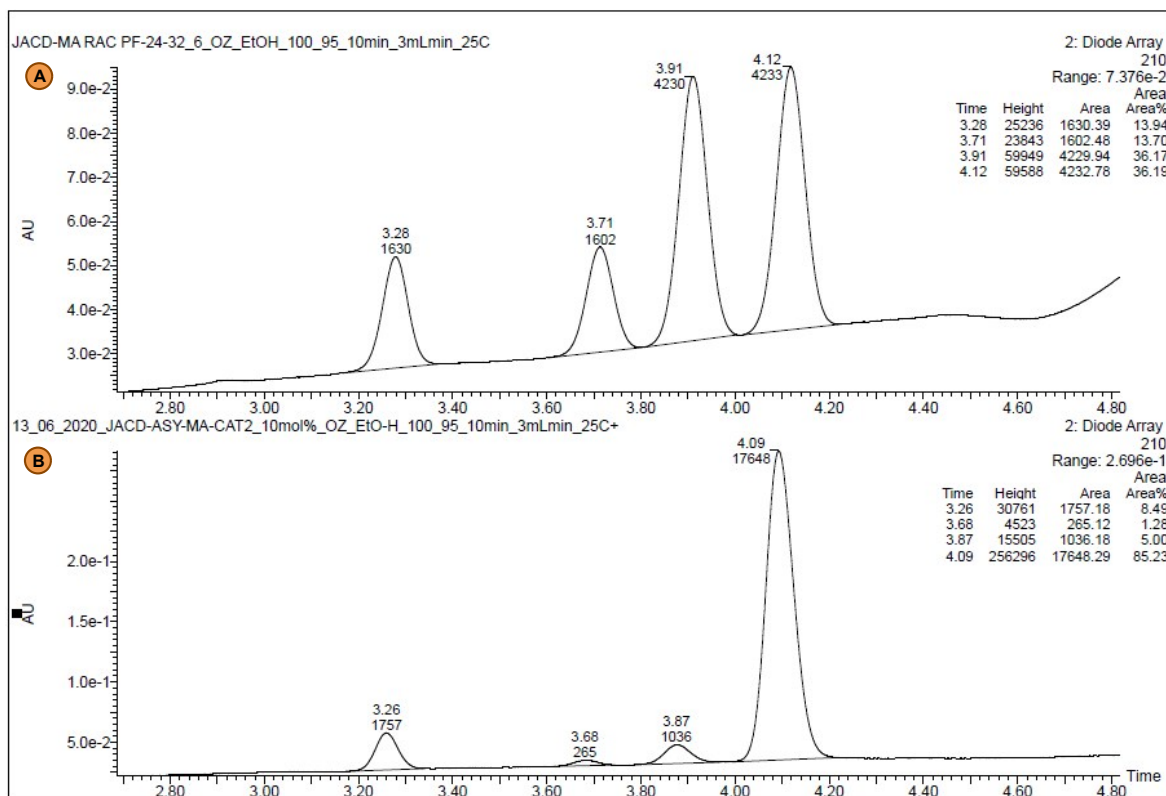
FIGURE 36. (a) Chiral UPC^2 of racemic 2-ethyl-4-nitro-3-phenylbutanal (**4a**); (b) Chiral UPC^2 of 2-ethyl-4-nitro-3-phenylbutanal (**4a**) obtained by the Michael reaction catalyzed by 10 mol% of compound **3b**. Trefoil CEL2, Grad: CO$_2$/EtOH 100-0% to 95-5 % in 10 min at 3 ml/min at 25°C. UV detection at 210 nm: **R$_t$**: (syn, minor) = 3.87 min, (syn, major) = 4.09 min. TABLE 2, Entry 2.
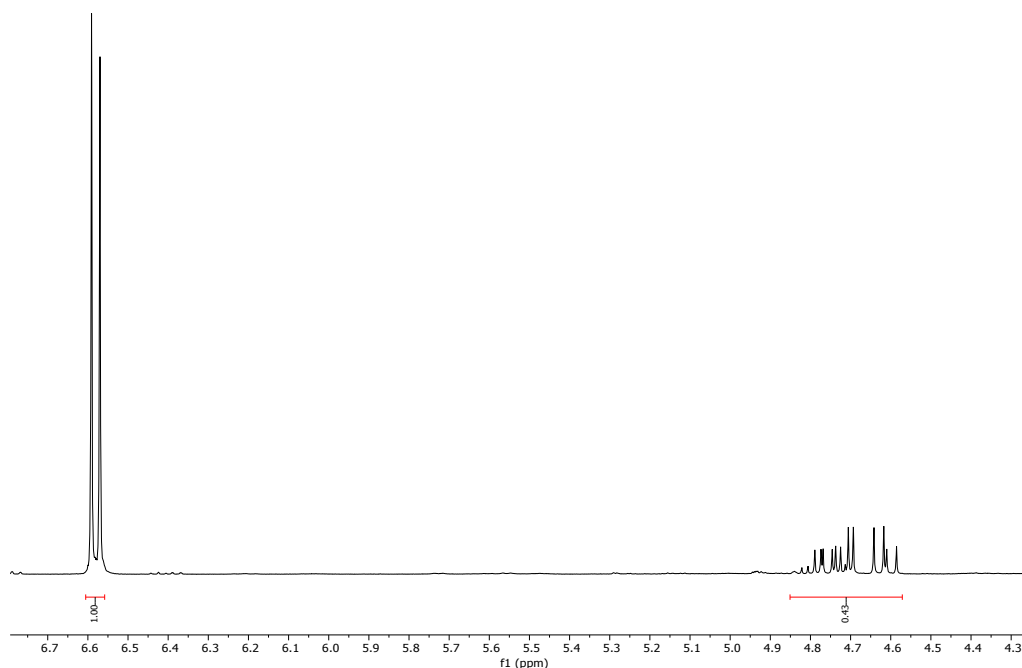
FIGURE 37. ^{1}H NMR of crude compound **4a** (400 MHz, CDCl$_3$) obtained by the Michael reaction catalyzed by 10 mol% of compound **3c** with 1, 2, 3-trimethoxybenzene as standard. Yield: 43%. TABLE 2, Entry 3.
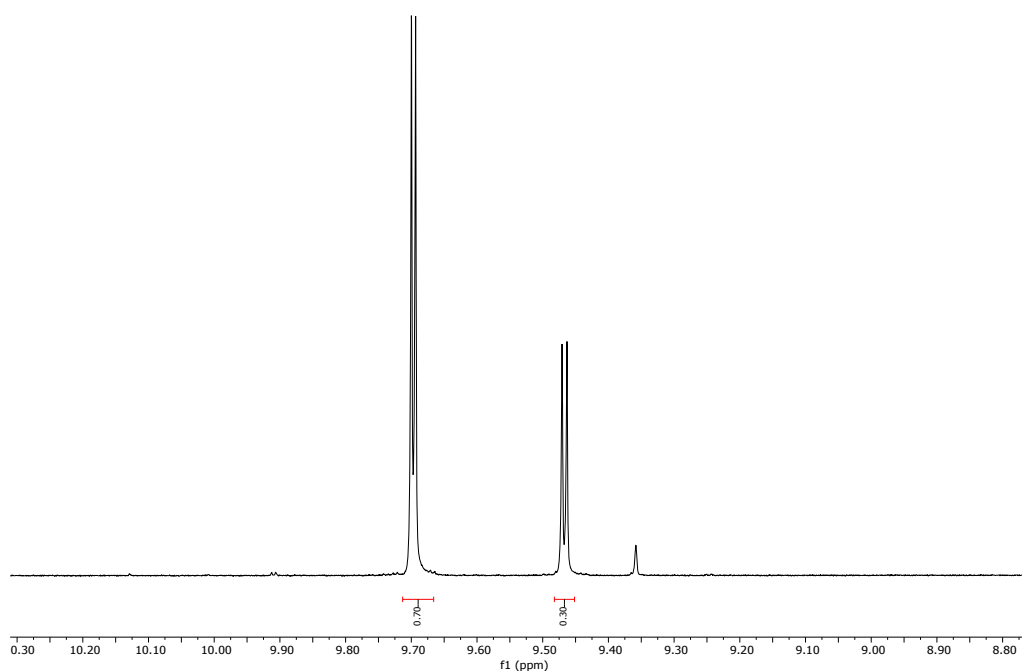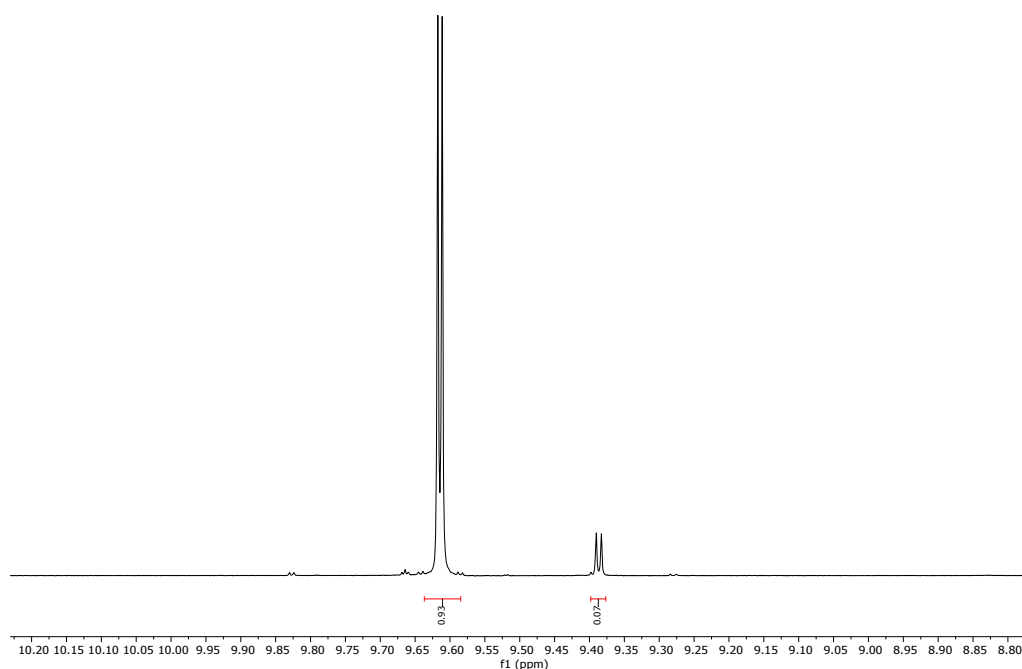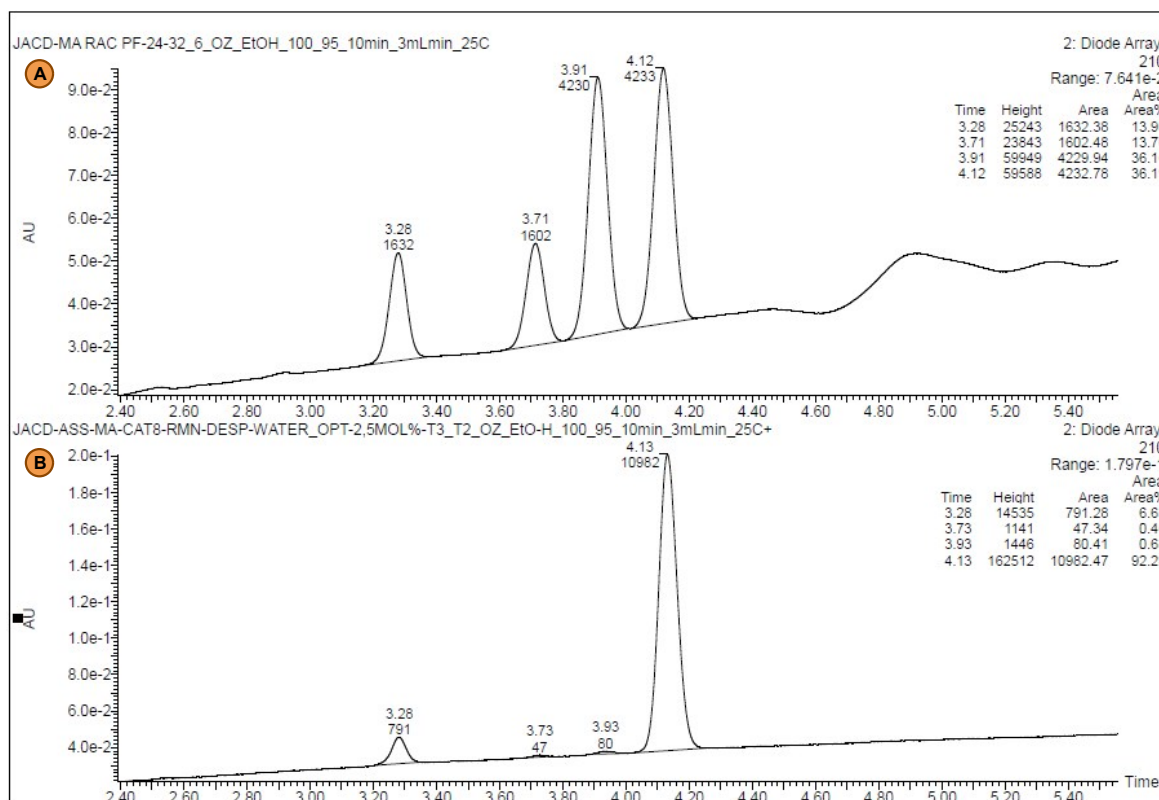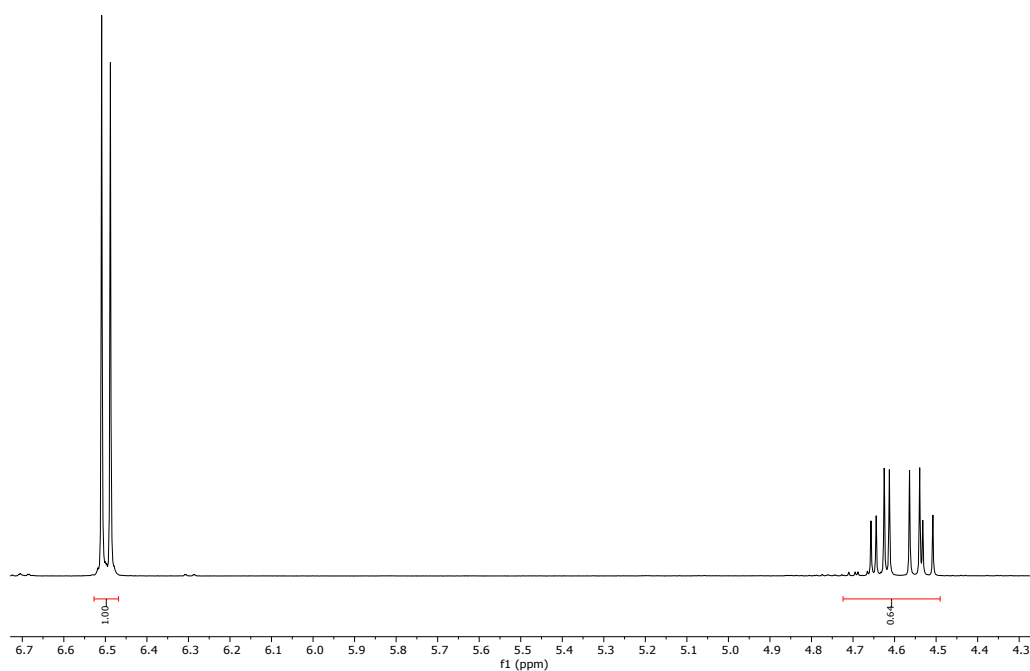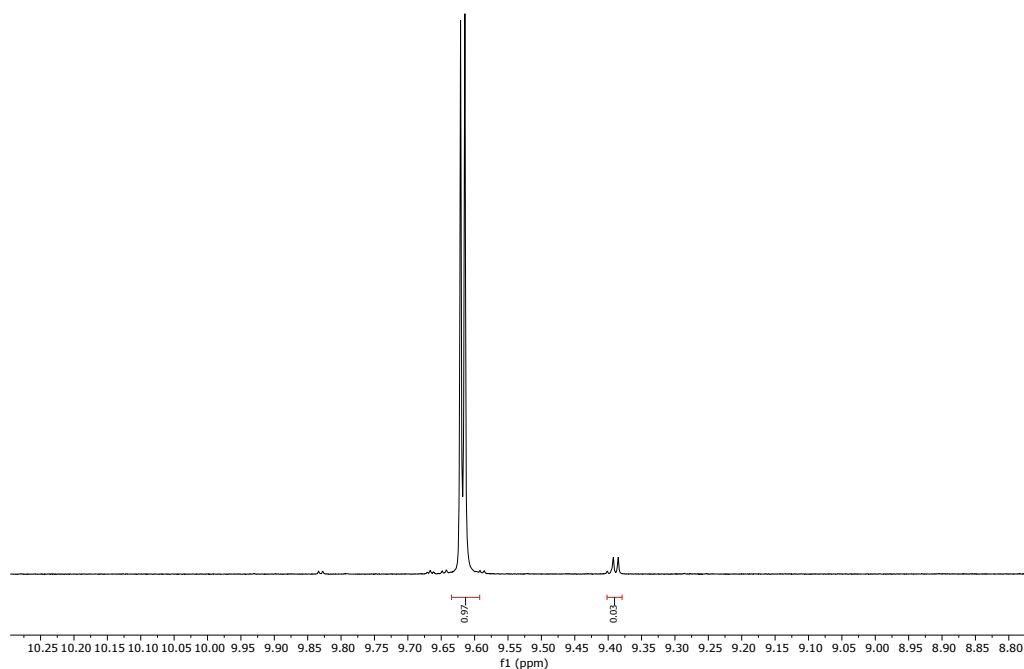
FIGURE 38. ^{1}H NMR of crude compound **4a** (400 MHz, CDCl$_3$) obtained by the Michael reaction catalyzed by 10 mol% of compound **3c**. Diastereoisomeric ratio (*syn/anti*): 70:30. TABLE 2, Entry 3.
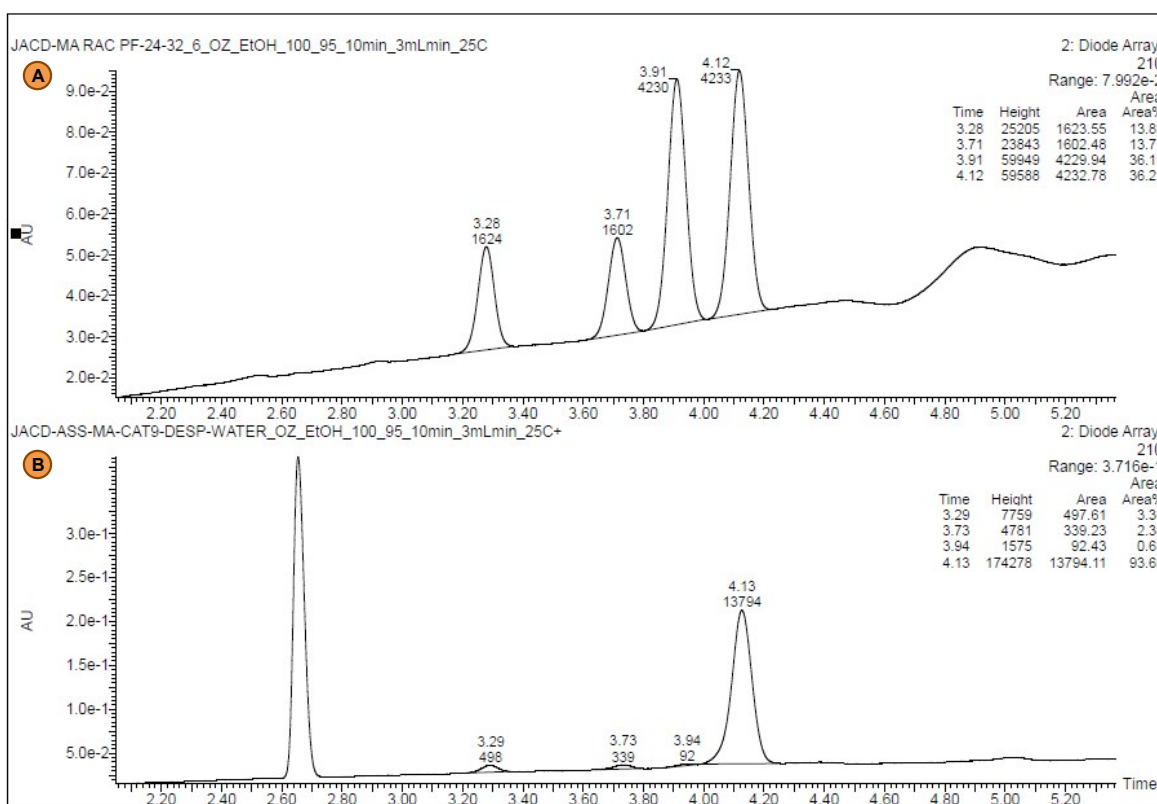
FIGURE 39. (a) Chiral UPC^2 of racemic 2-ethyl-4-nitro-3-phenylbutanal (**4a**); (b) Chiral UPC^2 of 2-ethyl-4-nitro-3-phenylbutanal (**4a**) obtained by the Michael reaction catalyzed by 10 mol% of compound **3c**. Trefoil CEL2**, Grad:** CO$_2$/EtOH 100-0% to 95-5 % in 10 min at 3 ml/min at 25°C. UV detection at 210 nm: **R$_t$:** (syn, minor) = 3.94 min, (syn, major) = 4.13 min. TABLE 2, Entry 3.
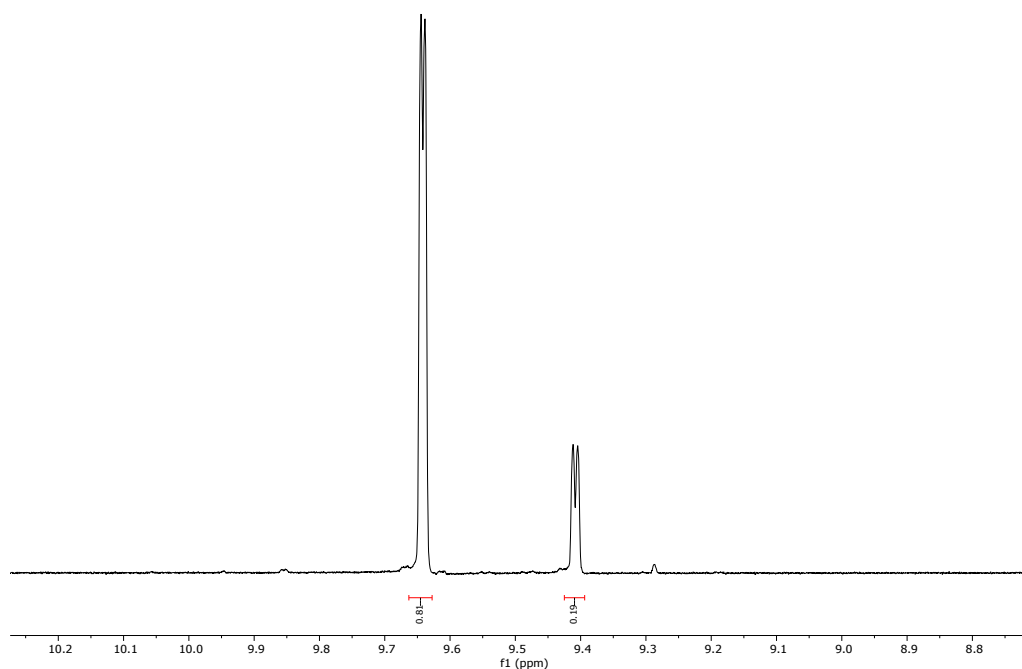
FIGURE 40. ^{1}H NMR of crude compound **4a** (400 MHz, CDCl$_3$) obtained by the Michael reaction catalyzed by 10 mol% of compound **3d**. Diastereoisomeric ratio (*syn/anti*): 81:19. TABLE 2, Entry 4.
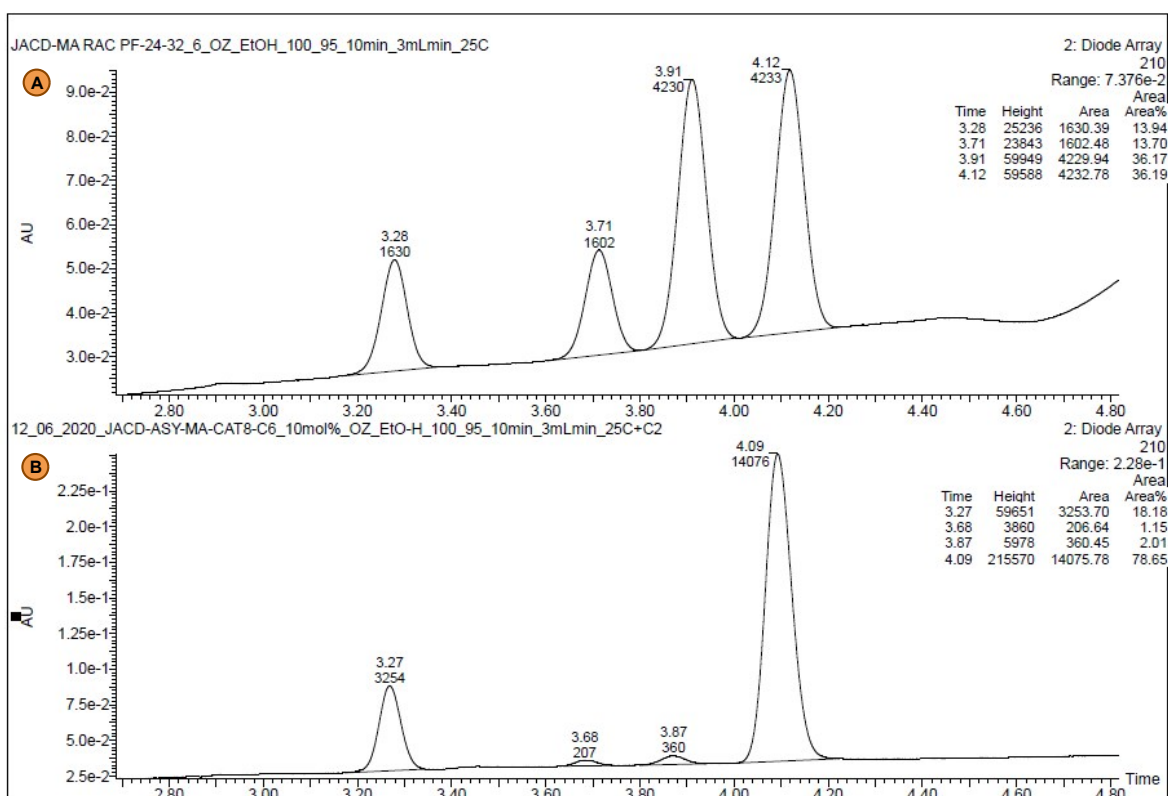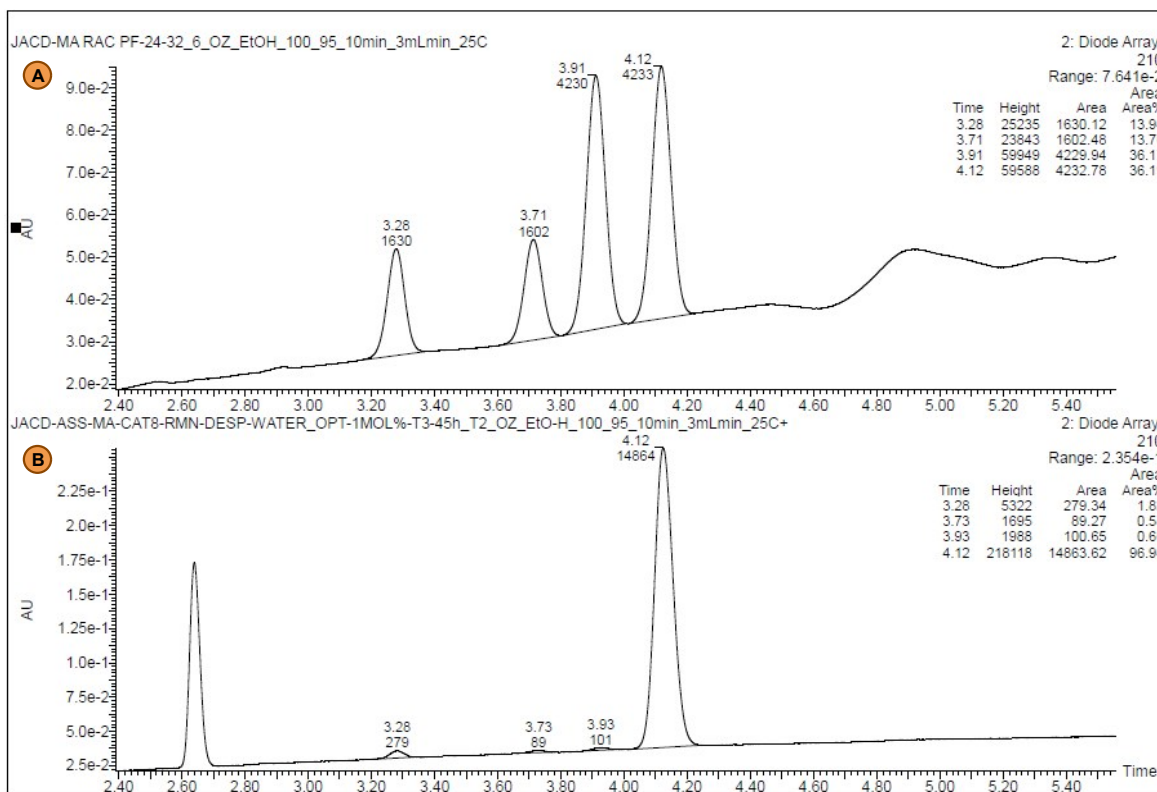

FIGURE 41. (a) Chiral UPC^2 of racemic 2-ethyl-4-nitro-3-phenylbutanal (**4a**); (b) Chiral UPC^2 of 2-ethyl-4-nitro-3-phenylbutanal (**4a**) obtained by the Michael reaction catalyzed by 10 mol% of compound **3d**. Trefoil CEL2, **Grad:** CO$_2$/EtOH 100-0% to 95-5 % in 10 min at 3 ml/min at 25°C. UV detection at 210 nm: **R$_t$**: (syn, minor) = 4.84min, (syn, major) = 5.18 min. TABLE 2, Entry 4.
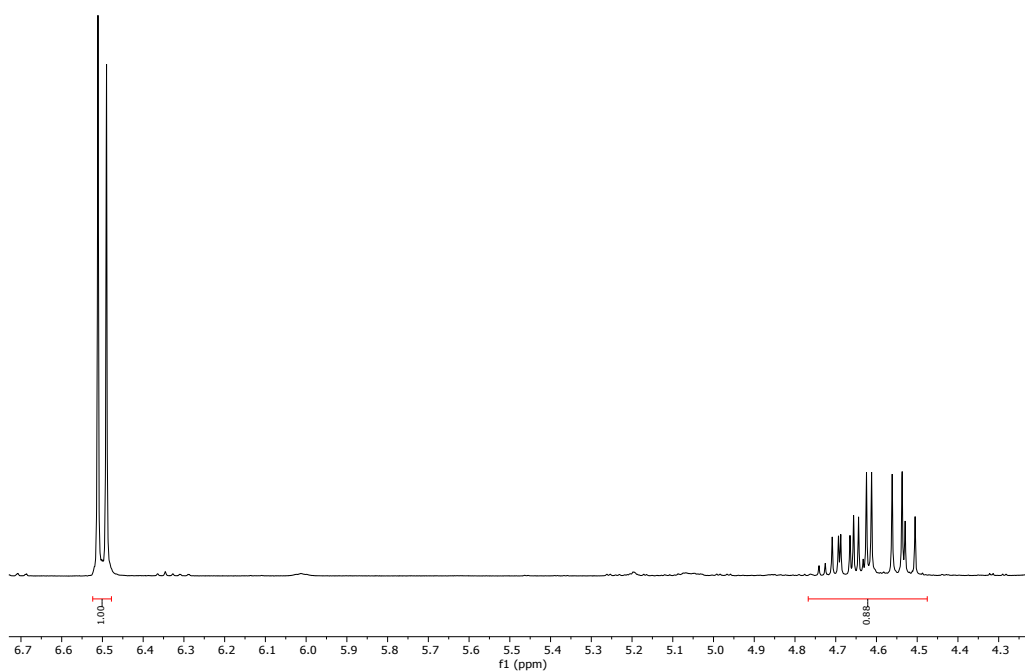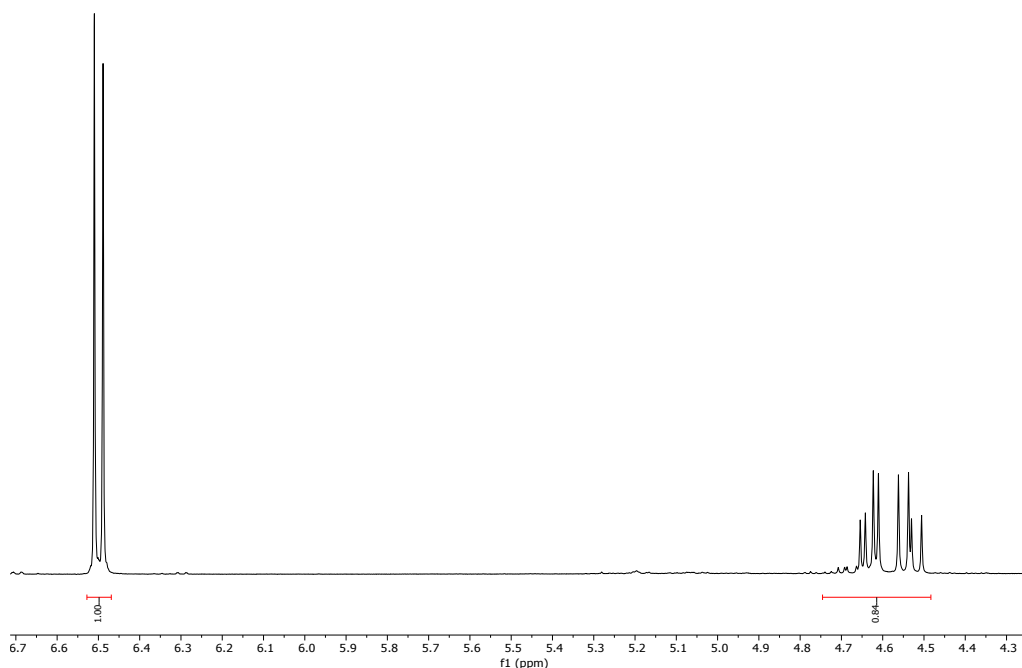
FIGURE 42. ^{1}H NMR of crude compound **4a** (400 MHz, CDCl$_3$) obtained by the Michael reaction catalyzed by 10 mol% of compound **3e** with 1, 2, 3-trimethoxybenzene as standard. Yield: 88%. TABLE 2, Entry 5.
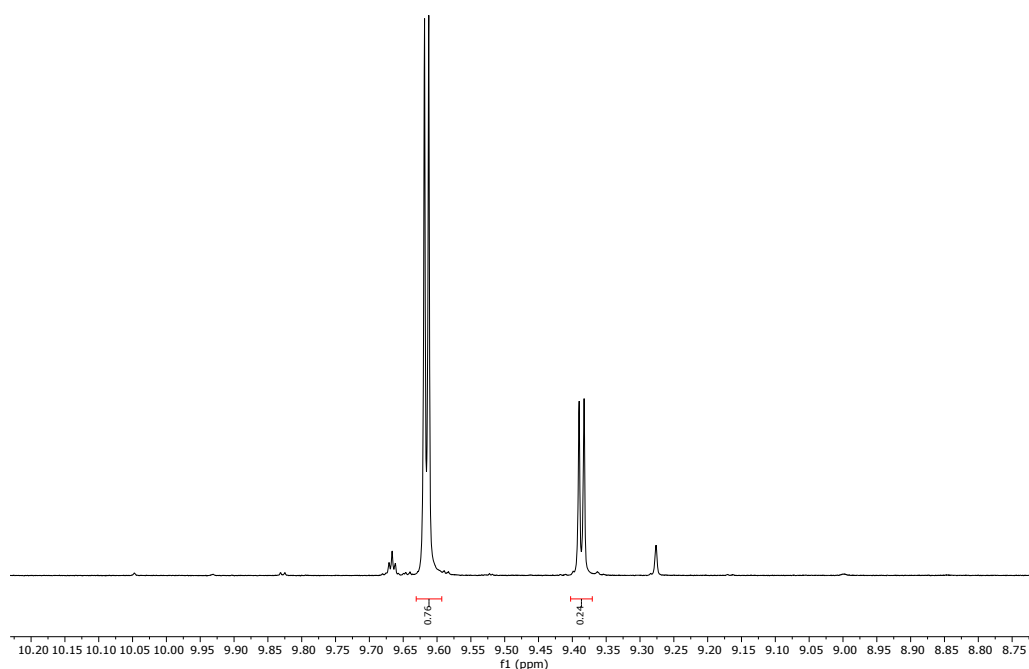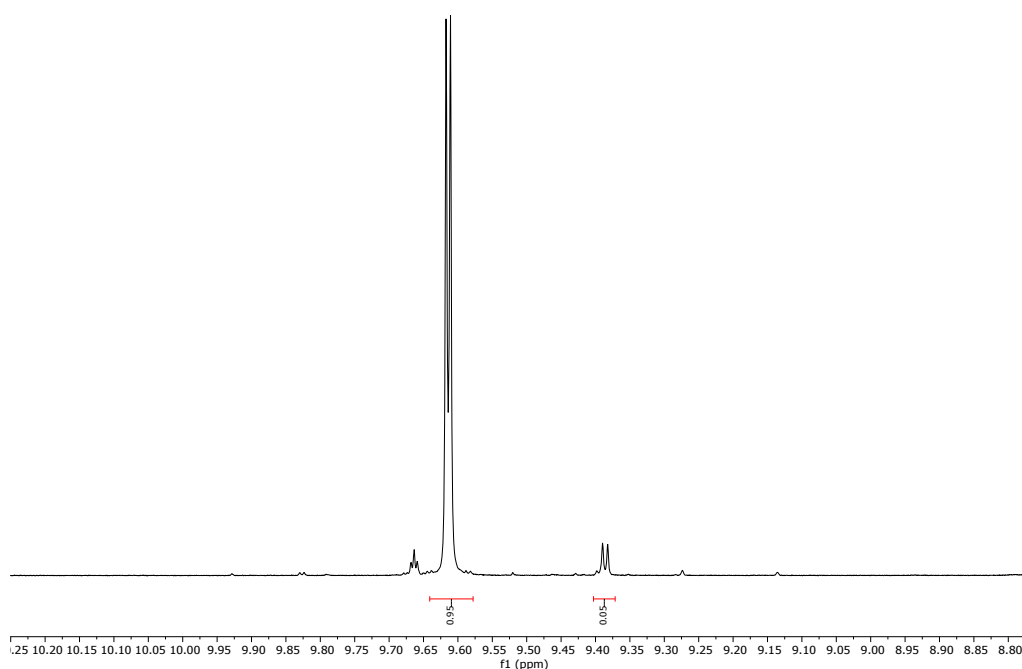
FIGURE 43. ^{1}H NMR of crude compound **4a** (400 MHz, CDCl$_3$) obtained by the Michael reaction catalyzed by 10 mol% of compound **3e**. Diastereoisomeric ratio (*syn/anti*): 76:24. TABLE 2, Entry 5.
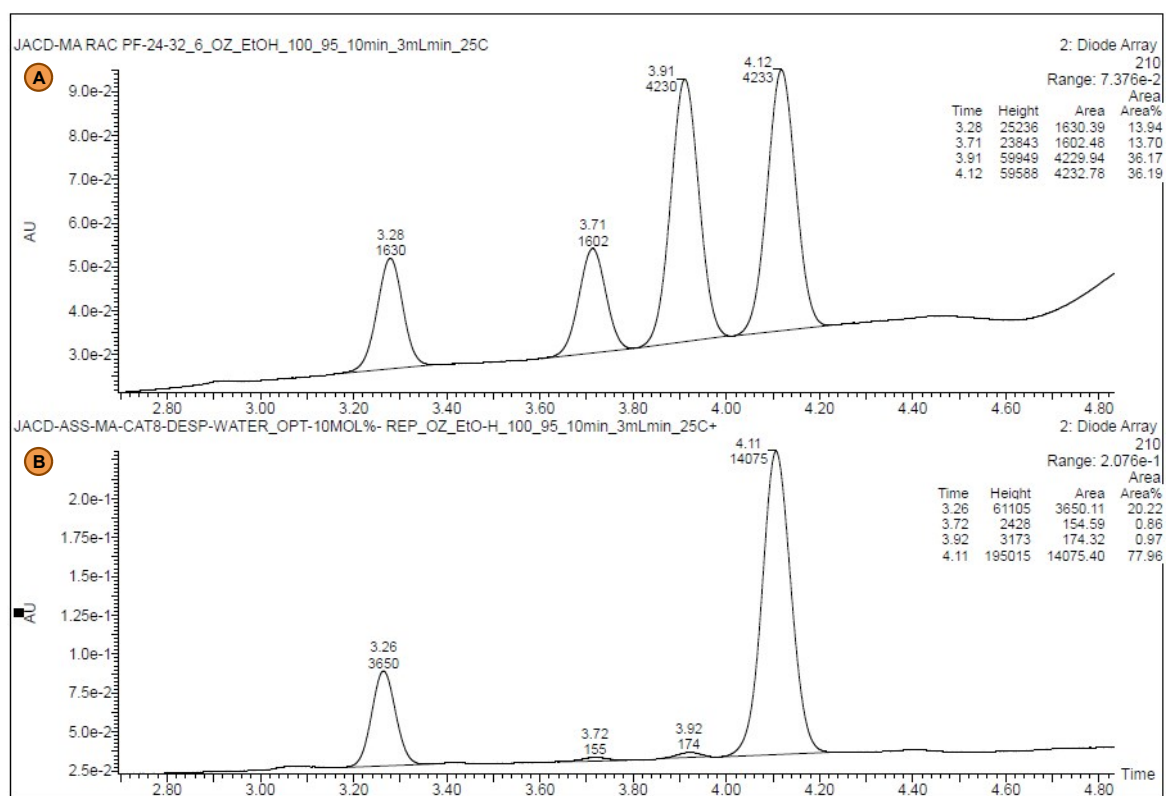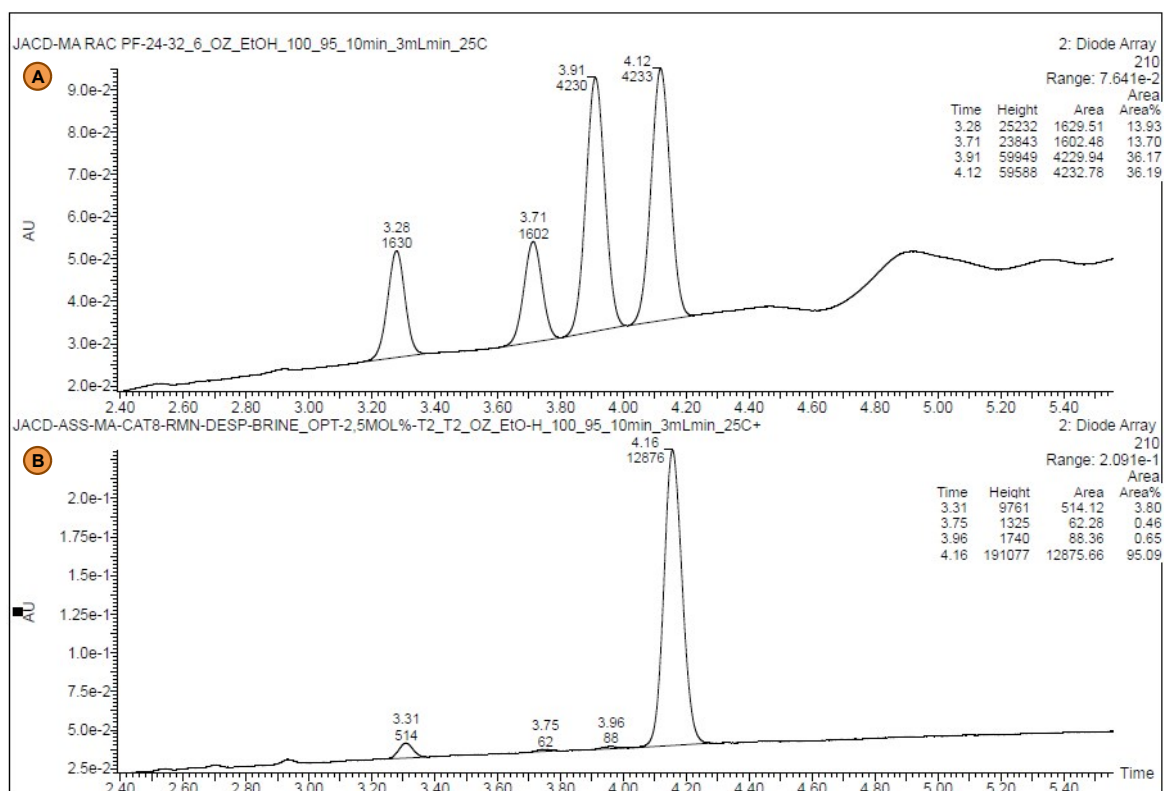

FIGURE 44. (a) Chiral UPC^2 of racemic 2-ethyl-4-nitro-3-phenylbutanal (**4a**); (b) Chiral UPC^2 of 2-ethyl-4-nitro-3-phenylbutanal (**4a**) obtained by the Michael reaction catalyzed by 10 mol% of compound **3e**. Trefoil CEL2, **Grad:** CO$_2$/EtOH 100-0% to 95-5 % in 10 min at 3 ml/min at 25°C. UV detection at 210 nm: **R$_t$**: (syn, minor) = 3.92 min, (syn, major) = 4.11 min. TABLE 2, Entry 5.
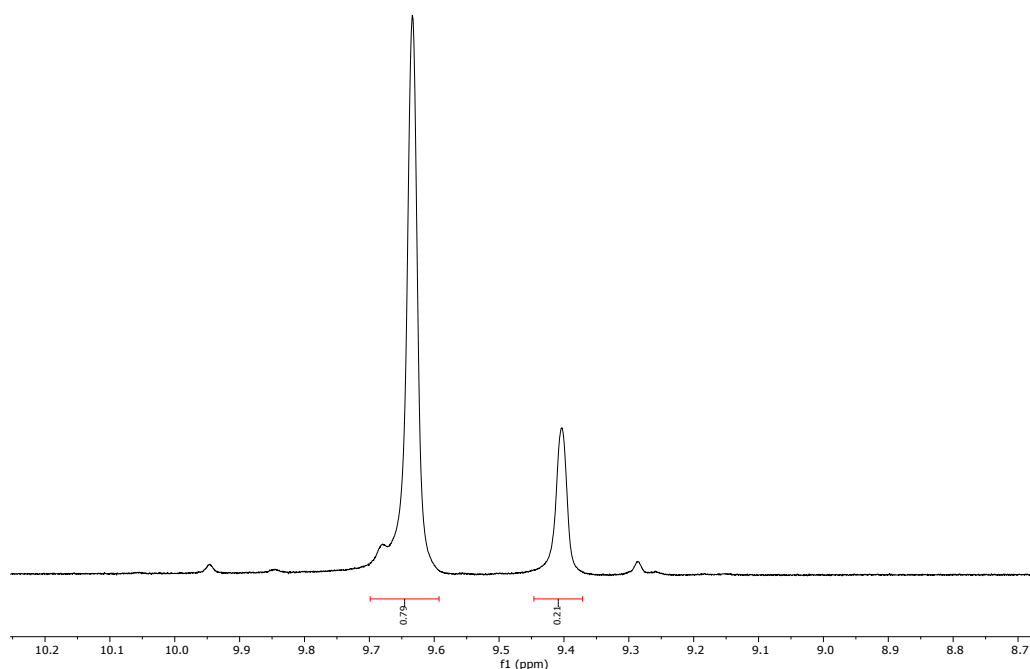
FIGURE 45. ^{1}H NMR of crude compound **4a** (400 MHz, CDCl$_3$) obtained by the Michael reaction catalyzed by 10 mol% of compound **3f**. Diastereoisomeric ratio (*syn/anti*): 79:21. TABLE 2, Entry 6.
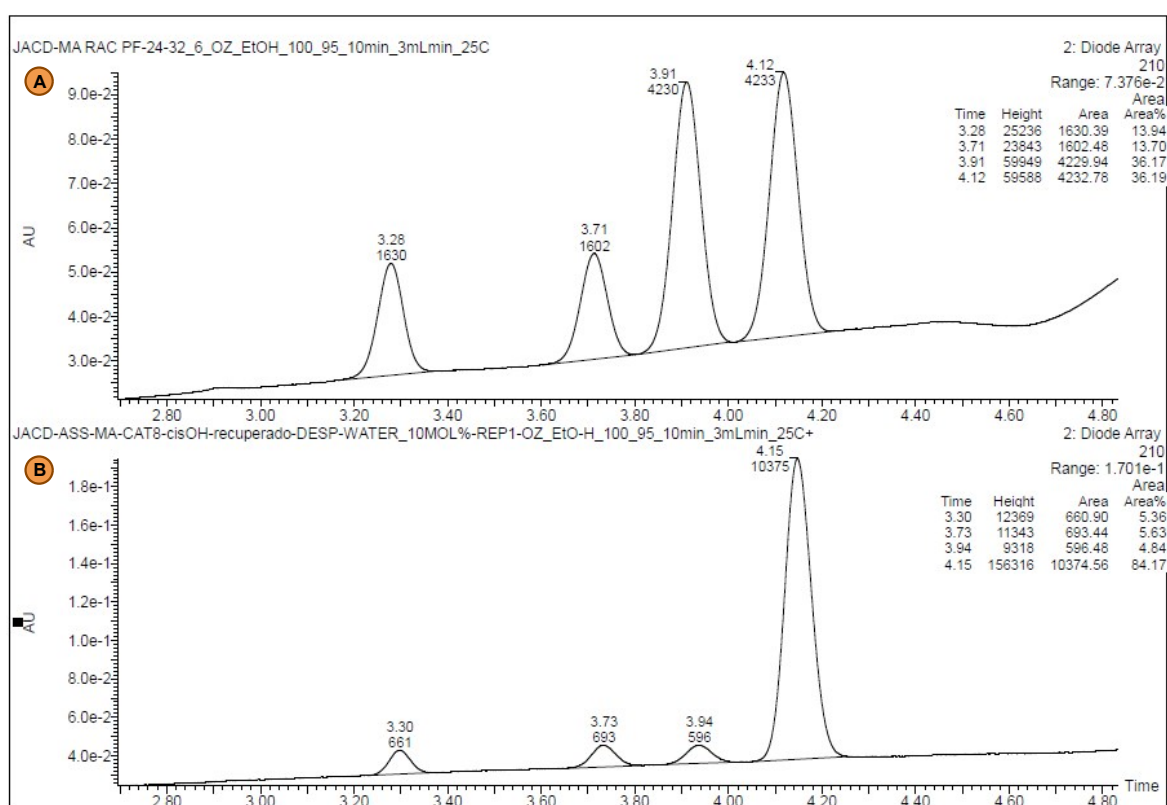
FIGURE 46. (a) Chiral UPC^2 of racemic 2-ethyl-4-nitro-3-phenylbutanal (**4a**); (b) Chiral UPC^2 of 2-ethyl-4-nitro-3-phenylbutanal (**4a**) obtained by the Michael reaction catalyzed by 10 mol% of compound **3f**. Trefoil CEL2, **Grad:** CO$_2$/EtOH 100-0% to 95-5 % in 10 min at 3 ml/min at 25°C. UV detection at 210 nm: **R$_t$**: (syn, minor) = 3.94 min, (syn, major) = 4.15 min. TABLE 2, Entry 6.
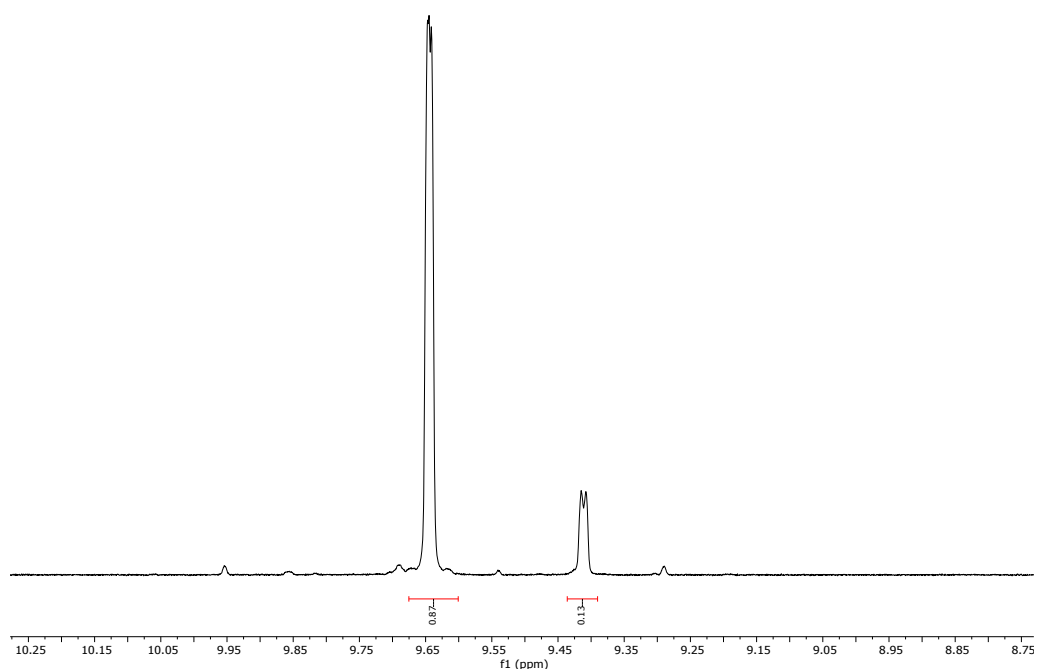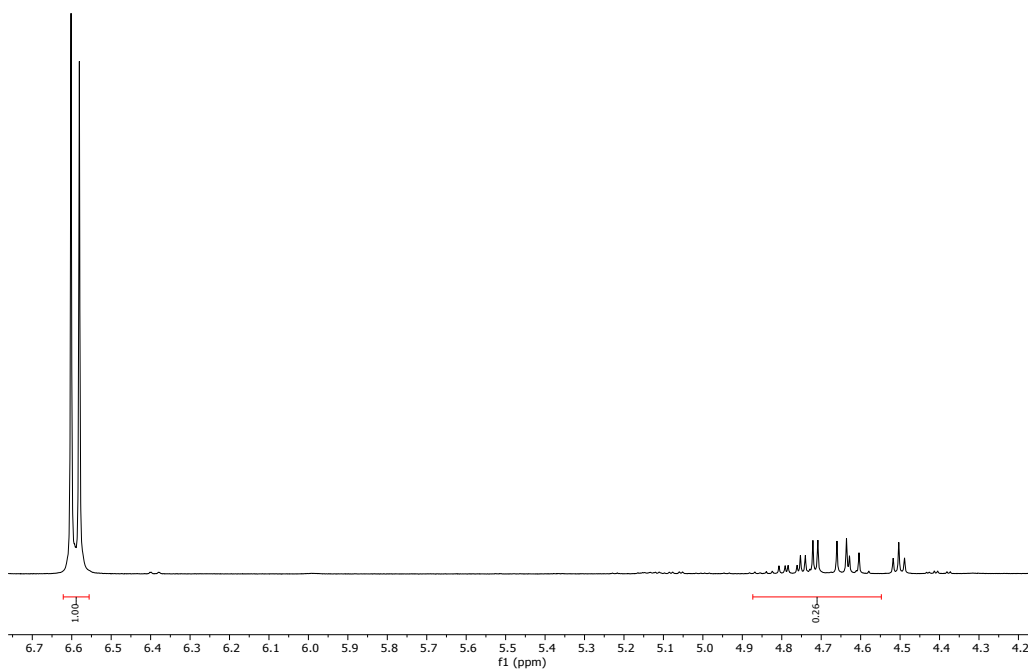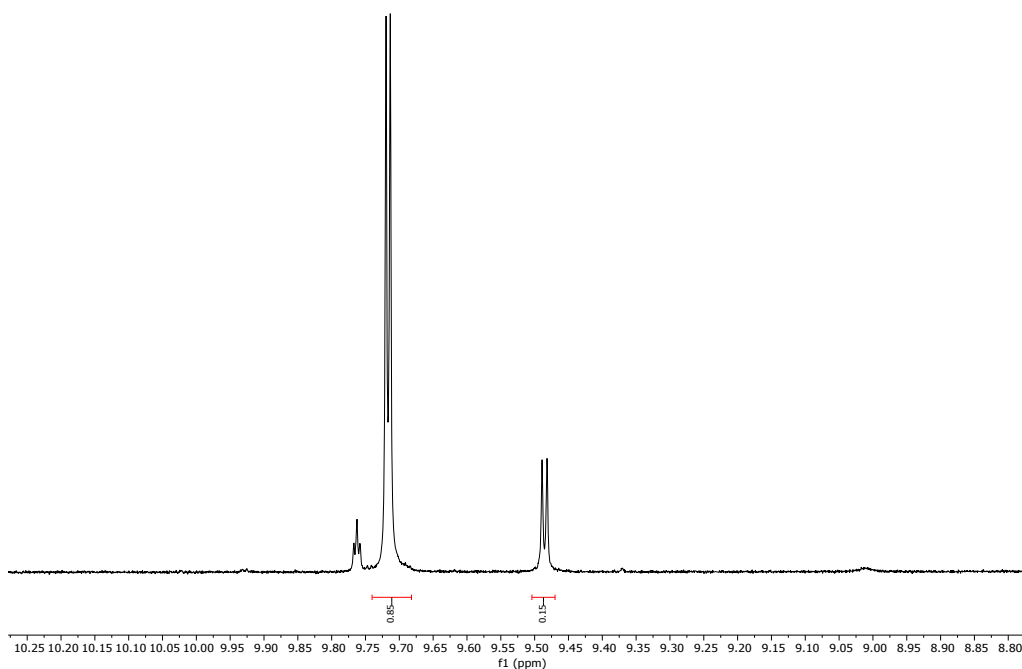
FIGURE 47. ^{1}H NMR of crude compound **4a** (400 MHz, CDCl$_3$) obtained by the Michael reaction catalyzed by 10 mol% of compound **3g**. Diastereoisomeric ratio (*syn/anti*): 87:13. TABLE 2, Entry 7.
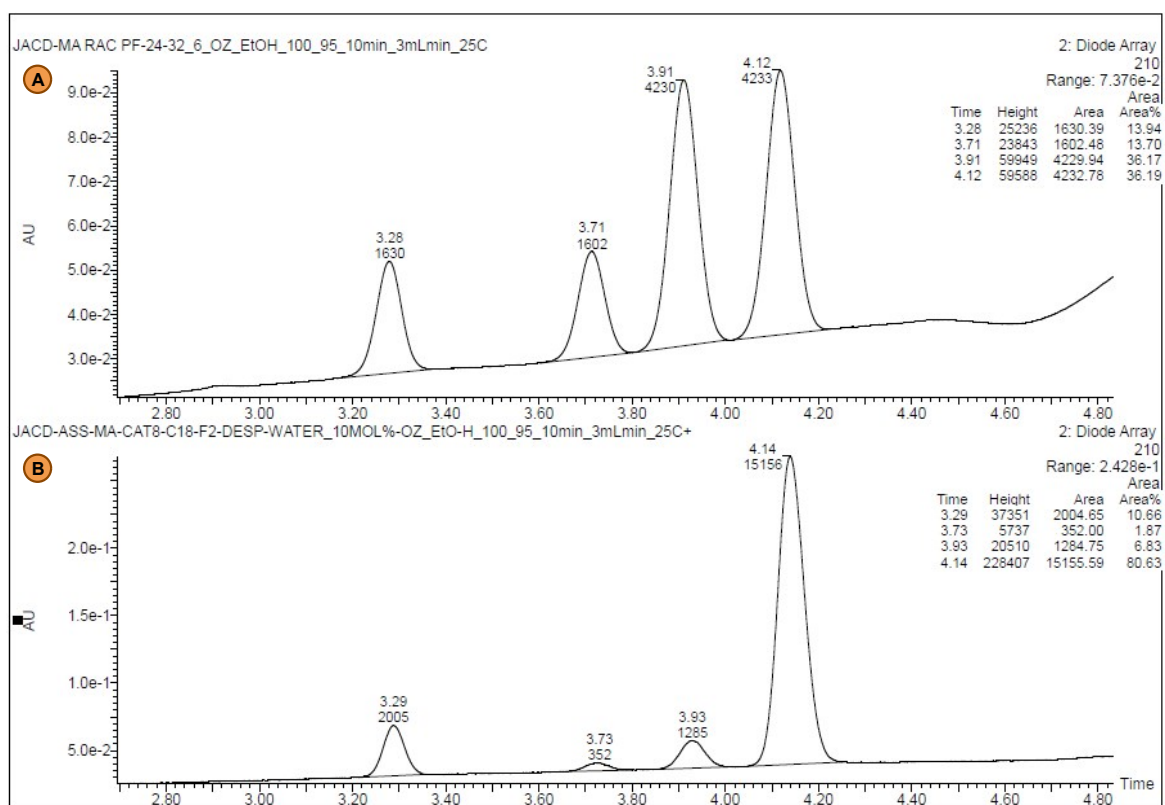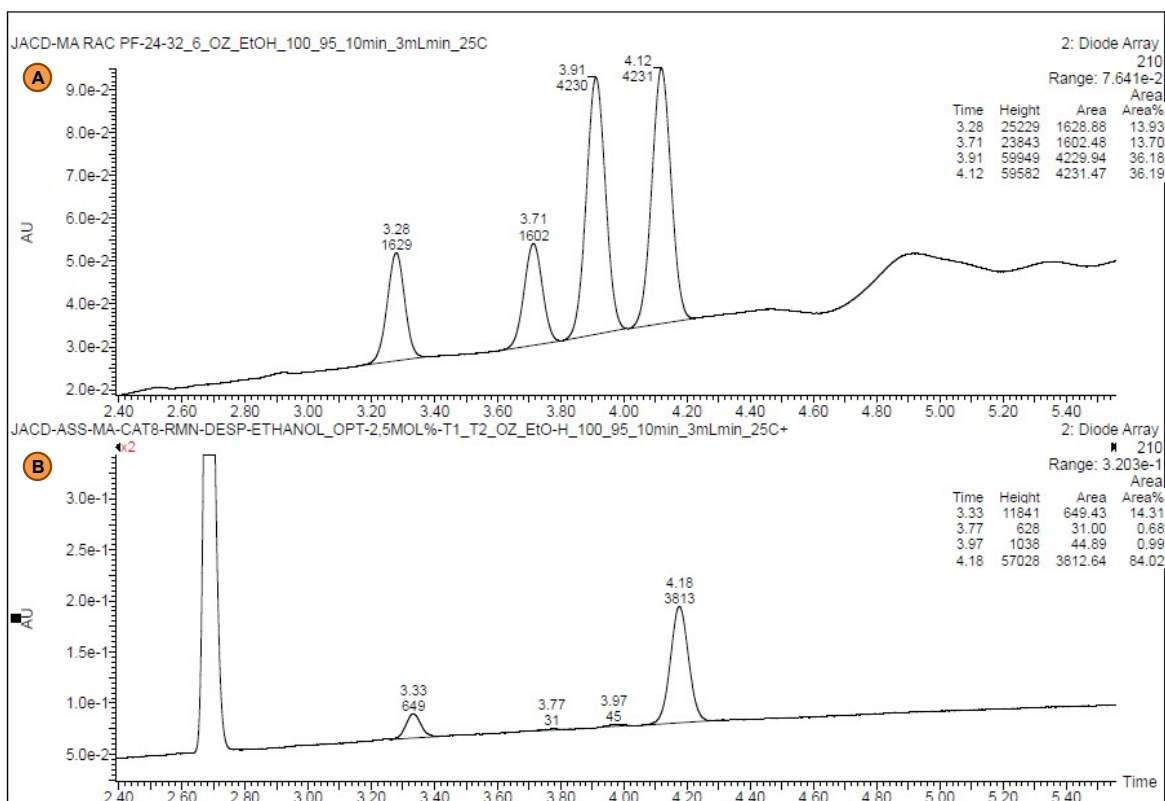

FIGURE 48. (a) Chiral UPC^2 of racemic 2-ethyl-4-nitro-3-phenylbutanal (**4a**); (b) Chiral UPC^2 of 2-ethyl-4-nitro-3-phenylbutanal (**4a**) obtained by the Michael reaction catalyzed by 10 mol% of compound **3g**. Trefoil CEL2, **Grad:** CO$_2$/EtOH 100-0% to 95-5 % in 10 min at 3 ml/min at 25°C. UV detection at 210 nm: **R$_t$**: (syn, minor) = 3.93 min, (syn, major) = 4.14 min. TABLE 2, Entry 7.
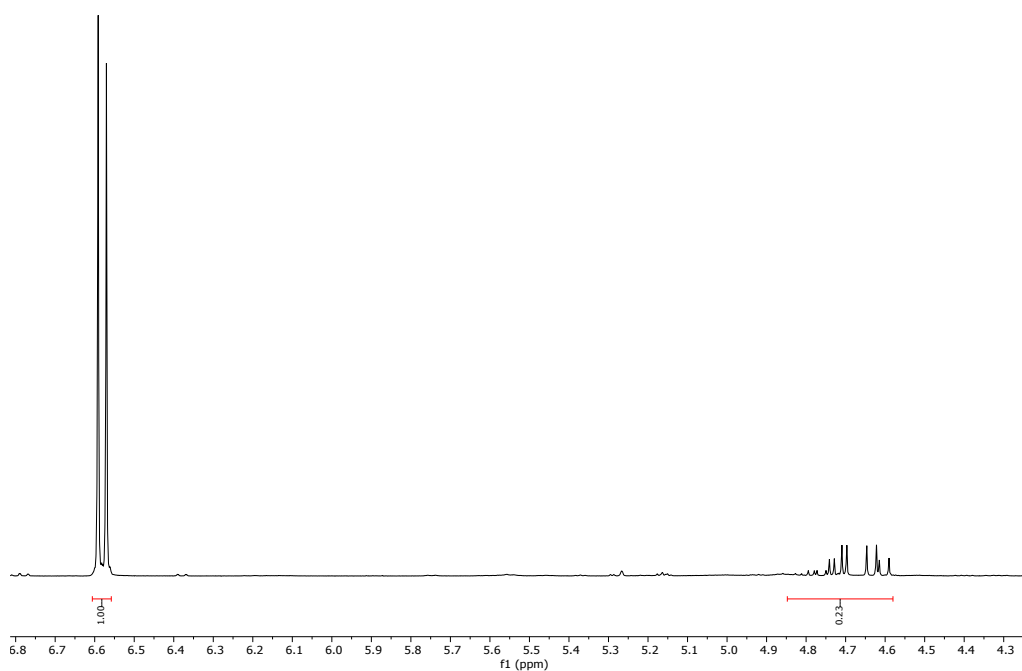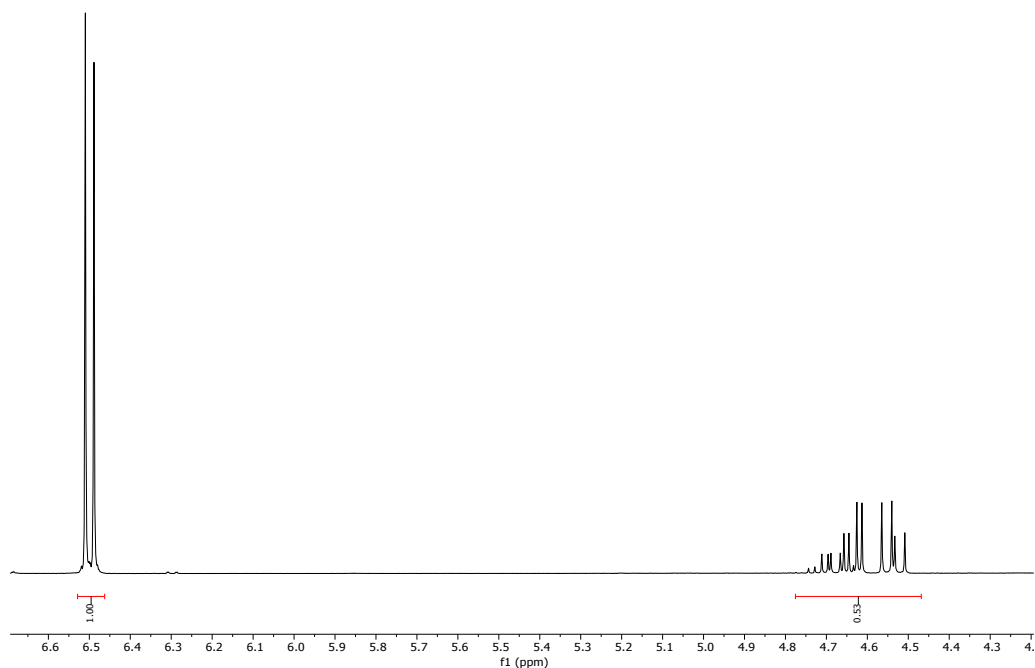
FIGURE 49. ^{1}H NMR of crude compound **4a** (400 MHz, CDCl$_3$) obtained by the Michael reaction catalyzed by 10 mol% of compound **3h** with 1, 2, 3-trimethoxybenzene as standard. Yield: 23%. TABLE 2, Entry 8.
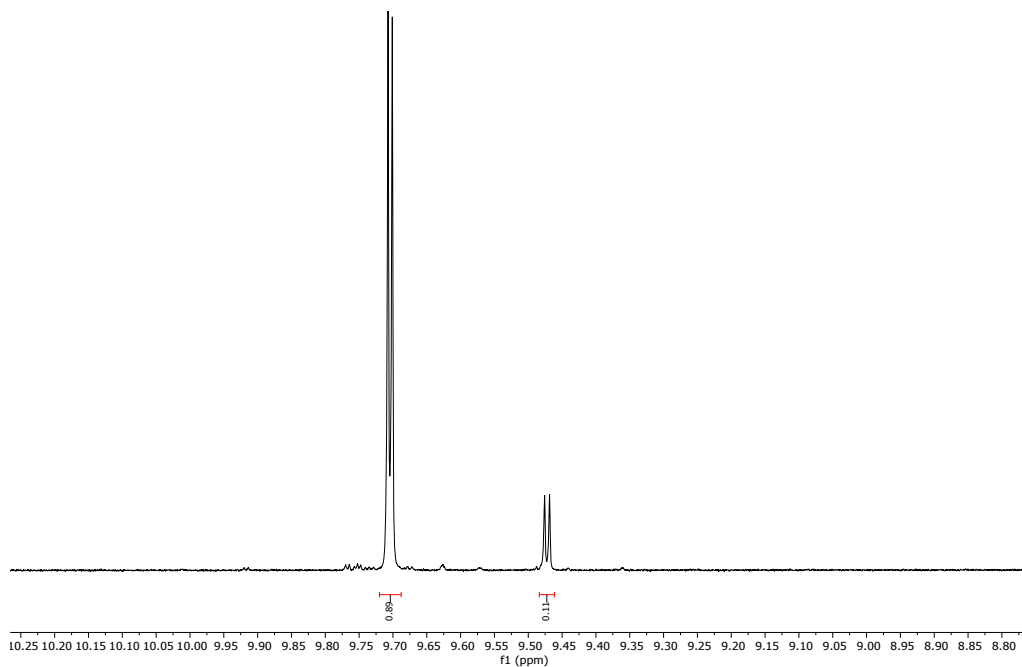
FIGURE 50. ^{1}H NMR of crude compound **4a** (400 MHz, CDCl$_3$) obtained by the Michael reaction catalyzed by 10 mol% of compound **3h**. Diastereoisomeric ratio (*syn/anti*): 89:11. TABLE 2, Entry 8.
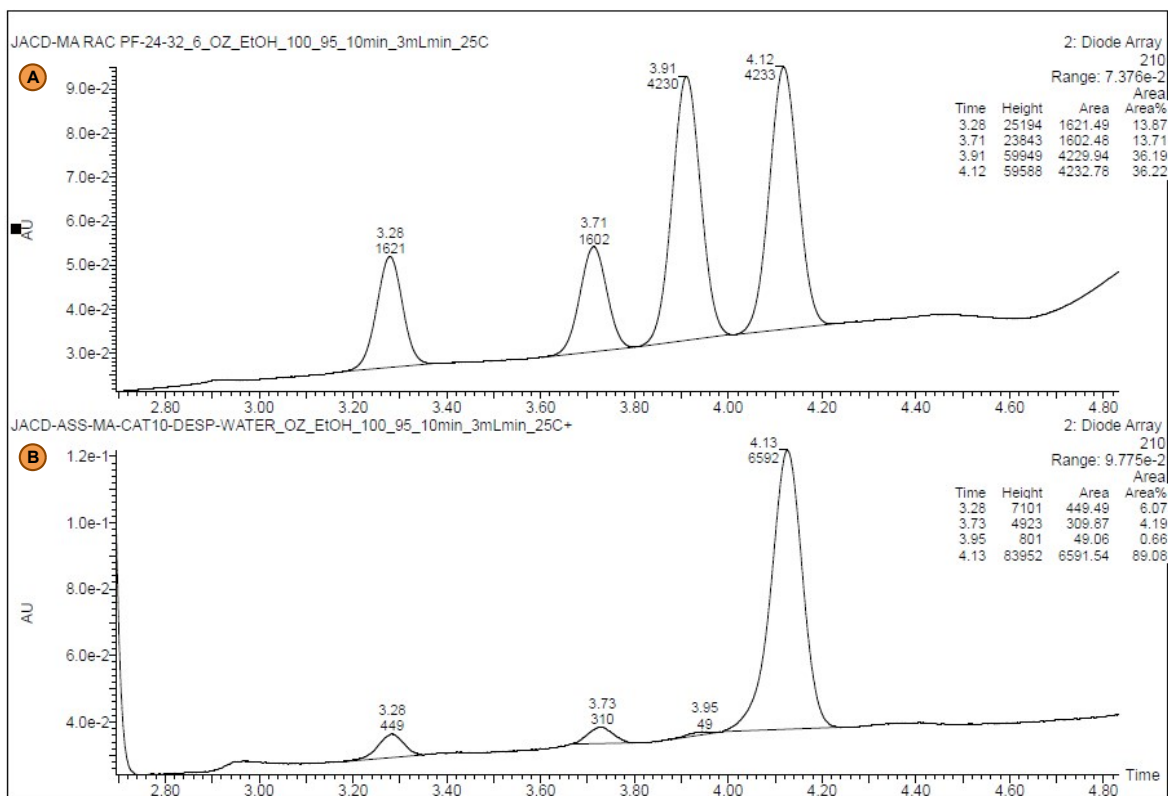
FIGURE 51. (a) Chiral UPC^2 of racemic 2-ethyl-4-nitro-3-phenylbutanal (**4a**); (b) Chiral UPC^2 of 2-ethyl-4-nitro-3-phenylbutanal (**4a**) obtained by the Michael reaction catalyzed by 10 mol% of compound **3h**. Trefoil CEL2, **Grad:** CO_2/EtOH 100-0% to 95-5 % in 10 min at 3 ml/min at 25°C. UV detection at 210 nm: **R$_t$**: (syn, minor) = 3.95 min, (syn, major) = 4.13 min. TABLE 2, Entry 8.
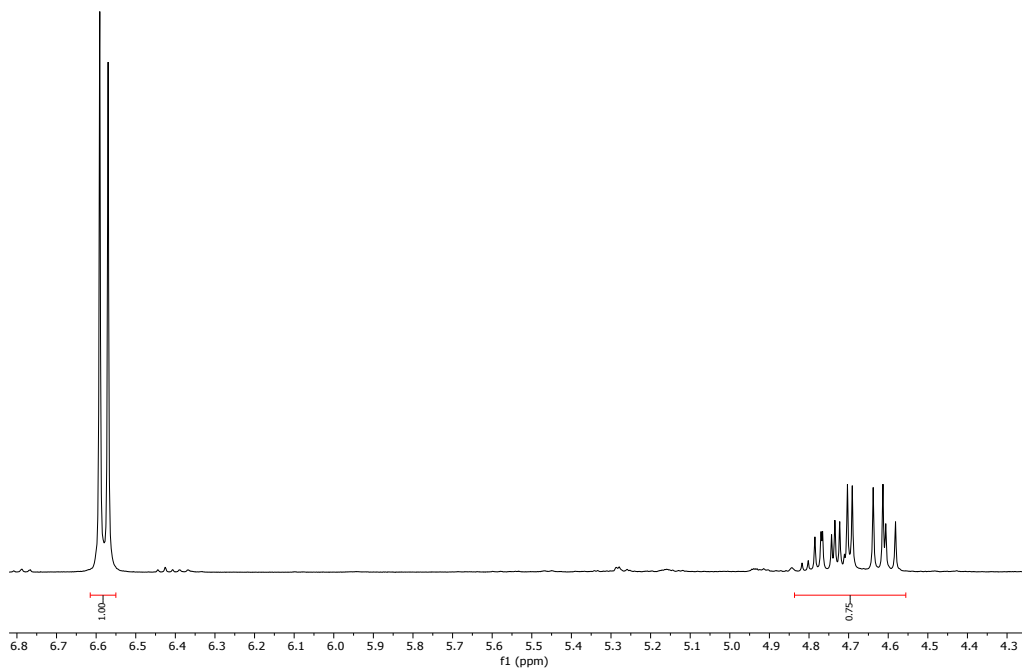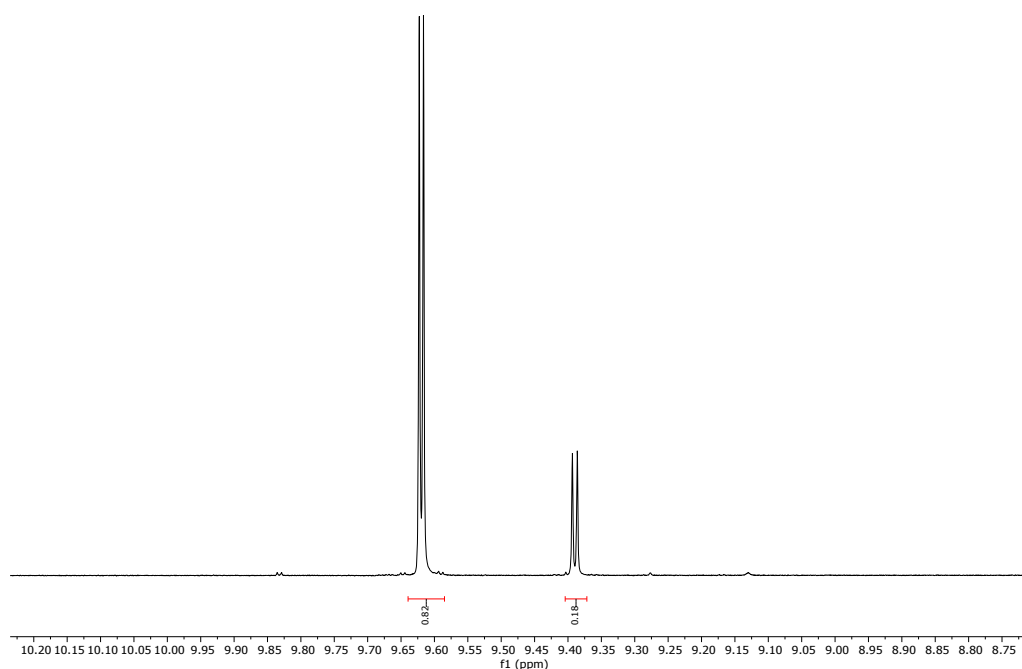

FIGURE 52. ^{1}H NMR of crude compound **4a** (400 MHz, CDCl$_3$) obtained by the Michael reaction catalyzed by 10 mol% of compound **3i** with 1, 2, 3-trimethoxybenzene as standard. Yield: 75%. TABLE 2, Entry 9.
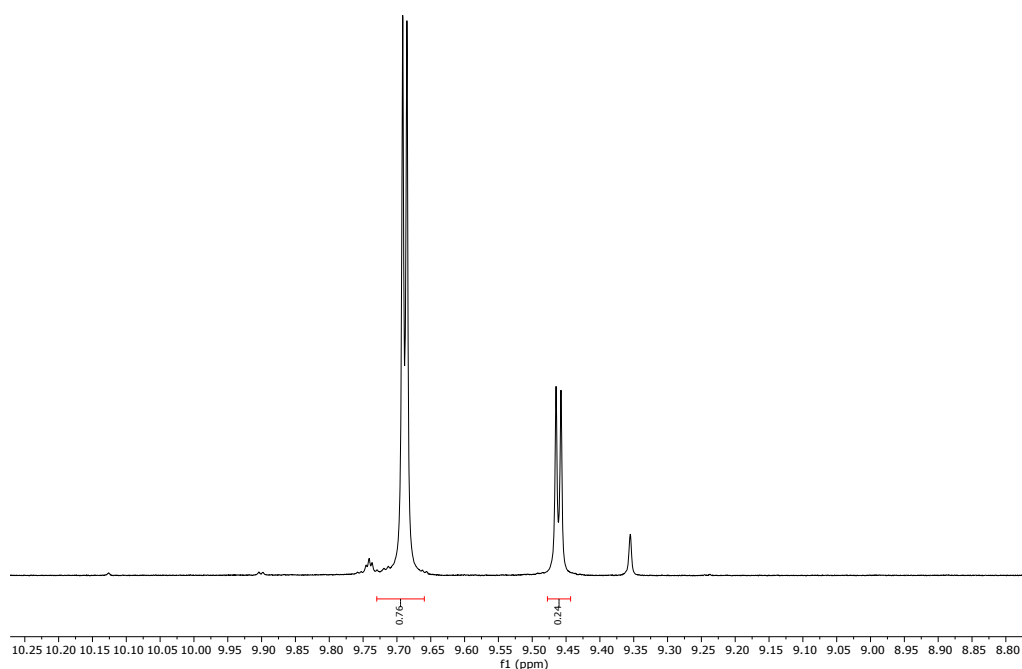
FIGURE 53. ^{1}H NMR of crude compound **4a** (400 MHz, CDCl$_3$) obtained by the Michael reaction catalyzed by 10 mol% of compound **3i**. Diastereoisomeric ratio (*syn/anti*): 76:24. TABLE 2, Entry 9.
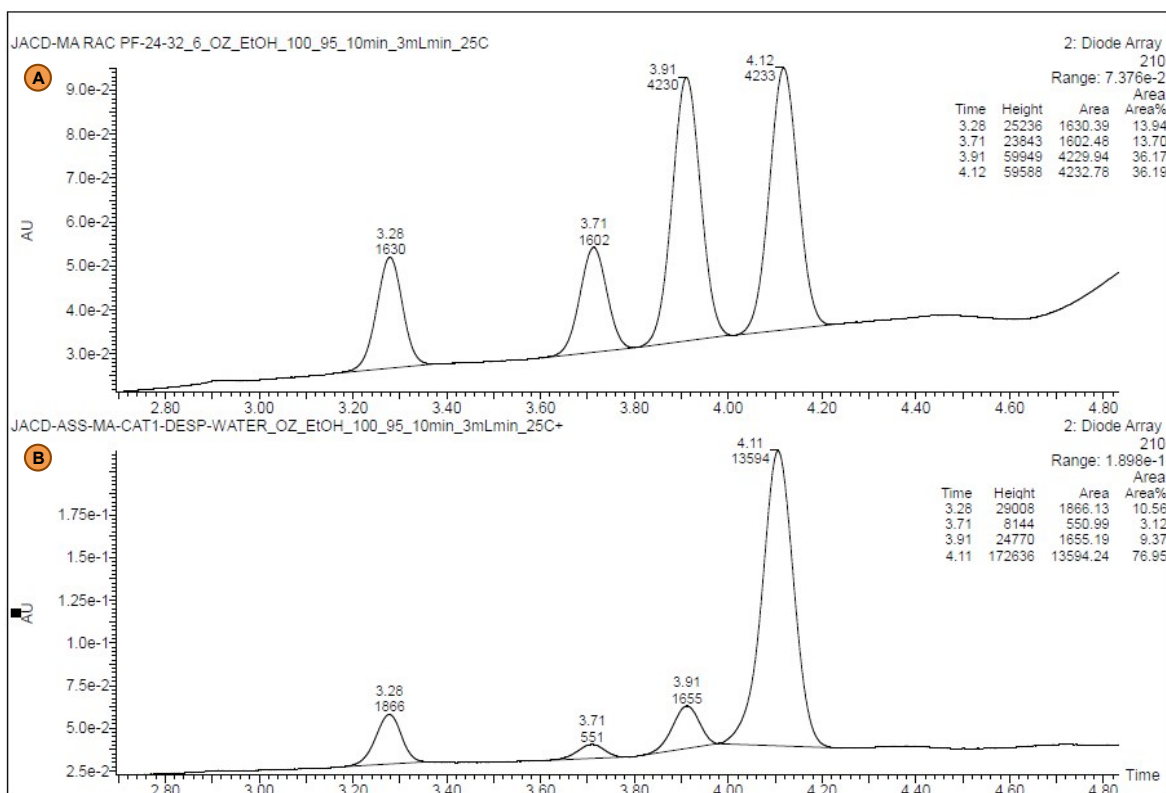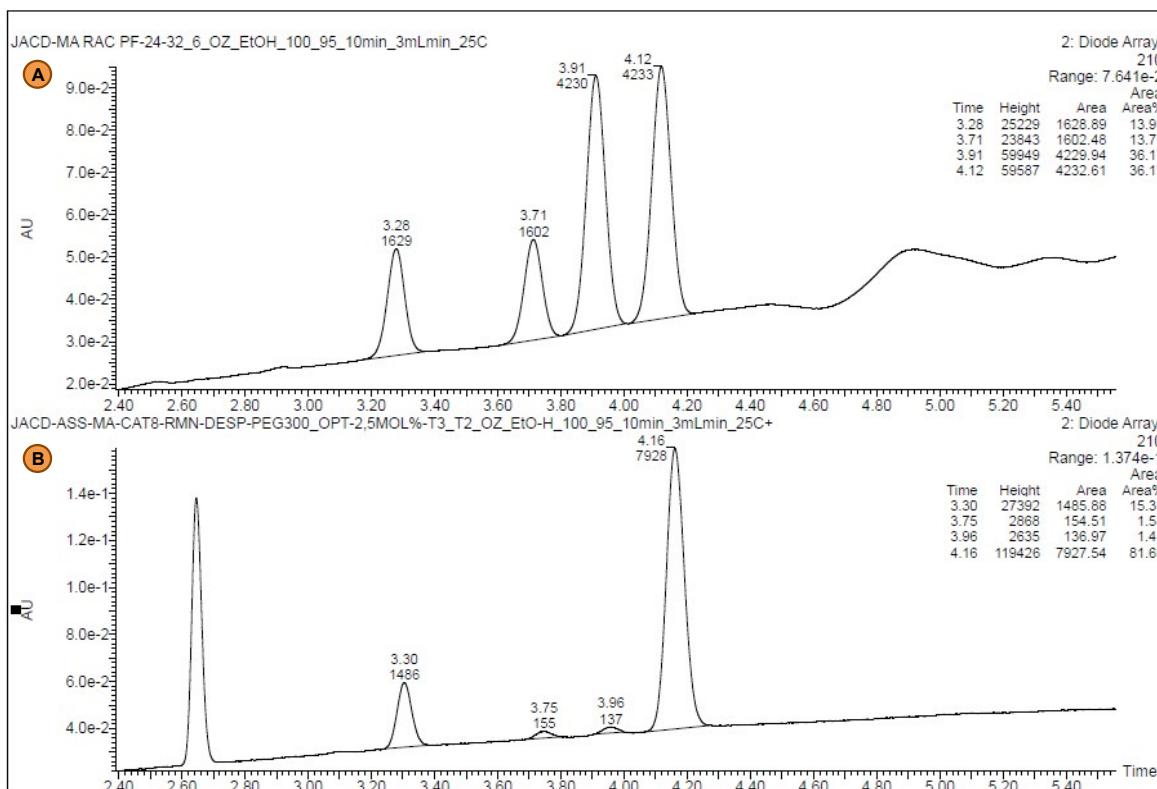

FIGURE 54. (a) Chiral UPC^2 of racemic 2-ethyl-4-nitro-3-phenylbutanal (**4a**); (b) Chiral UPC^2 of 2-ethyl-4-nitro-3-phenylbutanal (**4a**) obtained by the Michael reaction catalyzed by 10 mol% of compound **3i**. Trefoil CEL2, **Grad:** CO$_2$/EtOH 100-0% to 95-5 % in 10 min at 3 ml/min at 25°C. UV detection at 210 nm: **R$_t$**: (syn, minor) = 3.91 min, (syn, major) = 4.11 min. TABLE 2, Entry 9.
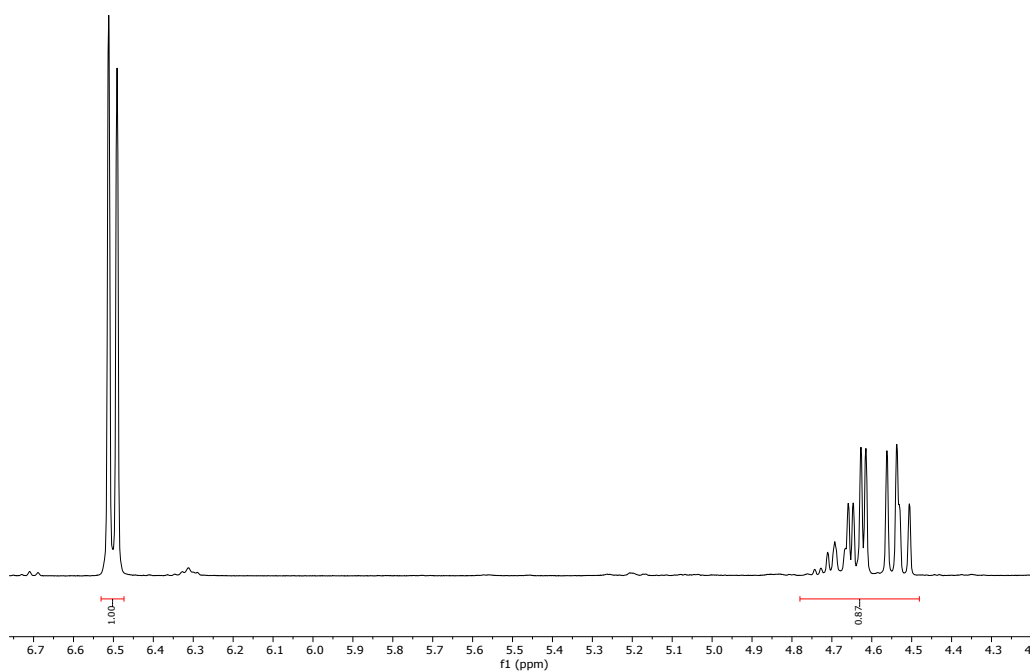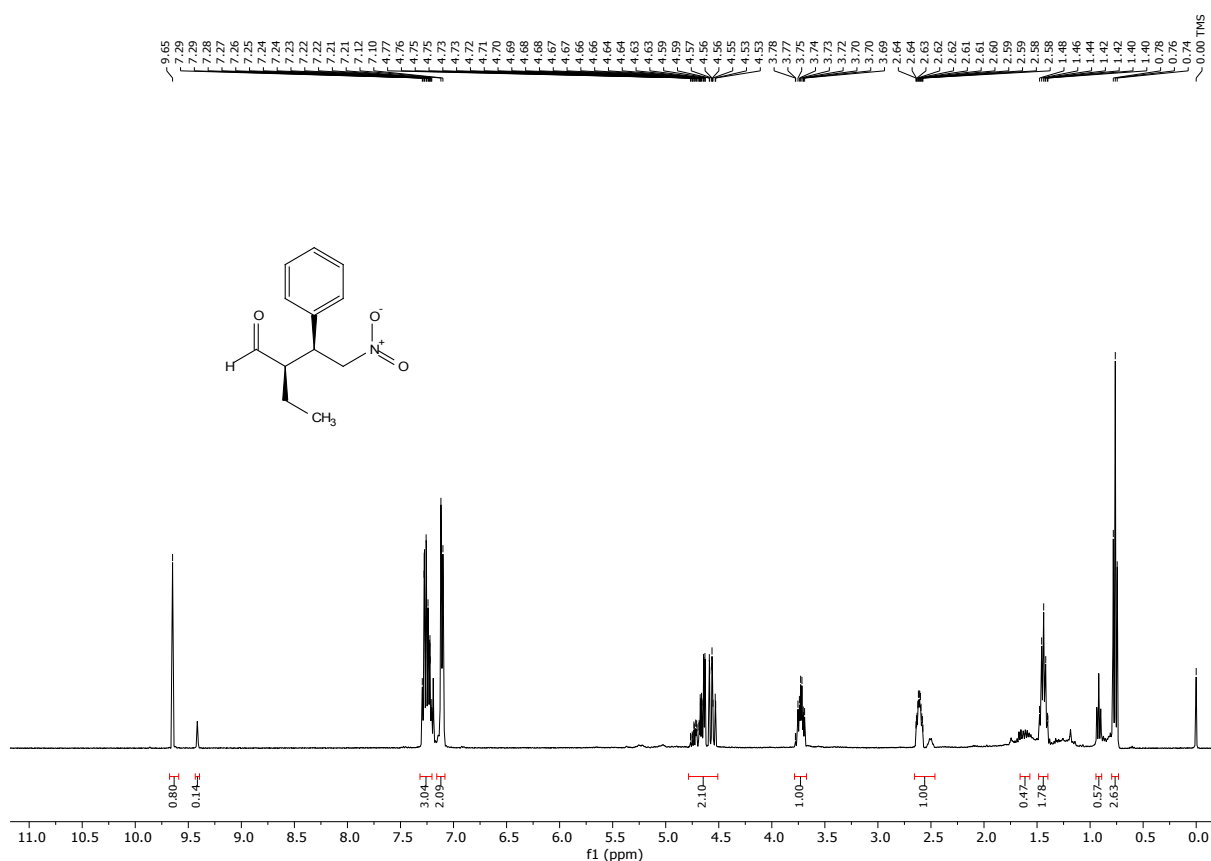
FIGURE 55. ^{1}H NMR of crude compound **4a** (400 MHz, CDCl$_3$) obtained by the Michael reaction catalyzed by 10 mol% of compound **3j** with 1, 2, 3-trimethoxybenzene as standard. Yield: 87%. TABLE 2, Entry 10.
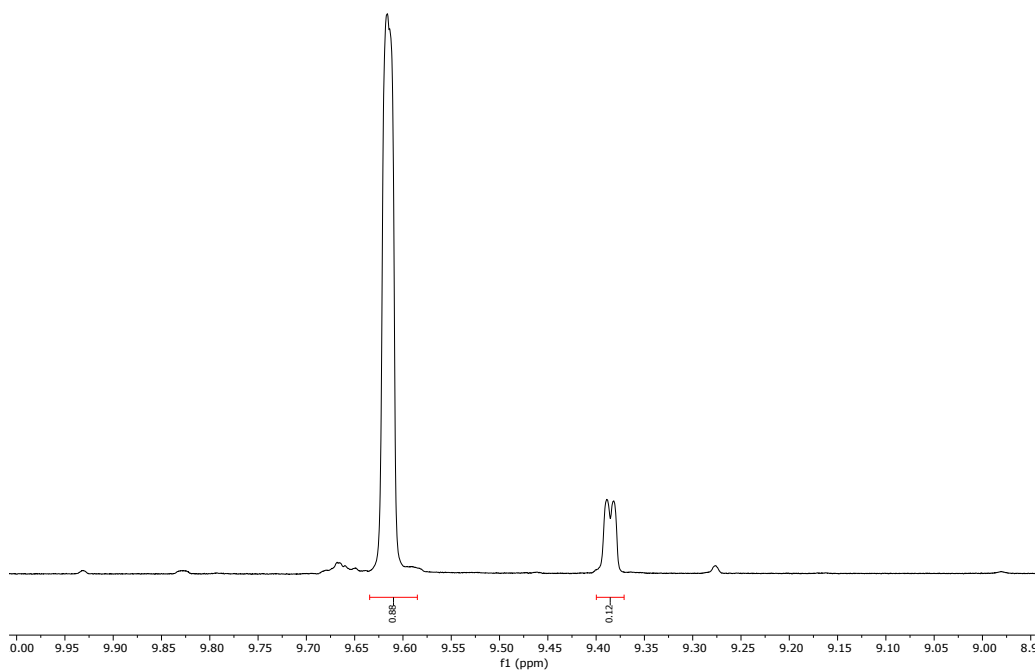
FIGURE 56. ^{1}H NMR of crude compound **4a** (400 MHz, CDCl$_3$) obtained by the Michael reaction catalyzed by 10 mol% of compound **3j**. Diastereoisomeric ratio (*syn/anti*): 88:12. TABLE 2, Entry 10.
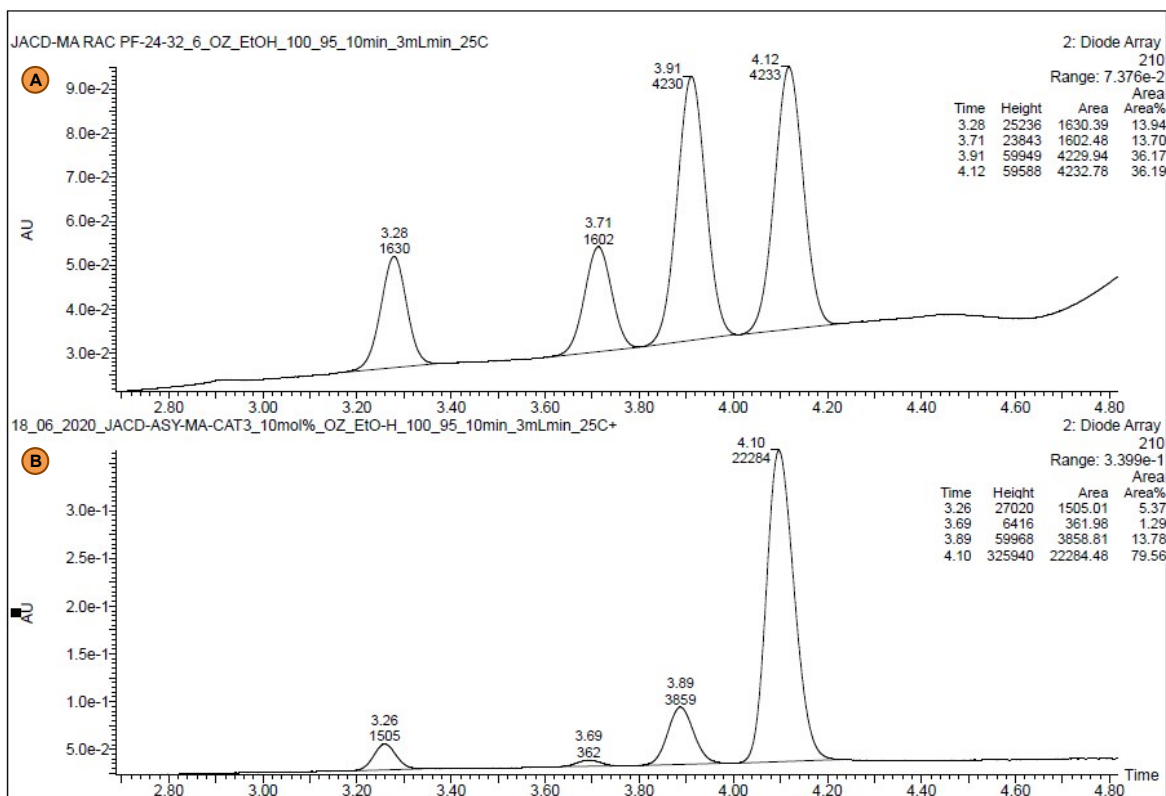
FIGURE 57. (a) Chiral UPC^2 of racemic 2-ethyl-4-nitro-3-phenylbutanal (**4a**); (b) Chiral UPC^2 of 2-ethyl-4-nitro-3-phenylbutanal (**4a**) obtained by the Michael reaction catalyzed by 10 mol% of compound **3j**. Trefoil CEL2, Grad: CO$_2$/EtOH 100-0% to 95-5 % in 10 min at 3 ml/min at 25°C. UV detection at 210 nm: Rt: (syn, minor) = 3.89 min, (syn, major) = 4.10 min. TABLE 2, Entry 10.
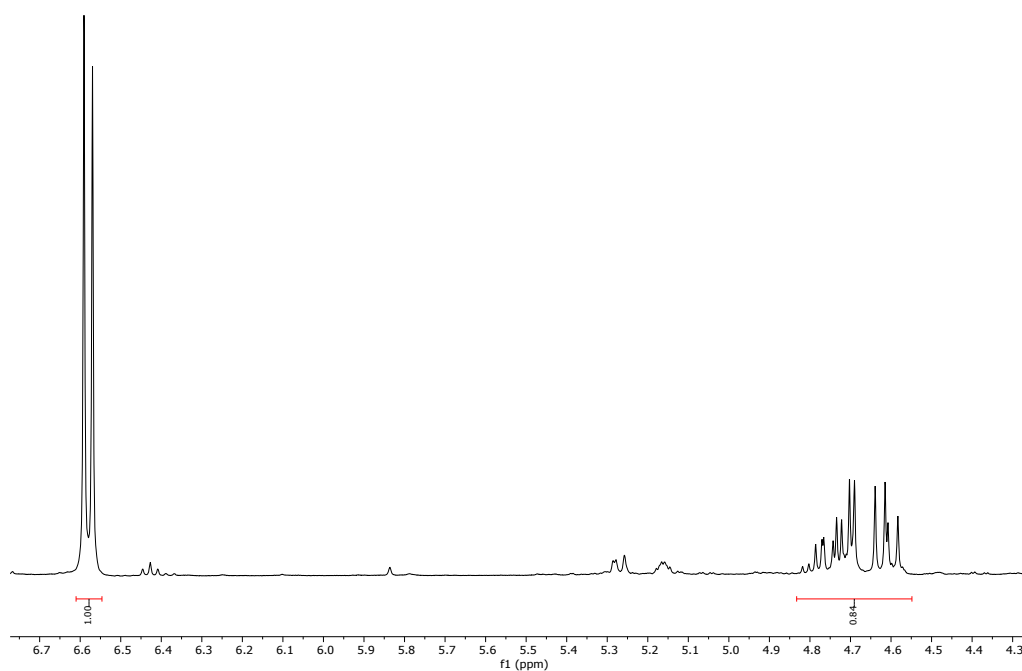
FIGURE 58. ^{1}H NMR of crude compound **4a** (400 MHz, CDCl$_3$) obtained by the Michael reaction catalyzed by 10 mol% of compound **3k** with 1, 2, 3-trimethoxybenzene as standard. Yield: 84%. TABLE 2, Entry 11.
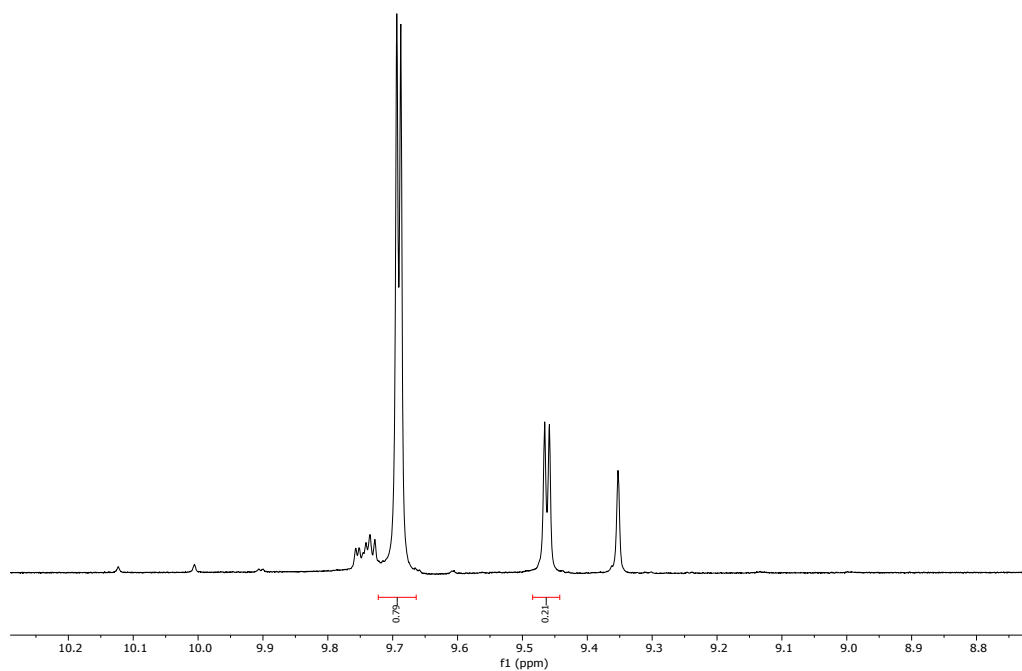
FIGURE 59. ^{1}H NMR of crude compound **4a** (400 MHz, CDCl$_3$) obtained by the Michael reaction catalyzed by 10 mol% of compound **3k**. Diastereoisomeric ratio (*syn/anti*): 79:21. TABLE 2, Entry 11.
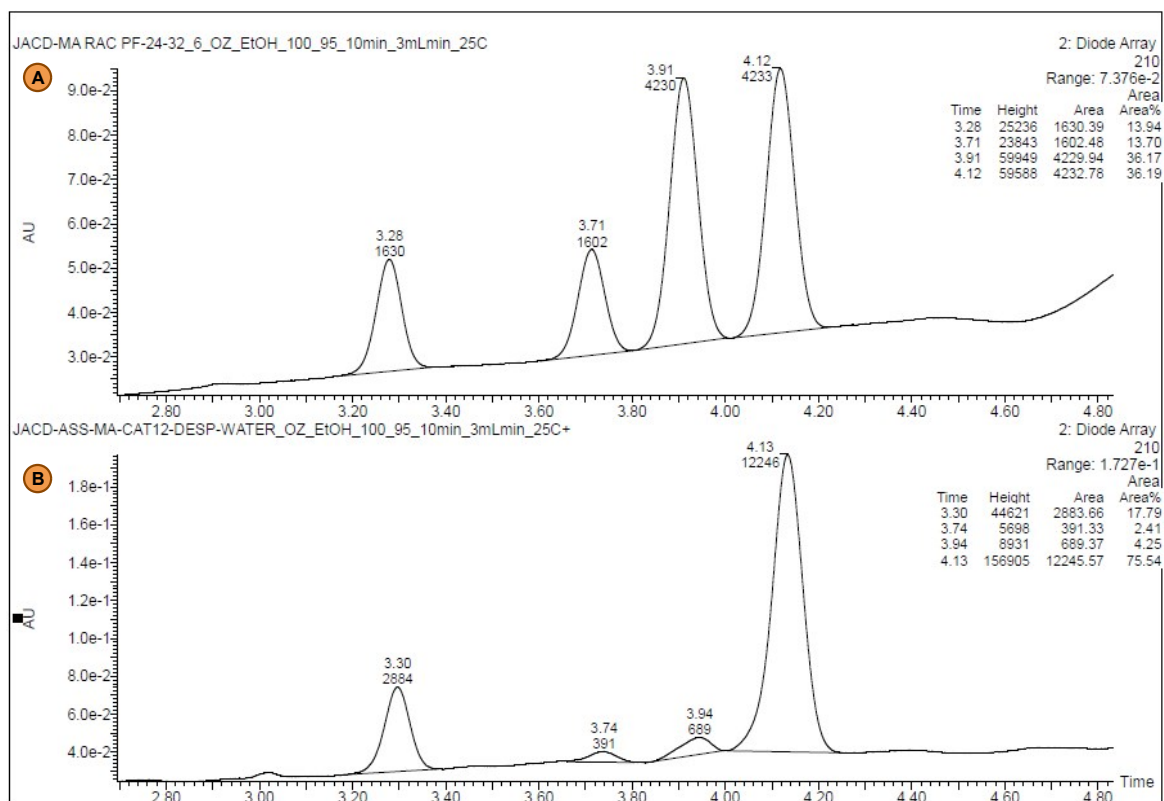
FIGURE 60. (a) Chiral UPC^2 of racemic 2-ethyl-4-nitro-3-phenylbutanal (**4a**); (b) Chiral UPC^2 of 2-ethyl-4-nitro-3-phenylbutanal (**4a**) obtained by the Michael reaction catalyzed by 10 mol% of compound **3k**. Trefoil CEL2, **Grad:** CO_2/EtOH 100-0% to 95-5 % in 10 min at 3 ml/min at 25°C. UV detection at 210 nm: R_t: (syn, minor) = 3.94 min, (syn, major) = 4.13 min. TABLE 2, Entry 11.

16. NMR Spectra and Chromatograms: Optimization

FIGURE 61. ^{1}H NMR of crude compound **4a** (400 MHz, CDCl$_3$) obtained by the Michael reaction catalyzed by 5 mol% of compound **3e** with 1, 2, 3-trimethoxybenzene as standard. Yield: 90%. TABLE 3, Entry 1.

FIGURE 62. ^{1}H NMR of crude compound **4a** (400 MHz, CDCl$_3$) obtained by the Michael reaction catalyzed by 5 mol% of compound **3e**. Diastereoisomeric ratio (*syn/anti*): 90:10. TABLE 3, Entry 1.

FIGURE 63. (a) Chiral UPC^2 of racemic 2-ethyl-4-nitro-3-phenylbutanal (**4a**); (b) Chiral UPC^2 of 2-ethyl-4-nitro-3-phenylbutanal (**4a**) obtained by the Michael reaction catalyzed by 5 mol% of compound **3e**. Trefoil CEL2, **Grad:** CO_2/EtOH 100-0% to 95-5 % in 10 min at 3 ml/min at 25°C. UV detection at 210 nm: **R$_t$**: (syn, minor) = 3.96 min, (syn, major) = 4.13 min. TABLE 3, Entry 1.

FIGURE 64. ^{1}H NMR of crude compound **4a** (400 MHz, CDCl$_3$) obtained by the Michael reaction catalyzed by 2.5 mol% of compound **3e** with 1, 2, 3-trimethoxybenzene as standard. Yield: 99%. TABLE 3, Entry 2.

FIGURE 65. ^{1}H NMR of crude compound **4a** (400 MHz, CDCl$_3$) obtained by the Michael reaction catalyzed by 2.5 mol% of compound **3e**. Diastereoisomeric ratio (*syn/anti*): 93:07. TABLE 3, Entry 2. TABLE 4, Entry 1.

FIGURE 66. (a) Chiral UPC^2 of racemic 2-ethyl-4-nitro-3-phenylbutanal (**4a**); (b) Chiral UPC^2 of 2-ethyl-4-nitro-3-phenylbutanal (**4a**) obtained by the Michael reaction catalyzed by 2.5 mol% of compound **3e**. Trefoil CEL2, **Grad:** CO$_2$/EtOH 100-0% to 95-5 % in 10 min at 3 ml/min at 25°C. UV detection at 210 nm: **R$_t$**: (syn, minor) = 3.93 min, (syn, major) = 4.13 min. TABLE 3, Entry 2. TABLE 4, Entry 1.

FIGURE 67. ^{1}H NMR of crude compound **4a** (400 MHz, CDCl$_3$) obtained by the Michael reaction catalyzed by 1 mol% of compound **3e** with 1, 2, 3-trimethoxybenzene as standard. Yield: 64%. TABLE 3, Entry 3.

FIGURE 68. ^{1}H NMR of crude compound **4a** (400 MHz, CDCl$_3$) obtained by the Michael reaction catalyzed by 1 mol% of compound **3e**. Diastereoisomeric ratio (*syn/anti*): 97:03. TABLE 3, Entry 3.

FIGURE 69. (a) Chiral UPC^2 of racemic 2-ethyl-4-nitro-3-phenylbutanal (**4a**); (b) Chiral UPC^2 of 2-ethyl-4-nitro-3-phenylbutanal (**4a**) obtained by the Michael reaction catalyzed by 1 mol% of compound **3e**. Trefoil CEL2, **Grad:** CO$_2$/EtOH 100-0% to 95-5 % in 10 min at 3 ml/min at 25°C. UV detection at 210 nm: **R$_t$**: (syn, minor) = 3.93 min, (syn, major) = 4.12 min. TABLE 3, Entry 3.

FIGURE 70. ^{1}H NMR of crude compound **4a** (400 MHz, CDCl$_3$) obtained by the Michael reaction catalyzed by 2.5 mol% of compound **3e** in Brine as a solvent; 1, 2, 3-trimethoxybenzene as standard. Yield: 84%. TABLE 3, Entry 4.

FIGURE 71. ^{1}H NMR of crude compound **4a** (400 MHz, CDCl$_3$) obtained by the Michael reaction catalyzed by 2.5 mol% of compound **3e** in Brine as a solvent. Diastereoisomeric ratio (*syn/anti*): 95:05. TABLE 3, Entry 4.

FIGURE 72. (a) Chiral UPC^2 of racemic 2-ethyl-4-nitro-3-phenylbutanal (**4a**); (b) Chiral UPC^2 of 2-ethyl-4-nitro-3-phenylbutanal (**4a**) obtained by the Michael reaction catalyzed by 2.5 mol% of compound **3e** in Brine as a solvent. Trefoil CEL2, **Grad:** CO$_2$/EtOH 100-0% to 95-5 % in 10 min at 3 ml/min at 25°C. UV detection at 210 nm: **R$_t$**: (syn, minor) = 3.96 min, (syn, major) = 4.16 min. TABLE 3, Entry 4.

FIGURE 73. ^{1}H NMR of crude compound **4a** (400 MHz, CDCl$_3$) obtained by the Michael reaction catalyzed by 2.5 mol% of compound **3e** in Ethanol as a solvent; 1, 2, 3-trimethoxybenzene as standard. Yield: 26%. TABLE 3, Entry 5.

FIGURE 74. ^{1}H NMR of crude compound **4a** (400 MHz, CDCl$_3$) obtained by the Michael reaction catalyzed by 2.5 mol% of compound **3e** in Ethanol as a solvent. Diastereoisomeric ratio (*syn/anti*): 85:15. TABLE 3, Entry 5.

S61

FIGURE 75. (a) Chiral UPC^2 of racemic 2-ethyl-4-nitro-3-phenylbutanal (**4a**); (b) Chiral UPC^2 of 2-ethyl-4-nitro-3-phenylbutanal (**4a**) obtained by the Michael reaction catalyzed by 2.5 mol% of compound **3e** in Ethanol as a solvent. Trefoil CEL2, **Grad:** CO_2/EtOH 100-0% to 95-5 % in 10 min at 3 ml/min at 25°C. UV detection at 210 nm: **R$_t$**: (syn, minor) = 3.97 min, (syn, major) = 4.18 min. TABLE 3, Entry 5.

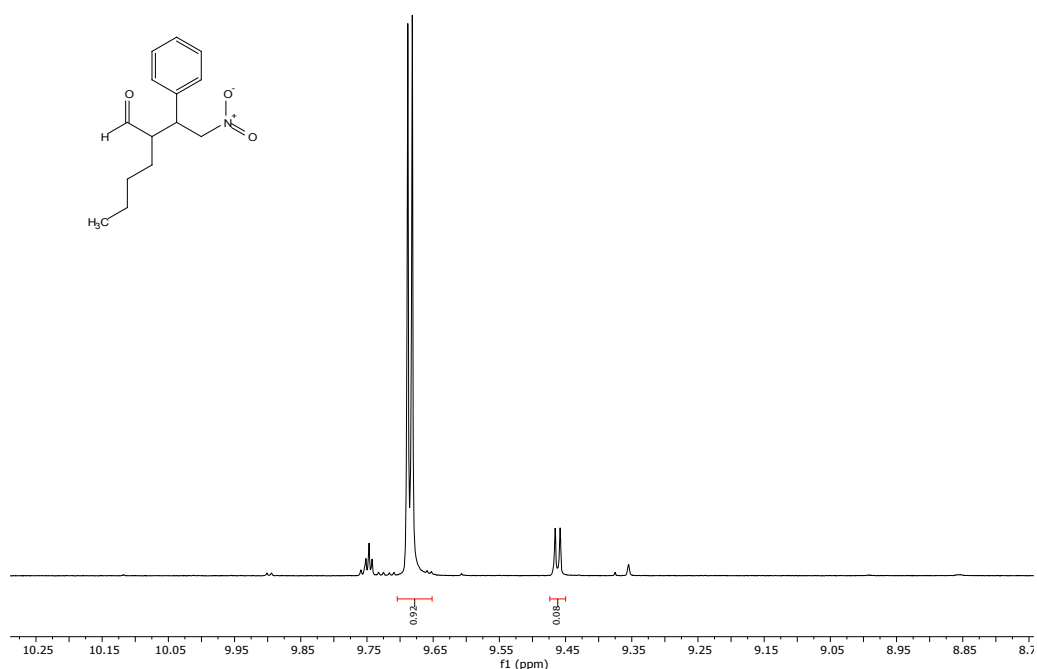**FIGURE 76.** ^{1}H NMR of crude compound **4a** (400 MHz, CDCl$_3$) obtained by the Michael reaction catalyzed by 2.5 mol% of compound **3e** in PEG-300 as a solvent; 1, 2, 3-trimethoxybenzene as standard. Yield: 53%. TABLE 3, Entry 6.

FIGURE 77. ^{1}H NMR of crude compound **4a** (400 MHz, CDCl$_3$) obtained by the Michael reaction catalyzed by 2.5 mol% of compound **3e** in PEG-300 as a solvent. Diastereoisomeric ratio (*syn/anti*): 82:18. TABLE 3, Entry 6.
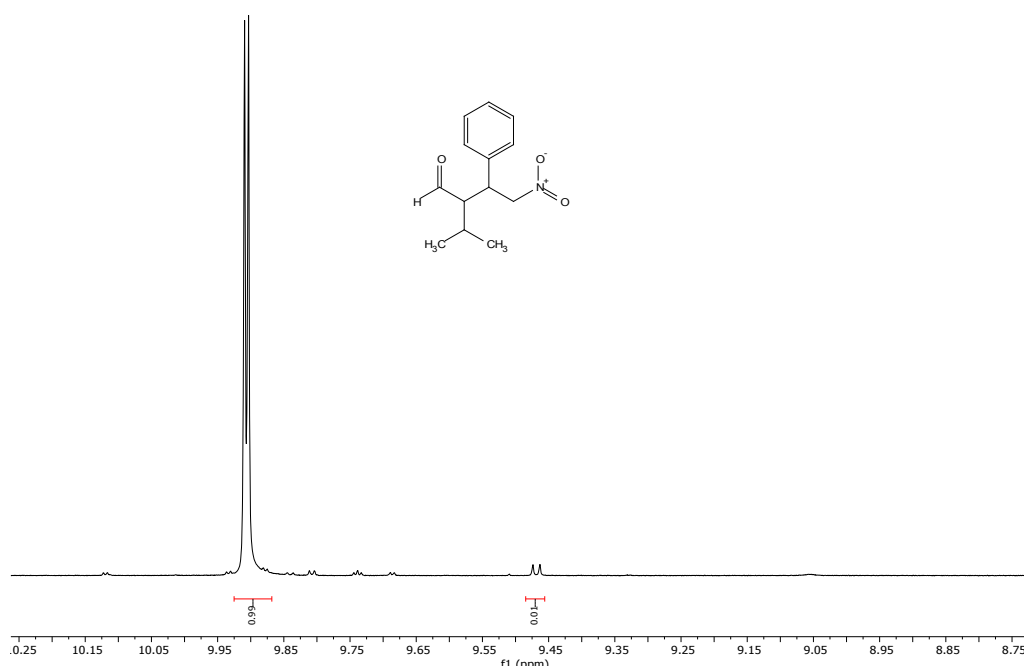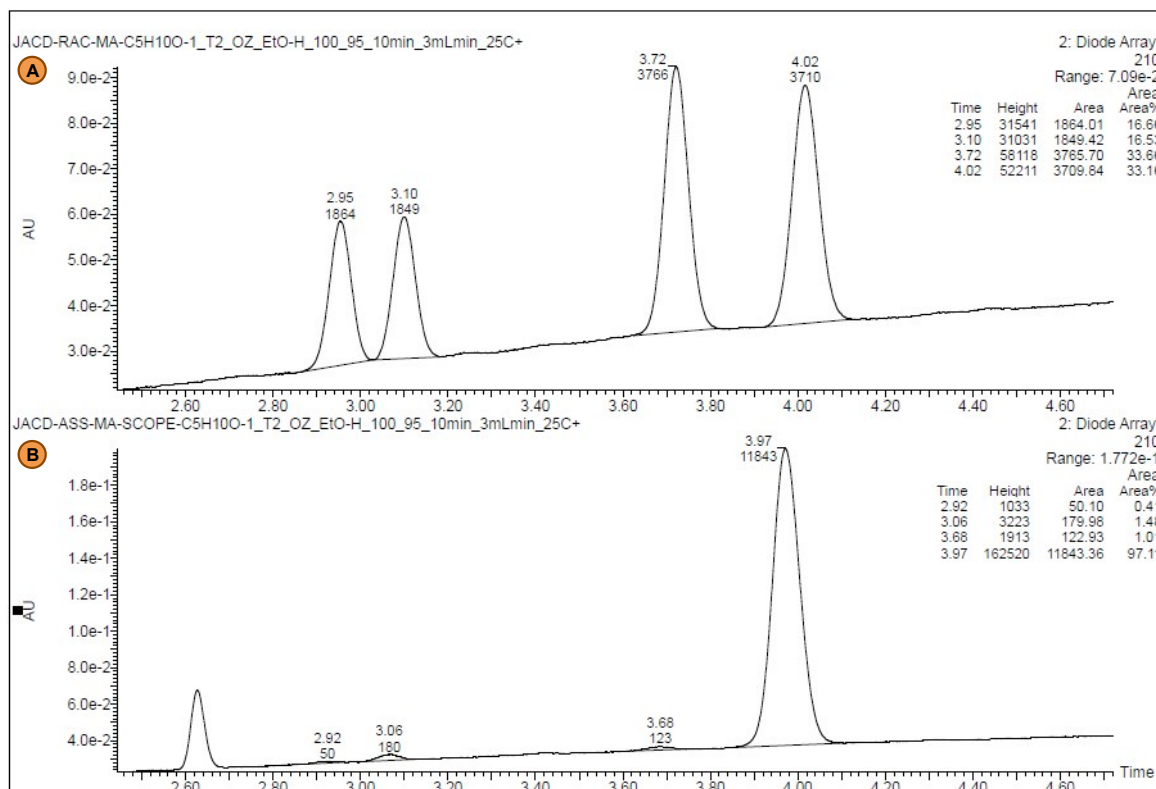

FIGURE 78. (a) Chiral UPC[2] of racemic 2-ethyl-4-nitro-3-phenylbutanal (**4a**); (b) Chiral UPC[2] of 2-ethyl-4-nitro-3-phenylbutanal (**4a**) obtained by the Michael reaction catalyzed by 2.5 mol% of compound **3e** in PEG-300 as a solvent. Trefoil CEL2, **Grad:** CO$_2$/EtOH 100-0% to 95-5 % in 10 min at 3 ml/min at 25°C. UV detection at 210 nm: **R$_t$**: (syn, minor) = 3.96 min, (syn, major) = 4.16 min. TABLE 3, Entry 6.

17. NMR Spectra: Scope

FIGURE 79. ^{1}H NMR of compound **4a** (400 MHz, CDCl$_3$). Diastereoisomeric ratio (*syn/anti*): 85:15.
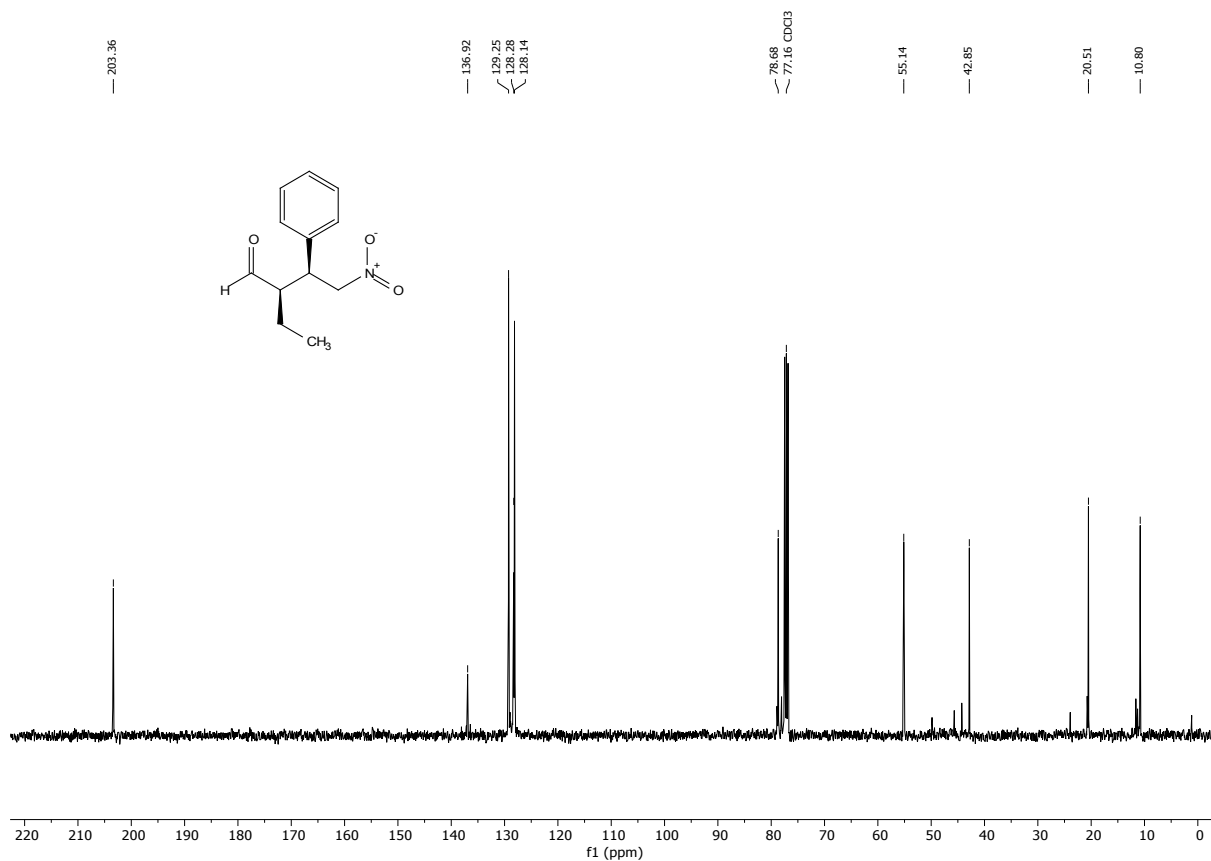
FIGURE 80. ^{13}C NMR of compound **4a** (100 MHz, CDCl$_3$).
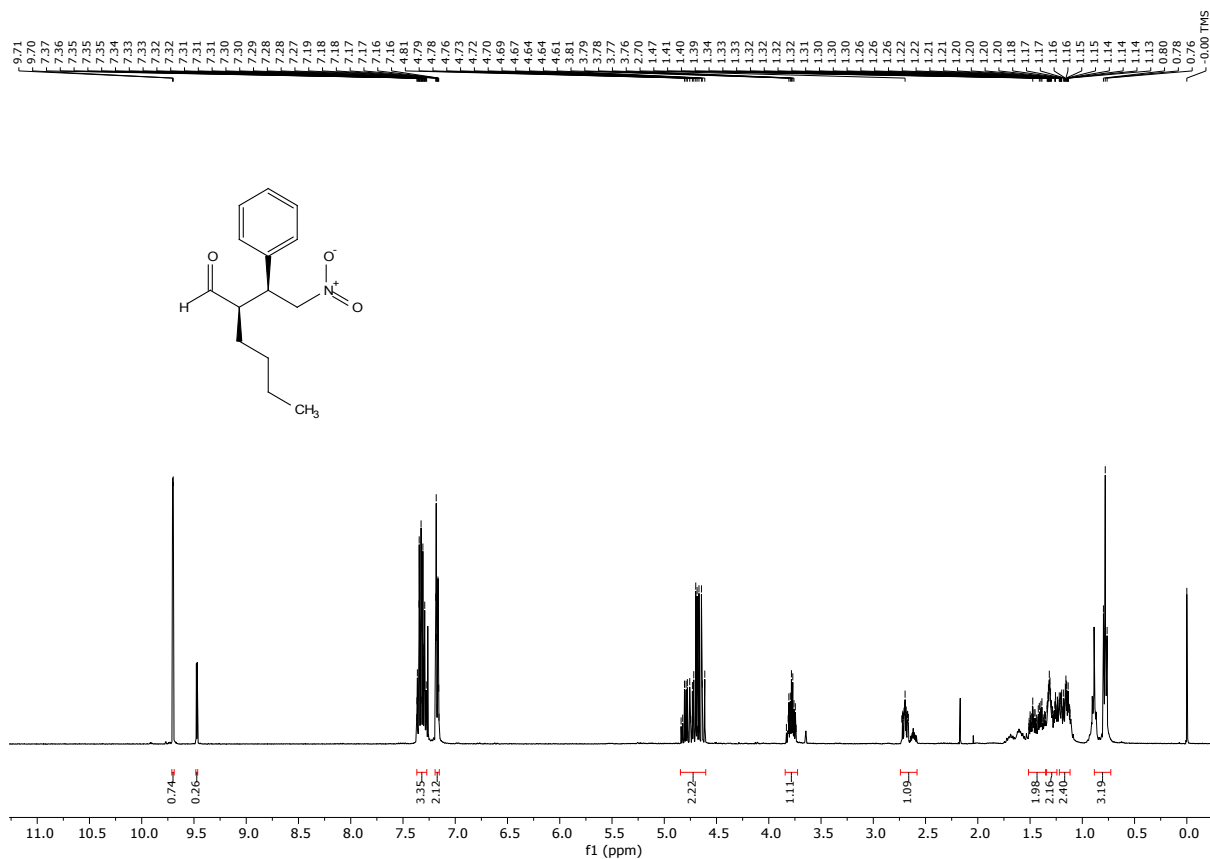
FIGURE 81. ¹H NMR of compound **4b** (400 MHz, CDCl₃). Diastereoisomeric ratio (*syn/anti*): 74:26.
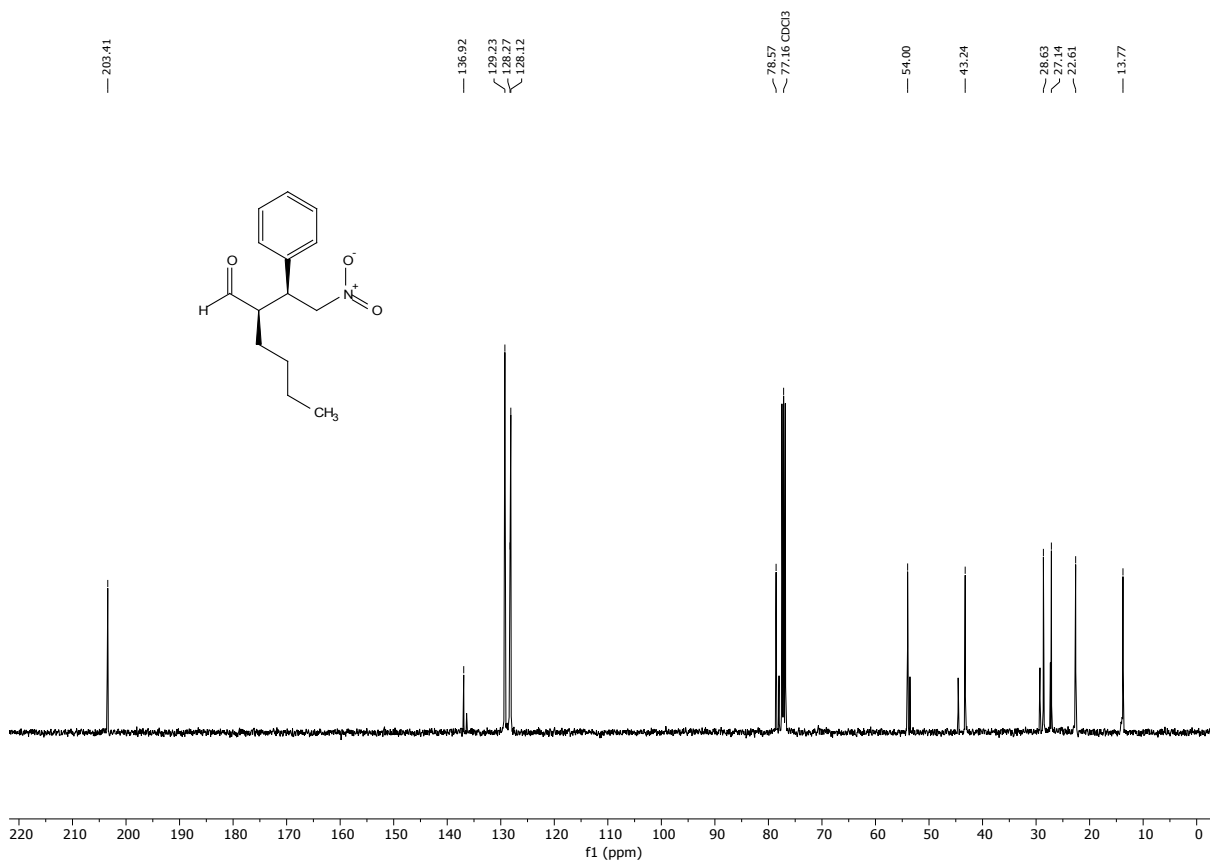
FIGURE 82. ¹³C NMR of compound **4b** (100 MHz, CDCl₃).

FIGURE 83. ¹H NMR of compound **4c** (400 MHz, CDCl₃). Diastereoisomeric ratio (*syn/anti*): 94:06.

FIGURE 84. ¹³C NMR of compound **4c** (100 MHz, CDCl₃).

S66
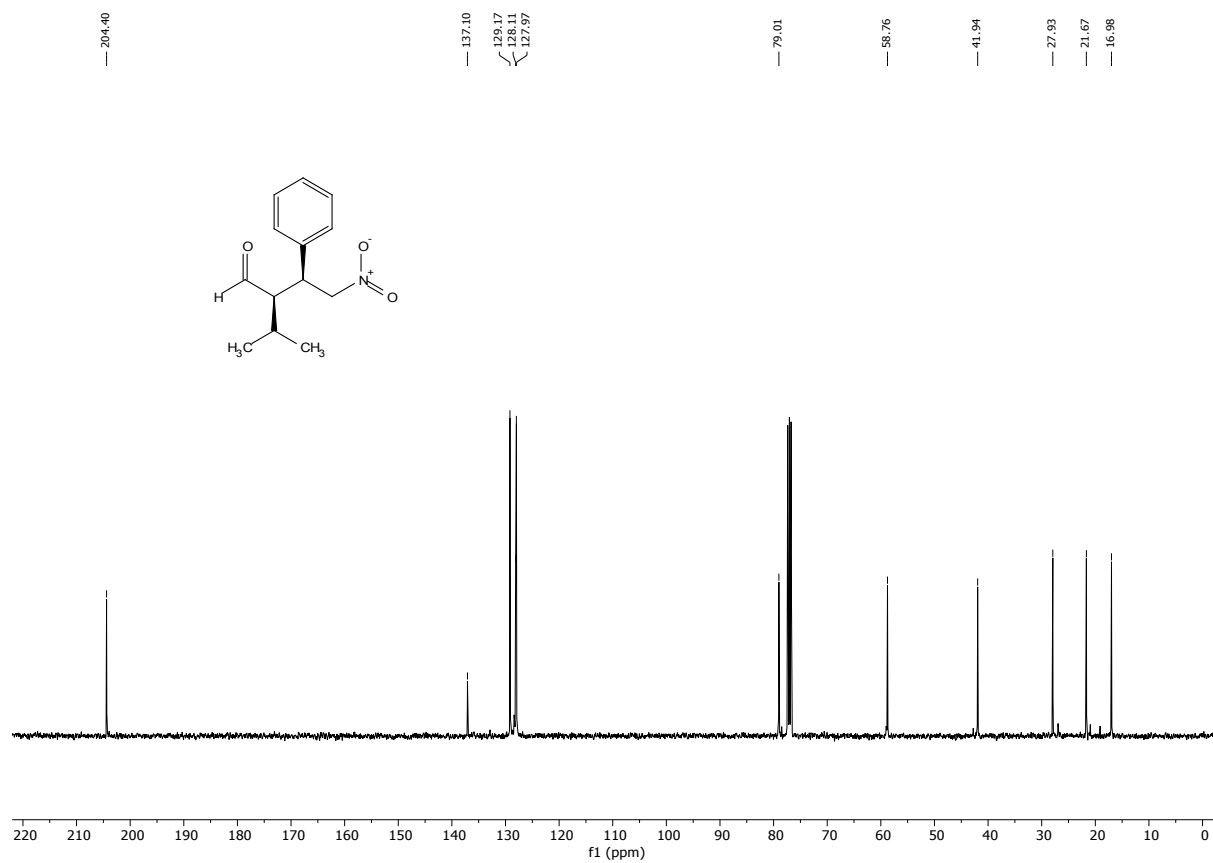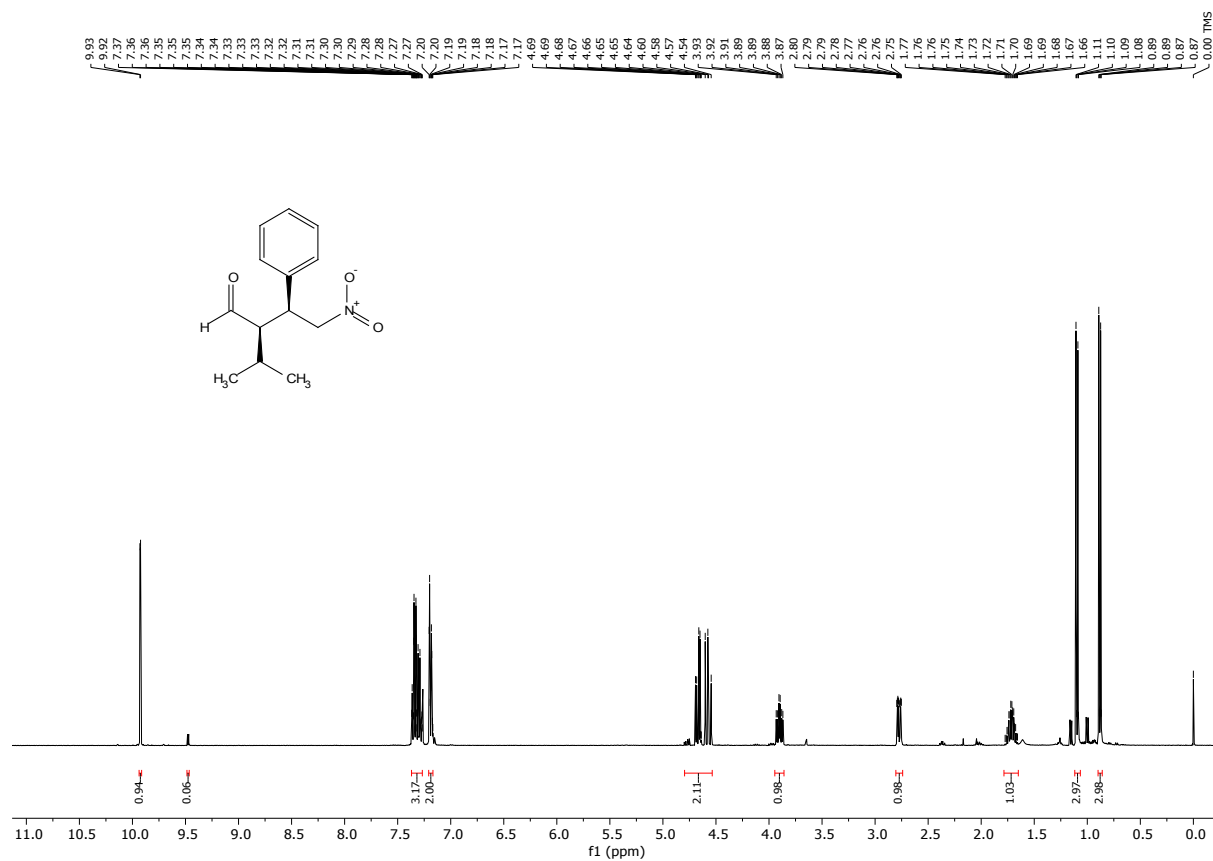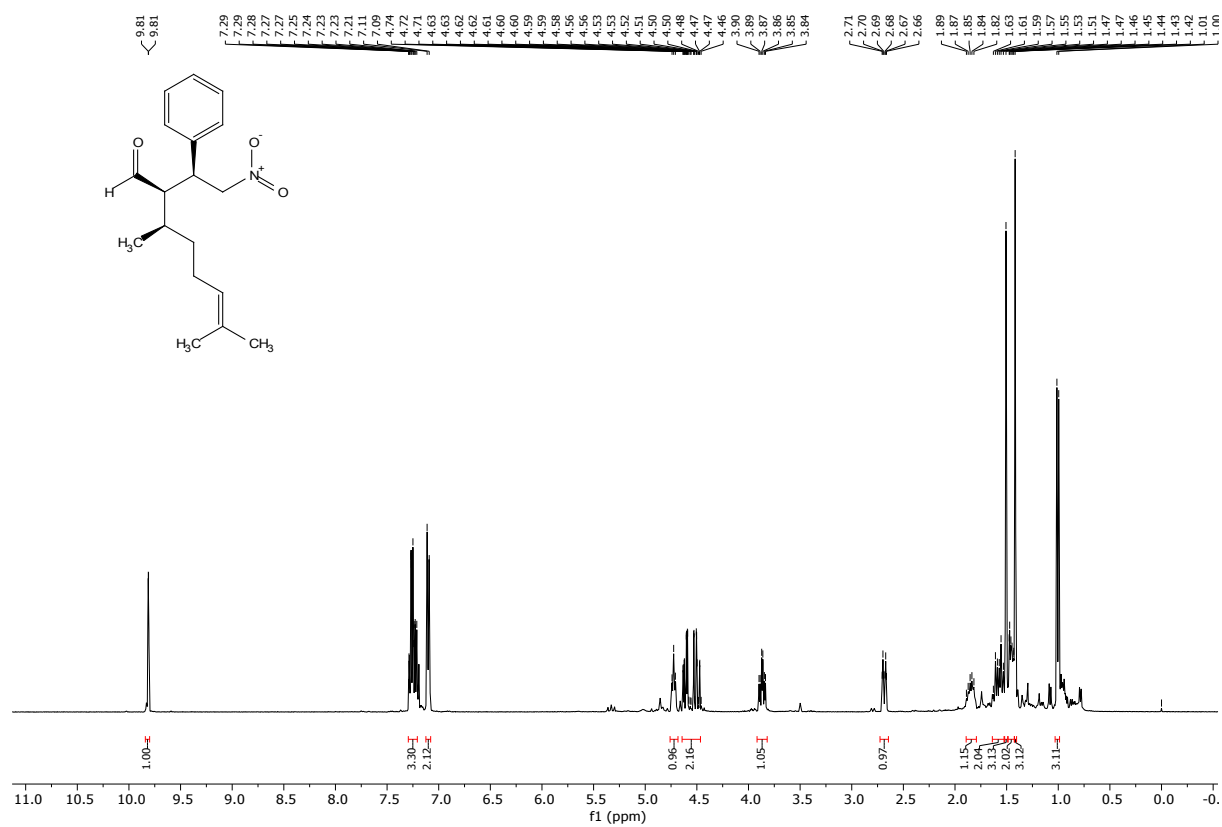
FIGURE 85. ^{1}H NMR of compound **4d** (400 MHz, CDCl$_3$). Diastereoisomeric ratio (*syn/anti*): 92:08.
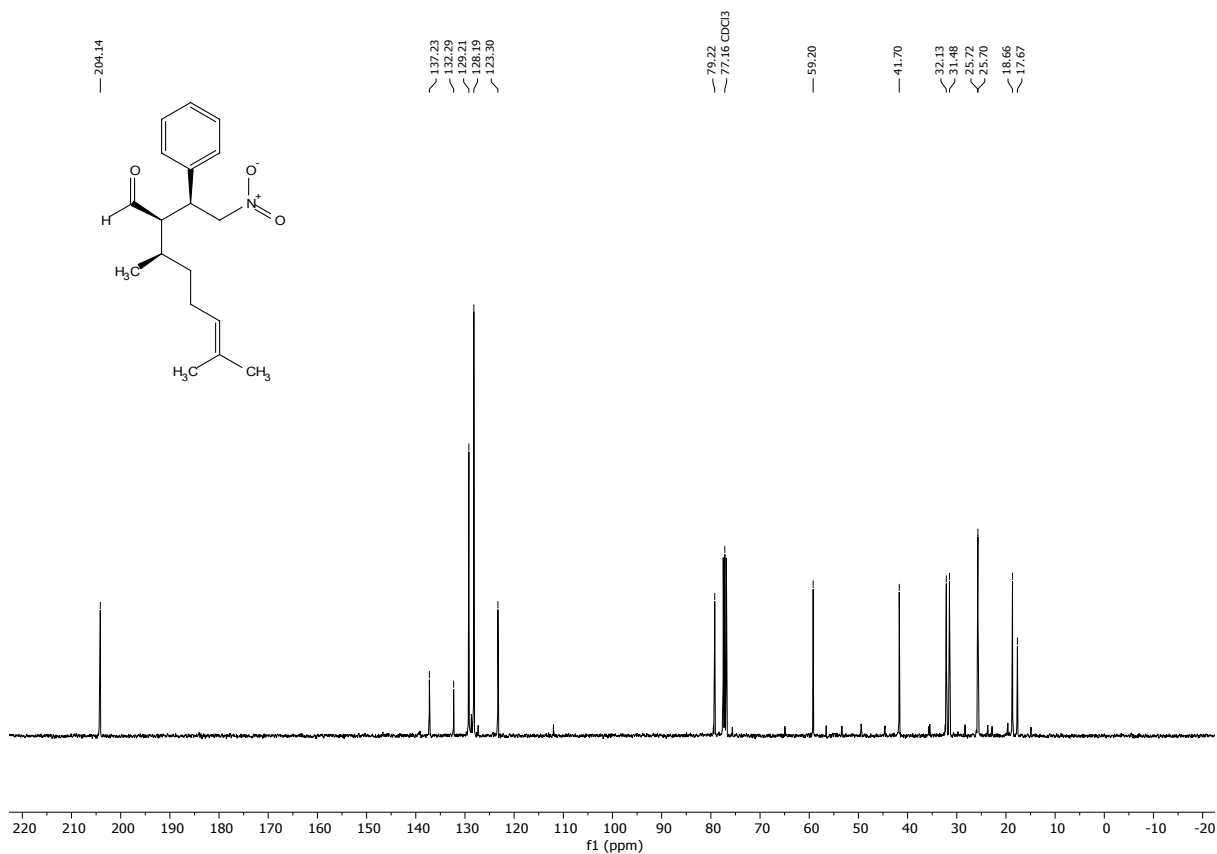
FIGURE 86. ^{13}C NMR of compound **4d** (100 MHz, CDCl$_3$).
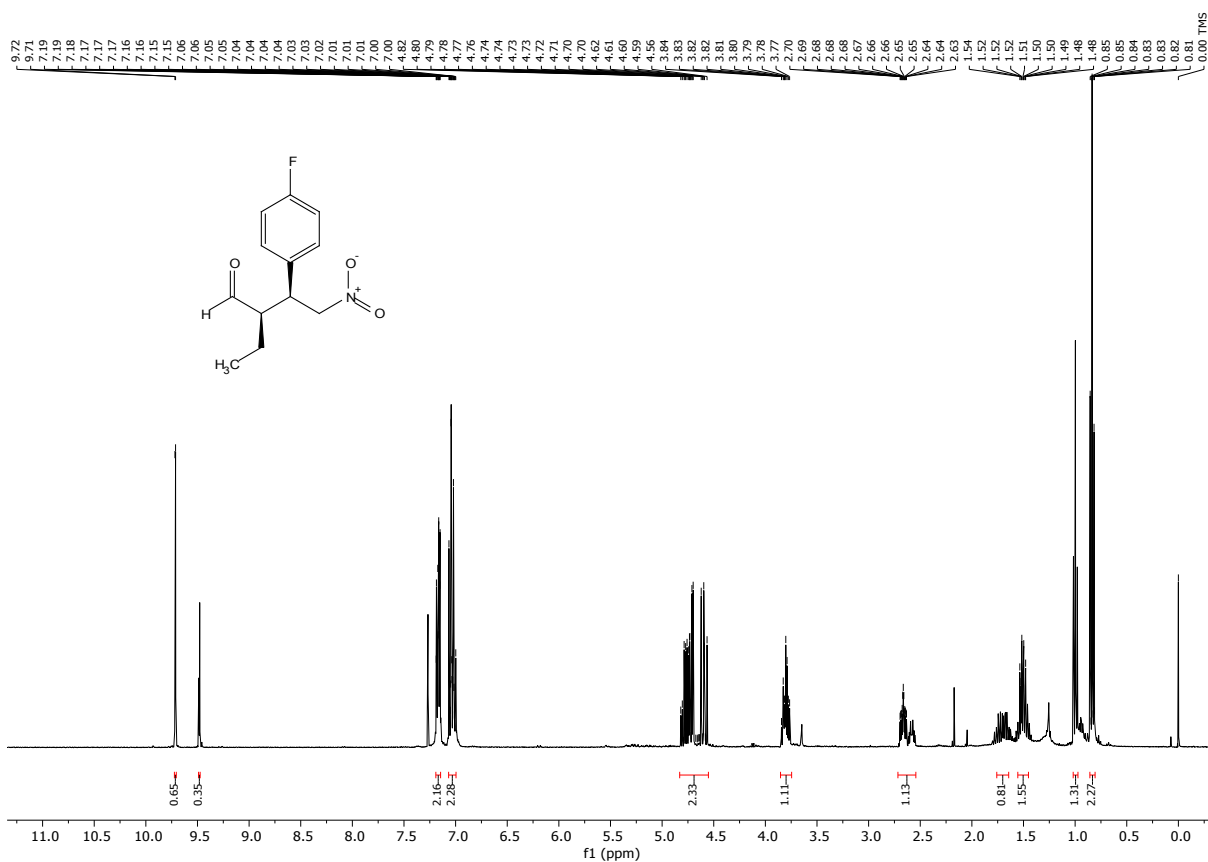
FIGURE 87. ^{1}H NMR of compound **4e** (400 MHz, CDCl$_3$). Diastereoisomeric ratio (*syn/anti*): 65:35.
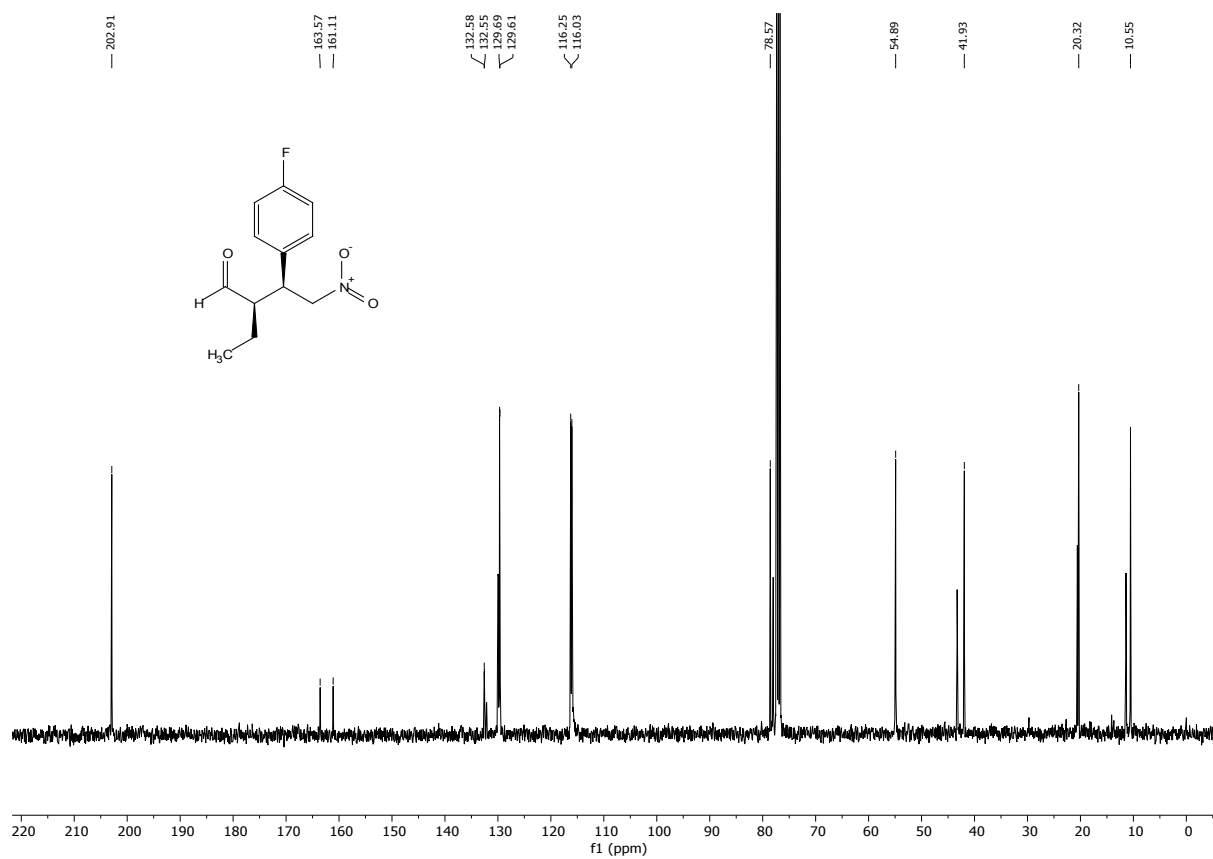
FIGURE 88. ^{13}C NMR of compound **4e** (100 MHz, CDCl$_3$).
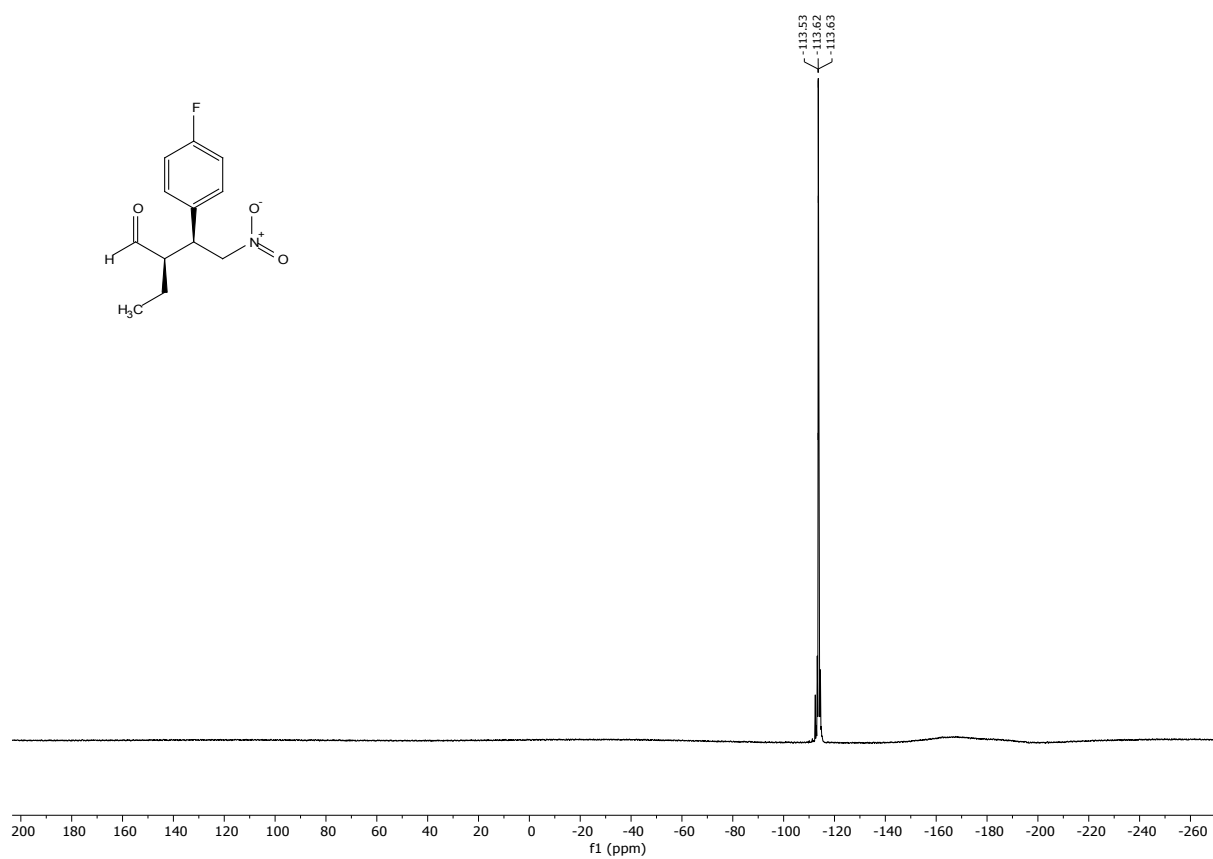
FIGURE 89. ^{19}F NMR of compound **4e** (377 MHz, CDCl$_3$).

FIGURE 90. ^{1}H NMR of compound **4f** (400 MHz, CDCl$_3$). Diastereoisomeric ratio (*syn/anti*): 72:28.

FIGURE 91. ^{13}C NMR of compound **4f** (100 MHz, CDCl$_3$).

FIGURE 92. ^{1}H NMR of compound **4g** (400 MHz, CDCl$_3$). Diastereoisomeric ratio (*syn/anti*): 64:36.

FIGURE 93. ^{13}C NMR of compound **4g** (100 MHz, CDCl$_3$).

FIGURE 94. ^{1}H NMR of compound **4h** (400 MHz, CDCl$_3$). Diastereoisomeric ratio (*syn/anti*): 67:33.

FIGURE 95. ^{13}C NMR of compound **4h** (100 MHz, CDCl$_3$).

FIGURE 96. ^{1}H NMR of compound **4i** (400 MHz, CDCl$_3$). Diastereoisomeric ratio (*syn/anti*): 88:12.
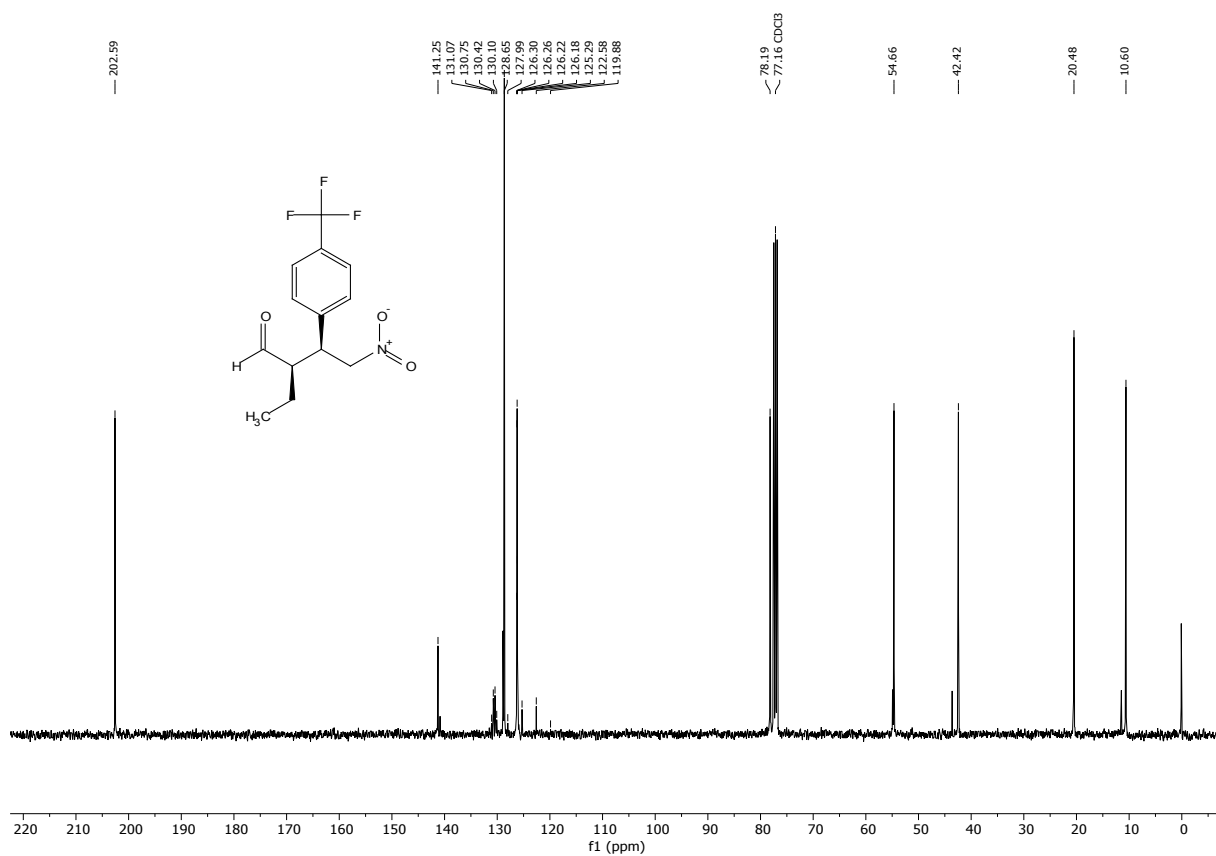
FIGURE 97. ^{13}C NMR of compound **4i** (100 MHz, CDCl$_3$).

S73

FIGURE 98. ^{19}F NMR of compound **4i** (377 MHz, CDCl$_3$).

FIGURE 99. ^1H NMR of compound **4j** (400 MHz, CDCl$_3$). Diastereoisomeric ratio (*syn/anti*): 66:34.

FIGURE 100. ^{13}C NMR of compound **4j** (100 MHz, CDCl$_3$).

FIGURE 101. ^{1}H NMR of compound **4k** (400 MHz, CDCl$_3$). Diastereoisomeric ratio (*syn/anti*): 89:11.
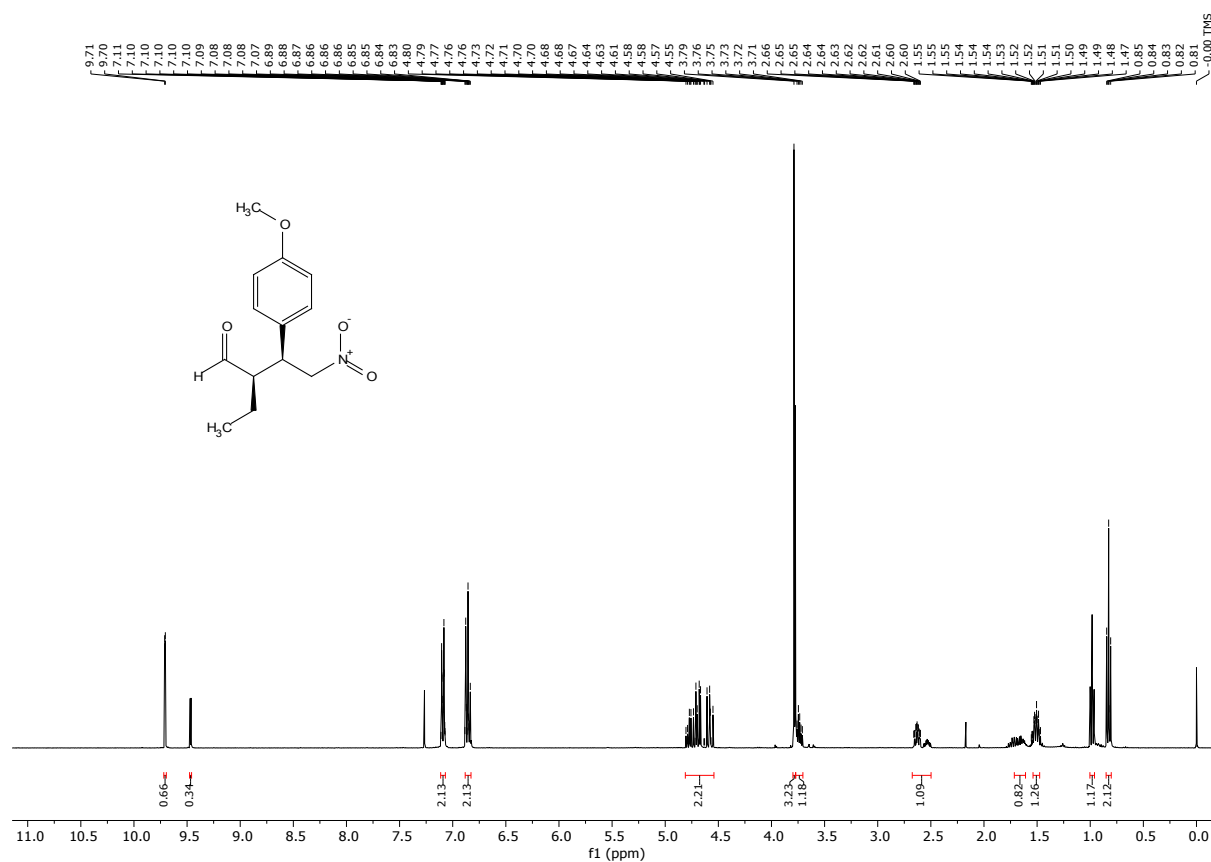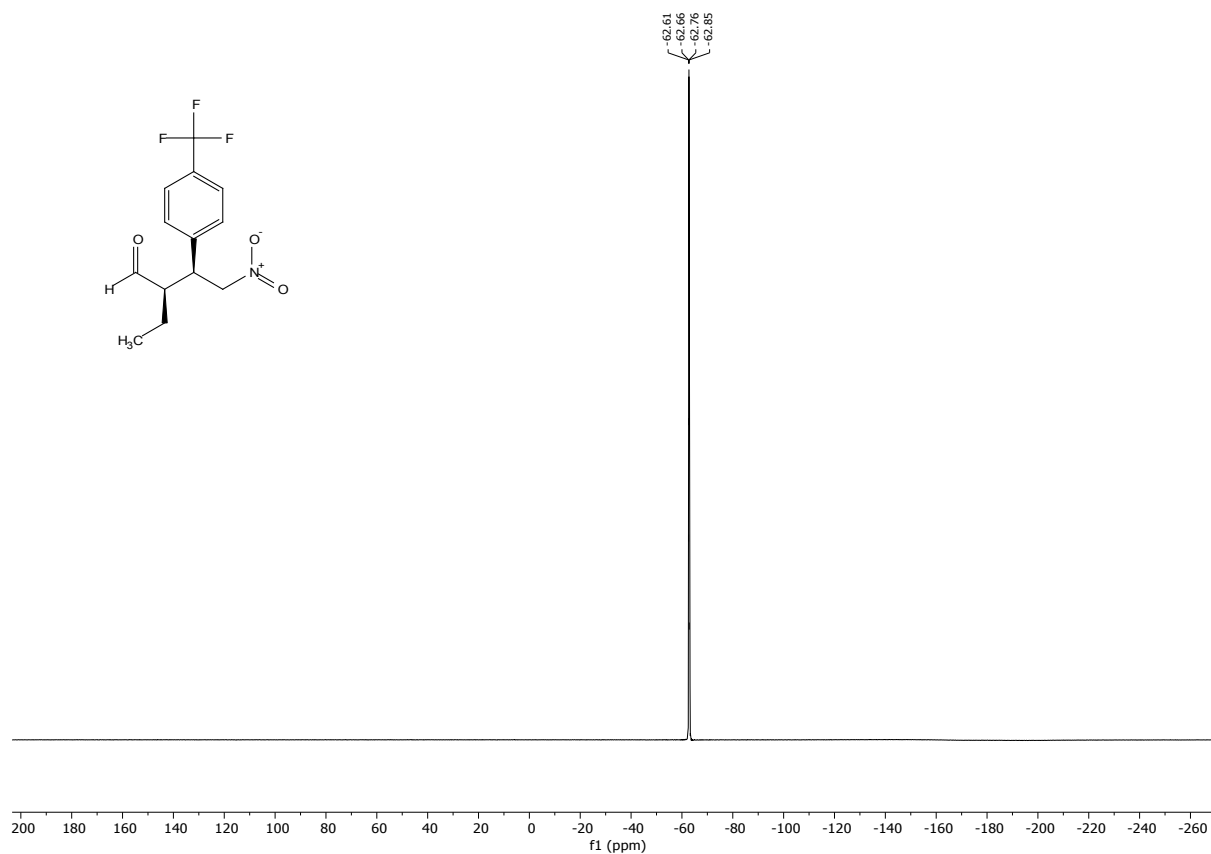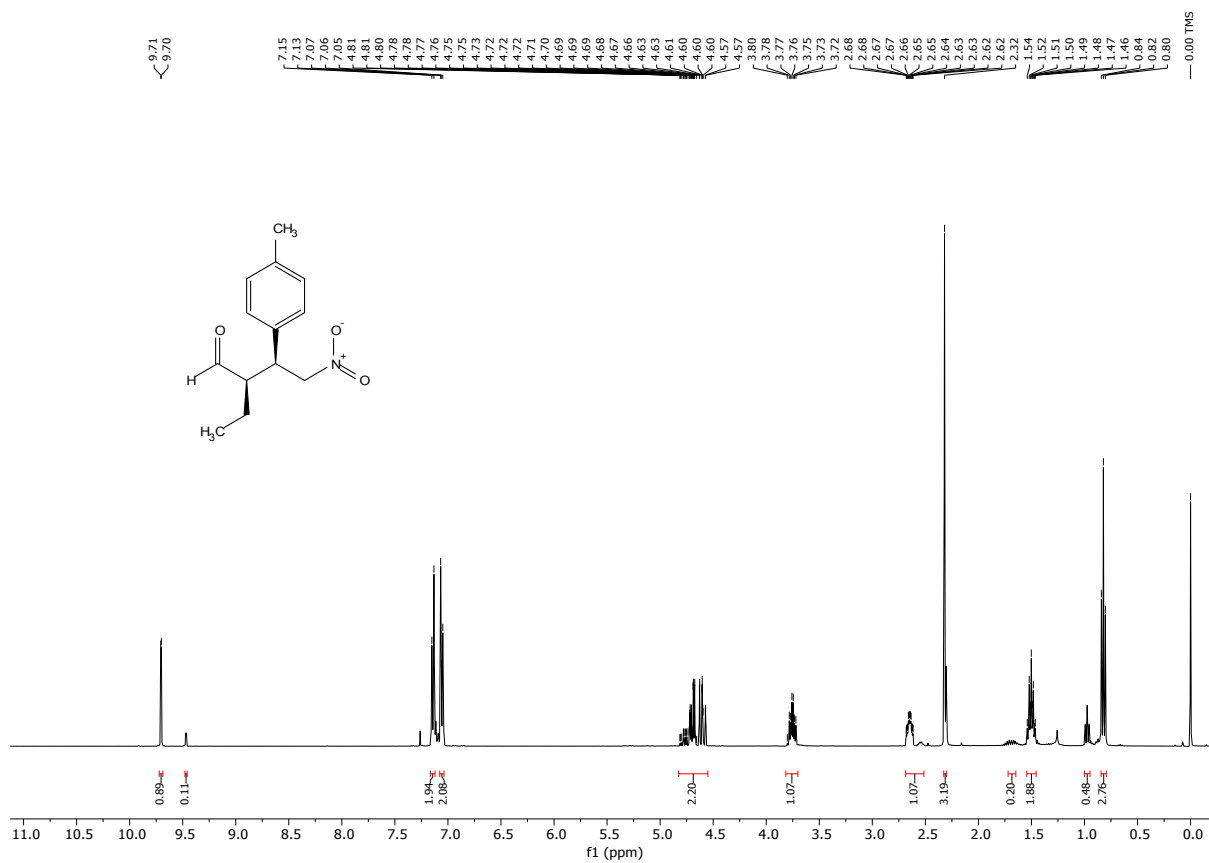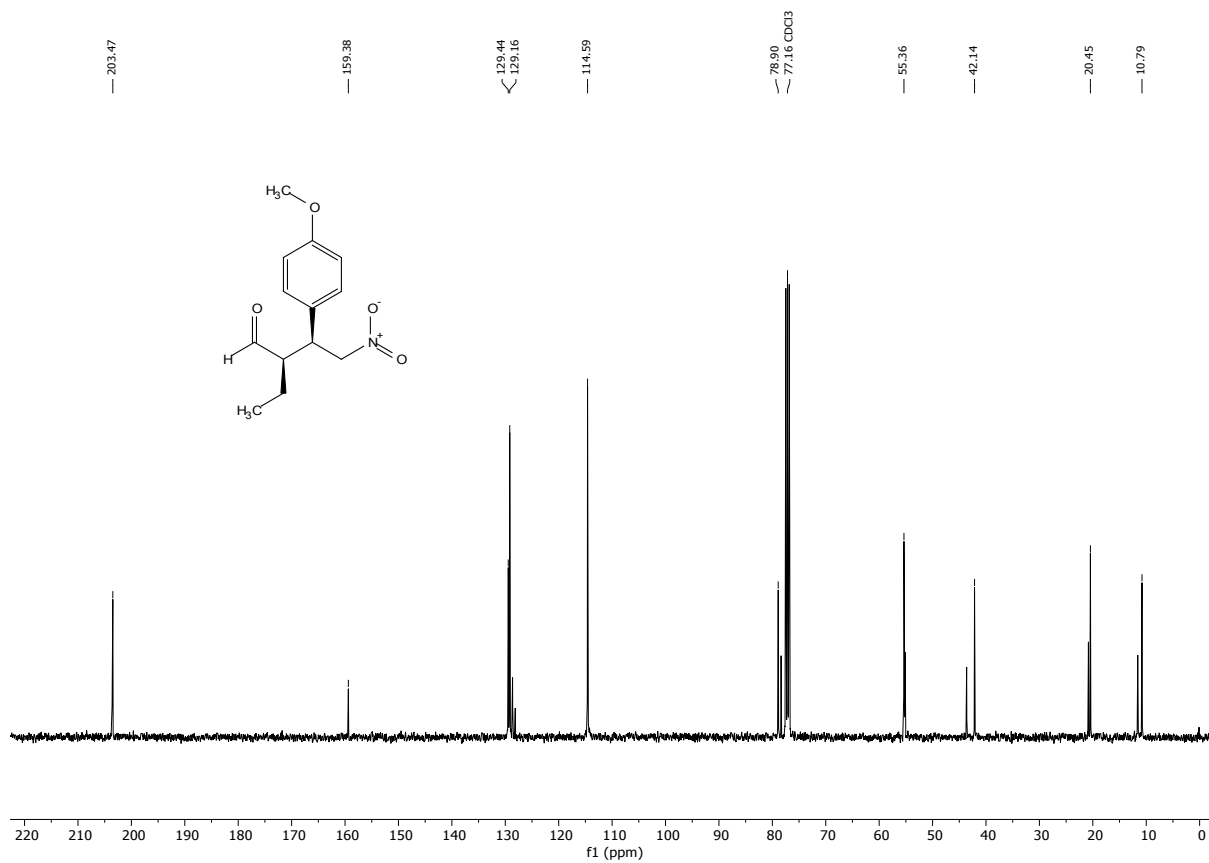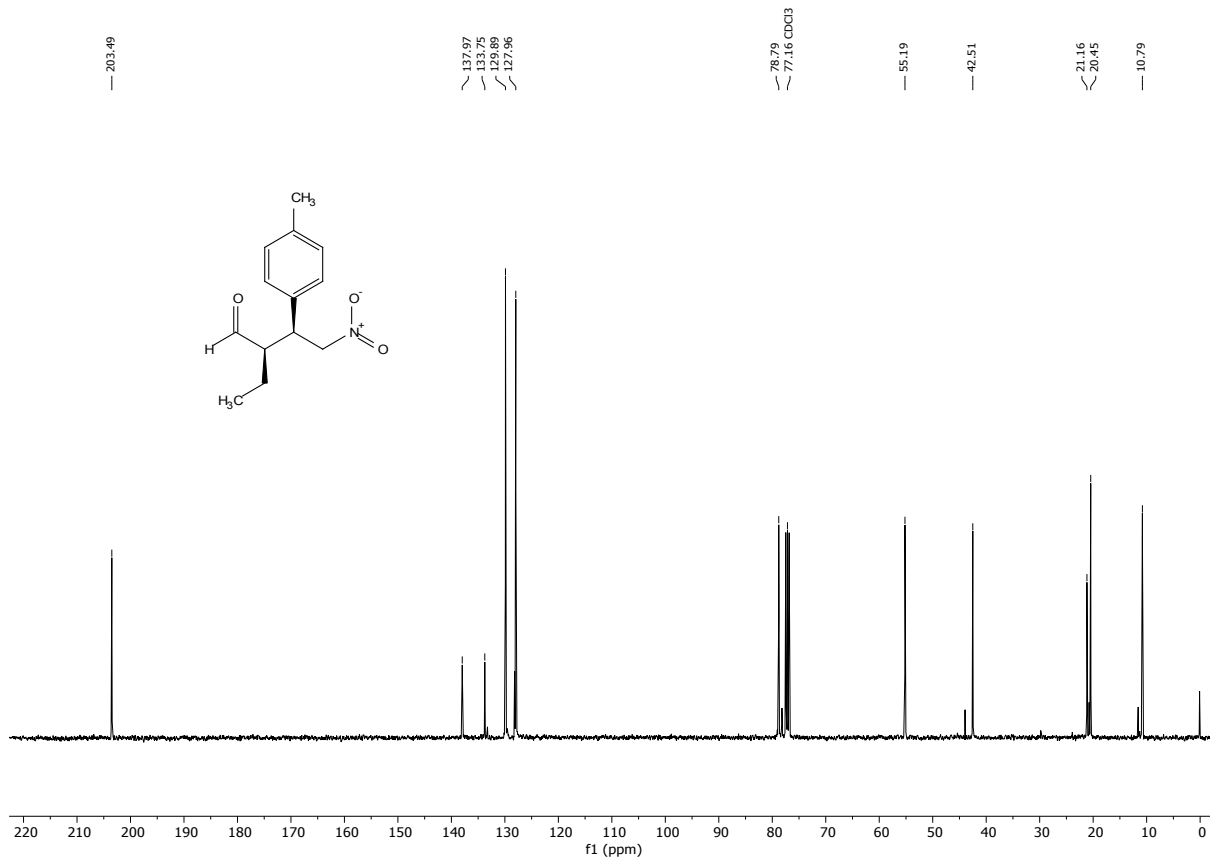
FIGURE 102. ^{13}C NMR of compound **4k** (100 MHz, CDCl$_3$).
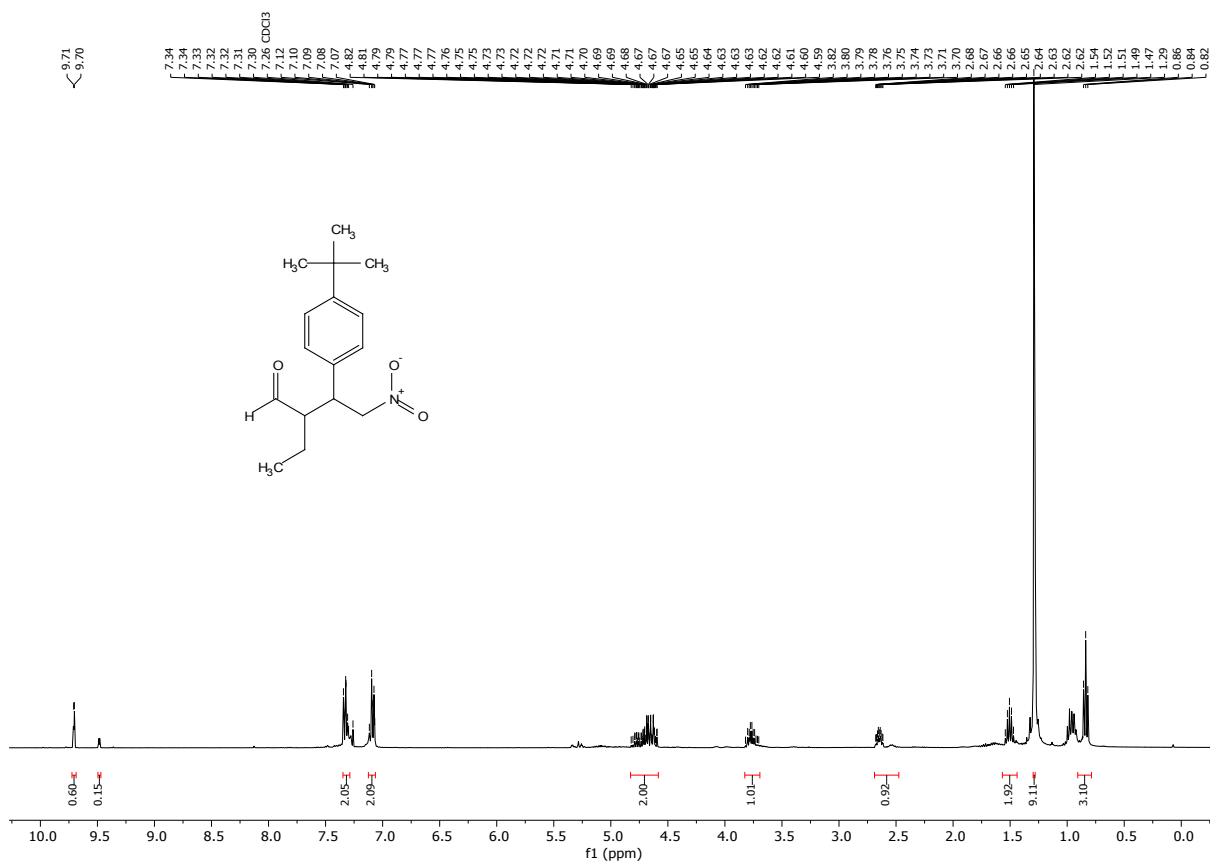
FIGURE 103. ^1H NMR of compound **4l** (400 MHz, CDCl$_3$). Diastereoisomeric ratio (*syn/anti*): 80:20.
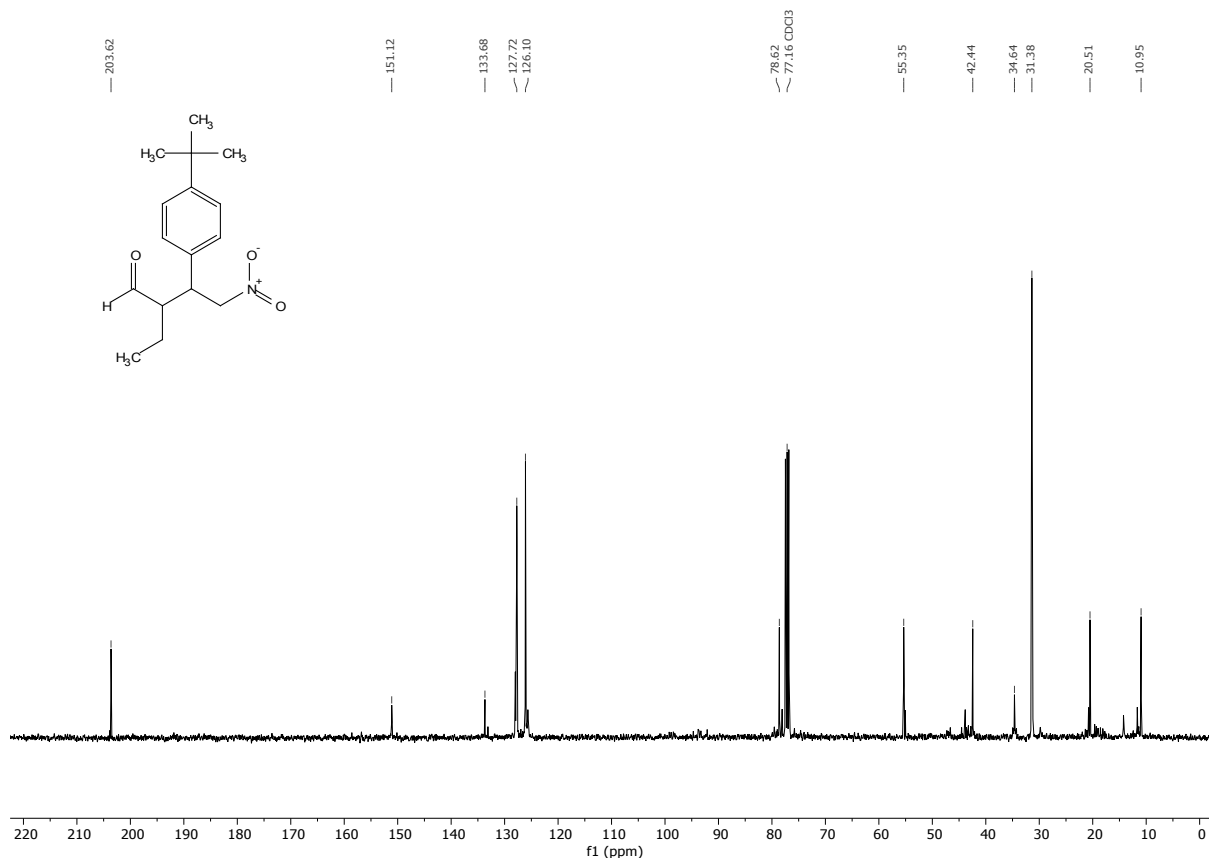
FIGURE 104. ^{13}C NMR of compound **4l** (100 MHz, CDCl$_3$).

FIGURE 105. ^{1}H NMR of compound **4m** (400 MHz, CDCl$_3$). Diastereoisomeric ratio (*syn/anti*): 74:26.

FIGURE 106. ^{13}C NMR of compound **4m** (100 MHz, CDCl$_3$).

FIGURE 107. ^{1}H NMR of compound **4n** (400 MHz, CDCl$_3$). Diastereoisomeric ratio (*syn/anti*): 87:13.

FIGURE 108. ^{13}C NMR of compound **4n** (100 MHz, CDCl$_3$).

FIGURE 109. ^1H NMR of compound **4o** (400 MHz, CDCl$_3$). Diastereoisomeric ratio (*syn/anti*): 80:20.
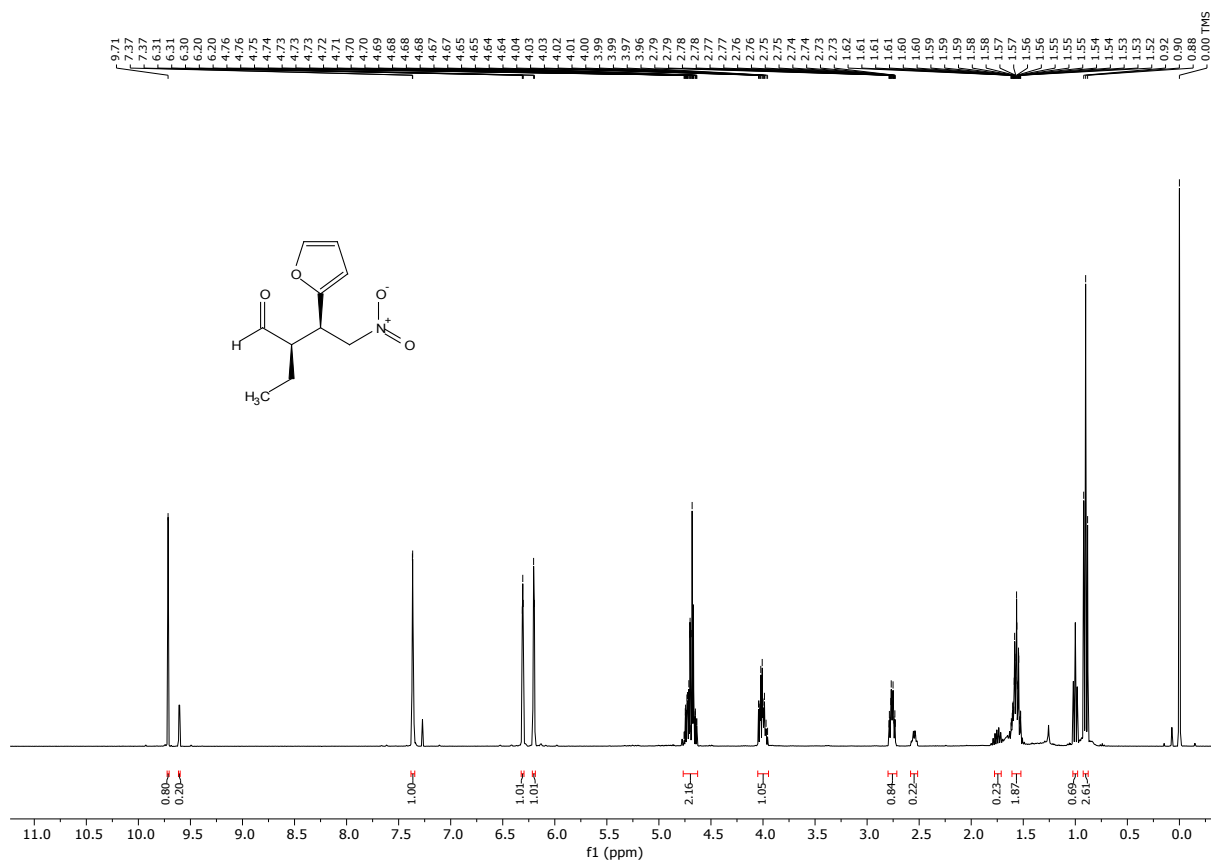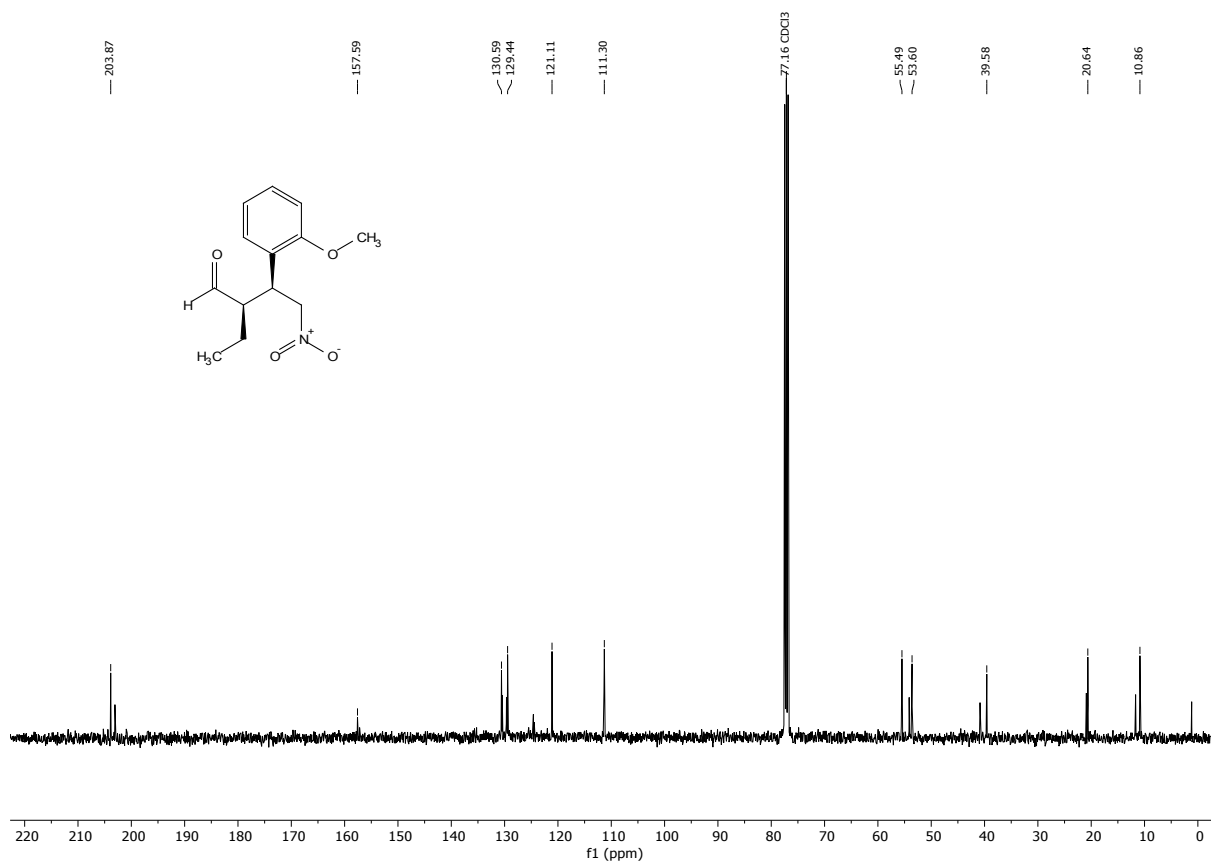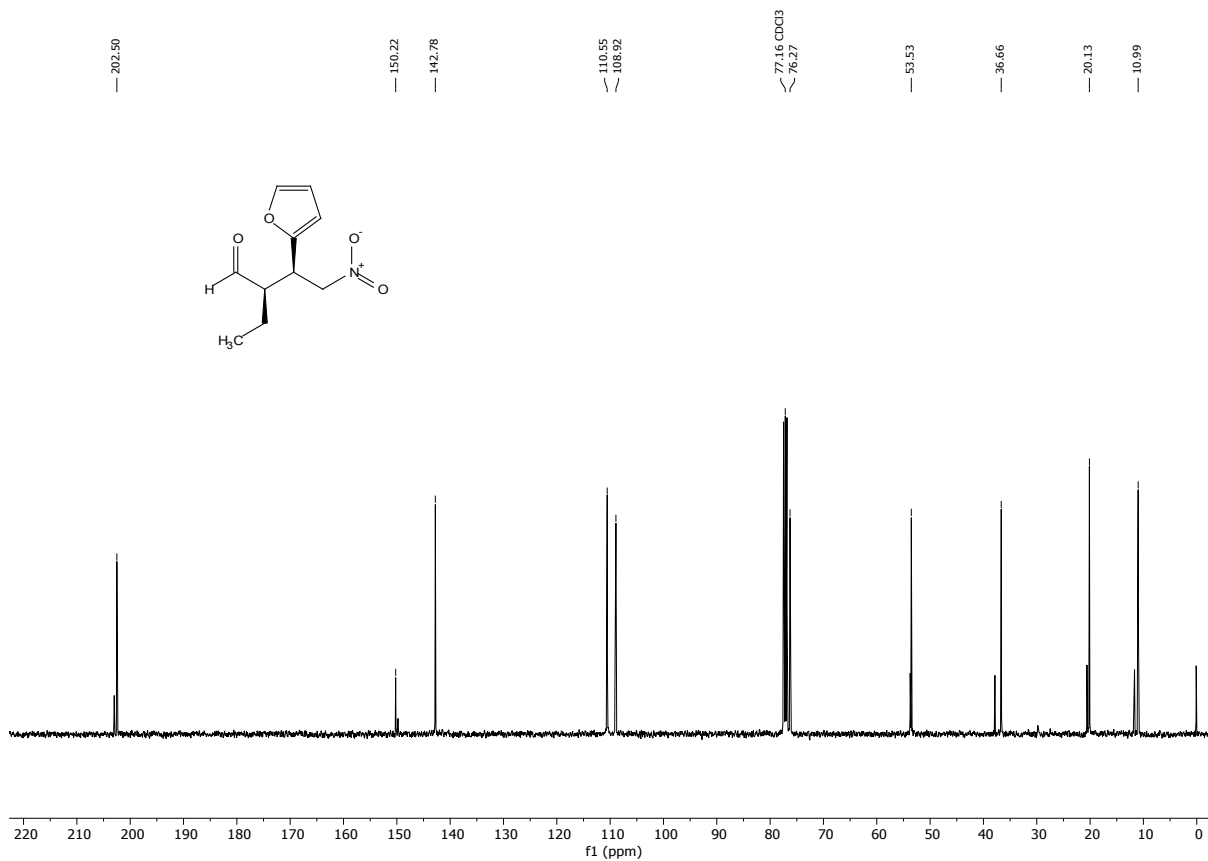
FIGURE 110. ^{13}C NMR of compound **4o** (100 MHz, CDCl$_3$).
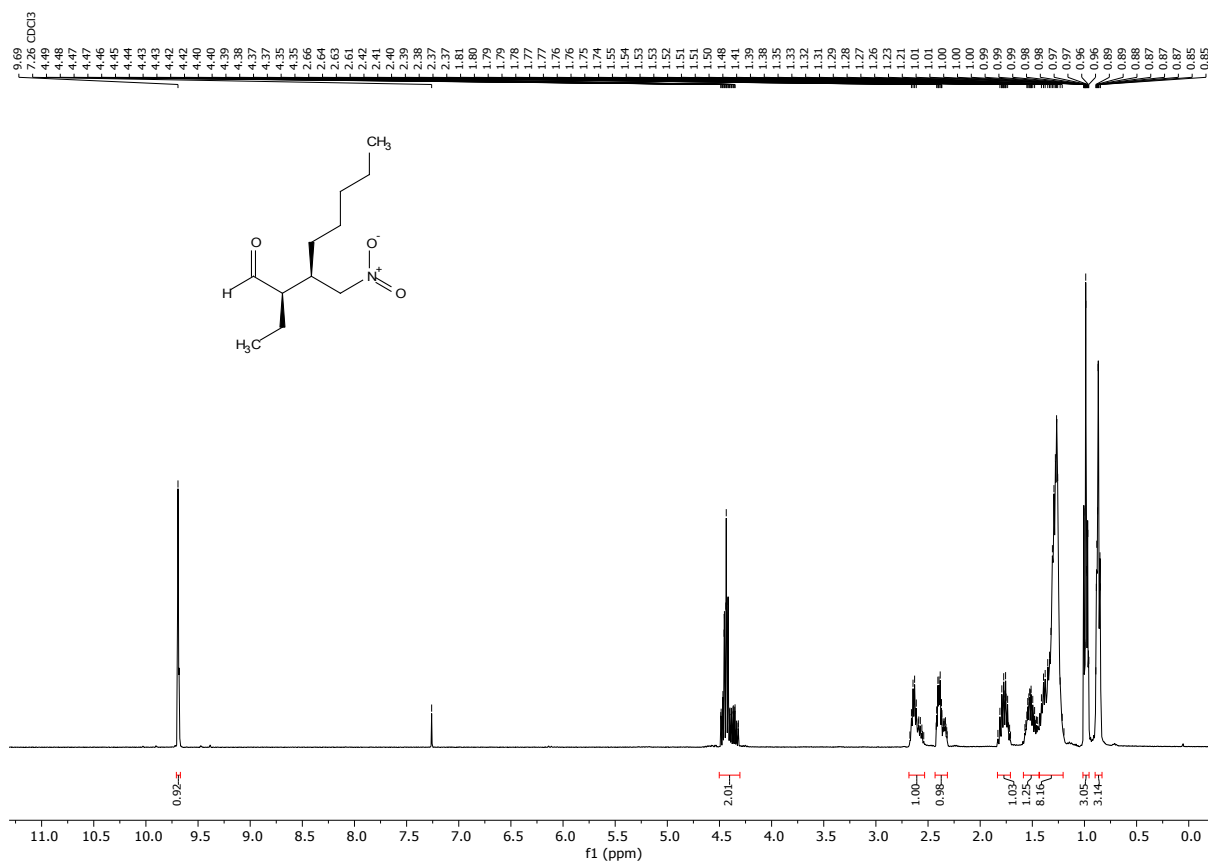
FIGURE 111. ^{1}H NMR of compound **4p** (400 MHz, CDCl$_3$). Diastereoisomeric ratio (*syn/anti*): 81:19.

S80
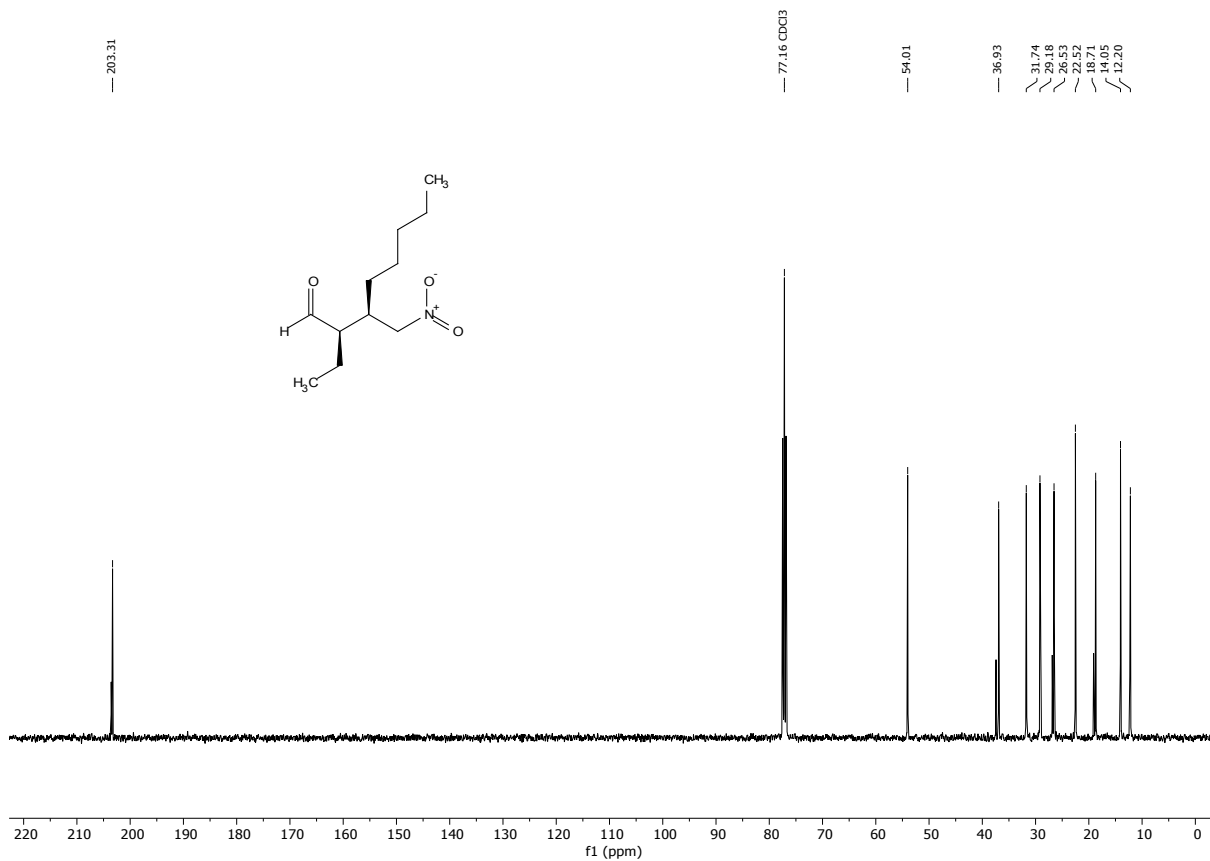
FIGURE 112. ^{13}C NMR of compound **4p** (100 MHz, CDCl$_3$).
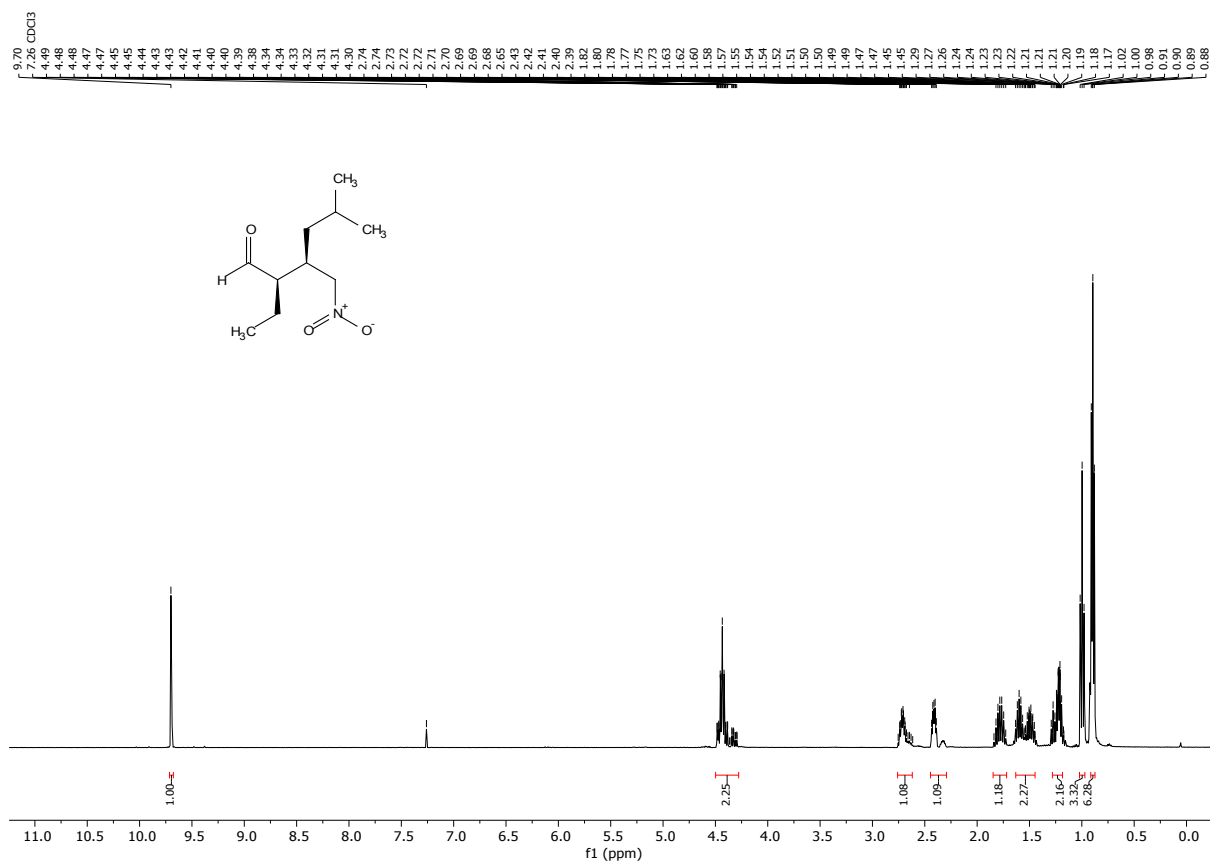
FIGURE 113. ^1H NMR of compound **4q** (400 MHz, CDCl$_3$). Diastereoisomeric ratio (*syn/anti*): 88:12.
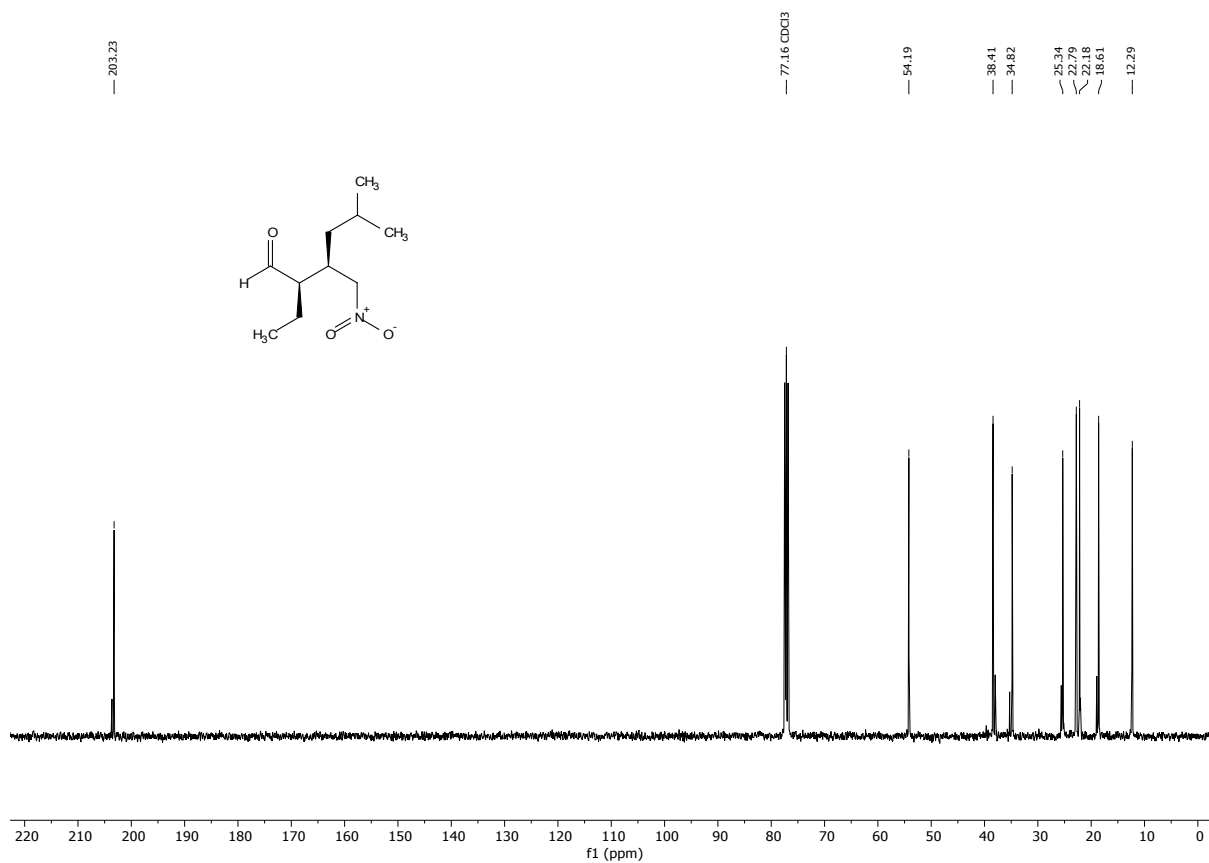
FIGURE 114. ^{13}C NMR of compound **4q** (100 MHz, CDCl$_3$).

18. NMR Spectra and Chromatograms: Scope

FIGURE 115. ^1H NMR of crude compound **4b** (400 MHz, CDCl$_3$) obtained by the Michael reaction catalyzed by 2.5 mol% of compound **3e**. Diastereoisomeric ratio (*syn/anti*): 92:08. TABLE 4, Entry 2.
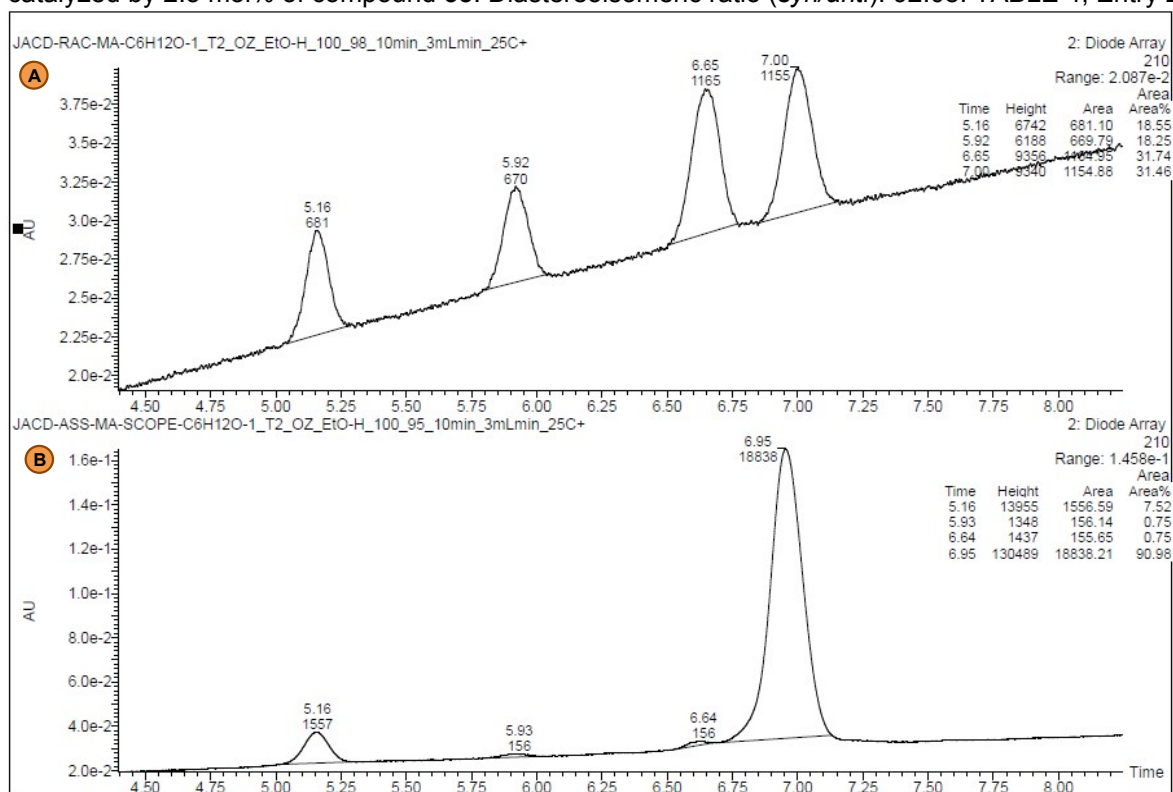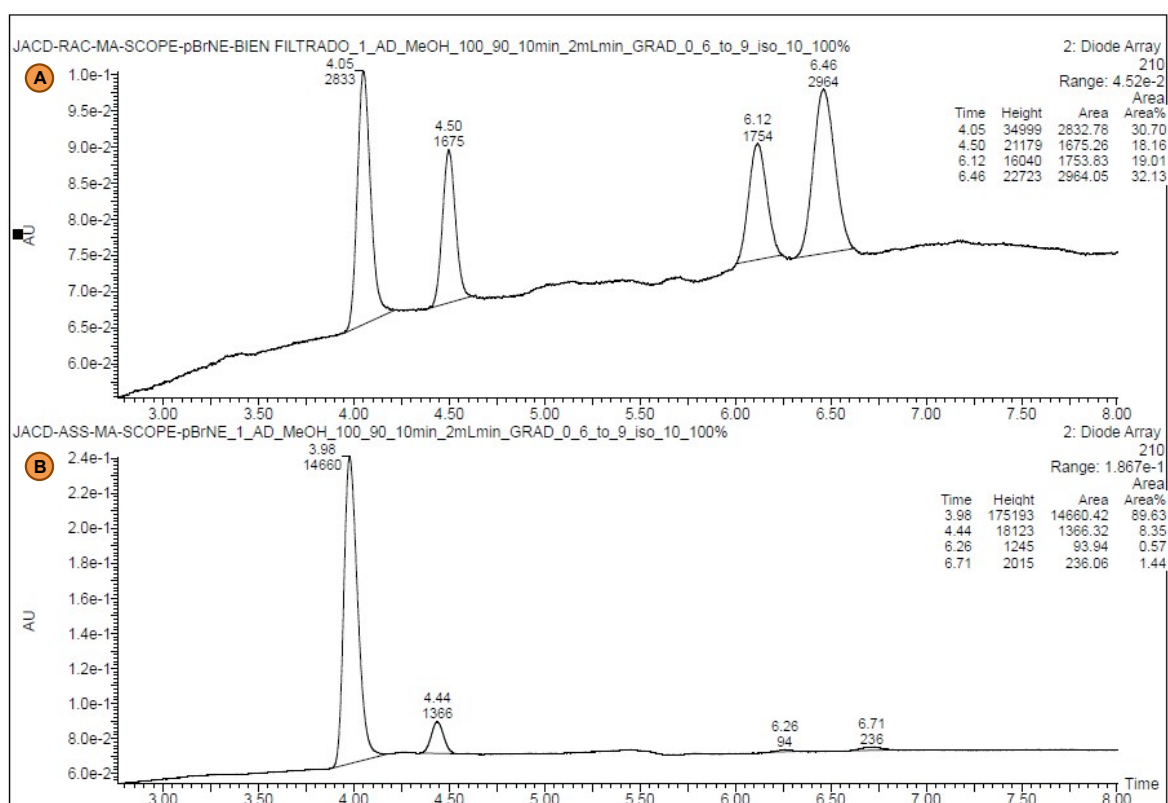

FIGURE 116. (a) Chiral UPC^2 of racemic 2-(2-nitro-1-phenylethyl) hexanal (**4b**); (b) Chiral UPC^2 of 2-(2-nitro-1-phenylethyl) hexanal (**4b**) obtained by the Michael reaction catalyzed by 2.5 mol% of compound **3e**. Trefoil CEL2, Grad: CO2/EtOH 100-0% to 95-5 % in 10 min at 3 ml/min at 25°C. UVdetection at 210 nm: **R$_t$**: (syn, minor) = 6.64 min, (syn, major) = 6.95 min. TABLE 4, Entry 2.
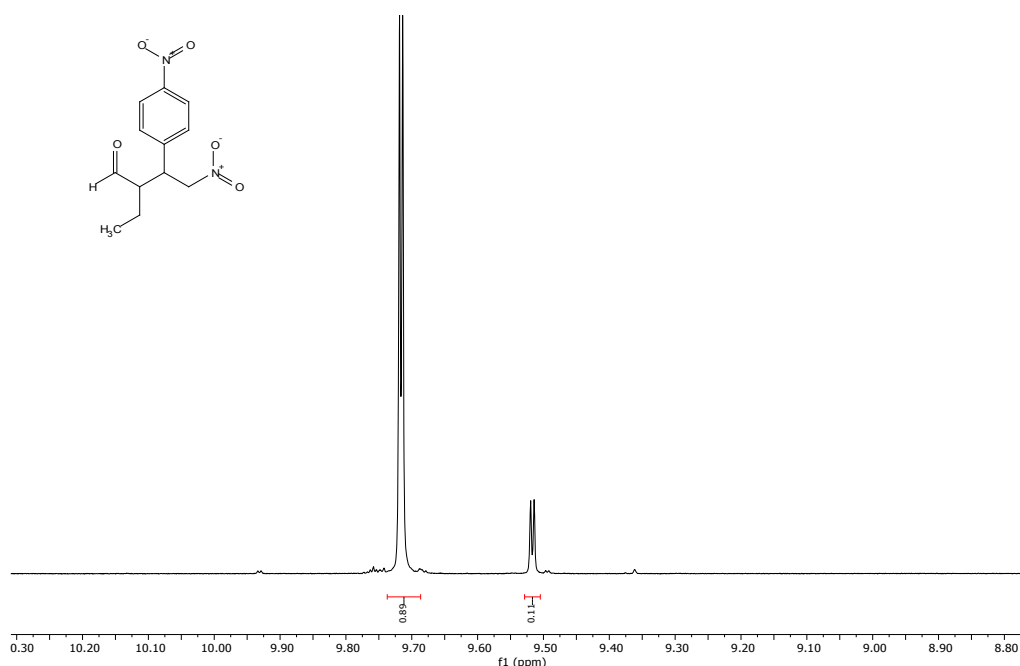
FIGURE 117. 1H NMR of crude compound **4c** (400 MHz, CDCl₃) obtained by the Michael reaction catalyzed by 2.5 mol% of compound **3e**. Diastereoisomeric ratio (*syn/anti*): 99:01. TABLE 4, Entry 3.
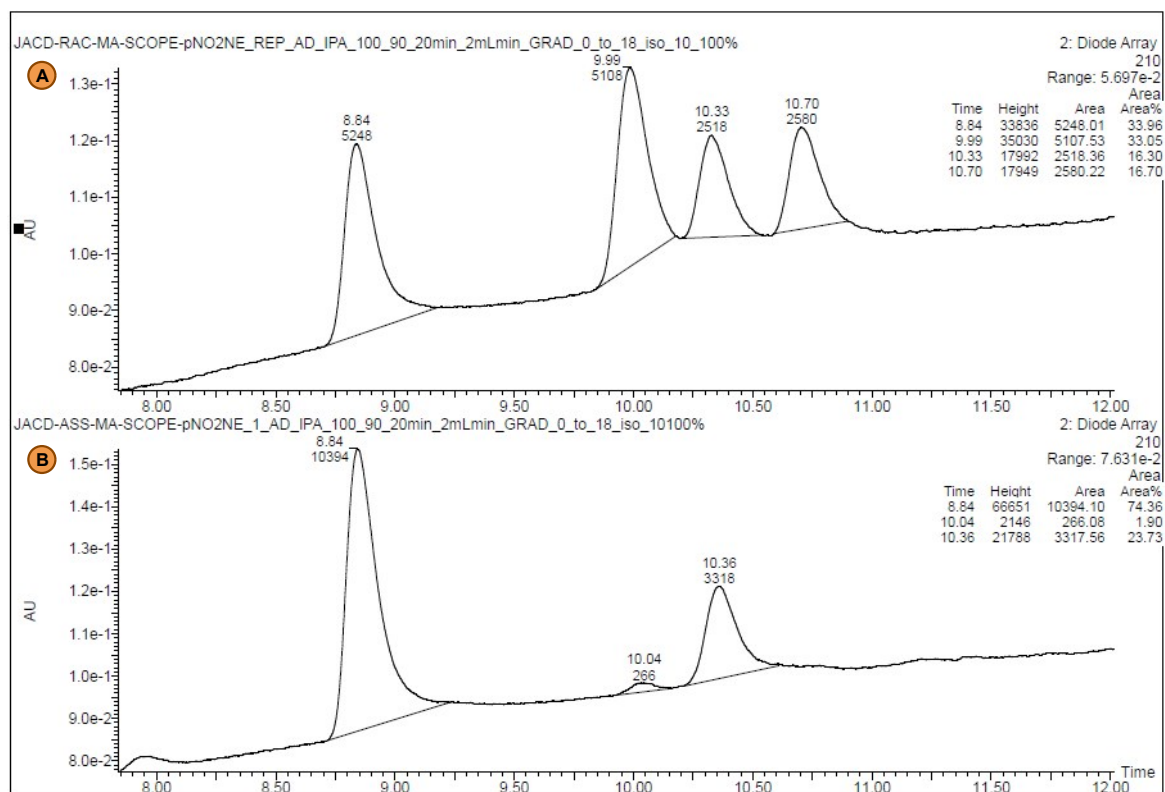

FIGURE 118. (a) Chiral UPC² of racemic 2-isopropyl-4-nitro-3-phenylbutanal (**4c**); b) Chiral UPC² of 2-isopropyl-4-nitro-3-phenylbutanal **4c** obtained by the Michael reaction catalyzed by 2.5 mol% of compound **3e**. Trefoil CEL2, **Grad:** CO_2/EtOH 100-0% to 95-5 % in 10 min at 3 ml/min at 25°C. UV detection at 210 nm: R_t: (syn, minor) = 3.68 min, (syn, major) = 3.97 min. TABLE 4, Entry 3.
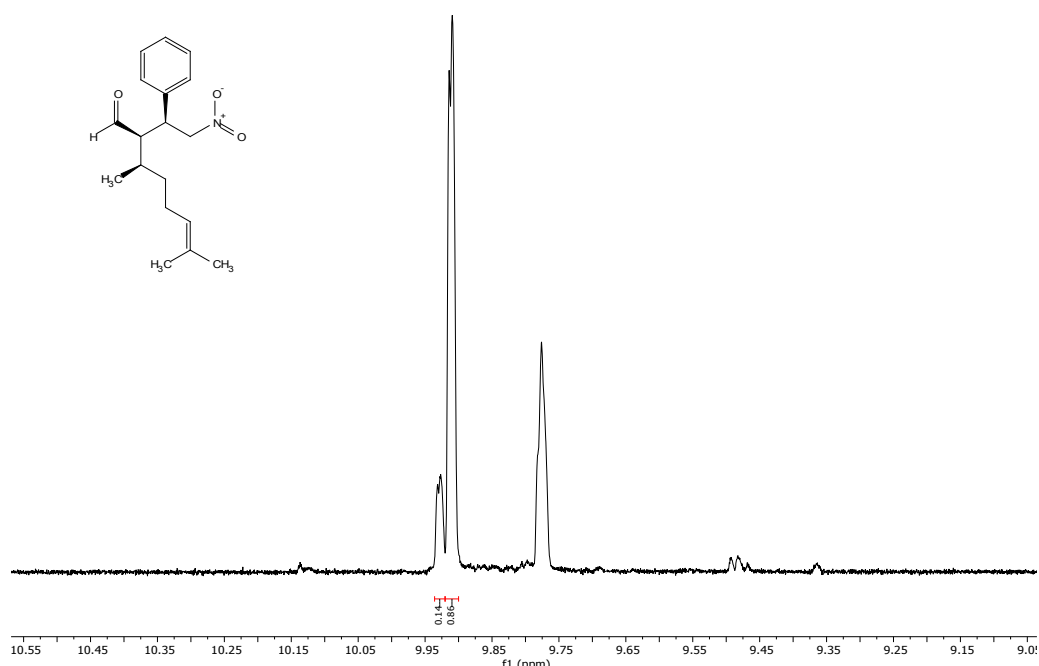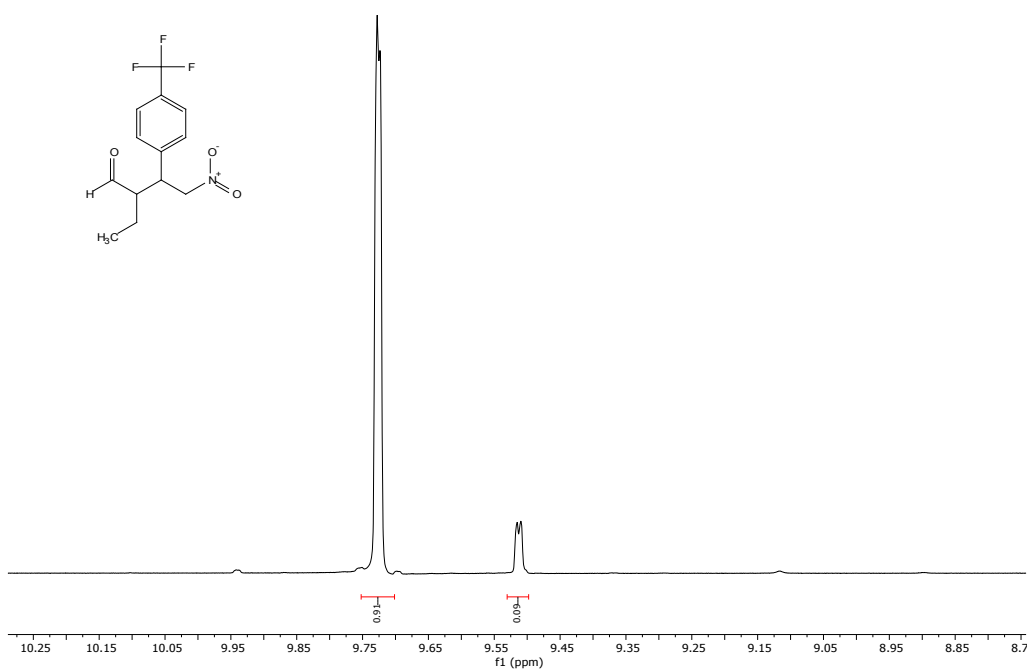
FIGURE 119. ^{1}H NMR of crude compound **4d** (400 MHz, CDCl$_3$) obtained by the Michael reaction catalyzed by 2.5 mol% of compound **3e**. Diastereoisomeric ratio (*syn/anti*): 86:14. TABLE 4, Entry 4.
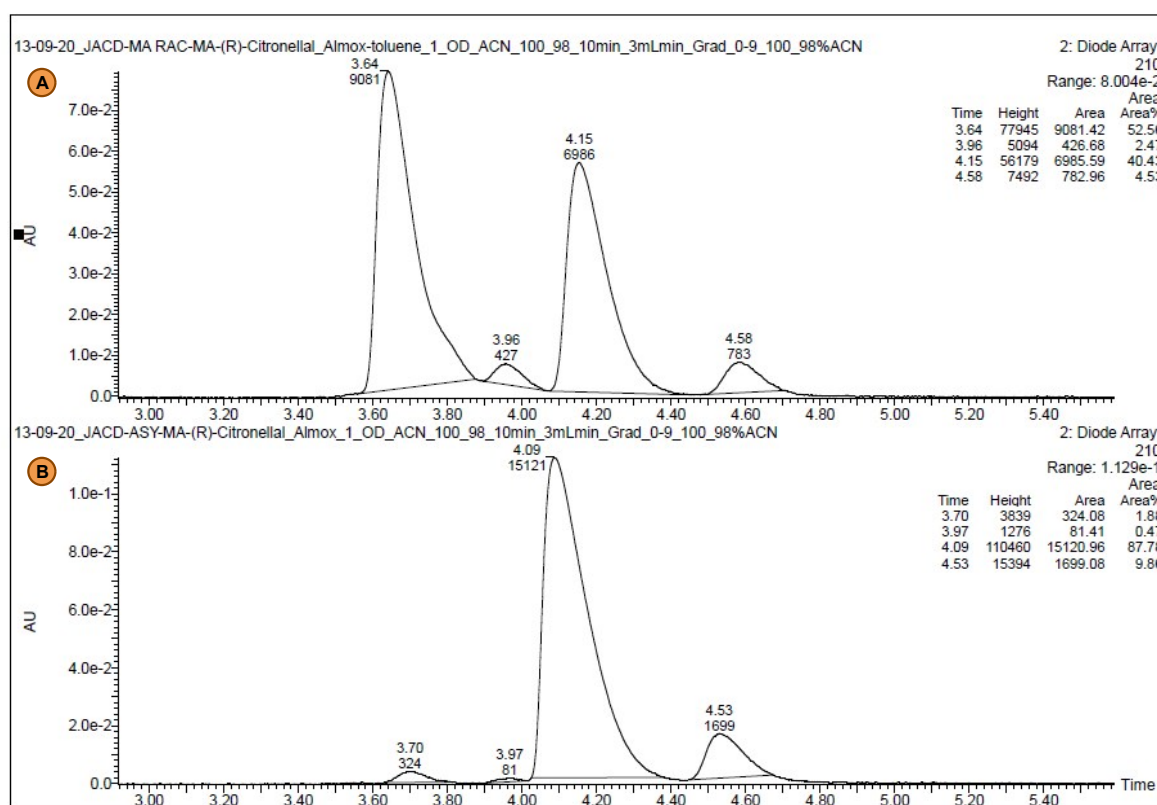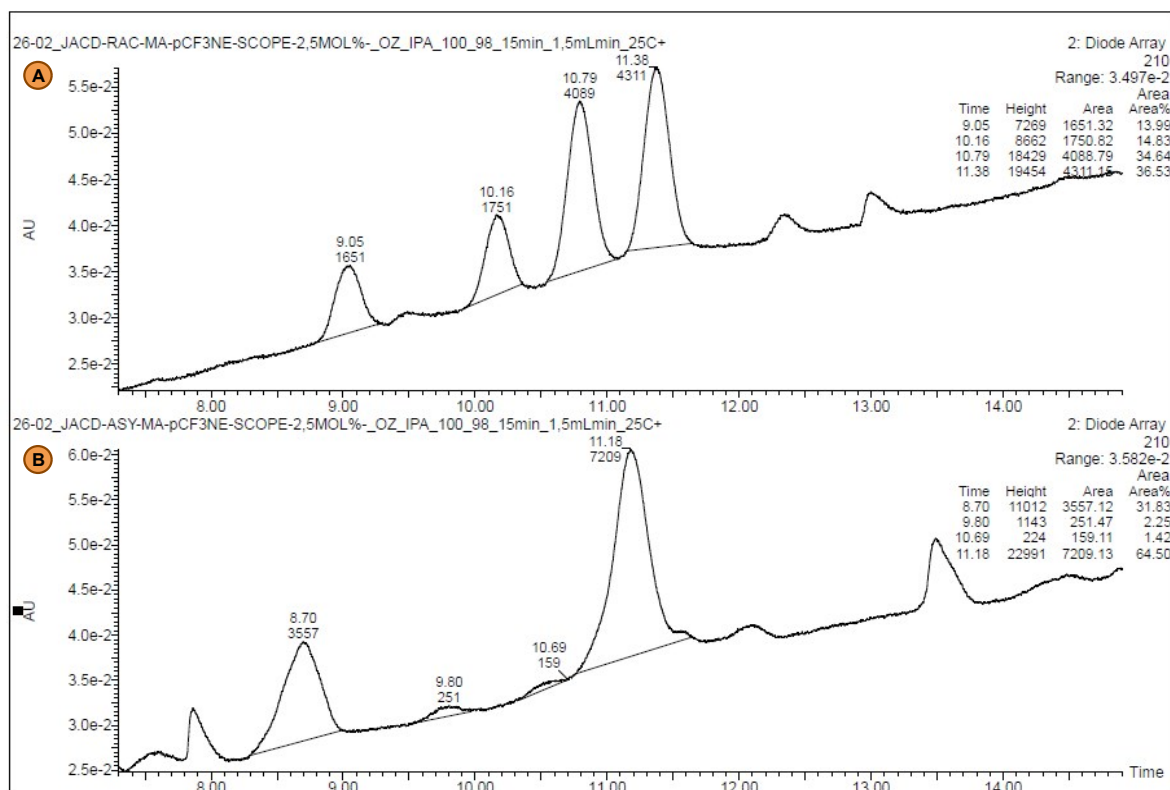

FIGURE 120. (a) Chiral UPC^2 of racemic 3,7-dimethyl-2-(2-nitro-1-phenylethyl)oct-6-enal (**4d**); (b) Chiral UPC^2 of 3,7-dimethyl-2-(2-nitro-1-phenylethyl)oct-6-enal (**4d**) obtained by the Michael reaction catalyzed by 2.5 mol% of compound **3e**. Trefoil CEL1, Grad: CO$_2$/ACN 100-0% to 98-2 % in 9 min; 100-0% in 1 min at 3 ml/min at 25°C. UV detection at 210 nm: **R$_t$**: (syn, minor) = 3.70 min, (syn, major) = 4.09 min. TABLE 4, Entry 4.
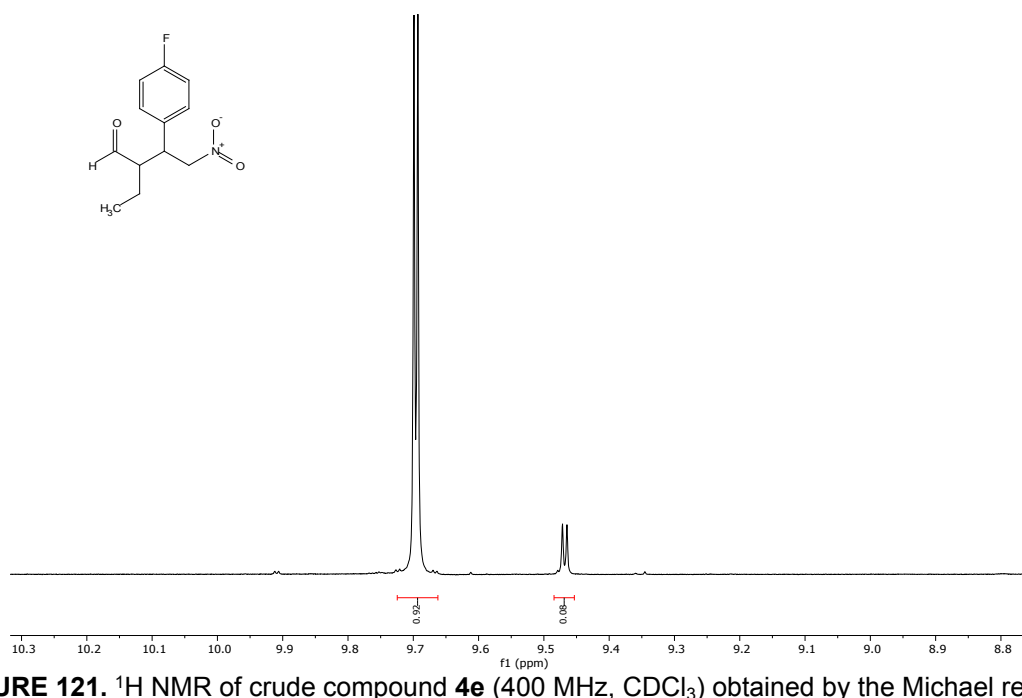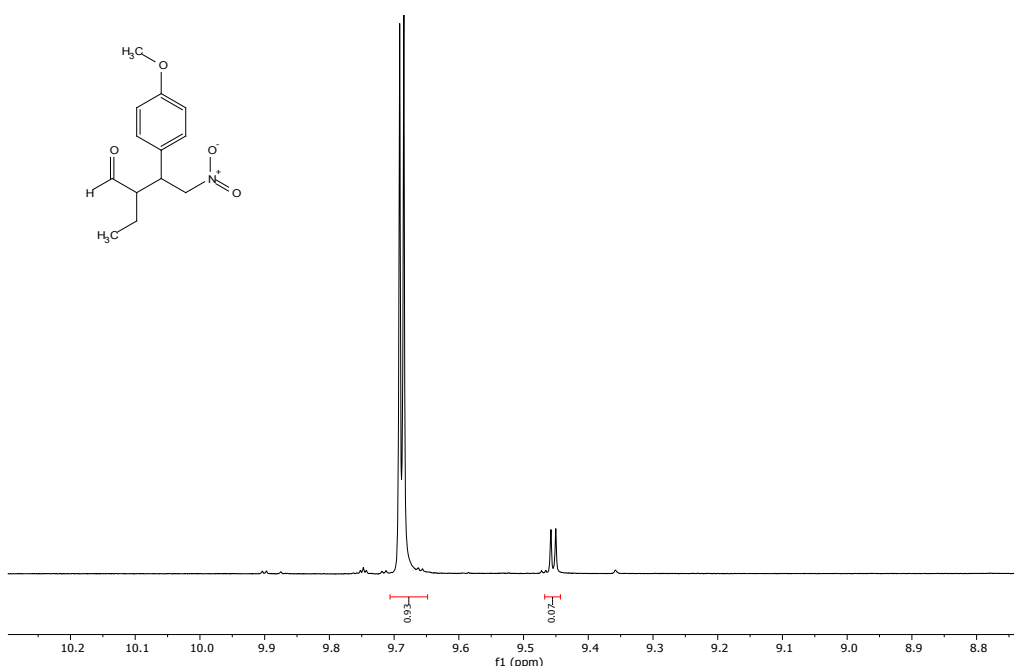
FIGURE 121. ^1H NMR of crude compound **4e** (400 MHz, CDCl$_3$) obtained by the Michael reaction catalyzed by 2.5 mol% of compound **3e**. Diastereoisomeric ratio (*syn/anti*): 92:08. TABLE 4, Entry 5.
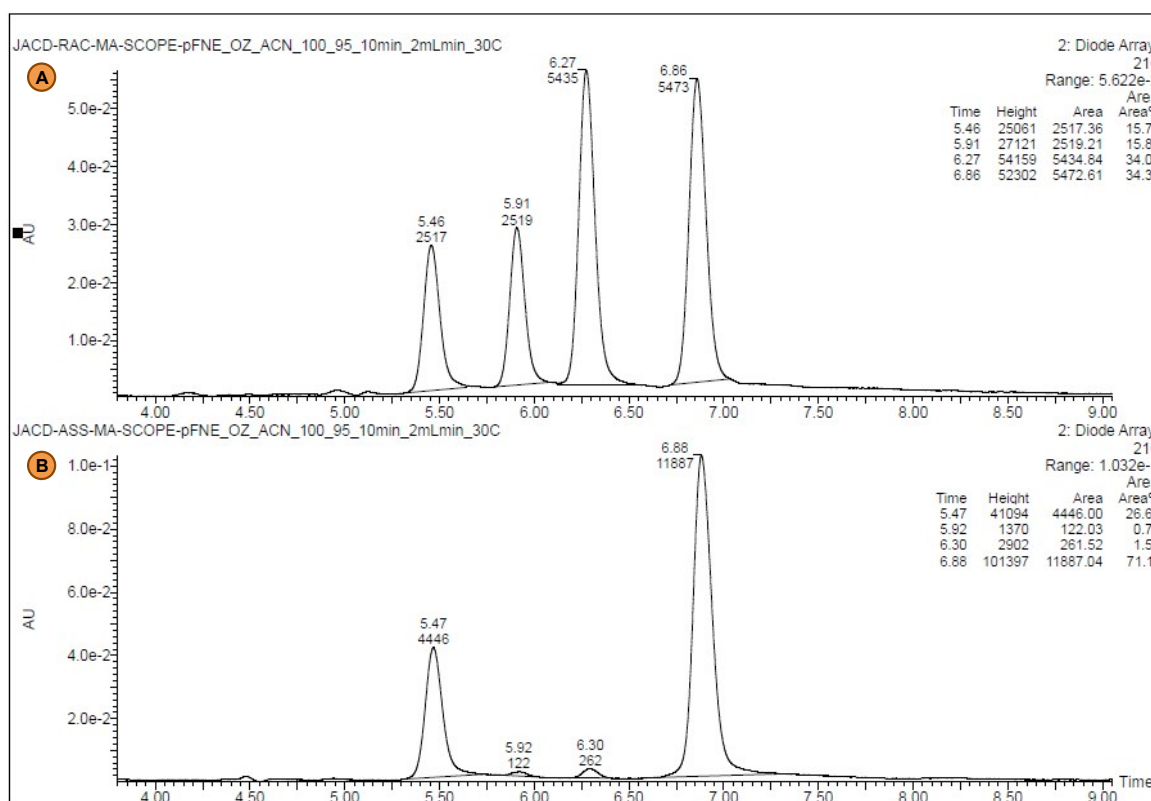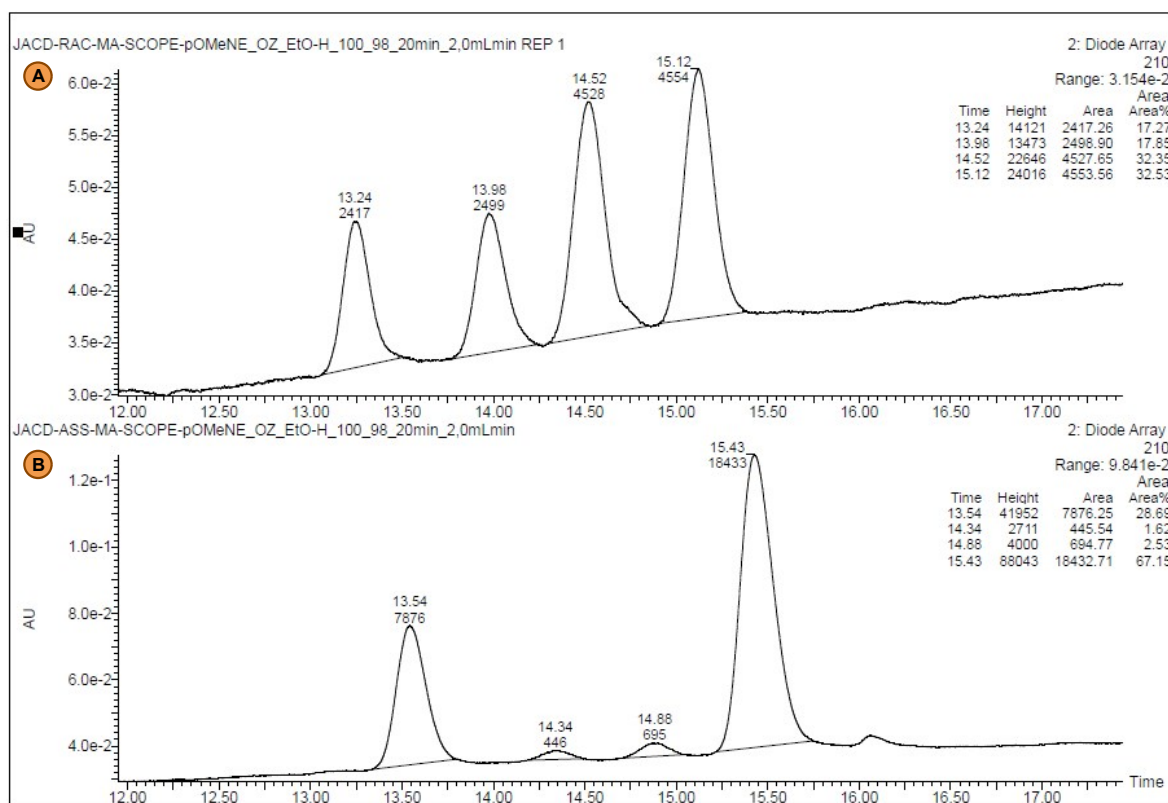

FIGURE 122. (a) Chiral UPC^2 of racemic 2-ethyl-3-(4-fluorophenyl)-4-nitrobutanal (**4e**); (b) Chiral UPC^2 of 2-ethyl-3-(4-fluorophenyl)-4-nitrobutanal (**4e**) obtained by the Michael reaction catalyzed by 2.5 mol% of compound **3e**. Trefoil CEL2, **Grad:** CO$_2$/EtOH 100-0% to 95-5% in 9 min; 100-0 % in 1 min at 2 ml/min at 25°C. UV detection at 210 nm: **R$_t$:** (syn, minor) = 6.30 min, (syn, major) = 6.88 min. TABLE 4, Entry 5.
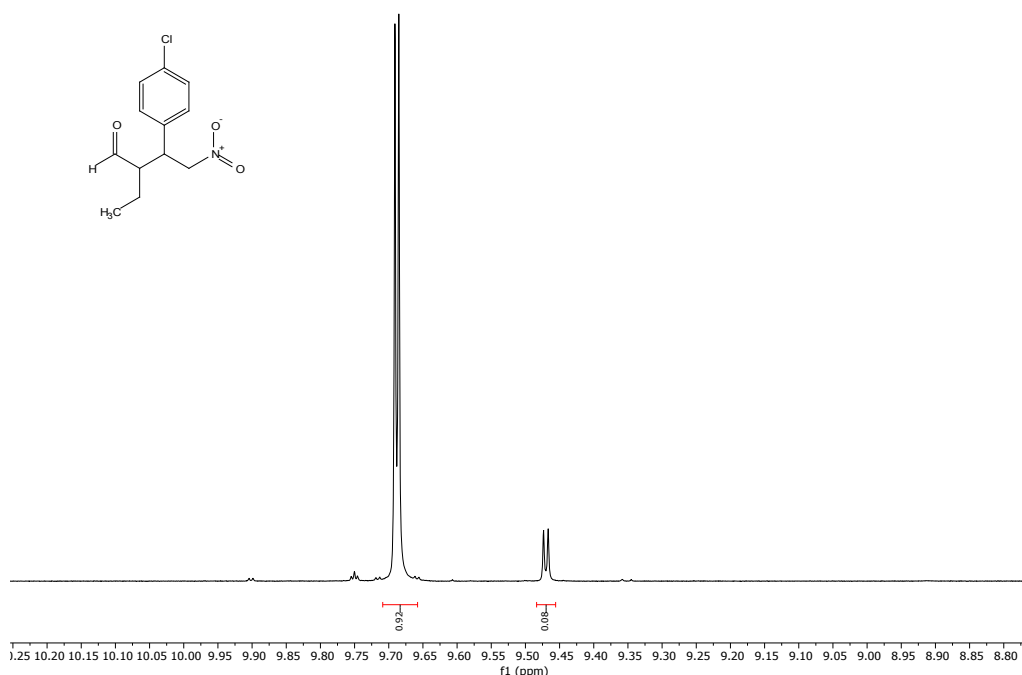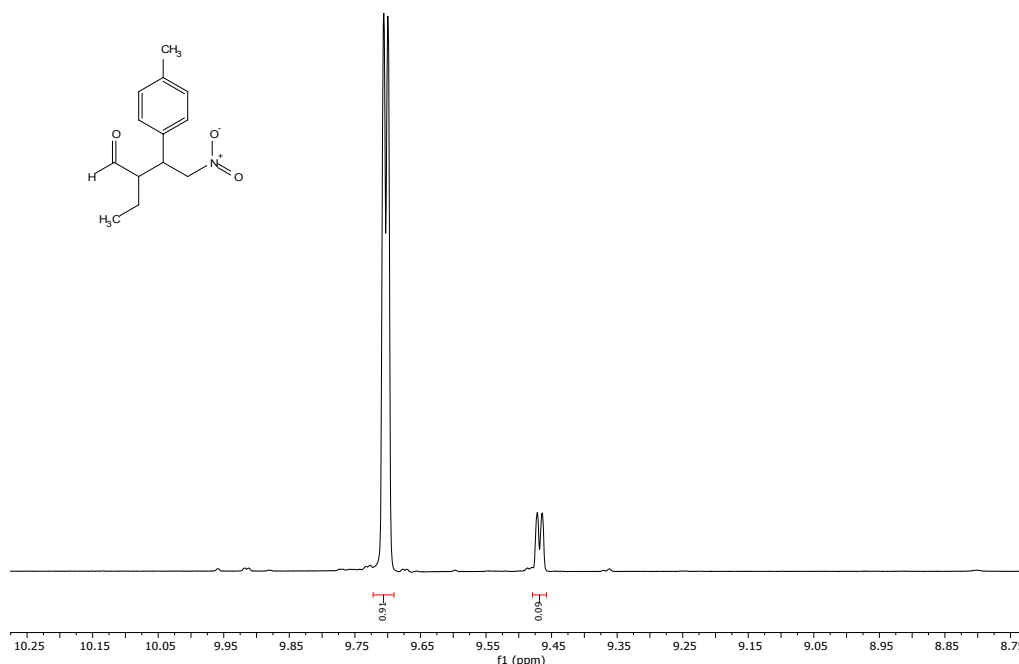
FIGURE 123. ^{1}H NMR of crude compoundcrude compound **4f** (400 MHz, CDCl$_3$) obtained by the Michael reaction catalyzed by 2.5 mol% of compound **3e**. Diastereoisomeric ratio (*syn/anti*): 92:08. TABLE 4, Entry 6.
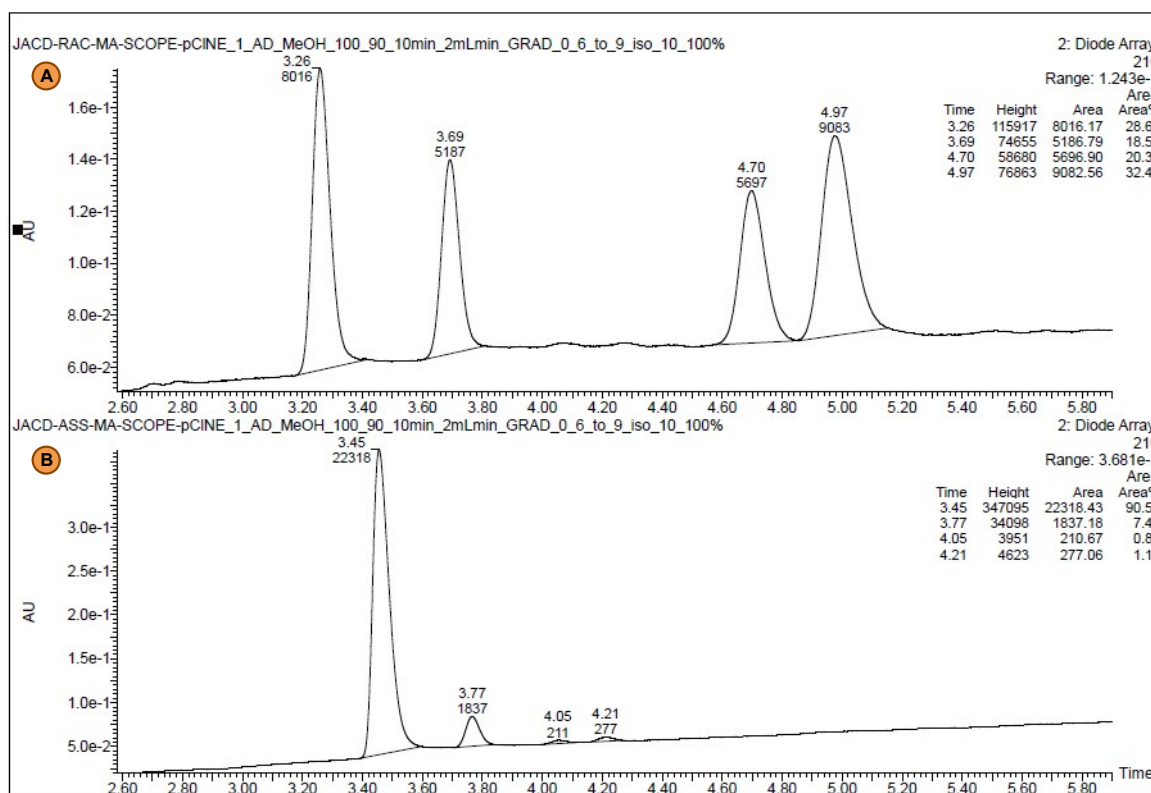
FIGURE 124. (a) Chiral UPC^2 of racemic 3-(4-chlorophenyl)-2-ethyl-4-nitrobutanal (**4f**); (b) Chiral UPC^2 of 3-(4-chlorophenyl)-2-ethyl-4-nitrobutanal (**4f**) obtained by the Michael reaction catalyzed by 2.5 mol% of compound **3e**. Trefoil AMY1, **Grad:** CO$_2$/MeOH 100-0% to 90-10 % in 6 min; 90-10 % in 3 min; 100-0 % in 1 min at 2 ml/min at 25°C. UV detection at 210 nm: **R$_t$**: (syn, major) = 3.45 min, (syn, minor) = 4.21 min. TABLE 4, Entry 6.
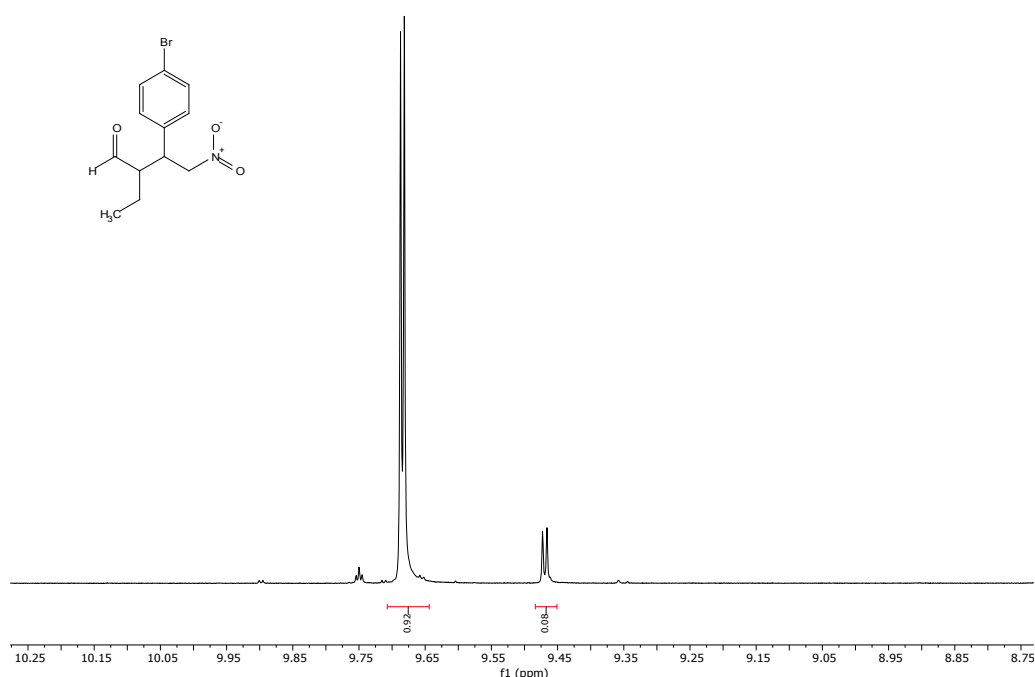
FIGURE 125. ^{1}H NMR of crude compound **4g** (400 MHz, CDCl$_3$) obtained by the Michael reaction catalyzed by 2.5 mol% of compound **3e**. Diastereoisomeric ratio (*syn/anti*): 92:08. TABLE 4, Entry 7.
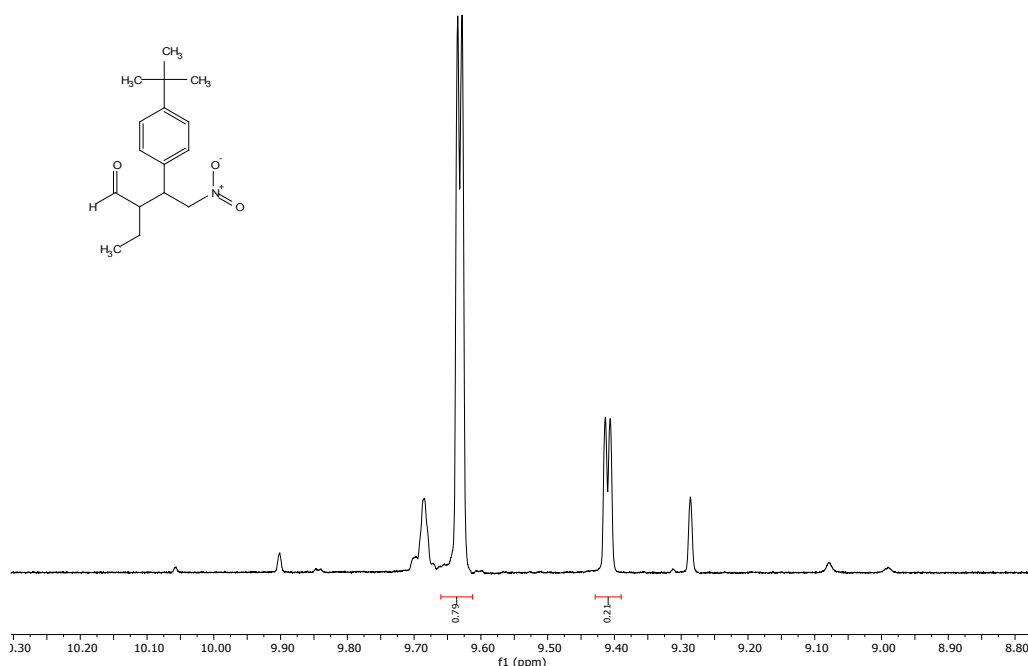

FIGURE 126. (a) Chiral UPC^2 of racemic 3-(4-bromophenyl)-2-ethyl-4-nitrobutanal (**4g**); (b) Chiral UPC^2 of 3-(4-bromophenyl)-2-ethyl-4-nitrobutanal (**4g**) obtained by the Michael reaction catalyzed by 2.5 mol% of compound **3e**. Trefoil AMY1, **Grad:** CO$_2$/MeOH 100-0% to 90-10 % in 6 min; 90-10 % in 3 min; 100-0 % in 1 min at 2 ml/min at 25°C. UV detection at 210 nm: **R$_t$**: (syn, major) = 3.98 min, (syn, minor) = 6.71min. TABLE 4, Entry 7.

FIGURE 127. ^{1}H NMR of crude compound **4h** (400 MHz, CDCl$_3$) obtained by the Michael reaction catalyzed by 2.5 mol% of compound **3e**. Diastereoisomeric ratio (*syn/anti*): 89:11. TABLE 4, Entry 8.
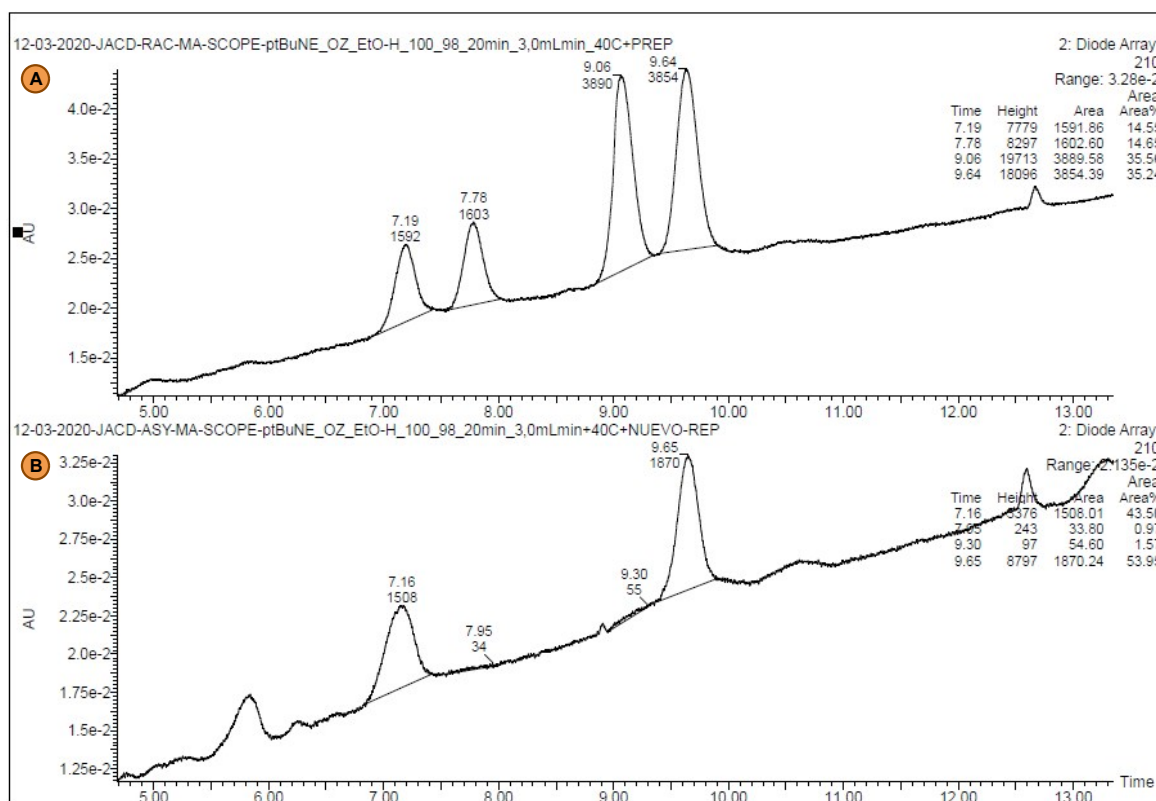

FIGURE 128. (a) Chiral UPC^2 of racemic 2-ethyl-4-nitro-3-(4-nitrophenyl) butanal (**4h**); (b) Chiral UPC^2 of 2-ethyl-4-nitro-3-(4-nitrophenyl) butanal (**4h**) obtained by the Michael reaction catalyzed by 2.5 mol% of compound **3e**. Trefoil AMY1, **Grad:** CO$_2$/IPA 100-0% to 90-10 % in 18 min; 90-10 % in 2 min at 2 ml/min at 25°C. UV detection at 210 nm: **R$_t$:** (syn, major) = 8.84 min, (syn, minor) = 10.04 min. TABLE 4, Entry 8.
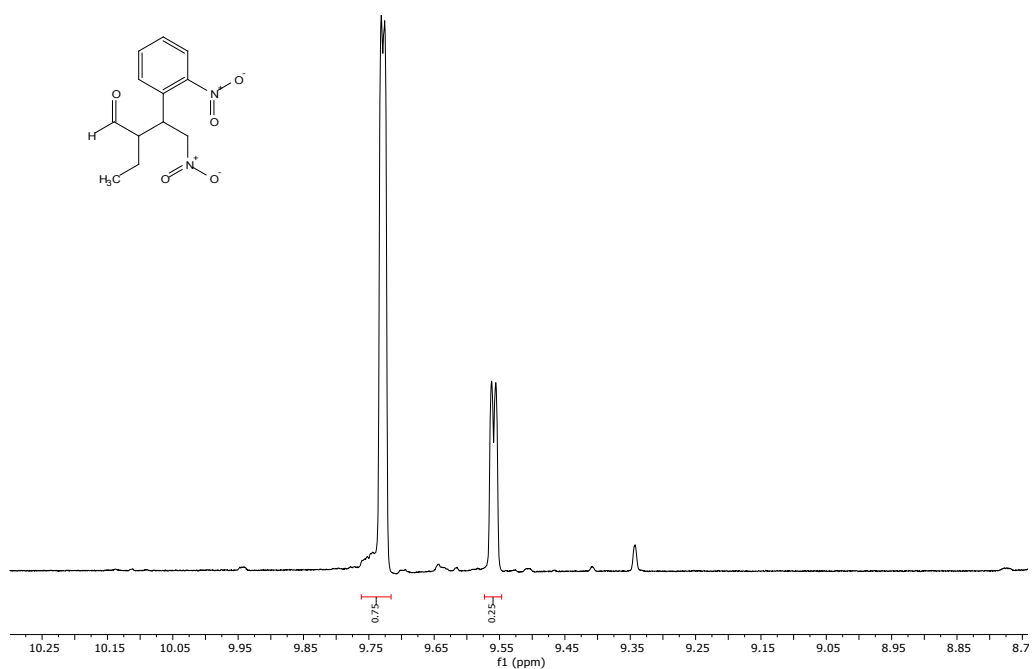
FIGURE 129. ^{1}H NMR of crude compound **4i** (400 MHz, CDCl$_3$) obtained by the Michael reaction catalyzed by 2.5 mol% of compound **3e**. Diastereoisomeric ratio (*syn/anti*): 91:09. TABLE 4, Entry 9.
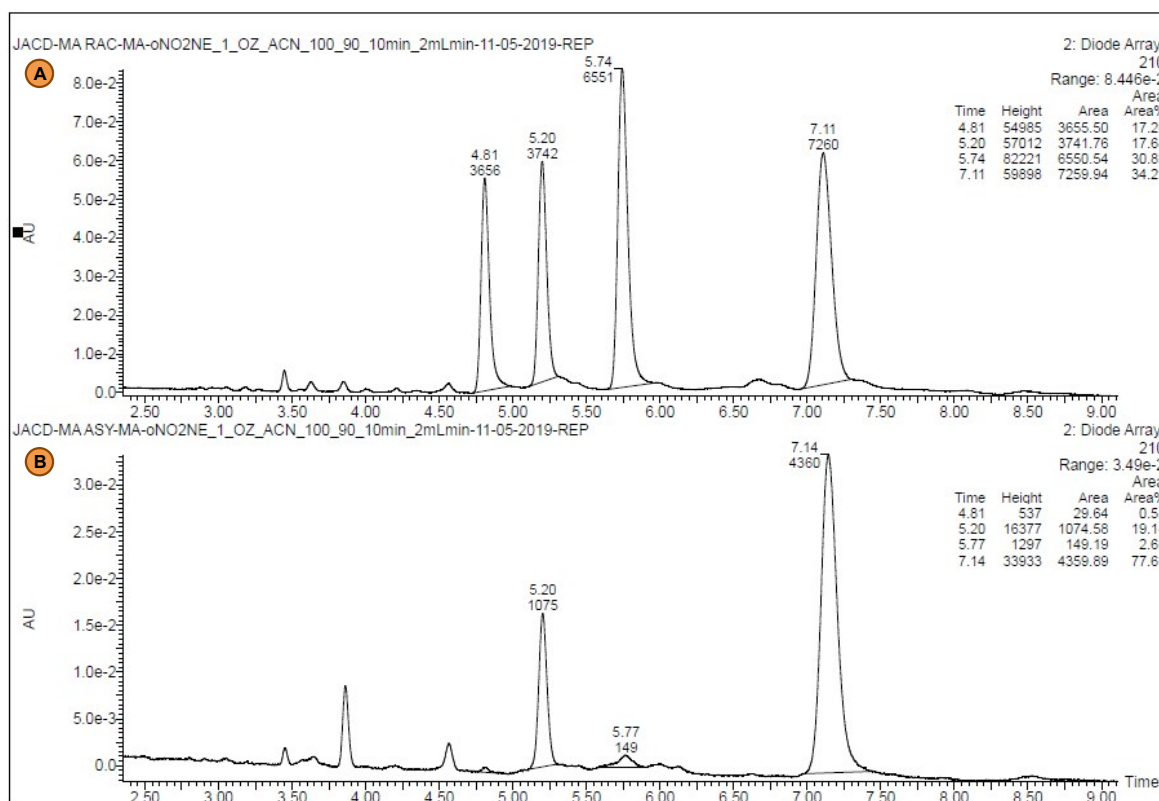

FIGURE 130. (a) Chiral UPC[2] of racemic 2-ethyl-4-nitro-3-(4-(trifluoromethyl)phenyl)butanal (**4i**); (b) Chiral UPC[2] of 2-ethyl-4-nitro-3-(4-(trifluoromethyl)phenyl)butanal (**4i**) obtained by the Michael reaction catalyzed by 2.5 mol% of compound **3e**. Trefoil CEL2, **Grad:** CO$_2$/IPA 100- 0% to 95-05 % in 14 min; 100-0 % in 1 min at 1.5 ml/min at 25°C. UV detection at 210 nm: **R$_t$**: (syn, minor) = 10.69 min, (syn, major) = 11.18 min. TABLE 4, Entry 9.
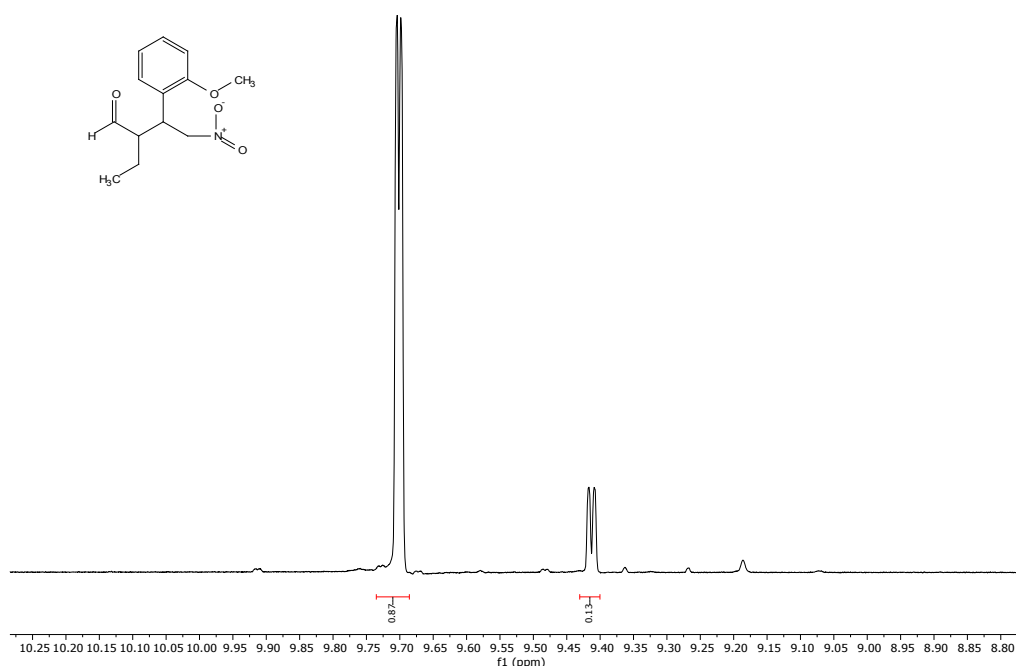
FIGURE 131. ^{1}H NMR of crude compound **4j** (400 MHz, CDCl$_3$) obtained by the Michael reaction catalyzed by 2.5 mol% of compound **3e**. Diastereoisomeric ratio (*syn/anti*): 93:07. TABLE 4, Entry 10.
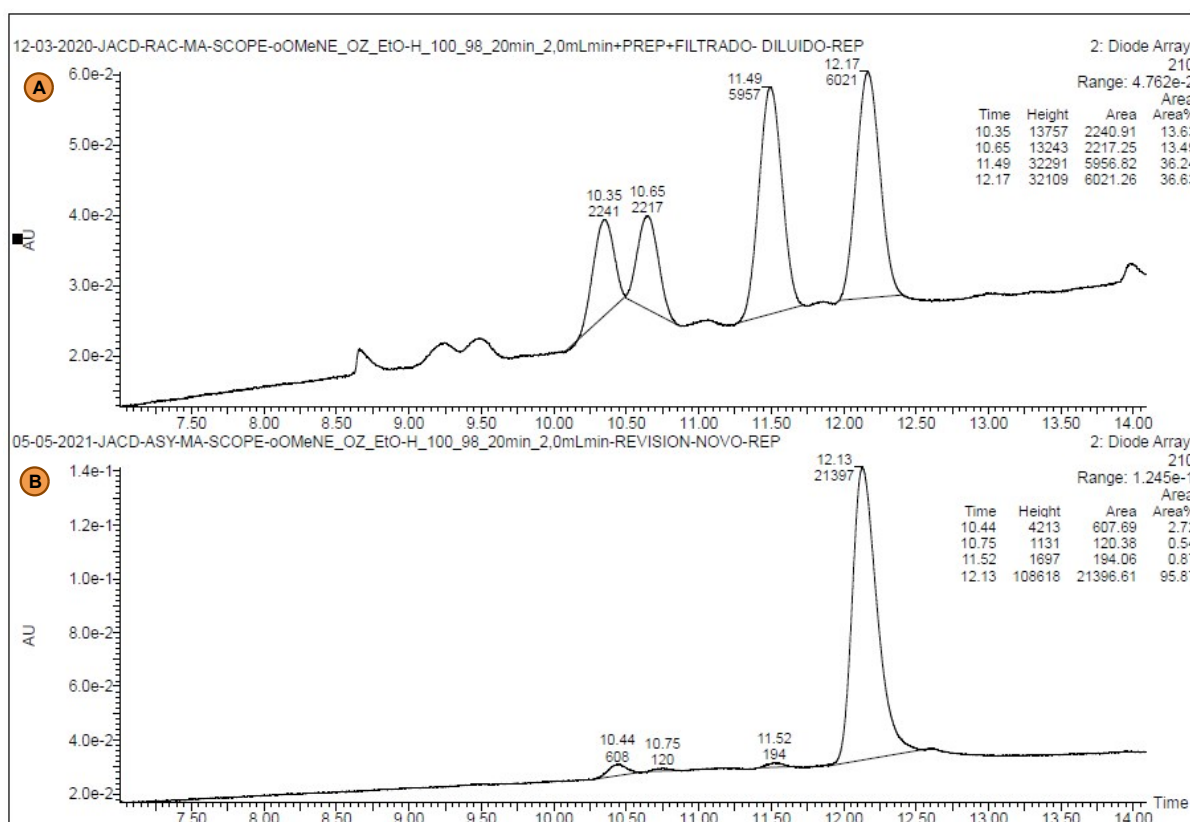

FIGURE 132. (a) Chiral UPC^2 of racemic 2-ethyl-3-(4-methoxyphenyl)-4-nitrobutanal (**4j**); (b) Chiral UPC^2 of 2-ethyl-3-(4-methoxyphenyl)-4-nitrobutanal (**4j**) obtained by the Michael reaction catalyzed by 2.5 mol% of compound **3e**. Trefoil CEL2, **Grad:** CO$_2$/EtOH 100-0% to 98-2 % in 19 min; 100-0 % in 1 min at 2.5 ml/min at 25°C. UV detection at 210 nm: **R$_t$**: (syn, minor) = 14.88 min, (syn, major) = 15.43 min. TABLE 4, Entry 10.
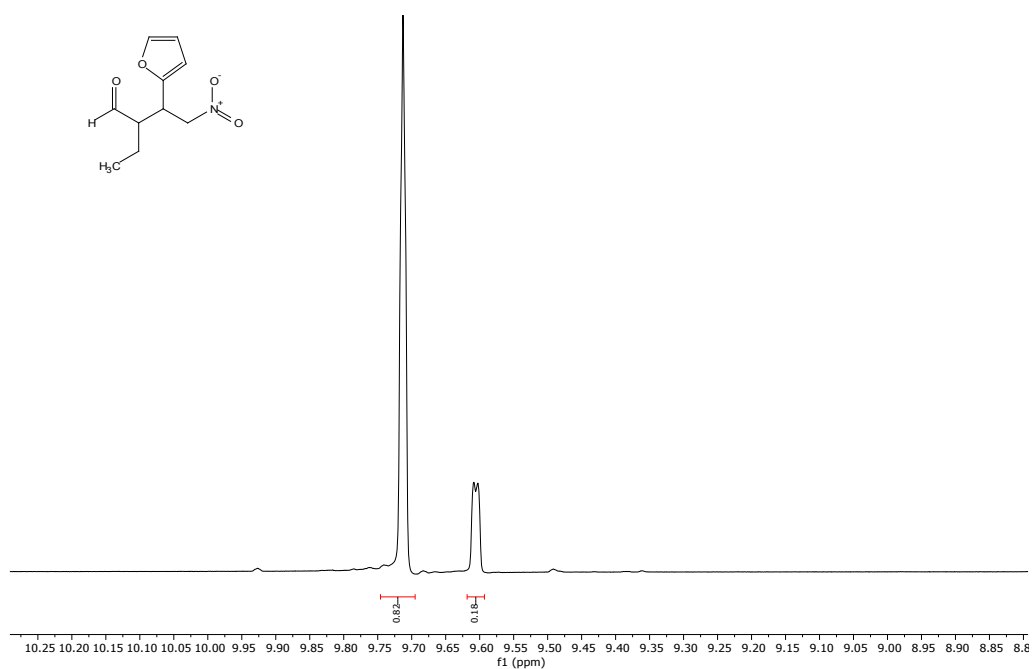
FIGURE 133. ^{1}H NMR of crude compound **4k** (400 MHz, CDCl$_3$) obtained by the Michael reaction catalyzed by 2.5 mol% of compound **3e**. Diastereoisomeric ratio (*syn/anti*): 91:09. TABLE 4, Entry 11.
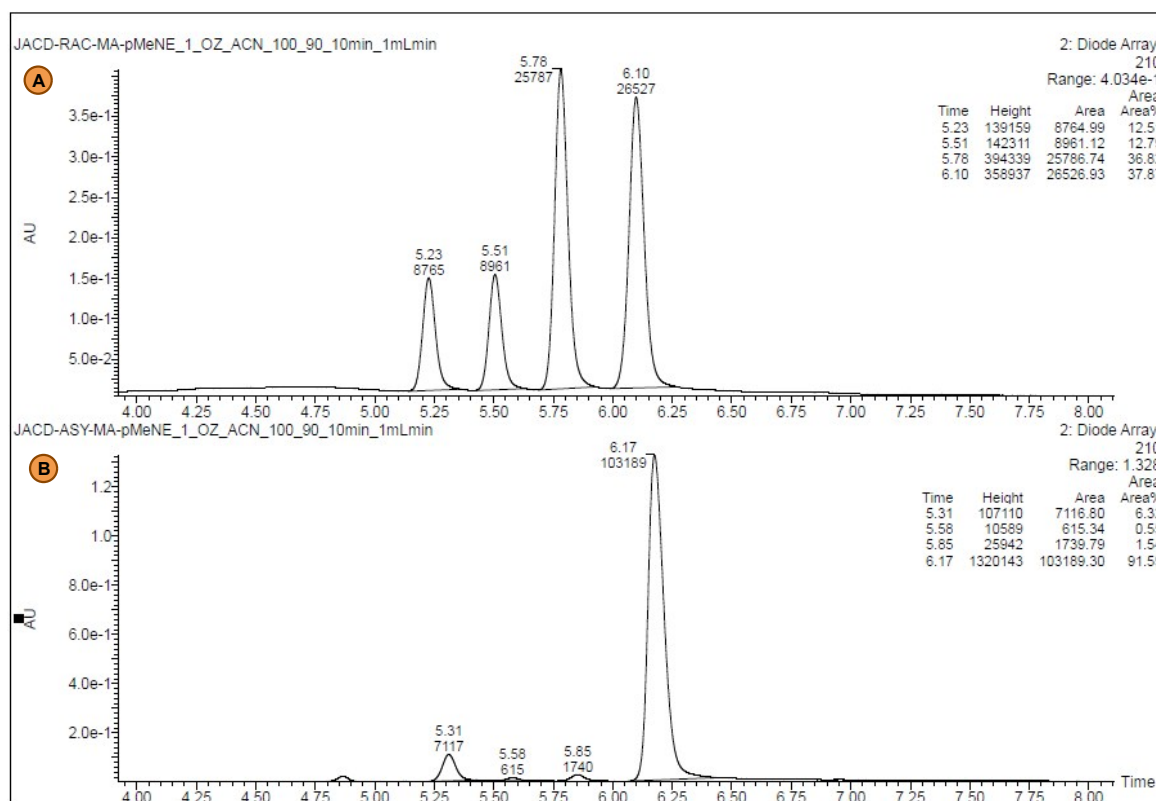
FIGURE 134. (a) Chiral UPC^2 of racemic 2-ethyl-4-nitro-3-(p-tolyl)butanal (**4k**); (b) Chiral UPC^2 of 2-ethyl-4-nitro-3-(p-tolyl)butanal (**4k**) obtained by the Michael reaction catalyzed by 2.5 mol% of compound **3e**. Trefoil CEL2, **Grad:** CO$_2$/ACN 100- 0% to 90-10 % in 5 min; 90-10 % in 4 min; 100-0 % in 1 min at 1 ml/min at 25°C. UV detection at 210 nm: **R$_t$**: (syn, minor) = 5.85 min, (syn, major) = 6.17 min. TABLE 4, Entry 11.

FIGURE 135. ^{1}H NMR of crude compound **4l** (400 MHz, CDCl$_3$) obtained by the Michael reaction catalyzed by 2.5 mol% of compound **3e**. Diastereoisomeric ratio (*syn/anti*): 79:21. TABLE 4, Entry 12.


FIGURE 136. (a) Chiral UPC^2 of racemic 3-(4-(tert-butyl)phenyl)-2-ethyl-4-nitrobutanal (**4l**); (b) Chiral UPC^2 of 3-(4-(tert-butyl)phenyl)-2-ethyl-4-nitrobutanal (**4l**) obtained by the Michael reaction catalyzed by 2.5 mol% of compound **3e**. Trefoil CEL2, **Grad:** CO$_2$/EtOH 100-0% to 98-02 % in 19 min; 100-0 % in 1 min at 3 ml/min at 40°C. UV detection at 210 nm: **R$_t$**: (syn, minor) = 9.30 min, (syn, major) = 9.65 min. TABLE 4, Entry 12.

FIGURE 137. ^{1}H NMR of crude compound **4m** (400 MHz, CDCl$_3$) obtained by the Michael reaction catalyzed by 2.5 mol% of compound **3e**. Diastereoisomeric ratio (*syn/anti*): 75:25. TABLE 4, Entry 13.
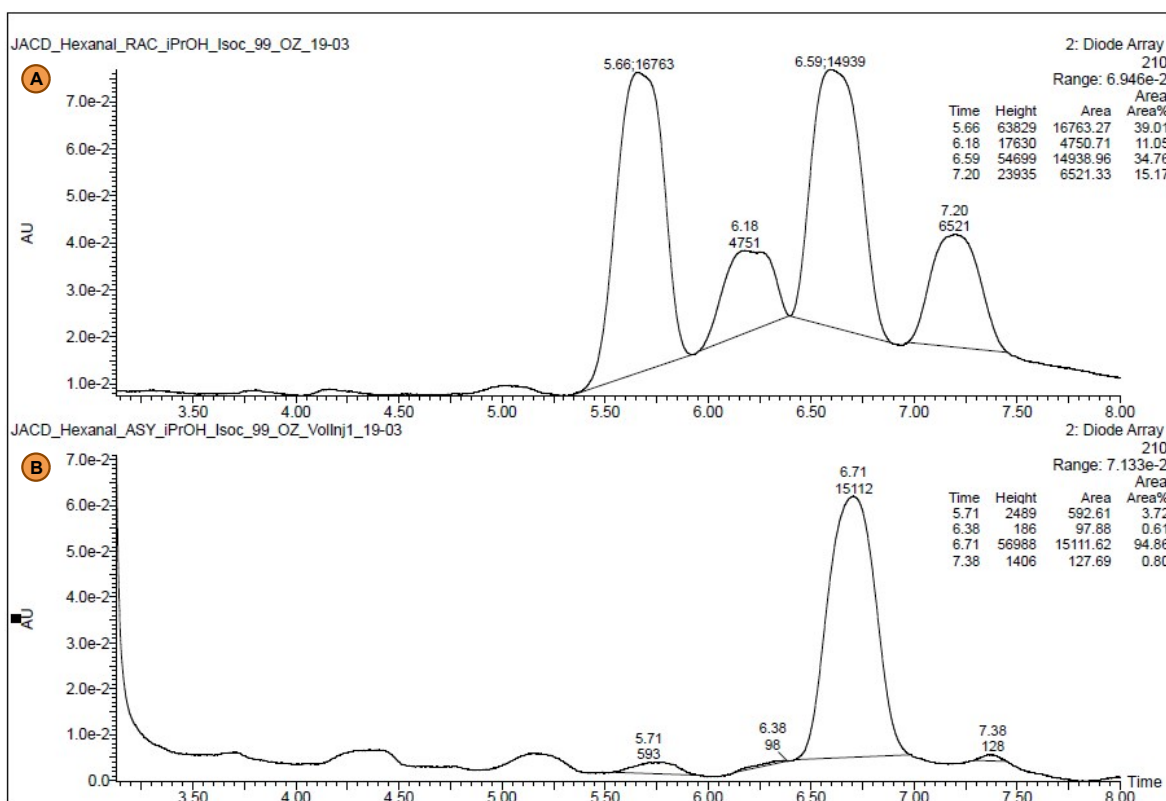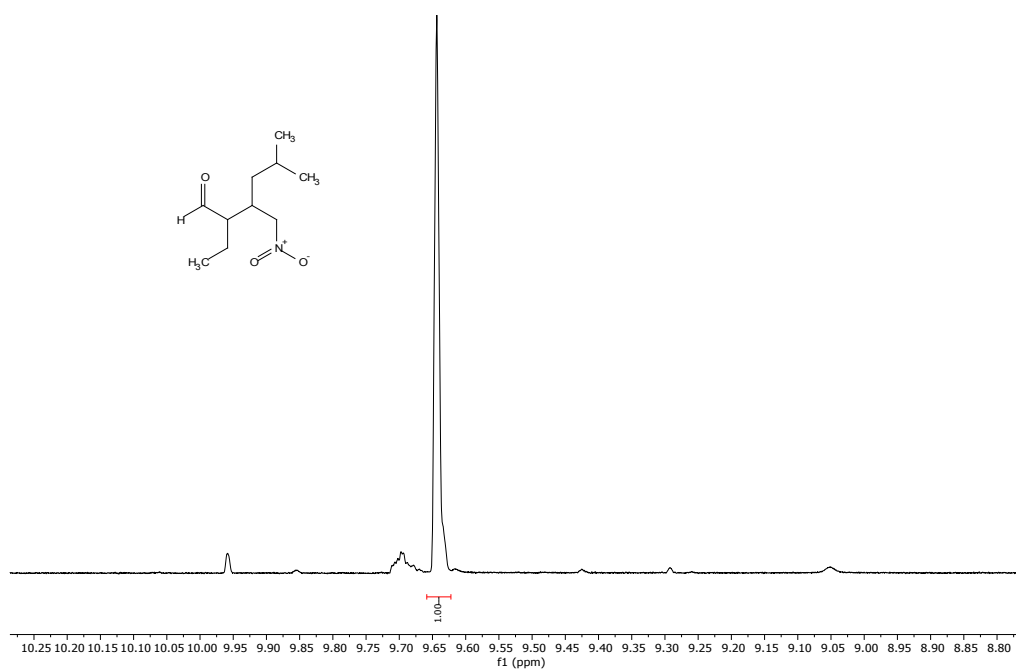

FIGURE 138. (a) Chiral UPC^2 of racemic 2-ethyl-4-nitro-3-(2-nitrophenyl)butanal (**4m**); (b) Chiral UPC^2 of 2-ethyl-4-nitro-3-(2-nitrophenyl)butanal (**4m**) obtained by the Michael reaction catalyzed by 2.5 mol% of compound **3e**. Trefoil CEL2, **Grad:** CO$_2$/ACN 100-0% to 90-10 % in 5 min; 90-10 % in 4 min; 100-0 % in 1 min at 2 ml/min at 25°C. UV detection at 210 nm: **R$_t$**: (syn, minor) = 5.77 min, (syn, major) = 7.14 min. TABLE 4, Entry 13.

S94

FIGURE 139. ^{1}H NMR of crude compound **4n** (400 MHz, CDCl$_3$) obtained by the Michael reaction catalyzed by 2.5 mol% of compound **3e**. Diastereoisomeric ratio (*syn/anti*): 87:13. TABLE 4, Entry 14.
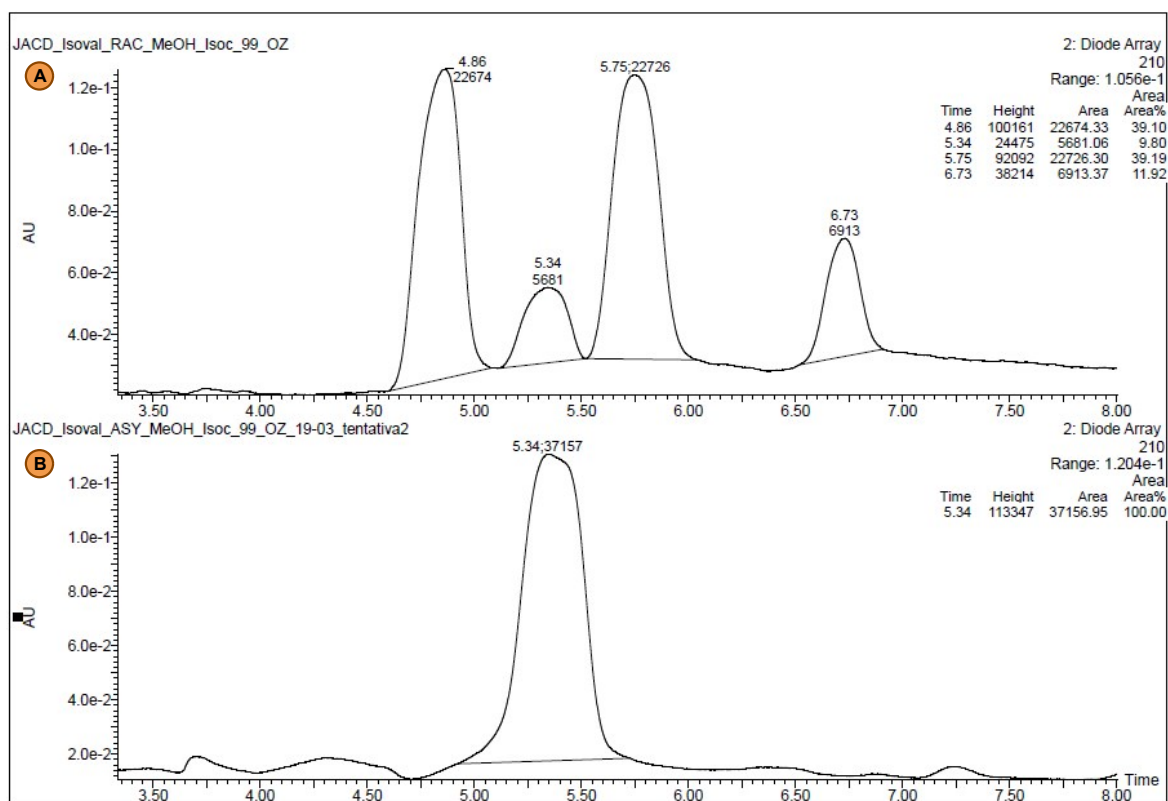

FIGURE 140. (a) Chiral UPC^2 of racemic 2-ethyl-3-(2-methoxyphenyl)-4-nitrobutanal (**4n**); (b) Chiral UPC^2 of 2-ethyl-3-(2-methoxyphenyl)-4-nitrobutanal (**4n**) obtained by the Michael reaction catalyzed by 2.5 mol% of compound **3e**. Trefoil CEL2, **Grad:** CO$_2$/EtOH 100- 0% to 98-02 % in 19 min; 100-0 % in 1 min at 2 ml/min at 25°C. UV detection at 210 nm: **R$_t$**: (syn, minor) = 11.52 min, (syn, major) = 12.13 min. TABLE 4, Entry 14.
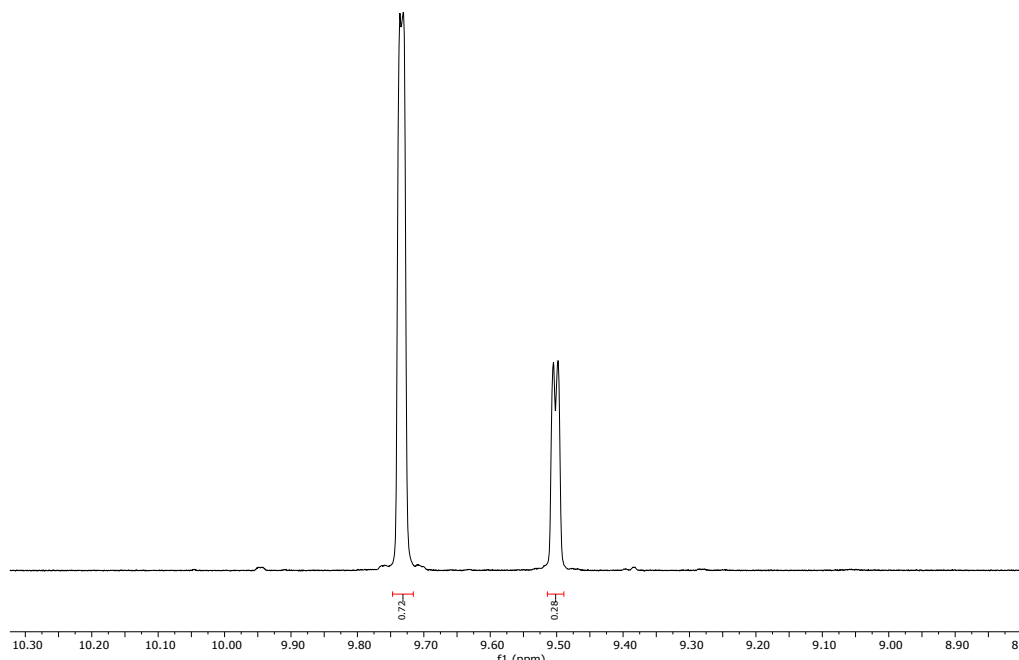
FIGURE 141. ^{1}H NMR of crude compound **4o** (400 MHz, CDCl₃) obtained by the Michael reaction catalyzed by 2.5 mol% of compound **3e**. Diastereoisomeric ratio (*syn/anti*): 82:18. TABLE 4, Entry 15.
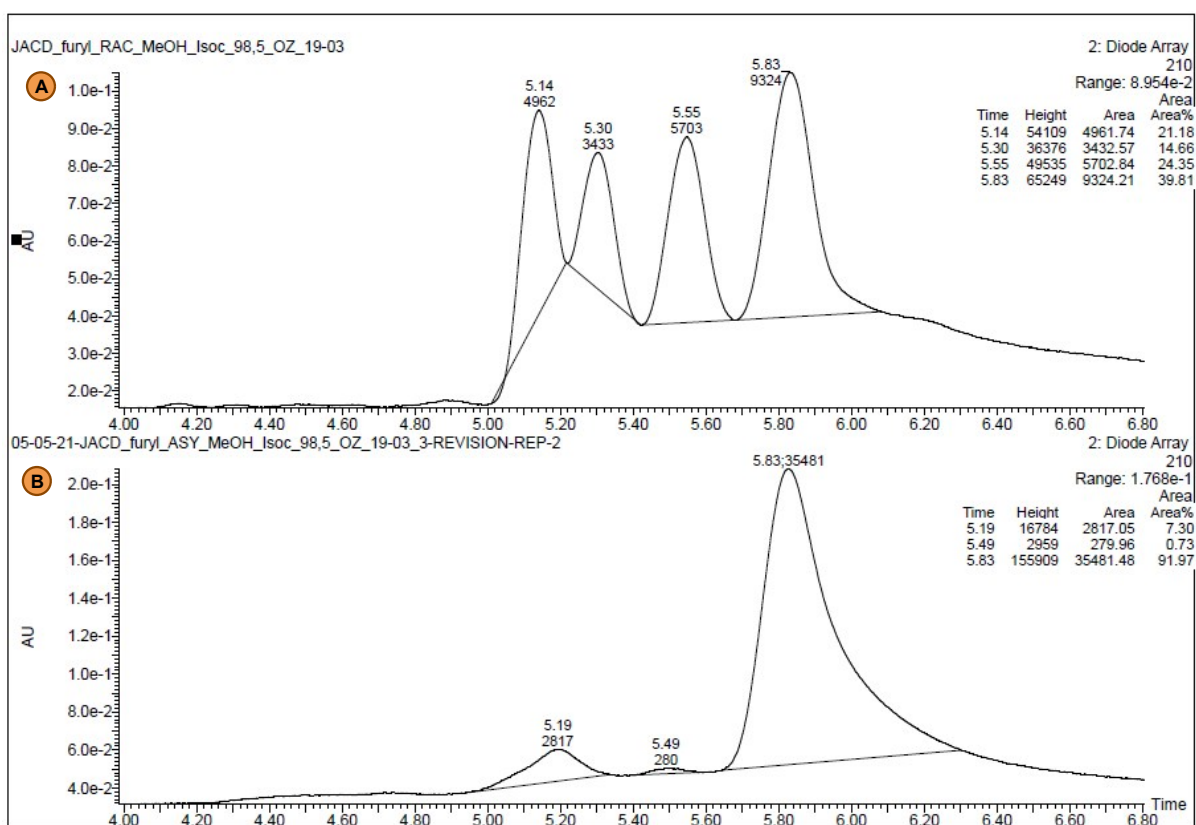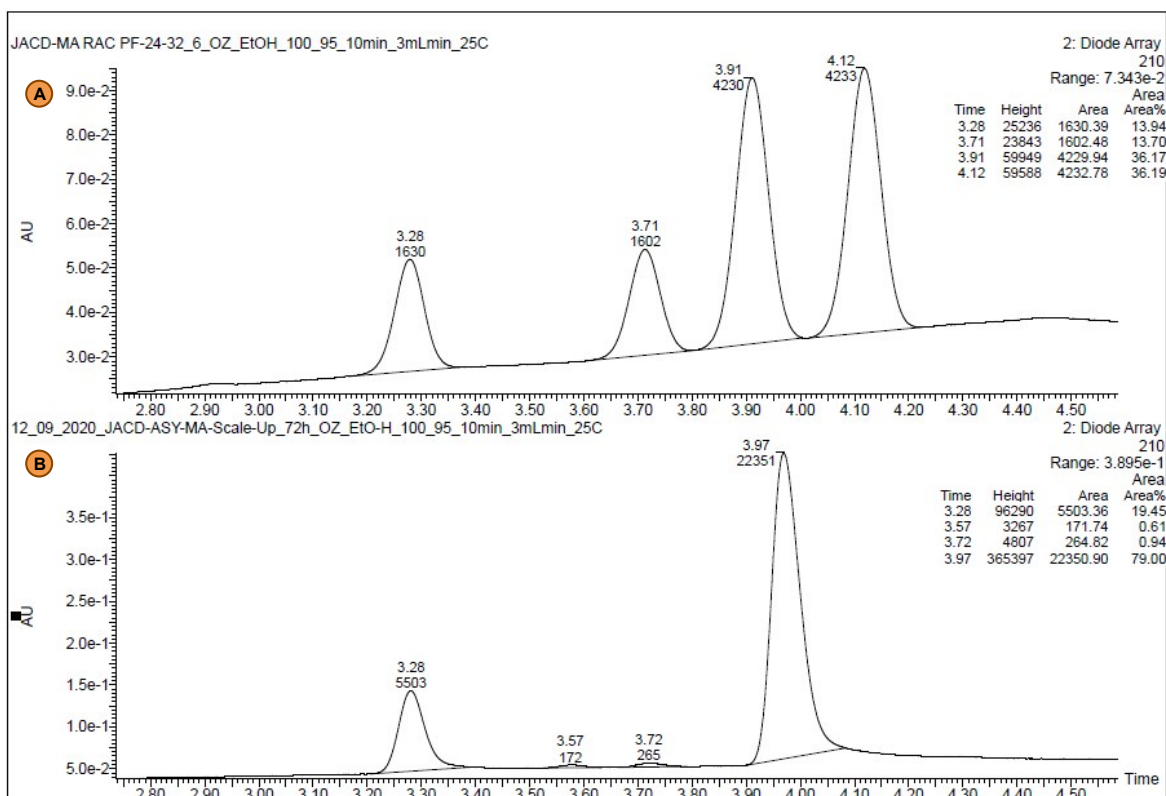

FIGURE 142. (a) Chiral UPC[2] of racemic 2-ethyl-3-(furan-2-yl)-4-nitrobutanal (**4o**); (b) Chiral UPC[2] of 2-ethyl-3-(furan-2-yl)-4-nitrobutanal (**4o**) obtained by the Michael reaction catalyzed by 2.5 mol% of compound **3e**. Trefoil CEL2, CO₂/MeOH 98.5-1.5 in 8 min at 1 ml/min at 35°C. UV detection at 210 nm: **R$_t$**: (syn, minor) = 5.49 min, (syn, major) = 5.83 min. TABLE 4, Entry 15.
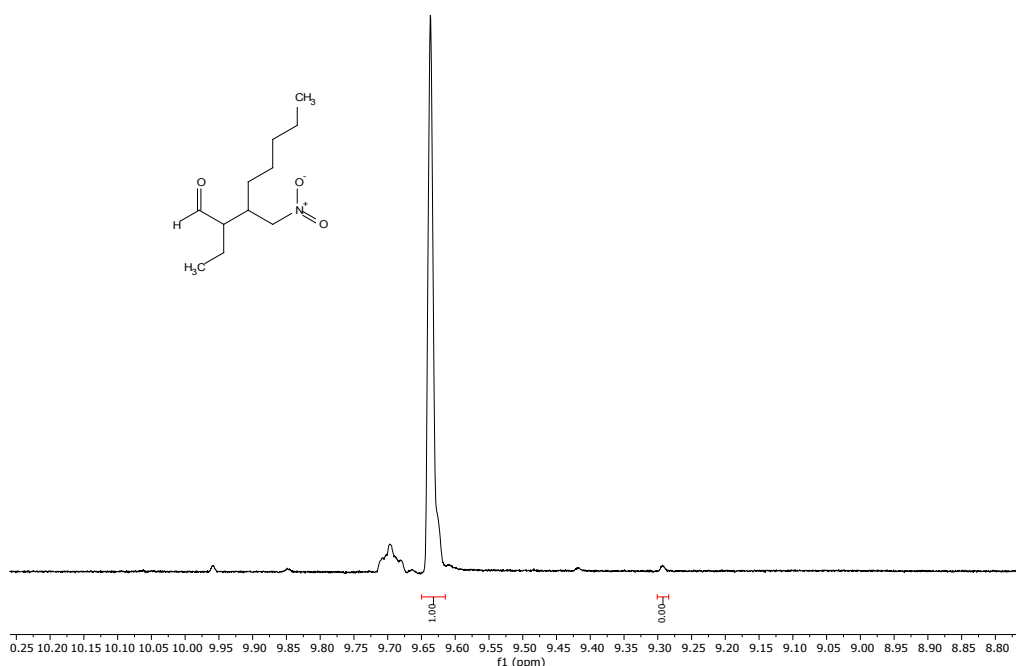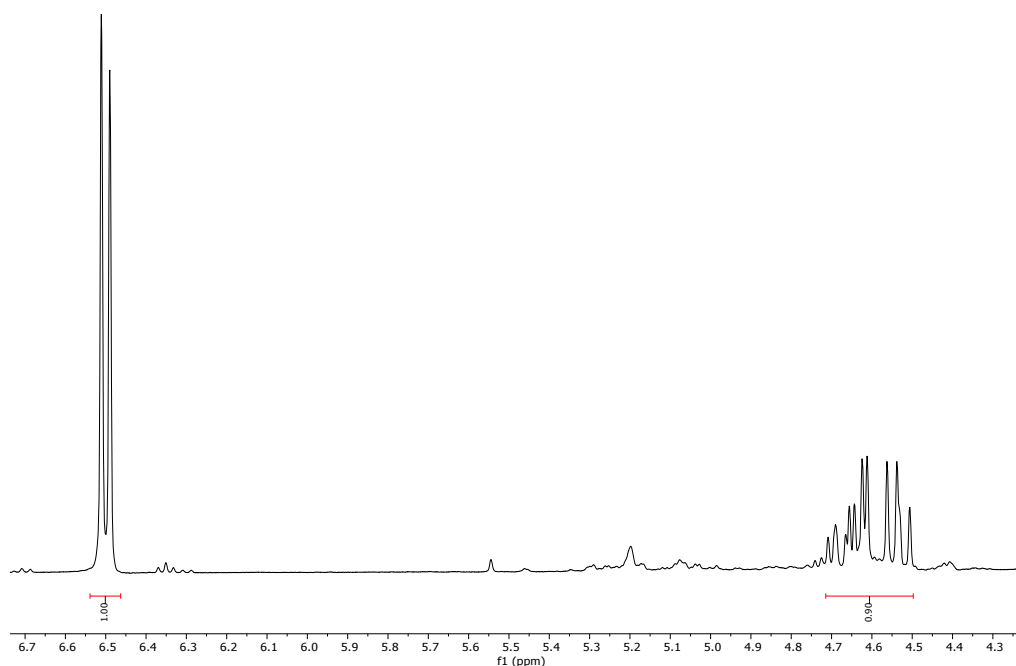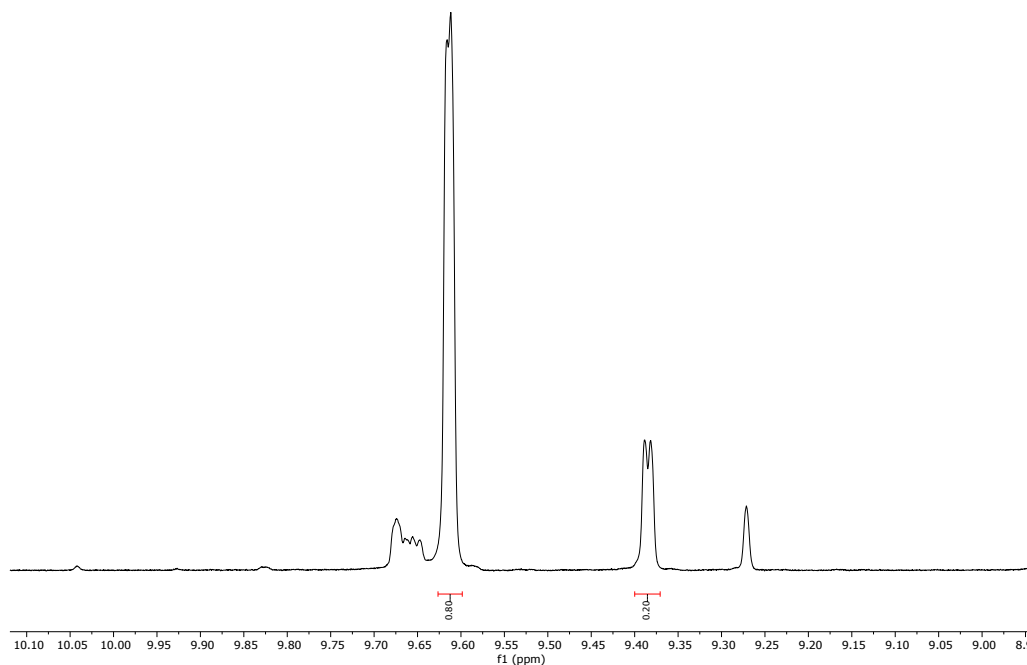
FIGURE 143. ^{1}H NMR of crude compound **4p** (400 MHz, CDCl$_3$) obtained by the Michael reaction catalyzed by 2.5 mol% of compound **3e**. Diastereoisomeric ratio (*syn/anti*): >99:1. TABLE 4, Entry 16.

FIGURE 144. (a) Chiral UPC^2 of racemic 2-ethyl-3-(nitromethyl)octanal (**4p**); (b) Chiral UPC^2 of 2-ethyl-3-(nitromethyl)octanal (**4p**) obtained by the Michael reaction catalyzed by 2.5 mol% of compound **3e**. Trefoil CEL2, CO$_2$/IPA 99-1 in 8 min at 1 ml/min at 35°C. UV detection at 210 nm: **R$_t$**: (syn, minor) = 5.71 min, (syn, major) = 6.71 min. TABLE 4, Entry 16.

FIGURE 145. ^{1}H NMR of crude of crude **4q** (400 MHz, CDCl$_3$) obtained by the Michael reaction catalyzed by 2.5 mol% of compound 3e. Diastereoisomeric ratio (*syn/anti*): >99:1. TABLE 4, Entry 17.
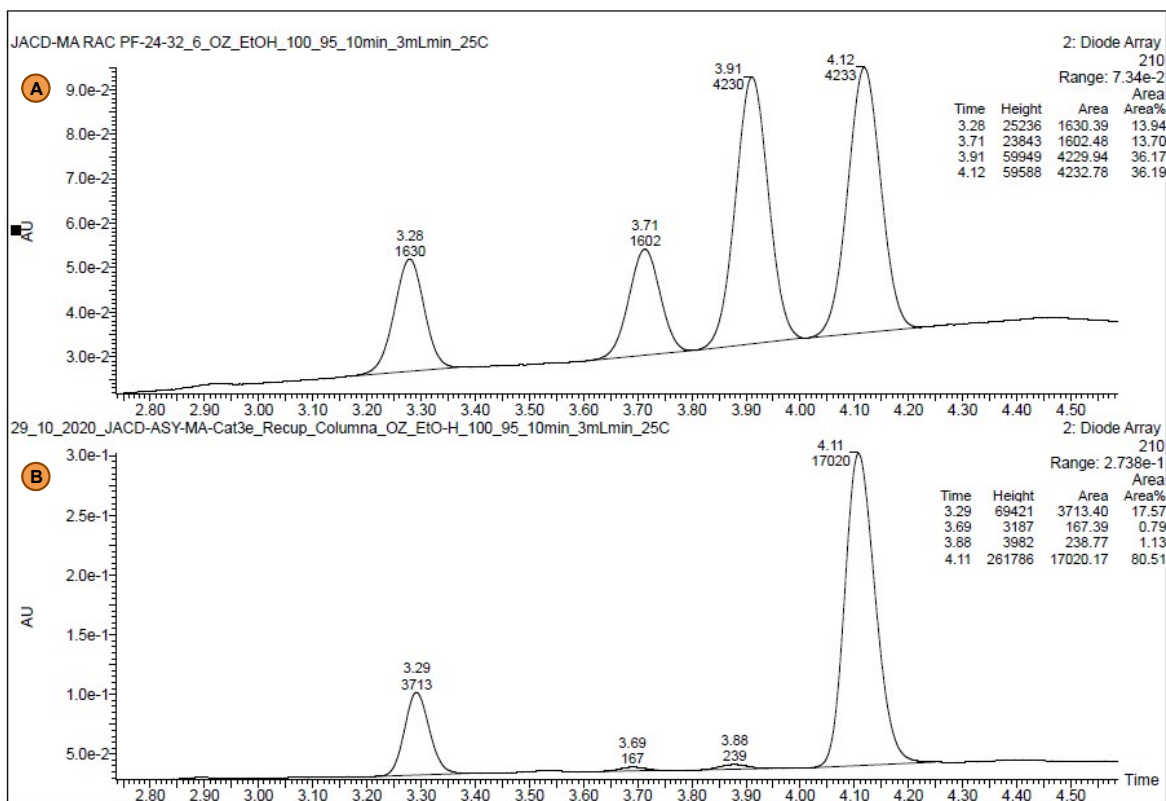

FIGURE 146. (a) Chiral UPC^2 of racemic 2-ethyl-5-methyl-3-(nitromethyl)hexanal (**4q**); (b) Chiral UPC^2 of 2-ethyl-5-methyl-3-(nitromethyl)hexanal (**4q**) obtained by the Michael reaction catalyzed by 2.5 mol% of compound **3e**. Trefoil CEL2, CO$_2$/MeOH 99-1 in 8 min at 1 ml/min at 35°C. UV detection at 210 nm: **R$_t$**: (syn, major) = 5.34 min. TABLE 4, Entry 17.
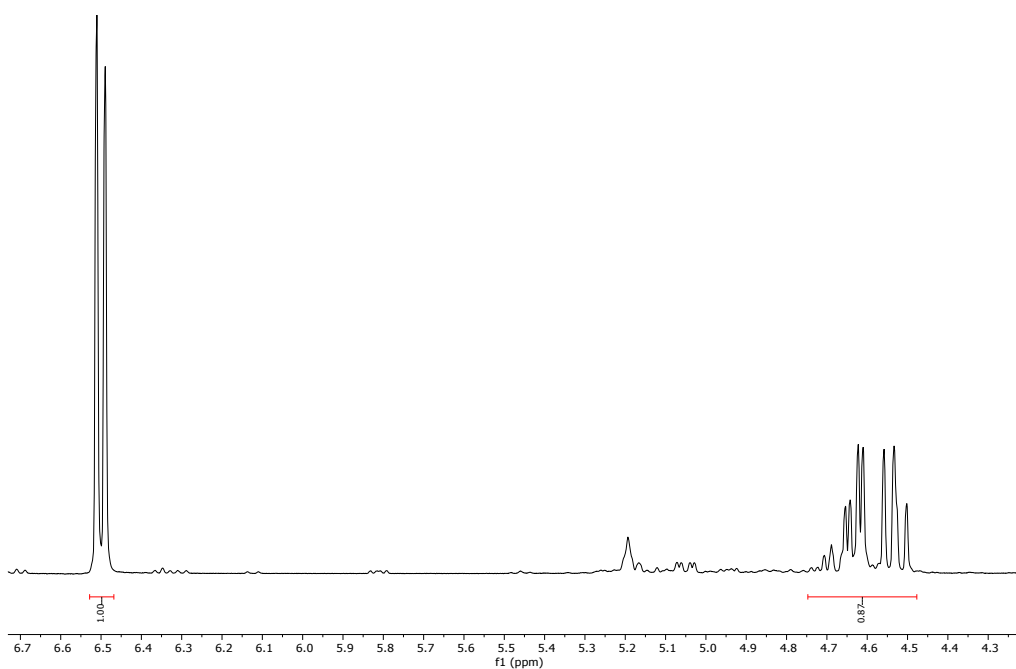
19. NMR Spectra and Chromatograms: Scale-Up

FIGURE 147. ^{1}H NMR of crude compound **4a** (400 MHz, CDCl$_3$) obtained by the Michael reaction catalyzed by 2.5 mol% of compound **3e** in a 2 mmol scale. Diastereoisomeric ratio (*syn/anti*): 72:28.

FIGURE 148. (a) Chiral UPC^2 of racemic 2-ethyl-4-nitro-3-phenylbutanal (**4a**); (b) Chiral UPC^2 of 2-ethyl-4-nitro-3-phenylbutanal (**4a**) obtained by the Michael reaction catalyzed by 2.5 mol% of compound **3e** in a 2 mmol scale. Trefoil CEL2, **Grad:** CO$_2$/EtOH 100-0% to 95-5 % in 10 min at 3 ml/min at 25°C. UV detection at 210 nm: **R$_t$**: (syn, minor) = 3.72 min, (syn, major) = 3.97 min.

20. NMR Spectra and Chromatograms: Catalyst recycle

FIGURE 149. ^{1}H NMR of crude compound **4a** (400 MHz, CDCl$_3$) obtained by the Michael reaction catalyzed by one-time recovered compound **3a** with 1, 2, 3-trimethoxybenzene as standard. Yield: 90%.
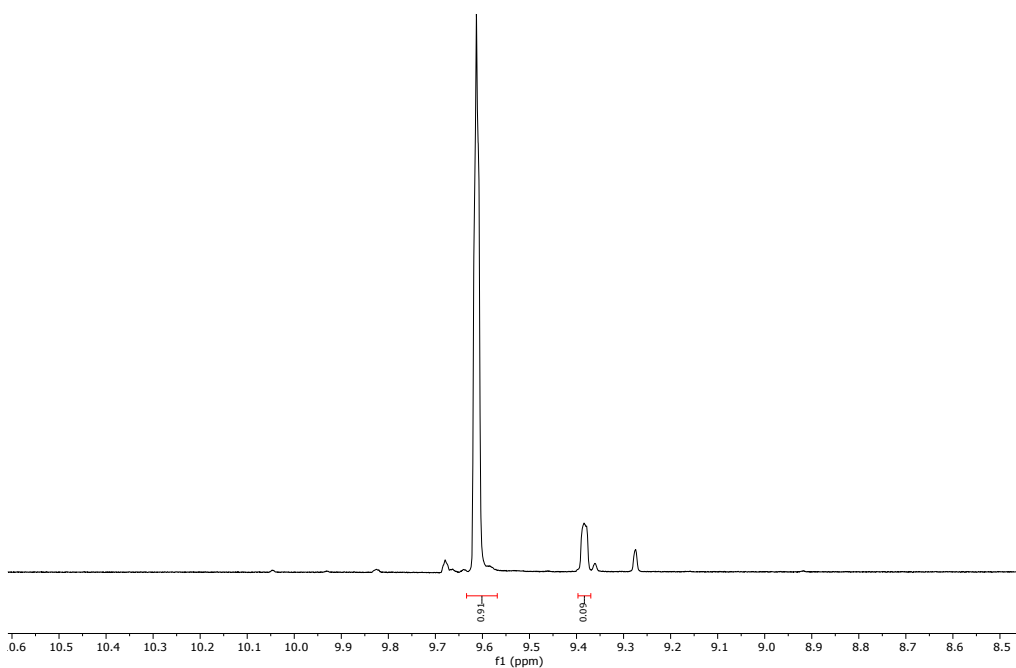

FIGURE 150. ^{1}H NMR of crude compound **4a** (400 MHz, CDCl$_3$) obtained by the Michael reaction catalyzed by one-time recovered compound **3a**. Diastereoisomeric ratio (syn/anti): 80:20.
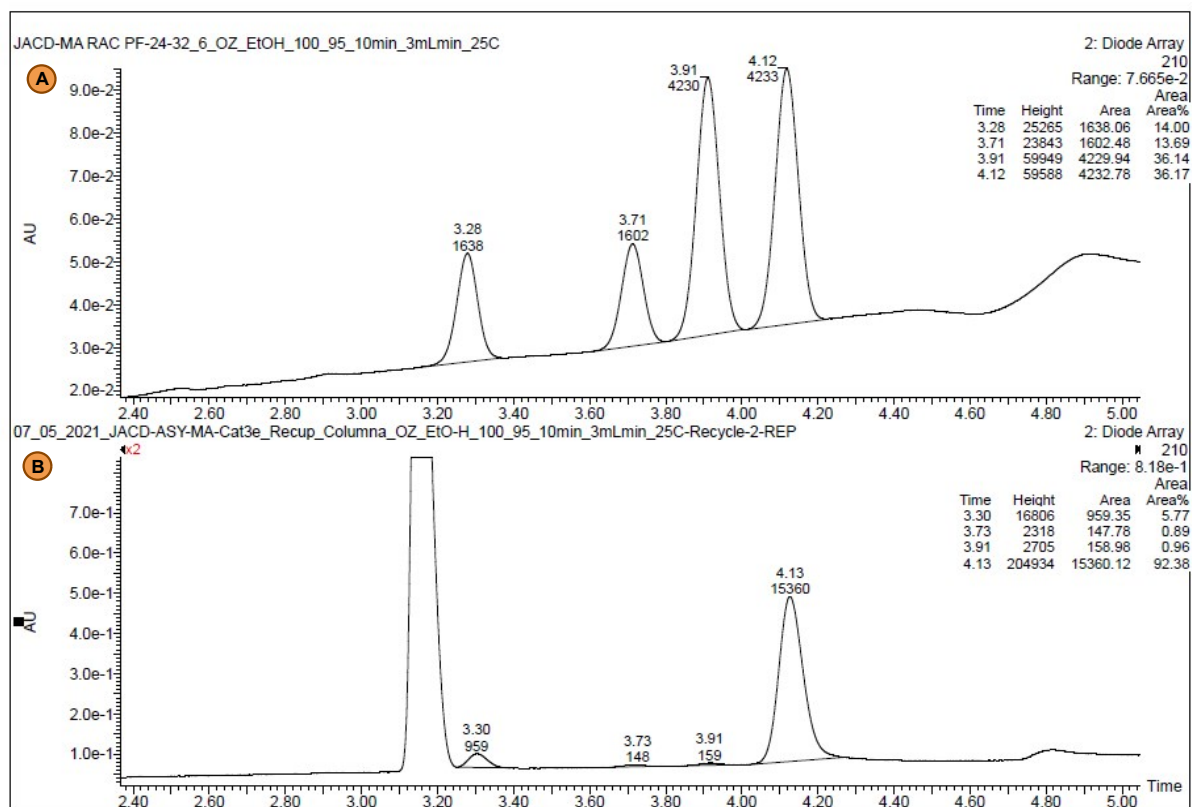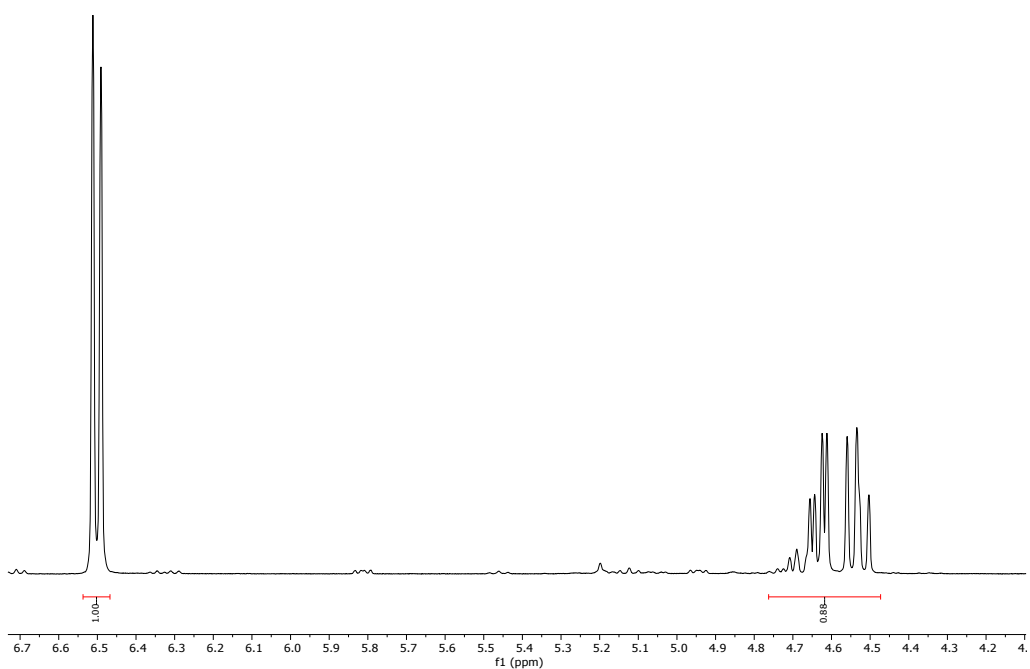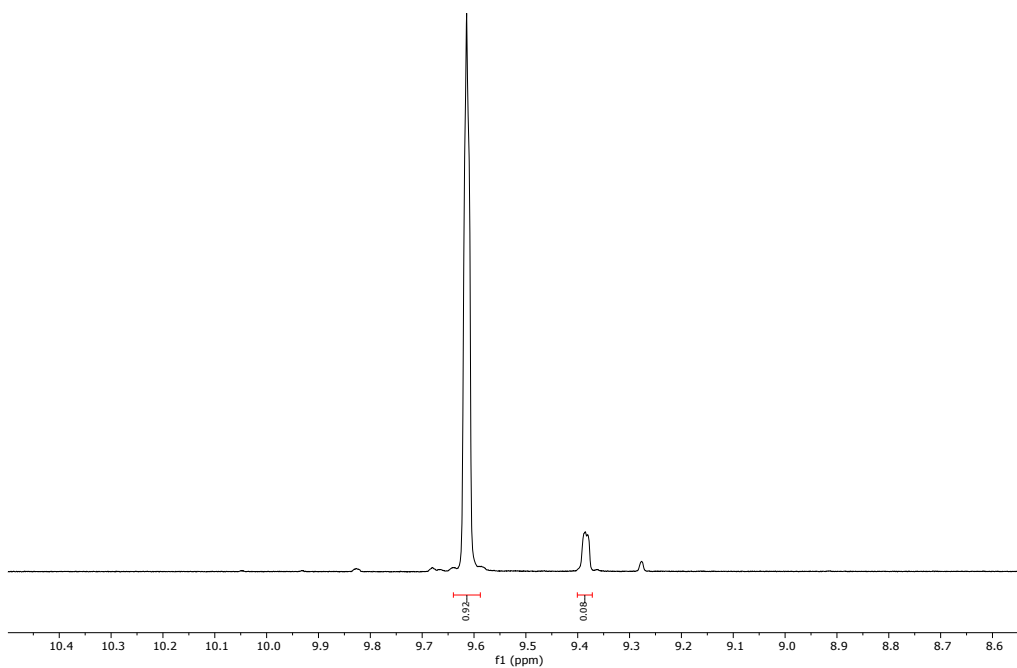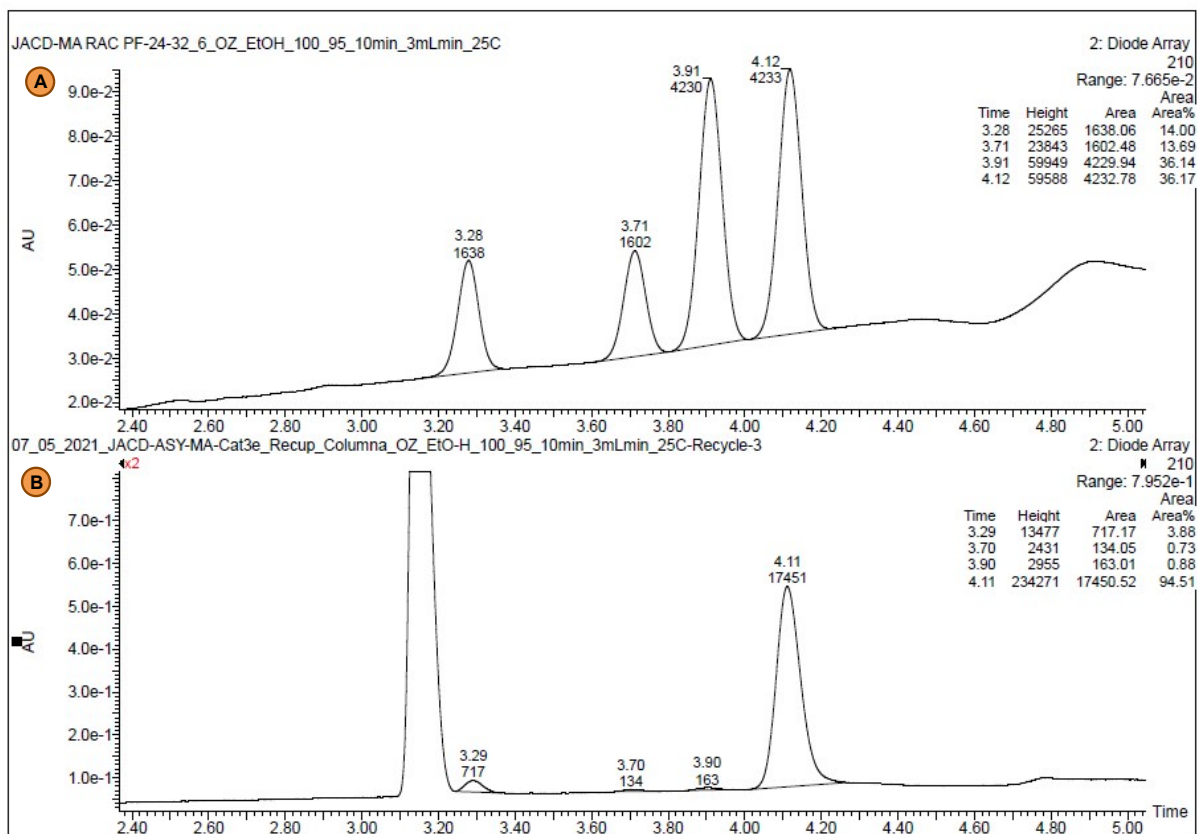
FIGURE 151. (a) Chiral UPC² of racemic 2-ethyl-4-nitro-3-phenylbutanal (**4a**); (b) Chiral UPC² of 2-ethyl-4-nitro-3-phenylbutanal (**4a**) obtained by the Michael reaction catalyzed by one-time recovered compound **3e**. Trefoil CEL2, **Grad:** CO_2/EtOH 100-0% to 95-5 % in 10 min at 3 ml/min at 25°C. UV detection at 210 nm: R_t: (syn, minor) = 3.88 min, (syn, major) = 4.11 min.

FIGURE 152. ^{1}H NMR of crude compound **4a** (400 MHz, CDCl$_3$) obtained by the Michael reaction catalyzed by two-times recovered compound **3a** with 1, 2, 3-trimethoxybenzene as standard. Yield: 87%.

FIGURE 153. ^{1}H NMR of crude compound **4a** (400 MHz, CDCl$_3$) obtained by the Michael reaction catalyzed by two-times recovered compound **3a**. Diastereoisomeric ratio (syn/anti): 91:09.

FIGURE 154. (a) Chiral UPC^2 of racemic 2-ethyl-4-nitro-3-phenylbutanal (**4a**); (b) Chiral UPC^2 of 2-ethyl-4-nitro-3-phenylbutanal (**4a**) obtained by the Michael reaction catalyzed by two-times recovered compound **3e**. Trefoil CEL2, **Grad:** CO_2/EtOH 100-0% to 95-5 % in 10 min at 3 ml/min at 25°C. UV detection at 210 nm: **R$_t$**: (syn, minor) = 3.91 min, (syn, major) = 4.13 min.
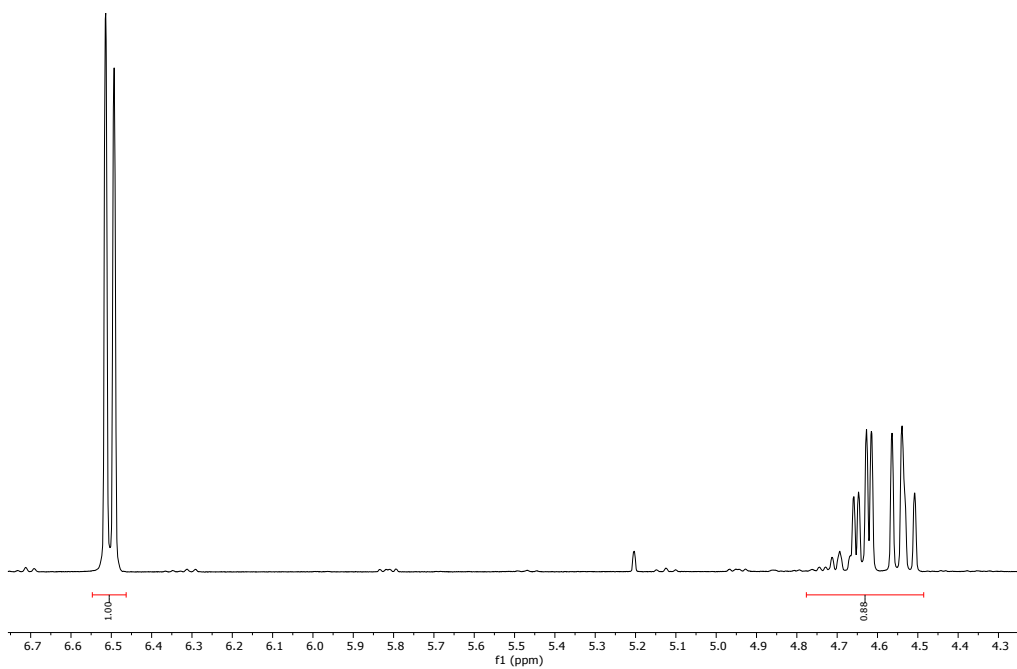
FIGURE 155. ^{1}H NMR of crude compound **4a** (400 MHz, CDCl$_3$) obtained by the Michael reaction catalyzed by three-times recovered compound **3a** with 1, 2, 3-trimethoxybenzene as standard. Yield: 88%.
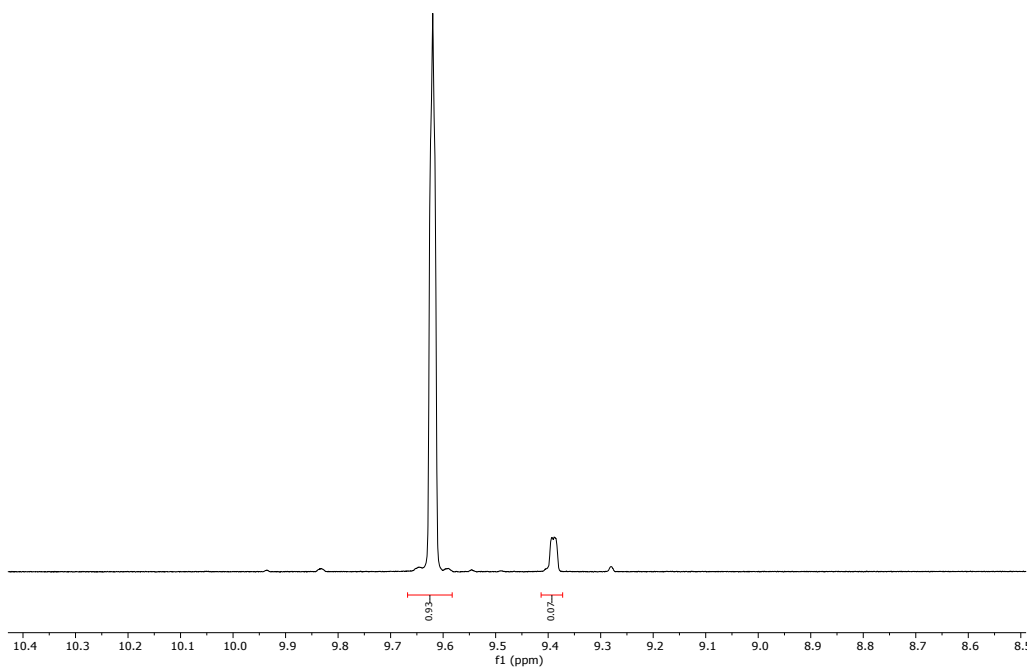

FIGURE 156. ^{1}H NMR of crude compound **4a** (400 MHz, CDCl$_3$) obtained by the Michael reaction catalyzed by three-times recovered compound **3a**. Diastereoisomeric ratio (syn/anti): 92:08.
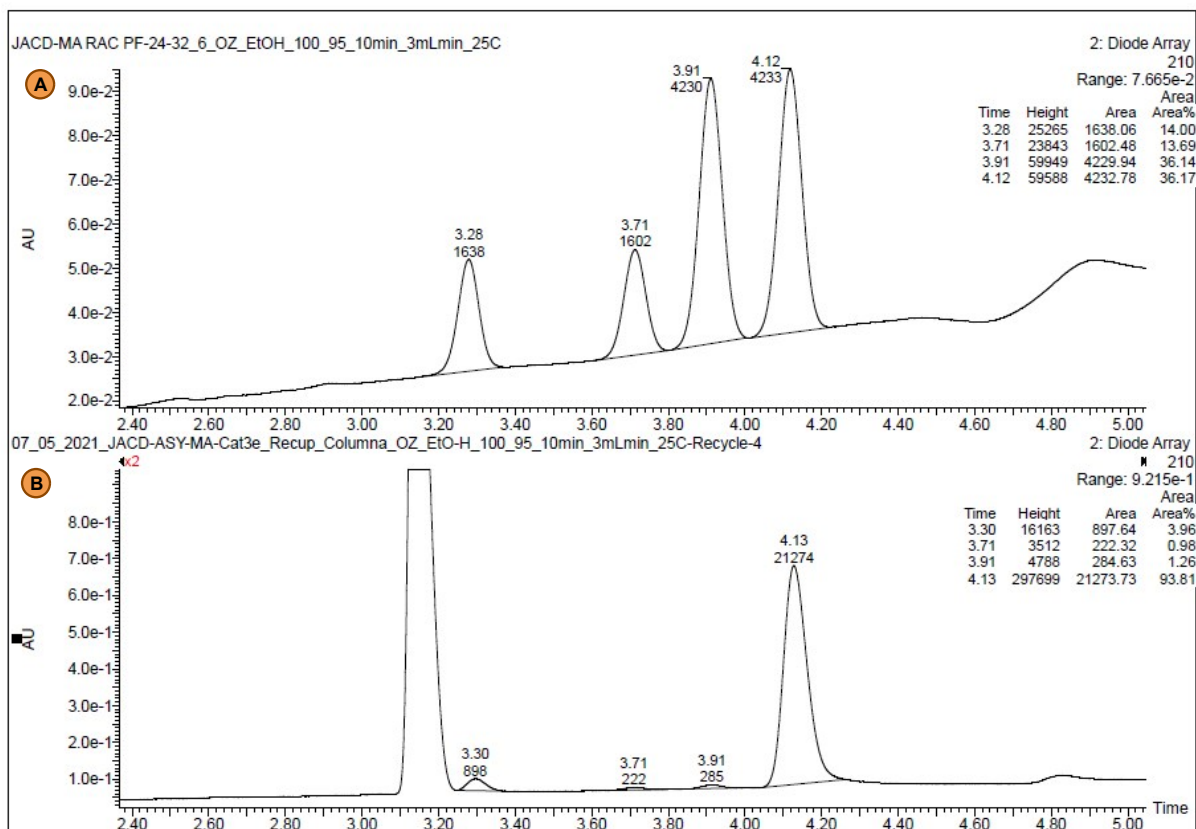
FIGURE 157. (a) Chiral UPC^2 of racemic 2-ethyl-4-nitro-3-phenylbutanal (**4a**); (b) Chiral UPC^2 of 2-ethyl-4-nitro-3-phenylbutanal (**4a**) obtained by the Michael reaction catalyzed by three-times recovered compound **3e**. Trefoil CEL2, **Grad:** CO_2/EtOH 100-0% to 95-5 % in 10 min at 3 ml/min at 25°C. UV detection at 210 nm: R_t: (syn, minor) = 3.90 min, (syn, major) = 4.11 min.

FIGURE 158. ^{1}H NMR of crude compound **4a** (400 MHz, CDCl$_3$) obtained by the Michael reaction catalyzed by four-times recovered compound **3a** with 1, 2, 3-trimethoxybenzene as standard. Yield: 88%.

FIGURE 159. ^{1}H NMR of crude compound **4a** (400 MHz, CDCl$_3$) obtained by the Michael reaction catalyzed by four-times recovered compound **3a**. Diastereoisomeric ratio (syn/anti): 93:07.

FIGURE 160. (a) Chiral UPC^2 of racemic 2-ethyl-4-nitro-3-phenylbutanal (**4a**); (b) Chiral UPC^2 of 2-ethyl-4-nitro-3-phenylbutanal (**4a**) obtained by the Michael reaction catalyzed by four-times recovered compound **3e**. Trefoil CEL2, **Grad:** CO$_2$/EtOH 100-0% to 95-5 % in 10 min at 3 ml/min at 25°C. UV detection at 210 nm: **R$_t$**: (syn, minor) = 3.91 min, (syn, major) = 4.13 min.

21. HRMS Spectra: Catalysts
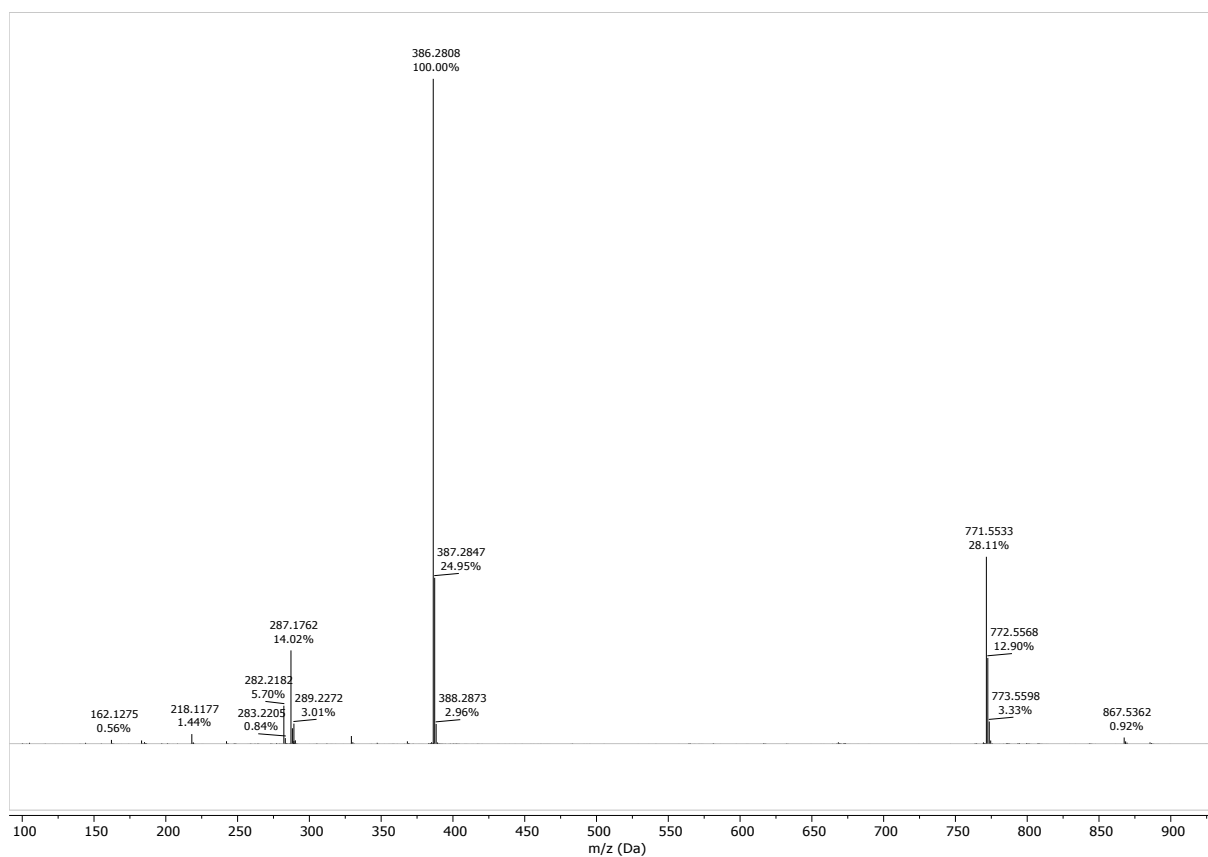
FIGURE 161. HRMS (ESI-Q-TOF) of compound **3a**; m/z: 386.2808. Calcd. for [M+H]$^+$:386.2802.
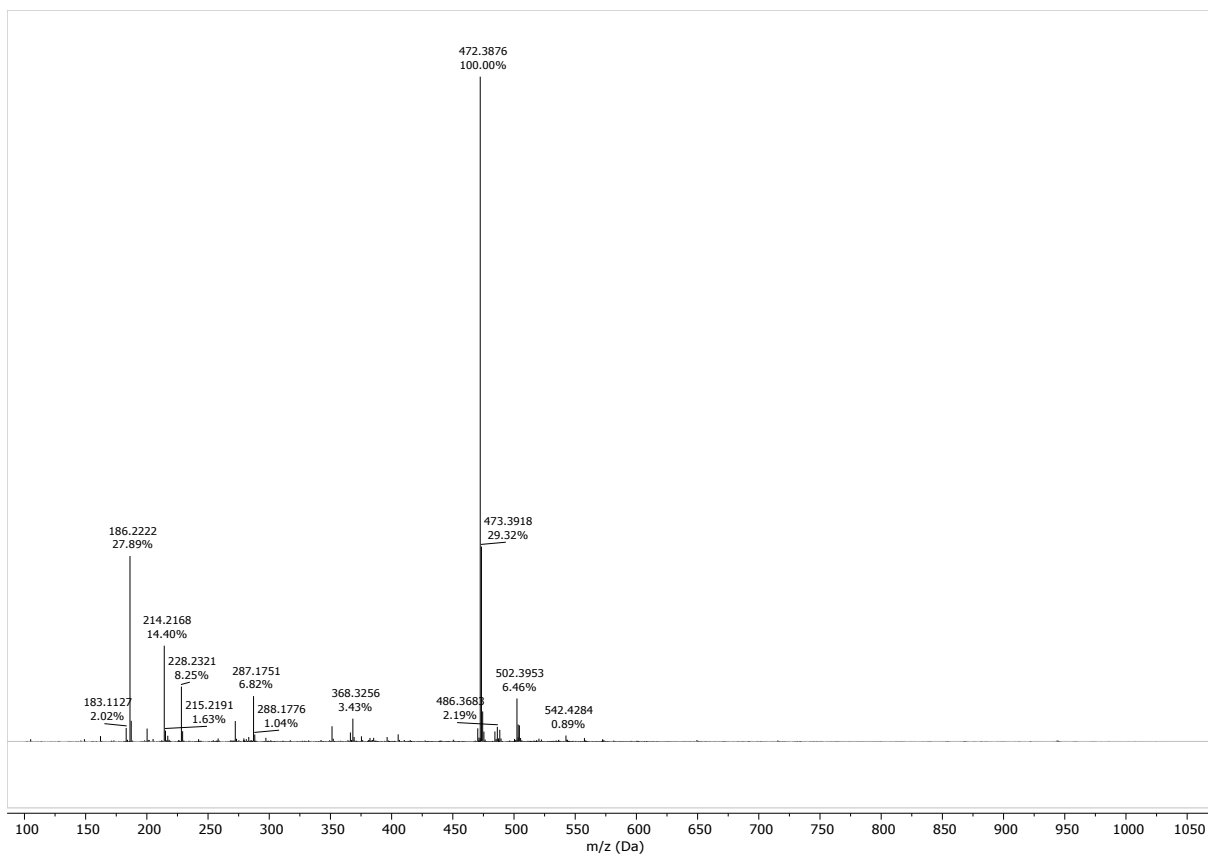
FIGURE 162. HRMS (ESI-Q-TOF) of compound **3b**; m/z: 472.3876. Calcd. for [M+H]$^+$: 472.3898.
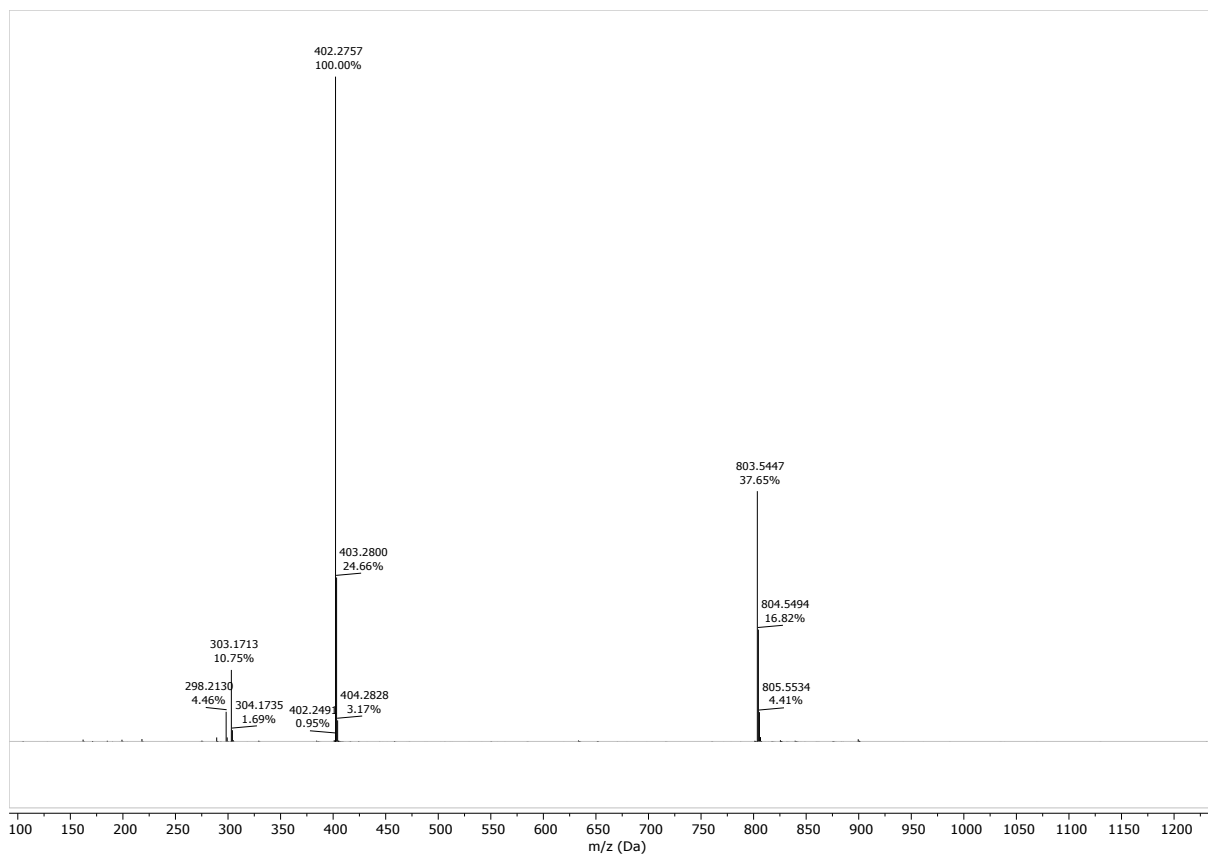
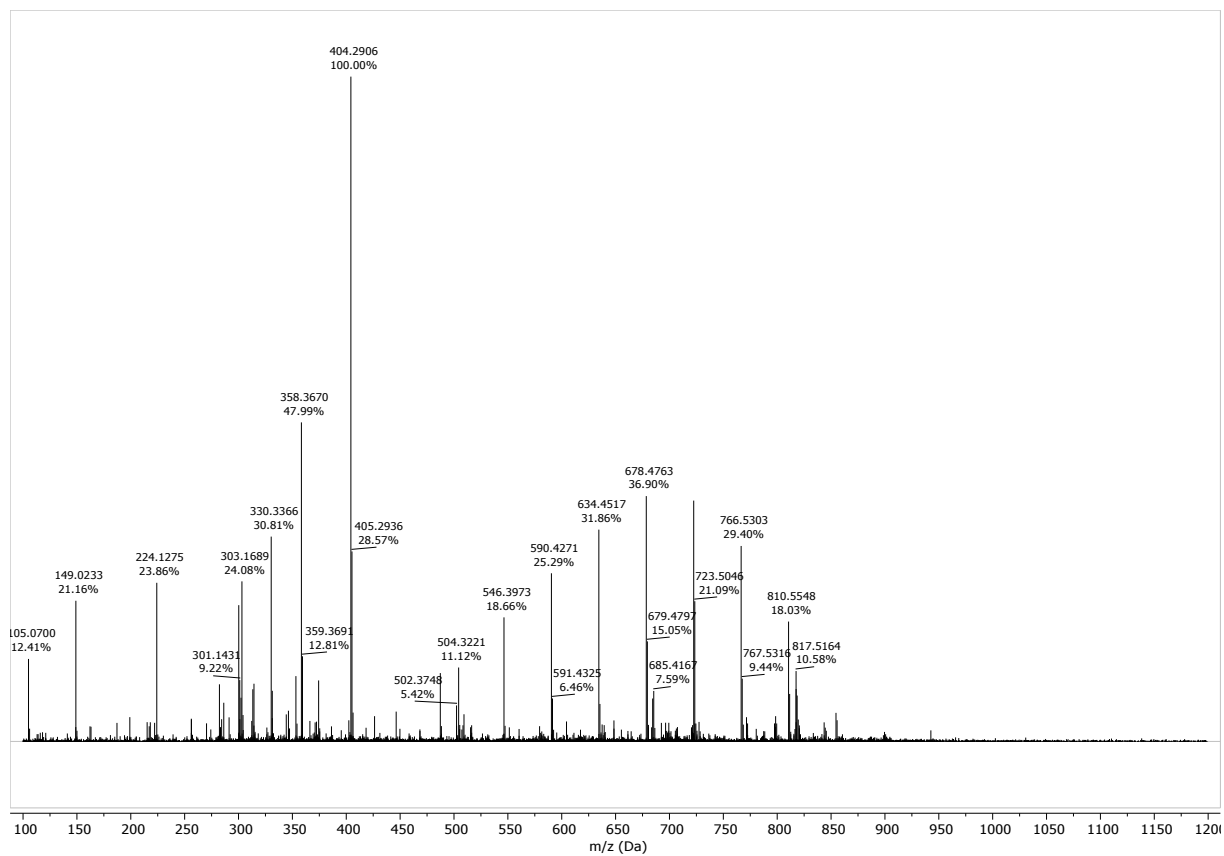**FIGURE 163.** HRMS (ESI-Q-TOF) of compound **3c**; m/z: 402.2757. Calcd. for [M+H]$^+$: 402.2751.

FIGURE 164. HRMS (ESI-Q-TOF) of compound **3d**; m/z: 404.2906. Calcd. for [M+H]$^+$: 404.2908.
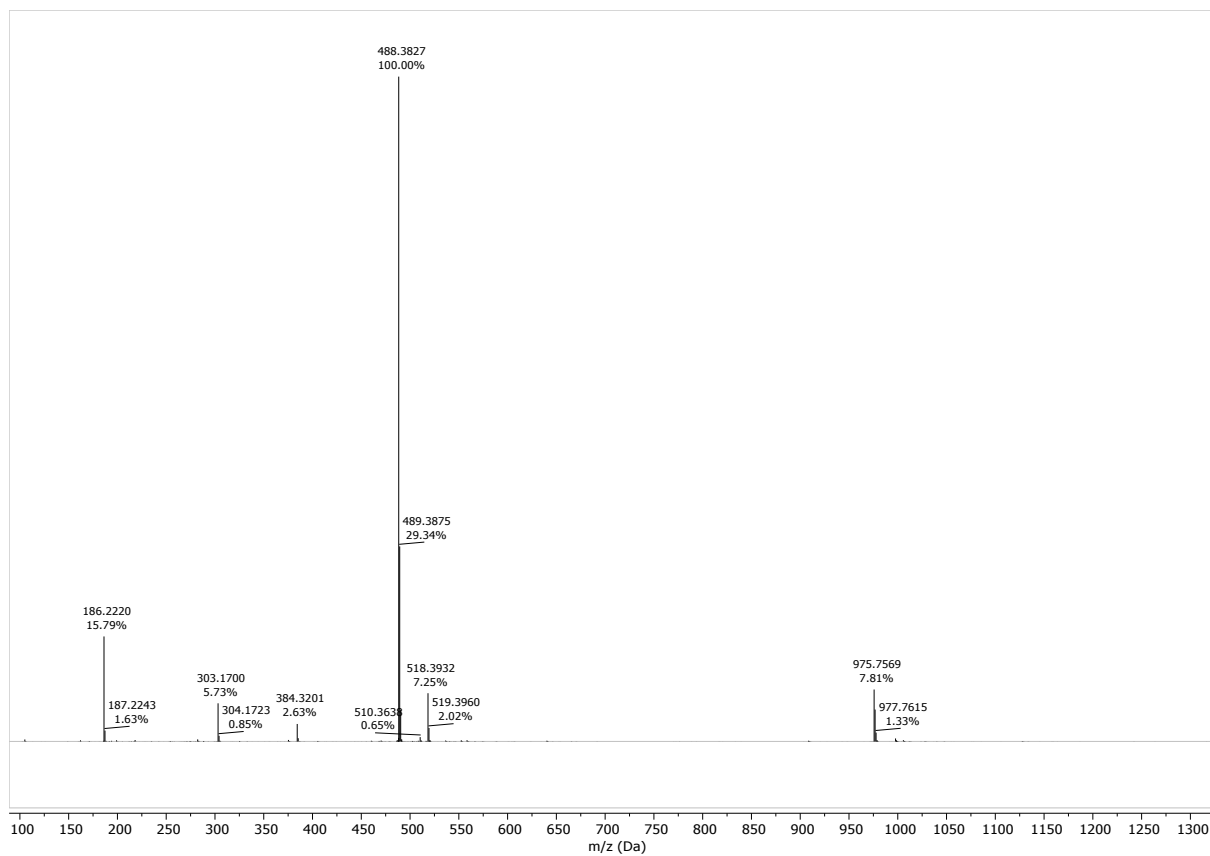
FIGURE 165. HRMS (ESI-Q-TOF) of compound **3e**; m/z: 488.3827. Calcd. for [M+H]$^+$: 488.3847.
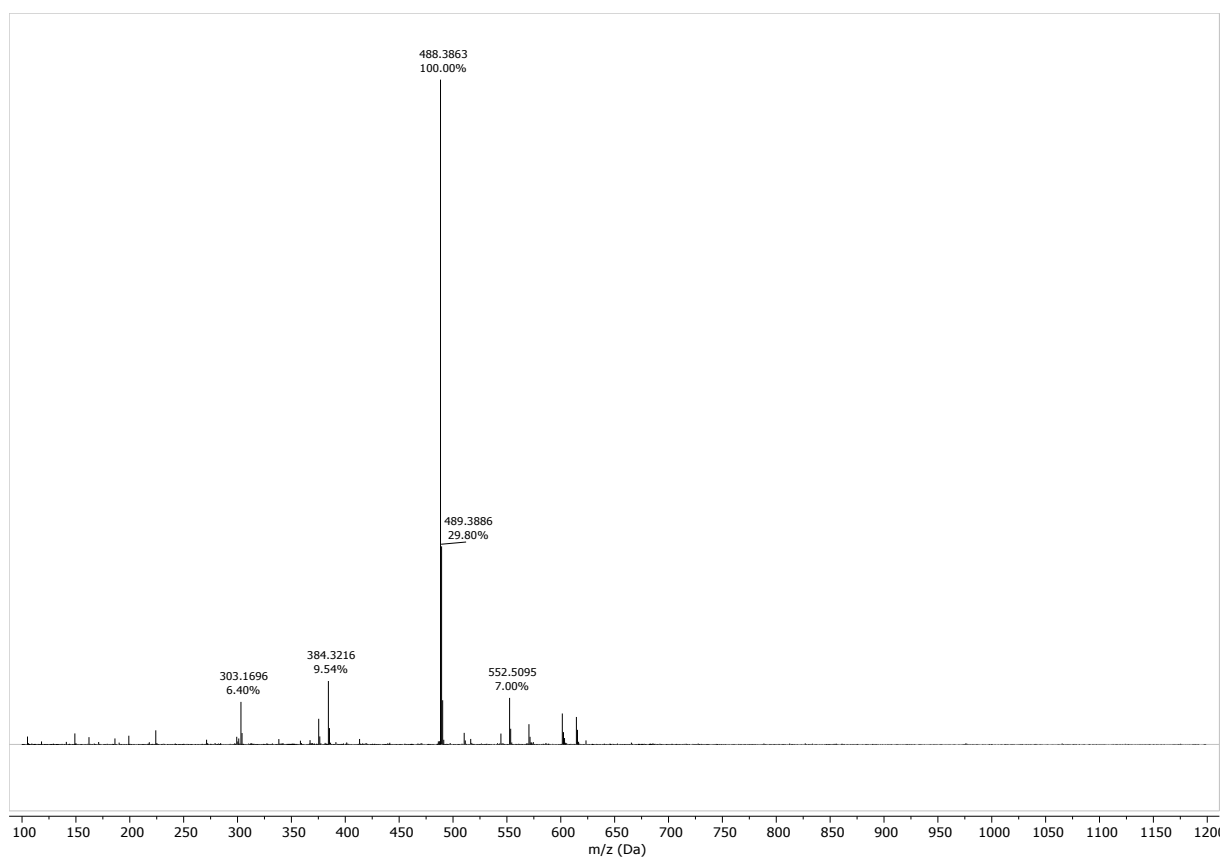
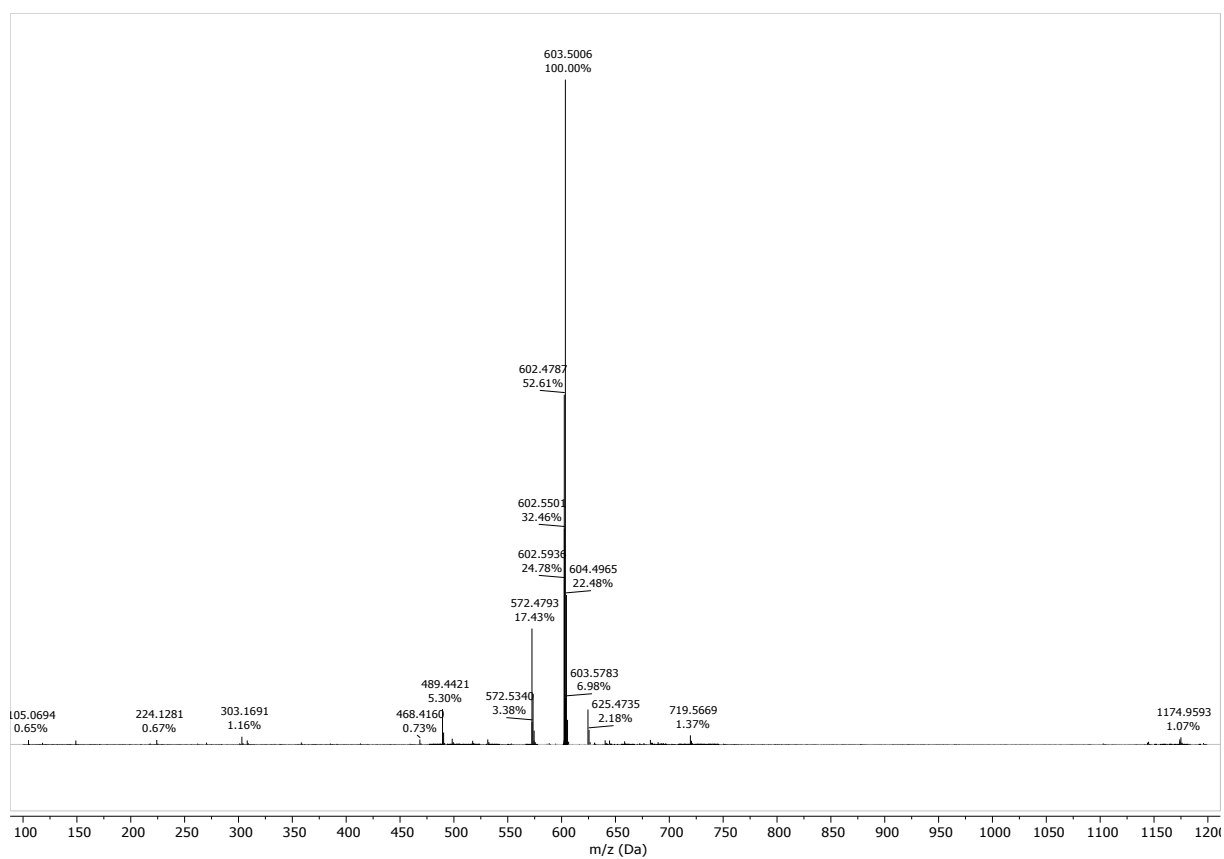**FIGURE 166.** HRMS (ESI-Q-TOF) of compound **3f**; m/z: 488.3863. Calcd. for [M+H]$^+$: 488.3847.

FIGURE 167. HRMS (ESI-Q-TOF) of compound **3g**; m/z: 603.5006. Calcd. for [M+CH3OH]$^+$: 603.4975.
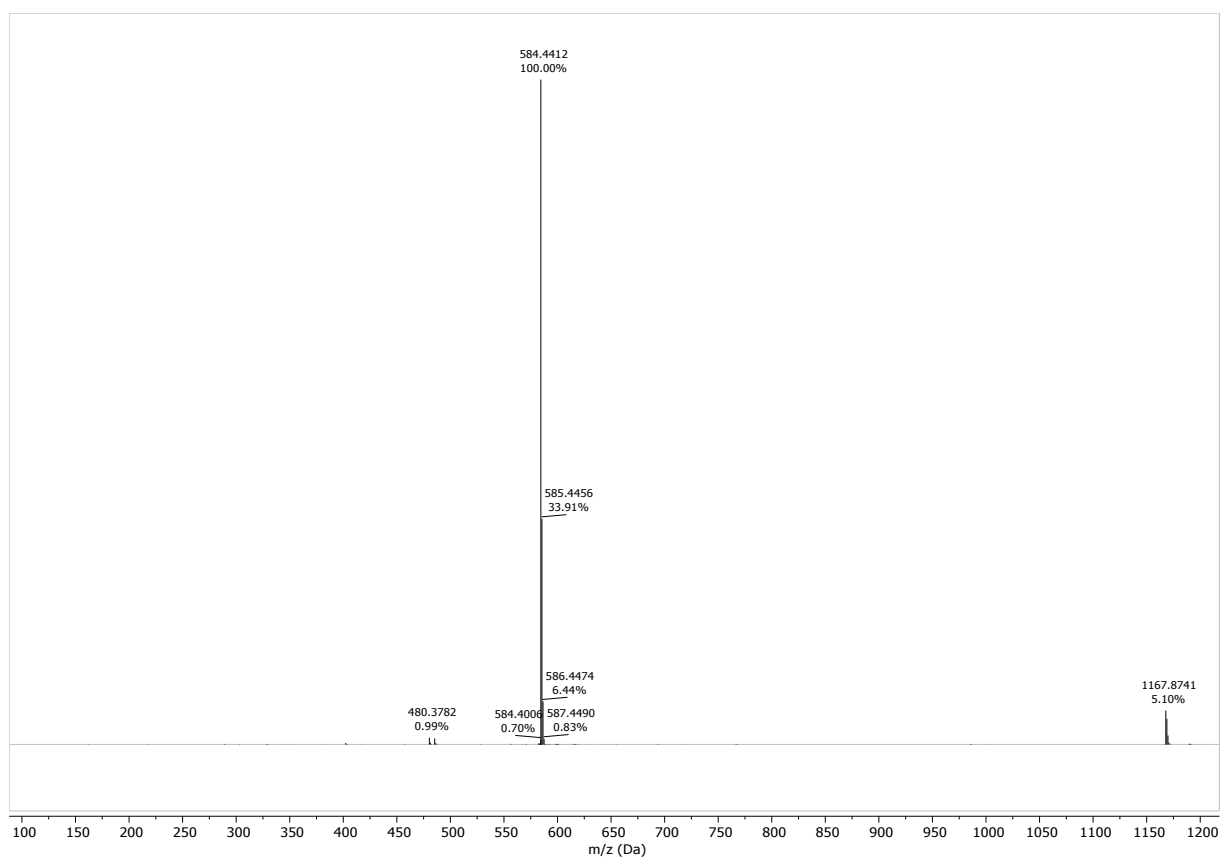
FIGURE 168. HRMS (ESI-Q-TOF) of compound **3h**; m/z: 584.4412. Calcd. for [M+H]$^+$: 584.4422.
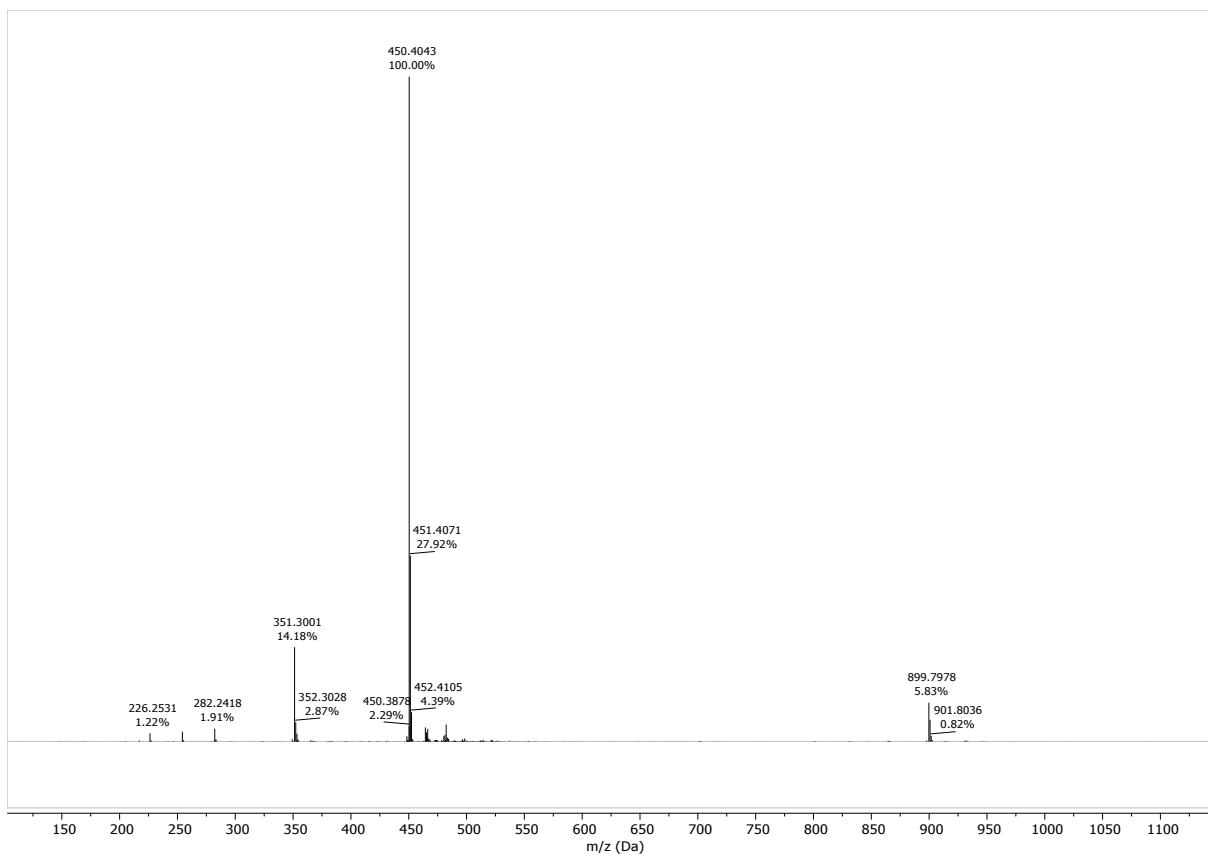
FIGURE 169. HRMS (ESI-Q-TOF) of compound **3i**; m/z: 450.4043. Calcd. for [M+H]$^+$: 450.4054.
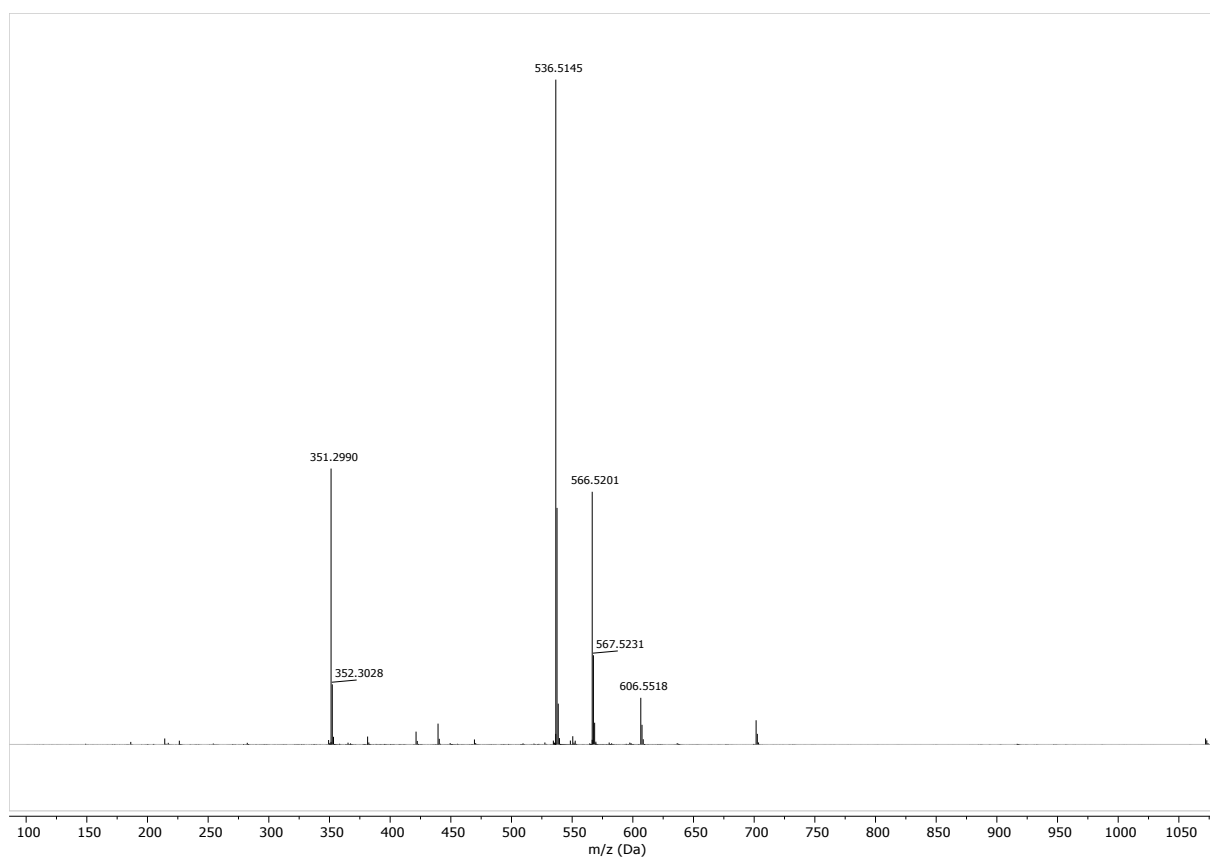
FIGURE 170. HRMS (ESI-Q-TOF) of compound **3j**; m/z: 536.5145. Calcd. for [M+H]$^+$: 536.5150.
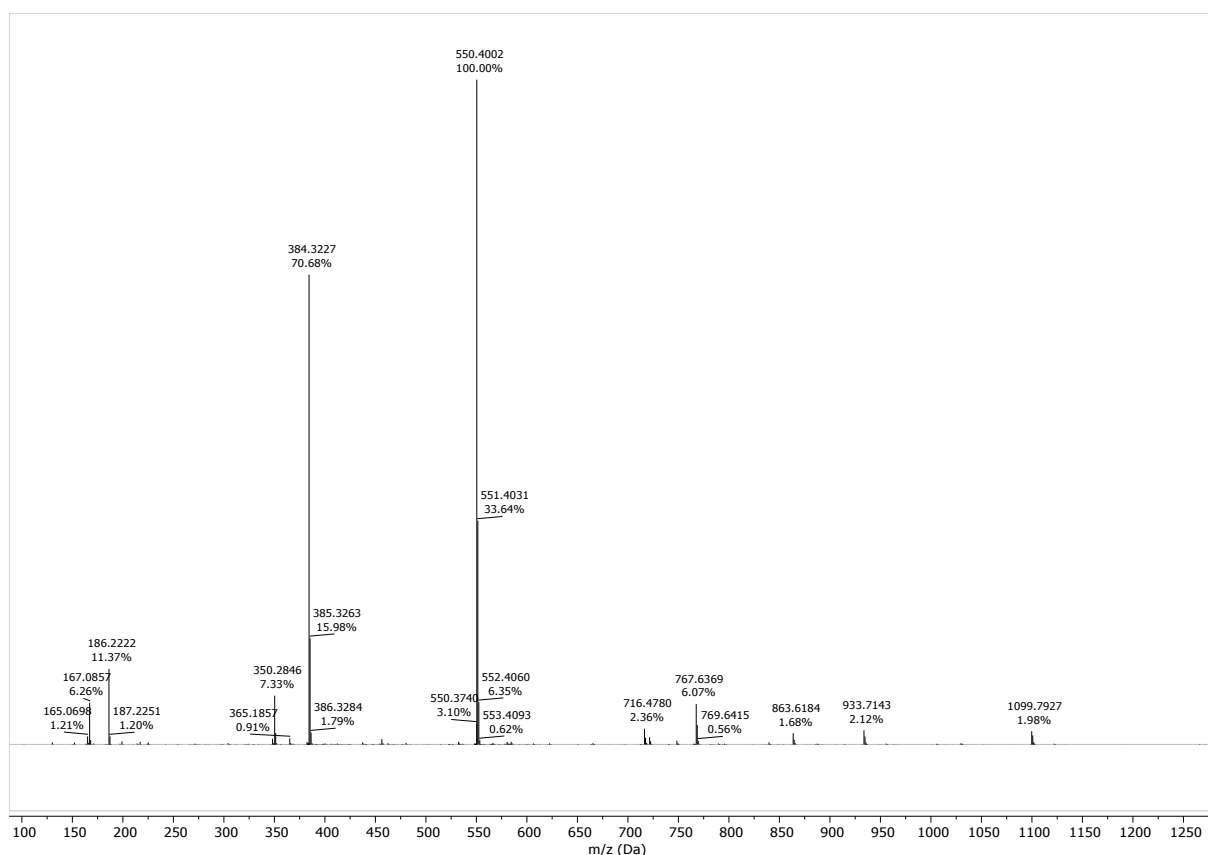
FIGURE 171. HRMS (ESI-Q-TOF) of compound **3k**; m/z: 550.4002. Calcd. for [M+H]⁺: 550.4003.

22. References

1   W. L. F. Armarego and C. L. L. Chai, *Purification of laboratory chemicals*, Butterworth-Heinemann, Fifth Edit., 2003.

2   G. R. Fulmer, A. J. M. Miller, N. H. Sherden, H. E. Gottlieb, A. Nudelman, B. M. Stoltz, J. E. Bercaw and K. I. Goldberg, *Organometallics*, 2010, **29**, 2176–2179.

3   K. A. Waibel, R. Nickisch, N. Möhl, R. Seim and M. A. R. Meier, *Green Chem.*, 2020, **22**, 933–941.

4   A. Madej, D. Paprocki, D. Koszelewski, A. Zadło-Dobrowolska, A. Brzozowska, P. Walde and R. Ostaszewski, *RSC Adv.*, 2017, **7**, 33344–33354.

5   A. F. De La Torre, D. G. Rivera, M. A. B. Ferreira, A. G. Correîa and M. W. Paixão, *J. Org. Chem.*, 2013, **78**, 10221–10232.

6   J. Dutta, N. Wakdikar and S. Tiwari, *Org. Biomol. Chem.*, 2017, **15**, 6746–6752.

7   H. Chen, X. Han, N. Qin, L. Wei, Y. Yang, L. Rao, B. Chi, L. Feng, Y. Ren and J. Wan, *Bioorganic Med. Chem.*, 2016, **24**, 1225–1230.

8   K. S. Feu, A. F. De La Torre, S. Silva, M. A. F. De Moraes Junior, A. G. Corrêa and M. W. Paixão, *Green Chem.*, 2014, **16**, 3169–3174.

9   W. Wang, J. Wang and H. Li, *Angew. Chemie - Int. Ed.*, 2005, **44**, 1369–1371.

10 L. G. Donadío, M. A. Galetti, G. Giorgi, M. Rasparini and M. J. Comin, *J. Org. Chem.*, 2016, **81**, 7952–7957.